Type 1 Insulin-like Growth Factor Signalling in Malignant Melanoma

Mark Goodfellow

MA VetMB CertVR DSAM DipECVIM-CA MRCVS

Submission for the degree of DPhil of Molecular Medicine at the

University of Oxford

Michaelmas 2012

Table of Contents

Abstract v
Acknowledgements vi
List of Figures vii
List of Tables ix

Table of Contents i
1. Introduction 1
1.1 Melanoma 1
1.1.1 Molecular Pathogenesis 1
1.1.2 Treatment 4
1.1.3 Conclusions 12
1.1.4 Comparative Aspects 12
1.2 The Wnt Pathway in Cancer 16
1.3 The IGF1R 20
1.3.1 IGF1R/IR hybrid receptors 21
1.3.2 IGF1R ligands and the regulation of their bioavailability 22
1.3.3 Signalling through the IGF1R 24
1.3.4 The role of IGF1R in tissue, development and disease 27
1.3.5 The role of IGF1R in cancer 30
1.3.6 IGF1R as a target for treatment of cancer 33
1.4 The role of the IGF1R axis in melanoma 38
1.5 The Role of the IGF1R Axis in the immune response 40
1.6 Aims of this project 42
2. Materials & Methods 46
2.1 Gene Nomenclature 46
2.2 Cell Culture 46
2.2.1 Cell Culture techniques. 46
2.2.2 Cell lines 47
2.2.3 Transfection of cultured cells 47
2.3 Growth Assays 51
2.3.1 CellTiter-Glo Luminescent Cell Viability Assay 51
2.3.2 Crystal Violet Assay 52
2.4 Treatments 55
2.5 Flow cytometry 55
2.5.1 Cell Surface Antigen Expression 58
2.5.2 Cell surface expression of murine Igf1r. 58

2.5.3 Analysis of Ploidy 59
2.5.4 Cell cycle analysis 59
2.5.5 Functional Immunological Assays 60
2.6 Immunofluorescence microscopy 67
2.7 Procedures for handling RNA 68
2.7.1 General Techniques 68
2.7.2 Extraction of Total RNA For qRT PCR 68
2.7.3 DNAase I Treatment and Reverse Transcription 68
2.7.4 Quantitative RT-PCR (qRT-PCR) 69
2.7.5 Extraction of RNA for gene profiling and miRNA quantification 74
2.7.6 Illumina gene arrays 75
2.7.7 miRNA quantification 75
2.8 Gene Silencing by RNA Interference 76
2.9 Procedures for handling DNA 77
2.9.1 Cloning of *Igf1r* shRNA into pENTR/H1/T0 Vector 77
2.9.2 Creation of a stable Tet R expressing cell line 81
2.9.3 Assay of β-Galactosidase activity 82
2.9.4 Cell based assay of Wnt pathway activation (SuperTop/FOP assay) 83
2.10 Protein Analysis 84
2.10.1 Lysis of harvested cells 84
2.10.2 Preparation of nuclear lysate 85
2.10.3 Protein quantification 85
2.10.4 SDS Polyacrylamide gel electrophoresis (SDS-PAGE) 86
2.10.5 Immunoblotting 87
2.11 Statistical analysis 89
3. Effects of IGF1R blockade on melanoma immunogenicity 90
3.1 Introduction 90
3.2 Results and Discussion 92
3.2.1 Effect of siRNA mediated Igf1r depletion on expression of MHC Class 1 ..... molecules in B16.F10 melanoma 92
3.2.2 Effect of IGF1 ligand stimulation on expression of MHC Class 1. 97
3.2.3 Effect of IGF1R depletion on MHC Class 1 expression in a panel of melanoma cell lines. 99
3.2.4 Effect of IGF1R inhibition on MHC Class 1 expression in B16.F10 ..... melanoma cells. 101
3.2.5 Effect of IGF1R depletion of B16.F10 cells on T cell proliferation and..... Cytokine production. 108
3.2.6 Effect of IFNɣ on the Immunogencity of B16.F10 melanoma 112

3.2.7 An inducible system for regulated Igf1r depletion in B16.F10 melanoma . 118
3.3 Conclusions 130
3.4 Future directions for investigation of the role of the Igf1r in the immunological response to tumour cells 131
4. IGF1R induced gene expression in human melanoma 134
4.1 Introduction 134
4.2 Experimental design 136
4.3 Results and Discussion 138
4.3.1 Selection of cell lines and experimental conditions. 138
4.3.2 Determination of growth inhibition by IGF1R small molecule inhibitor AZ12253801 145
4.3.3 Assessment of inhibition of basal IGF1R signalling by AZ12253801 148
4.3.4 Preparation of RNA for microarray analysis and miRNA qRT-PCR 154
4.3.5 miRNA qRT-PCR 155
4.3.6 Validation of miRNA of Interest 158
4.3.7 Bioinformatic analysis of microarray data 160
4.3.8 Screening for differential expression 161
4.3.9 Assessment of changes in expression of genes involved in immune recognition of tumour cells 165
4.3.10 Data mining for pathway representation and determination of an IGF1 induced gene signature. 166
4.3.11 *In silico* analysis of clinical melanoma datasets 169
4.3.12 Data mining for transcripts altered in a reciprocal fashion by IGF1R inhibition and stimulation. 175
4.3.13 Cluster analysis and Interactions of Genes of Interest 180
4.3.14 Validation of selected hits in four melanoma cell lines 183
4.4 Conclusions 191
4.4.1 HBP1 (HMG Box Protein 1) 192
5. HBP1 and IGF1R Signalling in human melanoma 200
5.1 Introduction 200
5.2 Results and Discussion 201
5.2.1 Effect of IGF1R depletion on *HBP1* mRNA 201
5.2.2 Quantification of HBP1 protein 203
5.2.3 Elucidation of the signalling pathway by which IGF1R affects *HBP1* transcription. 206
5.2.4 Effect of HBP1 depletion on cell cycle progression 220
5.2.5 Effect of HBP1 depletion on proliferation of A375 melanoma cells. 222
5.2.6 Expression of HBP1 in clinical melanoma – *in silico* analysis 224

5.2.7 Effect of IGF1R manipulation on known HBP1 transcriptional targets 225
5.2.8 Effect of HBP1 depletion on transcription of HBP1 target genes.....233
5.2.9 Optimisation of the TOPFLASH Assay in A375 melanoma cells. 236
5.2.10 Determination of the effects of IGF1R inhibition on transcription of Wnt..... target genes.....240
5.3 Conclusions.....244
5.3.1 Interaction of Wnt and growth factor pathways - future directions 246
6. Bibliography.....249

7. Appendices 1-6

Abstract

Novel therapeutic strategies are sorely required for malignant melanoma, which has been shown to overexpress the type 1 insulin-like growth factor receptor (IGF1R) compared to benign naevi. The IGF1R mediates many features of the malignant phenotype and is an attractive anti-cancer therapeutic target. Inoculation with IGF1R depleted tumour cells has been shown to upregulate MHC Class 1 expression and confer protection from tumour rechallenge *in vivo*. The initial aim of this project was to investigate effects of IGF1R depletion on MHC Class 1 expression and its functional significance in melanoma cells. *IGF1R* gene silencing, but not IGF1R inhibition, caused a significant increase in surface MHC Class 1 expression in one murine cell line, B16.F10, but 0/8 human melanoma cell lines. In B16.F10 cells, increased MHC Class 1 did not affect cell lysis or cytokine production by, or proliferation of, activated T lymphocytes *in vitro*. These results indicate that the increase in MHC Class 1 in melanoma cells is not of functional significance.

The main focus of this project then addressed a key issue relevant to clinical trials of IGF1R inhibition. Identifying features which render melanoma cells sensitive to IGF1R inhibitors is important to select patients suitable to receive this therapy. The approach was to define changes in gene expression after IGF1 or IGF1R inhibitor treatment of melanoma cells. Initial experiments were performed to select concentrations of IGF1 and IGF1R inhibitor AZ12253801, the latter based on GI_{50} concentrations. An IGF gene signature was created which was significantly correlated to Ki67 expression, a proliferation marker, in clinical datasets. This suggests a rationale for IGF1R targeting in clinical melanoma.

Gene expression profiling identified that IGF and IGF1R inhibition had reciprocal effects on expression of *HBP1*, a transcriptional repressor of prognostic significance in breast cancer. HBP1 was validated as an IGF1 regulated gene, and experiments using signalling inhibitors indicated that IGF1R regulates HBP1 via the PI3K pathway. HBP1 depletion did not influence effects of IGF1R inhibition on proliferation. However HBP1 induction appeared to mediate effects of AZ12253801 on inhibiting the WNT pathway, measured by TOP/FOP reporters, and HBP1 depletion enhanced basal and WNT-induced *NMYC* expression. *NMYC* has not previously been reported to be a Wnt/β catenin target gene in neoplastic cells. These results encourage further investigation into the effects of IGF1R in regulating HBP1, particularly with respect to dual IGF1R Wnt/β catenin targeting.

Acknowledgements

I would like to thank the Wellcome Trust for funding this Veterinary Research Training Fellowship and Dr Val Macaualy both for the opportunity to work in her laboratory and assistance given with this project. I would also like to thank Professor Cerenudolo and his team: Drs' Jon Silk, Mau Salio, Angus Stock and Carmen DeSanto for their indefatigable advice with the immunology portion of this project. Particular thanks must go to my fellow members of the IGF Lab: Megumi Takiguchi, Tamara Aleksic, Martin Kerr, Meenali Chitnis, Roger Ramcharan, Kunal Lodhia, Gao Shan and Philip Earwaker, I couldn't have done it without you.

And of course to Katie for her patience, endless support and encouragement.

List of Figures

1.1	The immunological synapse	9
1.2	The canonical Wnt/β-catenin pathway	17
1.3	The IGF1R axis	25
2.1	Cell growth determined on sequential days using the Cell Titer Glo Assay	53
2.2	Six well plate cell viability assay	54
3.1	Effect of Igf1r depletion on MHC Class 1 expression	94
3.2	Effect of Igf1r depletion on *Igf1r* expression and cell surface MHC 1	96
3.3	Effect of IGF1 treatment on cell surface MHC Class 1	98
3.4	Effect of IGF1R siRNA on MHC Class1 expression in a panel of melanoma cells	100
3.5	Effects of Igf1r inhibition with PPP on MHC Class 1 expression	103
3.6	Effects of AZ12253801 on Igf1r axis activation and MHC Class 1 expression	104
3.7	Effects of αIR3 (IGF1R blocking antibody) on MHC Class 1 expression	106
3.8	Effect of Igf1r depleted B16.F10 on T cell proliferation	110
3.9	Effect of Igf1r depleted B16.F10 on cytokine production by effector T cells	113
3.10	Cytotoxic T lymphocyte killing of IFNγ treated B16.F10 cells	115
3.11	Schematic overview of creation of a cell line with inducible shRNA expression	120
3.12	Expression of tetracycline regulatory protein (TETR) by B16.F10 clones	122
3.13	Effect of Igf1r siRNA or shRNA on Igf1r expression	126
3.14	Activity of the H1/T0 promotor in B16.F10 melanoma cells	129
4.1	IGF1R protein levels and surface expression in 4 chosen human melanoma cell lines	140
4.2	Effects of IGF1 on cell signalling in A375 melanoma	142
4.3	Effects of IGF1 on cell signalling in 3 melanoma cell lines	143
4.4	Effect of IGF1 on cyclin D expression in A375 cells	144
4.5	AZ12253801 inhibits growth of melanoma cells	147
4.6	Effect of AZ12253801 on IGF1 induced IGF1R and AKT phosphorylation	149
4.7	Effect of AZ12253801 on DNA content of A375 melanoma cells	151
4.8	Effec of AZ12253801 on DNA content of SKMel2, SKMel23 and SKMel28 melanoma cells	153
4.9	Analysis of changes in miRNA expression after IGF1R stimulation or inhibition in A375 cells	156
4.10	Effect of IGF1R stimulation or inhibition on miR-155, miR-20b and miR-200b	159
4.11	Dendrogram of sample clustering	163
4.12	Networks overrepresented in IGF1 induced gene sets at 3 and 24 hours	167
4.13	Correlation of IGF induced gene signature at 3 and 24 hours to Ki67	172

4.14	Correlation of melanoma IGF gene signature with prognosis in breast cancer	174
4.15	Heatmap of gene expression clustering 3 hours after AZ12253801 treatment	181
4.16	Heatmap of gene expression clustering 3 hours after IGF1 treatment	182
4.17	Gene chosen for validation have known relationships to components of the IGF1R signalling pathway	184
4.18	Selection of reference genes for validation studies	185
4.19	Validation in four melanoma cell lines of five transcripts reciprocally regulated after 3 hours of IGF1R stimulation or inhibition in A374 cells	187
4.20	Validation in four melanoma cell lines of three transcripts reciprocally regulated after 24 hours of IGF1R stimulation or inhibition in A374 cells	188
4.21	Validation in four melanoma cell lines of three transcripts which showed a large fold change in expression after IGF1 treatment in A375 cells	189
4.22	Schematic diagram of HBP1 with residues of known significance and published targets listed	191
5.1	The effects of IGF1R depletion on HBP1 expression	202
5.2	The effect of IGF1R axis manipulation on HBP1 protein expression	204
5.3	Effect of IGF1R stimulation or inhibition on phosphorylation of downstream molecules	207
5.4	U1026 inhibits MEK and ERK activation following IGF1 stimulation in A375 cells	210
5.5	LY294002 abrogates IGF1 induced AKT phosphorylation	211
5.6	Effect of U0126 and LY294002 on IGF1R mediated changes in HBP1 expression	213
5.7	Rapamycin inhibits IGF1 induced phosphorylation of S6 and p70-S6 Kinase	215
5.8	Effect of rapamycin on IGF1R mediated changes in HBP1 expression	216
5.9	Effect of FOXO dominant negative plasmid transfection on IGF1R mediated changes in HBP1 expression	219
5.10	HBP1 depletion has no effect on IGF1R mediated changes in cell cycle distribution of A375 melanoma cells	221
5.11	Effect of HBP1 depletion on growth of A375 melanoma cells	223
5.12	Expression of HBP1 is lower in proliferative melanoma	226
5.13	IGF1R manipulation influences HBP1 and CMYC expression	228
5.14	IGF1R manipulation is associated with temporal changes in HBP1 mRNA and reciprocal changes in target geen expression	229
5.15	IGF1R manipulation is associated with temporal changes in CDKN2A, MIF and NCF1 expression	230
5.16	HBP1 depletion results in an increase in NMYC, but not CMYC or CCND1, expression	235
5.17	WNT3A activates the Wnt/β-catenin pathway in A375 melanoma cells	238
5.18	Effect of AZ12253801 on WNT3A induced transcription is prevented by HBP1 depletion	241

5.19 NMYC expression is induced by WNT3A after HBP1 depletion 243

List of Tables

1.1 IGF1R inhibitory agent in Clinical Trials 35
2.1 Cell lines utilised in this project 48
2.2 Treatments applied to cells in culture 56
2.3 Antibodies used for Flow Cytometric analysis 57
2.4 Primer sequences and probe numbers of Human reference genes employed for qRT-PCR 70
2.5 Primer sequences and probe numbers of murine geens employed for qRT-PCR 71
2.6 Primer sequences and probe numbers of Human Genes of Interest employed for qRT-PCR 72
2.7 siRNA sequences employed for gene silencing 78
2.8 Antibodies used for Immunoblot analysis 88
3.1 Sequences of selected Igf1r shRNAs 124
4.1 Experimental Design 138
4.2 Genotype of Selected Melanoma cell lines 138
4.3 Gene transcripts chosen for further validation 176

1. Introduction

The focus of this thesis is the role of the insulin-like growth factor (IGF) axis in melanoma.

1.1 Melanoma

Melanoma is the most aggressive form of cutaneous neoplasia. The incidence and mortality of cutaneous melanoma in fair skinned human populations has been increasing worldwide for the last 30 years (World Health Organisation http://www.who.int/research/en/). This neoplasm has a multifactorial aetiology with environmental, genetic and host factors playing a role. Exposure to UVA and UVB, particularly in childhood is the primary aetiological factor and increased sun exposure or cosmetic tanning is likely the cause of the increasing global incidence (Lens and Dawes, 2004, Young, 2004). Inherited mutations predisposing to melanoma formation, such as that of *CDKN2A* have been identified but the incidence in the general population is low (Kamb et al., 1994, Hussussian et al., 1994, Satyamoorthy and Herlyn, 2003).

1.1.1 Molecular Pathogenesis

In 2000 Hanahan and Weinberg defined six properties of neoplastic cells which they designated the hallmarks of cancer; functional characteristics which are acquired during neoplastic transformation (Hanahan and Weinberg, 2000). Four additional properties were added in a subsequent paper (Hanahan and Weinberg, 2011). Numerous tumour suppressor genes and oncogenes are involved in the pathogenesis of melanoma and these confer properties identified as the *hallmarks of cancer*. As mentioned above familial mutations of

CDKN2A predispose to melanoma formation. However mutations in this gene are also common in spontaneous disease, being identified in half of primary melanoma and the majority of melanoma cell lines (Haluska et al., 2006a, Flores et al., 1996). The *CDKN2A* locus encodes two tumour suppressor genes, p16INK4A and p14ARF, which are involved in control of cell cycle progression and checkpoint regulation. p16INK4A binds to, and blocks the activity of, cyclin dependent kinase (CDK)-4 and -6 which are required to phosphorylate retinoblastoma protein (RB) and thus allow cell cycle progression into S phase (Lukas et al., 1995). In contrast p14ARF is an inhibitor of murine double minute protein (mdm2), itself a negative regulator of p53 (Gallagher et al., 2006). As such disruption of *CDKN2A* results in both the loss of RB and p53 mediated cell cycle control and therefore promotes *insensitivity to anti-growth signals* and *limitless reproductive potental.*

Changes in growth factor signalling are frequent events in melanoma. The role of the IGF1R and Wnt/β catenin signalling will be discussed separately but numerous other growth factors including hepatocyte growth factor, endothelial growth factor and basic fibroblast growth factor act in a paracrine or autocrine fashion on melanoma cells and these ligands and their receptors have roles in melanoma progression (De Wit et al., 1992, Halaban et al., 1992b, Fontijn et al., 2006, Mattei et al., 1994).

However it is changes in downstream signalling pathways which are the best characterised in melanoma. Analysis of somatic mutations in melanoma cell lines revealed a predominance of alterations in components of the MEK-MAPK pathways. The majority of primary melanoma and melanoma cell lines tested have constitutive activation of ERKs as a consequence of upstream activating mutations of *RAS* or *BRAF* (Satyamoorthy et al.,

2003). These mutations are thought to be early events in melanoma pathogenesis (Cohen et al., 2002), promote cell proliferation and survival (Wellbrock et al., 2004), and are associated with progressive disease (Dong et al., 2003).

Alterations in *RAS* genes are common in human cancer (Davies et al., 2002). In melanoma, mutations are almost exclusively found in *NRAS* and play a key role in melanoma pathogenesis (Chin et al., 1999, Chin et al., 1997). Indeed 20-30% of primary melanoma carry mutated *NRAS* (Omholt et al., 2002, Curtin et al., 2005). The most common mutations are found in the GTP binding domain, result in reduced GTPase activity, prolonged GTP binding and therefore constitutively active NRAS (Polakis and McCormick, 1993).

Mutations of *BRAF* are present in 50-70% of malignant melanoma (Davies et al., 2002, Shinozaki et al., 2004, Brose et al., 2002) typically in a mutually exclusive fashion with *NRAS* mutations (Haluska et al., 2006a). Clinically the incidence of *BRAF* mutations varies by clinicopathological subtype with a lower incidence (10%) in melanoma associated with chronic skin damage and higher (60%) in those without (Curtin et al., 2005). Mutations are principally in the activating segment and the single activating point mutation resulting in substitution of valine for glutamine at codon 600, hereafter designated *BRAF V600E*, is the most common (Wellbrock et al., 2004). This mutation, and others in the kinase domain, result in indpendant kinase activity, constitutively active ERK, *self sufficiency of growth* and, as established in murine studies, melanooncogenesis (Dhomen et al., 2009, Wan et al., 2004).

Further enhancement of cell signalling can occurs as a consequence of *PTEN* gene deletion or mutation resulting in activation of the PI3K/AKT signalling and this promotes cell survival and *evasion of apotosis* (Celebi et al., 2000, Goel et al., 2006). Interestingly *PTEN* mutations almost always occur in association with mutated *BRAF*, suggesting that this dual mutation can function in a similar fashion to a sole *NRAS* mutation (Haluska et al., 2006a). Indeed as *BRAF-V600E* is a common finding in benign naevi, this mutation is unlikely to be solely responsible for tumorigenesis (Pollock et al., 2003).

1.1.2 Treatment

Although the incidence of malignant melanoma is increasing, most cases are diagnosed at an early stage when complete surgical resection is curative. Indeed tumours of low Breslow thickness (Stages 0 and 1), which encompasses the majority of cases, have an excellent prognosis with a ten year survival of greater than 80% (Balch et al., 2009). In contrast thicker primary tumours (Stage 2) have an increased recurrence rate and patients presenting with nodal (Stage 3) or distant (Stage 4) metastases have a poor prognosis. In stage 3 patients survival rates depend on the number and nature of the nodal involvement, whilst Stage 4 patients have an average survival of only 6-10 months with 10% surviving longer than five years (Balch et al., 2009). Despite significant efforts and costly research, the treatment options for these patients with advanced disease remain limited. Furthermore as the incidence of melanoma has increased there has been an accompanying increase in the proportion of patients with advanced disease and thus a poor prognosis (Lens and Dawes, 2004).

1.1.2.1 Surgery and Chemotherapy

As described above surgical resection is the standard of care for low stage cutaneous melanoma and is typically curative. For those patients with metastatic disease non surgical therapies are appropriate but until recently were of limited efficacy. For example in the UK and USA the standard of care for stage 4 disease has been dacarbazine but responses to it and its oral analogue, temozolamide, are low (10% to 20%) with a median response duration of only 3 to 4 months (Middleton et al., 2007, Avril et al., 2004, Middleton et al., 2000, Eigentler et al., 2003). In fact no single agent or combination chemotherapy has been shown to improve overall survival in patients with advanced melanoma. Response rates are typically less than 20 percent and median response durations only four to six months. The inadequacy of conventional chemotherapy in advanced disease led to the exploration of numerous other treatment modalities, including immunotherapy, cancer vaccines and more recently, small molecule inhibitors. Although far from identifying an approach suitable for all patients, advances made and published during the time the research herein was being conducted have proved very beneficial for subgroups of patients. Furthermore, the mechanisms of action of these therapies are of direct relevance to the aims of this project, and are briefly outlined below.

1.1.2.2 Immunotherapy

Seminal experiments in cancer immunology in the 1950's revealed that "vaccination" of mice with irradiated MHC matched tumour cells could elicit a specific protective immunity to subsequent viable tumour challenge (Prehn and Main, 1957). In the case of melanoma occasional spontaneous regression has been reported and this phenomenon has been correlated with an anti-tumour immune response (Dissemond et al., 2003). These

observations led to the identification of tumour-specific antigens against which specific antitumour CD4+ and CD8+ T cells could be detected in melanoma patients (Pardoll, 2002). However melanoma typically progresses despite the presence of this immune response. A number of mechanisms have been postulated to explain this evasion of the immune response including escape from immune surveillance, via downregulation of MHC Class I molecules and inhibition of T cell activity via increased CTLA4 expression, and activity of CD25+ CD4+ regulatory T cells (Seliger, 2005). These will be discussed in more detail below, but the recognition that melanoma elicits an immune response associated with specific tumour antigens suggested that enhancement of the immune response might have therapeutic benefit. Present strategies of melanoma immunotherapy involve the enhancement of pre-existing host immunological responses directed at the tumour. No one therapy is suitable for all patients but certain agents have been shown to have clear benefits for subgroups of patients.

1.1.2.2.1 Interferon

Interferon, a cytokine produced by lymphocytes, monocytes and macrophages, has been postulated to have numerous beneficial mechanisms of action. Interferon has been suggested to increase dendritic cell response to melanoma associated antigens on tumour cells, enhance cell mediated cytotoxicity, increase T cell infiltration, increase antigen cross presentation, and have antiangiogenic and proapopotic properties (Tarhini et al., 2012). Used as an adjuvant therapy in Stage 2 and 3 disease. Interferon alpha is beneficial to a small subgroup of patients with microscopic not macroscopic lymph node metastases (Eggermont et al., 2005, Eggermont et al., 2008).

1.1.2.2.2 Cancer Vaccines

Cancer vaccines have been explored in melanoma, perhaps more than other tumour types, as a method of enhancing immune recognition and stimulating effective anti-tumour immune responses. This can occur by improving antigen presentation, inducing antibody production capable of killing melanoma cells by complement and antibody dependent cell mediated cytotoxicity and elicitation of durable effector memory T cell responses. Numerous strategies have been or are being trialled in melanoma patients including sole or combination peptide epitope vaccines (gp100, MART 1, Melan A, tyrosinase, MAGE A3), glycolipid vaccines (GM2), lysed whole cell vaccines, modified whole cell vaccines and dendritic cell vaccines (Soiffer et al., 2003) (Mitchell et al., 2007, Trefzer et al., Kirkwood et al., 2009, Eggermont A. M, 2010, Kirkwood et al., 2001) (Schwartzentruber et al., 2011, Hersey et al., 2004). As yet either as sole agents or in combination, results have not shown sufficient benefit for these strategies to be implemented in routine practice.

1.1.2.2.3 Adoptive cell therapy

An alternative strategy to challenging the immune system with exogenous tumour antigens is to isolate, activate and expand pre-existing antitumour lymphocytes *ex vivo*, before reintroduction into the patient. By collecting tumour infiltrating lymphocytes this technique selects for patient lymphocyte clones with individual tumour antigen specificity. This therapy has been associated with high response rates, durable remission and even cure, but the therapy is not yet widely available (Dudley et al., 2005, Koike et al., 2008).

During the time course of this thesis the results of trials of two novel strategies in the treatment of advanced melanoma were published, followed by further evidence of their efficacy (Hodi et al., 2010a, Chapman et al., 2011). These represented the first treatments to clearly improve overall survival in patients with advanced melanoma in randomised controlled trials.

1.1.2.2.4 CTLA4 Blockade

Presentation of tumour antigens is not sufficient alone for generation of an effective immune response. T cell activation is modulated by integration of stimulatory and inhibitory signals which coordinate the immunological response. Full T cell activation requires stimulation via two molecular interactions between the T cell and antigen presenting cell, across the so-called immunological synapse. Peptides derived from cleavage of either intracellular or phagocytosed extracellular proteins are displayed in the binding groove of a major histocompatibility complex molecule (MHC) Class I and II respectively. The T cell's unique receptor recognises its cognate ligand peptide only in the context of the MHC molecule. This interaction of the T cell receptor, its cognate peptide and MHC molecule initiates T cell activation (Figure 1.1). However full T cell activation requires a second co-stimulatory signal. This is generated by the interaction of CD80 molecules (B7-1) (and/or CD86 (B7.2)) on the antigen presenting cell and CD28 on the T cell which, amongst other effects, results in increased cytokine expression, including IL 2 (Alegre et al., 2001). Integration of both signals is required for T cell proliferation, acquisition of effector functions and migration to sites of antigen expression.

As mentioned above one of the mechanisms by which tumour cells fail to elicit an effective immune response is via the downregulation of surface MHC molecules and of co-

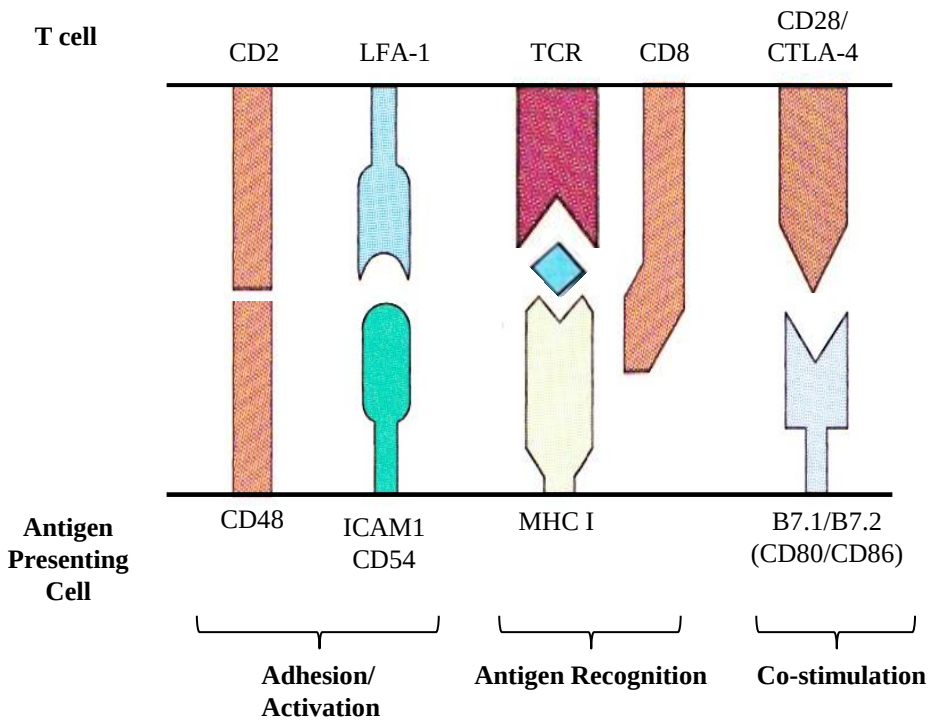


Figure 1.1 The immunological synapse. Endogenous antigen recognition by T cells requires processed antigen presentation in the context of an MHC Class 1 molecule by an antigen presenting cell. When a T cell encounters the appropriate MHC-peptide complex, conformational change enhances the affinity of lymphocyte functional antigen-1 (LFA-1) for intercellular adhesion molecules (ICAMs) and prolongs cell-cell contact. CD8 molecules increase the affinity of the T cell to MHC molecules ~100 fold. Interaction of CD28 with B7 molecules is required to provide co-stimulation which results in T cell activation. CTLA4 expression increases after T cell activation and limits CD28/B7 interactions thereby down regulating T cell function.

stimulatory molecules. Furthermore tumour growth generates inhibitory influences on T cell activation.

CTLA4 is a homologue of CD28 on the cytotoxic T cell and is an inhibitory receptor expressed only following T cell activation. The normal function of CTLA4 is to compete with CD28 in binding of B7 and therefore downregulate T cell activation by removing the co-stimulatory signal and triggering cell cycle arrest (Krummel and Allison, 1996, Chambers et al., 2001). In fact CTLA4 has a 500-2500 fold higher affinity for B7-1 and B7-2 than CD28 (Peggs et al., 2006). Overall the role CTLA4 is to limit response to autoantigens and prevent proliferation of single T cell clones specific to single epitopes, allowing a heterogenous population of anti-antigen T cell clones to develop (Egen et al., 2002). However in the case of melanoma, tumour specific antigens are principally auto-antigens, albeit lineage specific, and the restriction of T cell proliferation may prevent generation of an effective antitumour immune response. This suggests that blockade of the inhibitory effects of CTLA4 can potentiate effective immune responses against tumour cells. Indeed administration of CTLA4 blocking antibodies to tumour bearing mice inhibited tumour growth and was associated with activation of both CD4+ and CD8+ effector cells (Leach et al., 1996). Two fully humanised anti-CTLA4 monoclonal antibodies, ipilimumab and tremelimumab, have been developed, and ipilimumnab was FDA approved in March 2011. Treatment with ipilimumab significantly increases median overall survival in both previously untreated and previously treated patients with metastatic or unresectable melanoma (Hodi et al., 2010a). The responses are durable and may take some time to develop preceded by months of stable disease or even transient disease progression. Further improvement in survival times has been achieved through combination of CTLA4 blockade and dicarbazine chemotherapy (Robert et al., 2011).

Based on these results and others imilimumab has now become the standard of care for patients with advanced melanoma.

1.1.2.2.5 Inhibitors of the Mitogen Activated Protein Kinase Pathway.

The recognition of BRAF as an oncogene and thus a therapeutic target resulted in identification of compounds which could selectively inhibit BRAFV600E over wild type BRAF. *In vitro* the compound ultimately known as vemurafenib, suppressed ERK activation, tumour proliferation and, *in vivo*, caused tumour regression (Yang et al., 2010). Phase 3 clinical trials demonstrated that vemurafenib resulted in approximately 50% improvement in survival time over dacarbazine in advanced BRAFV600E melanoma (Chapman et al., 2011, McArthur et al., 2011). These results culminated in the approval of vermurafenib as a monotherapy for patients with *BRAF V600* mutation in the UK. Unfortunately most patients develop resistance to vemurafenib within 6 or 12 months, manifested by progressive disease, and a small group are refractory to initial treatment. The molecular mechanisms underlying vemurafenib resistance are numerous including gain of BRAFV600E copy number and, of relevance to this project, enhanced activity of the IGF1R/PI3K/AKT signalling cascade (Shi et al., 2012, Villanueva et al., 2010).

Other selective oncogenic BRAF inhibitors (Hauschild et al., 2012, Kefford et al., 2010) and selective MEK1 /2 inhibitors (Flaherty et al., 2012, Davies et al., 2007, Infante et al., 2010) have also been demonstrated to have efficacy in malignant melanoma.

1.1.3 Conclusions

The success of both vemurafenib and ipilimumab in treatment of advanced melanoma has altered the standard of care for this disease dramatically in the past 2 years and these agents have recently received approval from NICE (http://guidance.nice.org.uk) (Dummer et al., 2012). However resistance, particularly to vermurafenib, limits its long term use. As found with single agent chemotherapy, it is unlikely that sole therapy with a small molecule inhibitor or monoclonal agent will control or cure melanoma long term. Instead attention is now focusing on combination drug therapies. Combination therapies can either utilise different mechanism of cell killing, for example vemurafenib has been shown not to affect lymphocyte function so its use in combination with ipilimumab would be appropriate (Comin-Anduix et al., 2010). Alternatively combinations of drugs which target resistance mechanisms could be employed. Studies in our laboratory have shown that BRAFV600E melanoma is susceptible to IGF1R inhibition (Yeh et al., 2006) potentially useful in overcoming IGF1R mediated vemurafenib resistance (Villanueva et al., 2010).

1.1.4 Comparative Aspects

In domestic animals cutaneous melanoma is uncommon and its behaviour is usually unlike that in human patients. In dogs cutaneous melanoma accounts for ~6% of nonlymphoid cutaneous neoplasia (Bostock, 1986) and occurs with a low prevalence in horses and swine (Goldschmidt and Shofer, 1998, Goldschmidt et al., 1998). In contrast cutaneous melanoma is a rare disease of cat, cattle, sheep and goats (Goldschmidt et al., 1998).

In both dogs and horses cutaneous melanoma are tumours principally of haired skin and are almost exclusively benign. Lesions are most common on the head and eyelids of dogs

and ventrum and tail of horses (Meuten, 2002). Local treatment with surgical resection or cryotherapy is typically sufficient to control disease and there is no evidence to suggest progression to malignancy in neglected lesions (Withrow and Vail, 2007). Unlike the case in humans exposure to UV radiation is not considered to play a major role in pathogenesis. Instead a genetic predisposition to development of cutaneous melanoma appears to be the major factor in pathogenesis; there is an increased incidence in certain canine breeds (Vizsla, Miniature and Standard Schnauzers and Chesapeake Bay Retrievers), and in Arab and Lipizzaner horses (Foley et al., 1991). Although rare, malignant cutaneous melanoma is found at an increased incidence in certain breeds such as the miniature poodle (Bolon et al., 1990). Finally familial cutaneous melanoma found sporadically in horses and commonly in some breeds of swine (Sinclair (Hornel) miniature pig, Duroc and Duroc crosses) adds further weight to the importance of genetic factors (Bundza and Feltmate, 1990). Indeed melanoma in swine has been suggested as a suitable animal model for human disease (Borovansky et al., 2003) but whilst some are malignant, others spontaneously regress following an effective cell mediated immune response (Rambow et al., 2008b, Rambow et al., 2008a, Morgan et al., 1996), casting doubt on the utility of pigs as a model organism. In contrast cutaneous canine melanoma is not considered an appropriate model for human disease (Liu et al., 2011).

1.1.4.1 Canine Oral Malignant Melanoma

In canine patients oral melanoma is much more common than cutaneous disease, and is almost exclusively malignant (Dorn and Priester, 1976). Oral malignant melanoma is principally seen in older dogs (Ramos-Vara et al., 2000) particularly those with heavily pigmented oral mucosa (Dorn et al., 1968). Miniature poodles, cocker spaniels, Chow

Chow and Golden retrievers are over represented, again indicative of a genetic predisposition (Ramos-Vara et al., 2000). Although oral malignant melanoma is a rare disease of humans, and is not the subject of this thesis, the canine disease deserves mention as its pathology and recent developments in its treatment are of direct relevance.

1.1.4.2 Genetic mutations and IGF1R expression in canine melanoma

In common with human disease, mutations of tumour suppressor genes, particularly *p53, p21, p16 INK* and *PTEN* are features of canine oral malignant melanoma (Koenig et al., 2002) (Sakai et al., 2001). However unlike the case in human disease, *RAS* (Mayr et al., 2003, Richter et al., 2005, Escobar et al., 2004) and *BRAFV600* (Shelly et al., 2005) mutations are rare. *IGF1R* and IGF1R are expressed in the majority of primary tumours and canine melanoma cell lines. In cell culture IGF1 driven cellular proliferation and VEGF production can be prevented by IGF1R pharmacological inhibition (Thamm et al., 2010). Similar to the situation in human melanoma, the AKT and mTOR pathways are active in canine melanoma (Kent et al., 2009) and Wnt-β catenin signalling is often dysregulated (Han et al., 2010).

1.1.4.3 Treatment of Canine Oral Malignant Melanoma

Melanoma is the commonest oral tumour of dogs and metastases to local lymph nodes and distant sites are common at the time of diagnosis (Meuten, 2002). Surgery and radiotherapy can provide good control of local disease but strategies to manage distant metastases are poor. Overall the median survival time for dogs treated with surgery alone varies from 150-318 days with a one year survival of 35% (Harvey et al., 1981). Only modest improvements are achieved with adjuvant chemotherapy, such as carboplatin or

dacarbazine (Rassnick et al., 2001, Kitchell et al., 1994), or radiotherapy (Freeman et al., 2003, Blackwood and Dobson, 1996, Bateman et al., 1994b, Bateman et al., 1994a). Adjuvant carboplatin combined with radiotherapy following locoregional surgical control offers no benefit over radiotherapy alone (Murphy et al., 2005). In common with human disease, research and treatment trials have centred on exploiting the host's immune response. Immunomodulation with L-MTP (liposome muramyl tripeptide), IL2 and GM-CSF have shown promise but in most cases only Phase I trials have been completed (Quintin-Colonna et al., 1996, MacEwen et al., 1986, MacEwen et al., 1999, Dow et al., 1998). A notable exception is in the use of anti-melanoma vaccines. Use of gp100 whole cell tumour vaccine (Alexander et al., 2006) and dendritic cell vaccines (with human gp100 antigen) (Gyorffy et al., 2005) have proved as effective as conventional cytotoxic therapy. However it is trials with xenogeneic tyrosinase vaccines which have been most successful (Bergman, 2008, Bergman et al., 2006, Manley et al., 2011). Inoculation of tumour bearing dogs with a human xenogeneic tyrosinase DNA vaccine elicited production of anti-human tyrosinase antibodies, the majority of which cross reacted with canine tyrosinase, overcoming self tolerance, and resulting in tumour regression (Bergman et al., 2003, Liao et al., 2006). Ultimately the success of this vaccine in Phase 2 trials of 58 dogs with stage 2 or 3 oral melanoma following loco-regional control resulted in the United States Department of Agriculture licensing of "Oncept" in 2010 (Grosenbaugh et al., 2011). To date this remains the only licensed cancer vaccine in either dog or man, although the criteria for licensing drugs in companion animals are clearly less exacting than for humans.

1.2 The Wnt Pathway in Cancer

The Wnt signalling pathway is highly conserved and has a crucial role in the embryonic development of animal species. Components of the Wnt pathway act as either oncogenes or tumour suppressor genes and dysregulation of Wnt signalling is implicated in the majority of colorectal cancers, breast cancer and melanoma (Klaus and Birchmeier, 2008). In non neoplastic cells under basal conditions the β-catenin destruction complex, which includes Glycogen synthase kinase 3β (GSK3β), casein kinase 1α (CK1α), Axin, and adenomatous polypolis coli (APC), phosphorylates β-catenin which targets it for ubiquitylation and proteosomal degradation (Figure 1.2). On interaction of canonical Wnt ligands, WNT1 and WNT3A in melanoma, with a cell surface Frizzled receptor, members of the destruction complex are recruited to the membrane and are unavailable to bind β-catenin. Unphosphorylated β-catenin accumulates in the nucleus and associates with the TCF (T-cell factor) and LEF (lymphoid enhancer factor-1) transcription factor family to form transcriptionally active complexes (Korinek et al., 1997). Wnt target genes have a wide range of roles in cellular proliferation, differentiation, adhesion and signalling (Polakis, 2012). Cyclin D1 (*CCND1*) and *MYC* are among the best characterised (Gordon and Nusse, 2006). In the absence of a Wnt signal TCF/LEF family members interact with transcriptional co-repressors such as Groucho**,** which serve to repress Wnt signalling (Polakis, 2000).

Both genetic and biochemical mutations of Wnt pathway members can provide mechanisms for constitutive Wnt signalling. The best characterised are mutations or modifications of β-catenin which prevent GSK3β phosphorylation and thus proteosome mediated degradation, and mutations or reduced levels of Axin and APC. In colorectal

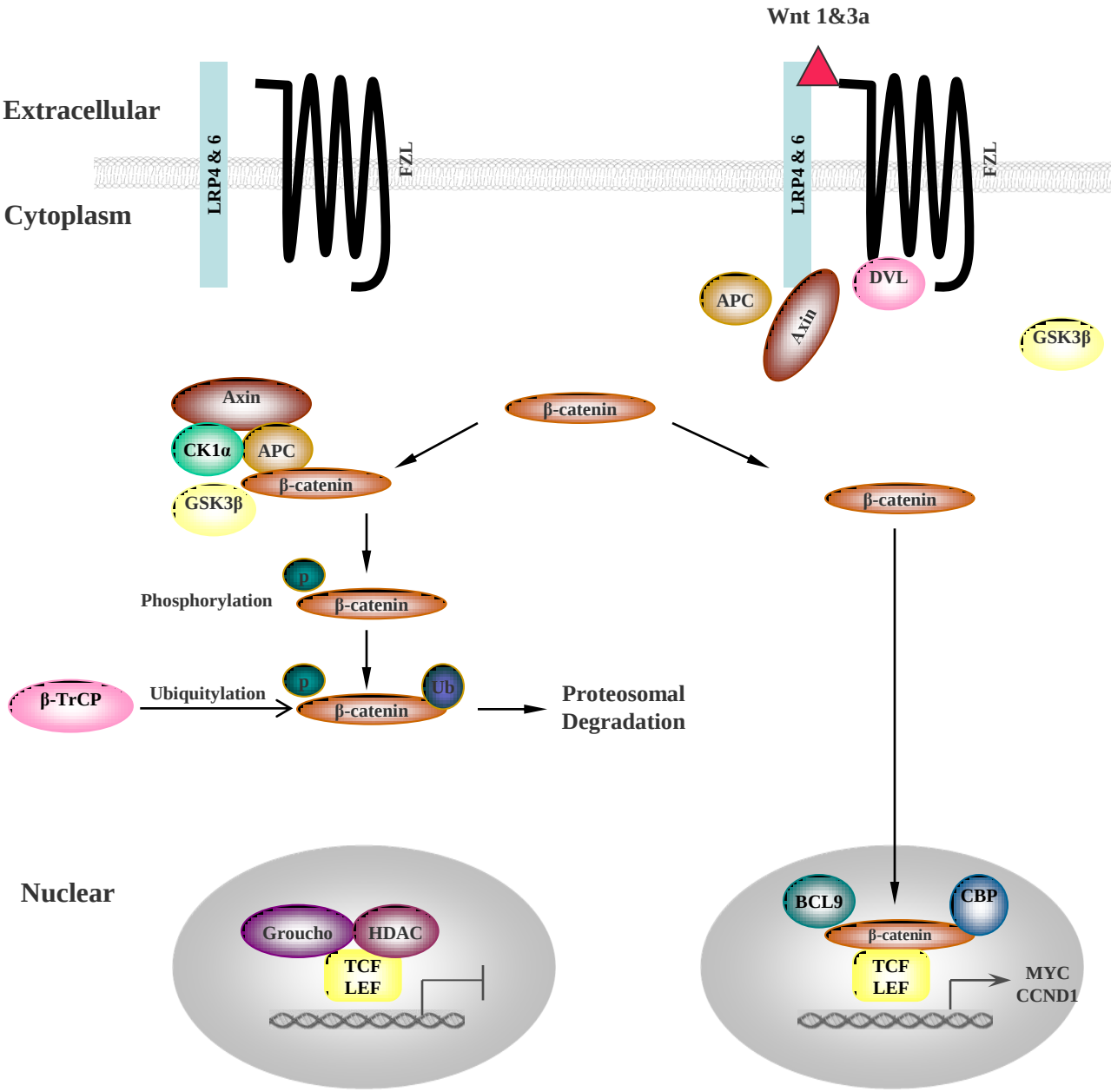


Figure 1.2 The canonical Wnt-β-catenin pathway. Left - In the absence of Wnt ligand, β-catenin is recruited to the destruction complex (comprising adenomatous polyposis coli (APC), Axin, glycogen synthase 3β (GSK3β) and casein kinase 1α (CK1α)). Following N terminal phosphorylation by GSK3β and CK1α and subsequent ubiquitylation by β transducin repeat-containing protein (β-TrCP), β-catenin is proteosomally degraded. Low levels of nuclear β-catenin ensure transcriptional repression of Wnt target genes by recruitment of the co-repressor Groucho to TCF and LEF transcription factors. **Right** - In the presence of canonical Wnt ligands, the destruction complex is inactivated and β-catenin accumulates and translocates to the nucleus. In the nucleus β-catenin forms a transcriptionally active complex with TCF and LEF transcription factors with coactivators such as B-cell CLL/lymphoma 9 protein (BCL9) and CREB binding protein (CBP), resulting in the transcription of Wnt target genes including *CCND1*and *MYC*.

carcinoma, breast cancer and oesophageal carcinoma high nuclear β-catenin is correlated to poor prognosis, and constitutive Wnt signalling results in increased expression of Wnt target genes which have documented roles in proliferation, angiogenesis, invasion and metastasis (Klaus and Birchmeier, 2008).

In addition to the so-called canonical Wnt pathway as described above, interaction of specific Wnt ligands, such as WNT5A, WNT5B and WNT11 in the case of melanoma, with Frizzled receptor family members can result in cell signalling cascades which do not involve β-catenin and indeed can inhibit signalling down the canonical pathway. Of the non canonical pathways, the Wnt5a/Ca^{2+} pathway is one of the best characterised and in addition to increasing cellular calcium it also acts to inhibit canonical Wnt signalling, possibly through promotion of β-catenin degradation (Weeraratna, 2005).

1.2.1.1 Wnt signalling pathways in melanoma

Mutations causing constitutive Wnt/β catenin signalling are rare in melanoma unlike the other cancer types described above (Pollock and Hayward, 2002, O'Connell and Weeraratna, 2009). In fact nuclear accumulation of β-catenin appears to be a normal feature of melanocytes, as staining is seen in almost all benign naevi (Rimm et al., 1999). This contrasts with other tissue types where nuclear β-catenin is associated with neoplastic progression. It has been suggested that Wnt signalling is crucial for homeostasis of melanocytes and indeed Wnt/β-catenin signalling drives expression of differentiation related genes, such as microphthalmia transcription factor, which play a key role in melanocyte development (Lucero et al., Takeda et al., 2000). As such it is not surprising that forced expression of constitutively active β-catenin in melanocytes is not sufficient to

induce melanoma in transgenic mice (Delmas et al., 2007). However the presence of β-catenin is critical for malignant transformation of melanocytes as it is required for suppression of p16INK4A (Cyclin dependent kinase inhibitor 2A - *CDKN2A*) leading to cell immortalisation, and then acts in concert with other oncogenes such as *NRAS* to promotes tumourigenesis (Delmas et al., 2007). These are early events in tumourigenesis and nuclear β-catenin staining is then lost on melanoma progression (Kageshita et al., 2001). Therefore activation of Wnt/β catenin signalling, denoted by nuclear β-catenin staining in patient tumours, is not a negative prognostic indicator as in breast cancer, but is actually associated with an improved prognosis (Chien et al., 2009). Experimentally forced expression of WNT3A in B16 melanoma cells results in reduced proliferation *in vitro* and reduced proliferation and metastasis *in vivo* (Chien et al., 2009). Similarly treatment with lithium chloride, an inhibitor of GSK3, results in reduced proliferation in human melanoma cell lines, including A375 (Chien et al., 2009).

Overall it appears that canonical Wnt signalling is important in early melanoma development but favours a less proliferative and less aggressive phenotype at later stages. In contrast non-canonical Wnt signalling is absent in melanocytes but becomes important following neoplastic transformation. Strong positive staining of WNT5A, a ligand of a non-canonical pathway, is a poor prognostic indicator in clinical cases of melanoma (Da Forno et al., 2008, Bittner et al., 2000) and transfection of WNT5A into melanoma results in an increased invasive potential (Weeraratna et al., 2002). Furthermore expression of WNT5A may contribute to the downregulation of the Wnt/β catenin signalling pathway following transformation, favouring a proliferative, motile and aggressive phenotype (Dissanayake et al., 2007, Chien et al., 2009).

1.3 The IGF1R

The IGF1R and the Insulin Receptor (IR) are members of the Receptor Tyrosine Kinase superfamily, high affinity cell surface receptors for hormones, growth factors and cytokines. Uniquely amongst the approximately 20 members of this family, the IGF1R and IR exist as disulfide linked dimers in the absence of ligand and undergo a conformational change on ligand binding, causing autophosphorylation (Adams et al., 2000). Other family members exist as monomers requiring ligand binding to promote dimerisation and activation. From an evolutionary perspective the IR and IGF1R share a common ancestory, and are part of a highly conserved system in vertebrates and invertebrates which coordinates cellular metabolism, growth and differentiation in response to the environment (Barbieri et al., 2003). Probably the role of the ancestral receptor was involved with cellular proliferation before gene duplication resulted in a division of labour and function, into carbohydrate metabolism and growth for the IR and IGF1R respectively.

The human IGF1R gene is constitutively expressed on almost every cell. The IGF1R is translated as a 1367 amino acid single-chain pre-proreceptor, from which a 30-residue signal peptide is cleaved resulting in the 220kDa pro-receptor. The pro-receptor is glycosylated, folded and dimerised post-translationally before processing in the Golgi apparatus generates α (~130 kDa) and β (~97 kDa) subunits. These subunits are assembled into half receptors (one α and one β subunit) which then associate on the cell surface and become disulphide-linked to produce the mature IGF1R, a holodimer comprised of two α and two β subunits. The two α subunits are entirely extracellular and form the ligand binding site. The two β subunits have extracellular, transmembrane and cytoplasmic domains. The cytoplasmic portion of the β subunit contains the tyrosine kinase catalytic

domain, phosphorylation of which is necessary for receptor activation, and two portions which mediate interaction with downstream signalling molecules; a juxta-membrane region and C terminal tail (Ward and Garrett, 2004). The IR is translated and assembled in a near identical fashion, except that alternate splicing of the IR gene at exon 11 results in two isoforms; IR_A and IR_B. The IR_B isoform principally binds insulin and regulates glucose uptake. The IR_A is a fetal isoform that lacks 12 amino acid residues encoded by exon 11 (Belfiore, 2007). IR_A can bind both insulin and IGF2 to promote cell proliferation and survival (Belfiore et al., 2009). The IGF1R shares approximately 70% sequence homology with the IR at the amino acid level, with ~50% homology at the ligand binding site and ~80% homology in the tyrosine kinase and substrate binding domains (Ullrich et al., 1986).

The type 2 IGF receptor (IGF2R), also known as the cation-independent mannose-6-phosphate receptor, is a ubiquitously expressed transmembrane glycoprotein with a large extracellular domain and a relatively short cytoplasmic tail. On the cell surface IGF2R exerts mitogenic effects (O'Dell and Day, 1998), but principally functions to sequester IGF2, through receptor mediated endocytosis and lysosomal degradation (Braulke, 1999) thus preventing it from activating the IGF1R (Arbet-Engels et al., 1999).

1.3.1 IGF1R/IR hybrid receptors

Due to the high degree of homology between the IR and IGF1R (Ullrich et al., 1986), two half receptors, one IGF1R and one IR, can heterodimerise, forming IR/IGF1R hybrid receptors (Belfiore et al., 2009, Pandini et al., 1999, Benyoucef et al., 2007). Indeed heterodimerization occurs at a similar frequency to homodimer formation. Typically, cells

express the IR and IGF1R at different levels favouring formation of holodimers of one type. However it has become clear that hybrid receptors occur commonly on cells expressing both receptor types, such as some neoplastic cells (Pandini et al., 1999). Furthermore IR_A is preferentially expressed by some neoplastic cells. In fact rather than considering the IR and IGF1R separately, perhaps it is more appropriate to consider neoplastic cells expressing a pool of receptors, containing varying proportions of the "classic" receptors (IR_A, IR_B, IGF1R) and all three permutations of hybrid receptor (IR_A-IR_B, IR_A-IGF1R, IR_B-IGF1R) (Sprynski et al., 2010). The IGF1R hybrid receptors have similar binding affinities for insulin, IGF1 and 2, irrespective of the IR monomer variant (Slaaby et al., 2006) resulting in further interplay between these two signalling pathways, which were previously considered distinct.

1.3.2 IGF1R ligands and the regulation of their bioavailability

The IGF1R is activated by binding of its ligands IGF1 and IGF2. These molecules are best considered as tissue growth factors as well as hormones. IGF1 is principally produced in the liver, and to a smaller degree in skeletal muscle, bone and cartilage, in response to growth hormone (Thissen et al., 1994). However other factors can also influence endocrine production such nutritional status (Thissen et al., 1994) and diet (Holmes et al., 2002). As such there can be significant variation in circulating IGF levels between individuals. Monozygotic twin studies suggest that such variation is ~50% genetically determined and ~50% determined by lifestyle (Harrela et al., 1996). At a tissue level local IGF expression results in both paracrine and autocrine actions (Pollak et al., 2004). IGF2 is expressed in both hepatic and extra-hepatic tissues but not under the regulation of growth hormone. The gene encoding IGF2 is imprinted, and is only expressed from the paternal allele (Eden et

al., 2001). As described previously IGF2R sequesters IGF2, for which it has a 100 fold greater affinity than does the IGF1R, thus preventing it from activating IGF1R (Arbet-Engels et al., 1999). The IR and IGF1R are specific for insulin and IGF1 and IGF2 respectively at physiological concentrations, although IR_A has a ~1.7x affinity for insulin compared to IR_B. Similarly IGF1R has a higher affinity for IGF1 than IGF2, although at high ligand concentrations cross-reaction does occur (Nissley et al., 1985).

Circulating IGF bioavailability is regulated by binding to high affinity IGF binding proteins (IGFBPs), of which there are six characterised forms (IGFBP1 to IGFBP6) (Firth and Baxter, 2002). The IGFBPs have an affinity for IGF ligands of the same order of magnitude as the IGF1R. As such, greater than 99% of circulating IGF1 is bound to IGFBPs the majority of which forms a trimeric complex with IGFBP-3 or IGFBP-5 and the acid labile subunit (ALS), a liver-derived GH-regulated glycoprotein (Frystyk, 2004) (Baxter, 1988). These ternary complexes enhance the circulating half life of IGFs from ~15 minutes to up to 16 hours, as they cannot cross endothelial membranes, nor can they activate IGF1R (Clemmons, 2007, Zapf et al., 1995). In contrast binary complexes formed by IGFs and the remaining IGFBPs (-1, -2, -4 & -6), or following dissociation of ALS from the ternary complexes, are able to cross endothelium and exert a biological effect. Dissociation of ALS from IGFBPs is poorly understood but may involve interaction of glycosaminoglycans on the endothelial cell surface. Similarly IGF ligand can be released by IGFBP proteolysis by proteases such as metalloproteases and caspases (Rajah et al., 1996). It should be noted some IGFBPs have well characterised IGF independent effects in addition to the role described above. For example IGFBP-3 has IGF independent growth inhibitory and proapoptotic actions in cancer xenografts, although the mechanism is poorly understood (Cohen, 2006).

A further group of IGFBP related proteins (IGFBP-rPs) have been characterised which share N terminal IGF binding domain homology with IGFBPs and which weakly bind IGF. Thus far ten of these cysteine rich proteins have been demonstrated to be involved in a wide variety of biological functions including growth regulation, but their involvement in regulation of IGF bioavailability remains unclear (Hwa et al., 1999).

Thus, activation of IGF1R by its ligands is tightly regulated by the complex interaction of IGFBPs, IGBFP-rPs, endothelial cells, tissue proteases and IGF2R.

1.3.3 Signalling through the IGF1R

IGF1R signalling involves a cascade of events which initiate two major downstream canonical signalling pathways, one regulating cell survival and mRNA translation, the other cellular proliferation (Figure 1.3). Binding of IGF ligand to the α subunit of IGF1R results in a conformational change in the intracellular portion of the β subunit resulting in trans-autophosphorylation of three tyrosine residues (Y1131, Y1135 and Y1136) within the kinase domain. Activated IGF1R recruits and phosphorylates tyrosine residues on insulin receptor substrates (IRS1-4) and Shc (Src homology/collagen) proteins, initiating the two major downstream canonical signalling pathways (Cheatham and Kahn, 1995, Saltiel, 1996, White, 1998, Byron et al., 2006).

Phosphorylated IRS1 serves as a docking protein to recruit and activate the regulatory and catalytic subunits of phosphoinositide 3-kinase (PI3K), leading to synthesis of phosphatidyl inositol-3,4,5-triphosphate (PIP_3) from PIP_2. PIP_3 activates phosphoinositide-

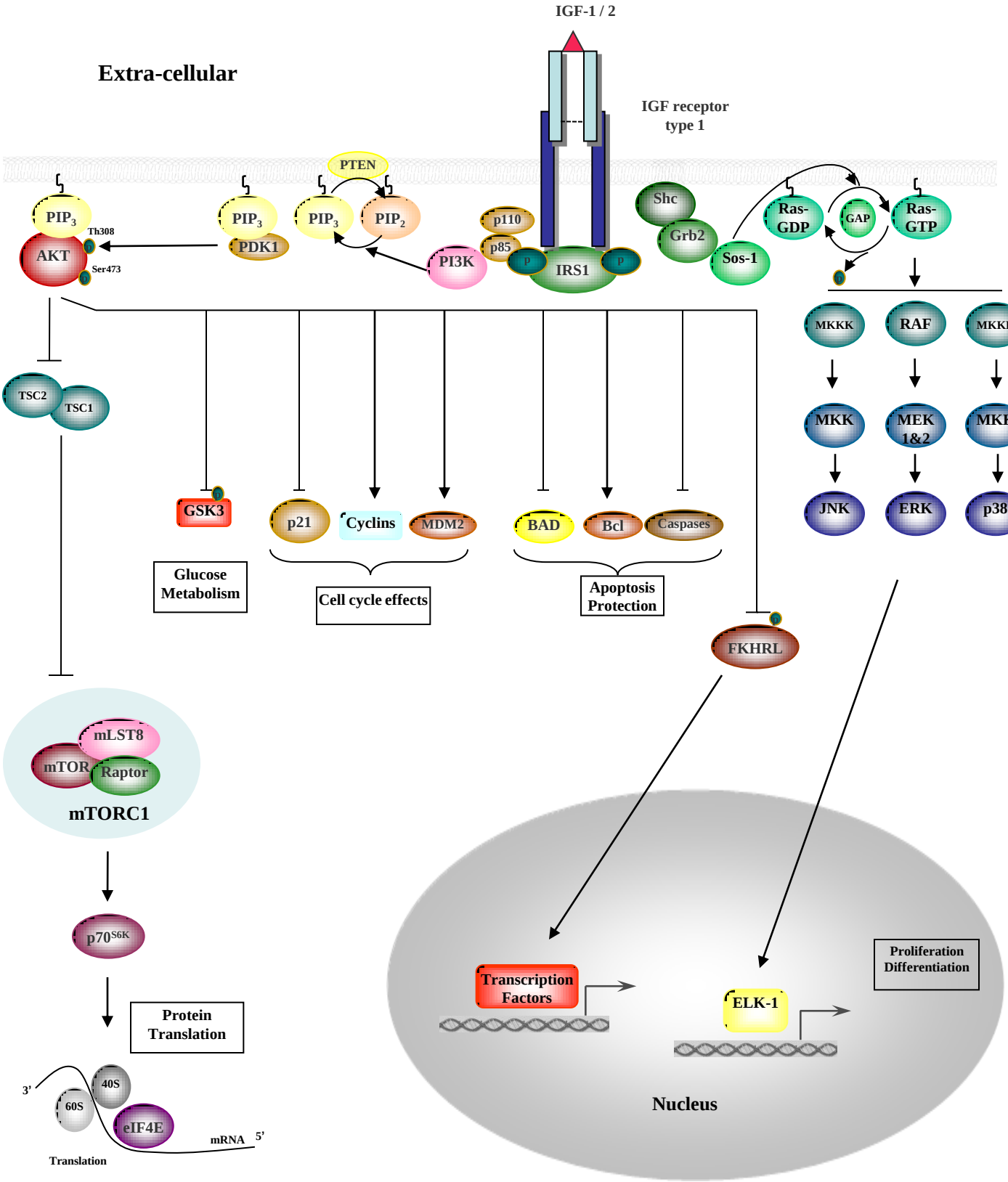


Figure 1.3 The IGF1R axis. The IGF1R mediates the malignant phenotype principally through the RAS/RAF/ERK and PI3K/AKT pathways resulting in effects on survival, apoptosis protection, cell cycle progression, proliferation, differentiation and metabolism. Particularly relevant to this project, transcription is influenced by both pathways, and mutations in these pathways (particularly *NRAS*, *BRAF and PTEN*) are common in melanoma.

dependent kinase-1 (PDK-1) which phosphorylates and thus activates downstream protein kinases, including membrane recruited AKT (Vanhaesebroeck and Alessi, 2000, Manning and Cantley, 2007). Signalling through the PI3K/AKT pathway mediates translation of proteins that promote proliferation principally via mammalian target of rapamycin complex 1 (mTORC1), and anti-apoptotic events via BCL2, caspase 9 and other members of the apoptosis regulatory mechanism (Vanhaesebroeck and Alessi, 2000).

In parallel recruitment of Shc leads to activation of the small G-protein RAS, via recruitment of growth factor receptor-bound protein 2 (GRB2), and son-of-sevenless (SOS). Ras activates the protein serine kinase RAF and thus the mitogen-activated protein kinase isoforms: extracellular signal-related kinases (ERKs), p38 and *cJun* N terminal kinase (JNK) (the MAPK cascade) (Davis, 1995), which results in proliferation.

Intracellular regulation of the IGF1R signalling pathway occurs at multiple levels, including within the cell membrane by SRC and protein phosphatases (O'Connor, 2003), and by negative feedback from downstream effectors: mTORC1, ERKs, JNK and p70 S6 Kinase.

In addition to these two principal signalling pathways IGF1R activation and the phosphorylation of IRS1 and 2 disrupts β-catenin/E cadherin complexes, allowing the B-catenin-IRS1 complex to translocate to the nucleus to drive transcription of β-catenin target genes, and disconnecting E-cadherin from the actin cytoskeleton favouring cell detachment and motility (Playford et al., 2000, Chen et al., 2005, Byron et al., 2006).

It must be noted that the downstream signalling cascades activated by insulin binding to the IR are strikingly similar to those of the IGF1R as might be expected given their shared evolutionary heritage. However the biological effects differ, due to differential expression of cellular components, individual cellular coordination, integration of downstream signalling events and differences in protein interaction (Mulligan et al., 2002). For example IRS1 is more efficiency phosphorylated by IR than by IGF1R, whilst the converse is true for IRS2 (Urso et al., 1999, Rakatzi et al., 2006). Similarly in mammary epithelial cells, which lack gluconeogenic enzymes, insulin results in cellular proliferation and inhibition of apoptosis rather than gluconeogenesis and glycogen deposition as it does in hepatocytes. In general IR_B activation can be thought of as resulting in glucose metabolism and cell proliferation, whereas IGF1R activation leads predominantly to mitogenesis, transformation and protection from apoptosis (Dupont and LeRoith, 2001, Nakae et al., 2001). However this distinction is not clear cut as physiological insulin can have mitogenic effects and in cells bearing a significant proportion of hybrid receptors the distinction between the IR and IGF1R signalling cascades are further blurred (Mashhedi et al., 2011).

1.3.4 The role of IGF1R in tissue, development and disease

Whereas IGF2 is the primary growth factor underpinning embryonic growth, IGF1 is the dominant fetal growth regulator in late gestation, and post natally (D'Ercole et al., 1980). *Igf1* or *Igf1r* null mice are born underweight, suffer increased perinatal mortality and only achieve ~60% of adult weight (Baker et al., 1993, Liu et al., 1993). A similar reduction in prenatal growth is seen following targeted disruption of the imprinted paternal allele of *Igf2* (DeChiara et al., 1991, DeChiara et al., 1990). Disruption of both *Igf1* and *Igf2* results

in more severe growth retardation, ~30%, than either alone (Liu et al., 1993). The fetal growth promoting effects of Igf1 and Igf2 are mediated by both Ir and Igfr as mice lacking both these receptors are more severely growth retarded than those lacking either receptor alone (Rother and Accili, 2000). As expected *Igf2r* knockout mice suffer embryonic overgrowth due to "excessive" action of Igf2 on Igf1r. Sporadically occurring IGF1 and IGF1R mutations have been documented in the human population which phenocopy those demonstrated experimentally (van Duyvenvoorde et al., 2010, van Duyvenvoorde et al., 2011). In contrast to the situation in adult and neoplastic tissues, hybrid receptors do not appear to play any significant growth-promoting role during embryogenesis (Lauro et al., 1999).

Post-natally IGF1R is required for the development and physiology of numerous cell types. In the pancreas IGF1 has a role in β cell growth and function (Ueki et al., 2006). Low serum IGF1 levels have been correlated with an increased risk of the subsequent development of diabetes mellitus (Saltiel and Kahn, 2001), presumably due to β cell compromise. Conversely supplementation of IGF1 to insulin resistant diabetics reduces insulin requirement (Kuzuya et al., 1993), possibly by enhancing β cell function, growth hormone suppression (Carroll et al., 1998), stimulation of glucose uptake into skeletal muscle (Dimitriadis et al., 1992) or cross talk between the IR and IGF1R signalling pathways. In the nervous system IGF1 is a neurotrophic peptide and neural survival factor, and has been implicated in the stimulation of neural activity and removal of amyloid β (Russo et al., 2005, Jarvis et al., 2007). As such, deficiencies in IGF1 signalling are implicated in the pathogenesis of numerous neuronal disorders involving amyloid accumulation including Alzheimer's disease (Puglielli, 2008). In the cardiovascular system the importance of role of IGF1 in the maintenance of health is indicated by its

dysregulation in diseases such as hypertension (Lembo et al., 1996), atherosclerosis (Delafontaine et al., 2004) and congestive heart failure (Vasan et al., 2003). Low circulating IGF1 levels are associated with an increased risk of ishaemic heart disease and cardiovascular mortality (Juul et al., 2002, Laughlin et al., 2004). Overall the global import of IGF1 is best illustrated by a recent meta-analysis which revealed increased mortality from cancer or heart disease for individuals with either high or low serum IGF1 (Burgers et al., 2011).

The IGF1 signalling system is also intimately interlinked with the generation and action of reactive oxygen species (ROS) and reactive nitrogen species (RNS). NADPH oxidase is amongst the primary enzymes responsible for generation of superoxide anions (O_2^-) in the mitochondria and IGF1R activation has been shown to activate one its component subunits NOX4 (Meng et al., 2008). Conversely IGF1R blockade inhibits the activity of NADPH oxidase (Cruzado et al., 2005). Furthermore IGF1R activation has been shown to mediate the actions of H_2O_2, the end product of O_2^- dismutation (Azar et al., 2006). Finally it has been shown that ROS induced oxidative stress of vascular smooth muscle cells results in an increase in IGF1 and IGF1R synthesis and a reduction in IGFBP4 synthesis, increasing the activity of the IGF1R pathway (Delafontaine et al., 2004, Du et al., 1999). Thus ROS generation appears essential to trigger IGF1 evoked signalling events and ROS induced oxidative stress can upregulate IGF1R activity.

More recently the role of IGF1R in regulation of life span has become recognised, initially from studies of *C.elegans* (Tissenbaum, 2012, Kenyon et al., 1993) and supported by the observations of increased lifespan in growth hormone deficient mice (Brown-Borg et al., 1996) and heterozygous *Igf1r* knockout mice (Holzenberger et al., 2003). In fact

functionally significant mutations in IGF1R have been found in human centenarians which may have contributed to their longevity (Suh et al., 2008). The precise mechanism by which the IGF1R axis contributes to longevity in mammals is unclear but may involve the relief of inhibition of action of forkhead transcription factor family (FOXO) and upregulation of antioxidant systems following the attenuation of IGF signalling (Willcox et al., 2008).

1.3.5 The role of IGF1R in cancer

Altered expression or regulation of IGF1R signalling has been implicated in the development and progression of cancer (Adams et al., 2000, Baserga, 2000) and endow cancer cells with a number of Hanahan and Weinberg's "*hallmarks of cancer*". Plasma IGF1 at the upper end of the normal range has been correlated with an increased incidence of colo-rectal (Pollak, 2000, Furstenberger and Senn, 2002, Yu and Rohan, 2000), and prostate (Rowlands et al., 2009, Roddam et al., 2008, Renehan et al., 2004) cancers. An association with other cancer types, for example breast cancer, is unclear due to conflicting evidence (Schernhammer et al., 2006, Hankinson et al., 1998, Hankinson and Schernhammer, 2003, Patel et al., 2008, Renehan et al., 2004). Conversely low IGF1 is associated with reduced cancer risk (Guevara-Aguirre et al., 2011) as is increased IGFBP3 in the case of colo-rectal cancer risk (Ma et al., 1999). These correlations suggest a high IGF environment favours, or selects for, the survival of pre-malignant or malignant lesions (Pollak et al., 2004).

Within the tumour microenviroment, IGF1 and IGF2 are released by many neoplastic cells in an autocrine fashion, or their release is induced in neighbouring cells to act in a

paracrine fashion, driving self proliferation and providing *self sufficiency in growth signalling* (Sporn and Roberts, 1985). In the case of Ewing's sarcoma the increased and decreased expression of IGF1 and IGFBP3 respectively, result in an autocrine loop (Benini et al., 2006). In the case of IGF2, loss of genomic imprinting within neoplastic cells results in increased IGF2 production which can promote tumour progression (Christofori et al., 1994, Christofori et al., 1995, Pravtcheva and Wise, 1998). This is particularly of relevance as IGF2 can act as a ligand both for IGF1R and also IR_A which, as described, is often expressed by neoplastic tissue and mediates cell survival (Vella et al., 2002, Sciacca et al., 2002). Furthermore tumour cell expression of proteases, such as prostate specific antigen, can increase local IGF tissue concentration through IGFBP proteolysis (Cohen et al., 1992).

The IGF1R plays a critical role in oncogenic cell transformation. R- cells, fibroblasts from *Igf1r* null mouse embryos, are refractory to oncogenic transformation by many viral and cellular oncogenes such as SV40 large T antigen, HRAS and EGFR (Sell et al., 1993). Re-introduction of Igf1r to R- cells "rescues" the cells and allows transformation (Sell et al., 1993, Sell et al., 1994). However R- cells can be transformed by GTPase deficient Gα13 protein (Liu et al., 1997) so IGF1R is not obligatory for acquisition of the neoplastic phenotype.

Over-expression of IGF1R has been demonstrated in a variety of cancers such as: colon (Hassan and Macaulay, 2002, Perer et al., 2000, Wu et al., 2002, Hakam et al., 1999), renal (Yuen et al., 2007), breast (Peyrat et al., 1988, Lee et al., 1998, Happerfield et al., 1997), pancreas (Hakam et al., 2003), bladder (Rochester et al., 2007), myeloma (Ge and Rudikoff, 2000), melanoma (All-Ericsson et al., 2002, Kanter-Lewensohn et al., 2000),

ovary (Yee et al., 1991) and prostate cancer (Hellawell et al., 2002). Furthermore IGF1R overexpression is correlated to an adverse prognosis in clear cell renal carcinoma (Parker et al., 2003), breast (Creighton et al., 2008), and ovarian (Parker et al., 2002) cancer suggesting that this alteration is of profound biological significance. Unlike the case with other receptors overexpressed in neoplasia, for example ERBB2 (Her2) (Eccles, 2011), gene amplification and activating mutations of IGF1R are rare, but have been reported in breast cancer and melanoma (Almeida et al., 1994, Adelaide et al., 2007). Several tumour suppressors including p53 (Werner et al., 1996), VHL (Yuen et al., 2007) and BRCA1 (Abramovitch and Werner, 2003, Maor et al., 2000) have been shown to suppress IGF1R expression likely accounting for the IGF1R upregulation in cancers that have lost tumour suppressor function.

Activation or overexpression, of IGF1R, IR and/or hybrid receptors, mediates many aspects of the malignant phenotype (Belfiore et al., 2009). Indeed experimentally forced expression of IGF1R, IGF and IRS have been documented to increase tumourigenesis, tumour growth, invasion and metastatic potential (Dearth et al., 2006, Wilker et al., 1999) whereas a reduction in IGF signalling slows progression (Lopez and Hanahan, 2002).

The IGF1R has a crucial role in *evading apoptosis*. The level of resistance to apoptosis is proportional to the expression of IGF1R (Resnicoff et al., 1995b). Conversely downregulation of IGF1R leads to apoptosis of tumour cells in anchorage-independent conditions *in-vitro* and *in-vivo* (Resnicoff et al., 1994a). The anti-apoptotic effects of IGF1R signalling are mediated principally through the IRS/PI3K/AKT pathway and involve inhibitory phosphorylation of pro-apoptotic factors, including the Bcl-2 associated death promoter BAD, Forkhead box transcription factors and caspase 9, and induction of

expression of anti-apoptotic proteins, including Bcl-2, Bcl-XL and NF-κB (Brazil et al., 2004). Additional "*hallmarks of cancer*" conferred by IGF1R activation or overexpression are increased cellular ability to *invade tissue and to metastasise*. This effect is mediated in part through the interaction between the IGF axis and E-cadherin as described in section 1.3.3 (Hazan et al., 2004, Playford et al., 2000), and IGF-induced secretion of matrix metalloproteinases (Zhang et al., 2003). Furthermore, IGFs promote *angiogenesis* by activating endothelial nitric oxide release by up regulating levels of hypoxia inducible factor α (HIFα) and Vascular Endothelial Growth Factor (VEGF) (Fukuda et al., 2002).

1.3.6 IGF1R as a target for treatment of cancer

As described above, the IGF1R plays important roles in transformation, apoptosis protection, invasion and metastasis and is therefore an attractive target for cancer treatment. In a variety of *in vitro* and *in vivo* models disruption of IGF signalling inhibits tumour growth, reduces metastasis and augments the efficacy of other anti-cancer treatments (Goya et al., 2004, Haluska et al., 2006b, Ji et al., 2007, Rowinsky et al., 2007, Cohen et al., 2005). In fact IGF1R targeting, perhaps due to the ability to affect multiple survival pathways, can circumvent downstream activating mutations which might be expected to negate the effects of IGF1R inhibition. For example previous work from our group suggested that PTEN mutant prostate cells (Rochester et al., 2005) and BRAFV600E mutant melanoma cells (Yeh et al., 2006) are sensitive to IGF1R gene silencing. IGF1R activation protects tumour cells against apoptosis induced by cytotoxic agents (Dunn et al., 1997) and IGF1R inhibition has been shown to enhance sensitivity to chemotherapy (Mitsiades et al., 2004, Scotlandi et al., 2005, Wu et al., 2006).

A variety of experimental strategies have been employed to block the function or expression of the IGF1R signalling cascade. IGF1R itself, as well as the ligand and downstream signalling components, are all attractive anticancer drugable targets. Whilst numerous strategies exist for disruption of IGF1R signalling experimentally, including RNA interference and antisense technologies (Riedemann and Macaulay, 2006), only those applicable to the clinic which have subsequently resulted in clinical trials, over 100 of which have been performed to date, are considered in detail below, and summarised in Table 1.1.

1.3.6.1 Antireceptor Antibodies (Blocking Antibodies)

Blocking antibodies are attractive therapeutic agents as they both block ligand receptor interaction and also may cause receptor internalisation and degradation (Sachdev et al., 2003, Maloney et al., 2003, Cohen et al., 2005, Burtrum et al., 2003, Jackson-Booth et al., 2003). Furthermore they offer specific targeting of the IGF1R and may mediate antibody dependent cellular cytotoxicity (Sachdev et al., 2003). The first antibody developed was αIR3, a mouse monoclonal antibody directed against the IGF1R (Kull et al., 1983). This antibody was subsequently shown to inhibit IGF1R activation and tumourigenecity in a number of *in vitro* and *in vivo* models (Macaulay et al., 1990, Arteaga and Osborne, 1989, Arteaga et al., 1989, Arteaga, 1992, Kalebic et al., 1994, Scotlandi et al., 1998). Numerous partial or totally humanised IgG_1 or IgG_2 antibodies directed against the IGF1R have subsequently been developed. Pre-clinical studies indicate that receptor downregulation through internalisation and degradation via the lysomoal/endocytic pathway is a more important feature than blocking ligand-receptor interaction (Li et al., 2000, Wu et al., 2005) and that these antibodies predominately affect the activity of the PI3K/AKT

	Agent	Phase*	No. of Trials†	Target
Monoclonal Antibodies	BI 836845	I	2	IGF1 & IGF2 Ligand
	MEDI-573	I	4	IGF1 & IGF2 Ligand
	AVE1642	II	3	IGF1R
	BII B022	I	3	IGF1R
	AMG479 (Ganitumab)	II	24	IGF1R
	CP 751 871 (Figitumumab)	III	8	IGF1R
	R1507 (Robatumumab)	II	5	IGF1R
	MK 0646 (Dalotuzumab)	II	4	IGF1R
	IMC-A12 (Cixutumumab)	II	22	IGF1R
	SCH 717454	II	4	IGF1R
Small molecule Inhibitors	OSI 906	II	6	IGF1R
	AXL 1717	II	3	IGF1R
	XL 228	I	2	TKI with activity against IGF1R, Src, FGFR & BCR-ABL
	BMS 754807	II	6	IR/IGF1R TKI
	Immunotherapy	I	1	IGF1R Antisense

Table 1.1 IGF1R Inhibitory agents in Clinical Trials listed at www.clinicaltrials.gov.

*- Denotes most progressed trial
†-Listed on 27/8/12
Tumour types enrolled in trials include – multiple myeloma, breast, solid, NSCC, Ewing's sarcoma, pancreas, ovarian, non Hodgkins Lymphoma, SCLC, Adrenocortical, SCC of lung, HNSCC, neuroendocrine. Hepatic, Thymoma, Thymic carcinoma, colon, mesothelioma, glioma,

canonical pathway (Shang et al., 2008). Subsequent clinical trials have evaluated IGF1R antibodies, as monotherapy or in combination with cytotoxic treatments, and have shown mixed results. Whilst some Phase II trials have reported responses, notably in Ewing's sarcoma (Olmos et al., 2010, Atzori et al., 2011), others have not (Reidy et al., 2010). None of these agents has thus far shown activity in unselected patients in Phase III trials, however one Phase III trial was abandoned due to excessive toxicity and lack of efficacy (Jassem, 2010, Basu et al., 2011). Hyperglycaemia has been reported regularly, not due to cross reactivity of the antibody with the IR but due to blockade of IGF1R on hypothalamic cells. In health IGF1 has a negative feedback effect on the hypothalamic pituitary axis, reducing GH release. When the hypothalamus senses a fall in circulating IGF1 levels, pituitary growth hormone production increases which stimulates hepatic IGF1 synthesis, peripheral insulin resistance and hyperinsulinaemia. Whether this toxicity will ultimately limit clinical use is less clear than the concerns regarding lack of efficacy.

1.3.6.2 Receptor Tyrosine Kinase Inhibitors

Small molecule receptor tyrosine kinase inhibitors block the kinase domain of the IGF1R, and prevent autophosphorylation in response to ligand stimulation. However unlike the monoclonal antibodies they do not alter IGF1R expression. Development of specific IGF1R inhibitors is complicated by the complete homology of the ATP binding cleft of the IR and IGF1R, but 15-30 fold selectivity for the IGF1R has been reported when IGF1R inhibitors are tested in intact cells (Garcia-Echeverria et al., 2004). Several IGF1R inhibitors have shown antineoplastic properties *in vitro* and *in vivo* in a range of cell types including fibrosarcoma and breast cancer (Scotlandi et al., 2005, Warshamana-Greene et

al., 2004, Mitsiades et al., 2004, Garcia-Echeverria et al., 2004) and some agents have subsequently entered clinical trials.

1.3.6.3 Anti-ligand Antibody (Ligand neutralisation)

Prevention of association of ligand and receptor offers an attractive method of inhibiting the IGF1R axis. Furthermore given the promiscuity of IGF1 and IGF2 ligands activating not only the IGF1R but also both IR_A and hybrid receptors, this strategy offers the ability to block all components of IGF driven signalling. Initial IGF neutralising antibodies demonstrated *in vitro* and *in vivo* inhibition of prostatic and hepatocellular carcinoma growth but cross reacted with insulin (Goya et al., 2004, Dransfield et al., 2010). A recently developed human IgG2 monoclonal antibody MEDI-573 binds both IGF1 and IGF2 but not insulin, and has been shown to inhibit IGF induced phosphorylation of IR_A, IGF1R and of downstream signalling components in mouse embryonic fibroblasts (MEF) which ectopically over express IGF1R alone or with IGF1 or IGF2. Furthermore this antibody inhibits the *in vivo* growth of MEF tumours, which are dependent on autocrine IGF stimulation (Gao et al., 2011). MEDI-573 is currently in Phase I clinical trials.

1.3.6.4 Conclusions

Whilst it is tempting to dismiss IGF1R blocking antibodies as a therapeutic strategy on the basis of the available evidence, the study designs have assessed additional benefit in the context of the standard, often poorly effective, chemotherapy treatment (Basu et al., 2011). An alternative approach selecting treatment combinations on the basis of pre-clinical evidence of superior efficacy might better demonstrate the utility of IGF1R blocking antibodies. For example in the case of melanoma, inhibition of the IGF1R can overcome

resistance to BRAF inhibition *in vitro* (Villanueva et al., 2010). Such a combination might prove more effective clinically than might be suggested by the reports described above. The key issue for effective use of IGF1R inhibitory drugs is the need for predictive biomarkers to identifying subsets of patients for whom this therapy would be most beneficial. For example it is well recognised that the mutation of the EGFR tyrosine kinase domain in pulmonary adenocarcinoma associated with sensitivity to gefitinib is most common in Asian, non smoking, females (Lynch et al., 2004). Similarly clinical trials typically recruit patients with advanced disease for whom there are poor therapeutic alternatives and any therapeutic benefit in early stage disease might be overlooked. For example, although the addition of figitumumab, offered no benefit over standard chemotherapy in advanced, previously treated, non small cell lung cancer (Jassem, 2010), the combination was more efficacious than standard chemotherapy in treatment-naïve patients (Gualberto and Karp, 2009).

1.4 The role of the IGF1R axis in melanoma

Melanoma pathogenesis is characterised by increasing growth autonomy and decreased requirement for, but enhanced response to, growth factors (Rodeck and Herlyn, 1988). Indeed the IGF1R axis is an important growth pathway in melanocytes (Halaban et al., 1992a, Halaban et al., 1992b) and transformation of melanocytes to melanoma is associated with an increased expression of IGF1R (Hoek et al., 2004, Easty and Bennett, 2000, Quong et al., 1994, Kanter-Lewensohn et al., 1998). A recent study implicates loss of miRNAs mir-376a and mir-376c during transformation in mediating the IGF1R upregulation (Zehavi et al., 2012) and IGF1R gene duplication has also been documented (Zhang et al., 1993). Early work suggested that growth of melanoma metastases is

independent of IGF1 (Rodeck et al., 1987b). However more recent work has demonstrated no difference in expression of IGF1R between primary lesions and metastases, and an active IGF1R axis in the latter (Xu et al., 2008, Easty et al., 2011).

There is substantial evidence that the IGF1R axis is required for survival, migration and proliferation of melanoma cells (Molhoek et al., 2011, Kanter-Lewensohn et al., 1998, Li et al., 2003, Neudauer and McCarthy, 2003, Shih and Herlyn, 1993, Furlanetto et al., 1993, Rodeck et al., 1987b, Herlyn et al., 1985, Stracke et al., 1988, Stracke et al., 1989, Satyamoorthy et al., 2001, Rodeck et al., 1987a, Hilmi et al., 2007). Furthermore proliferative effects are further increased synergistically by basic fibroblast growth factor and transforming growth factor β1, both of which are induced by IGF1 (Lazar-Molnar et al., 2000)

Melanoma cell lines and cultured primary cells are particularly sensitive to inhibition or downregulation of IGF1R, which causes growth arrest and apoptosis *in vitro* and *in vivo* (Werner and Le Roith, 1997, Dricu et al., 1997, Resnicoff et al., 1995a, Molhoek et al., 2011, Maloney et al., 2003, Yeh et al., 2006, Karasic et al., 2010, Lee et al., 2008). Of particular interest, inhibition of transplanted tumour growth is seen both in nude, immuno-incompetent, and in syngeneic mice. (Trabado et al., 2006, Resnicoff et al., 1994a, Kanter-Lewensohn et al., 1998, Furlanetto et al., 1993).

It has previously been thought that malignant melanoma cells are unable to produce IGF1 and rely on paracrine action of ligands produced by fibroblasts (Satyamoorthy et al., 2001, Satyamoorthy et al., 2002, Hilmi et al., 2007, Fleming et al., 1994). Indeed it has been suggested that insulin, acting via the IGF1R, is a more potent mitogen in melanoma cells

than IGF1 itself (Rodeck et al., 1987a, Rodeck et al., 1987b). However a recent study has not only demonstrated IGF1 production by both primary and melanoma cell lines, but also activation of IGF1R via an autocrine loop (Molhoek et al., 2011). Such an autocrine loop might explain the apparently contradictory correlation of low serum IGF1 with melanoma in two recent studies (Park et al., 2011, Santonocito et al., 2008).

It is also noteworthy that the IGF axis is strongly implicated in the development and progression of uveal melanoma, although the data regarding IGF1R expression and prognosis are contradictory (Economou et al., 2005, Al-Jamal and Kivela, 2011)

Overall these findings indicate that the IGF1R axis plays an important role in the pathogenesis of melanoma and that is also an attractive therapeutic target. Objective activity has been reported in a melanoma bearing patient in a Phase 1 trial of the IGF1R monoclonal antibody AVE1642 combined with conventional chemotherapy (Macaulay et al., 2012).

1.5 The Role of the IGF1R Axis in the immune response

There is evidence that manipulation of the IGF1R axis using nucleic acid based strategies and RNA interference (RNAI) may offer a means of increasing tumour immunogenicity, thereby overcoming *evasion from immune recognition*. Challenge of Igf1 or Igf1r depleted, irradiated, C6 glioblastoma cells to immunocompetent syngeneic rats resulted in complete regression of a pre-existing wild type tumour and protection from wild type tumour rechallenge (Trojan et al., 1993, Resnicoff et al., 1994b, Shevelev et al., 1997). Similar *in vivo* findings have been reported for other tumour types including, prostate carcinoma,

lung carcinoma, Ewing's sarcoma, embryonal carcinoma, hepatoma and breast cancer (Burfeind et al., 1996, Trojan et al., 1994, Lafarge-Frayssinet et al., 1997, Shevelev et al., 1997, Liu et al., 1998, Schillaci et al., 2006, Ellouk-Achard et al., 1998, Samani et al., 2001, Scotlandi et al., 2002). Of note similar inoculation of Igf1r depleted, irradiated, C6 glioblastoma cells into athymic nude rats does not protect from subsequent wild type tumour rechallenge (Resnicoff et al., 1996a), suggesting that manipulation of the IGF1R axis is capable of altering the immune response to tumour cells and this response is dependent on T lymphocytes. Indeed in immune competent hosts, CD8+ T lymphocyte infiltration has been documented in the regressing Igf1r or Igf1 depleted tumours but not wild type tumours (Lafarge-Frayssinet et al., 1997, Trojan et al., 1992, Trojan et al., 1993, Shevelev et al., 1997, Resnicoff et al., 1996b, Schillaci et al., 2006). Furthermore splenocytes harvested from mice challenged with Igf1r depleted breast cancer cells are reported to be capable of producing Class 1 cytokines Interferonɣ (IFNγ) and Tumour necrosis factor α (TNFα) on exposure to wild type breast cancer cells (Schillaci et al., 2006). Together these results implicate a role for the adaptive immune response.

Consistent with these findings, increased expression of MHC Class 1 molecules has been documented on glioma, hepatoma and embyronal carcinoma cells following IGF1 or IGF1R downregulation (Lafarge-Frayssinet et al., 1997, Ellouk-Achard et al., 1998, Upegui-Gonzalez et al., 1998, Ly et al., 2001, Ly et al., 2000, Szpechcinski et al., 2004, Trojan et al., 1996, Anthony et al., 1998). An increase in the surface expression of MHC Class 1 should render that tumour cell more likely to be recognised and destroyed by the adaptive immune system. Indeed IGF1 downregulation is reported to result in MHC Class I upregulation on manipulated glioma cells and generation of cytotoxic T lymphocytes (CTL) capable of killing wild type glioma cells *in vitro* (Trojan et al., 1993).

Several studies have documented changes in humoral immunity following IGF1 downregulation, specifically elevations in serum antibodies which are able to slow melanoma growth *in vitro* (Trabado et al., 2006, Trabado et al., 2007). Furthermore distant tumour regression has been observed in the rat C6 glioma model described above, when the Igf1r depleted cells were encapsulated in a subcutaneous diffusion chamber which prevented cell to cell contact (Resnicoff et al., 1995a). These findings have been replicated in twelve patients treated for malignant astrocytomas (Wongkajornsilp et al., 2001, Andrews et al., 2001). As cell–cell contact is prevented by a diffusion chamber, these experiments implicate mechanisms other than increased expression of MHC Class I molecules such as diffusion of apoptotic fragments and subsequent presentation by host dendritic cells or production of as yet uncharacterised immuno-peptides which interact with MHC Class I (Baserga et al., 1997b, Baserga, 2005, Resnicoff, 1998). Downregulation of IGF1 and IGF1R causes apoptosis and it has been documented that the proportion of apoptotic cells is greater *in vivo* than *in vitro* (Kooijman, 2006) (Ly et al., 2001, Ly et al., 2000, Resnicoff et al., 1995a).

1.6 Aims of this project

The interaction between manipulation of the IGF1R axis and tumour immunogenicity merits further investigation and melanoma is a promising candidate neoplasm, given the known role of immunotherapy in the treatment of this disease (Section 1.1.2.2). In a review paper Baserga's group documented immune effects of Igf1r downregulation in B1762.F10 murine melanoma but the results were not presented for analysis (Baserga et al., 1997b). Unpublished data from our laboratory (A.Yeh D.Phil Thesis, 2007)

demonstrated that siRNA-mediated depletion of the Igf1r in B16.F10 murine melanoma cells induced upregulation of surface MHC class 1 surface expression (H2-Db) by a mechanism other than increased transcription. This phenotype was not blocked by apoptosis inhibition, and appeared to be specific since it was not induced by depletion of the insulin (IR) or epidermal growth factor (EGF) receptors. However this preliminary work was in conflict with a contemporaneous report that Igf1 depletion of B16 melanoma cells did not cause a change in surface expression of MHC Class I ($H2\text{-}K^b$) (Trabado et al., 2006) and required further investigation.

In testing effects of IGF1R depletion on immune response to melanoma, it would also be important to develop an *in vivo* model in an immunocompetent animal. However IGF1R depletion is highly deleterious to tumour growth, presenting problems for *in vivo* assessment. Thus it would be useful to create a cell line in which the IGF1R could be depleted in a regulated manner by the induction of IGF1R specific shRNA. In addition to testing the effects on growth of the manipulated tumour, this would allow observation of any immune mediated effects on a distant (eg contralateral flank) wild type tumour.

It is also unclear to what extent immune effects are induced by clinically relevant strategies for targeting the IGF1R. Blocking monoclonal antibodies do cause IGF1R downregulation, whilst small molecule inhibitors of the IGF1R kinase domain, whilst blocking the intracellular signalling cascade, do not cause receptor downregulation. As such it is unclear if these clinically relevant strategies induce changes in neoplastic cells comparable to the effects of antisense or siRNA induced receptor depletion.

In considering IGF1R inhibition as a clinical strategy for treatment of melanoma it will be of critical importance to identify patients likely to benefit from IGF1R inhibitors. Identifying features which render melanoma sensitive to IGF1R inhibition will involve interrogation of the biology of IGF signalling in melanoma cells. Furthermore a translational approach may reveal signalling interactions that can inform rational combination therapies.

The pathways that transduce IGF signalling to the nucleus are reasonably well understood, as are the transcriptional targets of IGF1 signalling (Mulligan et al., 2002). However it is only relatively recently that the latter has been linked to response to anti-IGF1R therapies. Previous studies have investigated IGF induced patterns of gene transcription activated by IGF1, and have shown that an "IGF gene signature" is of prognostic significance in clinical cases of breast cancer (Creighton et al., 2008, Rajski et al., 2010). In addition, it is now clear that cancers commonly show dysregulation of another portion of the transcriptome, microRNAs (miRNAs) (Meister et al., 2004, Ma et al., 2007). These miRNAs are endogenous non-coding RNAs which negatively regulate expression of target genes at the post transcriptional level, via translational repression or mRNA cleavage. A single miRNA can control multiple gene targets in different cellular pathways and, as such, influence diverse biological processes. It is therefore possible that analysis of IGF-induced changes in miRNA profile may reveal novel pathway interactions or consequences of IGF1R manipulation. In addition miRNAs have several attractive features as biomarkers. miRNAs are stable in, and can be harvested from, archival formalin fixed paraffin embedded tissue, unlike mRNAs which can only be reliably retrieved from fresh frozen or specifically prepared (RNA later) tissue (Glud et al., 2009). As such miRNA signatures

promise to be robust, clinically useful biomarkers and indeed a miRNA signature has recently been correlated to survival in melanoma patients (Segura et al., 2010).

Thus it is hoped that an unbiased assessment of the transcriptional consequences of IGF1R activation or inhibition in melanoma may lead to identification of an IGF gene signature that correlates to clinical parameters including prognosis. Further interrogation of components of the gene signature may identify targets and pathways that influence sensitivity to IGF1R inhibition, and of relevance to this thesis, those which influence the immunogenicity of melanoma. Finally in the longer term, such a study it may provide information which may prove valuable in diagnosis, assessment of prognosis, rational treatment selection or monitoring efficacy of therapy.

Thus the aims of this project are to:

1. Assess the effects of IGF1R downregulation or inhibition on the immunogenicity of human and murine melanoma cells.
2. Define effects of IGF1R inhibition on the transcriptome of human melanoma cells.
3. Interrogate components(s) of the IGF gene signature to explore functional consequences of regulation by the IGF axis.

2. Materials & Methods

2.1 Gene Nomenclature

Human and murine gene and protein nomenclature used throughout this thesis is that of the Guidelines for Human Gene nomenclature (Wain et al., 2002) and the Mouse Genome Informatics Database (Eppig et al.) respectively.

2.2 Cell Culture

2.2.1 Cell Culture techniques.

Cultured cells were grown in sterile, mycoplasma-tested medium in tissue culture grade flasks, dishes and plates (Falcon/Nunc). All cell lines were maintained in a 37^{o}C humidified atmosphere of 5% CO_2 and 95% air or 10% CO_2 and 90% air. All cell lines were adherent and cultured in DMEM or RPMI-1640 supplemented with 10% fetal calf serum (FCS), penicillin (final concentration 100U/ml), streptomycin (100µg/ml) and Glutamine (6nM). For routine passage, cells were disaggregated using 3mM EDTA in PBS, washed in complete medium and an aliquot reseeded. For cryopreservation, disaggregated cells were resuspended in 10% dimethyl sulphoxide (DMSO), 50% FCS in the appropriate medium. This cell suspension was then aliquoted into sterile Nunc vials and cooled at 1^{o}C/min to -80^{o}C before transfer to liquid nitrogen. To recover frozen stocks, the frozen cell suspension was thawed rapidly to 37^{o}C before seeding into culture flasks containing complete medium which had been warmed and acclimatised in the appropriate CO_2 atmosphere. For the experiments described in chapters 4 and 5, all experiments were performed with cells of passage 4-5. Experiments described in chapter 3

were performed with cells of passage 3-10. During growth, cell lines were periodically checked for mycoplasma infection.

2.2.2 Cell lines

Cell lines utilised in this project are listed in Table 2.1. CHL-1, A375, A375M, SKMel28 and HMCB low passage cells were purchased from the American Type Culture Collection (ATCC); SKMel2, A2058, MM9 and MM25 cells were obtained from the Cancer Research UK Central Cell Services; SKMel23 were a kind gift from Professor V Cerundolo, (WIMM, UK) and B16.F10 from Dr Simon Davis, (WIMM, UK). A human colorectal cell line expressing the murine *Igf1r* (HT29-mIGF1r) had previously been generated in our laboratory (M. Takiguchi D.Phil Thesis 2008) and was used as a positive control in experiments assessing murine cell surface expression of *Igf1r*. A fast growing variant of human embryonic kidney cells transformed with the SV40 Large T-antigen, 293FT (Invitrogen), were utilised for production of lentivirus. Multiple aliquots were frozen at low passage.

2.2.3 Transfection of cultured cells

2.2.3.1 Transfection with RNA duplexes

Lipid mediated transfection reagent was used to introduce siRNA into cells as per manufacturer's guidelines. Two different protocols were employed during this project selected following optimisation experiments in the given cell lines and based on the cell plating format requirements for the planned experiment.

Cell Line	Cell type	Species	Culture Conditions	Routine Passage	Seeding Density for siRNA Transfection
B16.F10	Melanoma	Murine	RPMI 1640 in 5% CO_2	1:20 every 3rd day	$1.0x10^5$
CHL1	Melanoma	Human	DMEM in 10% CO_2	1:20 every 5th day	$2.0x10^5$
A375	Melanoma	Human	DMEM in 5% CO_2	1:20 every 5th day	$2.0x10^5$
SKMel2	Melanoma	Human	DMEM in 10% CO_2	1:10 every 5th day	$3.5x10^5$
SKMel23	Melanoma	Human	RPMI 1640 in 5% CO_2	1:20 every 3rd day	$2.5x10^5$
SKMel28	Melanoma	Human	DMEM in 5% CO_2	1:20 every 5th day	$2.0x10^5$
HMCB	Melanoma	Human	DMEM in 10% CO_2	1:20 every 3rd day	$2.5x10^5$
MM9	Melanoma	Human	RPMI 1640 in 5% CO_2	1:10 every 5th day	$3.5x10^5$
MM25	Melanoma	Human	RPMI 1640 in 5% CO_2	1:10 every 5th day	$3.5x10^5$
A2058	Melanoma	Human	DMEM in 10% CO_2	1:20 every 5th day	$2.5x10^5$
A375M	Melanoma	Human	DMEM in 10% CO_2	1:20 every 5th day	$2.0x10^5$
K1735	Melanoma	Murine	RPMI 1640 in 5% CO_2	1:20 every 5th day	$2.0x10^5$
HT29-mIgf-1r	Colorectal	Human	RPMI 1640 in 5% CO_2 *	1:3 every 7-10 days	-
293FT	Embryonic kidney	Human	DMEM in 10% CO_2 †	1:10 every 5th day	-

Table 2.1 Cell lines utilised in this project.

All culture media were supplemented with 10% fetal bovine serum (Helena Biosciences, Sunderland, UK). All cell lines were periodically tested for mycoplasma infection. Seeding density is given for forward transfection in a 6 well plate.

DMEM: Dulbecco's modified Eagle's medium,
RPMI: Roswell Park Memorial Institute
*: + 2.2mg/ml G418,
†: + 500µg/ml G418

2.2.3.1.1 Forward transfection

For the experiments described in Chapter 3, melanoma cells were seeded at a density chosen to result in 30-40% confluence after 24 hours. At this time cells were transfected with siRNAs using Oligofectamine (Invitrogen) as per the manufacturer's guidelines and as previously described (Bohula et al., 2003). Volumes to result in a 10nM siRNA transfection for cells in a 6cm dish are given in parentheses. Briefly Oligofectamine (4.5µl) was incubated with OptiMEM serum-free medium (Invitrogen) (150µl) for 10 minutes at room temperature. Similarly 20µM siRNA stock (0.5µl) was diluted with OptiMEM (560µl) appropriately to allow subsequent dilutions to achieve the desired final concentration of siRNA and incubated for 10 minutes at room temperature. The lipid and duplex mixtures were then combined and incubated together for a further 25 minutes at room temperature. This mixture was then diluted in OptiMEM (285µl) to achieve the final desired concentration of siRNA. Cell monolayers were washed twice with sterile PBS and the lipid/duplex complex (1ml) applied drop wise. After four hours incubation under usual culture conditions, complete medium and supplemental FCS were added to achieve a final concentration of 10% FCS. Transfected cells were collected after a further 24-48 hours for analysis.

2.2.3.1.2 Wet Reverse Transfection

For the experiments described in chapter 5, A375 melanoma cells were transfected with siRNA using DharmaFECT 1 (Thermo Scientific) as per the manufacturer's guidelines. Volumes to result in a 50nM siRNA transfection for cells in a single well of a 6 well plate are given in parentheses. Briefly 20µM siRNA stock (5µl) was diluted with serum free medium (495µl) and incubated for five minutes at room temperature. Concurrently

DharmaFECT I (5µl) was diluted with serum free medium (495µl) and similarly incubated. The duplex and lipid solutions were then mixed and incubated for a further 20 minutes. A suspension of cells in complete medium was prepared, containing sufficient cells to result in 50% confluence when plated (2 $x10^5$/ml), and equal volumes of cell suspension (1ml) and the siRNA:lipid complex solution (1ml) were added to wells of the culture plate. Following incubation for six hours at 37^oC the transfection medium was replaced with complete medium. Transfected cells were grown under usual conditions before further manipulation or analysis, typically 24-72 hours later.

2.2.3.2 Transfection of Plasmids

2.2.3.2.1 Nucleofection

Transient transfection of plasmid DNA by nucleofection was performed to test the efficacy of shRNA constructs. Transfection was achieved by nucleoporation using the Amaxa nucleofector 2b (Lonza) as previously described for the B16.F10 cell line ((Chou et al., 2009, Kadara et al., 2008)). Briefly 1.5 $x10^6$ B16.F10 cells, disaggregated by trypsinisation, were resuspended in 100µl Nucelofector solution V (Lonza) in electroporation cuvettes. Electroporation (nucleofection) was performed following addition of 2µg plasmid DNA as per the manufacturer's recommended protocol for B16.F10 cells (program P-20). The electroporated and transfected cell suspensions were immediately mixed with 500µl of pre-warmed cell culture medium and plated in prepared 6 well plates containing 1ml cell culture medium per well. Analysis was performed after 48 hours.

2.2.3.2.2 Lipid based transfection reagent

After comparing transfection efficiency of eGFP plasmids by flow cytometry using several different transfection reagents, FugeneHD (Promega) was determined to be the most efficacious reagent for transfection of A375 cells. Transfection was performed using a reagent:DNA ratio of 3:1 as described by the manufacturer's optimised protocol (http://www.promega.com/techserv/tools/FugeneHdTool/). Briefly $2x10^3$ A375 cells in 100µl complete medium were seeded into each well of a 96 well plate. For some experiments these cells underwent wet reverse transfection with siRNA, as described above, at this stage. On the following day ~50% confluence had been achieved. For each well a total of 0.1µg plasmid DNA was diluted with OptiMEM to a volume of 4.7µl and mixed thoroughly following addition of 0.3µl of FugeneHD. After incubation at room temperature for 30 minutes the DNA:lipid complex mixture was added to the plated cells drop wise. After 4 hours complete culture medium was added to a total volume of 200µl per well. Analysis was typically performed 24 hours after transfection.

2.3 Growth Assays

2.3.1 CellTiter-Glo Luminescent Cell Viability Assay

ATP induced luminescence, a measure of the number of metabolically active viable cells, was measured with the CellTiter-Glo Luminescent Cell Viability Assay (Promega) and Fluorstar Optima luminometer (BMG Labtech). Cells were lysed by addition of an equal volume of assay reagent directly to the culture medium. The reagent contains luciferin and a thermostable luciferase, which is activated by ATP. The resulting luminescence is read after 10 minutes incubation on a shaker at room temperature, and is proportional to the

amount of ATP, and thus the number of metabolically active cells present. One thousand cells per well were seeded, in triplicate, in 100µl complete culture medium into opaque walled 96 well plates (Grenier Bio-one). Twenty four hours after seeding, drug (AZ12253801) or vehicle were applied to triplicate wells and cell viability was serially assessed over the following days. Results were normalised to solvent treated cells (designated 100% growth). Using data from three independent experiments, curves were fitted to the data points using GraphPad Prism v5, and these curves were used to calculate the GI_{50}, the concentration of agent required to halve the growth of the cell population. The end point of each experiment was determined to have been reached when the same GI_{50} was recorded on sequential days (Figure 2.1).

2.3.2 Crystal Violet Assay

Quantification of DNA bound crystal violet allows visual assessment of cell growth in monolayer conditions. On solubilisation, the amount of crystal violet can be quantified spectrophotometrically and is proportional to cell mass (Aleksic and Feller, 2008). Growth in established monolayer conditions was determined by seeding $1x10^5$ cells into 6 well plates. Cells were allowed to proliferate to 50% confluence at which point treatment (AZ12253801 or vehicle) was added to duplicate wells. When the vehicle-treated wells reached 100% confluence, the cells were fixed and stained *in situ* with 0.1% crystal violet in 50% methanol for 20 minutes (Figure 2.2). After washing with water twice and air drying, protein bound dye was extracted with 10% acetic acid. Supernatant absorbance measured at 570nm was taken as representative of cell number. Readings were normalised to the absorbance of solvent-treated cells (designated 100% growth) and GI_{50} values calculated from dose response curves.

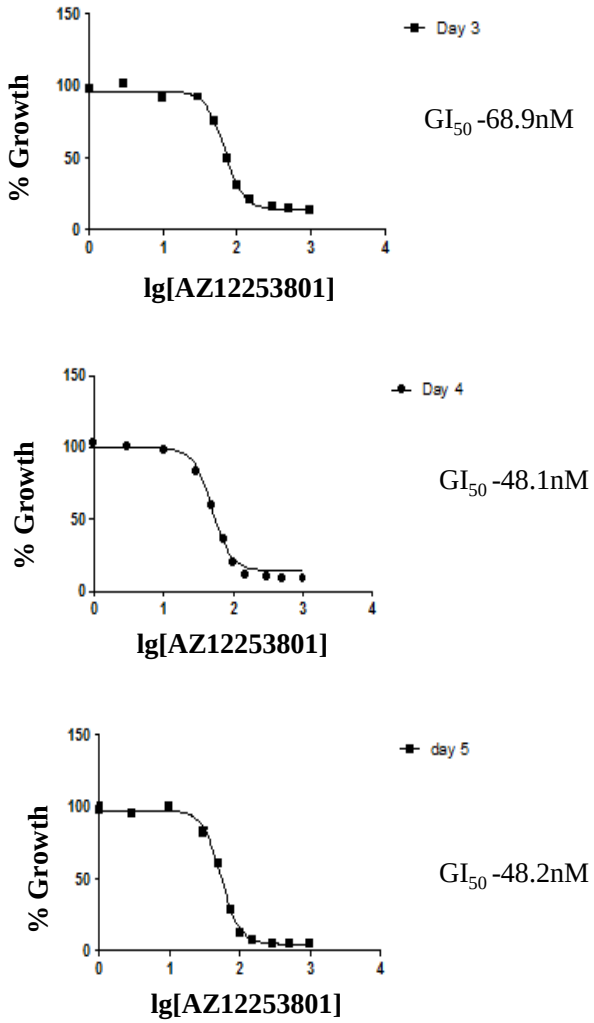


Figure 2.1 – Cell growth determined on sequential days using the CellTiter Glo Assay (Promega). The end point of each experiment was determined to have been reached when the same GI_{50} (concentration required to halve growth) was recorded on sequential days. In this representative example a GI_{50} of 48nM is recorded for A375 melanoma cells incubated with AZ12253801.

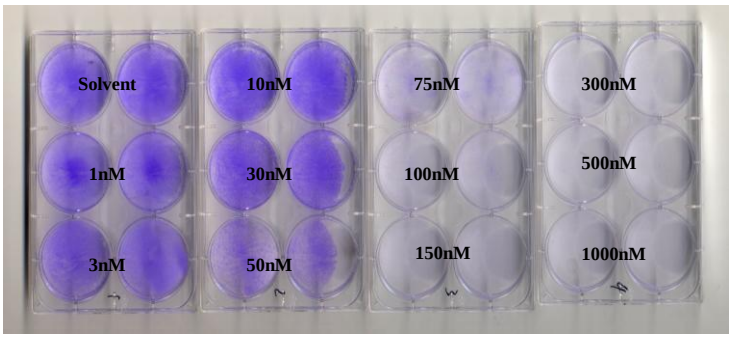


Figure 2.2 Six well plate cell viability assay after staining with crystal violet. Example shown - A375 cell treated with AZ12253801 until the solvent wells reached confluence. Wells were subsequently destained and A_{570} taken as a measure of cell number.

2.4 Treatments

Cells were treated with IGF1 or WNT3A ligands, small molecule inhibitors, or monoclonal antibodies as listed in Table 2.2. These compounds were prepared as stock concentrations, single use aliquots of which were stored at -20 or -80^{o}C until serial dilution in complete cell culture media to achieve working concentrations. In all cases the concentration of carrier was normalised across all experimental conditions to ensure that the final concentration of carrier was equivalent to that in the highest concentration of compound in each experiment. Carrier only treated cells served as controls. The concentration of DMSO was always less than 0.5% at the final concentration of compound.

2.5 Flow cytometry

Flow cytometry was used to measure cell surface expression of antigens, for functional T cell assays and for cell cycle analysis. Adherent cells were detached with 3mM EDTA in PBS prior to staining. Fluorescence analysis was performed on a FACS Calibur flow cytometer running Cell Quest software (BD Biosciences). Data analysis was performed using FlowJo 9 software. Unless otherwise stated centrifugation was performed at 4^{o}C, 2000rpm for 5 minutes. When live cell staining was performed, propidium iodide (10µg/ml) was added immediately before analysis and typically greater than 5 x10^{4} live cells were collected and analysed for each sample. Antibodies used for flow cytometry are detailed in Table 2.3.

Name	Target	Source	Diluent	Stock Solution	Working Concentration
AZ12253801	IGF1R	AstraZeneca	DMSO	10mM	0.1-1000nM
ADZ 1152-HQPA	Aurora B Kinase	AstraZeneca	DMSO	10mM	0.3-1000nM
U0126	MEK	Calbiochem	DMSO	100mM	1-50µM
LY294002	PI3K	Calbiochem	DMSO	10mM	10-100µM
Rapamycin	mTOR	Sigma	Methanol	5mM	1-50nM
SB203580	p38MAPK	Calbiochem	DMSO	2.65mM (1mg/ml)	1-100µM
SP600125	JNK	Calbiochem	DMSO	75.6mM	10-100µM
PPP	IGF1R	Merck	DMSO	5mM	0.5-25µM
α-IR3	IGF1R	Merck	PBS	100µg/ml	10-60nM
IGF1	IGF1R Ligand	Peptide Labs	HCl	10mM	1-50nM
WNT3A	Wnt Ligand	R&D Systems	PBS	200µg/ml	100-500ng/ml

Table 2.2 Treatments applied to cells in culture

Antibody	Product Number	Staining Concentration /1x10^6 cells	Fluorophore
H-2K^b	Santa Cruz 65382	1µg	FITC
H-2D^b	Cedarlane CL9001AP	1µg	Unconjugated mouse antibody
HLA-ABC	BD Pharmingen 555552	20µl	FITC
CD86	eBioscience 15-0862-81	1µg	PE-Cy5
CD221 (IGF1R)	BD Pharmingen 555999	20µl	PE
BrdU	Abcam 6326	15µl	Unconjugated rat antibody
Goat anti-mouse secondary antibody	Dako F0479	1:50	FITC
Goat anti-rat secondary antibody	Invitrogen 36930	1:250	AlexaFluor288

Table 2.3 Antibodies used for Flow Cytometric Analysis

2.5.1 Cell Surface Antigen Expression

Cells were washed in ice cold FACS buffer (PBS with 2% FCS) to reduce non specific antibody binding and equal numbers of cells (usually 10^6) were incubated with the relevant primary antibody diluted in 50-100µl FACS buffer for 30 minutes on ice, in the dark. If the primary antibody was directly conjugated to a fluorophore (FITC, PE, APC), the cells were washed twice in FACS buffer, resuspended in 200µl FACS buffer and analysed. If the primary antibody was not directly conjugated, the cells were washed twice in FACS buffer and incubated for a further 30 minutes in the dark on ice in 50-100µl conjugated secondary antibody in FACS buffer, washed twice again and resuspended 200µl FACS buffer for analysis. Background, non-specific, staining was determined by incubating an aliquot of each sample with the secondary antibody only, in the case of unconjugated primary antibodies, or with an irrelevant isotype conjugated antibody in the case of directly conjugated primary antibodies. Results were expressed as geometric mean fluorescent intensity (GMFI) determined by subtracting the GMFI of the isotype control, or secondary antibody alone control, from the GMFI of the specific antibody stained cells. Analysis of surface MHC Class 1 expression included a positive control in the form of cells treated for 24 hours with 20ng/ml human or murine interferon gamma (Peprotech), which has been shown to upregulate MHC Class 1 at a transcriptional level (Schroder et al., 2004).

2.5.2 Cell surface expression of murine Igf1r.

No antibodies could be identified commercially or in the literature that have successfully been used to detect cell surface Igf1r on murine cells. Preliminary experiments assessed multiple anti-human alpha subunit Igf1r antibodies, used in our laboratory for

immunoblotting and immunoprecipitation, but none were able to detect the Igf1r by flow cytometry. Successful detection was achieved using a previously published method which utilises biotinylated IGF1 ligand and a strepavidin-conjugated fluorophore (Xu et al., 1995). In brief, cells were serum-starved for one hour to displace native IGF1 from the Igf1r. Cells were then incubated on ice in a 100nM Hepes buffer (30mM NaCl, 5mM KCl, 1.2mM $MgSO_4$, 8.8mM Dextrose, 1% BSA) with 68nM biotinylated Des (1-3) IGF1 (Gropep, Australia) for 2 hours before labelling for 20 minutes with PE conjugated streptavidin. HT29-mIGF1r, a human colorectal cell line that over-expresses the murine Igf1r, previously produced in our laboratory (M.Takiguchi DPhil Thesis 2008), was used as a positive control. Staining specificity was assessed using competition with 100 fold excess of unlabelled Des (1-3) IGF1 (Gropep, Australia).

2.5.3 Analysis of Ploidy

Cells were washed in ice cold FACS buffer, resuspended in 400µl PBS and 3ml of ice cold 80% ethanol was added dropwise whilst gently vortexing the sample. After 12 hour fixation at -20^{o}C, cells were rehydrated with 10ml of FACS buffer, centrifuged and resuspended in 0.25% Triton in FACS buffer on ice for 10 minutes to permeabilise the cell membrane. Cells were washed with 10ml of FACS buffer, centrifuged and resuspended in PBS containing 10µg/ml propidium iodide and 100µg/ml RNAase A for analysis by flow cytometry.

2.5.4 Cell cycle analysis

Thirty minutes prior to harvesting, cells in culture medium were incubated with 10µM Bromodeoxyuridine (BrdU), a synthetic thymidine analogue that is incorporated into the

DNA of S phase cells. Cells were then harvested and fixed as described above (Section 2.5.3). Cells were rehydrated and permeabilised with 1ml 2M HCl 0.5% Triton for 30 minutes at room temperature. This acidification step breaks the hydrogen bonds between DNA strands allowing access to the integrated BrdU. Samples were then alkalinised with 1ml 0.1M sodium tetraborate to neutralise prior acidification, and fragment and destroy RNA. After centrifugation the cell pellet was resuspended in 100µl FACS Buffer and labelled with anti-BrdU primary antibody for 30 minutes at room temperature. The cells were washed twice in FACS buffer, resuspended in 100µl FACS buffer and incubated for a further 30 minutes with a conjugated secondary antibody, washed twice again and resuspended in 200µl FACS Buffer containing 40µg/ml propidium iodide for analysis.

2.5.5 Functional Immunological Assays

These assays rely on the principle of intracytoplasmic staining of live cells with Carboxyfluorescein succinimidyl ester (CFSE) or cell tracker orange (CTO). These molecules enter cells as non-fluorescent molecules and the action of intracellular esterases results in fluorescence, reduced ability to cross the cell membrane and longterm covalent binding to cellular proteins. As such, labelled cells can be identified and sequential halving of fluorescence is seen in daughter cells following cell division (Lyons and Parish, 1994). These assays used lymphocytes from transgenic C57BL/10 mice which expresses a T-cell receptor on >80% of peripheral lymphocytes that recognises αα366-374 (ASNENMDAM) of the nucleoprotein of influenza virus (A/NT/60/68) in the context of Class I MHC H2-D^b (Mamalaki et al., 1993).

2.5.5.1 Experimental animals

All mice were maintained in the Biological Services Unit, John Radcliffe Hospital, University of Oxford. Approval of care and use was obtained from the Clinical Medicine Ethical Review Committee, University of Oxford, under the authority of a UK Home Office Project License. Experiments used female C57BL/6 (hereafter referred to a B6) and C57BL/10 mice (hereafter referred to as F5 mice), aged 6–8 weeks. Experiments were conducted in full accordance with the United Kingdom Animal Procedure Act 1986 by individuals in possession of an appropriate personal license (Dr J.Silk, Dr M. Salio or Dr A.Stock)

2.5.5.2 VITAL Assay – *In Vitro* Killing Assay using CFSE/CTO

This assay was performed to assess how changes in MHC Class 1 expression of B16.F10 murine melanoma cells affected cell lysis induced by cytotoxic T lymphocytes. This assay compares specific T (effector) cell induced lysis of manipulated (target) cells with lysis of control (target) cells in a mixed population (Hermans et al., 2004). Prior staining with CFSE or CTO allows manipulated and control target cells to be distinguished and depletion of CFSE or CTO labelled target cells is indicative of T cell mediated cell destruction. Experiments required preparation of four cell populations.

Firstly a suspension of lymphocytes was produced from the spleen of an F5 mouse by maceration through a 100µm cell strainer. Intact cells were pelleted by centrifugation at 15000rpm for 5 minutes before resuspension and incubation for 5 minutes at room temperature in 2ml RBC lysis buffer (5 Prime). After quenching with 10ml complete culture medium, lymphocytes were pelleted by centrifugation, resuspended, counted and

plated at $2x10^6$ per well of a 6 well plate. In addition splenocytes from a B6 mouse were prepared identically and pulsed with 0.1µg/ml ASNENNDAM (Np) peptide for 1 hour, before washing in complete culture medium and resuspension. B6 splenocytes were then irradiated at 60 Gy and mixed with the F5 lymphocytes. IL-2 was added to a final concentration of 100U/ml. This mixed cell preparation was incubated at 37^{o}C for 7 days, the irradiated B6 splenocytes acting as antigen presenting cells to prime the effector F5 lymphocytes (*in vitro* priming). On day 7, the cell suspension was harvested and layered onto 10ml Lymphoprep (Axis-Shields) and centrifuged at 1800rpm for 20 minutes, without a brake for deceleration. Viable lymphocytes were collected from the liquid:polysaccharide interface and counted.

Secondly on the day of the experiment splenocytes were obtained from the spleen of a B6 mouse as described above, for use as a positive control.

Finally the 2 target cell populations were prepared from monolayer cultures of B16.F10 cells incubated with IFNɣ or solvent for 24 hours prior to disaggregation, by pelleting, centrifugation and resuspension in complete cell medium. Cells were then counted.

Each of the three preparations of target cells (control or IFNɣ- treated B16.F10, or positive control B6 cells) were divided into two equal aliquots and labelled by incubation with 1µM CFSE or 10 µM CTO in complete medium for 10 or 20 minutes respectively at 37^{o}C. Labelling was quenched by addition of 10ml FCS, and labelled cells were pelleted by centrifugation and resuspended in cell culture medium. The CFSE labelled cells were washed twice with complete medium before counting. The CTO labelled cells were incubated in complete medium for 20 minutes at 37^{o}C before washing twice and counting.

The labelled CFSE target cell aliquots were halved and one aliquot pulsed with Np peptide at a final concentration of 0.1µg/ml for 1 hour at 37^{o}C, then washed, pelleted and resuspended.

For each type of target cell, two cell mixtures were produced containing equal numbers of CTO labelled cells and either Np peptide pulsed or unpulsed CFSE labelled cells. 10^4 cells of each mixture were plated in round bottom 96 well plates, in duplicate. *In vitro* primed F5 lymphocytes were added to each well to achieve effector:target (E:T) ratios of 7:1, 3:1, 1:1 and 0:1. Duplicate plates were incubated for 24 hours at 37^{o}C. Cells were then pelleted by centrifugation and resuspended in 200µl FACS buffer. Analysis by FACS involved quantification of CFSE and CTO labelled live cell populations. Reduction of a peptide pulsed cell population in relation to the unpulsed control was interpreted as specific cell lysis (Hermans et al., 2004). In summary effector cells were incubated with a population consisting of 50% peptide pulsed target cells and 50% unpulsed (internal control) cells identified by differential cell labelling.

2.5.5.3 CFSE Proliferation Assay

This assay was employed to assess proliferation of CFSE-labelled lymphocytes (effectors) when incubated with B16.F10 melanoma cells (targets) that had been manipulated to influence MHC class 1 expression. When labelled with CFSE, division of lymphocytes can be documented by serial halving of the CFSE signal by flow cytometry (Lyons and Parish, 1994, Parish, 1999). Incubation of F5 lymphocytes with target cells in the absence of Np peptide act as a negative control to check specificity. Three different cell populations were prepared.

Firstly CD11c+ dendritic cells, prepared by Angus Stock, (WIMM) surplus to his experimental requirements were used as positive control cells. Briefly, CD11c+ cells were positively selected from collagenase treated splenic macerates from C57BL/6 mice using CD11c MACS microbeads and LS MACs columns (Miltenyi Biotec) as per manufacturer's instructions. The uniformity of the CD11c+ population was confirmed by positive FACS staining for MHC Class II and CD11c, comparing the macerate to the post enrichment sample. The positive control cells were counted, split into two fractions and one was pulsed for 60 minutes at 37^{o}C with Np peptide at a final concentration of 0.1µg/ml. Cells were then washed in complete cell medium and counted.

Secondly B16.F10 (target) cells were harvested 48 hours after siRNA transfection, counted and divided into two fractions. One fraction was pulsed for 60 minutes at 37^{o}C with Np peptide at a final concentration of 0.1µg/ml. Cells were then washed in complete cell medium and counted.

Finally, to generate lymphocyte effectors the spleen was harvested from an F5 mouse. A cell suspension was produced by maceration of the spleen through a 100µm cell strainer. CD8 + cells were harvested using a commercial kit (Dynal Mouse CD8 Negative Isolation Kit) according to manufacturer's instructions. Briefly splenocytes were resuspended at a concentration of 1x10^{8} cells/ml in Buffer 1 (PBS, 0.1% FCS, 2mM EDTA) with 20% FCS and incubated for 20 minutes at 4^{o}C with 100µl/ml of Antibody Mix. This antibody solution contained rat monoclonal antibodies directed against CD45R, CD11b, Ter-119, CD16/32 and CD4 and as such bound to CD4+ T cells, B cells, monocytes, NK cells, dendritic cells, erythrocytes and granulocytes. Meanwhile 4x10^{8} Dynal beads per 1x10^{8}

cells were washed three times and resuspended in 200µl Buffer 1. After incubation the cell:antibody mixture was diluted in Buffer 1, pelleted by centrifugation and resuspended in 400µl of Buffer 1. The cells were added to the bead suspension and incubated on a rolling, tilting mixer for 15 minutes at 4^{o}C. The mixture was then diluted with a further 1ml of Buffer 1 and placed onto the magnet apparatus (Dynal MPC). After standing for 2 minutes, the supernatant was transferred to a second tube and magnetic depletion was repeated. The final supernatant enriched for CD8+ T cells was diluted in complete culture medium with 10% FCS and cell number counted. Enrichment of CD8+ T cells was confirmed by flow cytometric assessment of the CD8+ population. CD8+ T lymphocytes were then labelled by incubation with 1µM CFSE in complete medium for 10 minutes at 37^{o}C, pelleted and washed twice in complete medium before resuspension and counting.

To set up the CFSE proliferation assay 5x10^{4} CFSE labelled CD8+ T cells in 100µl complete cell medium were plated in triplicate wells of a round bottomed 96 well plate and combined with appropriate numbers of Np pulsed or unpulsed B16.F10 melanoma cells in 100µl compete medium to achieve effector to target cell (E:T) ratios of 1:5, 1:2.5, 1:1.25, 1:1, 2:1, 4:1, 6:1, 8:1, 10:1, 12:1. Effector cells were also combined with Np pulsed or unpulsed CD11c+ cells at an E:T ratio of 3:1. Lymphocyte proliferation was assessed after 36 hours by flow cytometric quantification of CFSE signal.

2.5.5.4 Cytokine Assay

This assay was employed to assess cytokine production of *in vivo* primed lymphocytes (effectors) when incubated with B16.F10 melanoma cells (targets) that had been manipulated to influence MHC class 1 expression.

CD11c+ dendritic cells as positive control cells and B16.F10 target cells were prepared exactly as described in 2.5.5.3. To generate lymphocyte effectors the spleen was harvested from an F5 mouse which had been inoculated seven days previously with UV irradiated influenza virus strain PR8 (H1N1) containing the αα366-374 epitope. CD8+ lymphocytes were then isolated exactly as described in 2.5.5.3 but not labelled with CFSE.

To set up the cytokine assay $1x10^4$ CD8+ T cells in 100µl complete cell medium were plated in triplicate wells of a round bottomed 96 well plate and combined with appropriate numbers of Np pulsed or unpulsed CD11c+ cells or B16.F10 melanoma cells in 100µl compete medium to achieve effector to target cell (E:T) ratios of 16:1, 8:1, 4:1 and 1:1. Supernatant was harvested after 36 hours and stored at -80^{o}C until cytokine quantification. IFNɣ and TNFα concentrations were determined by ELISA.

Murine IFNɣ ELISA plates were prepared by incubating 100µl IFNɣ capture antibody (eBioscience R4-6A2) at a final concentration of 5µg/ml in carbonate-bicarbonate coating buffer (Sigma) in each well of a 96 well Maxisorp immunoplate (Thermo Scientific) overnight at 4^{o}C. Plates were washed three times in PBST (PBS, 0.05% Tween-20) and once in PBS before incubation with FCS buffer for 2 hours at room temperature. Final washing was performed as before. Triplicate 100µl sample aliquots were incubated in each well overnight at 4^{o}C in parallel with dilutions of IFNɣ (0.01-300U/ml) for construction of a standard curve. Wells were washed as before and 100µl of each sample was incubated with 0.5µg/ml biotin conjugated IFNɣ detection antibody (XMG1.2-Biotin) in PBST for 1 hour at room temperature. After further washing, 100µl of Extravidin peroxidise (Sigma) was added to each well and the plate was incubated for 1 hour at room temperature. After

final washing, 100µl of 3,3,5,5, tetramethylbenzidine (TMB) substrate was added to each well and incubated at room temperature. The reaction was stopped with 100µl of 1M H_2SO_4 when the lowest standard concentration of IFNɣ was slightly blue.

TNFα ELISA plates were prepared using the Mouse TNF alpha ELISA Ready-SET-Go kit (eBioscience) in manner identical to that above, except the coating buffer was 0.1M sodium pyrophosphate. A standard curve was generated using TNFα (2-1000pg/ml) in the same manner.

Cytokine concentration was determined with reference to the generated standard curves produced by reading at 450nm, and subtracting the reading at 570nm, on a plate reader (µQuant Universal Microplate Spectrophotometer, Northstar scientific).

2.6 Immunofluorescence microscopy

Cells were seeded onto glass coverslips and treated with drug (AZ1225308 or AZ1152-HQPA) or vehicle for two days. Coverslips were washed twice with ice cold PBS and fixed in 4% paraformaldehyde, 0.1% Triton in PBS for 20 minutes at room temperature. Prior to staining, cells were permeabilized with 0.5% Triton X-100/PBS for 5 minutes, washed in PBST for 5 minutes, and blocked in 5% FCS/PBS for one hour at room temperature. Cells were stained with primary antibody (Alpha tubulin 1:2000 (Abcam) and P-Histone H3 1:6000 (Millipore)) for 30 mins, washed three times with PBST and incubated with fluorophore conjugated secondary antibody (1:2000 Alexa Fluor 488 (Molecular Probes AF21206) or Alexa Fluor 555 (Molecular Probes AF31570)), for 12 hours in the dark. After washing in PBST five times, coverslips were mounted with ProLong Gold antifade reagent with DAPI (Molecular Probes). Preparations were

visualised with a Zeiss Axioshop 2+ fluorescence microscope and acquired with AxioVision software. Each experiment included a negative control, cells stained with secondary antibody in the absence of primary antibody.

2.7 Procedures for handling RNA

2.7.1 General Techniques

Work surfaces and equipment were cleaned with 100% ethanol and RNaseZap (Ambion) and all pipette tips used were filter tipped (Axygen). All other consumables were RNase-free. All solutions were prepared using nuclease free water (Ambion).

2.7.2 Extraction of Total RNA For qRT PCR

Total RNA was extracted using the RNeasy micro kit (Qiagen) according to manufacturer's directions. Briefly cell pellets were lysed in a high salt, β-mercaptoethanol, RNase containing buffer, and long RNAs (greater than 200nt) were selectively bound to a silica membrane. The RNA, effectively enriched for mRNA, was then eluted with nuclease free water. RNA immediately underwent DNAase I treatment and reverse transcription.

2.7.3 DNAase I Treatment and Reverse Transcription

Immediately following extraction and quantification, total RNAs were treated with DNA-free (AB Applied Biosystems) according to the manufacturer's protocol to remove contaminating DNA. RNA concentrations were assessed by Nanodrop spectrophotometry (Nanodrop technologies), and protein contamination was estimated from the ratio of

absorbance at 260:280nm and of solvent contamination at 230:260nm. An A260:280 and an A230:260 of 1.8-2.0 was considered to represent good quality RNA. Reverse transcription was then immediately performed. cDNA was synthesized from RNA by reverse transcription using the High Capacity cDNA Archive Kit (AB Applied Biosystems) according to the manufacturer's instructions. Briefly 5µg of total RNA was added to PCR reaction tubes and DEPC water added to a final volume of 25µl. A reverse transcriptase mastermix was prepared, comprised of 5µl of 10x RT Buffer, 5µl of 10x Random Primers, 2µl of 25x dNTPs, 10.5µl of DEPC water and 2.5µl of reverse-transcriptase per reaction. Twenty-five microliters of the reverse-transcriptase mastermix was added to each PCR reaction tube resulting in a final volume of 50µl. Reactions were incubated at 25^{o}C for 10 minutes, 37^{o}C for 2 hours and 4^{o}C for 10 minutes in a Peltier Thermo Cycler (MJ Research, Waltham, MA, USA). The resulting cDNAs were stored at -80^{o}C until analysis.

2.7.4 Quantitative RT-PCR (qRT-PCR)

2.7.4.1 Roche Universal probe Library

Primers for quantitative RT-PCR were designed using the Roche Universal Probe Library service (https://www.roche-applied-science.com) and were synthesised by Qiagen. Probes were purchased from Roche. Primer pairs and probe numbers are detailed in Tables 2.4, 2.5 and 2.6. Each 25µl qPCR reaction consisted of 20µl ABSOLUTE qPCR Master Mix (ABgene), 10pmol each of forward and reverse primers, 25µg cDNA and 1.25µl probe. Triplicate samples were analysed by real time qPCR on the Corbett Rotor Gene 3000 qPCR system (results presented in chapter 3) or Applied Biosystems Prism 7900HT system (results in chapter 4) under the following conditions: 2 minutes at 50°C, 10 minutes

Gene Name	Symbol	Forward Primer	Reverse Primer	Probe[a]
β-Actin	*ACTB*	cccagcacaatgaagatcaa	cgatccacacggagtacttg	63
β-2-Microglobulin	*B2M*	ttctggcctggaggctatc	tcaggaaatttgactttccattc	42
Glyceraldehyde-3-phosphate dehydrogenase	*GAPD*	agccacatcgctcagacac	gcccaatacgaccaaatcc	60
Hypoxanthine phosphoribosyl transferase 1	*HPRT1*	tgaccttgatttattttgcatacc	cgagcaagacgttcagtcct	73
Ribosomal protein L13a	*RPL13A*	ggccatcgtggctaaaca	ccttcacagcgtacgacca	3
TATA box binding protein	*TBP*	gctggcccatagtgatcttt	cttcacacgccaagaaacag	3
Ubiquitin C	*UBC*	cctgaccagcagaggttgat	tgttgtagtcagacagggtacga	11
Tyrosine 3-monooxygenase/ tryptophan 5-monooxygenase activation protein, zeta polypeptide	*YXHAZ*	gcaattactgagagacaacttgaca	tggaaggccggttaatttt	2
Flotillin 2	*FLOT2*	ctcagcttcaccatcaaggac	tcagcatctctctgcaccac	61
Heat shock 90-kDa protein 1, b	*HSPCB*	ggagaattctacaagagcctcact	tgaccttctacagaaaagtgcttg	48
Testis enhanced gene transcript	*TEGT*	atatggtcactcatttcattcagg	tcaatatcagggagcccaag	40
Tubulin alpha 6	*TUBA6*	ccccttcaagttctagtcatgc	attgccaatctggacacca	58

Table 2.4 Primer Sequences and Probe Numbers of Human "House Keeping Genes" employed for qRT-PCR

[a] : Universal ProbeLibrary number (Roche Diagnostics)

Gene Name	Symbol	Forward Primer	Reverse Primer	Probe[a]
Insulin-like Growth Factor Receptor 1	*Igf1r*	gagaatttccttcacaattccatc	cacttgcatgacgtctctcc	104
β-Actin	*Actb*	tgacaggatgcagaaggaga	cgctcaggaggagcaatg	106
Ubiquitin C	*Ubc*	gagttccgtctgctgtgtga	tcacaaagatctgcatcgtca	77
ɣ Actin 1	*Actg1*	cctagcacctagcacgatga	actcctgcttgctgatccac	11

Table 2.5 Primer Sequences and Probe Numbers of Murine genes employed for qRT-PCR

[a] : Universal ProbeLibrary number (Roche Diagnostics)

Gene Name	Symbol	Forward Primer	Reverse Primer	Probe[a]
v-myc myelocytomatosis viral related oncogene, neuroblastoma derived (avian)	*MYCN*	ccacaaggccctcagtacc	cctcttcatcatcttcatcatctg	55
v-myc myelocytomatosis viral oncogene homolog (avian)	*MYC*	gctgcttagacgctggattt	taacgttgaggggcatcg	66
Neutrophil cytosolic factor 1	*NCF1**	ctgcccgtcaaaccactt	ccgagatctacgagttccataaa	10
Cyclin-dependent kinase inhibitor 2A	*CDKN2A†*	gtggacctggctgaggag	ctttcaatcggggatgtctg	34
Macrophage migration inhibitory factor	*MIF*	tgttcatcgtaaacaccaacg	gtgcaccgcgatgtactg	3
Cyclin D1	*CCND1*	gaagatcgtcgccacctg	gacctcctcctcgcacttct	67
High Mobility Group -box transcription factor 1	*HBP1*	catgttatggtgctctgactgc	gctggtggtgttgtcgtg	37
unc-51-like kinase 1 (C. elegans)	*ULK1*	tcatcttcagccacgctgt	cacggtgctggaacatctc	26
Frequently rearranged in advanced T-cell lymphomas 2	*FRAT2*	gttcaaggtcacggtttgct	gaaaagactccggggtgagt	14
SIX homeobox 5	*SIX5*	aatgtgcacctcatcaactcc	gttggccaggaggaagttt	8
Chaperone, ABC1 activity of bc1 complex like (S. pombe)	*CABC1*	gaggggagctgatcatgg	aaaatattcttcatgtttatcctgacc	81
Leukemia inhibitory factor	*LIF*	tgccaatgccctctttattc	gtccaggttgttggggaac	26
Connective tissue growth factor	*CTGF¥*	gctcggtatgtcttcatgctg	agctgacctggaagagaacatt	71
Transducer of ERBB2, 1	*TOB1*	ggtccactcagcctttaacct	ttcattttggtagagccgaac	87
Interleukin 24 transcript 1	*IL24 t1*	gagggcagaagggtctgg	ccaagaagaattgaggctgct	69
Interleukin 24 transcript 2	*IL24 t2*	gagggcagaagggtctgg	gctgcagcaggaggttct	89
NADPH oxidase 4	*NOX4*	cgggagggtgggtatctaa	gctgacgttgcatgtttcag	66

Table 2.6 Primer Sequences and Probe Numbers of Human "Genes of Interest" employed for qRT-PCR

[a] : Universal ProbeLibrary number (Roche Diagnostics)
*: Also known as **p47phox**
†: Also known as **P16INK4A**
¥ : Also known as **IGFBP-8**

at 95°C and then 40 cycles of 15 seconds at 95°C and 1 minute at 60°C. Ct values for each triplicate were recorded in the exponential phase of the curve. Relative quantification of the gene of interest was derived using normalisation factors based on the geometric mean of 1-3 reference genes. The most stable reference genes under each experimental condition were chosen from a panel of 12 human and 3 mouse reference genes (Tables 2.4 and 2.5) based on an M score calculated using GeNorm software (http://medgen.ugent.be/~jvdesomp/genorm/) as previously described (Vandesompele et al., 2002). The reaction efficiency for each gene was calculated after obtaining standard curves for each PCR reaction, by making 10-fold serial dilutions covering the range equivalent to 50 to 0.5ng of RNA.

2.7.4.2 SYBR-Green based qPCR

Concerns with the variability of triplicate data produced using the above method prompted a change to use of a SYBR-Green based system, Sensimix SYBR (Bioline), for the experiments detailed in chapter 5. For primers designed as described in 2.7.4.1, trial PCR reactions and melting curves were performed to confirm a single PCR product was produced in the absence of the Roche probe. Additional primers designed using NCBI Primer-Blast (http://www.ncbi.nlm.nih.gov/tools/primer-blast/) to produce products less than 300bp, were purchased from Qiagen and are detailed in Table 2.6. qPCR was performed in a 384 well format using the Applied Biosystems Prism 7900HT system. Each 10µl reaction consisted of 5µl of 2x Sensimix SYBR (containing heat activated DNA polymerase, ultra-pure dNTP, $MgCl_2$ (6mM) and SYBR Green I), 2.5µl RNase free water, 0.5µl of 10µM equimolar primer pair mixture and 2µl of 10ng/µl cDNA. Triplicate samples were analysed by PCR under the following conditions: 10 minutes at 95°C and

then 40 cycles of 15 seconds at 95°C, 15 seconds at 55°C and 15 seconds at 72°C. Melting from 50^{o}C to 95^{o}C was performed to assess the uniformity of the PCR product.

2.7.5 Extraction of RNA for gene profiling and miRNA quantification

Total RNA was extracted using the mirVana kit (Applied Bioscience). This method employs both organic, acid-phenol:chloroform extraction and glass fibre filtration to preserve short RNA species including miRNA. The method was as described by the manufacturer except that trypsin was not used to detached monolayer cells and RNA was eluted in nuclease free water rather than the supplied EDTA (0.1mM). This former alteration was made after the observation that serum free complete culture medium used in the experiment would not block trypsin activity which would then degrade RNA and the latter was suggested to maximise efficiency of the subsequent assessment on microarray plates (personal communication Dr Christine Blancher). Briefly cell pellets were disrupted in a denaturing lysis buffer, incubated on ice for ten minutes before Acid-Phenol:Chloroform extraction of DNA. Ethanol was added to the aqueous, RNA containing, fraction and small RNAs (less than 200nt) were selectively bound to a glass-fiber filter. The RNA, effectively enriched for small RNA species including miRNA, was then eluted with nuclease free water. RNA concentration was assessed by spectrophotometry and purity was assessed using a microfluidics based platform (Agilent 2100 bioanalyser and RNA Nano 6000 kit). This analysis gives an indication of RNA purity, ribosomal RNA ratios and calculates an RNA Integrity number (RIN) based on sample integrity. RNA of a sufficient quality for microarray analysis required a RIN of greater than 7, 28S/18S ratio of greater than 1.6, A260/280 of 1.8-2.0 and A260/230 of

close to 1.8. Following extraction and confirmation of adequate purity RNAs were aliquoted and stored at -80^{o}C.

2.7.6 Illumina gene arrays

Illumina gene array analysis was carried out by Dr Christine Blancher, Microarray facility, Wellcome Trust Centre for Human Genetics, Oxford. RNA was labelled according to Illumina protocols for two rounds of amplification. Labelled RNAs were hybridized to Illumina HT12 v3.0 Beadchip arrays (Illumina, San Diego, USA). Two array chips were used, each bearing 12 samples.

The data were normalized by Robust Multiple-array Average (RMA) method and analyzed using Limma software (http://bioinf.wehi.edu.au/limma/) and the Ingenuity Pathway Analysis tool (Ingenuity systems Redwood City, CA). This analysis was performed by Mr Steve Taylor, Computational Biology Research Group, Weatherall Institute of Molecular Medicine, Oxford.

2.7.7 miRNA quantification

qRT-PCR was used to determine expression of the 754 commonest miRNAs using the recently developed Taqman MicroRNA assay cards A+B v3.0 (Applied Biosystems). Total RNA was reverse transcribed using the Taqman MicroRNA Reverse Transcription Kit (Applied Biosystems) and Megaplex RT Primers sets A+B (Applied Biosystems) as per manufacturer's instructions. Briefly 500ng RNA in 3µl was mixed with 10x Megaplex RT miRNA primers, 10mM dNTPs, 2U RNase inhibitor, 5mM MgCl and 75U Multiscribe reverse transcriptase in a total volume of 7.5µl and subjected to 40 cycles (16 ^{o}C for 16

minutes, 42°C for 1 minute and 50°C for 1 minutes) and 5 minutes at 85°C. Six microlitres of this Megaplex RT product was mixed with 444µl 2XTaqman Universal PCR Master Mix No AmpErase UNG and nuclease free water added to a total volume of 900µl. One hundred microlitres of PCR reaction mix was carefully pipetted into each of the 8 loading ports of the Taqman microfluidics array card. The loaded card was then centrifuged twice at 1200rpm for 1 minute at room temperature to distribute the PCR reaction mix through each of the 384 wells, which contain pre-aliquoted Taqman primers for miRNAs and endogenous controls. The card was then sealed using a purpose supplied device (Taqman Array Micro Fluidic Card Sealer). qRT PCR was then performed using Applied Biosystems 7900HT machine using a preset optimal cycling regime (2 minutes at 50°C [to activate UNG], 10 minutes at 95°C, 40 cycles of denaturation at 95°C for 15 seconds, and annealing and extension at 60°C for 1 minute). Ct values for each triplicate were recorded in the exponential phase of the curve. Results of the miRNA qRT-PCR were analysed using purpose designed Invitrogen software (Data Assist v2.0 http://www.invitrogen.com/site/us/en/home/Global/forms/dataassist-software-registration.html).

2.8 Gene Silencing by RNA Interference

Gene silencing was achieved using RNA interference (RNAi). Double stranded 21bp RNA homologous to the target gene introduced into cells mediates post-transcriptional gene silencing by binding and inducing cleavage of the corresponding mRNA by the Argonaute component of the RNA-induced silencing complex (RISC) cells (Elbashir et al., 2001, Rand et al., 2005).

The sequences used for RNAi experiments are detailed in Table 2.7. Non silencing control siRNA (Qiagen) was used as a control for non-specific effects of RNA transfection. The R4 duplex had been designed in our laboratory based on the findings of an antisense oligonucleotide array screen targeting an accessible region of IGF1R mRNA (Bohula et al., 2003). The R1 duplex had been designed in our laboratory using conventional criteria (Rochester et al., 2005). The HBP1 siRNA sequence was taken from a previously published report (Borrelli et al., 2010) and was found to be more effective than other commercially available HBP1 siRNA sequences. The sequence of each siRNA duplex was subjected to a BLAST search against the expressed-sequence-tagged library on the NCBI database to ensure targeting only of the desired transcript. siRNA duplexes were synthesised by Qiagen and were supplied as annealed HPLC-purified lyophilized pellets which were resuspended in RNase-free water (Qiagen) to a stock concentration of 20µM. Resuspended siRNAs were aliquoted, stored at -20^{o}C and subjected to no more than 4 freeze-thaw cycles.

2.9 Procedures for handling DNA

The procedures described in 2.9.1, 2.9.2 and 2.9.3 utilised reagents provided as part of the BLOCK-iT Inducible H1 RNAi Entry Vector Kit (Invitrogen) and the BLOCK-iT Inducible H1 Lentiviral RNAi System (Invitrogen).

2.9.1 Cloning of *Igf1r* shRNA into pENTR/H1/T0 Vector

2.9.1.1 Annealing reaction

Lyophilized single stranded (ss) oligonucleotides were resuspended in water to a final concentration of 200µM. For the annealing reaction 5µl of each of the top and bottom

Name	Target	Source	Sense & Antisense
R4	Hs+ Mm *IGF1R*	Bohula *et al*, 2003	CAAUGAGUACAACUACCGCTT GCGGUAGUUGUACUCAUUGTT
R1	Hs+ Mm *IGF1R*	Rochester *et al*, 2005	CGACUAUCAGCAGCUGAAGTT CUUCAGCUGCUGAUAGUCGTT
NSC	Non silencing control	Qiagen (1022076)	UUCUCCGAACGUGUCACGUTT ACGUGACACGUUCGGAGAATT
Q	Hs *IGF1R*	Qiagen (SI00017521)	GGAGAAUAAUCCAGUCCUATT UAGGACUGGAUUAUUCUCCAT
QM1	Mm *Igf1r*	Qiagen (SI01074017)	Not provided by manufacturer
QM2	Mm *Igf1r*	Qiagen (SI01074024)	
QM3	Mm *Igf1r*	Qiagen (SI01074003)	
QM4	Mm *Igf1r*	Qiagen (SI01074010)	GCUUCACAGUUUACUACAATT UUGUAGUAAACUGUGAAGCTG
HBP1	Hs *HBP1*	Borreli *et al*, 2010	GCUUGACUGUGGUACAGCATT UGCUGUACCACAGUCAAGCTT

Table 2.7 siRNA Sequences employed for Gene Silencing

All strands contained 19 nucleotides and two 3'deoxythymidines, as previously described (Elbashir *et al*., 2001)

strand oligonucleotides were incubated at 95^{o}C for 4 minutes in 2µl of 10X oligo annealing buffer and 8µl of DNase/RNase free water, followed by cooling for 10 minutes at room temperature. The resulting 50µM double stranded (ds) oligonucleotides were diluted to to a final concentration of 50µM for storage at -20^{o}C and a concentration of 500nM for analysis.

Annealing efficacy was checked by 4% agarose gel electrophoresis and demonstrated by the presence of a slower mobility species with twice the molecular weight of equal or greater intensity to that of the ss oligonucleotides.

2.9.1.2 Ligation and transformation

Five microlitres of 5nM ds oligonucleotide stock solution was incubated with 1.5ng pENTR/H1/T0 Vector, 1U T4 DNA ligase, 5x Ligation Buffer in total volume of 20µl reaction for 5 minute at room temperature. One shot Top10 Chemically Competent E.coli (Invitrogen) were transformed with ligated plasmid vector by heat-shock. Two microlitres of the ligation reaction were mixed with 50µl competent bacteria, chilled on ice for 30 minutes, heat shocked at 42°C for 45 seconds and placed on ice for 2 minutes. Bacteria were mixed with 250µl of SOC medium (Invitrogen) and incubated for 1 hour at 37°C with shaking at 200rpm. Bacteria were then plated onto prewarmed LB/kanomycin agar plates and incubated overnight at 37°C. Five colonies from each transformation were selected for analysis using a sterile plastic loop.

2.9.1.3 Preparation of Plasmid DNA

Plasmid DNA was extracted using Mini-prep or Maxi-prep kits (Qiagen). Bacterial colonies were picked, inoculated into 5ml of LB medium with 50µg/ml kanamycin and expanded overnight at 37^{o}C with shaking at 200rpm. Bacteria were pelleted by centrifugation at 6000g for 15 minutes at 4^{o}C and plasmid DNA was extracted as per the manufacturer's instructions. Briefly, cells were resuspended and lysed in an alkaline SDS buffer with RNase A before neutralisation. Following centrifugation the supernatant was applied to a column containing silica-gel, the DNA binding agent. The columns were washed twice with PE buffer containing ethanol and finally the plasmid DNA eluted in EB buffer. The maximum yield obtained was 20µg plasmid DNA.

2.9.1.4 Sequencing of Plasmid DNA

A restriction digest was performed to confirm insert presence. One microgram of DNA was incubated with the appropriate restriction enzyme in its provided buffer for one hour at 37^{o}C and analysed by 1% agarose gel electrophoresis. Plasmid DNA was supplied to the DNA Sequencing Service at the Weatherall Institute of Molecular Medicine, Oxford as 100-300ng/ml solutions for insert sequencing. Briefly insert sequences were amplified by PCR using H1 Forward (5'-TGTTCTGGGAAATCACCATA-3') and M13 Reverse (5'-CAGGAAACAGCTATGAC-3') primers using a DNA Engine Tetrad (Genetic Research Instruments). Automated sequencing was performed on a 48 capillary ABI 3730 Genetic Analyser (Applied Biosystems).

Sequences were analysed using free downloadable software (Sequence Scanner V1.0 software Applied Biosystems; http://appliedbiosystems.com). Plasmids with complete insert sequences were used for further experiments.

2.9.2 Creation of a stable Tet R expressing cell line

2.9.2.1 Production of Lentivirus

The pLenti4/BLOCK-iT DEST Gateway Vector Kit (Invitrogen) was used for the production of Lentivirus to introduce the pLenti6/TR plasmid containing the *TetR* gene into B16.F10 cells. Fetal calf serum functionally tested and shown to be free of tetracycline activity (Clontech) was used for these experiments. HEK293T cells were transfected with both expression plasmid (pLenti6/TR or pGFP Lenti) and viral packaging plasmids (Invitrogen viral packing plasmids) using Fugene6 (Roche). Briefly, 27µl of Fugene6 was incubated for 15 minutes at room temperature with the expression plasmid (2.3µg) and packaging plasmids (3µg total) in a total volume of 250µl OptiMEM (Invitrogen). This transfection mixture was added to monolayer cultures of HEK293T cells, at 80% confluence, in complete cell culture medium. After 24 hours the medium was replaced with fresh complete medium and after a further 48h the supernatant containing lentiviral particles was harvested, centrifuged at 1800rpm for 15 mins at +4^{o}C, and passed through a 0.45µm filter to remove intact cells. The supernatant was used immediately for infection and any residual stored at -80^{o}C.

2.9.2.2 Infection of B16.F10 cells with Lenti6/TR lentivirus.

Kill curves were performed using a range of concentrations of blasticidin, and the lowest concentration required to kill untransfected cells within 14 days (6µg/ml) was used

subsequently to select stable transfectants. $2x10^5$ B16.F10 cells were incubated for 24 hours with 2ml Lenti6/TR or positive control (pGFP Lenti) lentiviral supernatant in 6 well plates. This step differs from that recommended by the manufacturer who suggests quantifying the transducing units/ml of the viral supernatant by serial dilution, determining a multiplicity of infection (MOI) and subsequently using an MOI of 10 in definitive experiments. Typically, expression levels increase as MOI increases, and maximum TetR expression was desired. Therefore it was recommended to omit determination of MOI and use the viral supernatant undiluted (Dr M. Salio, personal communication). The day after transfection cells were cultured in complete medium for 24 hours before addition of blasticidin to a final concentration of 6µg/ml. Blasticidin supplemented medium was replaced every 48 hours for 14 days, or until blasticidin resistant colonies were identified. Resistant colonies were selected with a sterile pipette tip and expanded in complete medium containing 6µg/ml blasticidin. TetR expression was determined by immunoblotting and an aliquot of lysate from a previously prepared TetR expressing cell line, a kind gift from Dr Nick Platt was employed as a positive control.

2.9.3 Assay of β-Galactosidase activity

The β-galactosidase activity assay was performed to evaluate the efficiency of β Galactosidase shRNA transcription by the H1/T0 promotor and subsequent reduction in β Galactosidase production. $1.5\ x10^6$ B16.F10 cells were nucleofected with either a reporter plasmid, pcDNA 1.2/V5-GW/lacZ, alone or with the pENTR GW/H1/T0-lacZ2.1^{shRNA} plasmid in a 6:1 ratio as described in section 2.2.3.2.1. β-galactosidase activity was quantified after 48 hours using a β-Galactosidase Assay Kit (Invitrogen). This assay spectrophotometrically quantifies hydrolysis of ortho-nitrophenyl-β-D-galactopyranoside

(ONPG) to a yellow product (ONP) by β-galactosidase. Briefly cells were lysed in the supplied lysis buffer and by two freeze thaw cycles. An aliquot of lysate (10µl) was diluted to a final volume of 30µl with deionised water before addition of 70µl ONPG and 200µl Cleavage Buffer. After incubation at 37^{o}C for 30 minutes the reaction was stopped by addition of 500µl of Stop Buffer. Absorbance was measured at 420nm on a plate reader (µQuant Universal Microplate Spectrophotometer, Northstar scientific). A further small aliquot of each lysate underwent protein quantification as described in 2.10.3 and β galactosidase activity was corrected for protein content. Cells nucleofected in the absence of plasmid served as a negative control whilst β galactosidase (Sigma) alone served as a positive control.

2.9.4 Cell based assay of Wnt pathway activation (SuperTop/FOP assay)

The Super TOP/FOP Flash reporter assay was performed to evaluate TCF/LEF transcriptional activity induced by activated β-catenin as an end point of canonical Wnt signalling (Molenaar et al., 1996). The SuperTOPFlash plasmid contains 11 TCF/LEF binding sites upstream of a firefly luciferase gene and was a gift from Prof Yvonne Jones (Henry Wellcome Building for Genomic Medicine, Oxford). In the FOPFlash plasmid the TCF/LEF binding sites have been mutated to prevent β-catenin binding. The Renilla plasmid (pGL4.74[hRluc/TK]) contains a Renilla luciferase gene downstream from the herpes simplex virus thymidine kinase promoter. This plasmid acts as the internal control for assessment of transfection efficiency, and was a gift from Dr Lars Fugger (WIMM, Oxford). Twenty four hours prior to transfection, 2×10^{4} A375 cells in 100µl medium were seeded into opaque walled 96 well plates (Grenier Bio-one). Triplicate wells were transfected with either the TOPflash (firefly luciferase) reporter plasmid (0.1 µg/100 µl)

plus Renilla plasmid (1 ng/100 µl) or FOPflash plasmid (0.1 µg/100 µl) plus Renilla plasmid (1 ng/100 µl) using Fugene HD as described in section 2.2.3.2.2. After 24 hours, WNT3A was added to a final concentration of 250ng/ml for three hours. Both the firefly and the Renilla luciferase activities were measured using the Dual Luciferase Reporter Assay System Kit (Promega) according to manufacturer's instructions. This assay exploits the different evolutionary origins and substrates to independently quantify firefly and Renilla luciferase activity. Quantification of firefly luciferase is achieved through the addition of Beetle Luciferin in Luciferase reagent II. This reaction is then quenched and Renilla luciferase induced luminescence quantified after addition of coelenterazine in the 'Stop and Glo' reagent. Relative luminescence (SuperTOP/FOP activities) were calculated following the formula: TOP/FOP=(TOP firefly luciferase activity/renilla luciferase activity)/(FOP firefly luciferase activity/renilla luciferase activity). For some experiments A375 cells underwent wet reverse transfection as described in section 2.2.3.1.2 during initial well seeding.

2.10 Protein Analysis

2.10.1 Lysis of harvested cells.

For immunoblot analysis of protein levels, adherent cells were washed twice with ice-cold PBS and lysed directly in dishes on ice. The minimum volume of IGF1R lysis buffer (50mM HEPES, 100mM sodium chloride, 10mM EDTA, 4mM sodium pyrophosphate, 2mM sodium orthovanadate, 10mM sodium fluoride and 1% Triton-X-100, EDTA-free protease inhibitor cocktail (1.5mM Pefabloc (Roche) and phosphatase inhibitor cocktail I +II (Sigma)) necessary to harvest the cells was added (for example 500µl in a 10cm dish). After 10 minutes cells were scraped, the cell suspension/lysate collected and lysed on ice

for a further 20 minutes. Alternatively cells were scraped into cold PBS, centrifuged at 13000 rpm for 5 minutes at 4^{o}C and cell pellets frozen in liquid nitrogen before storage at -80^{o}C. Cell pellets were subsequently thawed on ice, resuspended in IGF1R lysis buffer and lysed on ice for 30 minutes. The resulting lysates were centrifuged at 13000 rpm for 10 minutes at 4^{o}C and the supernatant harvested and processed immediately. This protocol maximised preservation of protein phosphorylation status and protein yield. Residual sample was frozen immediately in liquid nitrogen for storage at -20^{o}C.

2.10.2 Preparation of nuclear lysate

For immunoblot of nuclear protein levels, adherent cells were washed twice with ice-cold PBS and lysed directly in dishes on ice. One ml of hypotonic lysis buffer (10mM Tris 7.5, 10mM KCl, 1mM EDTA, 1mM EGTA, 2mM $MgCl_{2,}$ EDTA-free protease inhibitor cocktail (1.5mM Pefabloc (Roche) and phosphatase inhibitor cocktail I +II (Sigma)) was added to each dish, cells were scraped, the cell suspension/lysate collected and dounced fifteen times on ice, then lysed for a further 15 minutes. The cell suspension was centrifuged at 3000rpm for 20 minutes at 4^{o}C. The nuclear pellet was then resuspended in IGF1R lysis buffer for 30 minutes on ice. The resulting lysates were centrifuged at 13000 rpm for 10 minutes at 4^{o}C and the supernatant harvested and processed immediately. Residual samples were frozen immediately in liquid nitrogen for storage at -20^{o}C.

2.10.3 Protein quantification

Soluble protein content was assessed using the BCA colourimetric assay (Thermo Scientific) read at 562nm on a plate reader (µQuant Universal Microplate Spectrophotometer, Northstar scientific) and extrapolated from a standard curve generated

from bovine serum albumin (0.1-2mg/ml). This assay quantifies protein content through the reduction of Cu^{2+} to Cu^{+} by peptide bonds and then bicinchoninic acid (BCA) chelates Cu^{+} to produce a purple coloured product.

2.10.4 SDS Polyacrylamide gel electrophoresis (SDS-PAGE)

SDS-PAGE was used to separate proteins according to electrophorectic mobility. Polyacrylamide gels were prepared using previously described techniques (Laemmli, 1970) using commercially available apparatus (Protean 3, Bio-Rad). Typically 7.5% resolving gels were prepared for analysis of proteins in the size range 40-180kDa. Briefly 30% acrylamide, 0.4% bisacrylamide stock (Protogel, National Diagnostics) was diluted appropriately with Tris/SDS buffer (0.1% SDS, 0.375M Tris-Cl pH 8.8). Acrylamide polymerisation was catalysed by addition of equimolar amounts of ammonium persulphate (Sigma) and Tetramethylethylenediamine (Sigma). Then 7.5ml of the resolving gel was poured between 8 x 10cm clean glass plates, 1.5mm apart and overlaid with isopropanol. After polymerisation the top of the gel was washed, dried and a stacking gel was added with a 1.5mm, 10 or 15 well comb. The stacking gel was prepared by diluting acrylamide stock with Tris/SDS buffer (0.1% SDS, 0.125M Tris-Cl pH 6.8) to result in a 5% acrylamide gel. Equivalent amounts of soluble protein, typically 20-50µg, were denatured in Laemmli buffer for 5 minutes at 95^{o}C, before loading into the wells within the stacking gel. Samples were analysed in parallel with a molecular weight marker (Full-Range Rainbow Marker, Amersham Biosciences). Proteins were electrophoresed at 125 volts for 90 minutes in running buffer (192 mM glycine, 25mM Tris-Cl, 0.1% SDS).

2.10.5 Immunoblotting

2.10.5.1 Semi-dry transfer of proteins to nitrocellulose membrane

Proteins separated by molecular size were transferred to nitrocellulose membrane by a semi-dry method. Six pieces of filter paper and one of nitrocellulose membrane (Hybond C Extra, Amersham), cut to the size of the resolving gel, were soaked in semi-dry transfer buffer (48mM Tris-Cl, 39mM glycine, 20% methanol, 1.3mM SDS (final pH 9.2)). Three pieces of the 3M filter paper were stacked on the base (anode) of the semi-dry transfer apparatus (Hoefer SemiPhor Transfer Unit, Amersham) followed by the membrane, the gel and the 3 remaining sheets of filter paper. This stack was gently compressed to extrude air bubbles. The top (cathode) of the transfer apparatus was replaced and a constant current (35mA per gel) applied for three hours.

2.10.5.2 Antibodies used for Immunoblotting

Following transfer of proteins and molecular weight marker to nitrocellulose, the membrane was blocked at room temperature, on a shaking platform for 1 hour, in 5% low fat milk or 5% BSA in PBS 0.05% Tween (PBST). The membranes were segmented by reference to the molecular weight marker depending on the proteins of interest and the portions incubated overnight at 4^{o}C with primary antibody in 5% BSA or milk in PBST. The antibodies used and their dilutions are detailed in Table 2.8. Following three ten minute washes in PBST the membrane portions were incubated for one hour with secondary antibody directed at the species of primary antibody employed and conjugated to horse-radish peroxidise (HRP). Following three further ten minute washes antibody bound protein was detected using enhanced chemoluminescence (ECL+, Amersham, UK), and the signal visualised on radiography film (Biomax MR, Kodak). This reagent produces

Antibody	Product Number	Primary Dilution	Molecular Wt (kDa)
p-IGF1Rβ (Tyr1135/1136)	CS #3024	1:1000 * a	95
IGF1R β	CS #3027	1:500 †	95
IGF1R α	SC #712	1:200 † b	130
p-AKT (Ser473)	CS #4051	1:1000 *	60
§ p-AKT (Ser473)	CS#9271	1:500 †	60
Total AKT	CS#9272	1:1000 *	60
p-ERK (Erk 1/2) (Thr202/Tyr204)	CS#4377	1:1000 *	42 & 44
Total ERK (Erk 1/2)	CS#9102	1:500 *	42 & 44
p-MEK 1/2 (Ser221)	CS#2338	1:1000 *	45
MEK 1/2	CS#4694	1;1000 †	45
p-S6 (Ser240/244)	CS#2215	1:5000 *	32
S6	CS#2217	1:1000	32
p - p70S6K (Thr389)	CS#9205	1:1000 *	70
p-GSK3 α (Ser 21) + β (ser9)	SC# 9331	1:1000 *	46 & 51
Phospho-p38 MAPK (Thr180/Tyr182)	CS#9211	1:1000 *	43
Phospho-SAPK/JNK (Thr183/Tyr185)	CS#9255	1:2000 †	46
p-β catenin	CS#9561	1:1000 *	92
Active β catenin	Millipore 05-665	1:10000 †	90
Total β catenin	BD 610154	1:5000 †	92
Cyclin D1	CS#2926	1:2000 †	36
HBP-1	SC#8484	1:200 ¥	76
TetR	Clontech 631110	1:1000 *	30
β-Actin	Ab #8224	1:10000 *	43
MCM2	Ab#4461	1:10000 *	100
β-tubulin	Sigma #T2046	1:20000 †	50

Table 2.8 Antibodies used for Immunoblot analysis

BD: BD Bioscience, CS: Cell Signalling, SC: Santa Cruz, Ab:Abcam,
†: Rabbit antibody in 5% BSA, *: Mouse antibody in 5% Milk, ¥: Goat antibody in 5% BSA.
§: Produced non specific band just above 60kDA in immunoblots from murine cells.
In all cases secondary antibody dilution was 1:10000 except a: 1:5000 and b: 1:2000.

luminescence by the oxidation of luminol by protein:antibody bound HRP. Radiographs were scanned and imported into Adobe Photoshop (Adobe). Densitometry quanitification was performed using Image J software. In all cases confirmation of loading of equivalent amounts of protein into each well was made by comparison to a reference protein, typically β-tubulin.

2.11 Statistical analysis

Prism v.5.0 (GraphPad) and Excel (Microsoft) graphing and statistical analysis software were used to plot and analyse data. Graphs were plotted to show mean values, and error bars depicting the standard error of the mean (SEM). The student's t-test and analysis of variance (ANOVA) with Bonferroni post test were used for the comparison of mean values between two and multiple (>2) data sets, respectively. A minimum of 95% level of significance (p value < 0.05) was used to define statistical significance.

3. Effects of IGF1R blockade on melanoma immunogenicity

3.1 Introduction

As described in the introduction, challenge of immunocompetent syngeneic rats with Igf1 or Igf1r depleted, irradiated, C6 glioblastoma cells resulted in complete regression of a pre-existing wild type tumour and protection from wild type tumour rechallenge (Trojan et al., 1993, Resnicoff et al., 1994b, Shevelev et al., 1997). Similar *in vivo* findings have been reported for other tumour types including: prostate carcinoma, lung carcinoma, Ewing's sarcoma, embryonal carcinoma, hepatoma and breast cancer (Burfeind et al., 1996, Trojan et al., 1994, Lafarge-Frayssinet et al., 1997, Shevelev et al., 1997, Liu et al., 1998, Schillaci et al., 2006, Ellouk-Achard et al., 1998, Samani et al., 2001, Scotlandi et al., 2002). Furthermore CD8+ T lymphocyte infiltration has been documented in the regressing tumours but not wild type tumours, implicating a role for the adaptive immune response (Lafarge-Frayssinet et al., 1997, Trojan et al., 1992, Trojan et al., 1993, Shevelev et al., 1997, Resnicoff et al., 1996b, Schillaci et al., 2006). Consistent with these findings increased expression of MHC Class 1 molecules, to a maximum of four fold, has been documented on glioma, hepatoma and embyronal carcinoma cells following IGF1 and IGF1R downregulation (Lafarge-Frayssinet et al., 1997, Ellouk-Achard et al., 1998, Upegui-Gonzalez et al., 1998, Ly et al., 2001, Ly et al., 2000, Szpechcinski et al., 2004, Trojan et al., 1996, Anthony et al., 1998). However alterations in MHC class I expression are not universally observed following Igf1r depletion, even in studies which document an antitumour protective effect associated with CD8+ cell infiltration (Schillaci et al., 2006). In summary, in some cell lines there is an immunological consequence of manipulating the IGF1R. Its significance and a mechanism by which it occurs are unclear.

In the case of melanoma protective effects of inoculation with IGF1 depleted B1762.F10 murine melanoma against future wild type tumour challenge are implied in a review paper (Baserga et al., 1997b). However in contrast no change in surface expression of MHC class I molecules (H2-Kb) was found on B16.F0 murine melanoma following antisense mediated Igf1r knockdown (Trabado et al., 2006, Trabado et al., 2007). However serum or splenocytes harvested from syngeneic mice inoculated with these manipulated B16.F0 cells retarded growth of wild type cells *in vitro* consistent with the generation of both humoral and cell mediated immunity (Trabado et al., 2006, Trabado et al., 2007).

Unpublished data from our laboratory demonstrated that siRNA-mediated depletion of the Igf1r in B16.F10 murine melanoma cells induced increased surface expression of MHC class 1 (H2-Db) by a mechanism other than increased transcription or change in cell size (A.Yeh DPhil Thesis, 2007). This phenotype was not blocked by apoptosis inhibition, and appeared to be specific since it was not induced by depletions of the insulin (IR) or epidermal growth factor receptors (EGFR). These results contrast with the published studies described above in the closely related cell line B16.F0 which found no change in surface MHC class 1 (H2-Kb) although H2-Db was not measured (Trabado et al., 2006, Trabado et al., 2007). Clearly further investigation is required to determine whether IGF1R manipulation of melanoma cells results in alterations in immunogenicity and if so by which mechanism.

The work described in this chapter aimed to further investigate the observed increase in MHC class 1 in B16.F10 following Igf1r siRNA mediated depletion and to characterise its consequences on tumour cell immunogenicity. Furthermore in order to test if Igf1r depletion affected the immune recognition of melanoma, it was considered important to

develop an *in vivo* model in an immunocompetent animal. However, IGF1R depletion is deleterious to tumour growth presenting problems for *in vivo* assessment. Thus it would be useful to create a cell line in which the IGF1R could be depleted in a regulated manner by the induction of IGF1R specific shRNA after measurable tumour growth had occurred. In addition to testing the effects on further growth of the manipulated tumour, this would allow observation of any distant (ie immune mediated) effects on a wild type tumour growing on the contralateral flank.

These two lines of work progressed in parallel; the results from the former informing the latter but are presented here serially for clarity.

3.2 Results and Discussion

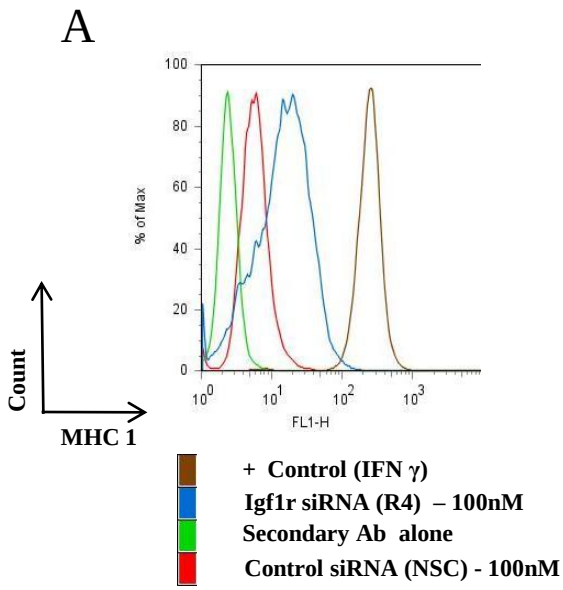
3.2.1 Effect of siRNA mediated Igf1r depletion on expression of MHC Class 1 molecules in B16.F10 melanoma

Previous results had documented an increase in surface expression of MHC Class 1 in B16.F10 melanoma cells following siRNA mediated Igf1r depletion. These experiments had used a relatively high concentration of a single IGF1R siRNA (A.Yeh DPhil Thesis, 2007). The first experiment in this project aimed to determine whether IGF1R downregulation with a variety of siRNA duplexes phenocopied the original findings. B16.F10 murine melanoma cells were transfected with control or one of six IGF1R siRNAs at a concentration of 100nM. Two of the IGF1R duplexes (R4 & R1) had been designed in our laboratory (Bohula et al., 2003, Rochester et al., 2005) and the remaining siRNA duplexes (designated QM1-4) and the non silencing control (NSC) were sourced commercially. Untransfected cells treated with Interferon gamma (IFNγ) for 24 hours

acted as a positive control when measuring MHC Class 1 expression, as IFNγ has previously been shown to upregulate MHC Class 1 expression at a transcriptional level (Eager et al., 1989). Untreated cells were analysed in parallel to allow comparison and normalisation across future experiments, and were included in all experiments described hereafter. Live B16.F10 cells were analysed forty eight hours after transfection by flow cytometry, following staining with the B22.249 antibody which recognizes stably folded H2-Db molecules on the cell surface. MHC Class I bound antibody was detected using a fluorophore conjugated secondary antibody.

IFNγ treatment resulted in a significantly enhanced (~300 fold) surface expression of H2-Db (hereafter referred to as MHC Class 1) molecules (Figure 3.1). It was found that B16.F10 expressed increased levels of MHC class 1 molecules on the cell surface following Igf1r knockdown with the R4 siRNA duplex, replicating the original data (A.Yeh DPhil Thesis, 2007). In total 3 of the 6 tested siRNA duplexes (R4, R1 and QM4) resulted in an increase in cell surface MHC Class 1 of between ~2 and 4 fold. Immunoblot analysis of parallel samples revealed that all 6 siRNAs were equally efficacious at depleting the Igf1r.

If increased MHC Class 1 expression was a consequence of Igf1r depletion, it was unclear why the 6 IGF1R siRNA duplexes had not all produced the same phenotype despite being equally efficacious at knocking down the Igf1r. The concentration of siRNA used was high, mimicking the original experimental conditions, and was suspected to be in excess of that required for Igf1r depletion. Increased transcription of MHC Class 1 has been documented as part of the Interferon response particularly to high concentrations of



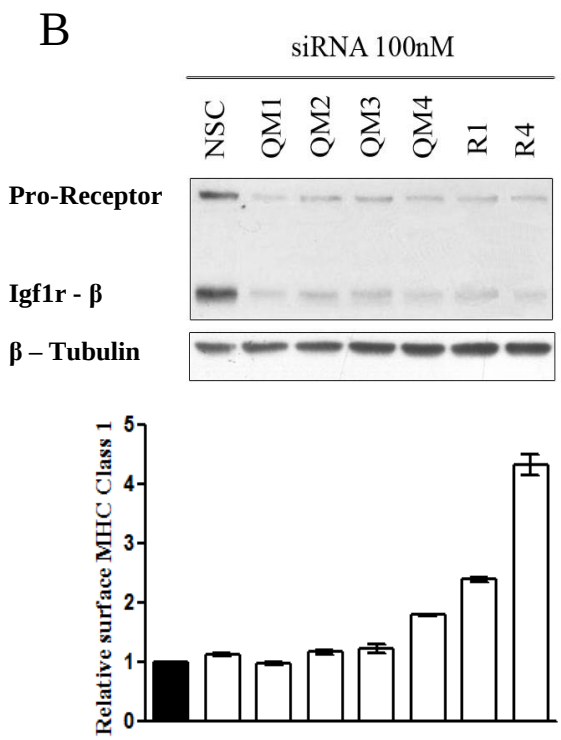


Figure 3.1 Effect of Igf1r depletion on MHC Class 1 expression. B16.F10 murine melanoma cells were transfected with 100nM Igf1r siRNAs (R4, R1, QM1, QM2, QM3, QM4) or non silencing control (NSC) and harvested after 48 hours. Cells treated with 20ng/ml IFNɣ for 24 hours served as positive controls. Cells were analysed by flow cytometry for MHC Class 1 (H2 D^b) surface expression and by immunoblot for Igf1r β subunit. **A)** Representative flow cytometry plot. Depletion of Igf1r in cells transfected with 100nm R4 siRNA results in an increase in MHC Class 1 expression compared to control transfectants..**B)** Bars represent geometric mean fluorescence (MHC Class 1) ±SEM from 3 independent experiments, normalised to untreated cells (black bar). Surface MHC class 1 increased following Igf1r depletion with 3 of 6 siRNAs. All 6 siRNAs were equally efficacious at depleting Igf1r.

"immunostimulatory" siRNAs. However this possibility was excluded given that transcription of MHC molecules and of four genes (oligoadenylate synthetase 1 & 2, IFN-stimulated gene 20 & myxovirus resistance gene) associated with an interferon response were not induced by transfection with 100nM of R4 siRNA (A.Yeh DPhil Thesis, 2007). However further assessment of the effects of reducing siRNA concentration would allow optimisation of Igf1r depletion for future experiments and would help to clarify whether changes in MHC Class 1 were attributable to Igf1r depletion alone rather than non-specific siRNA effects.

B16.F10 cells were transfected with each of the three IGF1R duplexes (R4, R1, QM4) which had been shown to increase surface MHC Class 1 at concentrations of 1, 10 and 100nM. All three duplexes caused a trend of increasing MHC Class 1 expression in a dose dependent manner (Figure 3.2A). The increase in MHC Class 1 was significant at 10 and 100nM of R4, and 100nM QM4, siRNAs compared to control transfected cells. On immunoblot all siRNA duplexes at all concentrations were seen to cause efficient Igf1r depletion to a similar degree. Quantitative RT-PCR (qRT-PCR) was performed to assess the efficacy of *Igf1r* depletion at the mRNA level. R4 and QM4 siRNAs were equally efficacious at depleting IGF1R mRNA at 1, 10 and 100nM (Figure 3.2B).

Thus these initial results confirmed the original observation of an increase in MHC Class 1 expression in B16.F10 cells transfected with the R4 IGF1R siRNA. Furthermore the magnitude of the increase was comparable to that reported in the literature for other cell types (Lafarge-Frayssinet et al., 1997, Ellouk-Achard et al., 1998, Upegui-Gonzalez et al., 1998, Ly et al., 2001, Ly et al., 2000, Szpechcinski et al., 2004, Trojan et al., 1996,

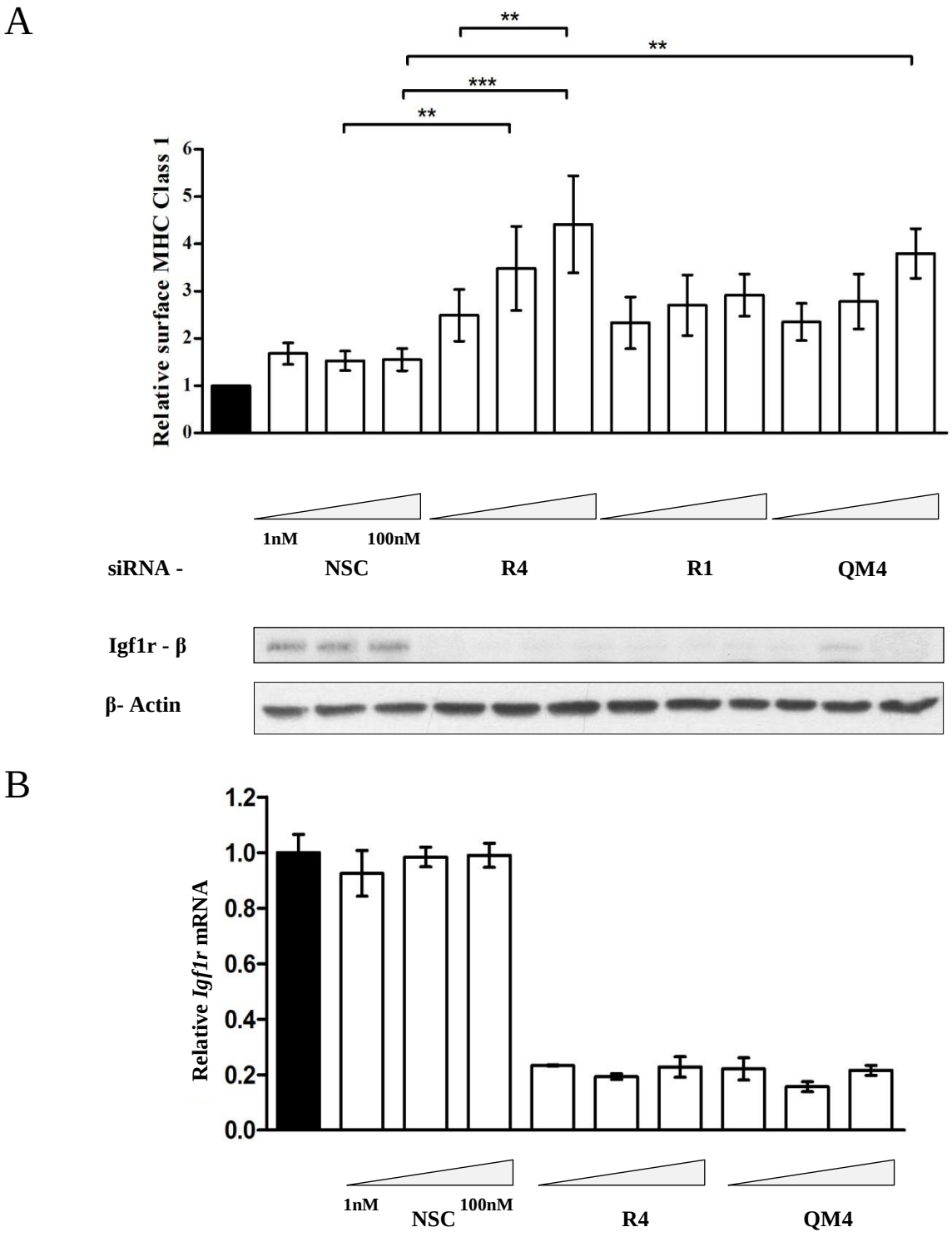


Figure 3.2 Effect of Igf1r depletion on *Igf1r* expression and cell surface MHC Class 1. B16.F10 melanoma cells were transfected with Igf1r siRNAs (R4,R1 & QM4) or non-silencing control (NSC) and MHC Class 1 expression analysed by flow cytometry, Igf1r by immnoblot and *Igf1r* mRNA levels by qRT PCR, relative to three house-keeping genes, after 48 hours. **A)** Bars represent geometric mean fluorescence (MHC Class 1) ±SEM from 3 independent experiments, normalised to untreated cells (black bar). Igf1r depletion caused a dose dependant increase in cell surface MHC Class 1 compared to control transfectants. Igf1r depletion was complete at all siRNA concentrations. **B)** Bars represent mean *Igf1r* mRNA ±S.E.M of values from 3 experiments, each in triplicate (9 data points) normalised to untreated cells (black bar). 1-100nM R4 and QM4 Igf1r siRNAs are equally efficacious at depleting *Igf1r* mRNA.
(** $p<0.01$, ***$p<0.001$ ANOVA).

Anthony et al., 1998). However this effect was only replicated with two of five additional siRNAs, despite similar efficacy of Igf1r depletion. To assess whether changes in MHC Class 1 expression were indeed linked to Igf1r it was decided to test the reciprocal effect by investigating the consequences of Igf1r activation.

3.2.2 Effect of IGF1 ligand stimulation on expression of MHC Class 1.

IGF1 has been shown to suppress MHC class 1 expression in rat thyroid cells and hair follicles (Giuliani et al., 2006, Saji et al., 1992, Ito et al., 2004). The next step was to examine if IGF1 treatment resulted in a change in MHC Class 1 expression in B16.F10 cells. A concentration of 50nM IGF was chosen as it is similar to the maximum circulating level in human adults (~10-58nM) (Thissen et al., 1994). B16.F10 cells were grown in serum free medium for 24 hours before incubation with solvent, complete medium (with 10% FCS) or 50nM IGF1 for 24 or 48 hours. In one IGF1 treated culture, the medium and IGF1 was replaced after 24h. MHC Class 1 expression was assessed as previously. Serum starvation or solvent treatment did not alter MHC Class 1 expression (Figure 3.3). Twenty four hour treatment with IGF1 ligand or complete medium significantly reduced MHC Class 1 expression. Treatment for 48h with replacement of the medium and IGF1 after 24 hours resulted in a significant reduction in MHC Class1 expression of a similar magnitude to treatment for 24 hours. The magnitude of the fall in MHC Class1 was modest in all conditions with a maximum reduction to 60% in cells treated with IGF1 for 24h. Cells treated for 48 hours had an MHC Class 1 expression intermediate between those treated for 24 hours and solvent treated cells. This may suggest that the reduction in MHC Class 1 following IGF1 stimulation is transient. These finding are in agreement to those in the literature in which IGF1 reduced transcription of MHC Class 1 in rat thyroid cells (Saji et

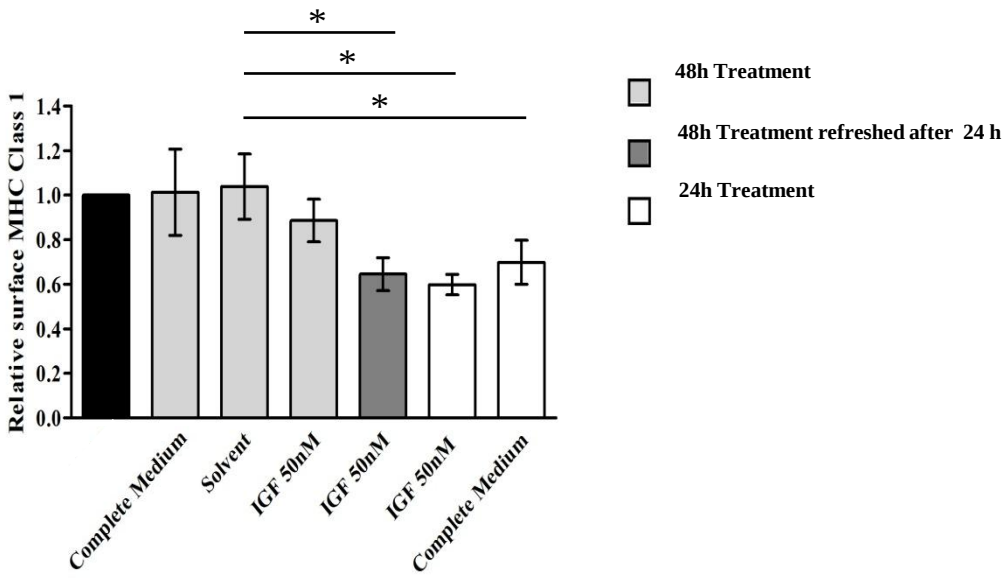


Figure 3.3 Effects of IGF1 treatment on cell surface MHC Class 1. B16.F10 melanoma cells deprived of serum for 12 hours, were grown in serum free medium with or without treatments for 48 hours. Treatments were applied for the full 48 hours (complete medium, solvent or IGF1 50nM), replaced after 24 hours (IGF1) or applied only for the final 24 hours (IGF1 or complete medium). MHC Class 1 expression was quantified by flow cytometry. Bars represent geometric mean fluorescence (MHC Class 1) ±SEM from 3 independent experiments, normalised to untreated cells (black bar). Serum starvation or solvent treatment did not alter surface MHC Class 1. Treatment with IGF1 or complete medium for 24 hours reduced MHC Class 1.

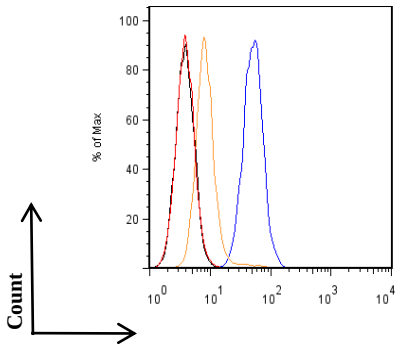
(* $P<0.05$ ANOVA)

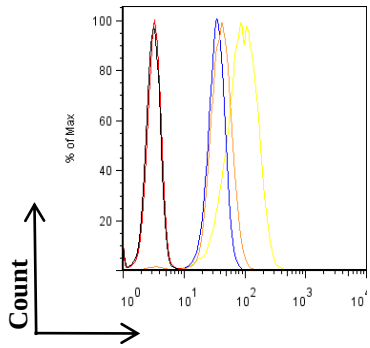
al., 1992, Giuliani et al., 2006). Furthermore these findings demonstrate that depleting and stimulating the Igf1r have reciprocal effects on MHC Class 1 expression in B16.F10 melanoma cells. As such further investigations into the observed increase in MHC Class 1with Igf1r depletion seemed warranted.

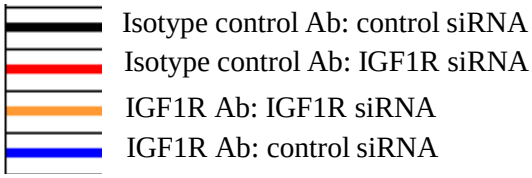
3.2.3 Effect of IGF1R depletion on MHC Class 1 expression in a panel of melanoma cell lines.

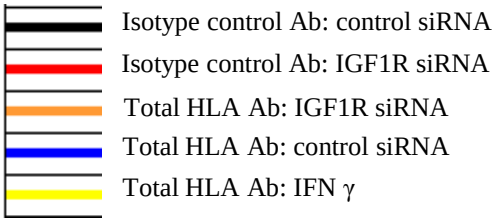
To determine whether the observed phenotype was a feature of all melanoma cells a total of 9 further melanoma cells lines, 8 human and 1 murine were analysed. To allow efficient screening, determination of surface IGF1R by flow cytometry was optimised. CHL-1 human melanoma cells were transfected with 100nM IGF1R (R4) or control (NSC) siRNA and assessed for cell surface IGF1R expression, by flow cytometry using a fluorophore conjugated IGF1R antibody. R+ cells, murine fibroblasts which over express the human IGF1R, were analysed in parallel by flow cytometry and acted as a positive control (Sell et al., 1994). Parallel cultures were assessed for total IGF1R, by immunoblot. Immunoblot analysis revealed near complete depletion of total IGF1R after 48 hours (Figure 3.4A). Results from the positive control (R+ cells) are not shown as differences in cell size meant it was not possible to analyse both controls and cells of interest with the same flow cytometer set up in a way which would allow graphical representation. Surface IGF1R after IGF1R depletion was quantified by flow cytometry as 17% of that of the control cells (Figure 3.4A). Given the correlation between immunoblot and flow cytometry, IGF1R expression in the human cell lines was assessed by flow cytometry alone in the following experiment. For the murine cell line assessment of Igf1r depletion was made by

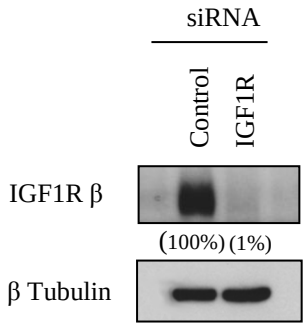
A











B

	ΔIGF1R (%)	Δ MHC 1 (%)
A2058	13 (3)	93 (5)
A375	18 (2)	103 (6)
A375M	19 (8)	131 (4)
CHL-1	17 (8)	101 (4)
MM9	14 (5)	64 (24)
MM25	15 (9)	163 (3)
SKMel 23	19 (5)	118 (5)
SkMel 28	12 (2)	98 (7)
K1735	See right	130 (4)

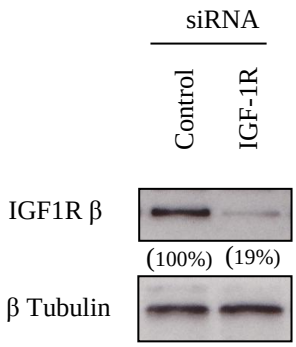


Figure 3.4 Effect of IGF-1R siRNA on MHC Class 1 expression in a panel of melanoma cell lines. Human and murine melanoma cell lines were transfected with 100nM IGF1R or control siRNA. After 48 hours the cell surface MHC Class1 and IGF1R quantified by flow cytometry and immunoblot (CHL-1 and K1735 only). R+ cells (murine fibroblasts which express hsIGF1R) and cells treated with 20ng/ml IFNγ for 24 hours served a positive controls for IGF1R and MHC class 1 expression respectively. Plot from R+ cells not shown (see text) **A)** Representative flow cytometry plot for CHL-1 human melanoma cells. Treatment with IGF1R siRNA reduced IGF1R expression to ~20% compared to control transfectants (left plot) but did not alter MHC Class 1 expression (right plot). IGF1R expression was negligible (1%) on immunoblot. **B)** ΔIGF-1R and Δ MHC 1 values represent relative expression following IGF1R depletion compared to control transfectants for 9 melanoma cell lines. Values are mean (± range) from two independent experiments. All cells showed reduced IGF1R expression but little change in MHC Class 1 expression following IGF1R depletion (left). In the case of the murine cell line K1735, Igf1r levels were assessed by densitometric quantification of immunoblot (right).

immunoblot analysis as no commercial antibody was found, despite large scale screening experiments, which was suitable for detection of murine Igf1r by flow cytometry.

The human and murine melanoma cell lines were transfected with 100nM of control or R4 IGF1R siRNA, which had been designed to be homologous to both the human and murine IGF1R mRNA transcript (Bohula et al., 2003). MHC Class 1 expression was determined after 48 hours with directly fluorophore conjugated H2-Kb antibody and total HLA antibody in the murine and human cell lines respectively, and IGF1R levels with a directly fluorophore conjugated anti-IGF1R antibody. IGF1R siRNA depleted surface IGF1R in human cells or total Igf1r in the murine cells to 12-20% of control levels (Figure 3.4B). Surface MHC Class 1 was not seen to change significantly in any cell line following IGF1R depletion to the extent previously observed in B16.F10 cells.

It appeared thus that the observed phenotype was specific, amongst the melanoma cell lines evaluated, to B16.F10 murine melanoma cells.

3.2.4 Effect of IGF1R inhibition on MHC Class 1 expression in B16.F10 melanoma cells.

To further assess whether the increase in MHC Class 1 was a consequence of IGF1R depletion rather than a non specific effect of some of the siRNAs, it was necessary to block the function of the IGF1R by different strategies. Furthermore although several studies have documented immunological consequences of IGF1R depletion with oligonucleotide based strategies, none had done so with more clinically applicable techniques, such as small molecule inhibitors or blocking antibodies (Burfeind et al., 1996, Trojan et al., 1994,

Lafarge-Frayssinet et al., 1997, Shevelev et al., 1997, Liu et al., 1998, Schillaci et al., 2006, Ellouk-Achard et al., 1998, Samani et al., 2001, Scotlandi et al., 2002).

Picropodophyllin (PPP) is an inhibitor of the kinase activity of the IGF1R and blocks receptor autophosphorylation as well as activation of both the PI3K/AKT and MAPK downstream signalling cascades (Girnita et al., 2004, Menu et al., 2006, Stromberg et al., 2006). It has no effects on IR function (Vasilcanu et al., 2004). B16.F10 cells were incubated with PPP or solvent for 48 hours before assessment of MHC Class 1 expression by flow cytometry. Parallel cultures were harvested for immunoblot analysis to determine the effects of PPP on phosphorylation of the downstream signalling molecule, AKT. Immunoblot confirmed that 2.5-25μM PPP reduced phosphorylation of AKT but had no effect on the expression of IGF1R itself, consistent with previously published reports (Figure 3.5) (Girnita et al., 2004, Menu et al., 2006, Stromberg et al., 2006, Vasilcanu et al., 2004). There was no effect of PPP on the surface expression of MHC Class 1 irrespective of dose.

AZ12253801 is a small molecule inhibitor of the IGF1R kinase domain which was undergoing pre-clinical assessment at the time of this study (Aleksic et al., 2010, Shaw et al., 2011). Permission was gained from AstraZeneca to assess its effects on MHC Class 1 expression. Preliminary experiments revealed that a dose of 30nM was sufficient to block IGF1 induced phosphorylation in B16.F10 cells (Figure 3.6A). B16.F10 cells were incubated with 30nM of AZ12253801 for 1, 12, 24 or 48 hours. Given that the stability of this drug in cell culture medium was unknown, in one dish treated for 48 hours, the medium and drug were replaced after 24 hours. In parallel B16.F10 cells were transfected with R1 and R4 siRNAs at a dose of 1nM to assess their effects on the phosphorylation of

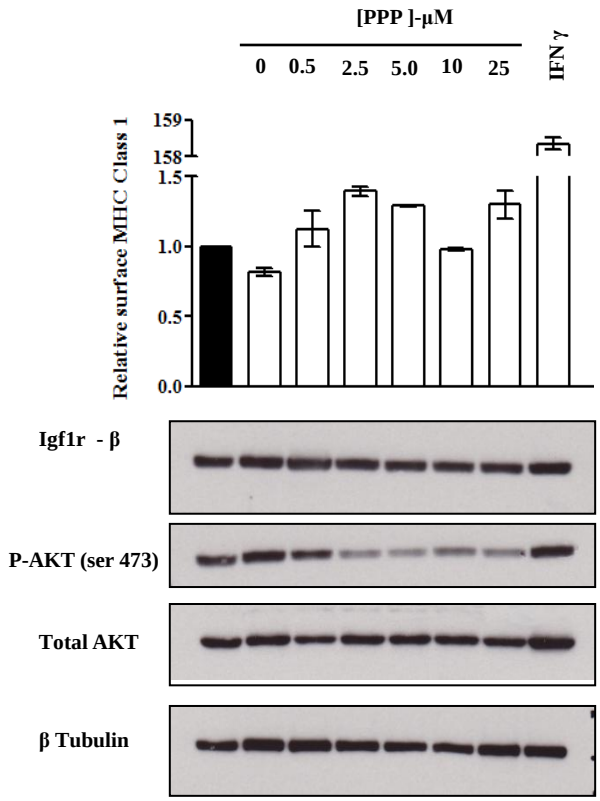


Figure 3.5 Effects of Igf1r inhibition with PPP on MHC Class 1 expression. B16.F10 cells were incubated for solvent or 0.5-25μM PPP. Cells treated for 24hours with 20ng/ml IFNγ served as positive controls. Cells were analysed by flow cytometry for cell surface MHC Class 1 expression and by immunoblot for Igf1r levels and AKT phosphorylation after 48 hours. Bars represent geometric mean fluorescence (MHC Class 1) ± range from 2 independent experiments, normalised to untreated cells (black bar). Immunoblot representative example from 2 independent experiments. PPP did not alter Igf1r expression but inhibited Igf1r signalling, assessed via basal AKT phosphorylation, at higher concentrations (2.5-25 μM). PPP treatment did not alter MHC Class 1 expression.

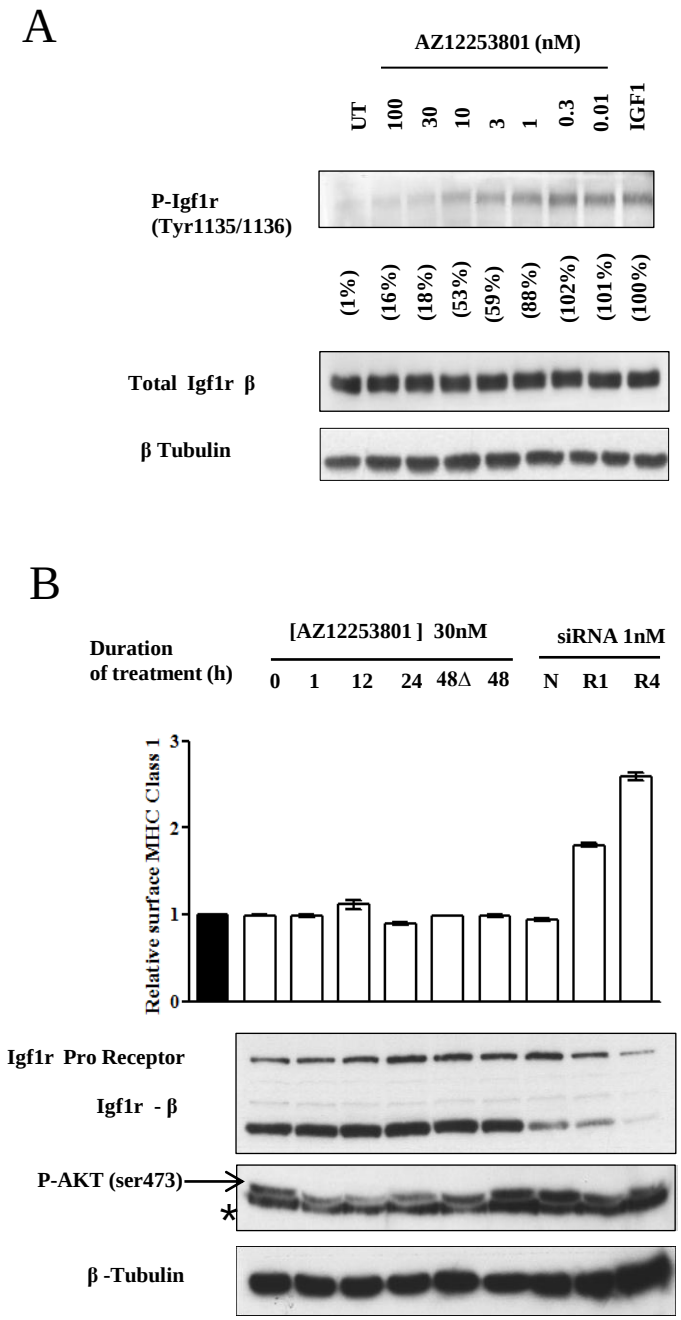


Figure 3.6 Effects of AZ12253801 on Igf1r axis activation and MHC Class 1 expression A) B16.F10 cells were serum deprived for 12 hours before incubation with AZ12253801 at a range of concentrations for 50 minutes. 10nM IGF1 was added for 10 minutes before assessment of Igf1r phosphorylation status by immunoblot. Values in parentheses represent densitometric quantification of immunblot. AZ12253801 blocked IGF1 induced phosphorylation of Igf1r in a dose dependant manner. **B)** B16.F10 cells were treated with 30nM AZ12253801 or solvent for 1, 12, 24, 48 hours (with (48Δ) and without media change), or transfected with control (N) or IGF1R (R1,R4) siRNAs. MHC Class 1 expression was assesed by flow cytometry and Igf1r protein and AKT phosphorylation by immunoblot after 48 hours. Bars represent geometric mean fluorescence (MHC Class 1) ± range from 2 independent experiments, normalised to untreated cells (black bar). Immunoblot representative example from two independent experiments. AZ12253801 did not alter Igf1r protein expression but did decrease basal phosphorylation of AKT to a greater extent than Igf1r depletion (arrowed band of immunoblot) (* represents non specific staining. This antibody Cell Signalling 9271 was not used for subsequent experiments). 30nM AZ12253801 did not cause in a rise in MHC Class 1 expression.

the downstream signalling molecule AKT. Incubation with AZ12253801 had no effect on Igf1r protein levels whilst transfection with siRNA caused marked Igf1r depletion as noted previously (Figure 3.6B). Incubation with AZ12253801 suppressed phosphorylation of AKT for 1-24 hours but had no effect on MHC Class 1 expression. The lack of effect on MHC Class 1 expression was thought unlikely to be as a result of a short drug half life as replenishment after 24 hours had no additional effect.

It was noted that unlike siRNA depletion, blocking the kinase activity of the Igf1r did not reduce Igf1r expression. Therefore a strategy which both blocked receptor signalling and depleted receptor protein levels would most closely replicate the effect of siRNA mediated depletion. The IGF1R blocking antibody αIR3 has previously been shown to compete with IGF1 for binding to the IGF1R and as such both blocks receptor activation and enhances receptor internalisation and degradation (De Leon et al., 1992). A variety of concentrations have been reported in the literature, the highest of which was 60nM (Sachdev et al., 2006). Therefore B16.F10 cells were incubated with 10, 30 or 60nM αIR3 or IgG for 24 or 48 hours and MHC Class 1 expression assessed by flow cytometry. Cells transfected with 10nM IGF1R (R4) siRNA were included as a positive control.
On immunoblot analysis, incubation with αIR3 reduced Igf1r protein levels moderately after 24h (Figure 3.7). After 48 hours incubation there was a recovery in Igf1r levels, perhaps explained by de novo synthesis and/or antibody depletion. Phosphorylation of AKT was seen to be reduced by all doses of αIR3 at 24 hours but not at 48 hours. Cell surface expression of MHC Class 1 was unchanged following incubation with αIR3.

Taken together, it was clear that experiments using small molecule kinase inhibitors or blocking antibodies did not replicate the phenotype seen following Igf1r depletion using

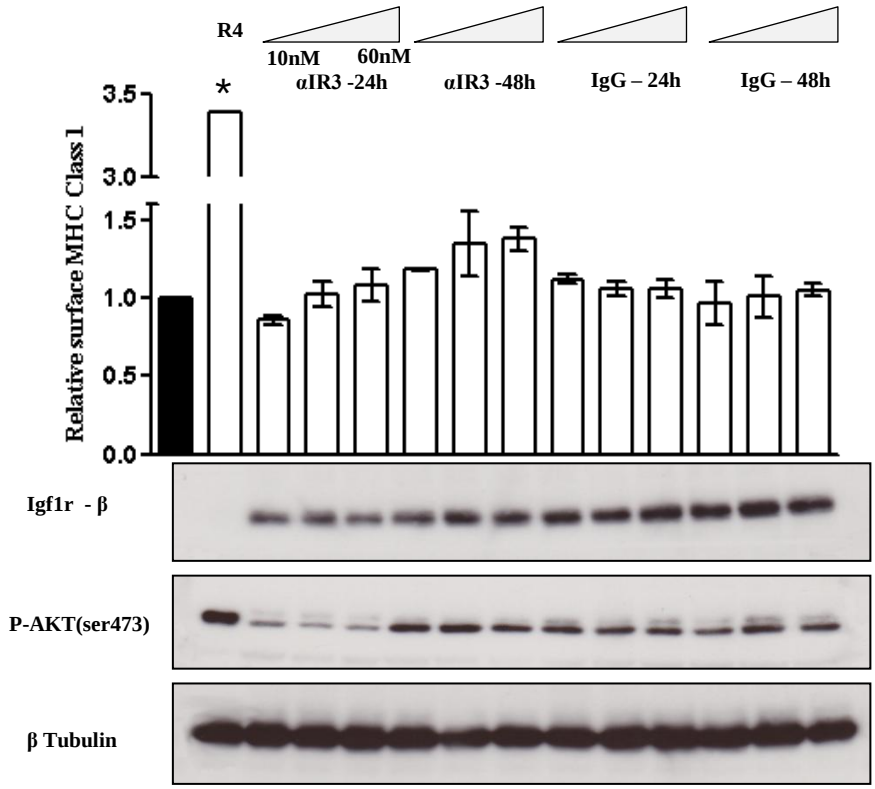


Figure 3.7 Effects of αIR3 (IGF1R blocking antibody) on MHC Class 1 expression B16.F10 cells were incubated for 24 or 48 hours with αIR3 blocking antibody or irrelevant IgG at a range of concentrations or transfected with 10nM IGF1R (R4) siRNA 48 hours prior to analysis. Cells were analysed by flow cytometry for cell surface MHC Class 1 expression and by immunoblot for Igf1r levels and AKT phosphorylation. Bars represent geometric mean fluorescence (MHC Class 1) ± SEM from 3 independent experiments, normalised to untreated cells (black bar). Immunoblot is a representative example from 3 independent experiments. Incubation with αIR3 for 24 hours moderately reduced Igf1r levels and inhibited downstream signalling (AKT phosphorylation). After 48 hours treatment, Igf1r and AKT phosphorylation status had returned to basal levels. αIR3 treatment did not affect MHC Class 1. IGF1R (R4) siRNA completely depleted Igf1r, resulted in increased basal AKT phosphorylation and caused a significant increase in MHC Class 1

(* $P<0.05$ one way ANOVA)

siRNA. Furthermore a statistically significant increase in MHC Class 1 had only been observed with three of the six tested IGF1R siRNAs and appeared to be unrelated to the efficiency of IGF1R depletion. Finally low doses (1nM) of these two siRNAs did not result in increased expression of MHC Class 1 despite depleting Igf1r at both the protein and mRNA level as effectively as higher concentrations. In short the increase of MHC Class 1 induced by these siRNAs was dose dependent across the range of concentrations tested whereas the efficiency at depleting the Igf1r was not.

These data cast doubt on whether the increase in MHC Class 1 was an IGF1R depletion related effect rather than a non specific effect of the siRNAs used. Non specific effects resulting from the introduction of siRNA into cells are recognized to have three separate origins; response against a lipid based cationic transfection agent, the interferon response and RISC dependent off target effects (Lin et al., 2005). On considering the above data, control cells exposed to the lipid transfection reagent did not exhibit the recorded phenotype. Furthermore previous work in our laboratory had shown that R4 siRNA did not induce transcripts associated with an interferon response, nor does it contain the immunostimulatory sequence 5'-UGUGU-3' or bear modifications such as triphosphate residues (A.Yeh DPhil Thesis, 2007). RISC associated off target effects are sequence-specific and are characterised by silencing of non target genes in a dose dependent method. It has been shown that only a minority of experimentally validated off target genes are identified by sequence alignment algorithms (such as BLAST) (Saxena et al., 2003). Many of the overlooked "off targets" had sequences in the 3' untranslated region (UTR) which matched the seed region of the siRNA (bases 2-7), in essence the siRNA seed region was acting as a miRNA. Therefore commercial producers of siRNAs now combine *in silico* sequence analysis with base modification and seed region analysis to minimise the

likelihood of non specific effects (Dharmacon technical support). On this basis it is interesting to note that two of the three siRNA sequences which produced an increase in MHC Class 1 were designed in our laboratory whereas 3 of the 4 commercially validated siRNAs did not produce this phenotype (Bohula et al., 2003, Rochester et al., 2005).

Rather than investigating the precise mechanism underlying the phenotype it was decided to determine if the increased surface expression of MHC Class 1 was of functional significance. If the phenotype resulted in increased recognition by immune effector cells then exploration of its mechanism was justified. Similarly given that in parallel with the above experiments, development of a B16.F10 cell with inducible Igf1r depletion for use in *in vivo* modelling was taking place, determining the consequences of the observed phenotype in an *in vitro* setting was justified, before commencing *in vivo* experiments.

3.2.5 Effect of IGF1R depletion of B16.F10 cells on T cell proliferation and Cytokine production.

As discussed in the introduction enhanced MHC Class 1 surface expression has been demonstrated to augment tumour immunogenicity (Ostrand-Rosenberg et al., 1989). Furthermore transfection of B16.F10 cells with MHC Class 1 molecules increases the immunogenicity of the cell line *in vivo* (Tanaka et al., 1988). The next series of experiments investigated whether the modest increases in surface MHC Class 1 observed in B16.F10 melanoma following Igf1r depletion were of functional significance in terms of proliferation of, and cytokine production by, T lymphocytes.

Using fluorescent cell staining dyes such as Carboxyfluorescein succinimidyl ester (CFSE), proliferation of T cells following activation can be monitored by the progressive halving of dye fluorescence within daughter cells following each cell division. The following CFSE T cell proliferation assay aimed to assess whether the increase in surface MHC Class1 following Igf1r depletion of B16.F10 cells led to increased recognition by, and thus proliferation of, CD8+ T cells.

These experiments utilised CD8+ T cells from syngeneic F5 transgenic mice which only recognise the Influenza nucleoprotein ASNENNDAM (Np) peptide when presented in the context of MHC Class 1 (type H2-Db) on an antigen presenting cell. B16.F10 melanoma cells were transfected with either 10nM IGF1R (R4) siRNA, the lowest concentration which caused significant MHC Class 1 increase, or control siRNA. After 48 hours these cells were harvested, pulsed with the antigenic Np peptide and incubated with CD8+ T cells at a range of ratios. B16.F10 cells not incubated with antigenic peptide acted as a control for specificity and Np peptide-pulsed CD11c+ dendritic cells were used as a positive control.

After 36 hours, T cells incubated with Np peptide pulsed CD11c dendritic cells had proliferated and undergone three cell divisions (Figure 3.8). The specificity of the assay was confirmed given that T cells incubated with unpulsed dendritic cells had not proliferated. Igf1r depletion resulted in the previously described increase in MHC Class 1 expression. However T cells incubated with Np peptide pulsed or unpulsed B16.F10 cells had not proliferated irrespective of B16.F10 MHC Class 1 expression.

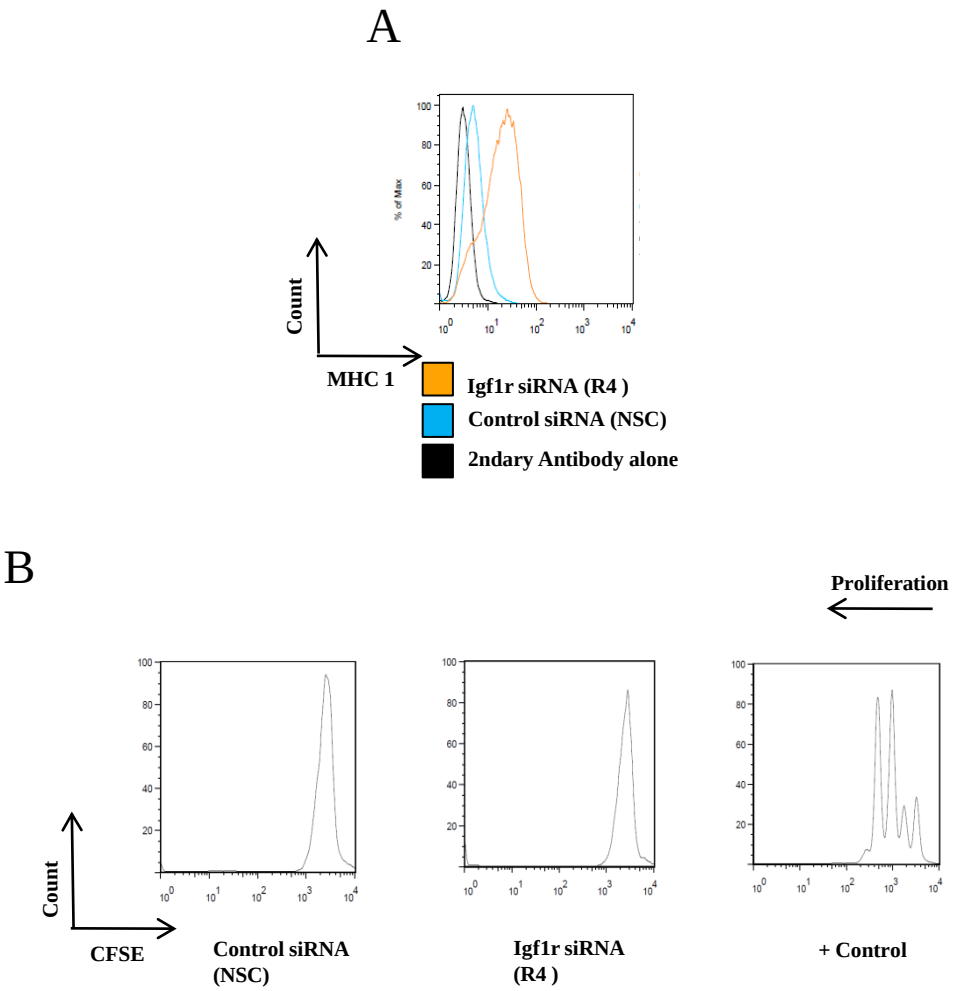


Figure 3.8 Effect of Igf1r depleted B16.F10 on T cell proliferation. B16.F10 cells were transfected with 10nM R4 (Igf1r) or NSC siRNAs and MHC class 1 levels quantified by flow cytometry after 48 hours.The cells were then pulsed with Np peptide and incubated with CFSE labelled CD8+ T lymphocytes at various Effector:Target (E:T) ratios. Np pulsed CD11c+ dendritic cells served as positive controls (at an E:T of 3:1). T cell proliferation was assessed after 36 hours by flow cytometric quantification of CFSE staining intensity. **A)** Igf1r depletion resulted in increased MHC class 1 expression compared to control transfectants . **B)** T cells incubated with peptide pulsed CD11c+ dendritic cells proliferated (3 divisions) as evidenced by sequential halving of CFSE fluorescence in daughter cells (right panel). T cell incubated with peptide pulsed B16.F10 cells did not proliferate irrespective of Igf1r depletion (E:T ratio of 1:1 shown as representative example). Graphs show representative results from one of two independent experiments.

Although the results of the preceding experiment suggested that B16.F10 cells were unable to initiate CD8+ T cell proliferation, this experiment had used naïve T cells, which had not previously encountered the specific antigen. These experimental conditions crudely replicate initial antigen presentation and it is likely that antigen presentation is more efficient in the complex immune milieu *in vivo*, for example involving professional antigen presenting cells and the additional cytokine stimuli provided by T Helper cells. Therefore the presence of increased surface MHC Class 1 molecules on Igf1r depleted B16.F10 cells might be of greater significance when considering the response of effector T cells which had previously been exposed to antigen and undergone clonal expansion (ie were primed). These effector cells might respond differently in the presence of B16.F10 (target) cells in terms of the production of type 1 cytokines or efficiency of cytotoxic cell killing. Indeed effector T cells are more efficient at cytokine production than induction of target cell lysis (Janeway CA Jr, 2001).

B16.F10 melanoma cells were transfected with 10nM IGF1R (R4) or control siRNA and harvested after 48 hours. Increase in MHC Class 1 in Igf1r depleted cells was confirmed and cells were pulsed with antigenic Np peptide before incubation at various effector:target (E:T) ratios with CD8+ T cells. Two types of T cell were utilised in this experiment in parallel, naïve CD8+ T cells and T cells that had been primed *in vivo* against the antigenic Np peptide. Bone marrow derived dendritic cells pulsed with Np peptide served as positive controls. After 36 hours incubation supernatant was analysed by ELISA for the presence of the type 1 cytokines; Interferon gamma (IFNɣ) and Tumour Necrosis Factor alpha (TNFα).

Target cells of any type which had not been pulsed by peptide did not induce cytokine production confirming specificity of the assay (Figure 3.9). Bone marrow derived dendritic cells which had been pulsed with Np peptide induced production of both cytokines in a dose dependent manner. Furthermore the cytokine production of primed CD8+ T cells was significantly higher than that of naïve T cells, confirming the efficiency of the *in vivo* priming protocol employed. B16.F10 cells did not induce cytokine production at any E:T ratio, irrespective of surface MHC Class 1 expression.

3.2.6 Effect of IFNɣ on the Immunogencity of B16.F10 melanoma

B16.F10 has been described to be a relatively non immunogenic tumour cell type and a variety of defects in the antigen presentation pathway have been described (Seliger et al., 2001). In the context of the previous experiment, antigenic peptide was bound directly onto MHC Class 1 molecules on the cell surface without the need for intracellular antigen processing and thus only deficiencies in immunologically relevant surface molecules are likely to be responsible for the lack of immunogenicity. It was considered that absence of a T cell response despite an increased MHC Class 1 expression might be limited by factors other than surface MHC Class 1. To test this hypothesis it was decided to assess the immunogenicity of B16.F10 cells which had a larger increase in surface MHC Class1 rather than the modest increase induced by Igf1r depletion. Indeed chemical treatment of B16.F10 cells which increase MHC Class 1 by the same degree as IFNɣ treatment have been shown to increase immunogenicity (Gorelik et al., 1985). IFNɣ treatment of B16.F10 cells has previously been shown to increase MHC Class 1 expression by a factor of 10^2 (Figure 3.1). In addition IFNɣ treatment further increases the immunogenicity of cells through promoting adhesion between the target cell and lymphocytes (Lloyd et al., 1996).

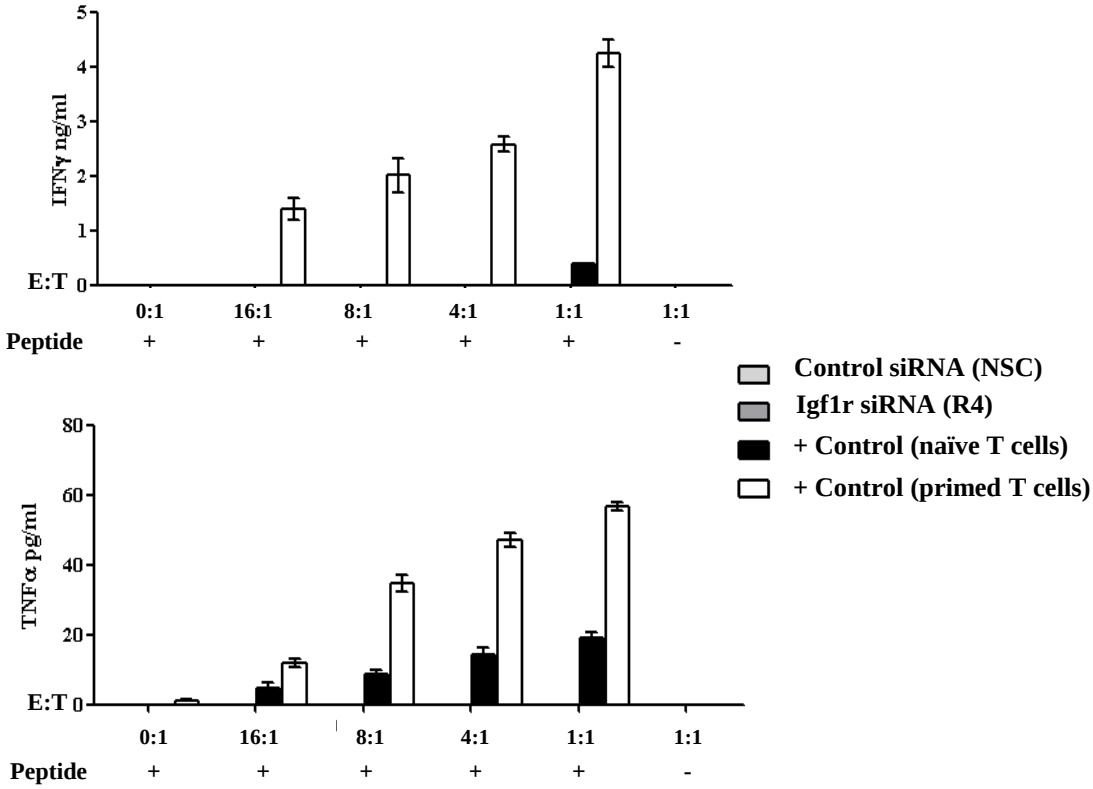


Figure 3.9 Effect of Igf1r depleted B16.F10 on cytokine production by effector T cell B16.F10 cells were transfected with 10nM R4 (Igf1r) or NSC siRNAs. After 48 hours cells and CD11c+ dendritic cells (positive controls) were pulsed with Np peptide and incubated with CD8+ T lymphocytes at various Effector:Target (E:T) ratios. T cells were either unprimed (naive) or harvested from a mouse challenged 7 days earlier with UV irradiated influenza virus strain PR8 (H1N1) containing the Np epitope. Type 1 cytokine (Tumour necrosis factor α (TNF-α) and Interferon gamma (IFN-γ)) concentration of the cell medium was assessed after 36 hours by ELISA. Histograms represent mean ± range cytokine concentration from two independent experiments. T cells incubated with unpulsed CD11c+ dendritic cells did not produce cytokines. Primed T cells incubated with peptide pulsed CD11c+ dendritic cells produced both TNF-α and IFN-γ. Cytokine production was reciprocally related to E:T. Naïve T cells produced IFNγ only at an E:T of 1:1 whereas TNFα production occurred at all E:T although at a lower level than production by primed T cells. Cytokines were not detected following T cell incubation with control or Igf1r depleted B16:F10 at any E:T ratio.

Cell mediated toxicity was traditionally measured by determining the ability of effector cells to lyse target cells labelled with radioisotopes (Wonderlich et al., 2001). A protocol which does not require handling of radioisotopes had been developed in our department and was employed in these experiments. The VITAL assay assesses the efficiency of cytotoxic lymphocyte mediated killing through selective depletion of fluorescently labelled, peptide pulsed, target cells in comparison to unpulsed target cells labelled with a different fluorescent cell marker dye (Hermans et al., 2004). B16.F10 cells were incubated with IFNɣ for 24 hours and surface MHC Class 1 expression was quantified by flow cytometry. These cells were then split into two aliquots and labelled with either CFSE or cell tracker orange (CTO) cell tracker dyes. Cells stained with CFSE were then pulsed with antigenic Np peptide. Equal numbers of unpulsed CTO stained cells and CFSE stained peptide pulsed cells were mixed before incubation with a pool of F5 lymphocytes at various E:T ratios. The lymphocytes had been primed *in vitro* and as such represented a heterogenous pool of effector and helper T cells. Peptide pulsed splenocytes marked with cell tracker dyes in an identical manner served as a positive control. Cytotoxic cell mediated killing was assessed after 4 and 24 hours by flow cytometry through documentation of a change in the ratio of CFSE and CTO labelled B16.F10 cells.

In the absence of lymphocytes the ratio of CFSE:CTO labelled positive control cells remained 1:1, reported as 0% mean specific lysis (Figure 3.10A). In unpulsed positive control cells a small degree of cell lysis was seen at high E:T ratios (Figure 3.10B). This represented background T cell toxicity towards the non syngeneic control cells which is not induced via peptide specific MHC1:TCR recognition. This was most likely explained by the presence of lymphocytes not bearing the TCR for the Np peptide which have been reported to make up a small proportion (<20%) of circulating lymphocytes in the F5

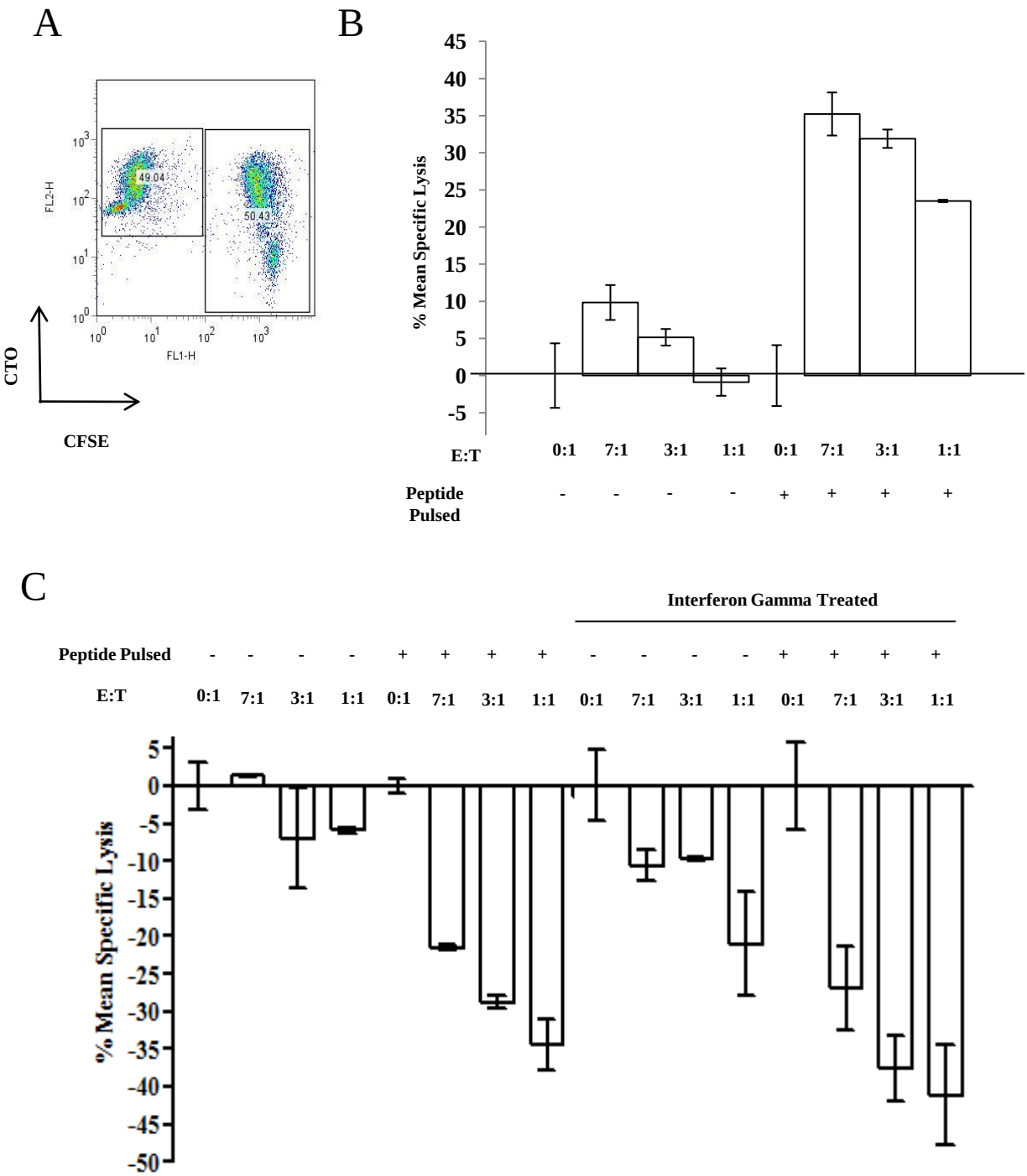


Figure 3.10 Cytotoxic T lymphocyte killing of Interferon Gamma treated B16.F10 cells. B16F10 cells were treated with solvent or 20ng/ml IFNγ for 24 hours. B6 splenocytes served as a positive control. Cells were split into two aliquots and labelled with Cell Tracker Orange (CTO) or CFSE. CFSE labelled cells were pulsed with Np peptide for 1 hour. Equal numbers of CTO and CFSE labelled cells were then incubated in different target:effector (E:T) ratios with *in vitro* primed CD8+ T lymphocytes for 24 hours. The relative proportion of Np pulsed and unpulsed cells was determined by flow cytometric separation by intracellular staining. % mean specific lysis was calculated as 100*(1- (%CFSE/%CTO cells)). Histograms represent mean (+/- range) from duplicate samples. **A)** Representative flow cytometry plot showing differentiation of the two cell populations. **B**) Mean specific lysis of Np peptide pulsed B6 splenocytes is proportional to E:T ratios. Minimal cell lysis is seen in the absence of NP peptide. **C)** Interferon gamma treatment of B16.F10 cells did not result in cell killing by cytotoxic T lymphocytes. Proliferation of CFSE stained B16.F10 cells (ie negative values for % mean specific lysis) at all tested E:Ts is greater following pulsing with peptide.

mouse (Mamalaki et al., 1993). Mean specific lysis of peptide pulsed control cells was significantly higher than unpulsed control cells and increased with E:T ratio (Figure 3.10B). B16.F10 cells, however, were not specifically lysed irrespective of whether or not they had been pulsed with peptide (Figure 3.10C). Futhermore IFNɣ treatment did not enhance lysis. On the contrary CFSE stained B16.F10 cells proliferated relative to CTO stained, peptide pulsed cells to a greater degree than unpulsed cells, and proliferation was highest at low E:T ratios. The reason for increased proliferation of peptide pulsed B16.F10 was unclear, but it is both dependent on cellular dye employed and on the presence of lymphocytes as it did not occur in their absence. That B16.F10 proliferation was reduced at high E:T ratios was most likely as a result of the cell culture medium being depleted more rapidly with higher numbers of lymphocytes. Whilst setting up this experiment with reciprocal dye combinations as described in the original methodology would have eliminated differential growth caused by cellular dyes, the observation that B16.F10 cells did not elicit CD8+ T cells mediated lysis rendered such an experiment unnecessary.

From these results it appeared that the immunogenicity of B16.F10 cells could not be increased by a 10^2 fold increase in MHC Class 1 expression induced by IFNɣ. Similar findings have previously been reported (Zoller, 1988). This suggested that factors other than, or in addition to, MHC Class 1 expression were limiting the immunogenicity of B16.F10 cells and that a modest increase in MHC Class 1 induced by depleting the Igf1r was unlikely to result in an immunological response measurable by these assays.

It was noted that upregulation of both MHC Class I and costimulatory molecules (B7) have been documented on IGF1R axis inhibition in embryonal carcinoma, breast

carcinoma and glioma cells (Schillaci et al., 2006, Trojan et al., 1996, Ly et al., 2000, Ly et al., 2001). Furthermore transfection of B7 molecules was required to render hepatoma and colon carcinoma cells immunogenic after IGF1 depletion (Liu et al., 2000). It was considered most likely that low or absent expression of co-stimulatory and adhesion molecules were limiting B16.F10 immunogenicity. B16.F10 cells have previously been shown to express negligible levels of the co-stimulatory molecules CD48, CD54, CD70 and CD86 (Zoller, 1988, Dezfouli et al., 2003). Of these CD54 (ICAM-1) and CD48 are adhesion molecules which bind to LFA-1 and CD2 respectively on the T cell surface and these interactions are responsible for the initial transient lymphocyte-target cell interaction. In the absence of the adhesion molecules CD48 and CD54, the initial transient binding of B16.F10 to the T cell is limited and this may dictate the frequency of immunological synapse formation even when MHC class 1 expression is increased (van der Merwe et al., 1995).

The immunogenicity of B16.F10 cells can be increased by upregulation of B7, CD54 and MHC Class 1, or transfection with MHC Class 1 or B7 molecules (Porgador et al., 1989, Dezfouli et al., 2003, Chen et al., 1994). However in the absence of factors which increase these surface molecules sufficiently B16.F10 remain poorly immunogenic. It was postulated that Igf1r depletion did not increase MHC Class 1 and/or costimulatory molecule expression sufficiently to render the cells immunogenic.

Together all of the findings presented above brought into question the utility of B16.F10 as a model system for evaluating the immunological consequences of IGF1R depletion *in vivo* given that the increase in MHC Class 1 was insufficient to increase cell immunogenicity. The utility of this model will be discussed further following description

of the progress made in development of the inducible system for regulated Igf1r depletion in B16.F10 cells.

3.2.7 An inducible system for regulated Igf1r depletion in B16.F10 melanoma

Previous studies have demonstrated that depletion of the IGF1R or IGF1 by nucleic acid or RNAi mediated strategies reduced the *in vivo* growth of a variety of tumours and that animals immunised with these modified tumour cells were protected against subsequent challenge with wild type tumour (Trojan et al., 1993, Resnicoff et al., 1994b, Shevelev et al., 1997, Burfeind et al., 1996, Trojan et al., 1994, Lafarge-Frayssinet et al., 1997, Liu et al., 1998, Schillaci et al., 2006, Ellouk-Achard et al., 1998, Samani et al., 2001, Scotlandi et al., 2002). However constitutive downregulation of the IGF1R is of detriment to the survival of tumour cells. Previous work in our laboratory had achieved stable short term IGF1R depletion in human MCF1 breast cancer cells but which was lost in the long term (Riedemann et al., 2007a, Riedemann et al., 2007b). The aim of this series of experiments was to create a murine melanoma cell line with regulated expression of an Igf1r short hairpin RNA (shRNA). This would enable a tumour inoculum to grow in syngeneic mice and then the Igf1r depleted at a set time point. The aim would then be to evaluate the consequences of Igf1r depletion on the growth characteristics of the manipulated tumour, and also to test any effect on growth of a distant, unmodified, tumour implanted in the contralateral flank. This approach could potentially enable testing of the hypothesis that manipulation of IGF1 signalling can influence immune responses, without focus on a specific mechanism. When these experiments commenced the results of the work presented in sections 3.2.1-3.2.6 were not yet available and it was anticipated that this

approach would also provide an opportunity to evaluate the interplay of MHC Class 1 expression and the IGF1R axis *in vivo.*

A wide variety of inducible shRNA systems have been developed for the long term stable expression of siRNA or shRNA under the influence of constitutively active promoters (Ventura et al., 2004, Ling and Arlinghaus, 2005). In these systems siRNA or shRNA sequences are cloned into expression constructs and retroviral or lentiviral vectors are then employed to facilitate efficient integration into the host genome and subsequent tissue specific expression. In more recently developed systems conditional expression of the siRNA or shRNA can be achieved through addition or removal of an exogenous drug which activates an otherwise silent promoter (Kappel et al., 2007, Shin et al., 2006, Pluta et al., 2007, Wiederschain et al., 2009, Rangasamy et al., 2008, Szulc et al., 2006). These systems vary in "leakiness", suboptimal gene control due to shRNA expression in the absence of the inducing agent (Wiznerowicz et al., 2006). They also fail if the chosen shRNA sequence is inefficient at causing mRNA depletion or if endogenous events such as promoter methylation, influence the inducible nature of expression (Szulc et al., 2006). A variety of single and dual vector based systems for conditional gene knockout were considered for this project and the strategem chosen utilised tetracycline regulated expression of a chosen shRNA from a H1/T0 RNAi cassette, causing a reduction in the expression of the target protein (BLOCK-iT Inducible H1 Lentiviral RNAi System. Invitrogen) (Kurita et al., 2010, Stauffer et al., 2007, Balamurugan and Said, 2006). In the absence of tetracycline, Tetracycline Repressor protein (TetR) is bound to, and inhibits transcription from, the H1/T0 promoter. In the presence of tetracycline, repression is released. Lentiviral infection is used to introduce the constructs into the target cells. An overview of the experimental strategy is presented in Figure 3.11. In short the

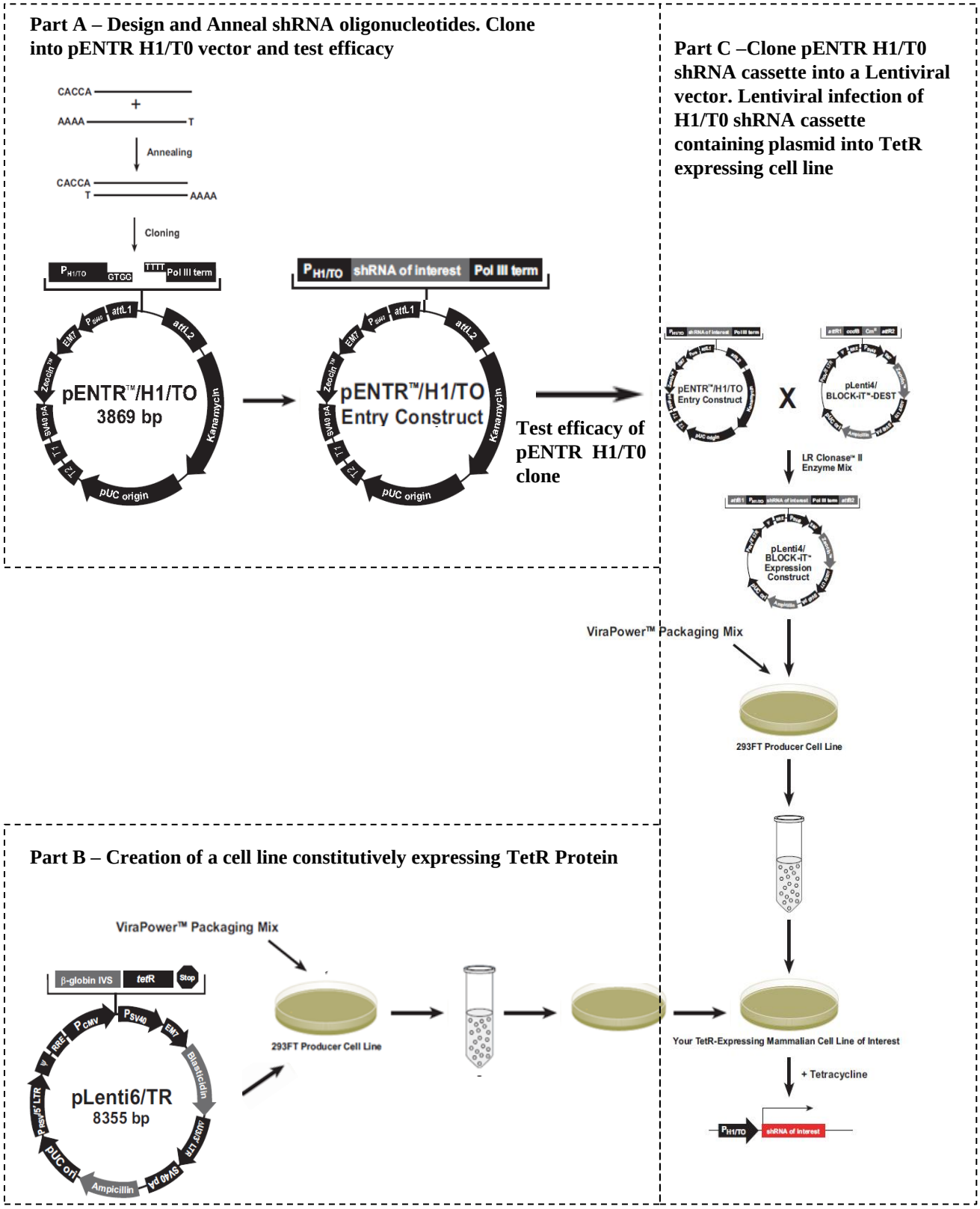


Figure 3.11 Schematic overview of creation of a cell line with inducible shRNA expression using the Invitrogen BLOCK iT Inducible H1 RNAi Lentiviral Kit. Briefly shRNA sequences are designed and cloned into pENTR H1/T0 vector. Following proof of efficacy the RNAi cassette is introduced into the cell line of interest via a lentiviral vector. To achieve tetracycline regulated expression of the RNAi cassette, a lentiviral vector is utilised to introduce the tetracycline regulatory protein (TetR) into the cell line of interest. Parts A and B have been performed and are described in the text.
(Schematic - Modified from Invitrogen product literature)

experimental stratagem involved 3 steps; creation of a B16.F10 cell line which constitutively expressed the TetR protein; selection, cloning and efficacy testing of the H1/T0 shRNAi cassette and finally introduction of the H1/T0 shRNAi cassette into the TetR expressing cell line.

3.2.7.1 Creation of a B16.F10 cell line constitutively expressing TetR

B16.F10 murine melanoma cells were infected with a pLenti6/TR lentiviral vector in which the CMV promoter drives constitutive expression of TetR. Blasticidin resistant clones were expanded and screened for expression of TetR by immunoblot. A previously derived TetR expressing cell line (a kind gift from Dr N. Platt) was employed as a positive control. A high level of TetR expression was recommended to achieve tight shRNA regulation (Invitrogen product literature). Of the selected clones ~60% expressed the TetR protein at a high level (Figure 3.12). On assessment it was seen that the selection procedure had resulted in some clones expressing different amount of Igf1r compared to the parental cell line. Those clones expressing similar Igf1r levels to the parental cell lines and high TetR expression (such as W) were considered suitable for further manipulation to achieve tetracycline regulated gene expression.

3.2.7.2 Selection, cloning and testing of Igf1r shRNA oligonucleotide sequences

The pENTR/H1/T0 plasmid contains the elements required for expression of a double stranded shRNA oligonucleotide under the control of the H1/T0 promotor. The human H1 promoter is recognized by RNA polymerase III, is said to be active in most mammalian cell types and controls high level constitutive expression (Invitrogen product literature). In

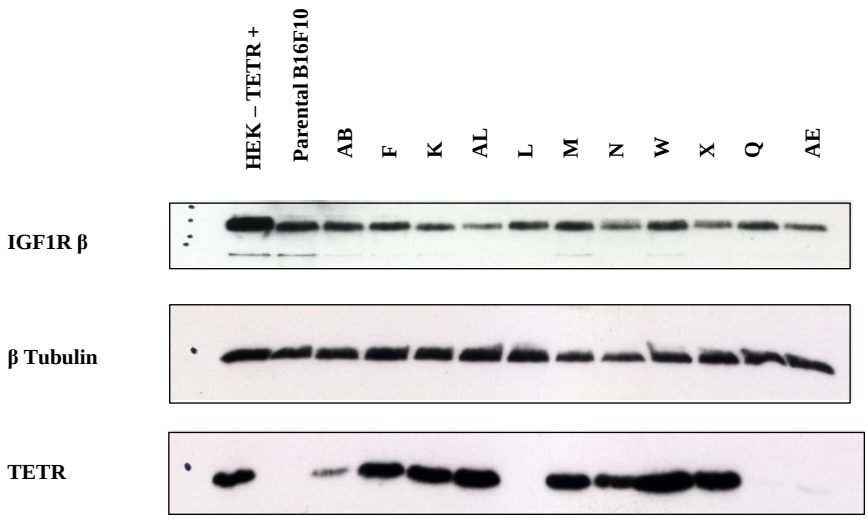


Figure 3.12 – Expression of tetracycline regulatory protein (TETR) by B16.F10 clones. B16.F10 cells were infected with a lentiviral vector carrying the pLenti6/TR plasmid and selected with blasticidin. TetR and Igf1r expression was quantified by immunoblot. HEK-TETR+, a protein lysate from a TETR expressing cell line served as positive control. Parental (uninfected) B16.F10 cells served as a negative control. Approximately 60% of the selected clones showed strong TetR expression. Some selected clones had reduced Igf1r expression compared to the parental cell line.

the H1/T0 cassette the H1 promoter has been modified to include two 19 nucleotide prokaryotic tet operator 2 (TetO2) sequences which bind TetR repressing transcription of the shRNA. Tetracycline binds with high affinity to TetR and causes a conformational change which prevents binding to TetO2, removing repression of shRNA transcription, resulting in target gene knockdown.

Putative IGF1R shRNA sequences were generated from siRNAs with known efficacy, review of the literature, from commercially available shRNAs and using RNAi design software (http://rnaidesigner.invitrogen.com/rnaiexpress/)(Dong et al., 2008, Yuan et al., 2008, Wang et al., 2007, Riedemann et al., 2007a, Lee et al., 2007b). Six of the 30 candidate shRNA sequences were chosen based on conventional siRNA design criteria and their spread across the IGF1R gene transcript (Table 3.1). In addition 2 control shRNAs were designed based on commercially available control siRNAs. All shRNAs contained the chosen Igf1r or control targeting sequence, a loop sequence 5'-CGAA-3' and then the reverse complement of the initial target sequence. In addition 5'-CACC-3' was added to the 5' end of the top strand and 5'-AAAA-3' to the 3' end of the bottom strand to allow directional cloning into the pENTR/H1/T0 vector. Single stranded DNA oligonucleotides were then synthesized, annealed and ds shRNAs cloned into the pENTR/H1/T0 vector. Individual clones were isolated, plasmid DNA extracted and the sequence of the H1/T0 RNAi cassettes verified by sequence analysis using H1 Forward and M13 Reverse priming sites of the pENTR H1/T0 vector.

In order to test the shRNA constructs it was necessary to achieve high efficiency transient transfection of the pENTR/H1/T0 plasmids into B16.F10 melanoma cells. Several transfection methods were assessed including nucleofection, lipid based transfection, with

NAME	Source	Target site	Parent Sequence	shRNA oligonucleotide sequence – "top" and "bottom" strands
R4	Bohula *et al*, 2003	639-657	CAATGAGTACAACTAC CGC	5'-CACCG*CAATGAGTACAACTACCGCCGAAGCGGTAGTTGTACTCATTG-3' 3'-C*GTTACTCATGTTGATGGCGGCTTCGCCATCAACATGAGTAACAAAA-5'
QM4	Qiagen siRNA	3189-3209	ATCCTAATGTATGAAA TTAAA	5'-CACCATCCTAATGTATGAAATTAAACGAATTTAATTTCATACATTAGGA§-3' 3'-TAGGATTACATACTTTAATTTGCTTAAATTAAAGTATGTAATCCTAAAA-5'
QM3		4970-4990ǂ	AACCTTAATGACAACA CTTAA	5'-CACCAACCTTAATGACAACACTTAACGAATTAAGTGTTGTCATTAAGG§-3' 3'-TTGGAATTACTGTTGTGAATTGCTTAATTCACAACAGTAATTCCAAAA-5'
I2	Invitrogen algorithm	1934-1952	GGAAAGATGTACTTTG CTTTC	5'-CACCGGAAAGATGTACTTTGCTTTCCGAAGAAAGCAAAGTACATCTTTCC-3' 3'-CCTTTCTACATGAAACGAAAGGCTTCTTTCGTTTCATGTAGAAAGGAAAA-5'
I 7		3455-3475	GCTGGTTATCATGCTG TATGT	5'-CACCGCTGGTTATCATGCTGTATGTCGAAACATACAGCATGATAACCAGC-3' 3'-CGACCAATAGTACGACATACAGCTTTGTATGTCGTACTATTGGTCGAAAA-5'
GL3	Genelink Algorithm	5010-5033ǂ	AATTGAGTCTCTTCGT TCTCTGC	5'-CACCAATTGAGTCTCTTCGTTCTCTGCCGAAGCAGAGAACGAAGAGACTCAA§-3' 3'-TTAACTCAGAGAAGCAAGAGACGGCTTCGTCTCTTGCTTCTCTGAGTTAAAA-5'
mNSC	Sigma Aldrich	Non Silencing control	CAACAAGATGAAGAGC ACCAA	5'-CACCG*CAACAAGATGAAGAGCACCAACGAATTGGTGCTCTTCATCTTGTTG-3' 3'-C*GTTGTTCTACTTCTCGTGGTTGCTTAACCACGAGAAGTAGAACAACAAAA-5'
NSC	Qiagen	Non Silencing control	TTCTCCGAACGTGTCA CGT	5'-CACCG*TTCTCCGAACGTGTCACGTCGAAACGTGACACGTTCGGAGAA-3' 3'-C*AAGAGGCTTGCACAGTGCAGCTTTGCACTGTGCAAGCCTCTTAAAA-5'

Table 3.1 – Sequences of selected Igf1r shRNAs
* - Additional G added for efficient transcriptional initiation by RNA Polymerase III and corresponding terminal C
ǂ - non coding exon
§ - Terminal Ts removed as will be provided by Polymerase III terminator

lipofectamine and Fugene, and calcium phosphate transfection methods. Nucleofection (Amaxa ^{TM}) using an eGFP plasmid achieved a transfection efficiency of ~87% and was found to be the most efficient and least toxic method of transfecting plasmid DNA into B16.F10 cells.

To assess efficacy of the plasmids in causing shRNA mediated depletion of the Igf1r, pENTR H1/T0-R4^{shRNA} and control plasmid pENTR H1/T0-NSC^{shRNA} were transfected into B16.F10 cells by nucleofection. eGFP plasmid was transfected alongside as a control for transfection efficiency. Cells were collected and analysed by immunoblot after 24 and 48 hours. There was no significant depletion of Igf1r despite strong positivity of eGFP infected control cells (Figure 3.13A).

It was possible that either the shRNA sequences were not efficacious or that immunoblotting was insufficiently sensitive to detect depletion of Igf1r in a subpopulation of transfected cells. It had previously been found that none of the tested antibodies had been suitable for detecting murine IGF1R by flow cytometry (section 3.2.3). Instead a previously published method was employed which quantified binding of a biotinylated Des 1, 3 -IGF ligand by streptavadin conjugated fluorophore (Xu et al., 1995). The technique was found to be sensitive and specific, signal being abrogated by incubation with 100 fold excess of unbiotinylated ligand. To test the sensitivity of this method in detecting depletion of the Igf1r, B16.F10 cells were transfected with a range of concentrations of IGF1R (R4) or control (NSC) siRNA and cell surface Igf1r quantified by flow cytometry and immunoblot after 48 hours. As previously documented Igf1r was seen to be effectively depleted on immunoblot by the R4 siRNA at concentrations of 100 and 1nM, and depleted to a lesser extent by 0.1nM and 0.01nM (Figure 3.13B). The results of

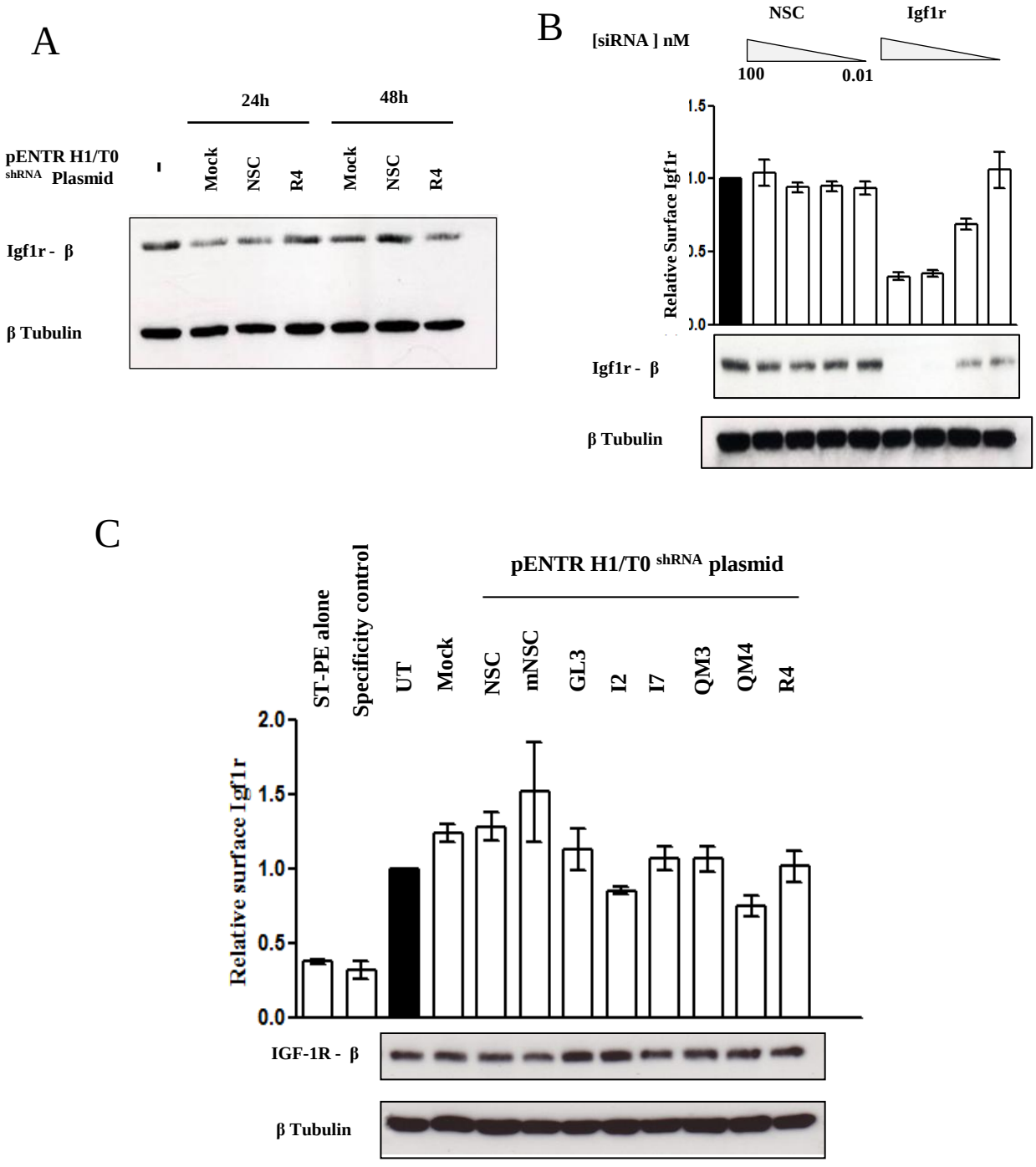


Figure 3.13 – Effect of Igf1r siRNA or shRNA on Igf1r expression. A) B16F10 cells were nucleofected with pENTR H1/T0 ^{shRNA} R4 and NSC plasmids. Igf1r expression was quantified by immunoblot after 24 and 48 hours. pENTR H1/T0 ^{shRNA} plasmid transfection did not alter Igf1r expression **A)** B16.F10 cells were transfected with 0.01-100nM Igf-1r or non silencing control (NSC) siRNA and after 48 hours the cell surface Igf1r was quantified by immunoblot and by flow cytometry using a biotinolyated ligand method (Xu e*t al*,1995). Bars represent geometric mean fluorescence (MHC Class 1) ±range from 2 independent experiments, normalised to untreated cells (black bar). 100 and 1 nM Igf1r siRNA depleted Igf1r completely on immunoblot and flow cytometry compared to control transfectants. 0.1 and 0.01nM siRNA depleted Igf1r in a dose dependant fashion. Igf1r levels measured by flow cytometry mirrored those seen on immunoblot. **C)** B16.F10 cells underwent nucleofection with each of 8 pENTR H1/T0 ^{shRNA} plasmids and Igf1r expression was assessed by immunoblot and flow cytometry after 48 hours. Fluorophore (ST-PE) alone and incubation with 100 fold excess of un-biotinolyated ligand served as controls. Bars represent geometric mean fluorescence (MHC Class 1) ±range from 2 independent experiments, normalised to untreated cells (black bar). Transfection with pENTR H1/T0 ^{shRNA} plasmids did not alter Igf1r expression.

flow cytometry similarly demonstrated reduction of surface Igf1r in a dose dependent manner and correlated to the Igf1r levels on immunoblot. Quantification of Igf1r by flow cytometry was thus considered to be suitable for identification of subpopulations of plasmid transfected cells which bear altered Igf1r expression.

B16.F10 cells were transfected by nucleofection with each of the 8 pENTR H1/T0 shRNAi plasmids and were analysed by flow cytometry and immunoblot after 48 hours. Untreated cells incubated with 100 fold excess of unbiotinolyated ligand, or streptavadin conjugated fluorophore alone served as controls for specificity. There was no significant reduction in average surface Igf1r expression or total Igf1r levels following transfection with any of the plasmids (Figure 3.13C). Furthermore the small dynamic range of the assay was insufficient to allow identification of subsets of cells expressing low Igf1r.

These initial tests failed to show depletion of the Igf1r in B16.F10 cells with pENTR H1/T0 shRNAi plasmids expressing the 6 chosen Igf1r shRNA sequences. There are numerous possible explanations for this finding including poor transfection efficiency of the relatively large plasmid, lack of the activity of the H1/T0 promoter in this cell line, selection of ineffective shRNA sequences or an inappropriate loop sequence. Although the product literature states that the H1/T0 promoter is active in most mammalian cell lines, a thorough search of the literature did not reveal previous evidence of activity in B16.F10 cells and only in one other murine cell line (Thurisch et al., 2009).

Two control plasmid were available for assessment of promoter function. Unfortunately the shRNA sequence for lamin within the pLenti4-GW/H1/T0-lamin^{shRNA} control plasmid provided with the Invitrogen kit was found by BLAST analysis to be homologous to

human but not murine lamin and as such could not be used to assess promoter activity. However a supplied LacZ2.1 ds oligonucleotide once cloned into the expression plasmid to produce a pENTR GW/H1/T0-lacZ2.1^{shRNA} plasmid was suitable for assessing activity of the H1/T0 promoter in B16.F10 cells.

B16.F10 cells were co-nucleofected with the pENTR GW/H1/T0-lacZ2.1^{shRNA} plasmid and a supplied reporter plasmid pcDNA 1.2/V5-GW/lacZ in a 6:1 ratio. β galactosidase activity was assessed after 72 hours spectrophometrically. Cells nucleofected with pcDNA 1.2/V5-GW/lacZ produced measurable β Galactosidase (Figure 3.14). There was no reduction in β Galactosidase production on co-nucleofection of the pENTR GW/H1/T0-lacZ2.1^{shRNA} plasmid.

Based on these results the H1/T0 promoter appeared to be unable to drive transcription of shRNA in B16.F10 cells, although failure of transfection of the relatively large pENTR GW/H1/T0-lacZ2.1^{shRNA} plasmid was also a possible explanation. Although not specifically investigated, it also seemed unlikely that the Igf1r shRNA sequences chosen were all ineffective. In particular R4 shRNA, designed to be homologous to both human and murine IGF1R, has previously shown efficacy, albeit in human cell lines, in our laboratory (Riedemann et al., 2007a). These factors could have been further investigated by selection from the literature of an shRNA sequence with known efficacy in the B16.F10 cell line, choice of a different promoter construct, cell sorting of cells cotransfected with the plasmid of interest and an eGFP plasmid and trialling of alternative shRNA and loop sequences. However given the results detailed in the earlier sections of this chapter it was concluded that the B16.F10 cell line may not represent an appropriate choice of model for testing the immunological consequences of Igf1r depletion *in vivo*.

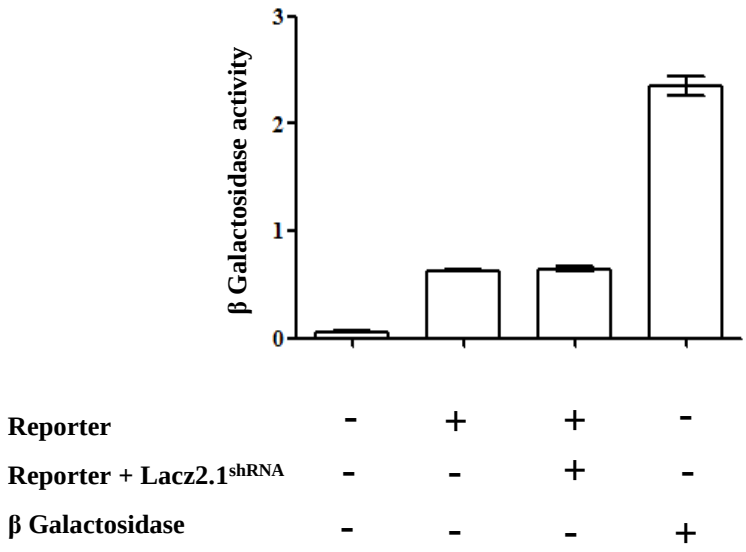


Figure 3.14. Activity of the H1/T0 promotor in B16.F10 melanoma cells. B16.F10 cells were nucleofected with either a reporter plasmid pcDNA 1.2/V5-GW/lacZ alone or in addition to the pENTR GW/H1/T0-lacZ2.1^{shRNA} in a 6:1 ratio. β Galactosidase activity was quantified after 48 hours. β Galactosidase (Sigma) served as positive control. Bars represent mean ±SEM β Galactosidase activity (arbitary units) from 3 independent experiments. Nucleofection of the pcDNA 1.2/V5-GW/lacZ resulted in β Galactosidase activity. pENTR GW/H1/T0-lacZ2.1^{shRNA} did not deplete β Galactosidase activity.

3.3 Conclusions

There are several reports in the literature that IGF1R depletion by oligonucleotide based strategies can increase the immunogenicity of tumour cells *in vivo* (Burfeind et al., 1996, Trojan et al., 1994, Lafarge-Frayssinet et al., 1997, Shevelev et al., 1997, Liu et al., 1998, Schillaci et al., 2006, Ellouk-Achard et al., 1998, Samani et al., 2001, Scotlandi et al., 2002). The experiments detailed in this chapter have thoroughly interrogated a preliminary finding made in our laboratory, that Igf1r depletion results in an increase in MHC Class 1 in B16.F10 melanoma cells. A dose dependent increase in MHC Class 1 expression was documented following Igf1r depletion with 3 of 6 Igf1r siRNAs, including the oligonucleotide used previously by Yeh. A reciprocal decrease in MHC Class 1 expression was found following incubation with IGF1 ligand. However doubt was cast on these findings given that: whilst the degree of MHC Class 1 expression was siRNA dose dependent the degree of Igf1r depletion was not, three other Igf1r siRNA did not result in an increase in MHC Class 1 despite efficacy at depleting the Igf1r, there was no significant change in MHC Class 1 in a panel of nine further melanoma cell lines, MHC Class 1 expression was unchanged with both kinase and blocking antibody inhibitors of the Igf1r and finally the change in MHC Class 1 was of no functional significance.

Concurrent experiments to generate an inducible shRNA system for *in vivo* testing of the hypothesis that IGF1R depletion has immunological consequences were problematic. Initial tests failed to demonstrate efficacy of plasmids expressing the chosen shRNA sequences. Before further investigation, the choice of cell line and utility of the proposed experiment were questioned given that the data described above had shown Igf1r depletion in B16.F10 cells resulted in a different phenotype compared to clinically relevant IGF1R inhibitors, and to other melanoma cell lines. Furthermore whilst the planned experiments

might interrogate the hypothesis, in the absence of the postulated mechanism to scrutinise, it was likely that they would add little to that already in the literature. Overall given the lack of biological consequences of the unique phenotype induced in B16.F10 cells and the relatively poor immunogenicity of the B16.F10 cell line it was decided that there was insufficient merit in continuing this part of the project.

During the time course of the above experiments the preliminary results of clinical trials of small molecule inhibitors of the IGF1R were becoming available. Therefore the emphasis of this project turned to assess the effects of clinically relevant IGF1R inhibitory drugs in human melanoma.

3.4 Future directions for investigation of the role of the Igf1r in the immunological response to tumour cells

Possible mechanisms for the reported ability of IGF1R depletion to cause an increase in tumour immunogenicity remain unclear. The documentation of an increase in MHC Class 1 and accumulation of CD8+ T cells in tumours following IGF1 or IGF1R depletion suggest involvement of MHC Class 1 mediated recognition of tumour cell antigens. However distant tumour regression, postulated to be caused by an immunological response, was also observed in a pilot clinical trial in which IGF1R depleted cells were contained in a diffusion chamber implanted distant to the primary tumour (Andrews et al., 2001). In this circumstance cell-cell contact between tumour and immune cells would be impossible and it is reasonable to suggest that diffusible elements were responsible for initiating the immunological response. It is possible to integrate both these findings and hypothesize about the mechanisms involved. Following inoculation of manipulated tumour cells, antigens are taken up by professional antigen presenting cells where they can be processed and cross presented in the context of MHC Class 1 molecules, resulting in a

CD8+ response. Indeed antigen presenting cells, particularly dendritic cells, are much more effective at generating a primary immune response than relatively non immunogenic tumour cells and tend to form the focus of immunological anti-cancer therapies.

Thus increased antigen presentation of manipulated tumour cells themselves is not a prerequisite for a CD8+ response. Why IGF1R depleted tumour cells should be more immunogenic than control cells is unclear. It could be postulated that IGF1R depletion results in an altered expression of tumour specific antigen or it may relate to another consequence of IGF1R depletion.

IGFs are well known to promote cell survival and IGF1R depletion results in apoptosis (Baserga et al., 1997a). Whilst apoptosis was classically considered to be an immunologically silent form of cell death it is increasingly recognised that anti-cancer therapies causing apoptosis or necrosis can have immunological consequences (Ullrich et al., 2007). Anthracycline, temozolomide treatment and irradiation have been shown to increase surface expression of calreticulin which increases phagocytosis of "apoptotic" cell fragments by dendritic cells. High mobility group box 1 (HMGB1) released during "apoptosis" prompts dendritic cell processing of phagocytosed antigens and the resultant priming of tumour antigen specific cytotoxic T cells (Gardai et al., 2005). Together these "eat me", "danger" signals and others have been shown to be responsible for immunological consequences of tumour cell death (Ullrich et al., 2007, Obeid et al., 2007a, Obeid et al., 2007b).

Further investigation into the immunological consequences of IGF1R manipulation should first determine if the previously described findings can be replicated using other methods of inhibiting the IGF1R as thus far all published work has employed oligonucleotide

techniques. Igf1r inhibition by small molecule inhibitors or blocking antibodies should be evaluated in model systems such as C6 glioma or breast cancer, in which inncoulation of IGF1R depleted tumour cells has previously been shown to result in regression of pre-existing tumours. Should other strategies fail to induce immunological consequences, as might be expected from the data presented herein, then it would seem appropriate to evaluate the differences in phenotype between Igf1r inhibited and Igf1r depleted cells to further explore the underlying mechanisms. In particular the induction of apoptosis which appeared to be more profound *in vivo* than *in vitro* (Resnicoff et al., 1995a) would be interesting to consider. Furthermore these model systems would also be more appropriate for the experiments planned with the inducible Igf1r shRNA system, as long as reliable Igf1r depletion could be achieved. The effect of IGF1R depletion on cell surface co-stimulatory and inhibitory molecules may also merit investigation, particularly given recent recognition of the efficacy in melanoma therapy of anti-CTLA4 and programmed cell death-1 (PD1) antibodies in blocking inhibitory signalling (Hodi et al., 2010b, Brahmer et al., 2012, Topalian et al., 2012).

4. IGF1R induced gene expression in human melanoma

4.1 Introduction

Present clinical strategies for targeting the IGF1R use blocking antibodies or small molecule inhibitors of the IGF1R kinase domain (Chitnis et al., 2008). Numerous compounds are in clinical trials as discussed in the introduction. However what is unclear is how to predict the likely efficacy of IGF1R inhibitory therapies in a given cancer, or even a given patient. For example IGF1R or *IGF1R* mRNA expression is predictive of response to IGF1R inhibition with monoclonal antibodies or small molecule inhibitors in some colorectal, breast and lung cell lines and patient biopsy specimens (Cao et al., 2008, Huang et al., 2009, Pitts et al., 2010, Gong et al., 2009, Zha et al., 2009) but not in others (Gualberto et al., 2010, Mukohara et al., 2009, Favoni et al., 1994, Spitz et al., 2002, Basu et al., 2011). In cell lines where IGF1R expression alone is not predictive of response, considering protein expression of other components of the IGF1R signalling cascade may allow identification of sensitive cells (Pitts et al., 2010). However there is clearly a need to develop a robust method to identify a subset of patients who would benefit from IGF1R inhibitory therapy. With this aim several studies have investigated the consequence of IGF1R activation or inhibition on gene expression in an attempt to identify a gene signature predictive of response to therapy. Three strategies have been employed: comparison of gene expression in cells sensitive and resistant to IGF1R inhibition (Pitts et al., 2010, Gualberto et al., 2010, Huang et al., 2009, Huang et al., 2008), assessment of gene expression following IGF1R stimulation (Rajski et al., 2010, Creighton et al., 2008) and assessment of gene expression after IGF1R inhibition (Bielen et al., 2011). In breast and colorectal cancer, gene signatures generated from these studies were predictive of response to IGF1R small molecule inhibition in tumour explant models (Pitts et al., 2010,

Litzenburger et al., 2011). In breast and lung cancer the generated gene signatures were predictive of prognosis in patients, providing further rationale for IGF1R inhibition in these tumour types (Creighton et al., 2008, Rajski et al., 2010, Gualberto et al., 2010). Furthermore these studies have suggested rational combination therapies to overcome resistance (Bielen et al., 2011, Huang et al., 2009). Notably the gene expression profiles had differed with cell type and only epithelial and mesenchymal neoplastic cells had been evaluated thus far (Rajski et al., 2010)

In the case of melanoma there is not a large body of *in vitro* and *in vivo* evidence supporting the IGF1R as a therapeutic target and as such the first strategy described above was inappropriate. Instead it was decided to combine the assessment of gene expression both after IGF1 treatment of melanoma cells and IGF1R inhibition with a small molecule inhibitor.

In addition it is now clear that cancers commonly show dysregulation of another portion of the transcriptome, microRNAs (miRNAs) (Meltzer, 2005). These miRNAs are endogenous non coding RNAs which negatively regulate expression of target genes at the posttranscriptional level, via translational repression or mRNA cleavage. A single miRNA can control multiple gene targets in different cellular pathways and, as such, influence diverse biological processes. Whereas mRNAs require translation and posttranslational modification, miRNAs are a direct functional product of the corresponding gene. As such miRNA signatures promise to be a robust, clinically useful biomarkers and indeed a miRNA signature has recently been correlated to survival in melanoma patients (Segura et al., 2010). To the author's knowledge no studies had described the effects of IGF1R

stimulation or inhibition on miRNA expression so such analysis might reveal novel pathway interactions or consequences of IGF1R manipulation.

This chapter details experiments to assess the transcriptional consequences of IGF1R activation or inhibition in a human melanoma cell line. It was anticipated that these experiments might lead to identification of novel gene targets and pathways which would inform IGF1R biology, assess IGF1R associated gene expression in a melanoma cell line and allow assessment of whether IGF1R induced gene expression in melanoma is of clinical relevance.

4.2 Experimental design

The aim of work described in this chapter was to identify a set of genes that were regulated by IGF1R which were either of individual interest in elucidating IGF1R biology or which, as an "IGF1 gene signature", could be used to interrogate clinical data.

Previous strategies have documented the change in gene expression on IGF1 stimulation of serum starved cells (Creighton et al., 2008, Pacher et al., 2007, Rajski et al., 2010). This removes the confounding effects of other mitogens in complete cell culture medium and evaluates only transcriptional changes induced by IGF1, but it is not physiological and may over emphasize the role of IGF1R signalling. Therefore it was decided to use a complementary strategy, evaluating the transcriptional consequences of IGF1R inhibition in melanoma cells growing in complete medium. The IGF1R small molecule inhibitor AZ12253801 and related compounds were undergoing pre-clinical assessment at the time

of this study and permission was gained from AstraZeneca for use of AZ12253801 (Aleksic et al., 2010, Shaw et al., 2011).

By exploiting these two complementary strategies it would also be possible to identify genes reciprocally regulated by IGF1R inhibition and stimulation. By this means it was hoped to avoid false positive results either as a consequence of "off target" effects of the inhibitor or as a result of serum deprivation. As such it was hoped that this experimental design would allow rapid identification of key genes involved in IGF1R biology in melanoma. This approach might also be expected to identify alterations in transcripts relevant to the clinical setting and might guide selection of the most pertinent treatment or combinatorial strategies.

Previous studies have examined IGF1 induced mRNA expression 3 and 24 hours after IGF1 stimulation and these time points have been suggested to represent direct and consequential effects of IGF1R signalling respectively (Creighton et al., 2008, Zha et al., 2009). The same time points were chosen for this study to allow comparisons to be made. An alternate approach would have been to choose time points based on the maximal change of a known transcriptional target of IGF1 signalling but it was felt this might influence the results unintentionally.

The aim of the experiment was to identify both mRNA and miRNAs regulated by IGF1R activation or inhibition in human melanoma cells. The experiment was thus designed with two parallel arms assessing the consequences of IGF1R inhibition or stimulation at 3 and 24 hours.

Cell preparation	Treatment	Total RNA collection
Serum starved	Solvent	3 & 24 hours
	IGF1	
Complete medium	Vehicle	
	AZ12253801	

Table 4.1 Experimental Design

4.3 Results and Discussion

4.3.1 Selection of cell lines and experimental conditions.

BRAF, *NRAS* and *PTEN* mutations are common in clinical cases of melanoma (Haluska et al., 2006a). Four melanoma cell lines were chosen (A375, SKMel2, SKMel23 & SKMel28) which bear a range of these mutations and were thus considered broadly representative of clinical melanoma (Table 4). After procurement and expansion of low passage cell stocks, *NRAS* and *BRAF* mutational status was assessed by PCR by Richard Lisle of the Department of Oncology, Oxford, and were confirmed to be as previously published (Table 4.2).

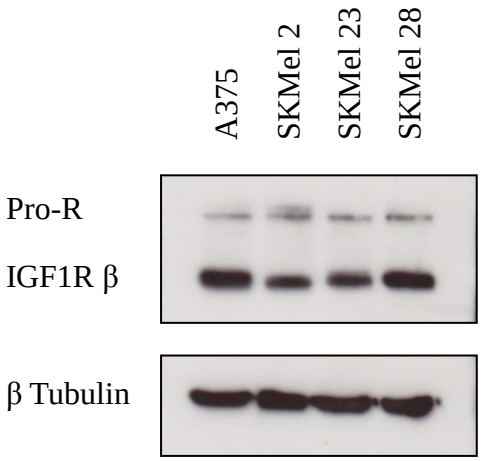
	NRAS	BRAF	PTEN	P53
A375	WT [1,2]	p. V600E [2]	WT [1]	WT [5]
SKMel2	p.Q61R [2]	WT [2]	WT [7]	p.G245S [6]
SKMel23	WT [1,2]	WT [2]	Deleted [1]	WT [5]
SKMel28	WT [1,2]	p.V600E [2]	p.T167A [1]	p.L145R [3,4,6]

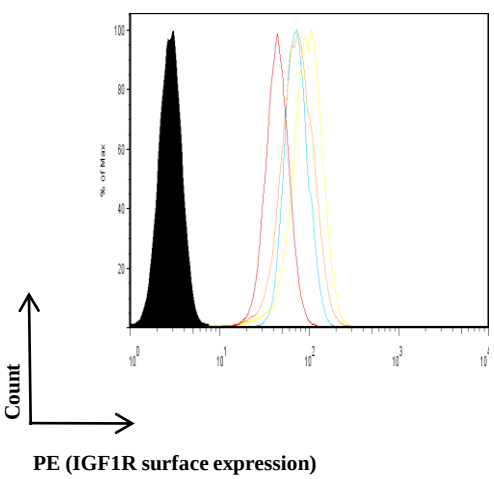
Table 4.2 Genotype of selected Melanoma cell lines. p. denotes protein amino acid substitution. [1] (Tsao et al., 2000), [2] (Tanami et al., 2004),[3] (Haluska et al., 2006a),[4] (Haapajarvi et al., 1999),[5] (Montano et al., 1994),[6] (Bae et al., 1996),[7] (Ikediobi et al., 2006)

Initial experiments assessed expression of IGF1R by the chosen cell lines. Based on data from other cell models it was postulated that relative cell expression of IGF1R might influence sensitivity to IGF1R inhibition or ligand stimulation (Cao et al., 2008, Gong et al., 2009). Total IGF1R was assessed by immunoblot, revealing that all cells expressed IGF1R, and A375 and SKMel28 cells expressed slightly higher levels than SKMel2 and SKMel23 (Figure 4.1). Cell surface IGF1R as quantified by flow cytometry showed higher levels on SKMel28, intermediate on SKMel2 and A375 and least on SKMel23 (Figure 4.1). This disparity between the relative IGF1R expression levels determined by the two methods was suspected to be due to differences in cell size. Macroscopically SKMel28 were clearly larger than the other cell types and SKMel23 smaller. This may account for some of the differences in cell surface IGF1R when quantified by flow cytometry. From this analysis it was clear that all four cell lines expressed IGF1R and were therefore suitable for further analysis.

The next experiments determined the concentrations of IGF1 to use in the transcriptional study. IGF1 concentration could have been chosen in one of two ways: either that which caused maximal receptor phosphorylation and downstream signalling or that which caused the maximal change in a known transcriptional target of IGF1. The former was chosen as the most unbiased way of assessing transcriptional consequences of IGF1R signalling and one which would allow direct comparison to previously published data.

After serum starvation each of the four cell lines was treated with IGF1 at a range of concentrations and cell aliquots harvested at 15 minutes, chosen as representative of immediate signalling events, and 3 and 24 hours, the time points chosen for the definitive experiment. IGF1R, AKT and MAPK phosphorylation status were assessed by





	Relative IGF1R surface expression
Isotype control	
SKMel 23	43.4 (2.3)
SKMel 2	71.1 (1.6)
SKMel 28	91.0 (3.1)
A375	71.2 (2.8)

Figure 4.1 IGF1R protein levels and surface expression in 4 chosen human melanoma cell lines. A375, SKMel2, SKMel23, SKMel28 cells were cultured in complete medium and analysed by immunoblot and flow cytometry for total and cell surface expression of IGF-1R. Immunoblot and flow cytometry plot representative examples of two independent experiments. Table shows relative IGF1R surface expression mean ± (range) normalised to cells stained with an isotype control antibody from two independent experiments. IGF1R expression varied between cell lines.

immunoblot. Figure 4.2 shows results at all time points for A375 cells. Given the similarity between cell lines in late signalling events Figure 4.3 shows results only at the 15 minute time point for SKMel2, SKMel23 and SKMel28. All cell lines were seen to respond to IGF1 stimulation, resulting in a dose dependent increase in IGF1R and AKT phosphorylation at the 15 minute time points. Phosphorylation of the IGF1R saturated at an IGF1 concentration of 8nM (50ng/ml). At 3 and 24 hour time points phosphorylation of the IGF1R was undetectable but phosphorylation of AKT persisted 24 hours after ligand stimulation. Total IGF1R levels showed a dose dependent reduction at 24 hours consistent with ligand driven receptor internalisation, which has been shown to be required for prolonged AKT activation (Romanelli et al., 2007). Basal phosphorylation of MAPK was seen in all cell lines with little or no response to IGF1 treatment.This was expected in those cell lines which have activating mutations of *NRAS* or *BRAF* (A375, SKMel2 & SKMel28) but was unexpected in SKMel23 which harbours wild type *NRAS* and *BRAF*. However it has previously been shown that many melanoma cell lines, including SKMel23, show MAPK activation as a consequence of BRAF gene amplification irrespective of mutational status (Tanami et al., 2004). These data demonstrated that 8nM of IGF1 was sufficient to activate the IGF1R signalling cascade and that this signal, in the form of phosphorylated AKT, persisted throughout the proposed time course of the experiment.

It was then necessary to determine whether the chosen concentration of IGF1 could induce a measurable transcriptional effect on a known transcriptional target of IGF1R signalling such as cyclin D1 (*CCND1*) (Klein and Assoian, 2008). A375 cells were treated with 8nM IGF1, or solvent, and cells collected for mRNA quantification and total protein analysis at 3 and 24 hours respectively. IGF1 induced an significant increase in *CCND1* mRNA at 3 hours and an increase in cyclin D1 protein at 24 hours (Figure 4.4).

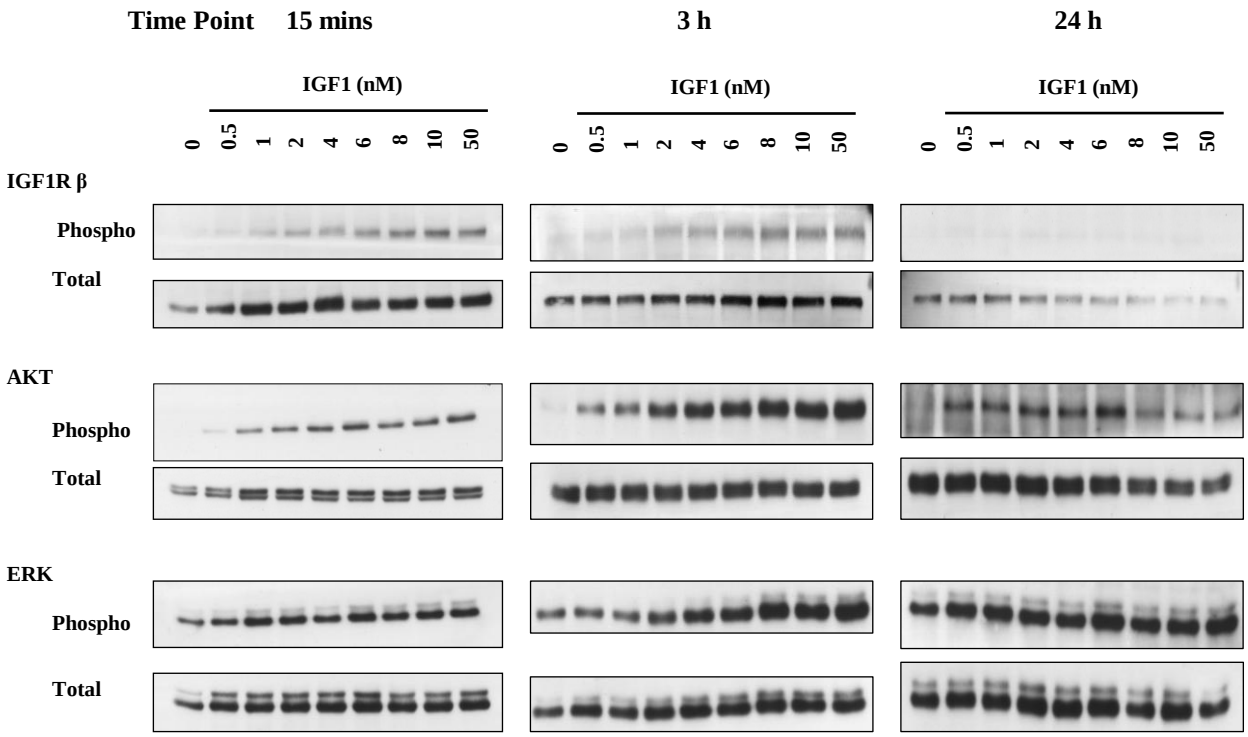


Figure 4.2 Effects of IGF1 on cell signalling in A375 melanoma cells. Serum starved A375 cells were treated with IGF1. Cells were harvested at 15 minutes, 3 hours and 24 hours and analysed by immunoblotting. IGF1R (Tyr,1135/1136), AKT(Ser473), and ERK (Thr202/Tyr204) phosphorylation were assessed by immunoblot. Immunoblots representative of two independent experiments. 8nM IGF1 caused a saturating phosphorylation of IGF1R for at least 3 hours and AKT phosphorylation for at least 24 hours.

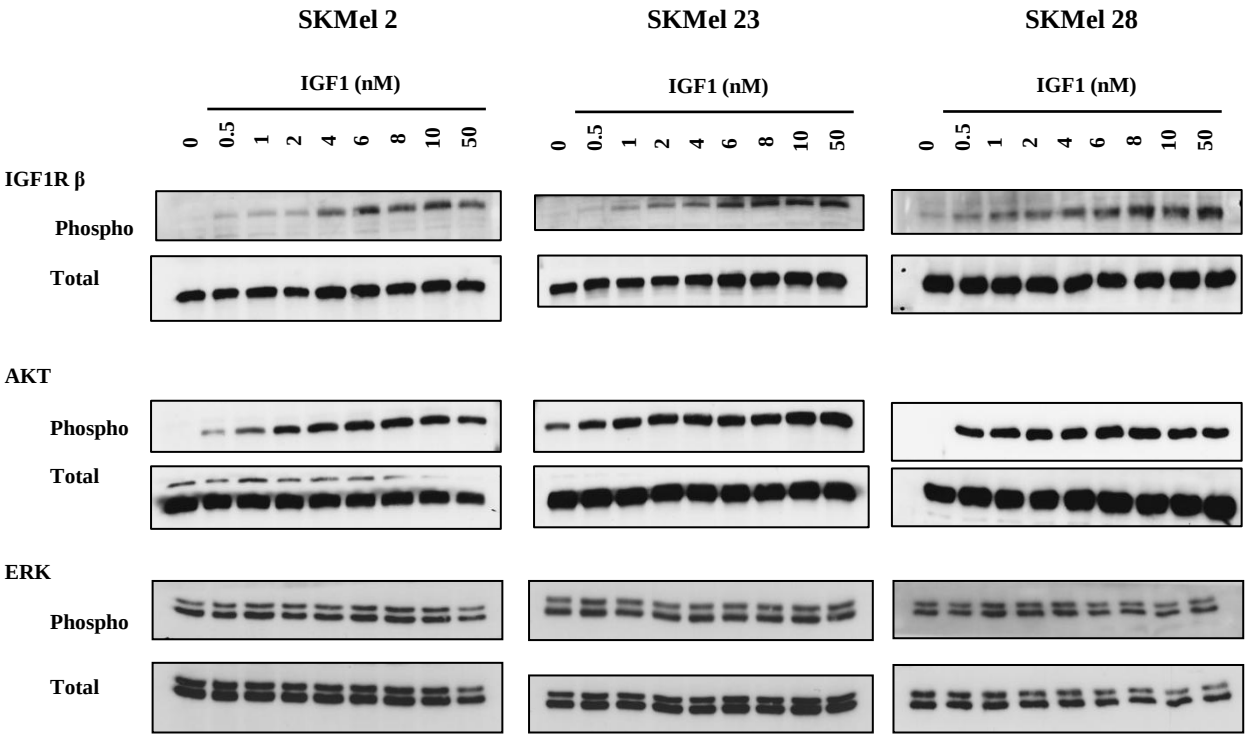


Figure 4.3 Effects of IGF1 on cell signalling in 3 melanoma cell lines. Serum starved SKMel2, SKMel23 and SKMel28 cells were treated with IGF1. Cells were harvested at 15 minutes. IGF1R (Tyr,1135/1136), AKT(Ser473), and ERK (Thr202/Tyr204) phosphorylation were assessed by immunoblot. Immunoblots representative of two independent experiments. 8nM IGF1 caused a saturating phosphorylation of IGF1R and AKT in all three cell lines. Basal phosphorylation of MAPK, unaffected by IGF1, was seen in all three cell lines.

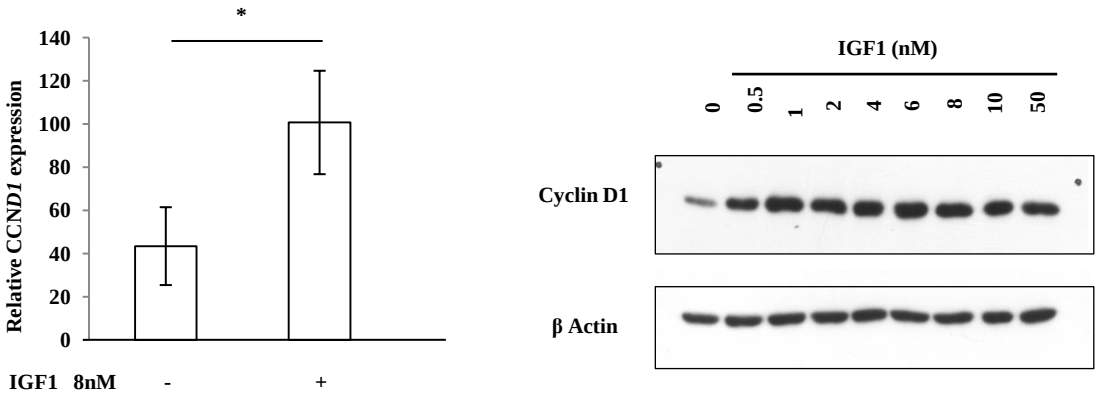


Figure 4.4 Effect of IGF1 on cyclin D1 expression in A375 cells. Serum starved A375 cells were treated with 8nM IGF1. Cells were harvested at 3 hours and 24 hours and analysed by qRT-PCR and immunoblot for *CCND1* mRNA and protein expression respectively. Histogram shows mean relative *CCND1* mRNA expression (±SEM) from two independent experiments in triplicate (6 data points). Immunoblot is a representative example from two independent experiments. IGF1 induced an increase in *CCND1* mRNA and protein at 3 and 24 hours respectively.

(*P<0.05 by paired t test).

In conclusion 8nM of IGF1 caused saturating phosphorylation of the IGF1R in all tested cell lines, accompanied by prolonged phosphorylation of AKT and a significant transcriptional effect. Using similar criteria 8nM had been chosen as the stimulating dose of IGF1 in previous studies assessing IGF1 regulated genes in breast cancer (Rajski et al., 2010, Creighton et al., 2008). During the time this work was being performed, results from our lab and others demonstrated that the IGF1R could translocate to the nucleus and influence transcription directly (Aleksic et al., 2010, Deng et al., 2011, Sehat et al., 2010, Warsito et al., 2012, Wu et al., 2012, Asmane et al., 2012, Hoa et al., 2012). In prostate cancer cell lines, this phenomenon has only been demonstrated with higher concentrations of IGF1 (30-50nM) (Aleksic et al., 2010) than had been determined for use in this study and it was anticipated that this experimental design would not allow identification of transcripts altered by nuclear IGF1R.

4.3.2 Determination of growth inhibition by IGF1R small molecule inhibitor AZ12253801

It was decided that the most appropriate concentration of inhibitor was one that resulted in a biologically relevant endpoint. The concentration required to suppress growth by 50% of the maximal response (GI_{50}) was considered more relevant to the response desired in a clinical situation, than a concentration required to suppress basal IGF1R phosphorylation, and had been used previously in a similar study (Huang et al., 2009). GI_{50} was established by two different methods of assessing the effect of AZ12253801 on cell proliferation. In a Cell Titer Glo assay (Promega) the signal is generated by ATP released from viable cells. It has been shown that the apparent degree of growth inhibition can vary with the duration of treatment exposure (Promega technical support – personal communication). Therefore growth inhibition assays were performed on sequential days until the same GI_{50} was

reported on serial days (Section 2.3.1). The GI_{50} for three cell lines (A375, SKMel2, SKMel28) was found to be similar (50-54nM), whilst that for SKMel23 was higher (113nM) (Figure 4.5A). Inhibition of growth appeared almost complete in A375, SKMel2 and SKMel23 cells but only partial in SKMel28. The technical restrictions of this assay meant that many cells were individual, rather than clustered, when exposed to the inhibitor. It was feared that this might render them more sensitive to the inhibitor and that this situation would not replicate that of the definitive experiment. Therefore a 6 well plate growth assay was also employed. Cells were allowed to grow to 50% confluence in 6 well plates before drug exposure, replicating the anticipated conditions of the definitive experiment. Cell number was then assessed colormetrically when the vehicle treated wells achieved confluence. In fact this assay generated similar GI_{50} values to those achieved in the Cell Titer Glo assays. (Figure 4.5B). A similar pattern was also observed in the completeness of the growth inhibition to that seen with Cell Titer Glo: there was substantial SKMel28 cell survival even at the highest concentrations of inhibitor. A possible explanation for this phenomenon is discussed in a subsequent section.

A concentrations of 50nM AZ12253801 (A375, SKMel2, SKMel28) and 115nM (SKMel23) were considered to represent the GI_{50} values for each cell line and were used in all future experiments. It is interesting to note that expression of IGF1R documented previously either by flow cytometry or by immunoblot (Figure 4.1) did not appear to correlate with the sensitivity to IGF1R inhibition. There is conflicting data in the literature regarding correlations between IGF1R expression and sensitivity to IGF1R inhibition (Huang et al., 2009, Pitts et al., 2010, Gong et al., 2009, Zha et al., 2009) (Gualberto et al., 2010, Mukohara et al., 2009, Favoni et al., 1994, Spitz et al., 2002, Cao et al., 2008). It is interesting that in this panel, a melanoma cell line with high IGF1R expression (SKMel28)

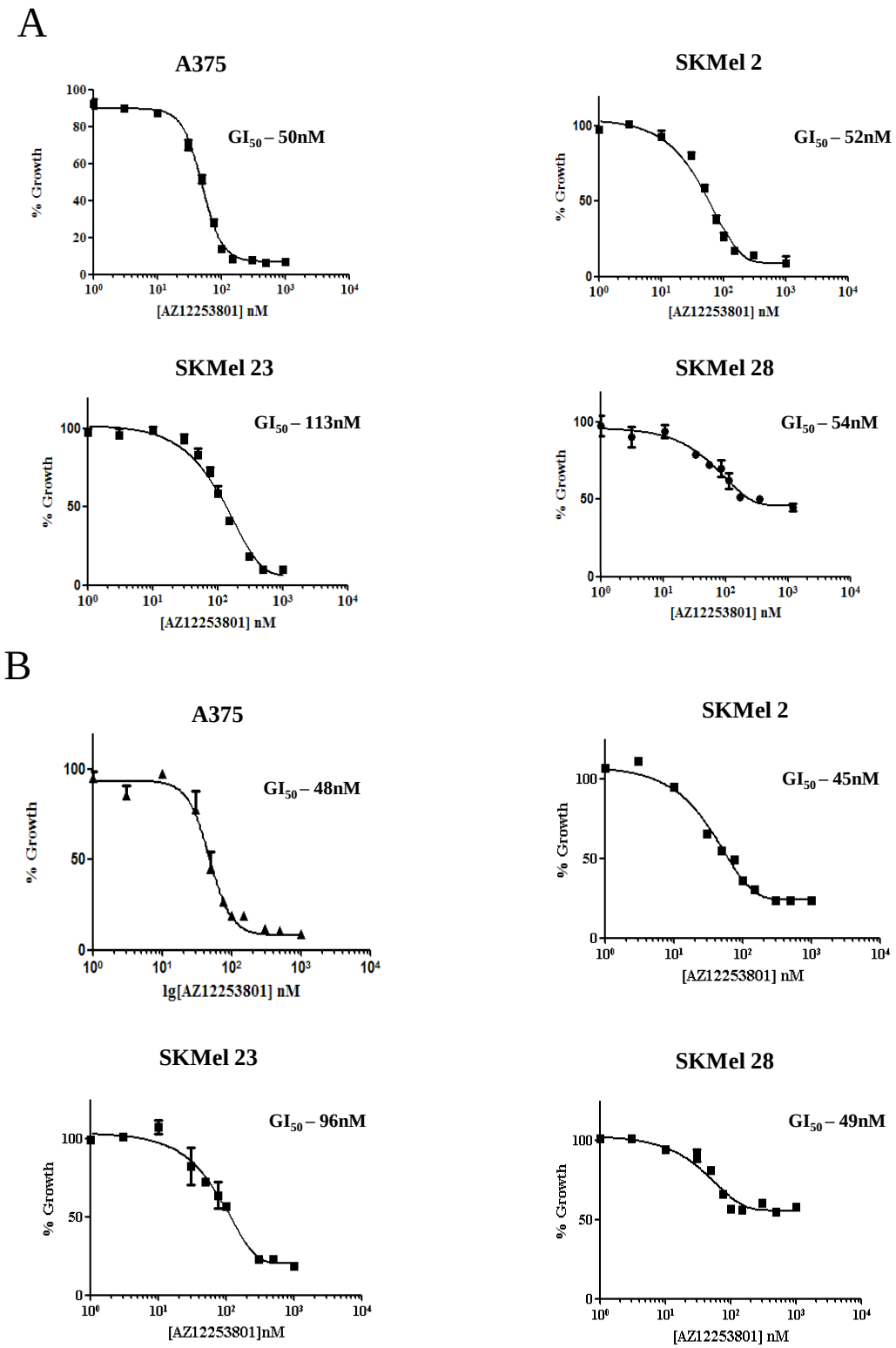


Figure 4.5 AZ12253801 inhibits growth of melanoma cells A) 10^3 cells were seeded into 96 well plates and treated after 24 hours with increasing concentrations of AZ12253801 or vehicle. Cell viability, taken as a measure of cell growth was measured using the Cell Titer Glo assay serially. Graph pad Prism v5 was used to fit the data points to a curve from which GI_{50} values were extrapolated. Graphs show data from 2 independent experiments performed in triplicate (6 data points) and show data from the day the saturating GI_{50} was reached. **B)** 10^4 cells were seeded into 6 well plates and treated with AZ12253801 or vehicle when they achieved 50% confluence. When the vehicle treated wells reached 100% confluence, cells were fixed, stained, dye solubilised and the absorbance (A_{590}) of supernatant taken as representative of cell number. Graphs show data from 2 independent experiments performed in duplicate (4 data points). GI_{50} is shown..

proved relatively refractory even to high concentrations of IGF1R inhibitor. Whether *RAS*, *RAF*, *PTEN* and p53 mutational status affects sensitivity of melanoma cells to IGF1R inhibition is presently the subject of another project in our laboratory.

4.3.3 Assessment of inhibition of basal IGF1R signalling by AZ12253801

It was necessary to assess the effects of the GI_{50} concentration of inhibitor to ensure that IGF1R signalling was indeed abrogated. Melanoma cells were treated with vehicle or AZ12253801 at its GI_{50} concentration and phosphorylation of IGF1R and AKT assessed after 3 and 24 hours. There was concern that it might not be possible to detect basal IGF1R and AKT phosphorylation, nor their reduction, under these conditions. Therefore high dose (50nM) IGF1, or solvent, was added to replicate samples 15 minutes before cell collection to assess the efficacy of the pre-existing AZ12253801 blockade. It was not possible to detect basal IGF1R phosphorylation in any cell line at either the 3 or 24 hour time points in solvent or inhibitor treated cells (Figure 4.6). Basal phosphorylation of AKT was observed in three of the cell lines (SKMel 23, SKMel28 and A375) and was inhibited after 3 or 24 hour treatment with AZ12253801. Phosphorylation of IGF1R in response to IGF1 was seen in all cell lines and was prevented by prior incubation with AZ12253801 for either 3 or 24 hours. IGF1 induced AKT phosphorylation was seen in all cell lines and could be blocked by AZ12253801 in all cells lines except A375. It was interesting that high dose IGF1 could overcome AZ12253801 induced IGF1R blockade in A375 cells, however AZ12253801 clearly suppressed basal AKT phosphorylation at both 3 and 24 hours, consistent with the relative sensitivity of this cell line to the IGF1R inhibitor in the experimental conditions proposed for gene expression analysis.

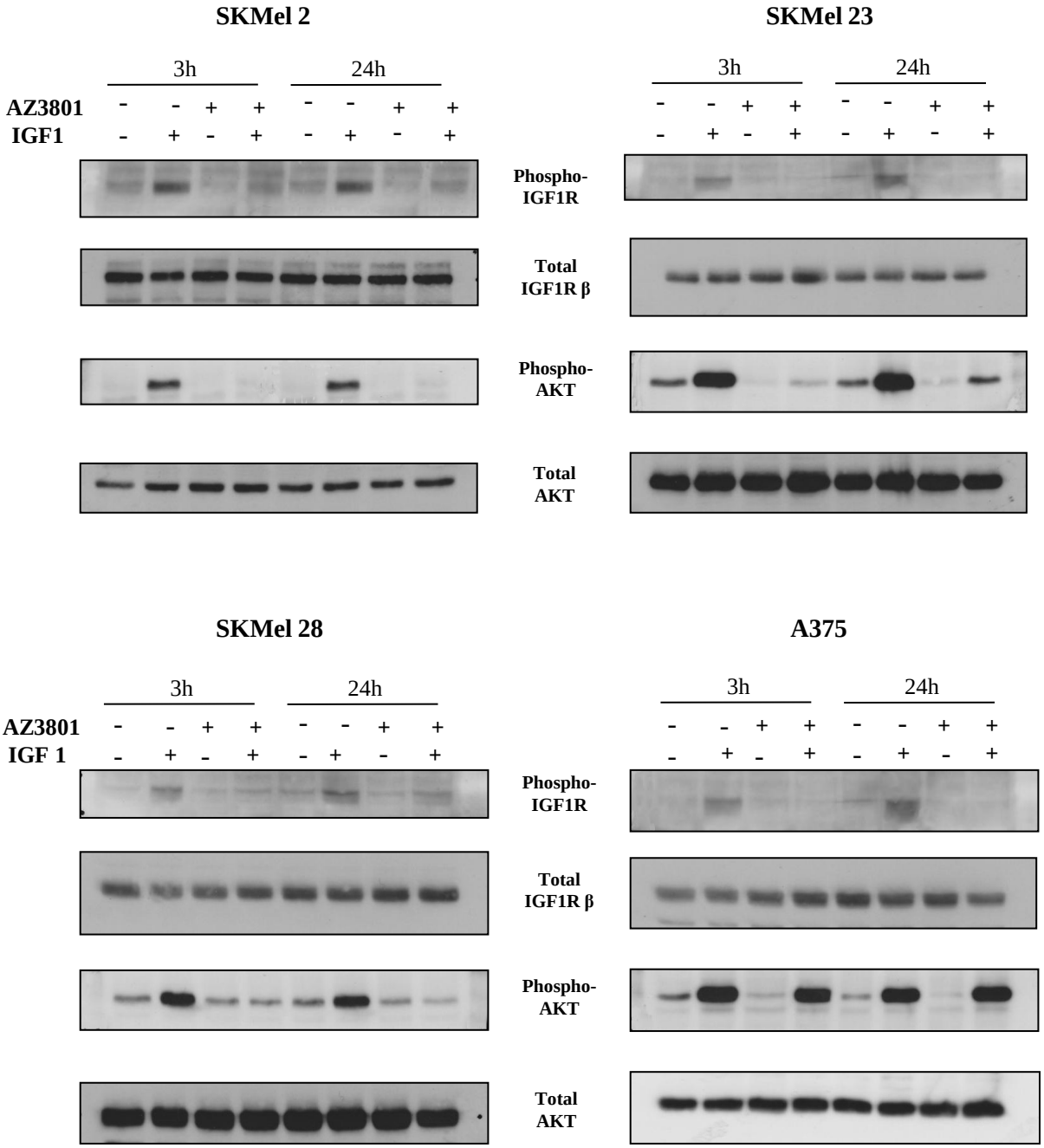


Figure 4.6 Effect of AZ12253801 on IGF1 induced IGF1R and AKT phosphorylation. Melanoma cells in complete cell medium were incubated with AZ12253801 at the previously identified GI_{50} concentrations (A375, SKMel2, SKMel23 – 50nM, SKMel23 - 115nM) for 3 and 24 hours before analysis of IGF1R and AKT phosphorylation by immunoblot. Replicate dishes were treated with 50nM IGF1 for 15 minutes prior to collection to induce IGF1R and AKT phosphorylation as a comparator. Immunoblots are representative experiments of 2 independent experiments. Basal phosphorylation of AKT was prevented by incubation with AZ12253801 in SKMel23 and A375 cells. IGF1 induced phosphorylation of IGF1R was prevented by AZ12253801 in all cell lines.

4.3.3.1 Characterisation of a known off target effect of AZ12253801

During the early stages of this project, we were given access to unpublished data from AstraZeneca revealing that high concentrations of AZ12253801 can induce a phenotype consistent with Aurora Kinase B inhibition. It is likely that both IGF1R and Aurora Kinase B have homology in the kinase domain, given that AZ12253801 has been shown to directly inhibit Aurora Kinase B in an *in vitro* kinase assay (Dr Elaine Kilgour, Astra Zeneca, personal communication) and that dual inhibition has been shown for other IGF1R inhibitors (Carboni et al., 2009). This off target effect does not necessarily preclude use of such drugs in the clinic as Aurora Kinase B is also a potential therapeutic target in anticancer therapy and specific small molecule inhibitors are undergoing clinical testing (Diamond et al., 2013, Lin et al., 2012, Bavetsias et al., 2012, Boss et al., 2011). In the context of the planned experiment which aimed to determine IGF1R specific effects on transcription, it was important to determine whether Aurora Kinase B inhibition was detectable at the chosen concentrations of AZ12253801. Aurora kinases regulate cell cycle transit from G_2 through cytokinesis. Specifically Aurora Kinase B is a chromosomal passenger protein that is involved in the attachment of the microtubules of the mitotic spindle to the centromere. Therefore inhibition of Aurora Kinase B was expected to result in failure of cytokinesis and polyploidy (Gadea and Ruderman, 2005).

A375 cells were treated with a range of concentrations of AZ12253801 for 48 hours and DNA content was assessed by flow cytometry, and cell morphology by immunofluoresence. A specific Aurora Kinase B inhibitor (ADZ 1152-HQPA), provided by AstraZeneca, acted as a positive control and produced polyploidy in the majority of A375 cells. AZ12253801 was seen to induce polyploidy in a dose dependent fashion (Figure 4.7). A large increase in the proportion of polyploid cells was observed at

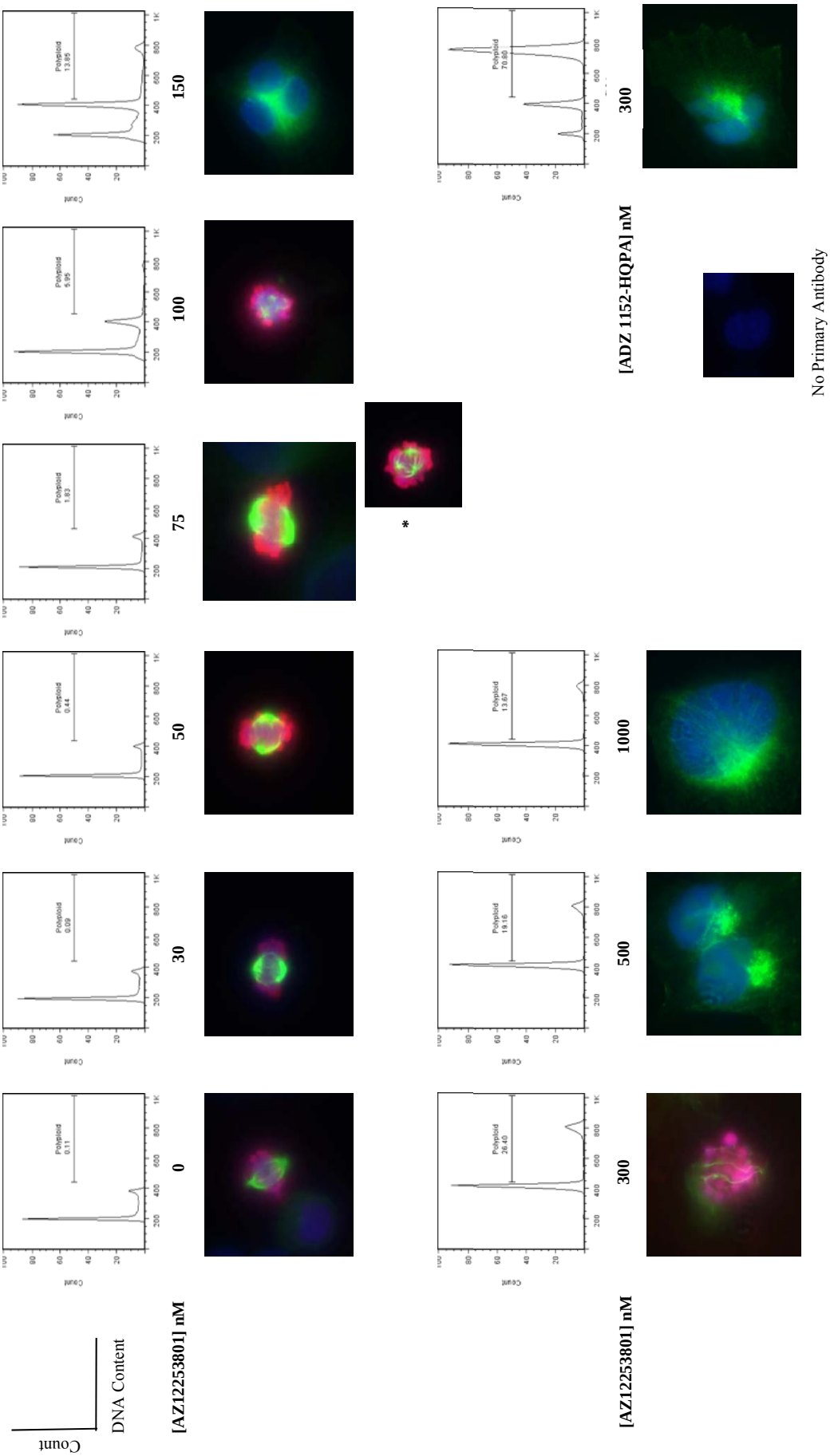
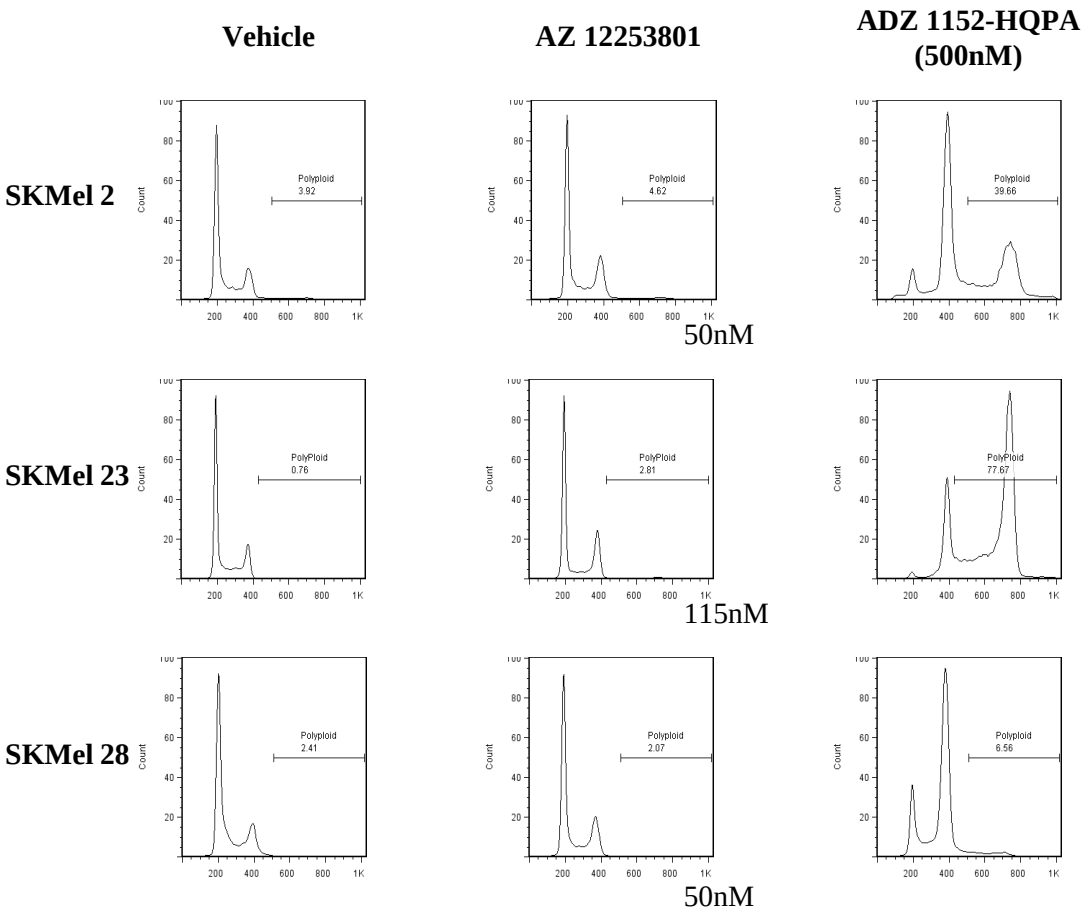


Figure 4.7 Effect of AZ12253801 on DNA content of A375 melanoma cells. A375 cells were treated for 48 hours with increasing concentrations of AZ12253801 or ADZ 1152-HQPA, an Aurora Kinase Inhibitor, before flow cytometric analysis for DNA content or immunocytochemical staining (βTubulin (green), Phospho-Histone H3 (red) or DNA (blue)). Significant polyploidy and abnormal mitotic figures were seen at concentrations of AZ12253801 above 100nM. Figures show typical metaphase mitoses. * Insert shows atypical mitosis seen in less than 1% of cells at 75nM AZ12253801.

concentrations of AZ12253801 over 100nM, with abnormal mitoses lacking obvious chromosomal alignment around centrioles. With increasing AZ12253801 concentration, cell size was seen to increase, and these large cells contained several poorly separated "nuclei" consistent with an Aurora Kianse B inhibited phenotype. The effects of AZ12253801 on Aurora Kinase B were assessed by flow cytometry in the three remaining cell lines (SKMel2 SKMel23 and SKMel28). After 48 hour incubation with AZ12253801, there was a dose dependent increase in the proportion of polyploid cells (Figure 4.8). In SKMel2 and SKMel28 cells there was little or no increase in polyploidy above baseline values at the GI_{50} concentration of AZ12253801 (50nM in each case). SKMel23 cells showed a modest increase in the proportion of polyploid cells at the GI_{50} of 115nM with a greater increase at 300nM than in the other cell lines. Given that polyploid cells comprised only 2-5% of cells at the GI_{50} concentrations, it was concluded that Aurora Kinase B inhibition was unlikely to produce significant false positive results in the planned assessment of the transcriptional effect of AZ12253801, and those which did result could potentially be eliminated by the reciprocal nature of the experimental design. It was interesting to note that SKMel28 was relatively refractory to polyploidy induced by the specific Aurora Kinase Inhibitor (AZD 1152 –HPQA) used as a positive control and by high concentrations of AZ12253801. Rather than developing polyploidy, SKMel28 cells underwent G_2 arrest only (Figure 4.8). This finding may explain why SKMel28 growth, assessed by Cell Titer Glo was not completely inhibited by AZ12253801 at high concentrations (Figure 4.5). The cells arrested in G_2 would still be viable and measured by the assay, whereas in the other cell lines polyploid cells and those undergoing mitotic catastrophe might be dying in response to AZ12253801.



% Polyploid cells	AZ12253801 (nM)										ADZ 1152-HQPA (nM)
	0	**3**	**10**	**30**	**50**	**75**	**100**	**115**	**150**	**300**	**500**
SKMel 2	3.9	3.6	3.6	3.9	4.6	5.8	14.0			24.3	39.7
SKMel 23	0.7	0.7	0.7	0.7	0.7	0.7	1.5	2.8	3.3	32.5	77.7
SKMel 28	2.4	1.8	2.0	2.4	2.1	2.2	2.4			5.1	6.6

Figure 4.8 Effect of AZ12253801 on DNA content of SKMel2, SKMel23, SKMel28 melanoma cells. Melanoma cells were treated for 48 hours with increasing concentrations of AZ12253801 or ADZ 1152-HQPA, an Aurora Kinase Inhibitor, before flow cytometric analysis for DNA content. Upper plots show vehicle treated cells, cells treated with AZ12253801 at the GI_{50} and cells treated with ADZ 1152 HQPA. Plots are representative example from 2 independent experiments. Lower table shows mean % polyploid cells from 2 independent experiments for each AZ12253801 concentration. AZ 12253801 at concentrations above the $G1_{50}$ caused polyploidy in SKMel2 and SKMel23 cells but caused G2/M arrest only in SKMel28 cells.

4.3.4 Preparation of RNA for microarray analysis and miRNA qRT-PCR

Based on the results of the previous experiments, A375 was chosen as the cell line to undergo full transcriptome analysis by microarray and miRNA qRT-PCR. A375 carries a single mutation (*BRAFV600E*) that is relevant to clinical melanoma, showed the most complete growth inhibition by AZ12253801 (Figure 4.5) and negligible polyploidy at the GI_{50} concentration (Figure 4.7).

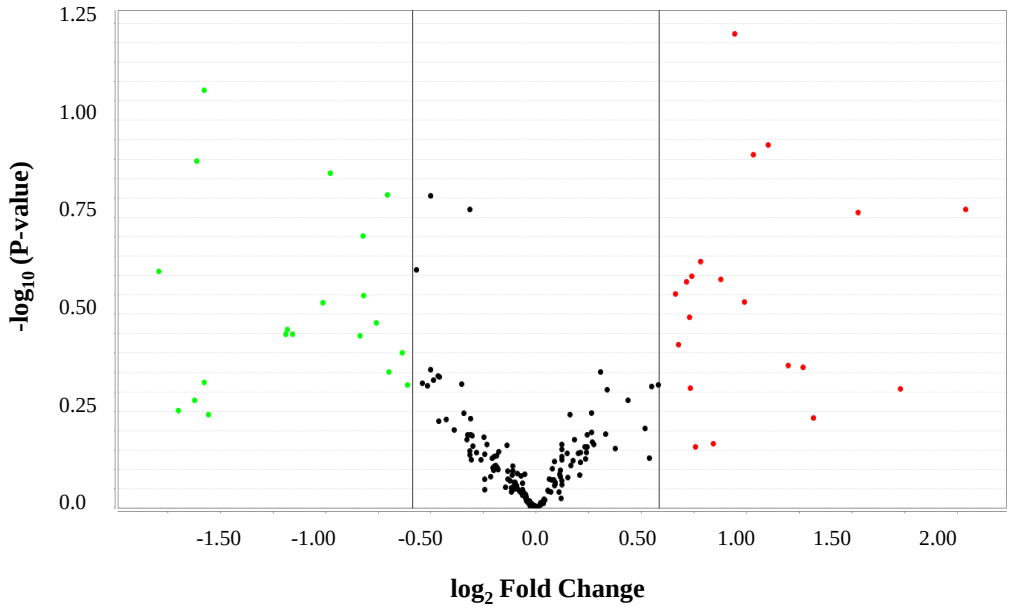
In three independent experiments, A375 cells were treated with IGF1 or solvent following overnight serum deprivation. Parallel cultures were grown in complete medium (with 10% FCS) and treated with 50nM AZ12253801 or vehicle as outlined in Table 4.1. After 3 and 24 hours total RNA was extracted and assessed for integrity. All RNAs met the quality control criteria of a RIN greater than 7, 28S/18S ratio of greater than 1.6, A260/280 of 1.8-2.0 and a A260/230 of close to 1.8. A transcriptional event (increase in cyclin D1 mRNA) was confirmed by qRT-PCR, at the three hour time point following IGF1 stimulation prior to submitting the samples for array analysis. Total RNAs were delivered to the Wellcome Trust Centre for Human Genetics, Oxford c/o Dr Christine Blancher for gene expression profiling using the Illumina Beadchip HT12 system.

Total RNA was prepared from the three other melanoma cell lines SKMel2, SKMel23 and SKMel28 under identical experimental conditions and retained for future validation studies. Aliquots of total RNA for all four cell lines were stored at -70^{o}C for future miRNA analysis.

4.3.5 miRNA qRT-PCR

Assessment of miRNA expression in A375 cells was determined in-house by qRT-PCR of the 754 commonest miRNAs using the recently developed Taqman MicroRNA assay cards A+B v3.0 (Orlova et al., 2011, Revel et al., 2011, Schepeler et al., 2012, Tombol et al., 2010). Results of initial microarray card runs were analysed by Invitrogen technical department (Dr E Geuns) and found to meet the expected performance criteria. In total 48 MicroRNA cards were used to produce miRNA expression profiles from the 3 experimental replicates of the 4 conditions at each timepoint. Not all miRNAs included on the cards amplified, and those that did not were considered to be absent or present at levels outside the detection range of the assay. As expected it was seen that fold changes in individual miRNAs were small and a cut off of a 50% change was used for screening purposes (Calin and Croce, 2006). When normalising miRNA expression to the endogenous controls provided on the microarray cards it was seen that no miRNAs met the criterion of reciprocity ($\log_2$ fold change of >+/-0.58 (absolute change of +/- 1.5)) and reached statistical significance ($-\log_{10}$(pvalue) of 1.30 ($p<0.05$)). For example, 24 hour treatment with IGF1 did not induce a significant change in any miRNA (Figure 4.9). On examination of the raw data it was seen that small differences in Ct values between experimental replicates which in the context of the small fold changes induced was responsible for the lack of significant differences. Furthermore it was seen that the microarray card endogenous controls (MammU6, RNU44, RNU48) varied across the experimental conditions. Such variation of "standard" miRNA endogenous controls has previously been documented (H.Gee DPhil Thesis) and it was clear an alternative method of normalisation was required. Using Genorm software the least variant miRNAs across the eight experimental conditions were determined. In all four comparisons, for example solvent verses IGF1 treated cells at 3 hours, the Genorm program reported 166 miRNAs,

A



B

miRNA	AZ25513801		IGF1	
	Fold Change	P-value	Fold Change	P-value
hsa-miR-155			0.315	0.044
hsa-miR- 20b	1.571	0.044		
hsa-miR-200b	1.925	0.014	0.568	0.018

Figure 4.9 Analysis of changes in miRNA expression after IGF1R stimulation or inhibition in A375 cells. A375 cells were treated with 50nM AZ12253801 or 8nM IGF1 and total RNA extracted after 3 and 24 hours. miRNA expression was determined using Taqman MicroRNA Assay Cards A+B V3.0 (Life technologies). **A)**. Volcano plot generated using Data Assist v2.0 (Invitrogen) software showing log_2fold change against $-log_{10}$(p value) for miRNAs affected by IGF1 treatment at 24 hours (red points log_2fold change >0.58, green points log_2 fold change <0.58). A similar plot was seen for miRNA at 3 hours. No miRNA meet the selection criteria: log_2 fold change of >±0.58 (absolute change of >±1.5) and a $-log_{10}$(pvalue) of 1.30 ($p<0.05$) **B)** Fold changes at 3 hours of miRNAs selected for validation based on a reciprocal change on IGF1R inhibition and stimulation (miR-200b normalised to miR31) or known relationship with genes of interest identified on microarray analysis (miR-155 & miR-20b normalised to MammU6, RNU44, RNU48 expression).

the maximum number calculable, with an M score <0.125, where transcripts with an M score <0.15 are considered suitably invariant for use as reference transcripts. This was further evidence that a significant proportion of miRNAs did not alter significantly on IGF1R manipulation. hsa-miR-186, hsa-miR-26a, hsa-miR-93 were chosen as the least variant miRNAs across all experimental conditions and the least variant miRNA within each comparison was identified, for example has-miR-31 comparing solvent and IGF1 treated samples at the 3 hour time point. However given the low M scores a large number of miRNAs could have served as reference miRNAs. The data were then normalised to each of these reference miRNAs and a list of miRNAs undergoing significant change was generated. These putative hits were assessed for consistency across the experimental replicates and those with an inconsistent direction of change eliminated. Finally the miRNAs were assessed for a reciprocal change in expression following IGF1R stimulation and inhibition. hsa-miR-200b at the three hour time point was identified as the only miRNA reciprocally regulated in any of the four experimental comparisons. Finally software which predicts putative targets of miRNA based on sequence analysis (Targetscan, Pictar) was used to identify miRNAs whose targets had been found to change significantly on microarray analysis (Table 4.1). hsa-miR-20b and hsa-miR-155 were selected for further validation on this basis. Both had significantly altered expression at the 3 hour time point following IGF1 or AZ12253801 treatment (Figure 4.9B).

The miR 200 family to which hsa-miR-200b belongs is frequently down regulated in cancers and has been shown to play a critical role in suppression of epithelial to mesenchymal transition (EMT), Wnt signalling, and resistance to EGFR inhibitors (Mongroo and Rustgi, 2010). Similarly hsa-miR-155 has been shown to have roles in regulation of apoptosis, differentiation and proliferation in breast cancer (Mattiske et al.,

2012). Finally hsa-miR-20b is a member of the miR-17 family which has been associated with suppression of apoptosis and proliferation via *MYC* (Olive et al., 2010).

4.3.6 Validation of miRNA of Interest

The three selected miRNAs, miR-200b, miR-20b and miR-155 were validated by performing PCR reactions on the original triplicate samples of independently derived cDNA using individual Taqman primers and normalising data to the expression of hsa-miR-31. There was no change in miRNA 20b expression across the experimental conditions (Figure 4.10). Expression of hsa-miR-155 varied between experimental replicates and only one experimental replicate showed an increased expression after AZ12253801 treatment. Expression of hsa-miR-200b decreased in two experimental replicates after AZ12253801 treatment, whilst replicates showed a conflicting direction of change following IGF treatment. Results from a colleague using the same microarray card system had similarly produced miRNA hits which could not be subsequently validated using individual miRNA primers (C. Blick DPhil Thesis).

On discussion with the manufacturer it became apparent that both the data generated in this project, and the experience reported to them from other users had led to the conclusion that the microarray cards had a low dynamic range, and were therefore of insufficient sensitivity to identify relatively modest changes in miRNA expression. This was frustrating because it is well documented that changes in miRNA are typically 1-2 fold, in contrast to the major changes often found in mRNA expression (Calin and Croce, 2006), and was not the manufacturer's advice at the time of microarray card procurement. Instead it was suggested that use of cluster analysis would facilitate recognition of broad families of miRNAs whose members could then be interrogated individually (Dr E Guens,

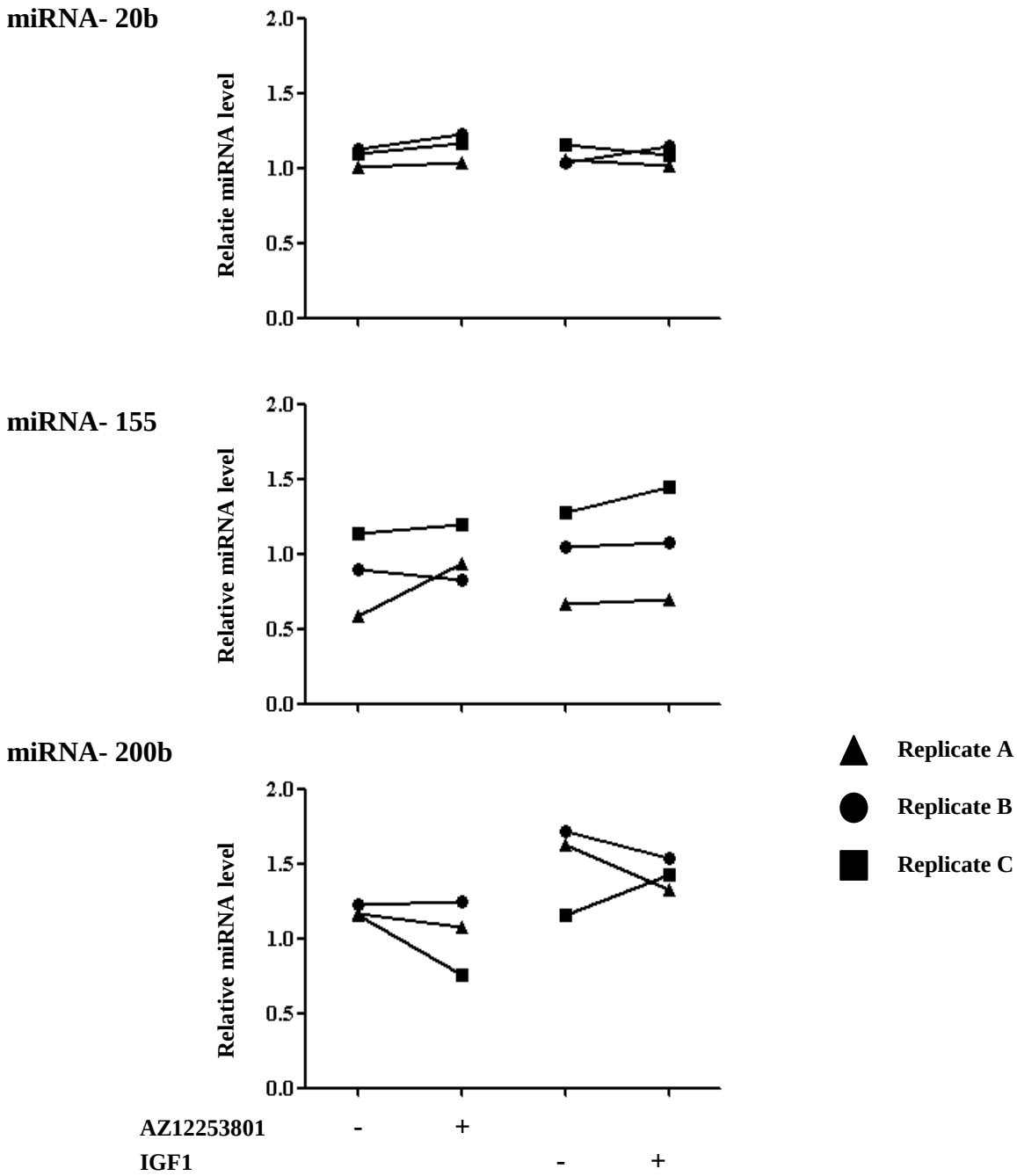


Figure 4.10 Effect of IGF1R stimulation or inhibition on miR-155, miR-20b and miR-200b expression. A375 cells were treated for 3 hours with 50nM AZ12253801 or vehicle, or ,after serum deprivation, with 8nM IGF1 or solvent. RNA was harvested and qRT-PCR for miRNA performed using individual Taqman primers. Graphs represent miRNA expression for the 3 independent biological replicates each of which was analysed by qRT PCR in triplicate and normalised to miR31.There was variation in miRNA expression between biological replicates. Overall no difference in miRNA expression was seen either following IGF1R inhibition or stimulation.

Invitrogen Technical Dept personal communication). Cluster analysis of the above data was performed but it did not identify any miRNA families which warranted further investigation. Furthermore given the discrepancy between the results produced by the Taqman Arraycards and the individual validation experiments, there was little confidence in the results produced by the Array cards. In light of this information it appears that the novel microarray card technology was not an appropriate technique to identify individual miRNAs regulated by IGF1R activation or inhibition, and that a bioinformatic deep sequencing technique would have been more suited to this purpose (Friedlander et al., 2008, Berezikov et al., 2006). Given the paucity of significant miRNA hits and a failure to validate the three chosen miRNAs, it was decided not to pursue this avenue of investigation further.

4.3.7 Bioinformatic analysis of microarray data

Normalisation and subtraction analysis of the raw data produced by microarray analysis was carried out by Dr Steve Taylor of the Computational Biology Group using the R statistical language with Bioconductor and LIMMA software package. Global normalisation, centring and scaling was successfully performed both within and between slides using standard techniques and will not be described here (Smyth, 2004, Smyth and Speed, 2003, Smyth et al., 2003). Differential expression was then determined between the data sets for IGF1R inhibitor and vehicle treated cells, or IGF1 and solvent treated cells at the 3 and 24 hour time points. Statistical analysis was performed and the data from the 10,000 most significant probes for each comparison presented in the form of a logarithmic fold change, moderated t statistic, p value and adjusted p value and B statistic (presented in Appendix 1-4). The author performed all subsequent analysis.

4.3.8 Screening for differential expression

Transcripts with a $\log_2$ fold change of ±0.38 (1.3 fold absolute change) were considered to have changed sufficiently to be of interest. The t statistic, p value (moderated t test) and p value adjusted for multiple testing are low power discriminatory tests as they interrogate individual transcripts alone, are strongly influenced by small standard deviations and were not considered further. The B statistic is generated by an Empirical Bayes approach which ranks transcripts to determine if the transcript is statistically significantly differentially expressed. It is effectively the logarithm of the ratio of probabilities that a transcript is differentially expressed, but is corrected for multiple testing by assuming that 1% of transcripts are differentially expressed.

$$Probability\ that\ a\ transcript\ is\ differentially\ expressed\ = \frac{e^B}{e^{B+1}}$$

$$Or\ more\ simply\ if\ B = 3 \quad P = \frac{e^3}{e^{3+1}} = 95.6\% \quad ie\ P \leq 0.044$$

Consequently transcripts with B≥ ±3 were considered to be significantly differentially expressed (Smyth, 2004).

Eleven transcripts were found to be differentially expressed following AZ12253801 treatment at the 3 hour time point and six transcripts at the 24 hour time point (Appenidx 1 and 2). In contrast 251 and 2861 transcripts were differentially expressed following IGF1 treatment after 3 hours and 24 hours respectively (Appendix 3 and 4). This is similar to the 2154 IGF1 regulated transcripts identified in the MCF7 breast cancer cell line after 24 hours (Creighton et al., 2008) and considerably more than 370 IGF regulated transcripts in stromal fibroblasts under similar experimental conditions (Rajski et al., 2010). Whilst it was anticipated that addition of a mitogen to serum starved cells would result in more transcriptional activity than inhibition of a single tyrosine kinase receptor, the degree of

the discrepancy was striking. Furthermore the fold changes in gene expression following IGF1R inhibitor treatment were generally small and of similar magnitude to those reported with NVP-AEW541, another small molecule inhibitor of the IGF1R, although this was used at a concentration of 5 X GI_{50} (Bielen et al., 2011).

The difference in magnitude of transcriptional changes induced by IGF1 and AZ1253801 is given further weight when considering the hierarchical clustering between the gene normalised expression of the individual samples (Figure 4.11). The gene expression profiles of the IGF1 treated sample at 24 hours (designated 8) and 3 hours (designated 4) clearly segregated from the corresponding solvent treated groups (7 and 3 respectively). In contrast AZ12253801 inhibitor treated gene expression at 3 (designated 1) and 24 hours (designated 5) clustered with the vehicle treated cells (2 and 6 respectively). Indeed in one case (2B) there was more similarity between one of the experimental replicates from vehicle treated cells and the inhibitor treated samples, than with the other vehicle treated samples (2A, 2C).

It is possible that signalling and transcriptional responses to AZ12253801 were attenuated by compensatory signalling via parallel signalling cascades. Such responses have been documented (Desbois-Mouthon et al., 2009). However given that it had been previously shown that AZ12253801 was capable of suppressing basal AKT phosphorylation after 3 and 24 hours exposure (Figure 4.6) it seemed likely that AZ12253801 treatment was likely to influence gene expression, at least via AKT inhibition. Irrespective of mechanism the conclusion which must be drawn is that inhibition of the IGF1R with AZ12253801 at a GI_{50} concentration had minimal effects on the transcriptome of A375 melanoma cells.

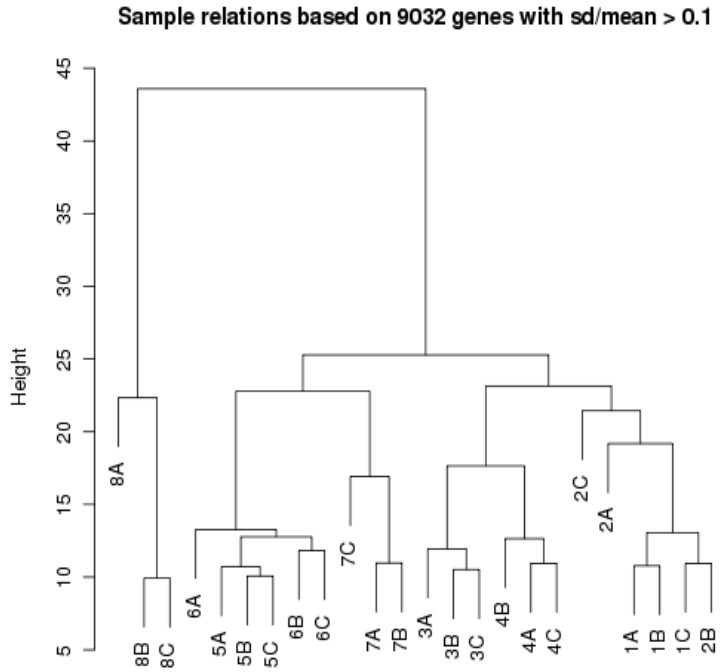


Figure 4.11 Dendrogram of sample clustering. Samples and replicates were assessed for hierarchical clustering on the basis of 9032 genes with a standard deviation/mean >0.1. Vehicle (1 & 5) and AZ12253801 treated (2 & 6) samples clustered together. In contrast Solvent (3 & 7) and IGF-1 treated (4&8) samples clustered separately.

KEY:

1 – Vehicle 2 –+ AZ12253801 3 – Solvent. 4 – + IGF-1	3H	5 – Vehicle 6 – + AZ12253801 7 – Solvent 8– + IGF-1	24H

A,B,C refer to the three biological replicates.

Transcripts altered by IGF1 treatment included previously published transcriptional targets of IGF1. Expression of *FOXO3* transcription factors were decreased on IGF treatment at 3h and *INSIG1* was increased at 24h (Essaghir et al., 2009, Stitt et al., 2004, Creighton et al., 2008). Similarly IGF1 altered expression of cyclins (*CCNA1, CCND1, CCNI*), cell division cycle proteins (*CDC20, CDC26, CDC42, CDC123, CDC14B*) and cyclin dependent kinases (*CDK19, CDKL3, CDKN1A, CDKN1B, CDKN2D*) (Creighton et al., 2008, Rajski et al., 2010). Finally *BCL-X(L)* which has recently been shown to be both induced by IGF1 and confer resistance to apoptosis in MeWo, another melanoma cell line, was seen to be increased in response to IGF1 in A375 cells (Hilmi et al., 2007). However BCL2 was unchanged and BIRC5 (survivin) decreased in contrast to the increases documented in MeWo cells. This was of interest as BCL2 and BCL-X(L) expression have been correlated to resistance to BMS-536924, an IGF1R small molecule inhibitor, in sarcoma cell lines (Huang et al., 2009).

Considering the components of the IGF1R signalling pathway itself, it was interesting to note that *CTCF* (*IGFBP-rP2*) showed altered expression in response to 3 hour IGF1 treatment (Appendix 3). Thus even at short time points there was evidence that IGF1R signalling is modulated by consequential transcriptional events. This pattern was more pronounced at 24 h when several other genes (*IRS2, AKT, SHC1, IGFBP1,3,6*) in the IGF1R cascade had showed altered expression, usually downregulation. Similar findings have been previously reported in MCF7 breast cancer cells, and probably represent feedback control of IGF1R signalling (Creighton et al., 2008, Pacher et al., 2007). Additionally IGF1 signalling had transcriptional consequences on other parallel signalling cascades including those activated by hepatocyte growth factor (HGF) and EGF. In toto three cytokines, two growth factors, eighteen kinases and thirty transcriptional regulators

showed altered expression at 3 hours, whereas at 24 hours ten cytokines, twenty G coupled receptors, eight growth factors and 64 kinases demonstrated altered expression.

Worthy of particular note, vascular endothelial derived growth factor (*VEGF*) was unchanged on IGF1 treatment of A375 cells unlike in breast cancer cell lines, primary human breast epithelial cells and fibrobasts (Pacher et al., 2007). Finally in addition to the screen hits previously known to be IGF regulated, several hits were either novel, or at least had not been highlighted in previous studies, and were of particular interest. These are discussed in a subsequent section.

4.3.9 Assessment of changes in expression of genes involved in immune recognition of tumour cells

As detailed in the previous chapter, depletion of the IGF1R using nucleic acid based technologies has been shown to increase the immunogenicity of tumour cells. During assessment of the transcripts altered in this experiment particular attention was paid to genes involved in immune recognition of tumour cells. The genes altered in expression by IGF1R inhibition did not involve those involved in tumour recognition. In contrast IGF1 treatment induced upregulation of many proteins involved with the unfolded protein response (*HSP90AA1, HSPA2, HSPA6, HSPA8, HSPA14, HSPA1A/1B, HSPA1L, HSPD1*), recognised as tumour antigens in melanoma or involved in antigen presentation (*TAP1, TAP2*). These changes might be expected to render cells more immunogenic after IGF1R activation. These findings were in contrast to previous work in our laboratory which had shown no changes in *TAP1* or *TAP2* expression after siRNA mediated depletion of IGF1R in CHL1 melanoma cells (A.Yeh DPhil Thesis). Given that increased immunogenicity of IGF1R inhibited cells has not previously been documented, these results would add further

justification to experiments such as outlined in the conclusions to Chapter 3. However one finding was consistent with the experimental results documented in Chapter 3. MHC Class1 expression (HLA-B) was reduced by IGF1 treatment and thus the changes documented in section 3.2.2 might be explained by transcriptional changes as previously reported (Saji et al., 1992, Ito et al., 2004, Giuliani et al., 2006).

4.3.10 Data mining for pathway representation and determination of an IGF1 induced gene signature.

Data from all transcripts with a B statistic greater than 3 were analysed through the use of Ingenuity Pathway Analysis software (Ingenuity Systems, Redwood City CA, USA). This allowed identification of gene sets present in the data with reference to a series of pathways/networks generated from the available literature. Of the 251 transcripts identified at 3 hours with a B value greater than 3, 232 were suitable for Ingenuity analysis, the remainder being either from duplicate probes or from genes not present in the Ingenuity reference dataset. As expected based on its biology and previous studies, gene sets identified as highly statistically significantly enriched within the data were principally concerned with cellular development, growth, gene expression, cell death (principally apoptosis) and the cell cycle (Figure 4.12) (Dupont et al., 2003, Creighton et al., 2008, Rajski et al., 2010). Of the genes present in these data sets, many were altered by IGF1. On consideration of canonical pathways represented within the dataset, p53, G_1/S checkpoint regulation and Wnt signalling have been previously reported in the literature (Rajski et al., 2010, Creighton et al., 2008). At the 24 hour time point 2345 transcripts of the 2607 with a B statistic greater than 3 were suitable for Ingenuity analysis. The networks identified as most significantly represented were similar to those at 3h but their relative significance had altered. Furthermore fewer transcripts within each pathway showed regulation by IGF1.

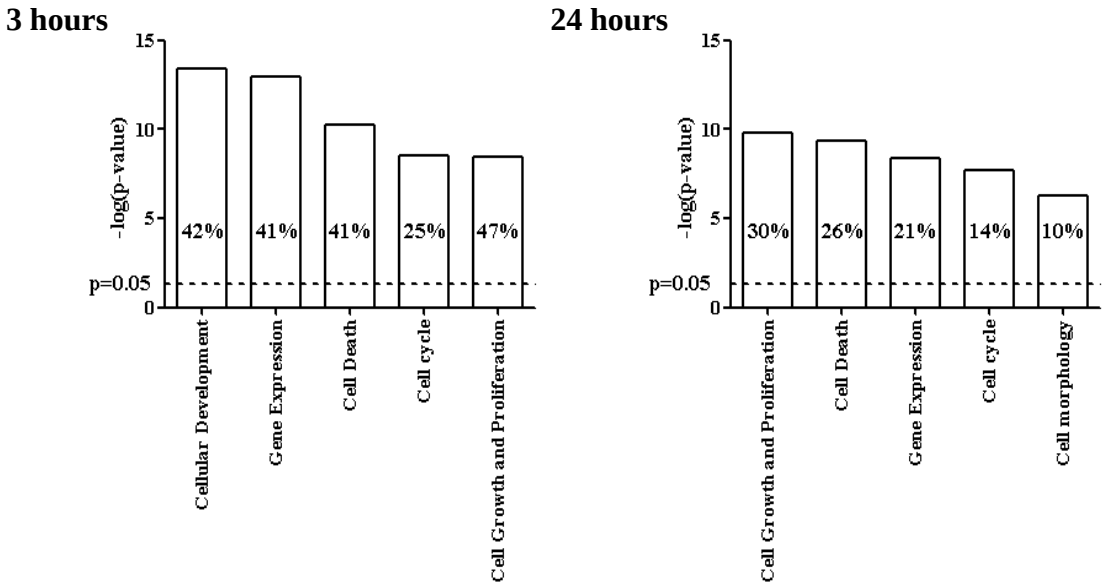


Figure 4.12 Networks overrepresented in IGF1 induced gene sets at 3 and 24 hours. Transcripts altered by IGF1 at 3 and 24 hours, with a B statistic greater than 3, were analyzed using Ingenuity software. The five most statistically significantly over represented gene networks at 3 and 24 hours are displayed. Percentages refer to the portion of total genes in the network whose transcription is altered by IGF1. Networks represented are similar at 3 and 24 hours and are those involved with cell proliferation and gene expression. Fewer genes in a given network are altered 24 hours after IGF1 stimulation than were affected at 3 hours.

Ubiquitination was a canonical pathway overrepresented in the dataset due to the substantial increase in Ubiquitin mRNA 24 hours following IGF1 treatment. This finding was surprising as IGF1 has previously been shown to suppress expression of Ubiquitin and ubiquitin ligases in muscle and perhaps warrants further attention in the future. Particularly because expression of elements of the ubiquitination pathway have previously been shown to correlate to sensitivity to IGF1R inhibition in colon cancer cell lines (Stitt et al., 2004, Fang et al., 2000, Zha et al., 2009). At both the 3 and 24 hour time points the disease network most statistically significantly expressed was "cancer" which was not surprising as this network comprises significant proportions of the cellular development, cellular growth, gene expression, cell death and the cell cycle networks.

The dominance of transcripts associated with cellular proliferation could be interpreted to indicate that IGF1R has a central, perhaps essential, role in this cellular process. However it must be noted that melanoma cells had been serum starved prior to IGF1 incubation and this is a distinctly non-physiological condition. In the reciprocal experiment in which IGF1R was inhibited, very few transcripts were significantly altered, suggesting that the contribution of IGF1R must be considered in context of availability of other ligands. Similarly the fall in the proportion of transcripts associated with cell proliferation at 24 hours does not indicate a temporal role of IGF1R signalling in cellular proliferation, rather that exposure to IGF1 may be insufficient to maintain proliferation in an otherwise mitogen free environment. It is particularly interesting to note that the expression of only 15 genes were altered in MCF7 cells overexpressing IGF1 compared with vector transfected cells (Pacher et al., 2007), in contrast to 2154 in serum deprived MCF7 cells stimulated with IGF1 (Creighton et al., 2008). This emphasises that gene expression induced by IGF1 depends on the cellular environment, and duration of mitogen exposure.

In spite of these reservations, it was clear that the transcripts identified on IGF1 stimulation at 3 and 24 hours were consistent with the predicted effects of IGF1 on cellular function and the previously described patterns of IGF1 induced genes. Within these functional groups were novel hits worthy of further investigation as discussed below. Overall transcripts with a B statistic greater than 3 were considered to represent the "IGF1 induced gene signature" in human melanoma cells at 3 and 24 hours and were used for the interrogation of clinical data sets. The IGF gene signature was separated into the IGF up regulated gene signature and IGF down regulated gene signature at each time point.

4.3.11 *In silico* analysis of clinical melanoma datasets

Given the similarities in gene expression between the generated data and that previously published it was also interesting to determine the similarity of the gene expression profiles, particularly because a published MCF breast cancer cell line IGF gene profile had been shown to be of prognostic significance in breast cancer (Creighton et al., 2008). The IGF1 induced breast cancer MCF7 gene signature was obtained from the authors and compared for similarity to the generated A375 IGF1 induced gene signatures. Analysis was performed by Dr Francesca Buffa (WIMM) using software designed in-house. Results were assessed for relevance by the author. *Italics* are used to distinguish the previously published MCF gene signature from that generated from A375 cells in this project.

The MCF IGF gene signature consisted of 1005 genes altered by IGF1 at both 3 and 24 hours. This was broken down into the *MCF7 IGF up regulated gene signature* and *MCF7 IGF down regulated gene signature* for comparison with those generated from A375. The *MCF7 IGF up regulated gene signature* consisted of 482 genes, 21 of which were shared

with the A375 IGF up regulated gene signature at 3 hours and 85 with the A375 IGF up regulated gene signature at 24 hours (Apendix 5). Similarly the *MCF7 IGF down regulated gene signature* consisted of 523 genes, 21 of which were shared with the A375 IGF down regulated gene signature at 3 hours and 73 with the A375 IGF down regulated gene signature at 24 hours (Appendix 6). As expected within these shared genes there were components of, and transcriptional targets of, the IGF1R signalling cascade such as *IRS2* and *INSIG1*. However it was interesting to note that components of the Wnt pathway such as frizzled family receptor 2 (*FZD2*) and 7 (*FZD7*), frequently rearranged in advanced T-cell lymphoma 1 (*FRAT1*) and 2 (*FRAT2*), HMG-box transcription factor 1 (*HBP1*) were also shared. Given that the relative significance of the canonical Wnt/β-catenin pathway differs between breast cancer and melanoma as discussed in the introduction, this was unexpected and is discussed further below.

The next analysis sought to assess whether the A375 IGF gene signature was of prognostic significance in melanoma. The Gene Expression Omnibus (GEO - http://www.ncbi.nlm.nih.gov/geo/) was interrogated for melanoma clinical data sets in which gene expression had been correlated to clinical parameters. Two data sets were identified: a data set of gene profiles of 38 melanoma metastases in which mitotic index had been correlated to patient survival (GSE19234) (Bogunovic et al., 2009), and a data set of 57 gene expression profiles from melanoma metastases in which four gene signatures were determined which correlated to patient survival (GSE22153) (Jonsson et al., 2010).

The A375 IGF gene signatures and details of the GEO datasets were provided to Dr Francesca Buffa for bioinformatic analysis. Specifically it was requested that the datasets be interrogated to assess whether the IGF gene signatures were correlated with any clinical

or histopathological parameters. Dataset interrogation was performed by Dr Buffa using software designed in-house. Results of analyses were provided by Dr Buffa and their relevance determined by the author. Given that each parameter was interrogated with respect to the IGF up regulated gene signature and IGF down regulated gene signature at each time point, only parameters significantly associated to the IGF gene signatures in a reciprocal fashion, or at more than one time point were considered relevant.

The IGF gene signatures did not correlate to any recorded parameters, including age, stage or survival, in the first dataset (GSE 19234). In the second dataset (GSE22153) the IGF signatures correlated to molecular subtype, CD3 immunohistochemistry ie T-cell infiltration and Ki67 score. The correlation with Ki67 score was reciprocal for the up and down regulated gene signatures and was considered further. At three hours, genes reduced in expression by IGF1 were expressed to a lower level in tumours with a Ki67 score >30% (Figure 4.13). Conversely genes increased in expression were expressed to a higher level in tumours with a Ki67 score >30%. Ki67 is a cell cycle dependent protein involved in cellular proliferation which can be detected in all phases of the cell cycle except G_0. As such the percentage of cells expressing Ki67 score is used as a measure of proliferation when assessing tumour samples histopathologically and has been correlated to prognosis in primary melanoma and metastatic melanoma lesions (Moretti et al., 1990, Pearl et al., 2007). In short the genes induced by IGF1 were correlated to a marker of cellular proliferation whose expression in metastases has previously been correlated to melanoma prognosis. It is therefore not unreasonable to suggest that IGF1R regulated genes may influence prognosis.

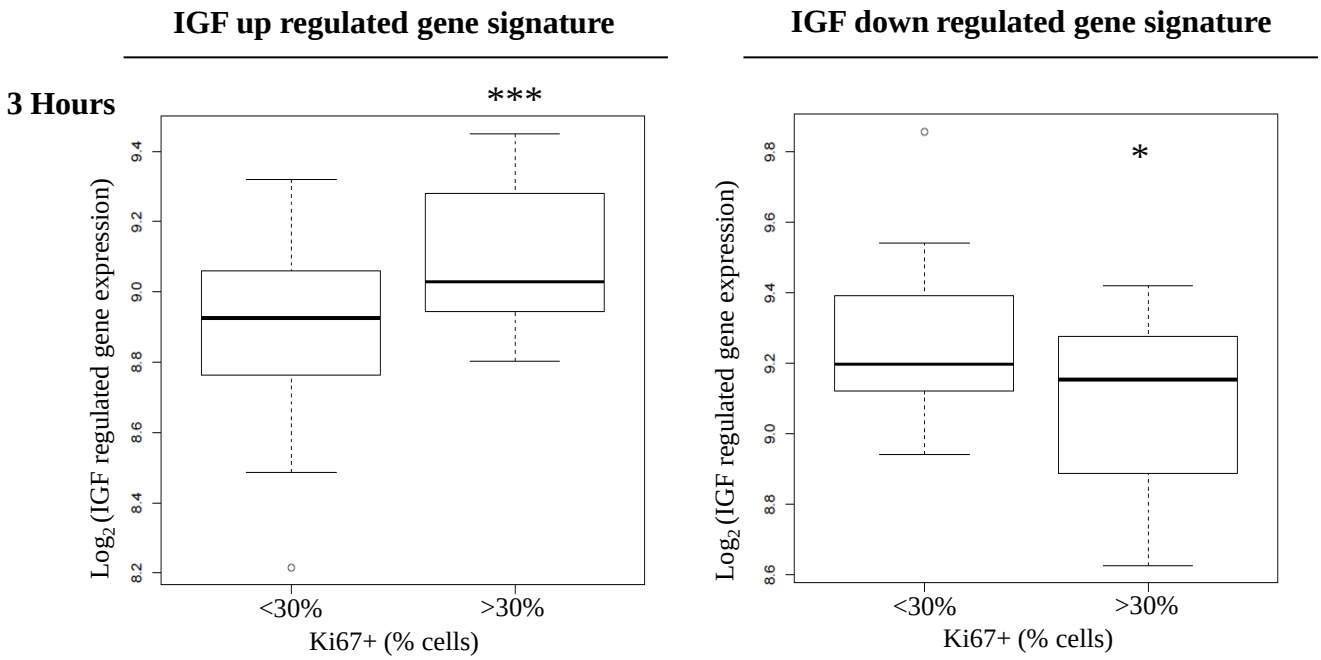


Figure 4.13 Correlation of IGF induced gene signature at 3 hours to Ki67. Gene expression of Ki67% high (>30%) and low (<30%) melanoma metastases from GEO dataset GSE 22153 were compared to the IGF up and down regulated gene signatures at 3 hours. IGF up and down regulated genes at 3 hours were expressed to a greater and lesser degree respectively in high Ki67% tumours compared to low Ki67% tumours

* P<0.05, *** P<0.005 by Kruskal Wallis Chi squared test

Thus the A375 IGF gene signature had been shown to correlate to Ki67, a well characterised melanoma prognostic marker, and there was marked similarity between the A375 IGF gene signature and the MCF IGF gene signature, which itself was of prognostic significance in breast cancer. Given that only 2 relatively small melanoma datasets had been available to assess correlations with survival, it was decided to assess the prognostic relevance of the A375 IGF gene signature in breast cancer. Five GEO breast cancer datasets were identified, representing a total of 897 cases: GSE 6532 (separated into two cohorts KI and OXF) (Loi et al., 2007), GSE6532 (Loi et al., 2007), GSE9165 (Loi et al., 2008), GSE1456 (Pawitan et al., 2005) and GSE2034 (Wang et al., 2005). The IGF up regulated and down regulated gene signatures at 3 and 24 hours were assessed for correlation to recurrence free survival in the identified datasets. In all four analyses the A375 melanoma IGF gene signature was correlated to prognosis in breast cancer. In particular there was an association between the IGF down-regulated gene signature at 3hr and reduced risk of relapse, and the IGF up-regulated gene signature at 24hr and increased likelihood of relapse (Figure 4.14).

Overall bioinformatic analysis had shown that the devised IGF gene signature was correlated to Ki67, a prognostic marker in melanoma, and to prognosis in breast cancer. The findings in breast cancer were considered to validate the A375 gene signature. However of more importance was the suggestion that IGF induced changes in gene transcription were correlated to a clinically significant parameter in melanoma, providing additional rationale for targeting the IGF1R in melanoma.

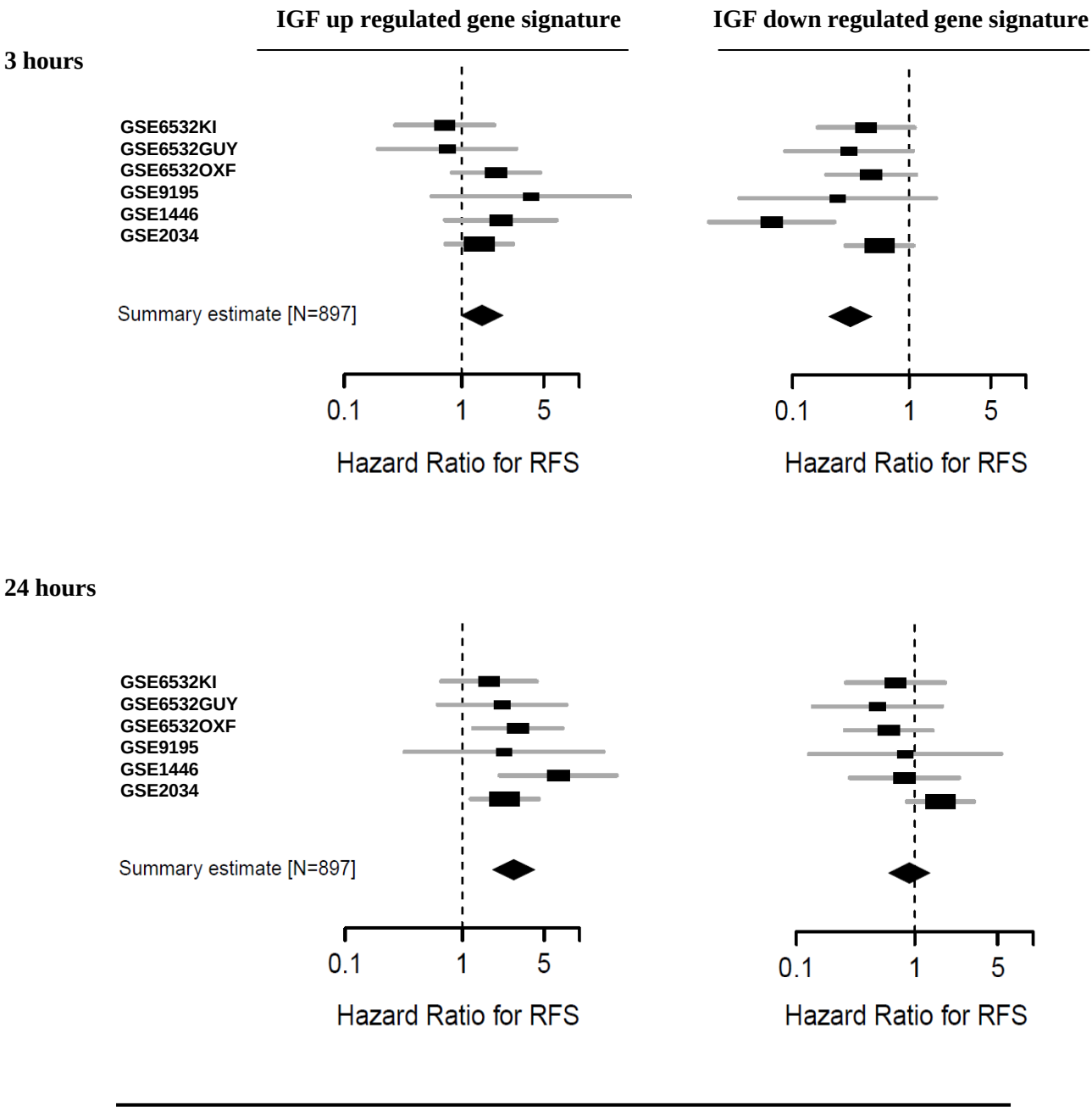


Figure 4.14 Correlation of melanoma IGF gene signature with prognosis in breast cancer. Six datasets of gene expression from breast cancer biopses were assessed for expression of the A375 melanoma IGF up regulated and down regulated gene signatures at 3 and 24 hours and expression correlated to the hazard ratio for relapse free survival (RFS ie the likelihood of relapse) The IGF up and down regulated gene signatures for 3 hours were correlated to an increased and decreased likelihood of relapse. The IGF up regulated gene signature for 24 hours was correlated to an increased likelihood of relapse.

4.3.12 Data mining for transcripts altered in a reciprocal fashion by IGF1R inhibition and stimulation.

The experimental design allowed identification of genes whose expression was affected in a reciprocal way by IGF1 ligand and IGF1R inhibitor treatment. This was considered the most appropriate strategy for identifying transcripts which were likely to be affected during clinical treatment with an IGF1R inhibitor, whilst excluding any transcripts affected through a mechanism other than inhibition of IGF1R itself.

Of the genes differentially expressed at 3 hours following AZ12253801 inhibitor treatment, five were found to be reciprocally regulated by IGF1 (Table 4.3). Similarly two genes were found to be reciprocally regulated at 24 hours. It was noteworthy that in all of these cases of reciprocal change, IGF1R inhibition had increased transcription and IGF1 stimulation reduced transcription. In contrast IGF1 stimulation tended to increase transcription in the majority of significantly altered transcripts, at least at the 3 hour time point. The reason for this observation that reciprocally regulated targets opposed the general pattern of change is unclear but it implies that the transcripts regulated by IGF1R inhibition were not reduced as a result of direct withdrawal of IGF1 driven transcription.

The seven genes which had been identified as reciprocally altered could be categorised as those involved with apoptosis; Interleukin 24 (*IL-24),* NADPH Oxidase 4 (*NOX4),* Chaperone activity of bc1 complex-like, mitochondrial *(CABC)* and Unc-51-like kinase 1 (*ULK1*); the Wnt signalling pathway, *HBP1* and *FRAT2*, and melanoma progression, SIS homeobox 5 (*SIX5*) (Table 4.3). All had been previously implicated to a greater or lesser extent in cancer biology.

	AZ12253801 Treatment		IGFI Treatment			
	log_2 Fold Change	**B-statistic**	**log_2 Fold Change**	**B-statistic**	**ILMN_Gene**	**Definition**
3h						
	0.677	4.508	-1.828	21.718	HBP1	HMG-box transcription factor 1 (HBP1), mRNA.
	0.522	4.022	-0.650	7.455	SIX5	SIX homeobox 5 (SIX5), mRNA.
	0.481	3.335	-0.747	10.154	CABC1	ABC1 activity of bc1 complex homolog (S. pombe) (CABC1) mRNA.
	0.451	4.259	-0.967	17.218	FRAT2	Frequently rearranged in T-cell lymphomas 2 (FRAT2), mRNA.
	0.424	4.961	-0.695	13.405	ULK1	unc-51-like kinase 1 (C. elegans) (ULK1), mRNA.
			1.953	19.783	CTGF	Connective tissue growth factor (CTGF), mRNA.
			1.626	20.892	LIF	Leukemia inhibitory factor (LIF), mRNA.
			-0.716	7.367	TOB1	Transducer of ERBB2, 1 (TOB1), mRNA.
24h						
	0.741	5.718	-0.738	6.910	IL24	Interleukin 24 (IL24), transcript variant 1, mRNA.
	0.599	6.776			IL24	Interleukin 24 (IL24), transcript variant 2, mRNA.
	0.623	3.781	-1.278	16.771	NOX4	NADPH oxidase 4 (NOX4), mRNA.

Table 4.3 Gene transcripts chosen for further validation. Genes with a B statistic >3 and a log_2 fold change >+/-0.38 were chosen for further investigation on the basis of a reciprocity of change on AZ12253801 and IGF-1 treatment at either the 3 or 24 hour time points. B statistic refers to the log odd ratio of a gene being differentially expressed, B>3 is equivalent to P<0.04. Seven transcripts met these criteria (*HBP1, SIX5, CABC, FRAT2, ULK1, IL24 v1* & *NOX4*). Of these, two (*CABC1* & *ULK1*) chosen at the 3 hour time point remained statistically significantly altered 24h after IGF1 treatment. Four additional transcripts were chosen for validation; *IL24 v2* was one of only 4 genes altered by AZ12253801 treatment at 24 hours, *CTCF* and *LIF* transcripts showed the largest fold change of all genes on IGF1 treatment at the 3 hour time point and *TOB1* expression had previously been correlated to sensitivity to IGF1R inhibition (Zha *et al*, 2009).

4.3.12.1 Reciprocally altered genes of interest associated with apoptosis (*IL-24, NOX4, CABC, ULK*)

Interleukin 24 (IL24) is a cytokine, also known as the tumour suppressor protein melanoma differentiation-associated 7 (MDA7), whose expression is lost with neoplastic transformation of melanocytes (Fisher et al., 2003). IL24 has anti-tumour activity in nude mice bearing human cancer xenografts and selectively induces apoptosis in many human cancer cell lines, including melanoma, without effect on normal cells (Fisher et al., 2007). Whilst *IL24 transcript variant 1* showed the reciprocity of change demanded by the selection criteria, *IL24 transcript 2* did not. However given that there were so few genes which showed altered gene expression following AZ12253801 treatment at 24 hours, it was appropriate to validate both variants.

Nicotinamide adenine dinucleotide phosphate (NADPH) oxidase 4 (NOX4) has previously been shown to mediate the antiapoptotic effect of growth factors including IGF1 via the production of reactive oxygen species (Vardatsikos et al., 2009). Whilst IGF1 has been shown to increase NOX4 protein level this was not a transcriptional effect (Meng et al., 2008). Antisense depletion of NOX4 has been shown to inhibit proliferation in melanoma cells (Brar et al., 2002) and NOX4 promotes pancreatic cancer cell survival (Lee et al., 2007a). In contrast to these previous findings *NOX4* mRNA was reduced by IGF1 and increased by inhibition of IGF1R in A375 melanoma cells.

Chaperone activity of bc1 complex-like, mitochondrial (CABC1) is a mitochondrial protein that functions in an electron-transferring membrane protein complex in the respiratory chain. Inhibiting CABC1 expression partially suppresses p53-induced

apoptosis (Iiizumi et al., 2002). *CABC1* had not previously been documented as an IGF1 regulated gene.

UNC-51 -like kinase encoded by *ULK1* is a downstream target of mTOR and is involved in autophagosome formation (Mizushima, 2010). Increased expression of ULK1 has been associated with malignant transformation and negative prognosis in squamous cell carcinoma of the oesophagus, and depletion of ULK1 protects melanoma cells from apoptotic stimuli (Jiang et al., 2011, Wong et al., 2010).

4.3.12.2 Reciprocally altered genes of interest associated with Wnt/β-catenin signalling (*FRAT2, HBP1*)

FRAT2 and FRAT1 are dishevelled (DVL) binding proteins which mediate the dissociation of GSK-3 from axin, disrupting the β-catenin destruction complex following Wnt activation (Li et al., 1999). Up-regulation of FRAT1 and 2 have been documented in gastric carcinoma and are implicated in carcinogenesis through activation of Wnt signalling (Saitoh and Katoh, 2001).

HBP1 is a transcriptional repressor involved in the suppression of Wnt signalling and of cell proliferation (Sampson et al., 2001). HBP1 prevents binding of TCF/LEF family members to DNA, inhibiting Wnt/β-catenin induced transcription. In addition HBP1 is implicated in the loss of RAS induced senescence which accompanies neoplastic transformation (Zhang et al., 2006) and the HBP1 target macrophage migration inhibitory factor (MIF) is over expressed in prostate cancer (Chen et al., 2010). Decreased transcription of HBP1 had previously been described in response to both IGF1 and insulin (Palsgaard et al., 2009), but increased expression had not previously been reported in response to IGF1R inhibition.

4.3.12.3 Reciprocally altered gene of interest associated with melanoma progression (*SIX5*)

Homeobox protein SIX5 is a transcription factor encoded by *SIX5* which is involved in regulation of cellular differentiation particularly during organogenesis (Fougerousse et al., 2002). It activates IGFBP5 expression but has not been previously been described as an IGF1 regulated gene (Sato et al., 2002). IGFBP5 has been associated with melanoma metastasis and is described as a biomarker for melanoma progression (Xi et al., 2006).

4.3.12.4 Other genes of interest

In addition to selecting these reciprocally altered genes, it was noted that IGF1 had induced large $\log_2$fold increases in two additional genes of interest (Table 4.3). Leukaemia inhibitory factor (LIF) is a cytokine that has been implicated in modulation of the immune response, induction of cancer cachexia and either the stimulation and inhibition of tumour growth, depending on the cell type (Szepietowski et al., 2004, Mori et al., 1991).

Connective tissue growth factor (CTGF) is a member of a group of growth factors which in addition to trophic effects (Brigstock, 2003) bear an IGF binding domain. As such CTGF is an IGFBP-related protein, has the alternate designation IGFBP-rP2 (Kim et al., 1997) and acts to antagonise the effects of IGF1. Previously IGF1 treatment of bovine mammary epithelia was reported to decrease production of CTGF, whereas in the data presented above IGF1 stimulation increased *CTGF* mRNA (Zhou et al., 2008). In the case of LIF there were no reports of an association with IGF signalling, in the case of CTGF the data obtained differed to that in the literature. Both of these hits were selected for further validation.

Finally validation of *TOB1* was considered appropriate (Table 4.3). *TOB1* encodes a member of the tob/btg1 family of anti-proliferative proteins which has previously been shown to be down regulated by IGF1 (Creighton et al., 2008, Zha et al., 2009). Of clinical interest, TOB1 expression is a negative prognostic indicator in breast cancer (Helms et al., 2009) and its expression has previously been shown to be correlated to sensitivity to an IGF1R monoclonal antibody in breast and colorectal cancer cell lines (Zha et al., 2009). On this basis TOB1 was considered worth evaluating as a potential predictor of melanoma response to anti-IGF1R therapy.

Interestingly four of the genes chosen for further validation, *CTGF, FRAT2, HBP1, ULK1*, were shared between the A375 and MCF7 IGF gene signatures (Section 4.3.11) (Appendix 5 & 6). As such it was anticipated that validation and further investigation of these genes might inform IGF1R biology in melanoma and in other tumour types.

4.3.13 Cluster analysis and Interactions of Genes of Interest

Cluster analysis was performed on the genes with a B statistic greater than 0 at the three hour time point both for inhibitor and ligand treated cells. The cluster analysis of the genes regulated in inhibitor treated cells is limited by the paucity of significant hits (Figure 4.15). However, it can be seen that the genes of interest chosen on the basis of reciprocity clustered to distinct areas of the IGF1 induced gene heat map whilst those chosen on the basis of large fold changes were distant (Figure 4.16). Whilst it was not intended to select gene targets by such criteria, it was both interesting and reassuring that genes selected on the basis of their expression after inhibitor treatment had similar changes in expression patterns on IGF stimulation.

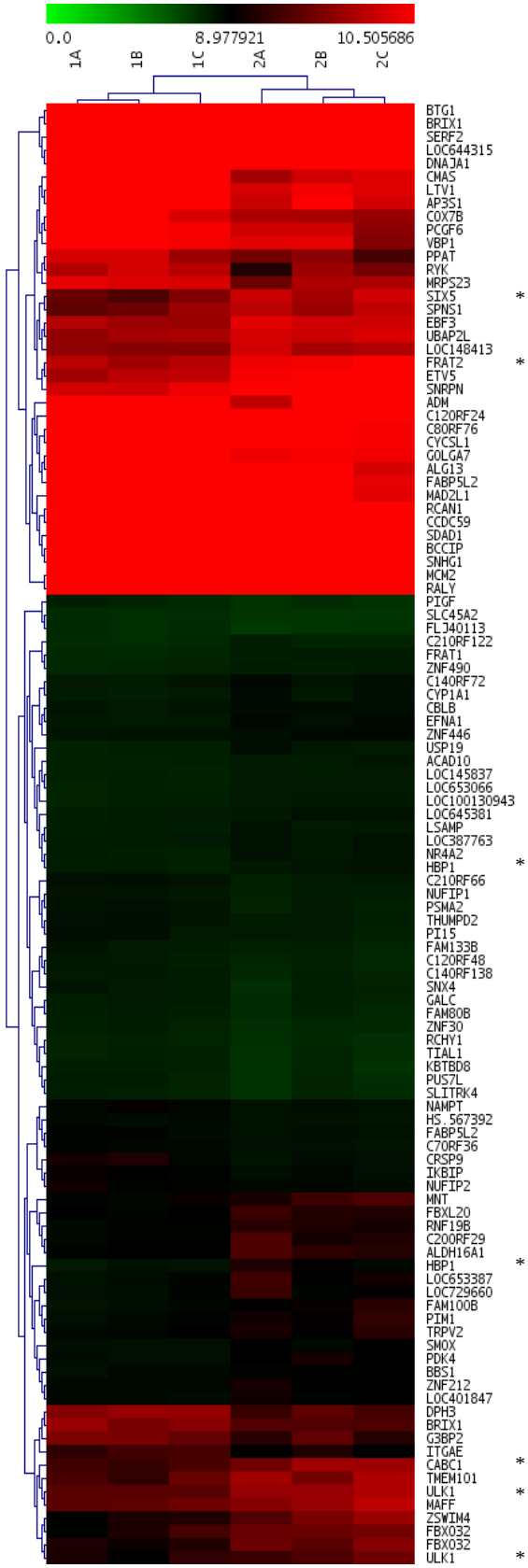


Figure 4.15 Heat Map of gene expression clustering 3 hours after AZ12253801 treatment. All genes with a B statistic >0 were subjected to hierarchical clustering analysis. Asterisks mark transcript chosen for further validation. Where transcripts appear on multiple occasions this indicates multiple probes used in the initial analysis or transcript variants.

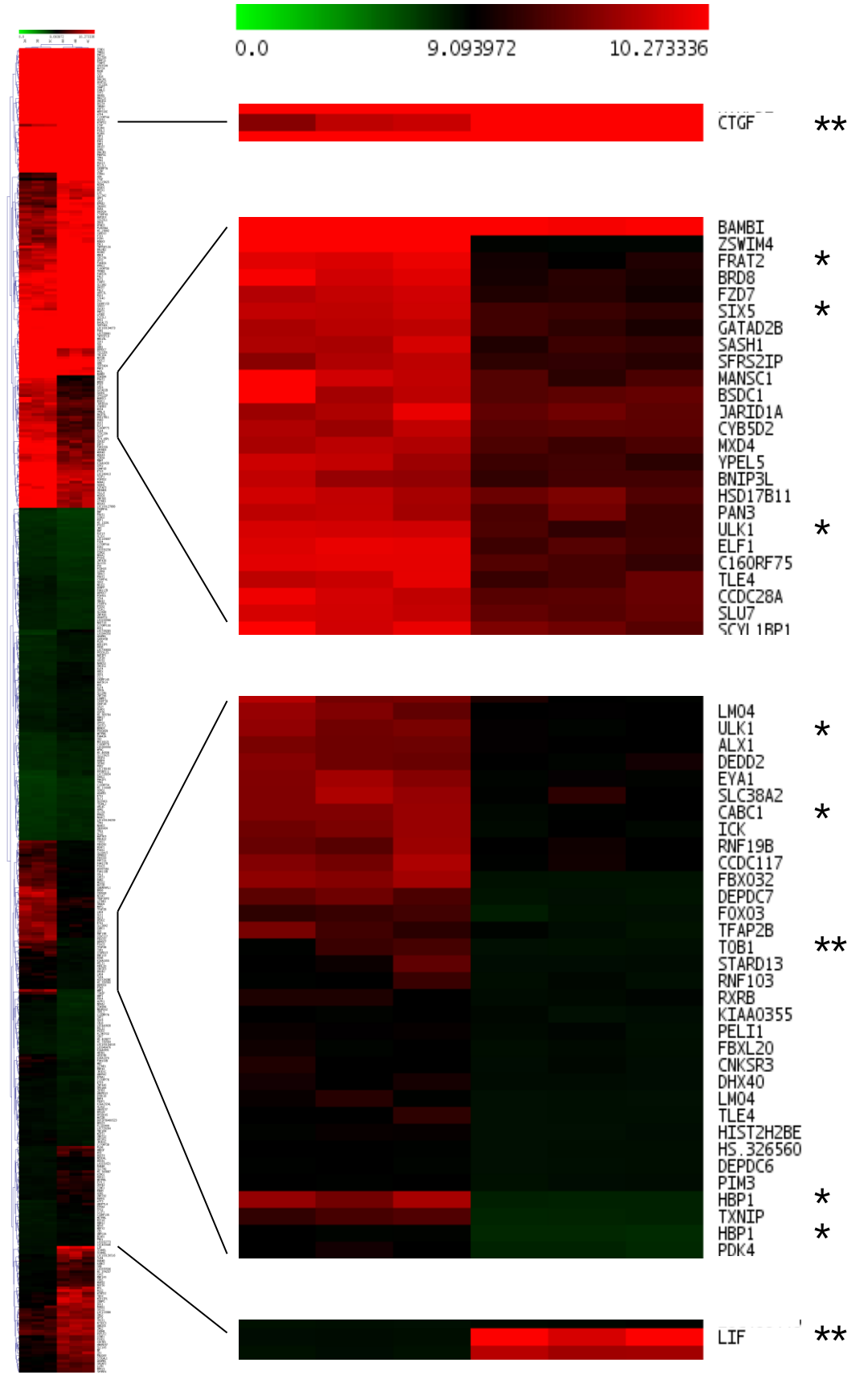


Figure 4.16: Heat Map of gene expression clustering 3 hours after IGF-1 treatment. All genes with a B statistic >0 were subjected to hierarchical clustering analysis. * marks transcript chosen for further validation based on reciprocal regulation by IGF1 and IGF1R inhibition. ** marks transcripts chosen for validation based on other criteria (see text). Where transcripts appear on multiple occasions this indicates multiple probes used in the initial analysis or transcript variants.

Further consideration of the known interactions, relationships or antagonisms between the protein products of the selected genes of interest revealed that they could all be related to a small number of "hub" molecules, AKT, β-catenin, cyclin d1, mTOR, TP53 and GSK3β, with well characterised interactions with the IGF1R (Figure 4.17). This suggested that in cases where there were no published data to support an interaction between the IGF1R and a gene of interest, for example FRAT2, the commonality of interaction, in this case with the Wnt signalling pathway, merited further investigation.

4.3.14 Validation of selected hits in four melanoma cell lines.

Quantitative RT PCR was used to validate the changes observed in the selected genes of interest in A375 cells, and in the further three melanoma cell lines by an alternative method. In order to select appropriate reference (house keeping) genes, fold change data for all probes of 14 common reference genes were obtained from the microarray results. Analysis using the GeoNorm algorithm (Vandesompele et al., 2002) allowed identification of the least variable reference genes (Figure 4.18). All reference genes had very low variability (M scores ≤ 0.05) and would have been suitable. The three most stable genes, *RPLPO, GAPD,* and *ACTB* were selected for normalisation of qRT-PCR data.

qRT-PCR was used to assess expression of the ten genes of interest with respect to the three reference genes in the original RNA samples extracted from A375 cells. All three experimental replicates were analysed under all four experimental conditions at the appropriate time point. In the case of those genes which had not shown reciprocal regulation, all experimental conditions were included in the analysis for completeness. Following completion of the A375 validation qRT-PCRs and preliminary analysis of the results, the genes of interest were analysed in cDNAs from the three other melanoma cell

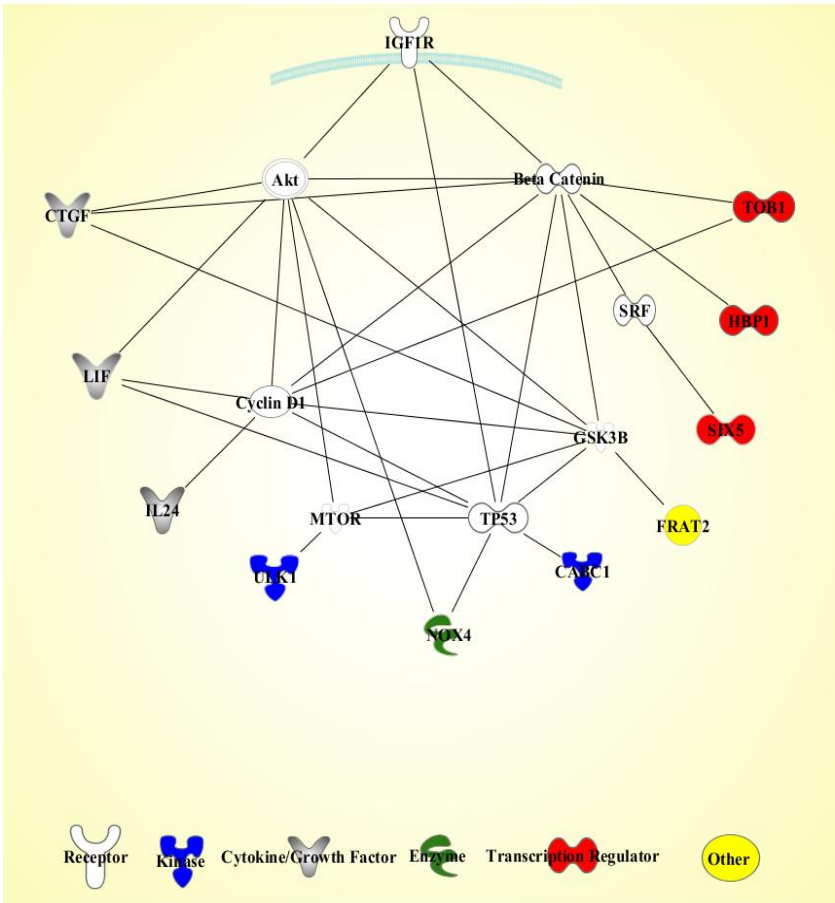


Figure 4.17: Genes chosen for validation have known relationships with components of the IGF1R signaling pathway. An interaction network was constructed using Ingenuity software and information taken from the literature which was not present in the Ingenuity database for the ten genes chosen for validation. Lines do not always represent direct interaction. It was seen that all ten genes had known relationships or interactions with well characterized elements of IGF1R signaling, although induction of these genes had not necessarily been previously associated with IGF1 stimulation.

HBP1 ,HMG-box transcription factor 1: IL-24,Interleukin 24: ULK1,Unc-51-like kinase 1: CTCF, Connective Tissue Growth Factor: LIF, Leukaemia Inhibitory Factor: TOB1,Transducer of ERBB2: NOX4, NADPH Oxidase 4: FRAT2, Frequently arranged in T cell lymphomas 2:CABC1,Chaperone activity of bc1 complex-like, mitochondrial: SIX5, SIS homeobox 5.:SRF ,Serum Response Factor .

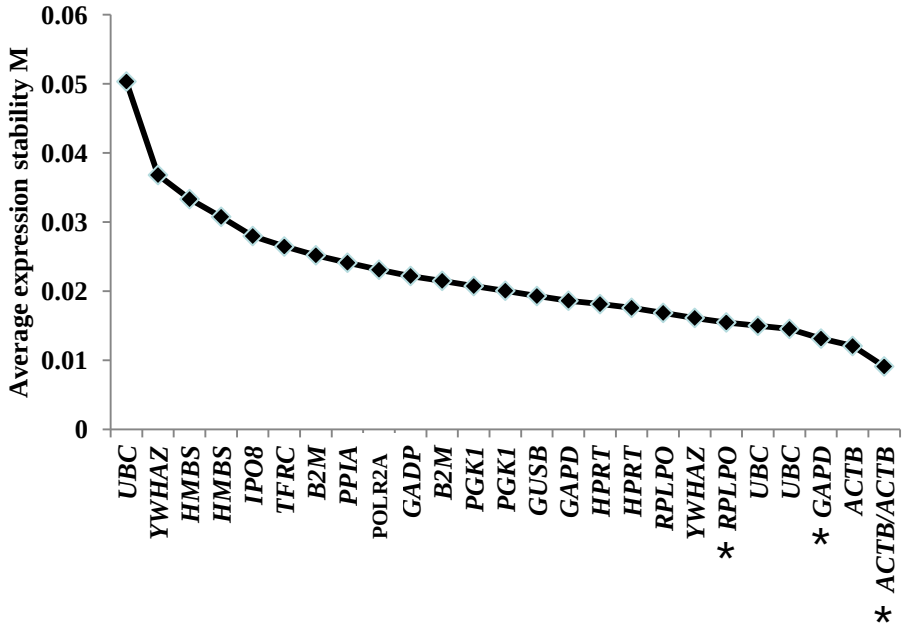


Figure 4.18: Selection of Reference genes for validation studies. Fold change data for 14 common reference genes at the 3 hour time point from all samples underwent GeNorm analysis. The average expression stability was calculated and the least variant genes, under these experimental conditions, was identified by serial subtraction. All genes were seen to be sufficiently invariant to act as reference genes having M scores ≤0.05. M values ≤0.15 are deemed to be sufficiently invariant for use as reference genes (Vandesompele *et al*, 2002).

*= Reference genes selected.

UBC, Ubiquitin C: *YWHAZ*, tyrosine3-monooxygenase: *HMBS* , hydroxymethybilane synthase: *IPO8*, Importin 8: *TFRC*, Transferrin receptor: *B2M*, beta -2-microglobulin: *PPIA*, peptidylpropyl isomerase A: *POLR2A*, polymerase (RNA) II polypeptide A: *GADP*, Glyceraldehyde-3-phosphate dehydrogenase: *PGK1*, phosphoglycerate kinase: *GUSB*, glucuronidase beta: *HPRT*, hypoxanthine phosphoriribosyl-transferase: *RPLPO*, ribosomal protein large PO: *ACTB*, beta actin.

lines, SKMel2, SKMel23, SKMel28, again normalising to *RPLPO*, *GAPD*, and *ACTB* in the same way. For clarity the results are presented together (Figures 4.19, 4.20 & 4.21).

In A375 cells, reciprocal change on IGF1R inhibition or stimulation was seen to a similar extent in all seven genes, *HBP1*, *FRAT2*, *CABC*, *SIX5*, *ULK1*, *IL24 v1* and *v2*, and *NOX4*, confirming the reciprocity identified by microarray analysis. While the fold changes induced by IGF1 stimulation were significant in all cases, IGF1R inhibition resulted in a significant change in only three genes, *HBP1*, *IL24 v1* and *NOX4* (Figures 4.19 & 4.20). On consideration of the three additional genes of interest, *CTCG*, *LIF*, and *TOB1*, significant changes were seen on IGF1 stimulation similar in extent to those documented by microarray analysis in all three cases, and the lack of regulation by AZ12253801 was confirmed (Figure 4.21).

Gene expression changes in SKMel2, SKMel23 and SKMel28 were less consistent. In the case of *HBP1*, *CABC1* and *NOX4* the changes in gene expression were similar to those observed in A375 cells for all three cell lines, but significance was not reached in all cases (Figures 4.19 & 4.20). Similarly IGF induced FRAT2 downregulation was observed in all cell lines but the change was not significant in SKMel28. On consideration of the remaining genes of interest, *ULK1*, *CTCG*, *LIF*, *TOB1* and *IL24 v1*, one or more cell lines had changes in gene expression which opposed those observed in A375 in one or more of the experimental conditions, although most of these changes did not achieve statistical significance. In the case of *IL24 v2* the increase in gene expression following IGF1 treatment of SKMel23 was statistically significant, in contrast to the significant decrease that occurred in A375 under the same conditions. Furthermore the robust increase in

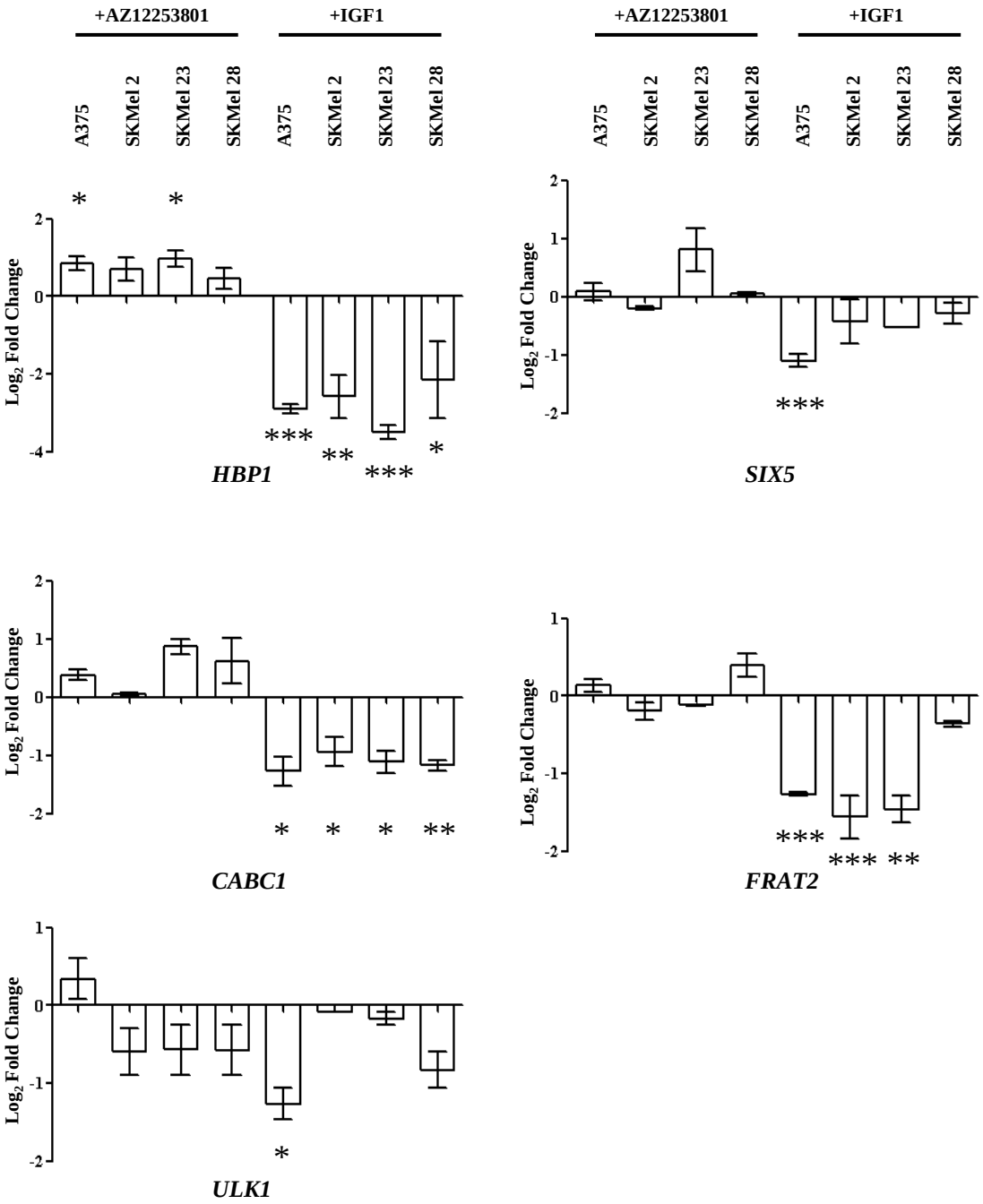


Figure 4.19 Validation in four melanoma cells of five transcripts reciprocally regulated after 3 hours IGF1R stimulation or inhibition in A375 cells. Melanoma cells were treated with 50nM AZ12253801 or vehicle or, following serum deprivation, with 8nM IGF1 or solvent and gene expression determined by qRT-PCR after 3 hours. Histograms represent mean log2fold change in expression (±SEM) compared to solvent or vehicle treated cells from three independent experiments. HBP1 was reciprocally regulated in A375 and SKMel23 cells and showed a consistent direction of change in all 4 cell lines.

(* P<0.05, **P<0.01 *** P<0.005 by one way ANOVA)

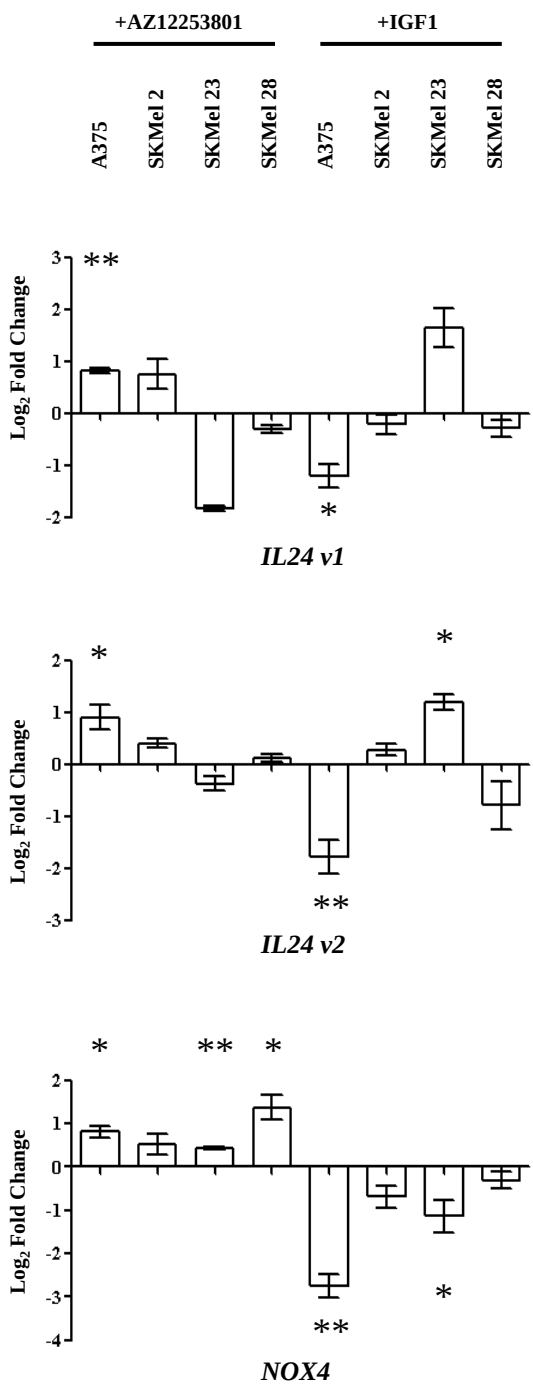


Figure 4.20 Validation in four melanoma cells of three transcripts reciprocally regulated after 24 hours of IGF1R stimulation or inhibition in A375 cells. Melanoma cells were treated with 50nM AZ12253801 or vehicle or, following serum deprivation, with 8nM IGF1 or solvent and gene expression determined by qRT-PCR after 3 hours. Histograms represent mean log2fold change in expression (±SEM) compared to solvent or vehicle treated cells from three independent experiments. *IL24v1*, *IL24v2* and *NOX4* were all reciprocally regulated by IGF1R stimulation and inhibition in A375 cells. *NOX4* was reciprocally regulated by IGF1R stimulation and inhibition in SKMel23 cells.

(* P<0.05, **P<0.01 by one way ANOVA)

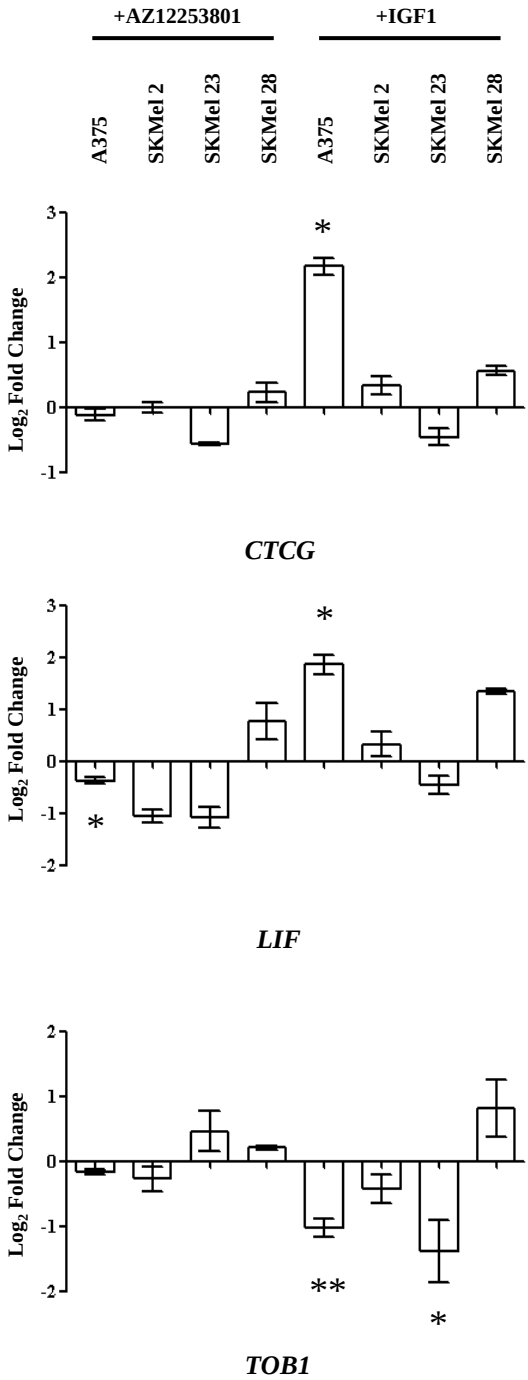


Figure F. Validation in four melanoma cells of three transcripts which showed a large fold change in expression after IGF1 treatment, or were of particular interest, in A375 cells. Melanoma cells were treated with 50nM AZ12253801 or vehicle or, following serum deprivation, with 8nM IGF1 or solvent and gene expression determined by qRT-PCR after 3 hours. Histograms represent mean log2fold change in expression (±SEM) compared to solvent or vehicle treated cells from three independent experiments. IGF1 induced a large fold change in expression of *CTCG* and *LIF* in A375 cells but not in other cell lines.

(* P<0.05, **P<0.01 by one way ANOVA)

expression of *CTCG* and *LIF* was not observed in any cell lines, although there was a modest upregulation in IGF treated SKMel28 cells.

Taken together these data demonstrated that the reciprocal changes in *HBP1* and *NOX4* expression observed in A375 following IGF1R manipulation were robustly reproduced in SKMel2, SKMel23 and SKMel28 cells. The IGF induced changes observed in *FRAT2* and *CABC* expression were also considered to be consistent across the cell lines.

It was concerning that despite apparently consistent changes in gene expression, statistically significant differences were not always observed. Further scrutiny of the qRT-PCR data shed light on this anomaly. Although variation in Ct was consistently within 0.5 cycles for any given technical triplicate, there was substantial variation within this range. This variability was then compounded by production of a normalisation factor for a given gene comparison which was influenced by the variability of the three technical replicates of the 3 reference genes. Ultimately this resulted in a large standard deviation when the final gene expression of all three experimental replicates were compared, and limited the statistical power that could be achieved. Initially this variation was thought to be as a result of human technical error as the qRT-PCRs were performed on 384 well plates into which reagents were pipetted manually. A series of trial experiments revealed that Ct values were equally variable when pipetting was robot automated. Given that all genes analysed exhibited the same variability, it was unlikely that suboptimal primer sequences were to blame. Instead attention turned to the third variable in the Universal probe system (Roche), the fluorescent probes. Ultimately it was discovered that a reaction using a SYBR green system with the same samples and primers produced consistent Ct values, whereas the universal probe system exhibited the degree of variability seen previously. It was unclear

which feature of the probes, either the oligonucleotide or the fluorophore, was the cause of this variability. Instead qRT-PCR was performed using SYBR green for all future experiments.

4.4 Conclusions

The results presented in this chapter document the changes in gene expression as assessed by microarray following IGF1R manipulation in a melanoma cell line A375. In agreement with the previous literature, large numbers of genes (>2000) had altered expression following IGF1 treatment, and of these the majority were concerned with cellular proliferation, cell cycle regulation, apoptosis and gene expression (Creighton et al., 2008, Rajski et al., 2010, Pacher et al., 2007). An IGF1 induced gene signature was produced and interrogation of clinical data sets revealed a correlation to Ki67 positivity of melanoma tumour samples, which is itself of prognostic significance. As such these data are further evidence for a rationale of IGF1R targeted strategies in melanoma. Further investigation is required to determine if the IGF1 induced gene signature predicts response to anti-IGF1R antibodies and small molecule inhibitors in melanoma cells as has been shown for other cell types (Litzenburger et al., 2011, Creighton et al., 2008).

In total the expression of only seventeen genes was altered following 3 or 24 hour IGF1R inhibition by the small molecule inhibitor AZ12253801. This is in contrast to the more significant transcriptional effects of IGF1R inhibitor NVP-AEW541 in a Wilms' tumour model (Bielen et al., 2011), although in that study, gene expression was quantified after treatment with IGF1R inhibitor at 5 x GI_{50}, rather than 1 x GI_{50} as used here. This suggests that transcriptional consequences of IGF1 stimulation cannot be directly

extrapolated to the situation of IGF1R inhibition. Furthermore, on this basis of this data, it could be suggested that that anti-cancer effect of IGF1R inhibitors may be more likely to be attributed to translational or post-translational effects than transcriptional effects. Of the genes whose expression was altered by IGF1R inhibition, seven were found to be regulated in a reciprocal fashion by IGF1R stimulation. qRT-PCR validation reactions confirmed all of the documented changes in A375 cells. On assessment in a further 3 cell lines, only 2 genes (*HBP1*, *NOX4*) were found to be consistently influenced by IGF1R inhibition or stimulation in a similar manner to that observed in the A375 cell line. The involvement of NOX4 in IGF biology has been previously explored in vascular smooth muscle cells, contributing to IGF-induced cell migration and production of reactive oxygen species (Vardatsikos et al., 2009, Meng et al., 2008).

The finding that HBP1 expression is reciprocally regulated by IGF1 and IGF1R inhibition represented a novel result.

4.4.1 HBP1 (HMG Box Protein 1)

HBP1 was originally identified as a suppressor of the potassium transport defective phenotype of mutant Saccharomyces cerevisiae (Lesage et al., 1994). Subsequently HBP1 was shown to be a binding partner of retinoblastoma protein (RB) and was characterised as a High Mobility Group box (HMG) box transcriptional repressor (Lavender et al., 1997, Tevosian et al., 1997, Shih et al., 1998). The family of HMG box proteins are transcription factors, and proteins involved with DNA replication and repair which are characterised by a 75 amino acid DNA binding domain (Stros et al., 2007). Further investigation has revealed HBP1 to have a diverse range of targets and to act as both a suppressor and promoter of gene transcription. HBP1 regulates expression of many genes involved in cell

cycle regulation, such as *NMYC*, and inhibits G_1 to S phase progression (Tevosian et al., 1997). Loss, depletion or inactivation of HBP1 promotes cell proliferation and invasiveness in melanoma, breast and prostate cancers *in vitro* (Eskandarpour et al., 2009, Chen et al., Paulson et al., 2007). In contrast overexpression of HBP1 slows growth in cell culture of a variety of cell types and promotes differentiation (Yao et al., 2005). As such HBP1 is best described as a growth suppressor, differentiation factor and tumour suppressor gene. As shall be described, abrogation of HBP1 activity has been correlated to aggressive tumour phenotype *in vivo*.

4.4.1.1 Factors known to influence HBP1 expression

The regulators of HBP1 expression are poorly understood. HBP1 is induced by terminal differentiation of many cell types in which it acts as a proliferation barrier (Xiu et al., 2003). The p63 transcription factor and mir 17-5p have recently been shown to suppress *HBP1* expression in keratinocytes and breast cancer cells respectively (Borrelli et al., 2010, Li et al., 2010). Stimulation of serum starved myoblasts with IGF1 (100 nM) or insulin (100 nM) for 4 hours resulted in a ~3 and ~1.5 fold decrease in *HBP1* expression respectively (Palsgaard et al., 2009). However HBP1 is not increased in streptozotocin-diabetic rats (Villafuerte et al., 2004). It seems unlikely that *HBP1* is an insulin regulated gene given this finding, and that HBP1 tissue distribution is ubiquitous and not restricted to insulin responsive tissues (Lesage et al., 1994). The question of whether *HBP1* is an IGF induced gene is less clear. HBP1 is a binding partner to the insulin response element of IGFBP-3 but this observation is of unknown significance (Villafuerte et al., 2004). It is also interesting to note that many of the gene targets of HBP1, such as *CMYC* and *CCND1*

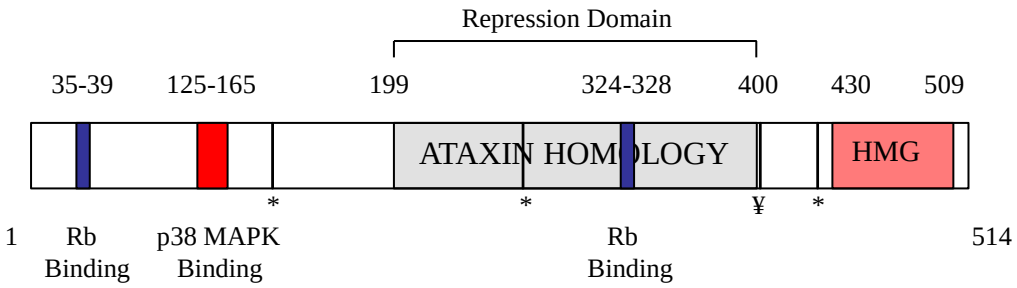
are also gene targets of IGF1 signalling. Despite these tentative associations, a role of IGF signalling in influencing HBP1 expression is unknown.

4.4.1.2 Role of HBP1 in the regulation of the Cell cycle.

HBP1 acts, via its gene targets, to prevent G_1 to S phase progression. HBP1 interacts selectively with RB and related family member p130, inhibitors of cell proliferation, which bind the E2F transcription activator. HBP1, RB, and P130 levels are found to be upregulated during differentiation and under conditions of cell cycle arrest in muscle, adipocytes, erythroid and other cell types (Yee et al., 1998, Tevosian et al., 1997). Overexpression of HBP1 inhibits G_1 and S phase progression and the appropriate ratio of RB to HBP1 is necessary for progression though differentiation of hepatocytes (Shih et al., 2001) and keratinocytes (Borrelli et al., 2010). As such under normal cellular conditions HBP1 acts as a proliferation barrier promoting terminal differentiation of tissues.

4.4.1.3 HBP1 as a transcription factor and tumour suppressor gene.

HBP 1 possesses a sequence specific HMG-motif DNA binding domain which initiates DNA bending, to allow assembly of multi-component transcription factor complexes (Figure 4.22). In addition HBP1 possesses an AXH (Ataxin homology) ”repressor” domain which mediates repression of gene transcription both independently of, and modulated, by RB and p130 binding. Binding of histone deacetylase (HDAC) to this repressor region is necessary for HBP1 mediated repression of transcription. A diverse range of target genes has been identified for HBP1. Of particular relevance to this project are transcription factors that regulate cellular proliferation, cell growth and differentiation (Figure 4.22). Inhibition of E2F induced *NMYC* transcription is prevented by direct



¥ - serine 401, phosphorylated by p38 MAPK (Xiu, Kim et al. 2003)
* - Lysine 171, 297,305,307,419, acetylated by histone acetyltransferase p300 & CBP (Wang, Pan et al. 2011)

Gene Name	***Gene symbol***	**Transcriptional effect**	**Binding site**		
			DNA	**TCF LEF**	
Cyclin D1	*CCND1*	-	Y	Y	(Tetsu *et al*, 1999; Sampson *et al*, 2001)
CMYC	*CMYC*	-	Y	Y	(He *et al*, 1998; Escamilla-Powers *et al*, 2010)
NMYC	*NMYC*	-	Y		(Tevosian *et al*, 1997)
p47 phox (neutrophil cytosolic factor)	*NCF1*	-	Y		(Berasi *et al*, 2004)
		+			(Teng 2009)
Histone H1^{o}	*H1F0*	+	Y		(Lemercier *et al*, 2000)
Myeloperioxidase	*MPO*	+	Y		(Lin *et al*, 2001)
Cyclin dependant kinase inhibitor 2A - p16^{INK4A}	*CDKN2A*	+	Y		(Li *et al*, 2010)
CD2	*CD2*	+			(Zhuma *et al*, 1999)
Cyclin dependant kinase inhibitor 1A - p21	*CDKN1A*	-	Y		Gartel *et al*, 1998)
Macrophage migration inhibitory factor	*MIF*	-	Y		(Chen *et al*, 2010)

Figure 4.22 Schematic diagram of HBP1 with residues of known significance and published targets listed.

binding of HBP1 to the *NMYC* promoter (Tevosian et al., 1997). In the case of *CCND1* and *CMYC* HBP1 represses transcription both by direct binding to the gene promoter and through binding to, and inhibition of activity of, the TCF/LEF transcriptional activators (Sampson et al., 2001). Finally HBP1 appears to bind CMYC directly preventing association with its target promoters (Escamilla-Powers et al., 2010). Clearly given these gene targets HBP1 acts in a number of ways as a global suppressor of Wnt signalling. As previously described, constitutive activation of Wnt signalling is implicated in the pathogenesis of many cancers (Polakis, 2000). By implication loss of HBP1 or abrogation of its function would be expected in such circumstances.

4.4.1.4 Interactions with MAPK pathway

Expression of oncogenic RAS induces premature senescence in human fibroblasts through activation of the RAF/MEK/ERK and MKK3/P38 MAPK pathways (Wang et al., 2002). HBP1 is required for RAS mediated senescence of primary cells by direct DNA binding to the promoter of *CDKN2A* enhancing its transcription (Zhang et al., 2006, Li et al., 2010). Acetylation of the HBP1 repression domain further enhances *CDKN2A* expression (Wang et al., 2011). As might be expected, depletion of HBP1 in the face of oncogenic RAS promotes tumorigenesis of primary cells (Li et al., 2010).

In contrast in neoplastic cells, notably melanoma, constitutive activation of the RAS/RAF pathway drives cellular proliferation. In melanoma cells depletion of constitutive active NRAS resulted in an increase in HBP1 and reduced cell cycle proliferation (Eskandarpour et al., 2009). The P38 MAPK and JNK pathways are, like the RAF/ERK pathway, downstream of RAS. Unlike the RAF/ERK pathway whose activation mediates cell

proliferation, the P38 MAPK and JNK pathways are mediators of stress responses that usually lead to growth arrest or apoptosis. HBP1 is both a substrate and binding partner of p38 MAPK but not of other members of the MAPK family (Xiu et al., 2003). Phosphorylation of serine 401 of HBP1 by p38 MAPK increases HBP1 protein half life resulting in cell cycle arrest (Xiu et al., 2003). These findings parallel those with another inhibitor of G_1 progression, p21. As such modulation of HBP1, like that of p21, by P38 MAPK is a mechanism by which P38 MAPK negatively influences G_1 progression (Xiu et al., 2003).

4.4.1.5 Other gene targets of HBP1 and interactions with EGFR pathway

The *P47PHOX* gene encodes the regulatory subunit for NADPH oxidase, neutrophil cytosolic factor (NCF1). In non immune cells the generation of radical oxygen species (ROS) by the NADPH complex is a consequence of mitogenic stimulation with growth factors, such as EGF (Sauer et al., 2001). Following stimulation of the EGFR HBP1 represses transcription of *P47PHOX* inhibiting ROS production which contributes to the inhibition of cell cycle progression (Berasi et al., 2004, Huang et al., 2006). Conversely HBP1 depletion results in a significant increase in *P47PHOX* expression in mouse lymphoid endothelial cells (Teng, 2009). In *P47PHOX* knockout mice or following siRNA mediated NCF1 (P47PHOX) depletion *in-vitro, HBP1* levels significantly increase (Li et al., 2010). Therefore HBP1 appears to be an important mechanism involved in regulation of endothelial reactive oxygen species by NADPH oxidase.

HBP1 has also been described an activator of the myeloperoxidase gene, Histone $H1^o$ and CD2 promoters (Lin et al., 2001, Zhuma et al., 1999, Lemercier et al., 2000). A wide

variety of additional genes show altered expression following manipulation of HBP1 expression in keratinocytes and the K562 (erythroleukaemic) cell line (Borrelli et al., 2010, Yao et al., 2005).

4.4.1.6 HBP1 and cancer

The diverse set of gene targets suggests HBP1 has multiple mechanisms for affecting G_1 progression and suppressing oncogenic pathways. Constitutive Wnt signalling is a well characterised feature of breast cancer and, as postulated above, HBP1 loss or abrogation would be expected in such circumstances. Paulson *et al* recently identified the presence of ten functionally defective HBP1 mutants or complete absence of HBP1 in a cohort of patients with invasive breast cancer, and reduced HBP1 activity was correlated to tumour recurrence (Paulson et al., 2007). Subsequent *in vitro* studies revealed that HBP1 depletion increased Wnt signalling, proliferation and invasiveness in breast cancer cell lines. Further supportive evidence from the same laboratory concerns the green tea compound epigallo-catechin galate (EGCG) which has been shown to retard breast cancer xenograft growth in animal models and stabilizes *HBP1* mRNA resulting in HBP1-dependent repression of Wnt signalling (Fujiki et al., 2002, Kim et al., 2006).

In the case of prostate cancer, low HBP1 and increased expression of macrophage inhibitory factor, a direct HBP1 target gene, is associated with a decrease in relapse free survival. Conversely HBP1 overexpression repressed growth and invasion of prostate cancer cell lines (Chen et al., 2010).

It is clear that loss of functional HBP1 plays an important role in some cancers. Therefore it can be postulated that exploitation of HBP1 mediated repression of cell proliferation may be of therapeutic benefit. Investigation of the significance of IGF induced changes in HBP1 expression in human melanoma cells are detailed in the next chapter.

5. HBP1 and IGF1R Signalling in human melanoma

5.1 Introduction

The HMG transcription factor *HBP1* had been identified, as described in Chapter 4, as a gene reciprocally regulated by IGF1R activation and inhibition. Whilst *HBP1* had been previously shown to be decreased by both IGF1 and insulin in myoblasts (Palsgaard et al., 2009), this is, to the author's knowledge, the first report that IGF1R inhibition is capable of increasing *HBP1* transcription. This finding suggested a possible novel interaction of the IGF1R and Wnt signalling pathways, involving HBP1.

As described in the previous chapter, HBP1 plays an important role in cell cycle progression, acting in a reciprocal fashion to the E2F transcription factor. Over-expression of HBP1 has been shown to repress *NMYC* and *CCND1* transcription, Wnt/β catenin signalling and cell cycle progression (Yee et al., 1998, Tevosian et al., 1997, Sampson et al., 2001). Conversely clinically loss of HBP-1 activity is associated with invasive breast cancer (Paulson et al., 2007) consistent with the findings that Wnt/β catenin signalling is a negative prognostic indicator in breast cancer (Lin et al., 2000).

However as described previously, the roles of the canonical and non-canonical Wnt signalling pathways in melanoma are complex and temporal. Whilst Wnt/β catenin signalling is a pre-requisite for melanocyte transformation, its continued activity is detrimental to tumour progression (Kageshita et al., 2001). Instead following transformation non-canonical Wnt pathways, such as those stimulated by WNT5A, contribute to the downregulation of Wnt/β catenin target genes and favour a proliferative, metastatic phenotype (Weeraratna et al., 2002, Bittner et al., 2000, Da Forno et al., 2008).

Thus, the canonical Wnt pathway plays different roles in melanoma and breast cancer. Whilst non canonical Wnt pathways, particularly that stimulated by WNT5A, represent a therapeutic target in melanoma, inhibition of canonical Wnt/β catenin signalling might favour an aggressive phenotype, in direct contrast to the case in breast cancer. Therefore it is possible that a change in HBP1 expression induced by IGF1R inhibition may limit the efficacy of IGF1R inhibiting therapies in melanoma, and dual targeting might be predicted to enhance observed phenotypic effects.

As such it was important to understand the biological significance of changes in *HBP1* expression following manipulation of IGF1R activity. Specifically, the aims were firstly to validate the relationship between IGF1R and HBP1 using gene silencing, secondly to determine the mechanism by which IGF1R signalling affects *HBP1* transcription, and finally to assess the relative role of HBP1 in regulating phenotype and gene expression in the context of IGF1R inhibition and Wnt/β-catenin signalling.

5.2 Results and Discussion

5.2.1 Effect of IGF1R depletion on *HBP1* mRNA

Initial experiments determined if other methods of manipulating the IGF1R influenced *HBP1* transcription. A375 cells were transfected with IGF1R or control siRNA. After 48 hours IGF1R protein and *IGF1R* and *HBP1* mRNA levels were determined by immunoblot and qRT-PCR respectively. *IGF1R* mRNA was significantly depleted and IGF1R total protein markedly reduced following transfection with IGF1R siRNA (Figure 5.1). *HBP1* mRNA was increased by a factor of approximately 1.75 following IGF1R depletion, similar to the two fold increase seen 3 hours after AZ12253801 treatment as detailed in the previous chapter (Figure 4.19). Given that increase in *HBP1* mRNA had been

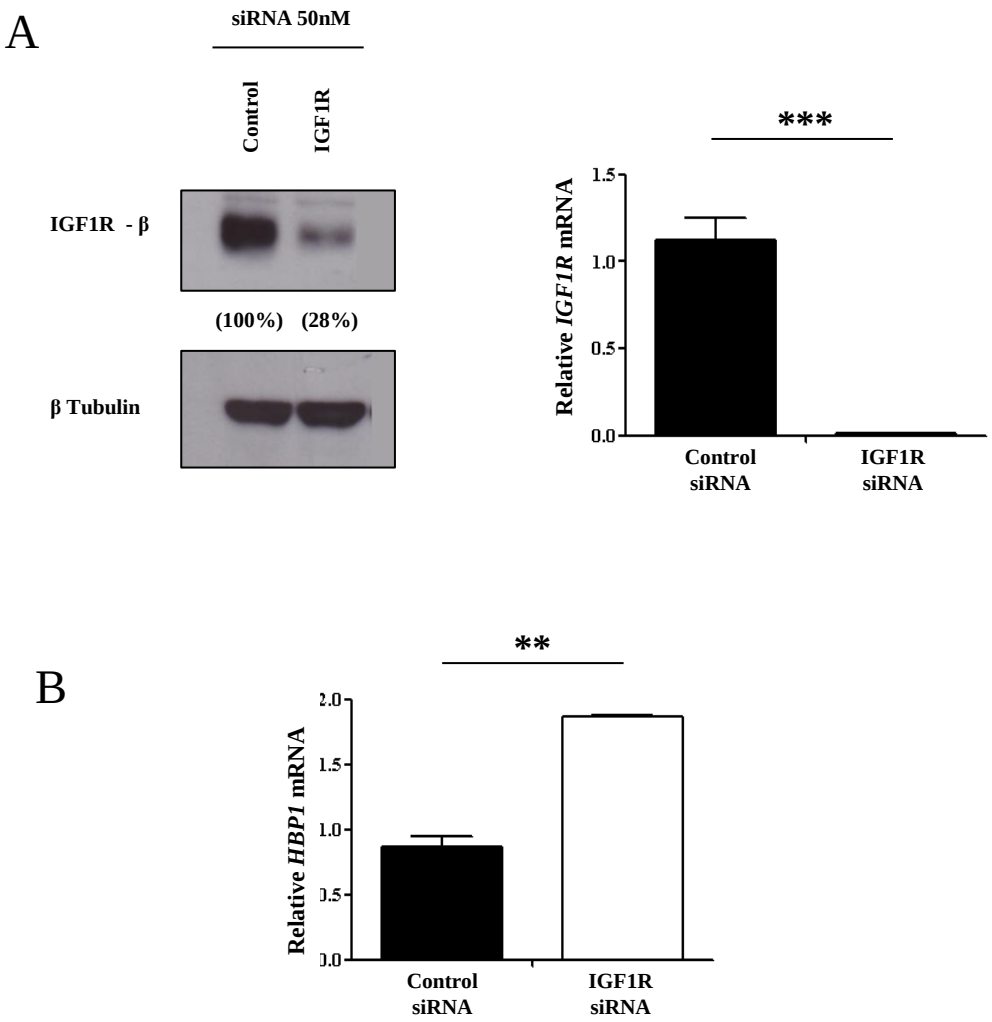


Figure 5.1 The effect of IGF1R depletion on HBP1 Expression. A375 melanoma cells were reverse transfected with 50nM IGF1R or control siRNA. IGF1R protein and *IGF1R* and *HBP1* mRNA were quantified after 48 hours by immnoblot and q RT-PCR. Histograms represent mean relative change (±range) in mRNA normalised to control siRNA treated cells from 2 independent experiments. **A)** IGF1R protein and mRNA are significantly depleted following IGF1R siRNA. Immunoblot is a representative example and identical results were obtained in two independent experiments. Values in parentheses represent densitometric quantification. **B)** *HBP1* mRNA is significantly increased following IGF1R depletion.

(** P<0.01, *** P<0.005 by one way ANOVA)

demonstrated with two methods of reducing IGF1R signalling, and that a reduction in *HBP1* mRNA followed IGF1 stimulation, these results confirmed that *HBP1* transcription was influenced by IGF1R signalling.

5.2.2 Quantification of HBP1 protein

Whilst alterations in *HBP1* transcription following IGF1R manipulation had been demonstrated, there was no information on changes in protein level or half life, nor was the latter documented in the literature. Several antibodies are commercially available and these were trialled for detection of HBP1 on immunoblot. A375 cells were treated for three hours with AZ12253801 or vehicle or, following overnight serum deprivation, with IGF1 or solvent. Whole cell extracts were prepared and RNA extracted from parallel dishes for qRT-PCR to assess *HBP1* mRNA levels. All sourced antibodies produced poor results with faint or no bands within a heavily stained background, irrespective of the method of cellular lysis. Given that HBP1 is a transcription factor and thus a nuclear protein, immunoblot of A375 nuclear extract was performed in an effort to increase specificity of detection. This produced an immunoblot that showed several distinct bands without marked background staining (Figure 5.2A upper). It was unclear which of the bands observed represented HBP1. Whilst the datasheet for the antibody documented a band at 76kD, the predicted size of HBP1 based on amino acid sequence is 54 kD. Within this range there were four distinct bands. Whilst the band at ~54kD demonstrated changes in protein level predicted by the mRNA data (Figure 5.2A lower), a reduction following IGF1 stimulation and an increase following AZ12253801 treatment, the changes were very modest and it was unclear which band, if any, represented HBP1.

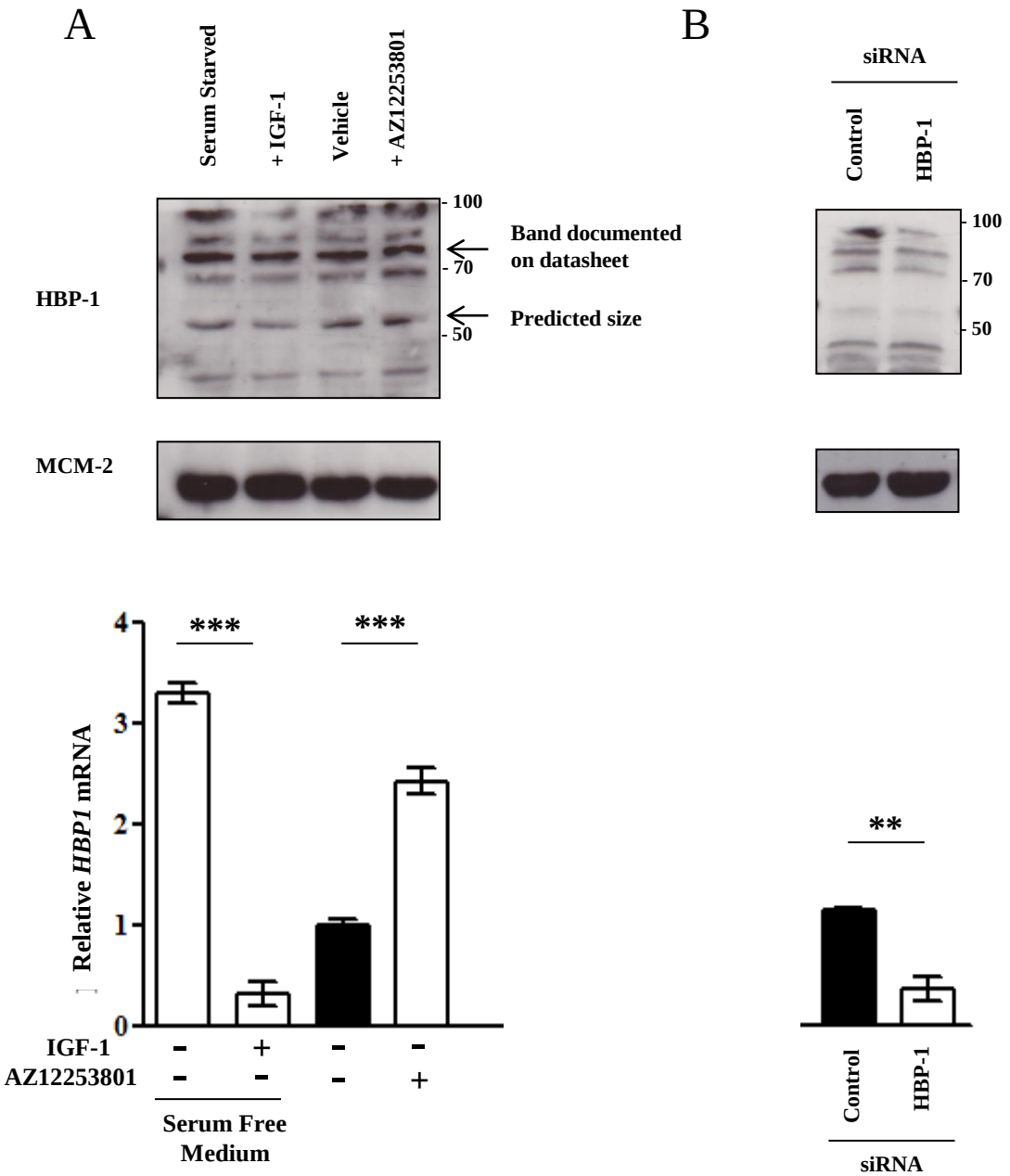


Figure 5.2 The effect of IGF1R axis manipulation on HBP1 protein expression. **A)** A375 melanoma cells in complete culture medium were incubated for 3 hours with 50nM AZ12253801 or, following overnight serum deprivation, with 8nM IGF1. HBP1 expression was assessed by immunoblot of nuclear lysate and qRT-PCR. Immunoblot was performed with 2 HBP1 antibodies (SC 8488 & SC 25390). In 3 independent experiments SC 8488 produced a superior, and identical result, and a representative example is shown. Histograms represent mean relative change (±SEM) in mRNA normalised to control conditions from 3 independent experiments. Significant changes in *HBP1* expression following IGF1R manipulation were not duplicated on immunoblot. It was unclear which of the multiple bands represents HBP1. **B)** A375 melanoma cells were reverse transfected with 50nM HBP1 or control siRNA and HBP1 expression assessed by immunoblot of nuclear lysate and qRT-PCR after 48 hours. A representative immunoblot is shown, identical results were achieved in 3 independent experiments . Histograms represent mean relative change (±SEM) in mRNA normalised to control conditions from 3 independent experiments. HBP1 siRNA significantly reduced *HBP1* expression. There was no change in the intensity of the putative HBP1 bands on immunoblot following siRNA mediated HBP1 depletion . (** P<0.01, *** P<0.005 by one way ANOVA)

In order to further explore the utility of this antibody for detecting changes in HBP1 protein levels by immunoblot it was necessary to deplete HBP1 with siRNA to determine whether this reduced intensity of any of the previously documented bands. Three HBP1 siRNAs were sourced: two from a commercial manufacturer were of unknown efficacy and one was synthesized from a published sequence (Borrelli et al., 2010). Forward, reverse and double transfection strategies were trialled in A375 at a variety of siRNA concentrations. In all cases qRT PCR was performed for *HBP1* mRNA after 48 hours. *HBP1* mRNA was reduced by 70-85% by the most effective siRNA reverse transfected at 50nM and this protocol was used for subsequent experiments. This degree of *HBP1* mRNA depletion equals or is superior to that documented in the literature using RNA interference (Borrelli et al., 2010, Wang et al., 2011, Li et al., 2010, Paulson et al., 2007). Higher siRNA concentrations or double transfection protocols did not improve *HBP1* mRNA depletion. As shall be discussed below, it is possible that the process of transfection itself acted as a drive to HBP1 expression. In full medium *HBP*1 mRNA was reduced by the chosen HBP1 siRNA to ~15% that of control cells (Figure 5.2B). Attempts to improve mRNA depletion using alternate transfection reagents and double transfection protocols were unrewarding. Immunoblot of nuclear lysates following cell treatments as described above revealed that all of the bands previously documented were present at equal intensity following control or HBP1 siRNA transfection (Figure 5.2B). The band at ~54kD was reduced to an equal extent in both control and HBP1 siRNA transfected cells despite significantly different *HBP1* mRNA levels.

From these results it was clear that all trialled antibodies were inadequate for HBP1 protein detection and it would be necessary to rely solely on *HBP1* mRNA quantification in future experiments. It was noted that in the literature immunoblotting for endogenous

HBP1 had been performed in only one study using an antibody generated in-house (Kim et al., 2006). Attempts to obtain this reagent were unsuccessful. Other studies had measured HBP1 by immunoblotting for tagged HBP1 transgenes (Escamilla-Powers et al., 2010, Wang et al., 2011, Chen et al., 2010).

5.2.3 Elucidation of the signalling pathway by which IGF1R affects *HBP1* transcription.

In order to explore the molecular mechanism by which IGF1R affects *HBP1* transcription it was necessary to identify the consequences of IGF1 or AZ12253801 treatment on downstream components of the IGF1R signalling cascades MEK/MAPK/ERK and PI3K/AKT. Recently it has been reported by our lab and others that IGF1R can translocate to the nucleus and effect transcription (Aleksic et al., 2010, Sehat et al., 2010, Warsito et al., 2012, Sarfstein et al., 2012). This raised the possibility that nuclear IGF1R could regulate HBP1 directly by binding to regulatory sequence in the HBP1 gene. However, in prostate cancer cell models, nuclear IGF1R translocation was induced by relatively high IGF1 concentrations (30-50nM), but not by lower IGF1 levels (1-10nM) that maximally activate the canonical downstream signalling pathways (Aleksic et al., 2010). If these observations are relevant to melanoma cells, this would suggest that HBP1 regulation by 8nM IGF1 is unlikely to involve nuclear IGF1R.

A375 cells were treated for 3 hours with AZ12253801 or vehicle or, following serum deprivation, with IGF1 or solvent, as described previously and cell lysates immunoblotted for phosphorylated components of the PI3K/AKT/mTOR and MEK/MAPK signalling cascades (Figure 5.3A). Following serum starvation, there was no detectable phosphorylation of IGF1R, AKT or P70 S6Kinase. In contrast MAPK and S6 were basally

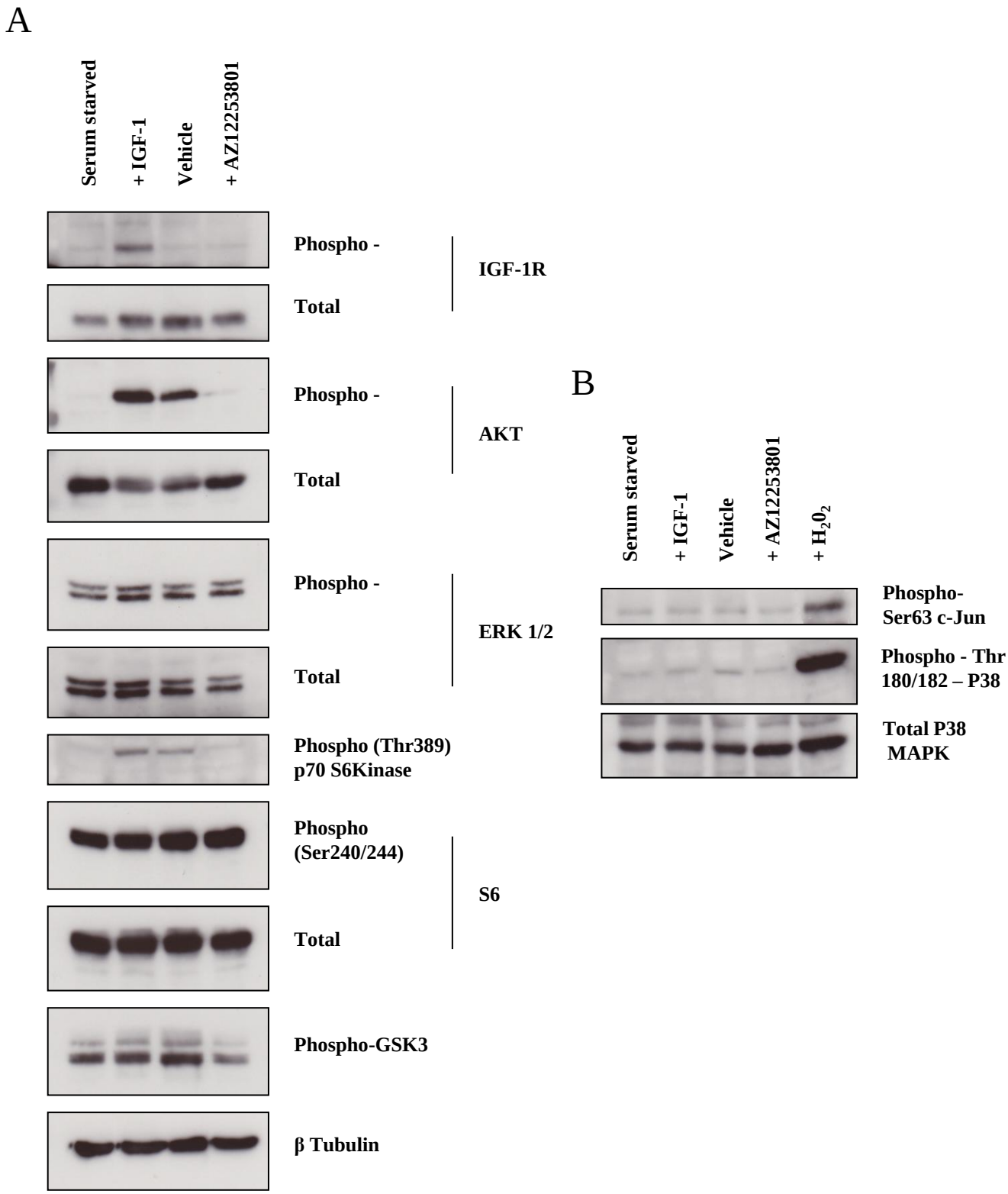


Figure 5.3 Effect of IGF1R stimulation or inhibition on phosphorylation of downstream molecules. A375 melanoma cells in complete culture medium were incubated for 3 hours with 50nM AZ12253801 or, following overnight serum deprivation, with 8nM IGF1. Phosphorylation status of downstream molecules was assessed by immunoblot. Similar results were seen in 2 independent experiments. **A**) IGF1R, AKT and P70 S6kinase were phosphorylated following IGF1 treatment. Basal phosphorylation of AKT and P70 S6Kinase was abrogated by IGF1R inhibition. **B)** Cells were treated as described in A). Cells treated with 1μM H_20_2 for 30 minutes served as a positive control. Phosphorylation of c-Jun and P38 MAPK were not observed basally or after IGF1R manipulation .

phosphorylated in serum starved cells. Basal phosphorylation of MAPK was consistent with previous observations (Figure 4.3) and was attributed to constitutively active BRAFV600E in this cell line. Phosphorylation of S6 following activation of p90S Kinase by MAPK has been reported and this could contribute to basal S6 phosphorylation in this cell line (Pende et al., 2004). Future experiments suggested that additional or alternate mechanisms also existed.

Following treatment with IGF1, phosphorylation of IGF1R, AKT and S6 Kinase was documented, indicating activation of the PI3K/AKT/mTOR signalling cascade. Conversely in full medium basal phosphorylation of AKT and S6 Kinase was reduced following incubation with AZ12253801.

It was also necessary to consider the JNK and P38 signalling cascades, particularly the latter given that HBP1 is phosphorylated by P38 MAPK (Xiu et al., 2003). A375 cells were treated as before or with H_20_2 as a positive control. Phosphorylation of both JUN and P38 MAPK was induced by H_20_2 but manipulation of the IGF1R had negligible effect (Figure 5.3B).

Collectively these data confirmed the previous findings that in A375 cells manipulation of IGF1R influenced activity of the PI3K/AKT/mTOR signalling cascade and that there were further effects downstream of mTOR. In contrast there was no effect on the ERK, P38 MAPK and JNK pathways. As such further experiments were not performed to test effects of inhibiting P38 MAPK on IGF-regulated HBP1 expression, as activation of this pathway was not detectable in A375 cells under basal conditions or following IGF1R manipulation.

5.2.3.1 Testing effects of MEK and PI3K inhibition on *HBP1* expression

The next set of experiments used chemical inhibitors of components of the PI3K/AKT and MEK/ERK pathways, initially performing dose-response experiments to check for target inhibition. Whilst IGF1R manipulation appeared to have no effect on ERK phosphorylation in A375 cells (Figure 5.3A), depletion of NRAS has been shown to increase *HBP1* expression and it was therefore interesting to determine whether inhibition of ERK phosphorylation would influence *HBP1* transcription (Eskandarpour et al., 2009). Serum starved A375 cells were pre-treated for 4 hours with increasing concentrations of U0126 and LY294002, inhibitors of MEK and PI3K respectively, and in the last 15 minutes were stimulated with 8nM IGF1. Concentration ranges of each compound were chosen with reference to the literature (Itoh et al., 1999, Ge et al., 2002, Sumimoto et al., 2006). Cell lysates were then immunoblotted for active upstream and downstream pathways components. IGF1 induced IGF1R phosphorylation confirmed that the ligand was bioactive (Figure 5.4). Both MEK and ERKs were basally phosphorylated in serum free medium and there was no additional effect of IGF1. Phosphorylation of both MEK and ERKs decreased in a dose dependent manner with increasing U0126 concentration. Whilst ERK 1/2 phosphorylation was abolished at ≥5μM U0126, residual MEK phosphorylation remained. In contrast, AKT was not phosphorylated in serum starved cells and S473 phosphorylation was robustly induced on stimulation with IGF1. There was an LY294002 induced dose dependent decrease in AKT phosphorylation with complete abolition at 75 μM (Figure 5.5).

Using the selected concentrations of inhibitors, it was now possible to determine the effect of MEK and PI3K inhibition on IGF1 and AZ12253801 induced changes in HBP1 transcription. A375 cells were treated with AZ12253801 or vehicle or, following serum

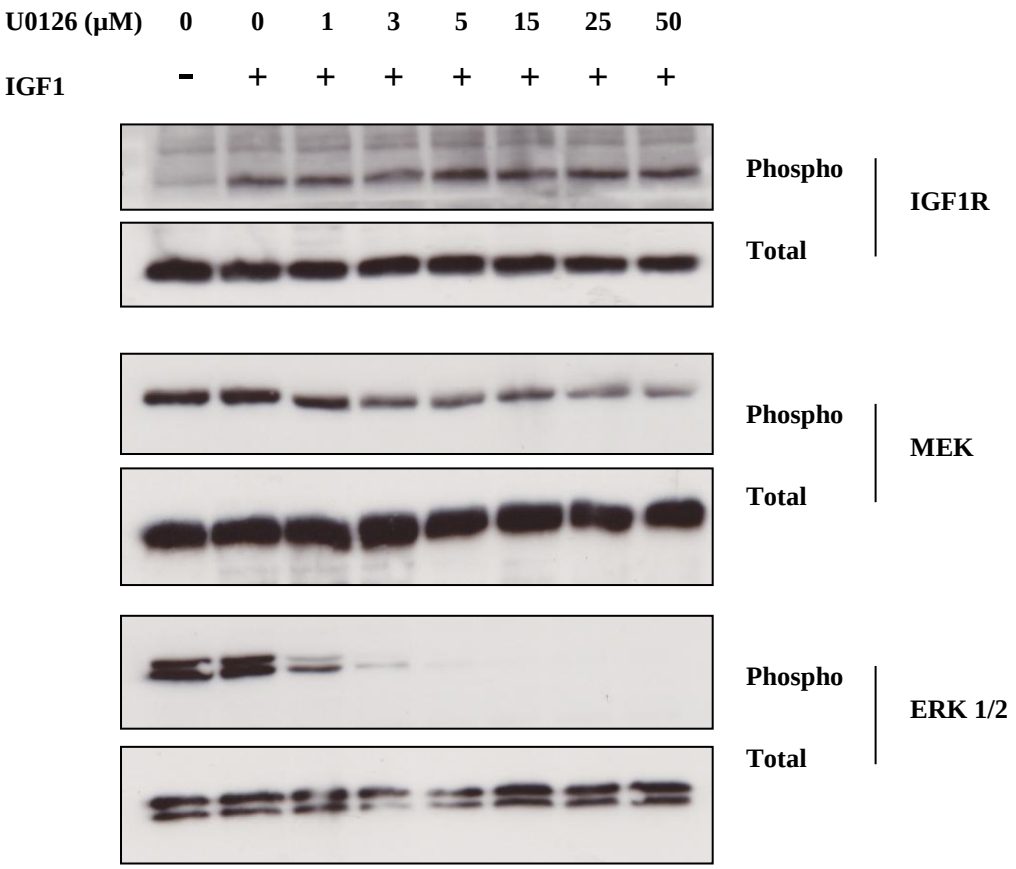


Figure 5.4 U0126 inhibits MEK and ERK activation following IGF1 stimulation in A375 cells. Serum deprived A375 cells were incubated U0126 for 4 hours and then treated with 8nM of IGF1 for 15 minutes. Phosphorylated and total forms of IGF1R, MEK and ERK were quantified by immunoblot. U0126 inhibits IGF1 induced MEK and ERK phosphorylation in a dose dependant manner. 15µM U1026 completely inhibited IGF1 induced ERK phosphorylation and reduced MEK phosphorylation.

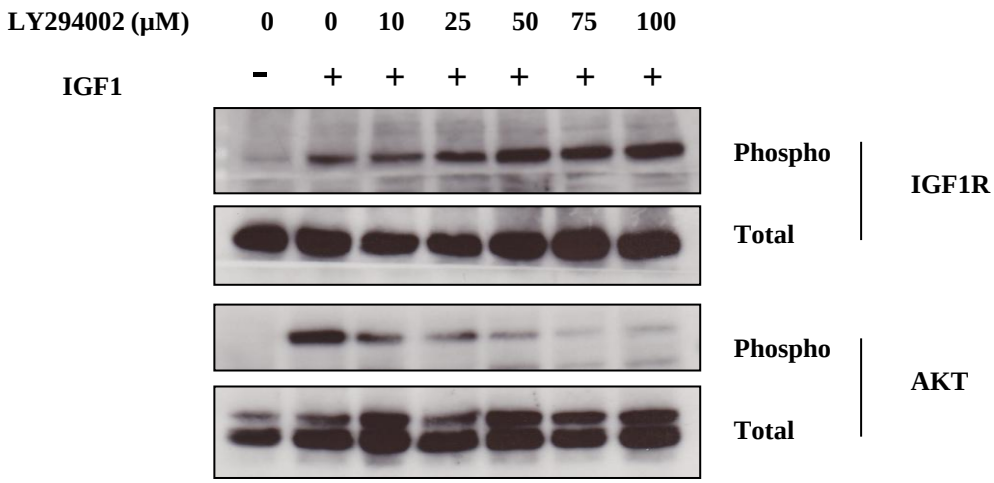


Figure 5.7 LY294002 abrogates IGF1 induced AKT phosphorylation. Serum deprived A375 cells were incubated with LY294002 for 4 hours and then treated with 8nM of IGF1 for 15 minutes. Phosphorylated and total forms of IGF1R and AKT were quantified by immunoblot. LY294002 inhibits IGF1 induced AKT phosphorylation in a dose dependant manner.75μM LY294002 completely inhibited IGF1 induced AKT phosphorylation.

deprivation, with IGF1 or solvent, with or without 15µM U1206 or 75µM LY294002. Total RNA was extracted and qRT-PCR for *HBP1* mRNA performed. In the absence of U0126, IGF1 induced significant reduction in *HBP1* mRNA as previously documented and unexpectedly addition of U0126 to serum starved cells resulted in a significant increase in *HBP1* mRNA (Figure 5.6A left). In compete medium U1026 enhanced the AZ12253801 induced increase in HBP1 (Figure 5.6A right). These observations may suggest that constitutive ERK activity lowers basal *HBP1* transcription. This finding may be of significance when utilising treatments which abrogate basal MAPK phosphorylation and would be explored should further experiments reveal that changes in *HBP1* transcription resulted in a phenotypic effect.

Whilst MEK inhibition did not prevent IGF1 induced changes in *HBP1* expression, the PI3K inhibitor LY294002 significantly increased *HBP1* mRNA and prevented the IGF1 induced reduction (Figure 5.6B left). Similarly incubation of cells in full medium with LY294002 resulted in a significant increase in *HBP1* mRNA, with no further increase following addition of AZ12253801 (Figure 5.6B right). These data suggested that IGF1R mediated effects on *HBP1* mRNA are mediated via the PI3K/AKT pathway.

5.2.3.2 Testing effects of mTOR inhibition on *HBP1* expression

It had previously been shown that IGF1 and AZ12253801 affected phosphorylation of P70 S6 Kinase, one of the most well characterised substrates of mTOR, itself a downstream effector of AKT (Figure 5.3). mTOR has effects on both translation, via P70 S6 Kinase and 4E-BP1, the eukaryotic initiation factor 4E (eIF4E) binding protein 1 and transcription via p70 S6 Kinase, and was thus a potential regulator of *HBP1* mRNA (Hay and

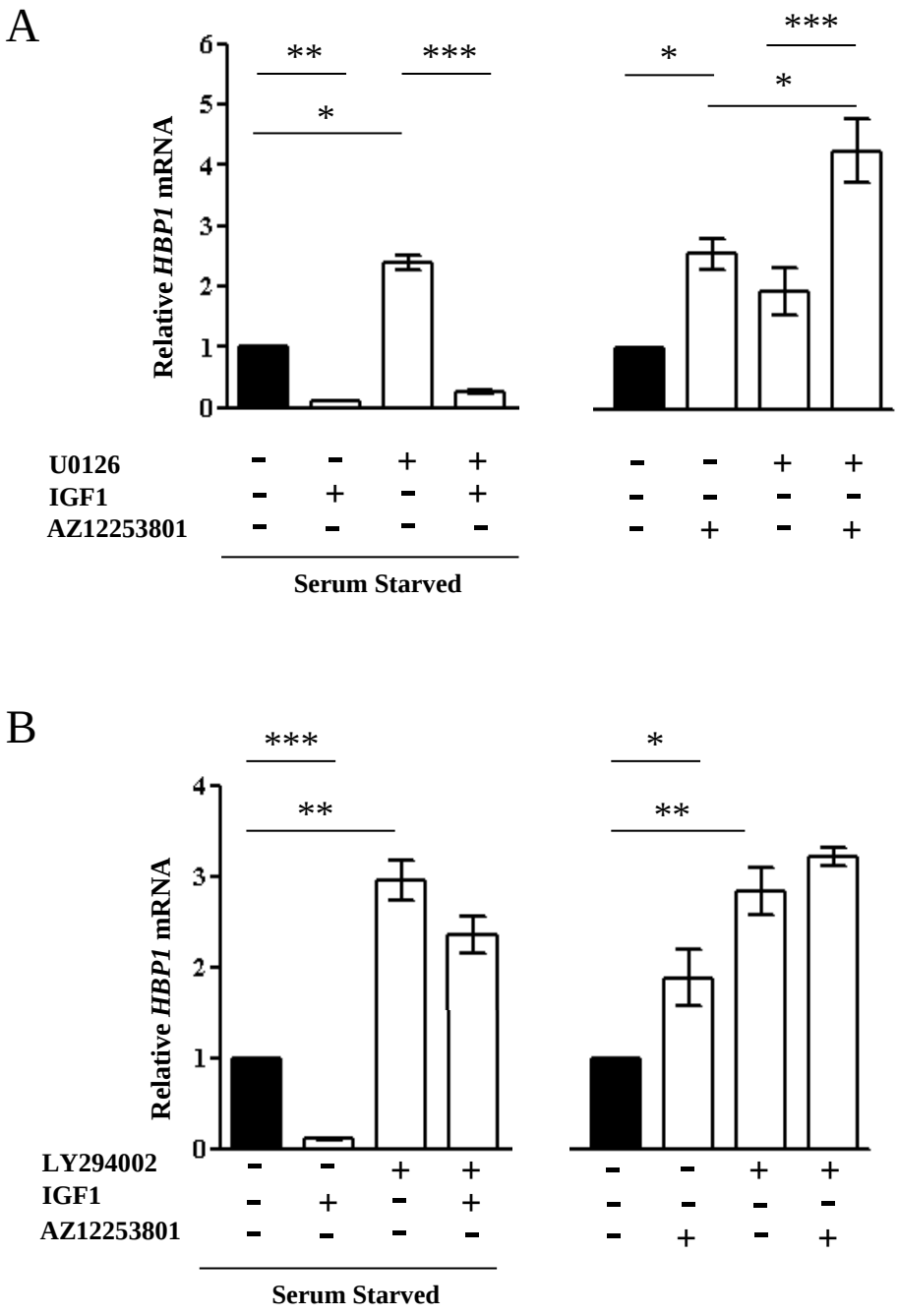


Figure 5.6 Effect of U0126 and LY294002 on IGF1R mediated changes in *HBP1* expression. A375 cells were treated with 15µM U0126 or 75µM LY294002 for 1 hour followed by 3 hours treatment with 8nM IGF1 or 50nM AZ12253801. Cells treated with IGF1 had been serum deprived overnight prior to inhibitor addition. HBP1 expression was quantified by qRT PCR. Histograms represent mean relative change (±SEM) in mRNA normalised to control cells (black bar) from 3 independent experiments. **A)** U0126 significantly increased *HBP1* expression in serum deprived cells and cells in complete medium. U0126 did not prevent changes in *HBP1* expression caused by IGF1R manipulation. **B)** LY294002 significantly increase in *HBP1* expression in serum deprived cells and cells in complete medium. Pretreatment with LY294002 prevented an IGF1 induced decreased, and AZ12253801 induced increase, in *HBP1* expression.

(*P<0.05, ** P<0.01, *** P<0.005 by one way ANOVA)

Sonenberg, 2004, Zaragoza et al., 1998, Hannan et al., 2003). Furthermore mTOR is known to modulate the transcription of some IGF induced genes such as *RNA POL1*, and effects of mTOR on increasing mRNA stability have been postulated (James and Zomerdijk, 2004, Vaira et al., 2006). Thus mTOR could affect *HBP1* protein levels either via translation or by increasing *HBP1* transcript stability. Furthermore mTOR is involved in the regulation of Rb phosphorylation and thus E2F activity, so it seemed plausible that mTOR might also regulate HBP1 (Usui et al., 2000).

Serum starved A375 cells were incubated with increasing concentrations of rapamycin, an inhibitor of mTORC1, to test effects on IGF induced activation of mTOR effectors. In serum starved cells P70 S6 Kinase was unphosphorylated, whilst S6 was basally phosphorylated, as had been previously documented (Figure 5.7). Addition of IGF1 resulted in phosphorylation of P70 S6 Kinase, with a minor increase in phosphorylation of S6. Rapamycin caused complete abrogation of the phosphorylation of P70 S6 Kinase but residual S6 phosphorylation was observed even at high concentrations.

The next experiment tested the effects of rapamycin on *HBP1* expression. A375 cells were treated with AZ12253801 or, following serum deprivation, with IGF1 with or without 5nM rapamycin. In the absence of rapamycin, IGF1 and AZ12253801 induced significant reduction and increase in *HBP1* mRNA respectively as previously documented (Figure 5.8). Treatment with rapamycin increased basal *HBP1* expression but did not alter the relative magnitude of the IGF1 induced reduction. Pretreatment with rapamycin partially abrogated the increase in *HBP1* expression following AZ12253801 treatment. These results were not consistent with mTOR mediating an increase in *HBP1* mRNA halflife.

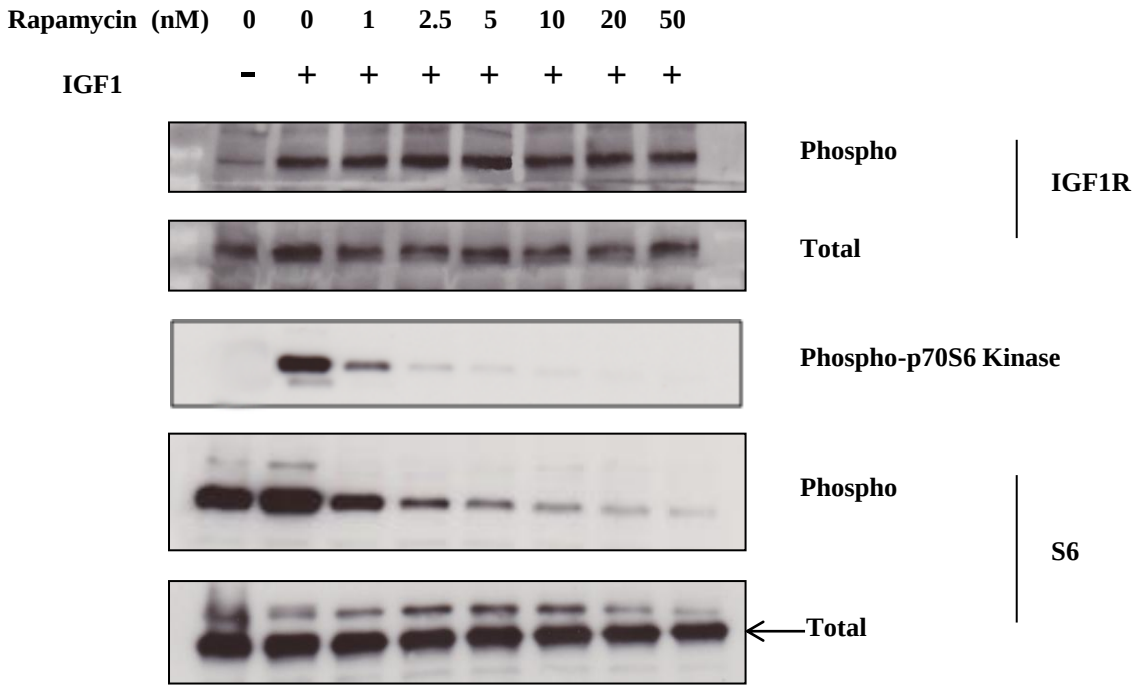


Figure 5.7 Rapamycin inhibits IGF1 induced phosphorylation of S6 and p70-S6 Kinase. A375 cells were serum deprived overnight, treated with rapamycin for 4 hours and then treated with 8nM of IGF1 for 15 minutes. Phosphorylated and total forms of IGF1R, p70S6 Kinase and S6 were quantified by immunoblot. Rapamycin inhibited IGF1 induced phosphorylation of p70S6 Kinase and S6 in a dose dependant manner. 5nM rapamycin completely inhibited p70S6 Kinase but weak phosphorylation of S6 persisted even at high doses.

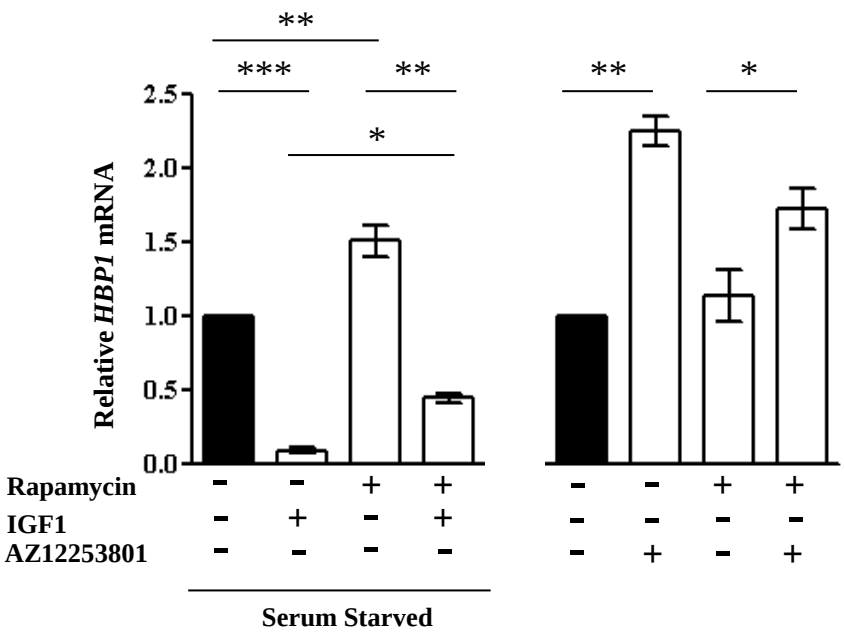


Figure 5.8 Effect of rapamycin on IGF1R mediated changes in *HBP1* expression. A375 cells were treated with 5nM rapamycin for 1 hour followed by 3 hours treatment with 50nM IGF1 or AZ12253801. Cells treated with IGF1 had been serum deprived overnight prior to inhibitor addition. HBP1 expression was quantified by qRT PCR. Histograms represent mean relative change (±SEM) in mRNA normalised to control cells (black bar) from 3 independent experiments. Rapamycin significantly increased *HBP1* expression in serum deprived cells and cells in complete medium. Rapamycin did not prevent or affect the magnitude of changes in *HBP1* expression caused by IGF1R manipulation.

(*P<0.05, ** P<0.01, *** P<0.005 by one way ANOVA)

Taken together, it appeared that rapamycin had induced minor modifications in the HBP1 response to IGF1, but had not completely abolished it, unlike the PI3K inhibitor LY294002 (Figure 5.6B). It was concluded that the effects of IGF1R manipulation on *HBP1* expression were mediated downstream of PI3K, by an effector other than mTORC1. AKT is directly downstream of PI3K and has numerous substrates (Manning and Cantley, 2007). To reduce the number of potential molecules for investigation, the HBP1 gene promoter was interrogated.

In silico analysis of *HBP1* revealed numerous transcription factor binding motifs immediately upstream of the transcription start site (www.sabiosciences.com). Of particular interest were CMYC and NMYC, known gene targets of HBP1 and the Forkhead box family members FOXO1, 1A, 3, 3A, 3B and 4. Overexpression of FOXO3 has previously been demonstrated to increase expression of *HBP1* in a prostate carcinoma cell line and HBP1 has been described as a FOXO3A regulated gene on this basis (Essaghir et al., 2009, Hegde et al., 2007, Modur et al., 2002b). FOXO3 has been shown to be phosphorylated following IGF1 stimulation, excluding it from the nucleus and preventing the initiation of transcription (Davila and Torres-Aleman, 2008, Li et al., 2008). Therefore it was possible that FOXO family members could mediate the effects of IGF1R manipulation on *HBP1* transcription. There is marked redundancy within FOXO family members and as such siRNA mediated depletion of individual family members was unlikely to yield meaningful results (Hosaka et al., 2004). To the author's knowledge there is no pan-FOXO inhibitor. Instead a previously characterised dominant negative plasmid encoding the DNA binding domain of FOXO4 (FOXO4DN) was obtained (a kind gift from Dr T. Kress) (Medema et al., 2000). Transfection of the dominant negative plasmid into A375 cells resulted in a marked phenotypic change with a slowing of cell growth and

an increase size. This observation was unexpected as overexpression of FOXO family members has been shown to suppress cellular growth (Medema et al., 2000). However it was not possible to detect HA tagged FOXO4DN by immunoblotting in A375 transfectants and there was no change in basal *HBP1* or *HBP1* upregulation in response to AZ12253801 (Figure 5.9). As such efficient transfection could not be confirmed. The originating laboratory reported similar problems, had obtained the plasmid from elsewhere and, unfortunately, the plasmid sequence was unknown to them. Had time allowed, sequencing of the plasmid would have enabled confirmation of the coding sequence of the insert and use of RT PCR to confirm construct expression. This would have allowed experiments to assess whether FOXO family members mediate IGF1R induced changes in *HBP1* expression. Should FOXOs have been implicated as the downstream effector of AKT responsible for modulating *HBP1* transcription, the identity of the specific FOXO family member could be ascertained by chromatin immunoprecipitation using antibodies for each FOXO, followed by PCR for FOXO binding sites in the HBP1 promoter.

The results of these experiments suggested that changes in HBP1 expression following IGF1R manipulation were mediated via the PI3K pathway. Further experiments to interrogate the role of FOXOs were hampered by technical issues. Although the mechanism was not fully understood, it was appropriate to determine whether changes in HBP1 were of biological significance in melanoma. Two approaches were taken to address this question. Firstly experiments were conducted to investigate the significance of IGF1R mediated changes in HBP1 on cellular phenotype and expression of known HBP1 gene targets *in vitro*. Secondly publically available databases were interrogated to determine whether HBP1 expression is altered in clinical cases of melanoma.

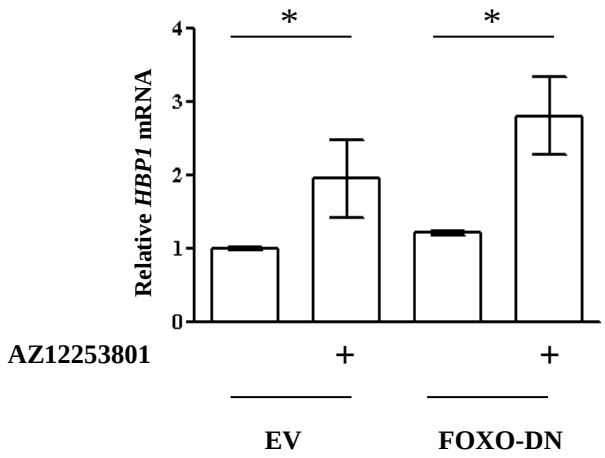


Figure 5.9 Effect of FOXO dominant negative plasmid transfection on IGF1R mediated changes in *HBP1* expression. A375 cells were transfected with a FOXO4 dominant negative plasmid or empty vector. After 48 hours cells were treated with 50nM AZ12253801 for 3 hours and *HBP1* expression was assessed by qRT-PCR. Histograms represent mean relative mRNA (±range) normalised to untreated cells transfected with empty vector, from 2 independent experiments. FOXO4DN did not affect AZ12253801 induced expression of *HBP1*.

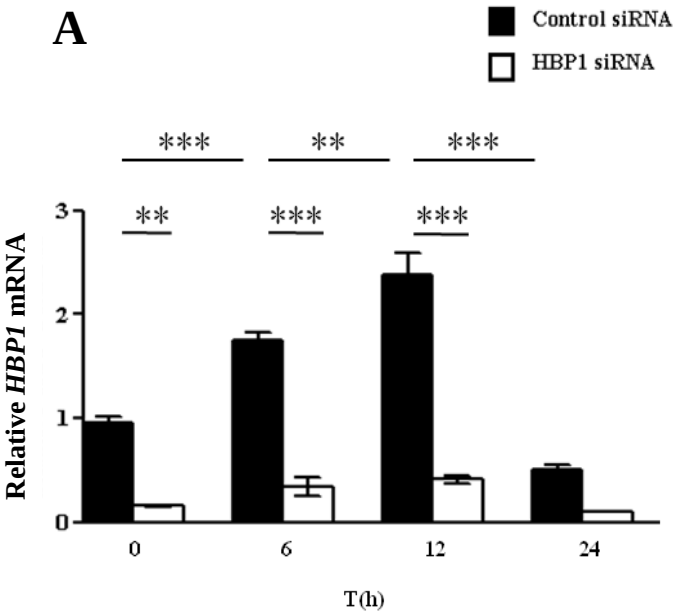
(*P<0.05 by one way ANOVA)

5.2.4 Effect of HBP1 depletion on cell cycle progression.

It had previously been demonstrated that overexpression of HBP1 resulted in G_1/S cell cycle arrest in C33A (cervical carcinoma), C2C12 (murine myoblast), hepatocytes and K562 erythroleukaemic cells (Tevosian et al., 1997, Shih et al., 2001, Yao et al., 2005). It was therefore interesting to determine what role IGF1R mediated changes in HBP1 played in the cell cycle progression of A375 melanoma cells.

A375 cells were reverse transfected with either HBP1 or control siRNA. After 48 hours the cells were serum deprived for 12 hours before addition of IGF1. Cell cycle distribution was determined using the BrdU/PI flow cytometry method at the time of serum deprivation (0h), 6 and 12 hours after serum deprivation, and 12h after IGF1 addition (24h). Total RNA was harvested from parallel samples and *HBP1* mRNA levels quantified by qRT-PCR.

In cells transfected with control siRNA, *HBP1* mRNA significantly increased both 6 and 12 hours after serum deprivation and declined following addition of IGF1 (Figure 5.10A). HBP1 mRNA was significantly reduced at the 0, 6 and 12h timepoints in HBP1 siRNA transfected cells. Residual *HBP1* mRNA levels in HBP siRNA transfected cells followed a similar, if attenuated, pattern in response to serum deprivation and IGF treatment as the control transfected cells but there was no significant change over the course of the experiment. After addition of IGF1 there was no significant difference in *HBP1* mRNA between control and HBP1 siRNA transfected cells. The similar pattern of change in *HBP1* mRNA in control and HBP1 siRNA transfected cells suggested even in the face of *HBP1* depletion with siRNA, starvation and IGF1 treatment were potent stimuli affecting *HBP1* mRNA levels.



B

	T (h)	Phase of the Cell cycle (%) G0/ G1	Early S	Late S	Total S	G2/ M
Control siRNA	0	56.4	20.7	15.6	36.3	7.3
	6	64.9	10.9	15.2	26.1	9.1
	12	78.7	9.7	6.1	15.8	5.5
	24	52.4	20.6	16.8	37.4	10.2
HBP1 siRNA	0	59.1	16.0	16.4	32.4	8.5
	6	64.9	11.3	13.6	24.9	10.3
	12	79.3	9.5	5.4	15.0	5.7
	24	55.7	22.5	12.4	34.9	9.4

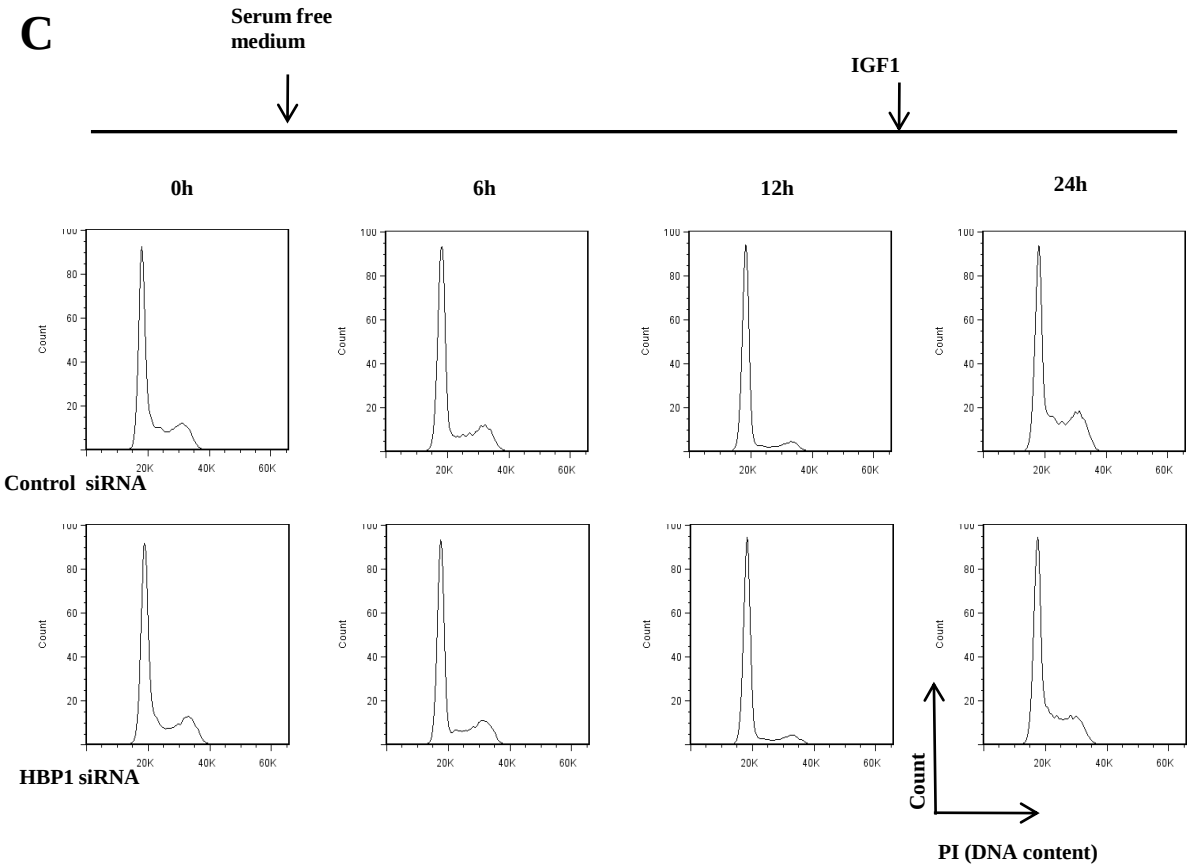


Figure 5.10 HBP1 depletion has no effect on IGF1R mediated changes in cell cycle distribution of A375 melanoma cells. A375 cells were serum deprived 48 hours after siRNA mediated *HBP1* depletion. Samples were collected at the time of serum deprivation (T=0), 6, 12 and 24 hours later. 8nM IGF1 was added after 12 hours **A)** *HBP1* expression was quantified by qRT-PCR. Histograms represent mean relative (±SEM) in mRNA normalised to control conditions from 3 independent experiments. HBP1 expression increased in control transfectants after serum deprivation but not in HBP1 depleted cells. **B)** Cell cycle distribution was determined by flow cytometry using BrdU incorporation. Values represent mean % from 3 independent experiments. % cells in phases of the cell cycle did not alter after HBP1 depletion. **C)** Representative cell cycle distribution plots. Similar plots were obtained in 3 independent experiments.

(**P<0.01, *** P<0.005 by one way ANOVA)

following serum deprivation, control siRNA transfected cells accumulated in $G_{1,}$ with a restoration of S and G2/M populations following IGF1 addition (Figure 5.10B & C). The cell cycle distribution profile of HBP1 depleted cells was not significantly different to control siRNA transfected cells at any time point.

It was concluded from this experiment that HBP1 has little role in controlling the cell cycle progression of A375 cells and that serum deprivation represents a strong drive to *HBP1* transcription, even in the face of siRNA mediated depletion.

5.2.5 Effect of HBP1 depletion on proliferation of A375 melanoma cells.

Wnt/β catenin signalling has been shown to reduce the proliferation of A375 melanoma cells (Chien et al., 2009, Widlund et al., 2002). Given that HBP1 inhibits transcription of Wnt/β catenin gene targets it was postulated that depletion of HBP1 would further decrease cell proliferation by removing repression of the Wnt/β catenin pathway. In addition given that *HBP1* expression is increased by inhibition or depletion of the IGF1R, and that IGF1R inhibition decreases cell proliferation it was possible that HBP1 antagonises, at least in part, effects of IGF1 on cell proliferation.

The next experiments tested effects of HBP1 depletion on the anti-proliferative effects of AZ12253801. A375 cells were reverse transfected with HBP1 or control siRNA and AZ12253801 was added 48 hours later. Proliferation was assessed a further three days later by the Cell Titer Glo method. Parallel samples were harvested for assessment of *HBP1* mRNA by qRT PCR which confirmed significant *HBP1* depletion (Figure 5.11A). Treatment with AZ12253801 inhibited cell proliferation to ~65% of control transfectants, consistent with previous results (Figure 4.5). However HBP1 depletion had no additional effect on proliferation nor on growth inhibition by AZ12253801 (Figure 5.11B).

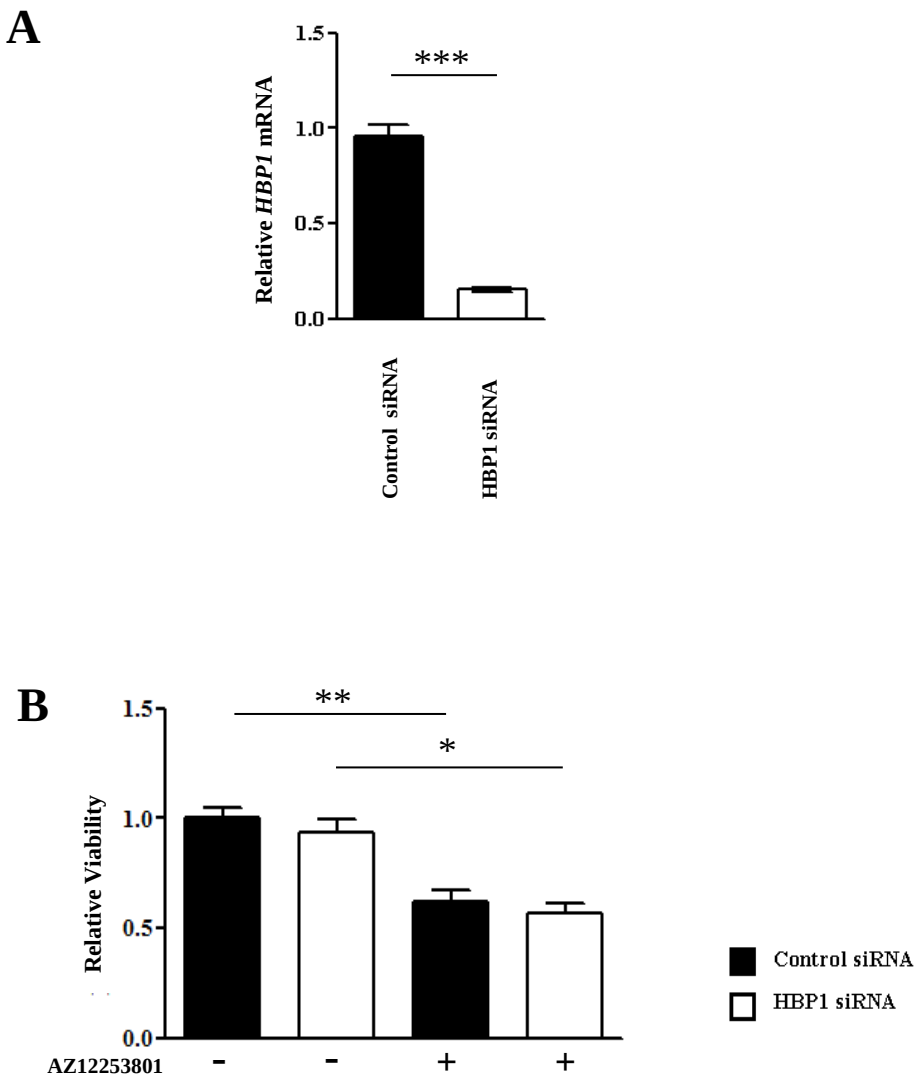


Figure 5.11 Effect of HBP1 depletion on growth of A375 melanoma cells. A) HBP1 or control siRNA transfected cells were treated with vehicle or 50nM AZ12253801 24 hours after transfection. **A)** *HBP1* expression was quantified by qRT-PCR. *HBP1* expression was significantly reduced 72 hours following siRNA mediated HBP1 depletion. **B)** Cell viability, in duplicate wells, was assessed by Cell Titer Glo assay 48 hours after treatment. Histograms represent mean relative viability(±SEM) normalised to control conditions from 3 independent experiments, each with 3 data points. AZ12253801, but not *HBP1* depletion, inhibited cell viability.

Treatment (*P<0.05, **P<0.01, *** P<0.005)

These results demonstrated that HBP1 depletion had no effect on proliferation of A375 melanoma cells and did not influence the growth inhibitory effect of AZ12253801. These results suggest HBP1 does not diminish the effects of IGF1R on growth of A375 cells. There was no increase in proliferation of A375 cells following HBP1 depletion suggesting that in complete medium HBP1 does not inhibit action of mitogenic pathways for example Wnt/β catenin. The role of HBP1 in Wnt/β-catenin signalling in A375 melanoma is investigated further in a subsequent section.

5.2.6 Expression of HBP1 in clinical melanoma – *in silico* analysis

Given that loss of HBP1 function and expression had previously been associated with invasive disease in patients with breast cancer (Paulson et al., 2007), it was interesting to investigate if there was any association between HBP1 expression and melanoma progression. Analysis of the melanoma datasets available via the Oncomine portal (www.oncomine.org) revealed five in which a comparison between melanoma and benign naevi was possible. In one dataset HBP1 expression was significantly lower in melanoma compared to benign naevi (P=0.004) (Talantov et al., 2005). In those clinical datasets where patient data was available there was no correlation between HBP1 expression and any clinical parameter, such as survival.

The same clinical melanoma datasets as described in Chapter 4, GSE19234 (Bogunovic et al., 2009) and GSE22153 (Jonsson et al., 2010) deposited at The Gene Expression Omnibus were interrogated for correlation of HBP1 expression to clinical parameters. Data interrogation was performed by Dr Francesca Buffa and relevance of the results determined by the author. HBP1 expression was not correlated to any clinical parameters in the first dataset (GSE19234). In the second dataset tumours with a high Ki67 score

(>30%) had significantly reduced HBP1 expression compared to low Ki67 tumours. (Figure 5.12). As described in Chapter 4, Ki67 is used as a marker for cellular proliferation and is of prognostic significance in melanoma. That HBP1 expression is lower in aggressive tumours, as it the case in breast cancer (Paulson et al., 2007), provided further evidence that manipulation of HBP1 expression might be of therapeutic benefit.

5.2.7 Effect of IGF1R manipulation on known HBP1 transcriptional targets

From the results presented in 5.2.4 and 5.2.5 it appeared that either HBP1 played little role in cell cycle progression or proliferation of A375 cells, or that compensatory changes following HBP1 depletion were preventing observation of a phenotype. In order to better understand the consequences of IGF1R induced changes in *HBP1* expression, experiments were performed to assess the temporal changes in *HBP1* mRNA and that of its best characterised gene targets following IGF1R manipulation. The aim was to understand how expression of *HBP1* and selected HBP1 target genes varied following IGF axis manipulation.

A375 cells were incubated with AZ12253801 or vehicle or, following serum deprivation, with IGF1 or solvent, and total RNA was harvested prior to, and at intervals following treatment addition. qRT-PCR was performed for *HBP1* and 6 gene targets of HBP1 identified from the literature: *CCND1, CMYC, NMYC, CDKN2A, NCF1* and Macrophage inhibitory factor (*MIF)*(Tevosian et al., 1997, Tetsu and McCormick, 1999, Sampson et al., 2001, He et al., 1998, Escamilla-Powers et al., 2010, Berasi et al., 2004, Li et al., 2010, Gartel et al., 1998, Chen et al., 2010).

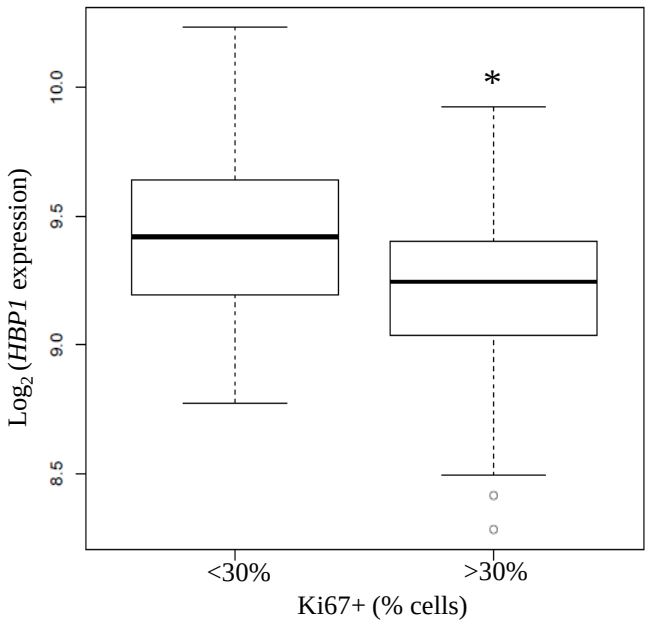


Figure 5.12 Expression of HBP1 is lower in proliferative melanoma. Gene expression of *HBP1* was assessed in KI67% high (>30%) and low (<30%) melanoma metastases from GEO dataset GSE 22153. *HBP1* expression was lower in high Ki67% tumours compared to low Ki67% tumours

(*P<0.05 by Kruskal-Wallis chi squared test)

HBP1 mRNA was significantly higher in serum deprived cells compared to cells in full medium at the start of the experiment and remained unchanged over the course of the experiment (Figure 5.13A). *HBP1* mRNA was significantly decreased one hour following addition of IGF1 and remained significantly reduced at all time points with a nadir at 3 hours and a non significant rise in *HBP1* mRNA between 12 and 24 hours. In contrast *HBP1* mRNA rose significantly within 2 hours of AZ12253801 treatment to a level which was sustained until a trend to further increase at 12 and 24 hours (Figure 5.13B). However in vehicle treated cells *HBP1* mRNA significantly increased between the 12 and 24 hour time points to a greater degree than in AZ12253801 treated cells. The cause of this rise in *HBP1* mRNA in vehicle treated cells is unclear. It could have been a consequence of increasing cellular confluence, as this was the only treatment group in which cell proliferation proceeded uninhibited throughout the experiment.

Notably in this experiment *HBP1* mRNA was significantly higher 24 hours after AZ12253801 treatment than in vehicle treated cells. This observation contrasts with the findings of the microarray experiment detailed in the previous chapter, in which *HBP1* expression was not significantly increased 24 hours after addition of AZ12253801. These experiments differ only in the size of the culture vessels; it is postulated that in the case of the microarray experiment, the rise in *HBP1* mRNA in vehicle treated cells was similar to that in AZ12253801 by the 24 hour time point. This may have resulted in HBP1 not being identified as a transcript altered by 24 hour treatment with AZ12253801.

Expression of HBP1 target genes (*CCND1, CMYC, NMYC, CDKN2A, NCF1* and *MIF*) over the time course of the experiment will be displayed as graphs (Figure 5.14 & 5.15). For clarity gene expression in control cells (serum starved (solvent treated) or cells in

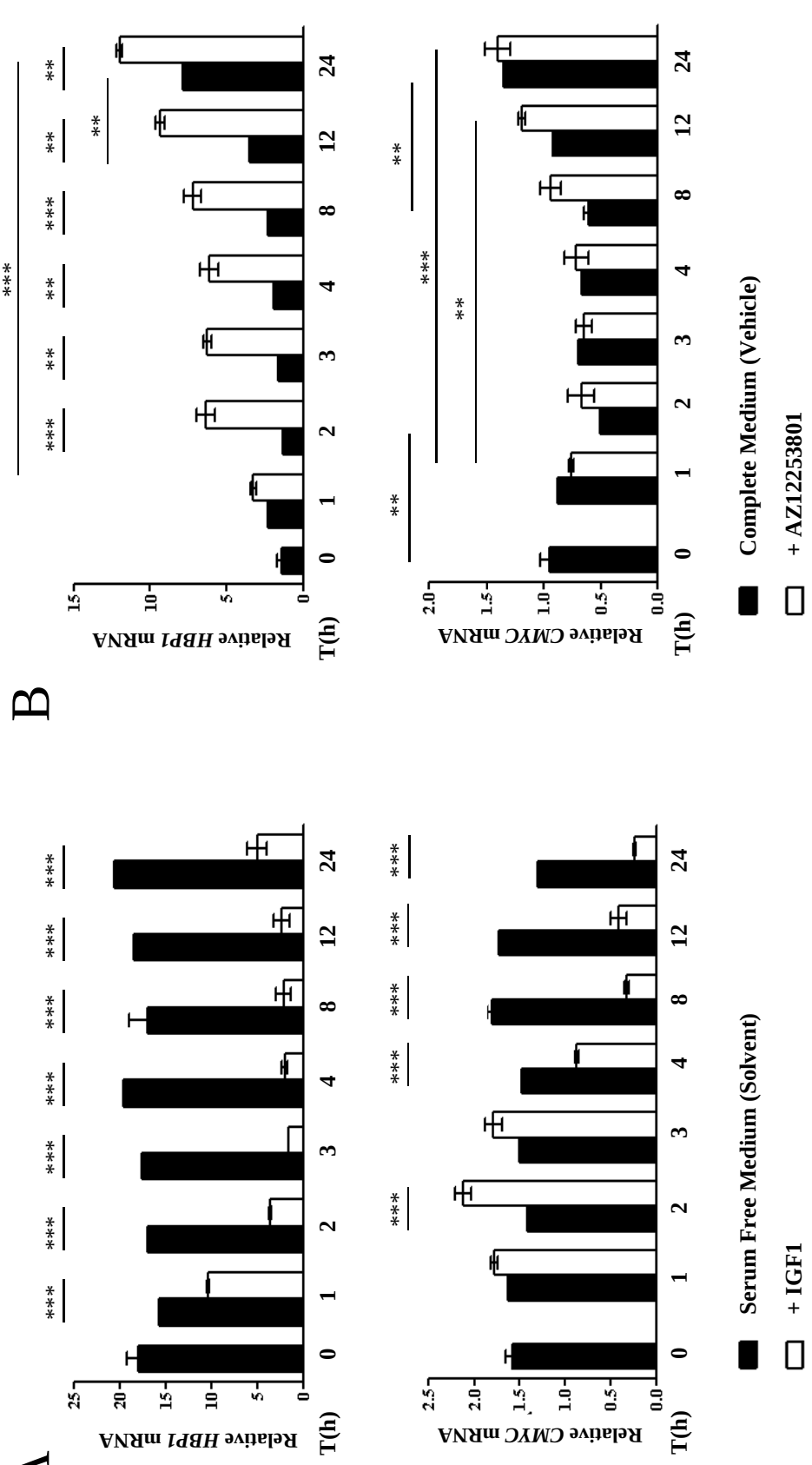


Figure 5.13 IGF1R manipulation influences *HBP1* and *CMYC* expression. A375 melanoma cells were treated with vehicle or 50nM AZ12253801 or, following overnight serum deprivation, with 8nM IGF1 or solvent. Expression of *HBP1* and *CMYC* were assessed by qRT-PCR at the start of the experiment and after 1,2,3,4,8,12 and 24 hours. Histograms represent mean relative expression (±SEM) from 3 individual experiments normalised to cells in full medium at T=O. *HBP1* expression in serum deprived cells fell rapidly after addition of IGF1, whereas expression gradually increased in AZ12253801 treated cells. *CMYC* expression increased transiently after IGF1 addition before falling below initial levels. *CMYC* expression was not significantly affected by AZ12253801.
(** P<0.01, *** P<0.005 by one way ANOVA).

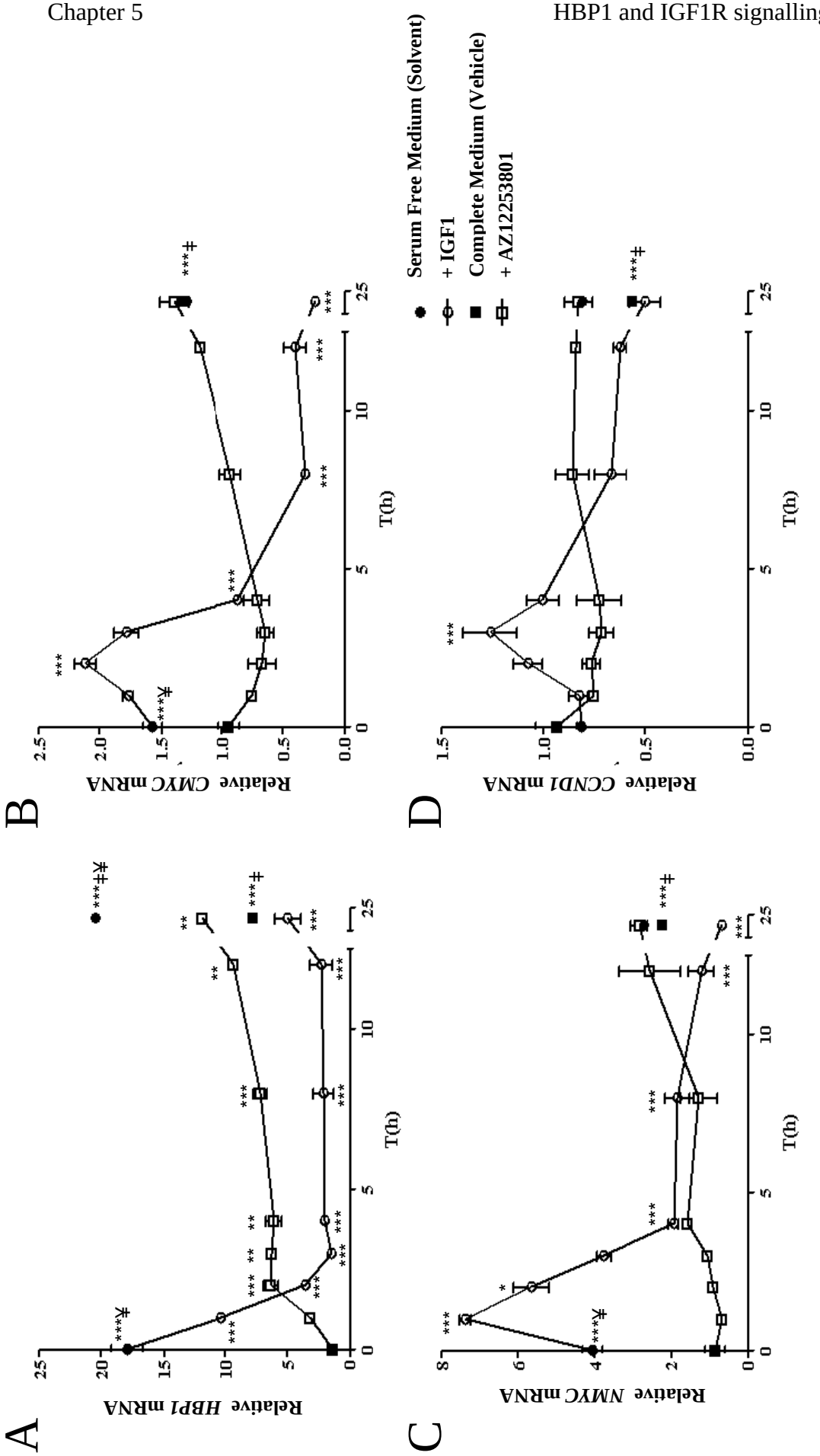


Figure 5.14 IGF1R manipulation is associated with temporal changes in *HBP1* mRNA and reciprocal changes in target gene expression. A375 melanoma cells were treated with vehicle or 50nM AZ12253801 or, following overnight serum deprivation, with 8nM IGF1 or solvent. Expression of *HBP1*, *CMYC*, *NMYC* and *CCND1* was assessed by qRT-PCR at the start of the experiment and after 1,2,3,4,8,12 and 24 hours. Graphs represent represent mean relative gene expression (±SEM) from 3 independent experiments normalised to cells in full medium at T=O. For clarity gene expression of serum deprived and vehicle treated cells are shown only at time points T=0 and T=24. Asterisks represent significant difference between gene expression of control and treated cells at a given time point, between serum deprived and vehicle treated cells (¥) or for control cells over the time course of the experiment (ǂ).*HBP1* expression fell and *CCND1*, *NMYC* and *CMYC* expression increased after IGF1 treatment. Data in A) and B) replicate that in Figure 5.13 (** P<0.01, *** P<0.005 by one way ANOVA).

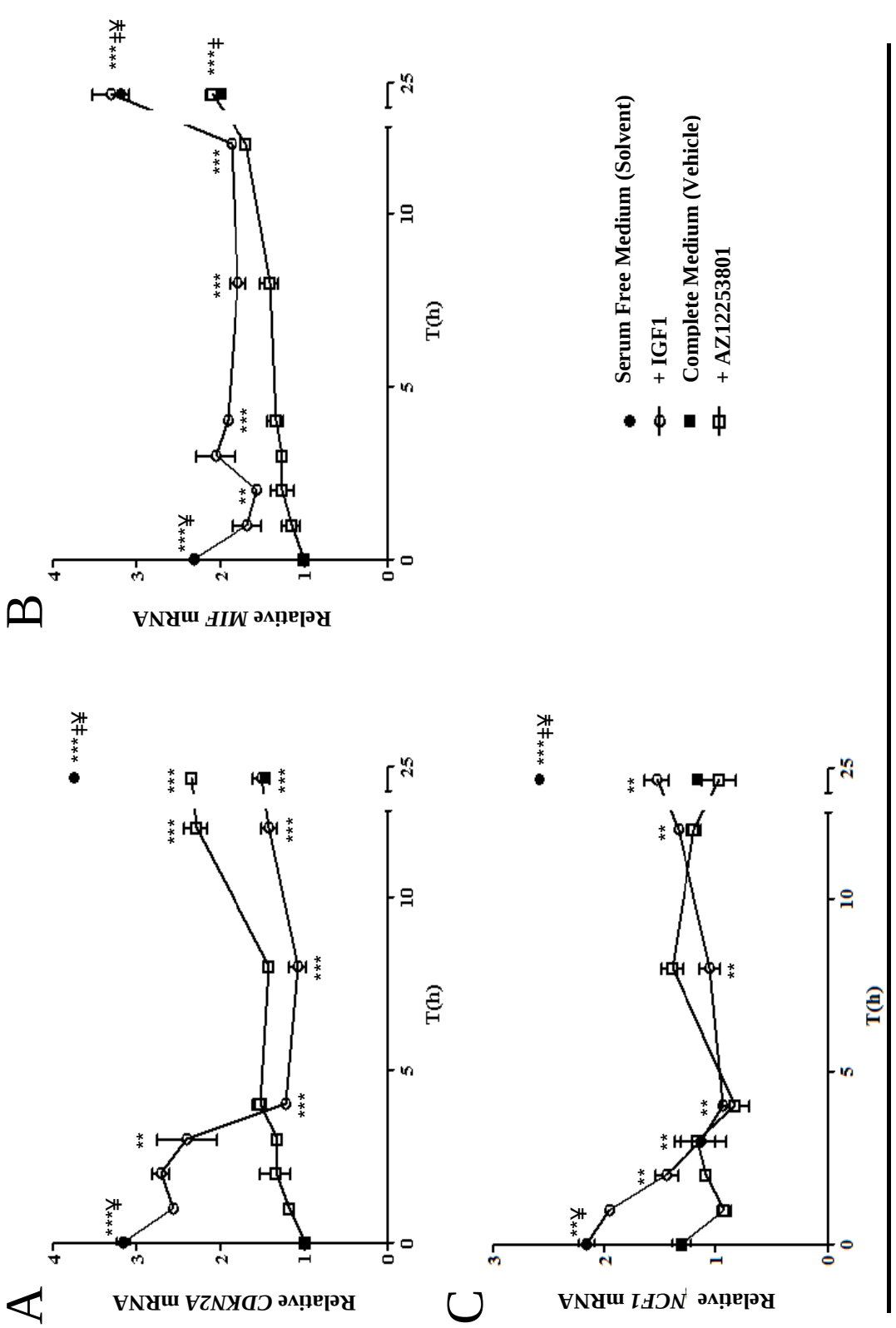


Figure 5.15 IGF1R manipulation is associated with temporal changes in *CDKN2A*, *MIF* and *NCF1* expression. A375 melanoma cells were treated with vehicle or 50nM AZ12253801 or , following overnight serum deprivation, with 8nM IGF1 or solvent. Expression of *CDKN2A*, *MIF* and *NCF1* was assessed by qRT-PCR at the start of the experiment and after 1,2,3,4,8,12 and 24 hours. Graphs represent represent mean relative gene expression (± SEM) from 3 independent experiments normalised to cells in full medium at T=O. For clarity gene expression of serum deprived (solvent) and vehicle treated cells are shown only at time points T=0 and T=24. Asterisks represent significant difference between gene expression of control and treated cells at a given time point, between serum deprived and vehicle treated cells (¥) or for control cells over the time course of the experiment (ǂ).Gene expression fell after addition of IGF1 before significantly increasing at late time points. *CDKN2A* expression is significantly increased 24 hours after AZ12253801 treatment.

(** P<0.01, **** P<0.005 by one way ANOVA).

complete medium (vehicle treated)) are displayed only at the 0 and 24 hour time points as these varied little over the time course of the experiment. As an illustration *HBP1* and *CMYC* expression in both control and manipulated cells are displayed in Figure 5.13 and for manipulated cells only in Figure 5.14. In serum starved, solvent treated, cells there was no significant change in *CMYC* expression over the time course of the experiment. In contrast in vehicle treated cells in complete medium there was a significant fall in *CMYC* expression at 2 hours followed by a significant increase at 24 hours, CMYC expression at 24 hours was not significantly different to that at 0 hours (Figure 5.14).

Following IGF1R manipulation, expression of HBP1 target genes (*CCND1, CMYC, NMYC, CDKN2A, NCF1* and *MIF*) appeared to fall in two groups with common temporal patterns. The first group comprised *NMYC, CMYC,* and *CCND1* (Figure 5.14). *NMYC* and *CMYC* expression was significantly higher in serum starved cells compared to those in complete medium at the start of the experiment but had fallen to similar levels by the 24 hour time point. Cells in complete medium showed a significant rise in *NMYC* and *CMYC* expression during the course of the experiment whereas *CCND1* expression fell significantly. *CCND1, CMYC* and *NMYC* expression was significantly increased 1-3 hours following IGF1 addition then reduced between the 4 and 24 hour time points. Expression fell significantly below that of the serum deprived (solvent treated) cells by 24 hours, in the case of *NMYC* and *CMYC* this fall was significant. *CMYC* and *CCND1* expression followed a similar pattern following AZ12253801 treatment. Expression initially fell to a nadir at 3-4 hours followed by a rise to a maximum at 24 hours but gene expression was not significantly different to control cells in complete medium at each time point.

As such, in IGF1 treated cells these genes displayed an expression profile as might be expected if HBP1 was repressing expression, and the fall in HBP1 on IGF1 treatment

removed this inhibition. The increase in *HBP1* expression on AZ12253801 treatment was somewhat less, and no significant change in target gene expression was detected.

CDKN2A, NCF1 and *MIF* comprised a second group of HBP1 target genes, in which gene expression followed that of *HBP1* (Figure 5.15). *CDKN2A, NCF1* and *MIF* expression was significantly higher in serum starved, solvent treated, cells compared to those in complete medium (vehicle treated) at the start and end of the experiment. Furthermore there was a significant increase in *CDKN2A, NCF1* and *MIF* expression over the time course of the experiment in serum starved, solvent treated, cells. In the case of *CDKN2A* this is not unexpected as this molecule is an inhibitor of cyclin D mediated cell cycle progression, and would be expected to be expressed with prolonged serum starvation. Expression of all three genes fell significantly in the 4 hours following IGF1 addition and remained low thereafter. In vehicle treated control cells in complete medium *MIF* expression increased over the time course of the experiment whereas *CDKN2A* and *NCF1* expression did not. There was a trend to increased expression during the latter half of the experiment similar to that seen in serum starved, solvent treated, cells. In AZ12253801 treated cells *CDKN2A* and *MIF* expression gradually increased but this was only significant for *CDKN2A* after 12 hours. *NCF1* expression was unchanged following the addition of A12253801.

Changes in target gene expression in control cells over the time course of the experiment may have been due to factors such as cell confluence and medium depletion. In some cases these confounding factors may have acted to diminish the changes observed following IGF1R manipulation. However overall it was clear that the greatest changes in *HBP1* mRNA occurred in the 4 hours following IGF1 or AZ12253801 treatment and that significant changes in HBP1 target gene expression also occurred in this period. Furthermore although *HBP1* mRNA expression remained low for at least 24 hours

following IGF1 treatment, expression of genes repressed by HBP1 only transiently increased and subsequently expression fell below baseline levels. The change in expression of these target genes was also of a smaller magnitude than that of HBP1 itself. Irrespective of the half life of the HBP1 protein, there are clearly other influences on expression of genes repressed by HBP1 that can oppose the influence of HBP1.

Given that IGF1 is likely to affect transcription of shared IGF1 and HBP1 target genes such as *CMYC* and *CCND1* by multiple mechanisms, not only via HBP1, it was necessary to manipulate expression of HBP1 itself in order to elucidate its contribution to IGF signalling. *NMYC* and *CMYC* had demonstrated the expected reciprocity of change if HBP1 was repressing their expression, and the greatest changes in expression following IGF1R activation and inhibition (Figure 15.14). Therefore it was appropriate to concentrate further investigations on the first group of gene targets identified above.

5.2.8 Effect of HBP1 depletion on transcription of HBP1 target genes

NMYC, *CMYC* and *CCND1* are the best characterised gene targets of HBP1 and are also regulated by the IGF1R signalling pathway via multiple signalling cascades. For example IGF1R activation can affect *CCND1* expression via a variety of mechanisms, such as via E2F, activating transcription factor 2 (ATF2), nuclear factor Kappa B and fos related antigen 1 (FRA1) (Klein and Assoian, 2008). Therefore HBP1 gene silencing was used to determine whether the changes observed in HBP1 target gene transcription were attributable to IGF1 induced changes in HBP1 rather than IGF1R mediated effects via alternate pathways and effectors.

A375 cells were reverse transfected with HBP1 or control siRNA. After 48 hours cells were treated for three hours with AZ1223801 or vehicle, or, following serum deprivation,

with IGF1 or solvent. Total RNA was harvested and *HBP1*, *CMYC*, *NMYC* and *CCND1* expression was determined by qRT-PCR. *HBP1* expression was high in serum starved, solvent treated control transfectants and fell significantly on addition of IGF1 (Figure 5.16A). HBP1 expression was significantly reduced by HBP1 siRNA with only a minor further fall following addition of IGF1. In vehicle treated control transfectants in full medium *HBP1* was up regulated by AZ1223801 treatment, and this response was abrogated by *HBP1* depletion.

It was noted that in control transfectant cells serum deprivation had induced a 1.5 fold increase in *HBP1* expression (Figure 5.16A) compared to the 2.5 fold increase previously observed in untransfected cells (Figure 5.2). It was possible that the process of tranfection itself was inducing *HBP1* expression and that IGF1R axis induced changes might be blunted in comparison to those seen in untransfected cells. This might offer an explanation as to why, despite repeated attempts, *HBP1* could not be depleted below 15% of levels in control cells. This could be further explored by comparing *HBP1* expression in untransfected, control siRNA transfected and mock transfected cells.

In serum deprived control transfectants IGF1 treatment resulted in a significant increase in *CCND1* and *CMYC* expression (Figure 5.16B & D). Basal *CMYC* and *CCND1* expression, and the increase following IGF1 treatment were unchanged by *HBP1* depletion. In vehicle treated cells in complete medium *CCND1* and *CMYC* expression were unchanged by addition of AZ12253801 or HBP1 depletion.

In serum deprived cells *NMYC* expression fell on IGF1 treatment (Figure 5.16C). *HBP1* depletion resulted in a significant increase in *NYMC* expression, which fell to similar levels to that of control transfectants after IGF1 treatment. In complete medium there was no change in *NMYC* expression on addition of AZ12253801.

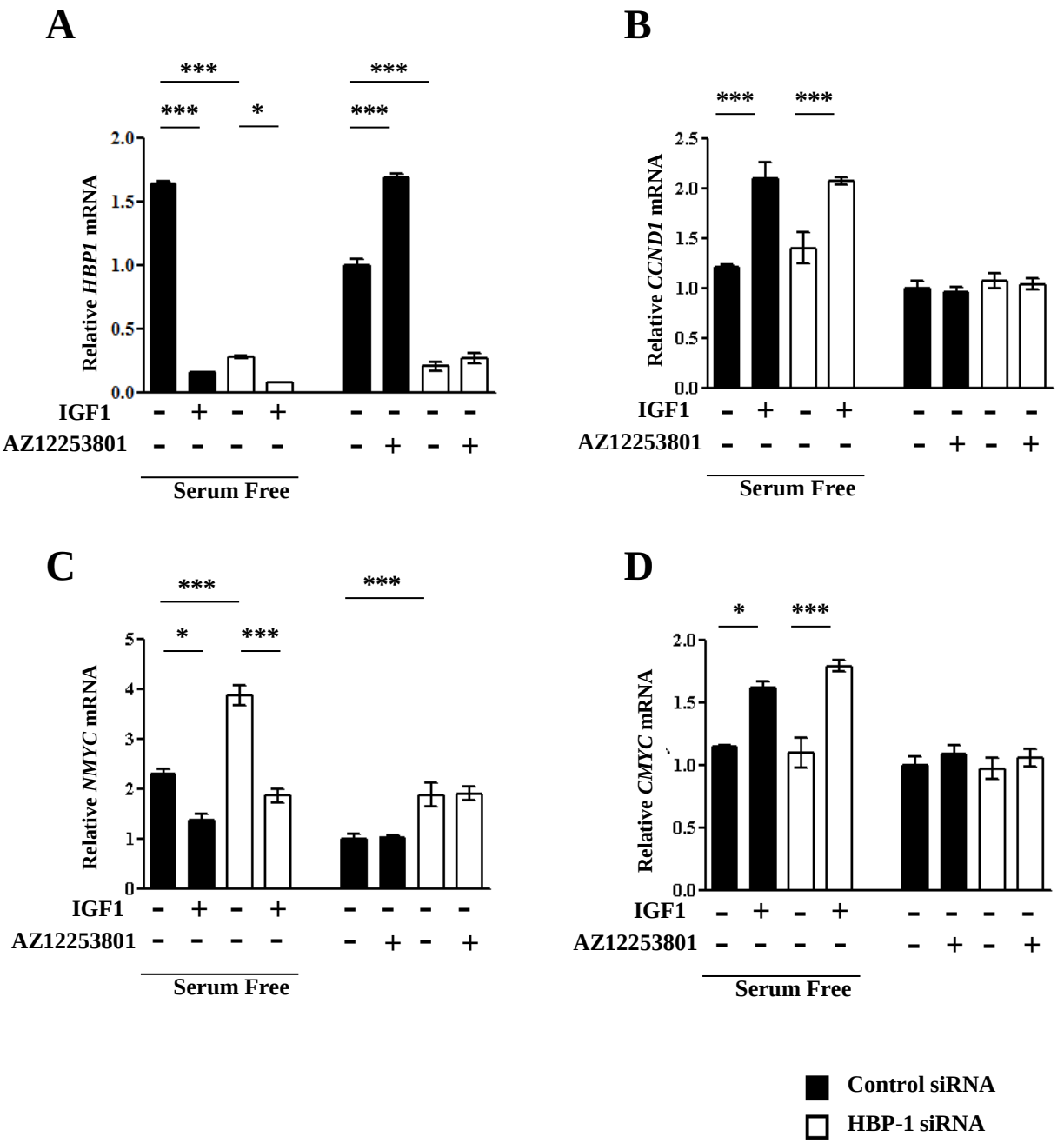


Figure 5.16 HBP1 depletion results in an increase in *NMYC*, but not *CMYC* or *CCND1* expression. HBP1 or control siRNA transfected A375 cells were treated for 3 hours with vehicle or 50nM AZ12253801 or, following overnight serum deprivation, with 8nM IGF1 or solvent. *HBP1, NMYC, CMYC, CCND1* expression was quantified by qRT-PCR. Histograms represent mean relative (±SEM) mRNA normalised to vehicle treated, control siRNA transfectants from 3 independent experiments. *HBP1* depletion significantly reduced *HBP1* expression and prevented IGF1R mediated changes in expression. *HBP1* depletion did not affect IGF1 induced *CMYC* and *CCND1* expression. *HBP1* depletion increased *NMYC* expression but did not alter the effect of IGF1R manipulation on *NMYC* expression.

(*P<0.05, **P<0.01, *** P<0.005 by one way ANOVA).

The increase in *CMYC* and *CCND1* mRNA and a decrease in *NMYC* mRNA 3 hours after IGF1 stimulation were expected from the previous results (Figure 5.14). Additional samples collected at an earlier time point might have determined whether HBP1 depletion affected the induction of *NMYC* mRNA that had been previously observed one hour after IGF1 treatment (Figure 5.14). However the fact that *NMYC* expression in HBP1 depleted cells exceeded that of control cells in both serum deprived and full medium conditions suggested that HBP1 was acting as a repressor of *NMYC* transcription under basal conditions.

Given that HBP1 depletion had no effect on *CMYC* and *CCND1* expression it was concluded that in A375 melanoma cells either HBP1 did not have a significant role in regulation of these genes, or that HBP1 induced effects were obscured by compensatory changes. In addition whilst it was clear that HBP1 was acting as a repressor of *NMYC* transcription, observation of IGF1R induced effects on *NMYC* transcript was dependent on the time of sampling (Figures 5.14 & 5.16).

Based on the results of this experiment it seemed likely that further elucidation of the consequences of IGF1R induced changes in HBP1 levels would be complicated by a number of factors, including the ability of IGFs to influence target gene transcription in a variety of ways, as previously discussed for *CCND1* (Klein and Assoian, 2008). Furthermore it was clear that the target gene mRNA varied temporally. As such a more linear reporter system was required which might minimise these confounding effects.

5.2.9 Optimisation of the TOPFLASH Assay in A375 melanoma cells.

SuperTOP is well characterised reporter construct in which β-catenin-TCF/LEF binding to a luciferase promoter enables quantification of activation of the Wnt/β-catenin pathway

(Molenaar et al., 1996). HBP1 has been characterised as an inhibitory binding partner of TCF and LEF transcriptional activators (Sampson et al., 2001). As such use of a SuperTOP reporter offered a linear system to assess effects of IGF axis and HBP1 manipulation on Wnt/β catenin signalling.

It was first necessary to determine whether A375 cells could respond to Wnt ligand with an increase in active β-catenin. A375 cells were serum deprived overnight before addition of a range of concentrations of WNT3A, chosen with reference to those used in the literature (Biechele et al., 2010, Bryja et al., 2007). Cell lysates were prepared after three hours and immunoblot performed for the inactive (phosphorylated), active (unphosphorylated) forms and total β-catenin. Active β-catenin was seen to be induced in a dose dependent manner (maximally by 250ng/ml WNT3A) and phosphorylated β-catenin reduced by 500ng WNT3A (Figure 5.17A). Active β-catenin levels were low in cells growing in full medium and serum starved cells, suggesting that the Wnt/β-catenin pathway is relatively inactive in A375 cells under normal cell culture conditions.

The SuperTOPFlash (SuperTOP) reporter plasmid consists of eight TCF response elements upstream of firefly luciferase cDNA. Binding of β-catenin to the TCF sites results in firefly luciferase production. A second control plasmid FOPFlash (FOP) is identical except for mutations of the TCF binding sites which are thus incapable of β-catenin binding. FOP serves to document any background luciferase production and demonstrates specificity of response to β-catenin (Molenaar et al., 1996).

Initial assays optimised the conditions for use of the TOP/FOP assay to report activity of the Wnt/β-catenin pathway. After 24 hours A375 cells transfected with SuperTOP or FOP control plasmid were incubated with WNT3A for 3 hours. Cells transfected with the FOP plasmid showed no change in luciferase activity in response to WNT3A (Figure 5.17B). In

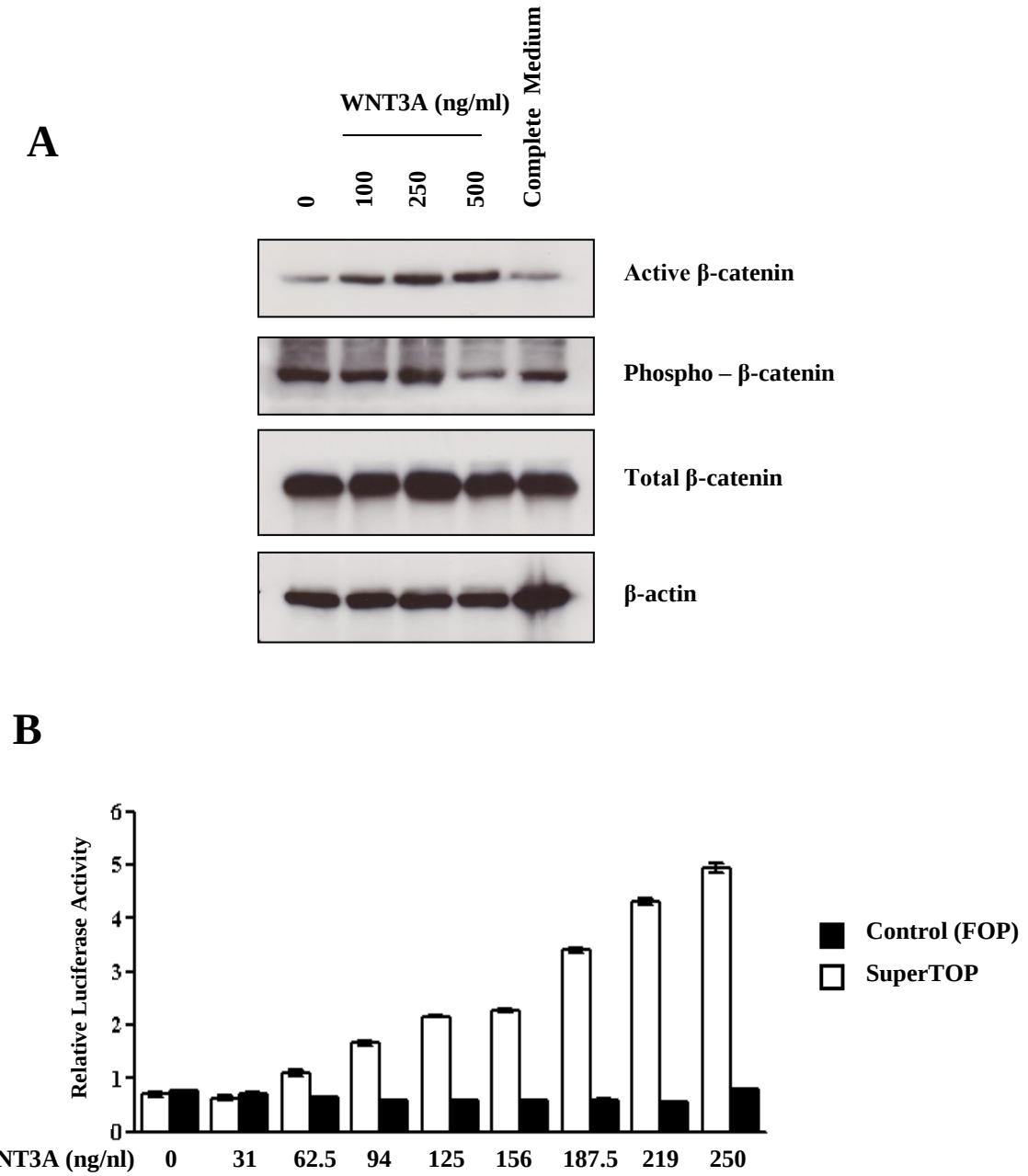


Figure 5.17 WNT3A activates the Wnt/β catenin pathway in A375 melanoma cells. A) Serum deprived A375 melanoma cells were treated with increasing concentrations of WNT3A. Phosphorylated, unphosphorylated and total β catenin were determined by immunoblot. WNT3A activates β catenin in A375 cells**. B)** A375 cells were transfected with SuperTOP or FOP plasmids with a transfection control renilla plasmid in a 10:1 ratio. Wnt/β catenin mediated luciferase transcription was assessed 24 hours after plasmid transfection following 3 hour incubation with WNT3A. Histograms represent mean relative (±SEM) luminesence normalised to renilla luminescence from 3 replicates. WNT3A caused a dose dependant increase in luciferase activity in cells transfected with SuperTOP reporter plasmid. A375 cells transfected with FOP plasmid showed low basal luminescence which did not increase in response to WNT3A.

contrast luciferase activity increased with WNT3A concentration in a dose dependent manner in cells transfected with SuperTOP. It was concluded that components of the Wnt/β-catenin signalling pathway were present in A375 cells and could be activated by WNT3A. WNT3A at a concentration of 250ng/ml was sufficient to induce a robust measurable luminescence, had also induced a detectable increase in active β-catenin (Figure 5.17A), and this concentration was used in subsequent experiments.

Reporter activity induced by WNT3A was assessed in two conditions previously shown to induce *HBP1* mRNA (Figure 5.2). A375 cells transfected with SuperTOP or FOP were either treated with AZ12253801 for 3 hours or serum starved overnight, prior to addition of WNT3A. Cells in full medium served as a comparator. In the absence of WNT3A, or in cells transfected with FOP plasmid, negligible luciferase activity was recorded (Figure 5.18A). All subsequent results refer to cells transfected with SuperTOP. A significant increase in luciferase activity was seen in all conditions following addition of WNT3A. The luminescence was greatest in WNT3A treated cells in full medium, significantly lower in cells treated with AZ12253801 and lower still in serum deprived cells, although the differences were not great. Based on previous results (Figure 5.2) HBP1 expression would be expected to be lowest in cells in full medium, highest in serum deprived cells and intermediate in cells treated with AZ12253801. Thus it appeared that activity of the Wnt/β-catenin pathway reported by SuperTop was proportional to the expected expression of HBP1.

To elucidate whether HBP1 was responsible for the repression of WNT3A induced transcription, it was necessary to deplete HBP1. A375 cells were reverse transfected with HBP1 or control siRNA 24 hours prior to transfection with SuperTOP or FOP plasmids. After a further 24 hours luciferase activity was determined following incubation with

AZ12253801, WNT3A or both for 3 hours. Total RNA was extracted from parallel WNT3A treated wells and *HBP1* mRNA quantified.

In the absence of WNT3A, or in cells transfected with FOP plasmid, negligible luciferase activity was recorded (Figure 5.18B). All subsequent results refer to cells transfected with SuperTOP. Following incubation with WNT3A luciferase activity was significantly higher in HBP1 depleted cells compared to control transfectants (Figure 5.18B left). In control transfectants AZ12253801 treatment resulted in a significant decrease in WNT3A driven luminescence. In contrast in HBP1 depleted cells there was no change in WNT3A driven luminescence following AZ12253801 treatment. HBP1 siRNA transfection was seen to have significantly reduced *HBP1* mRNA compared to control cells (Figure 5.18B right). AZ12253801 treatment increased *HBP1* mRNA in control cells but had no effect in cells following HBP1 depletion, as had previously been documented.

From these experiments it appeared that AZ12253801 upregulated HBP1 resulting in reduced WNT3A driven reporter activity. Conversely depletion of HBP1 resulted in an increase in SuperTop reporter activity, supporting the suggestion that AZ12253801 induced HBP1 up-regulation mediated effects of the IGF1R inhibitor on Wnt/β catenin pathway activation. The next step was to assess whether manipulation of the IGF1R axis, and thus HBP1, affected transcription of known WNT3A target genes.

5.2.10 Determination of the effects of IGF1R inhibition on transcription of Wnt target genes

Forty eight hours after reverse transfection with control or HBP1 siRNA, A375 cells in full medium were incubated with WNT3A for 3 hours. Parallel samples were similarly WNT3A treated following prior incubation for 1 hour with AZ12253801 or vehicle. Total RNA was extracted for quantification of *HBP1, NMYC, CMYC* and *CCND1* expression.

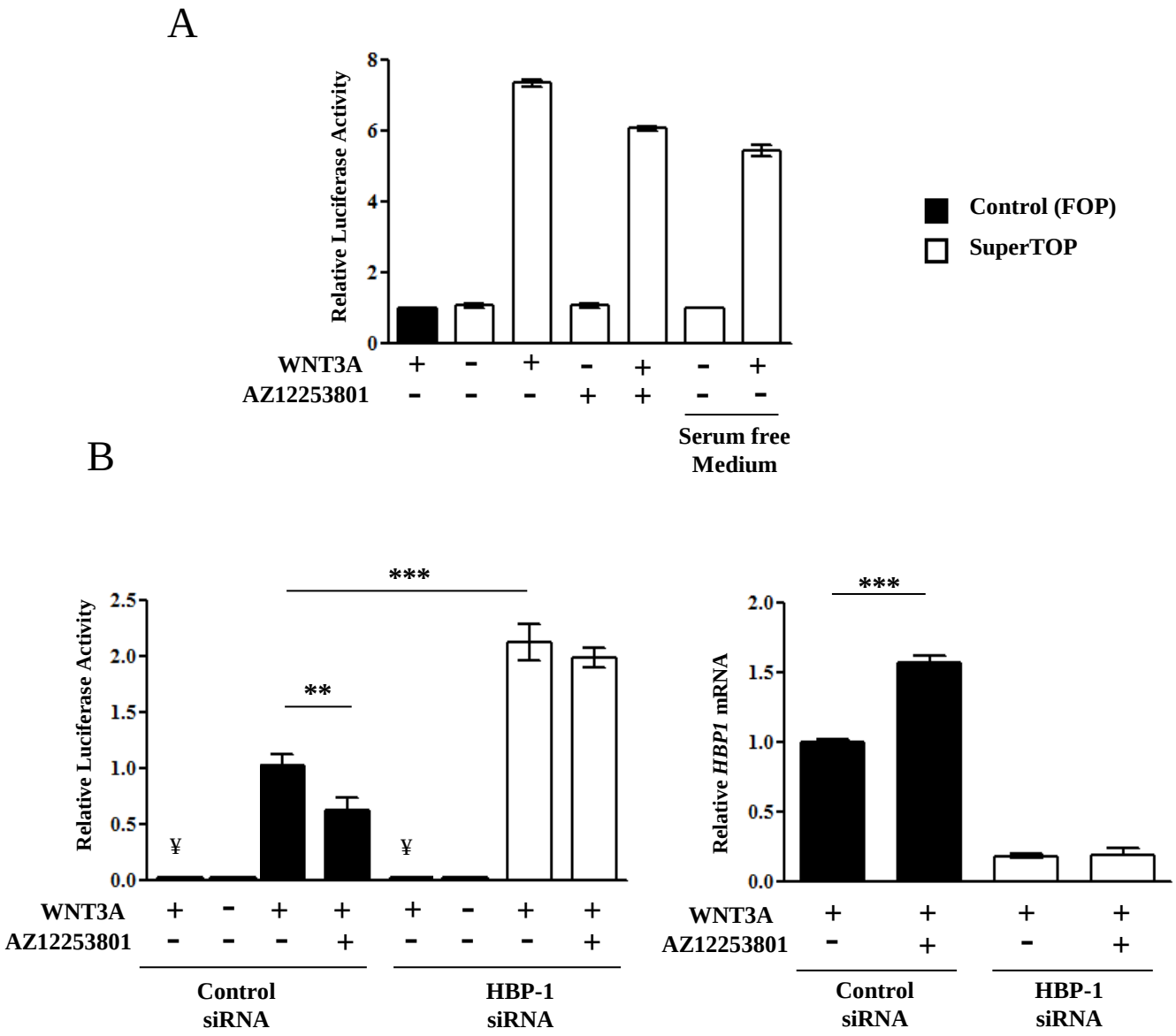


Figure 5.18 Effect of AZ12253801 on WNT3A induced transcription is prevented by HBP1 depletion. A) A375 cells were transfected with SuperTOP or FOP plasmids with a transfection control renilla plasmid in a 10:1 ratio. Wnt/β catenin mediated luciferase transcription was assessed 24 hours after plasmid transfection following 3 hour incubation with 250ng/ml WNT3A in serum deprived cells, cells treated for 1 hour with 50nM AZ12253801 and cells in full medium. Histograms represent mean relative luminesence (±range) normalised to renilla luminescence from 2 independent experiments with 3 replicates (6 data points). WNT3A induced luciferase activity was significantly lower in AZ12253801treated and serum deprived cells. **B left)** HBP1 or control siRNA transfected cells were transfected with SuperTOP/FOP and renilla plasmids 48 hours after siRNA transfection. Wnt/β catenin mediated luciferase transcription was assessed 24 hours after plasmid transfection following 3 hour incubation with 250ng/ml WNT3A cells treated with 50nM AZ12253801 for 1 hour. Histograms represent mean relative change (±SEM) in luminescence normalised to control renilla luminescence from 3 independant experiments with 3 replicates (9 data points). WNT3A did not result in luciferase activity in cells transfected with FOP. WNT3A induced luciferase activity was reduced by AZ12253801. *HBP1* depletion increased WNT3A induced luciferase activity, which was not abrogated by AZ12253801. **B right)** Duplicate dishes were analysed for HBP1 expression by qRT PCR. Histograms represent mean relative expression (±SEM) normalised to control transfectants from 3 independent experiments .

(**P<0.01, *** P<0.005 by one way ANOVA).

CMYC and *CCND1* are well characterised target genes of the Wnt/β-catenin pathway and HBP1 has been shown to affect their transcription both through direct DNA binding and via inhibition of TCF/LEF (He et al., 1998, Tetsu and McCormick, 1999, Shtutman et al., 1999). NMYC has been demonstrated to be a Wnt/β-catenin target gene in the embryo and was included for interest and because it had been the only gene whose expression had been significantly affected by HBP1 depletion in previous experiments (ten Berge et al., 2008, Kuwahara et al., 2010).

In cells transfected with control siRNA, *HBP1* expression was induced by AZ12253801 as previously documented (Figure 5.19A). Treatment with WNT3A did not alter basal *HBP1* expression but modestly reduced the increase in *HBP1* expression in response to AZ12253801, suggesting that the drive to *HBP1* transcription caused by IGF1R inhibition may be antagonised by active Wnt/β-catenin signalling. In the face of HBP1 depletion neither WNT3A nor AZ1223801 induced significant changes in *HBP1* mRNA levels.

At the tested time-points, *CCND1* mRNA was unchanged irrespective of HBP1 depletion, WNT3A or AZ12253801 treatment (Figure 5.19B). *CMYC* was upregulated by WNT3A, but neither basal nor WNT induced *CMYC* expression was influenced by AZ12243801 treatment or HBP1 depletion (Figure 5.19C). In contrast *NMYC* expression was unaffected by WNT3A or AZ12253801 in control transfectants (Figure 5.19D). HBP1 depletion upregulated *NMYC* expression, with a further significant increase in *NMYC* mRNA on addition of WNT3A which was not altered by prior incubation with AZ12253801.

From the results of this experiment it was concluded that in A375 cells transcription of *CCND1* is not increased by Wnt/β-catenin signalling. This was unexpected given the well-recognised identification of *CCND1* as a Wnt/β catenin target gene in other cell models. In contrast Wnt stimulation did increase *CMYC* transcription, but this effect was not

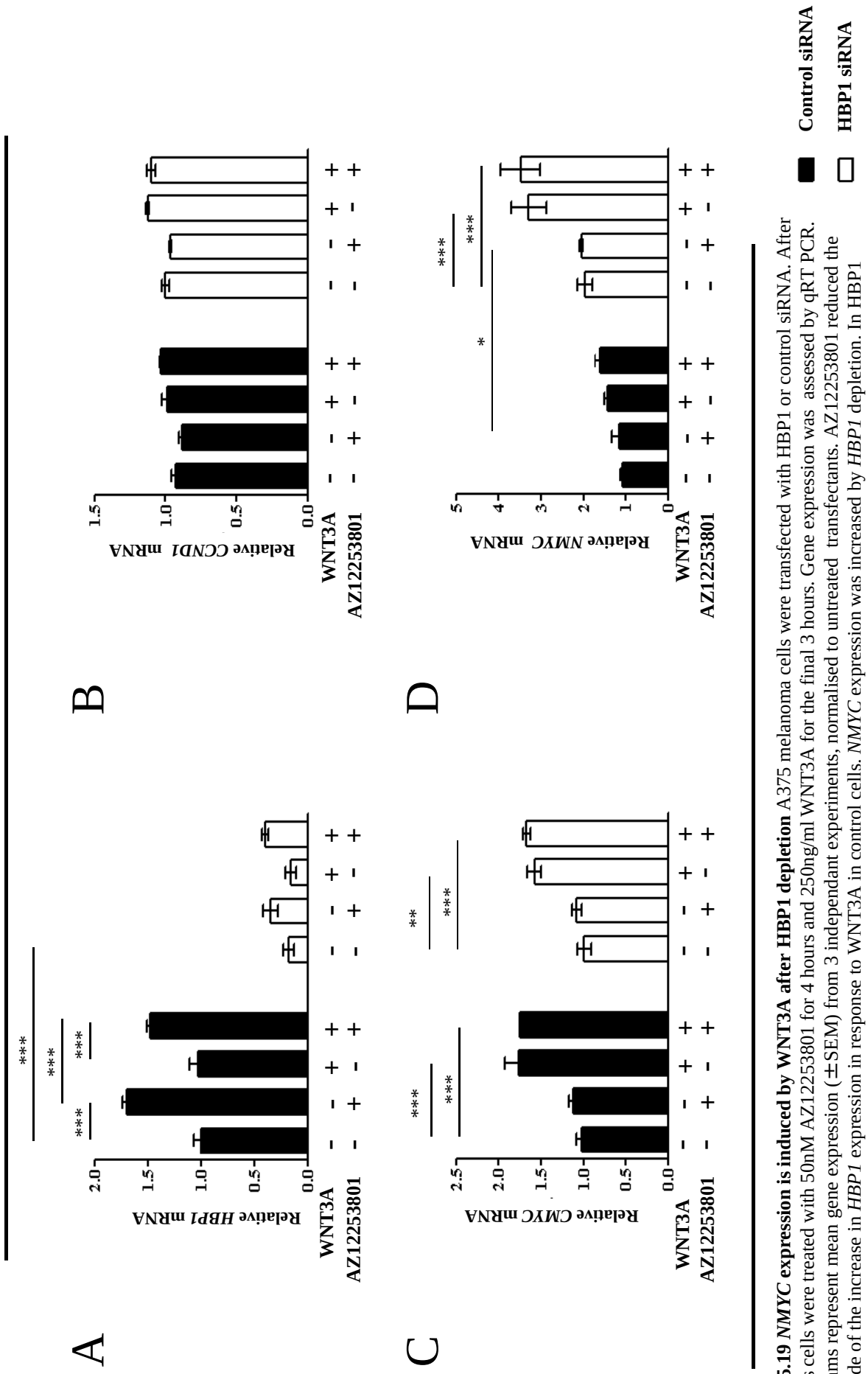


Figure 5.19 *NMYC* expression is induced by WNT3A after HBP1 depletion A375 melanoma cells were transfected with HBP1 or control siRNA. After 48 hours cells were treated with 50nM AZ12253801 for 4 hours and 250ng/ml WNT3A for the final 3 hours. Gene expression was assessed by qRT PCR. Histograms represent mean gene expression (±SEM) from 3 independant experiments, normalised to untreated transfectants. AZ12253801 reduced the magnitude of the increase in *HBP1* expression in response to WNT3A in control cells. *NMYC* expression was increased by *HBP1* depletion. In HBP1 depleted, but not control cells, WNT3A induced *NMYC* expression.
(* P<0.05, ** P<0.01, *** P<0.005 by one way ANOVA)

influenced by IGF1R inhibition or HBP1 depletion. To the author's knowledge *NMYC* has been described as a Wnt target gene only in embryonic cells and tissue not in terminally differentiated or cancer cells (Kuwahara et al., 2010, ten Berge et al., 2008). In this experiment Wnt/β-catenin stimulation did not affect *NMYC* expression in control cells and it might have thus been concluded that *NMYC* is not a Wnt related gene. However following depletion of HBP1 *NMYC* expression was induced by WNT3A. This suggested that *NMYC* is a Wnt target gene in A375 melanoma cells but its expression is prevented under basal conditions by HBP1 and this repression can be released on HBP1 depletion. It is not known whether HBP1 represses *NMYC* expression indirectly via TCF/LEF inhibition, as is the case with *CCND1* and *CMYC*, in addition to via direct promoter binding, as previously published, and it would be interesting to explore this further (Tevosian et al., 1997, Tetsu and McCormick, 1999, Sampson et al., 2001, He et al., 1998, Escamilla-Powers et al., 2010).

Although this final experiment did not demonstrate that transcription of Wnt target genes could be decreased by IGF1R inhibition, as had been hypothesized following the results documented in section 5.2.9, the unexpected finding of *NMYC* as a Wnt/β-catenin target was a novel and intriguing finding.

5.3 Conclusions

HBP1 had previously been identified as a gene downregulated by IGF and insulin in myoblasts *in vitro* but not by insulin *in vivo* (Palsgaard et al., 2009, Villafuerte et al., 2004). Furthermore the distribution of HBP1 expression throughout tissues of the body was not thought to be consistent with an insulin induced protein (Lesage et al., 1994). In this chapter it has been shown that *HBP1* mRNA expression in A375 melanoma cells is

induced by serum deprivation and to a lesser degree by blocking of IGF1R signalling, both by receptor depletion or small molecule inhibition. It has been shown that IGF induced changes in *HBP1* mRNA levels are effected via the PI3K pathway, but not via mTOR. Whilst the final effector was not identified, the forkhead family of transcription factors are possible candidates based on the available literature and presence of binding sites in the *HBP1* promotor (Modur et al., 2002a, Hegde et al., 2007, Essaghir et al., 2009). Attempts were made to assess the relative contribution of HBP1, and thus by inference the relative importance of changes induced by IGF1R manipulation, on cellular phenotype. Depletion of HBP1 did not alter cell cycle distribution or proliferation of A375 cells, nor alter the growth retarding effects of inhibiting the IGF1R.

Expression of several of the gene targets of HBP1: *NMYC, CMYC* and *CCND1* were shown to be increased following IGF1 treatment as would be expected if HBP1 mediated repression was withdrawn. Of these only *NMYC* had significantly increased expression following depletion of HBP1. As such it appears under basal conditions that *NMYC* transcription may be limited by HBP1 and thus an increase in HBP1 as a result of IGF1R inhibition has no additional effect.

In advanced melanoma, inactivation of the Wnt/β-catenin pathway is a feature of progressive disease. The data presented above suggest that there is little role for Wnt/β-catenin driven gene transcription in A375 melanoma cells under basal conditions given that transcription of *CMYC, NMYC* and *CCND1* was not affected by WNT3A. However depletion of HBP1 resulted in an increased transcription of *NMYC*. In addition, following HBP1 depletion, WNT3A results in a further increase in *NMYC* transcription, above that that resulting from HBP1 depletion alone. Taken together these results suggest that in A375 melanoma cells in normal cell culture conditions *NMYC* transcription in response to

Wnt/β-catenin is prevented by HBP1. Or it might be stated that the most significant role of HBP1 in A375 melanoma cells identified in this series of experiments is the suppression of *NMYC* transcription.

In conclusion it is clear that changes in HBP1 following IGF1R manipulation are not solely responsible for changes in the expression of the examined HBP1 target genes. These findings may offer further insight into understanding the interaction of the Wnt/β-catenin and IGF1R signalling pathways.

5.3.1 Interaction of Wnt and growth factor pathways - future directions

On studying the Wnt/β-catenin and IGF1R signalling pathways there are obvious common molecules, including GSK3β, and transcriptional end points. IGF1 promotes transcription of the same proto-oncogenes, *CMYC* and *CCND1* as Wnt/β-catenin (He et al., 1998, Shtutman et al., 1999, Sun and Jin, 2008). In addition IGF or insulin stimulation of a number of cell types activates β-catenin/TCF responsive genes, and in some cases an accumulation of β-catenin, confirming an interaction between the two pathways (Satyamoorthy et al., 2001, Verras and Sun, 2005, Desbois-Mouthon et al., 2001, Gherzi et al., 2006). However the molecular mediators for pathway cross talk have not been fully elucidated. Insulin enhances β-catenin nuclear translocation and the binding of β-catenin to TCF binding motifs in the *CMYC* gene promoter can be blocked by inhibition of PI3K but not by AKT or mTOR (Sun and Jin, 2008). Therefore an element downstream of PI3K, but not AKT, is suspected to mediate this crosstalk. A potential role has been postulated for the 14-3-3 family of proteins but this is as yet unclear (Tian et al., 2004). The findings presented above represent another contribution to this puzzle. In particular if crosstalk

exists between the IGF/insulin and Wnt/β-catenin signalling pathways, mechanisms for negative feedback would be expected.

Control of HBP1 levels by mitogenic stimuli such as IGF1 suggest a mechanism by which Wnt/β-catenin medicated gene transcription is modulated and provides further evidence of coordination between the two signalling pathways in the control of transcription and translation of common gene targets. Whilst there are no known mechanisms by which HBP1 could enhance nuclear translocation of β-catenin, it can affect the binding of β-catenin to TCF and of the β-catenin/TCF complex to gene promoters (Sampson et al., 2001). The mediator of IGF1R effects on HBP1 expression could not be identified following these experiments, but the results indicate a downstream effector of PI3K which as mentioned above is the pathway previously implicated in insulin/Wnt cross talk (Tian et al., 2004).

With respect to cancer treatment, knowledge of signalling pathway interactions offers a suggestion of novel therapeutic combinations and treatment strategies. Indeed this was the basis on which the screening experiment described in Chapter 4 was performed. The fortuitous discovery of HBP1 as an IGF1R regulated gene and one which can be upregulated by clinically relevant IGF inhibitors suggest further study in this area is required, particularly since loss, depletion or inactivation of HBP1 promotes cell proliferation and invasiveness in melanoma, breast and prostate cancers *in vitro* (Eskandarpour et al., 2009, Paulson et al., 2007, Chen et al., 2010).

In the case of melanoma the evidence of IGF1R inhibition as a treatment strategy remains incomplete and the Wnt/β-catenin pathway is of minor significance in advanced disease

(Kageshita et al., 2001). In contrast there is a large body of evidence regarding the dependence of breast cancer cells on IGF1R and constitutive Wnt signalling (Creighton et al., 2008, Howe and Brown, 2004). If inhibition of the IGF1R can produce sustained HBP1 increase in cancers which are dependent on Wnt/β-catenin driven proliferation, this therapy might effectively target two proliferative pathways at once.

As such it may be informative to repeat the experiments detailed in this chapter in a cancer cell types in which IGF1R and Wnt/β-catenin signalling have known and dominant roles in proliferation. It could be postulated that combined IGF1R and Wnt/β-catenin directed therapies might be expected to have a combined anti –proliferative effect, and might limit development of resistance to monoagent therapy. Indeed this has recently been shown in a breast cancer model (Liu et al., 2012). In the face of HBP1 non-functional mutants, such as recently identified in a cohort of breast cancer patients (Paulson et al., 2007), IGF1R induced changes in HBP1 expression would likely be ineffective at altering Wnt driven proliferation. However inhibition of the common molecules shared between the IGF1R and Wnt/β-catenin pathways, such as mTOR, might offer a therapeutic benefit. Certainly the role of IGF1 axis in regulating expression of HBP1 warrants further investigation in light of the potential therapeutic applications.

6. Bibliography

ABRAMOVITCH, S. & WERNER, H. (2003) Functional and physical interactions between BRCA1 and p53 in transcriptional regulation of the IGF-IR gene. *Horm Metab Res,* 35**,** 758-62.

ADAMS, T. E., EPA, V. C., GARRETT, T. P. & WARD, C. W. (2000) Structure and function of the type 1 insulin-like growth factor receptor. *Cell Mol Life Sci,* 57**,** 1050-93.

ADELAIDE, J., FINETTI, P., BEKHOUCHE, I., REPELLINI, L., GENEIX, J., SIRCOULOMB, F., CHARAFE-JAUFFRET, E., CERVERA, N., DESPLANS, J., PARZY, D., SCHOENMAKERS, E., VIENS, P., JACQUEMIER, J., BIRNBAUM, D., BERTUCCI, F. & CHAFFANET, M. (2007) Integrated profiling of basal and luminal breast cancers. *Cancer Res,* 67**,** 11565-75.

AL-JAMAL, R. T. & KIVELA, T. (2011) Prognostic associations of insulin-like growth factor-1 receptor in primary uveal melanoma. *Can J Ophthalmol,* 46**,** 471-6.

ALEGRE, M. L., FRAUWIRTH, K. A. & THOMPSON, C. B. (2001) T-cell regulation by CD28 and CTLA-4. *Nat Rev Immunol,* 1**,** 220-8.

ALEKSIC, T., CHITNIS, M. M., PERESTENKO, O. V., GAO, S., THOMAS, P. H., TURNER, G. D., PROTHEROE, A. S., HOWARTH, M. & MACAULAY, V. M. (2010) Type 1 insulin-like growth factor receptor translocates to the nucleus of human tumor cells. *Cancer Res,* 70**,** 6412-9.

ALEKSIC, T. & FELLER, S. M. (2008) Gamma-secretase inhibition combined with platinum compounds enhances cell death in a large subset of colorectal cancer cells. *Cell Commun Signal,* 6**,** 8.

ALEXANDER, A. N., HUELSMEYER, M. K., MITZEY, A., DUBIELZIG, R. R., KURZMAN, I. D., MACEWEN, E. G. & VAIL, D. M. (2006) Development of an allogeneic whole-cell tumor vaccine expressing xenogeneic gp100 and its implementation in a phase II clinical trial in canine patients with malignant melanoma. *Cancer Immunol Immunother,* 55**,** 433-42.

ALL-ERICSSON, C., GIRNITA, L., SEREGARD, S., BARTOLAZZI, A., JAGER, M. J. & LARSSON, O. (2002) Insulin-like Growth Factor-1 Receptor in Uveal Melanoma: A Predictor for Metastatic Disease and a Potential Therapeutic Target. *Invest. Ophthalmol. Vis. Sci.,* 43**,** 1-8.

ALMEIDA, A., MULERIS, M., DUTRILLAUX, B. & MALFOY, B. (1994) The insulin-like growth factor I receptor gene is the target for the 15q26 amplicon in breast cancer. *Genes Chromosomes Cancer,* 11**,** 63-5.

ANDREWS, D. W., RESNICOFF, M., FLANDERS, A. E., KENYON, L., CURTIS, M., MERLI, G., BASERGA, R., ILIAKIS, G. & AIKEN, R. D. (2001) Results of a pilot study involving the use of an antisense oligodeoxynucleotide directed against the insulin-like growth factor type I receptor in malignant astrocytomas. *J Clin Oncol,* 19**,** 2189-200.

ANTHONY, D. D., PAN, Y. X., WU, S. G., SHEN, F. & GUO, Y. J. (1998) Ex vivo and in vivo IGF-I antisense RNA strategies for treatment of cancer in humans. *Adv Exp Med Biol,* 451**,** 27-34.

ARBET-ENGELS, C., TARTARE-DECKERT, S. & ECKHART, W. (1999) C-terminal Src kinase associates with ligand-stimulated insulin-like growth factor-I receptor. *J Biol Chem,* 274**,** 5422-8.

ARTEAGA, C. L. (1992) Interference of the IGF system as a strategy to inhibit breast cancer growth. *Breast Cancer Res Treat,* 22**,** 101-6.

ARTEAGA, C. L., KITTEN, L. J., CORONADO, E. B., JACOBS, S., KULL, F. C., JR., ALLRED, D. C. & OSBORNE, C. K. (1989) Blockade of the type I somatomedin receptor inhibits growth of human breast cancer cells in athymic mice. *J Clin Invest,* 84**,** 1418-23.

ARTEAGA, C. L. & OSBORNE, C. K. (1989) Growth inhibition of human breast cancer cells in vitro with an antibody against the type I somatomedin receptor. *Cancer Res,* 49**,** 6237-41.

ASMANE, I. N., WATKIN, E., ALBERTI, L., DUC, A., MAREC-BERARD, P., RAY-COQUARD, I., CASSIER, P., DECOUVELAERE, A.-V. R., RANCHÃ¨RE, D., KURTZ, J.-E., BERGERAT, J.-P. & BLAY, J.-Y. (2012) Insulin-like growth factor type 1 receptor (IGF-1R) exclusive nuclear staining: A predictive biomarker for IGF-1R monoclonal antibody (Ab) therapy in sarcomas. *European journal of cancer (Oxford, England : 1990),* 48**,** 3027-3035.

ATZORI, F., TABERNERO, J., CERVANTES, A., PRUDKIN, L., ANDREU, J., RODRIGUEZ-BRAUN, E., DOMINGO, A., GUIJARRO, J., GAMEZ, C., RODON, J., DI COSIMO, S., BROWN, H., CLARK, J., HARDWICK, J. S., BECKMAN, R. A., HANLEY, W. D., HSU, K., CALVO, E., ROSELLO, S., LANGDON, R. B. & BASELGA, J. (2011) A phase I pharmacokinetic and pharmacodynamic study of dalotuzumab (MK-0646), an anti-insulin-like growth factor-1 receptor monoclonal antibody, in patients with advanced solid tumors. *Clin Cancer Res,* 17**,** 6304-12.

AVRIL, M. F., AAMDAL, S., GROB, J. J., HAUSCHILD, A., MOHR, P., BONERANDI, J. J., WEICHENTHAL, M., NEUBER, K., BIEBER, T., GILDE, K., GUILLEM PORTA, V., FRA, J., BONNETERRE, J., SAIAG, P., KAMANABROU, D., PEHAMBERGER, H., SUFLIARSKY, J., GONZALEZ LARRIBA, J. L., SCHERRER, A. & MENU, Y. (2004) Fotemustine compared with dacarbazine in patients with disseminated malignant melanoma: a phase III study. *J Clin Oncol,* 22**,** 1118-25.

AZAR, Z. M., MEHDI, M. Z. & SRIVASTAVA, A. K. (2006) Activation of insulin-like growth factor type-1 receptor is required for H2O2-induced PKB phosphorylation in vascular smooth muscle cells. *Can J Physiol Pharmacol,* 84**,** 777-86.

BAE, I., SMITH, M. L., SAEED SHEIKH, M., ZHAN, Q., SCUDIERO, D. A., FRIEND, S. H., O'CONNOR, P. M. & FORNACE, A. J. (1996) An Abnormality in the p53 Pathway following Î³-Irradiation in Many Wild-Type p53 Human Melanoma Lines. *Cancer Research,* 56**,** 840-847.

BAKER, J., LIU, J. P., ROBERTSON, E. J. & EFSTRATIADIS, A. (1993) Role of insulin-like growth factors in embryonic and postnatal growth. *Cell,* 75**,** 73-82.

BALAMURUGAN, K. & SAID, H. M. (2006) Role of reduced folate carrier in intestinal folate uptake. *Am J Physiol Cell Physiol,* 291**,** C189-93.

BALCH, C. M., GERSHENWALD, J. E., SOONG, S. J., THOMPSON, J. F., ATKINS, M. B., BYRD, D. R., BUZAID, A. C., COCHRAN, A. J., COIT, D. G., DING, S., EGGERMONT, A. M., FLAHERTY, K. T., GIMOTTY, P. A., KIRKWOOD, J. M., MCMASTERS, K. M., MIHM, M. C., JR., MORTON, D. L., ROSS, M. I., SOBER, A. J. & SONDAK, V. K. (2009) Final version of 2009 AJCC melanoma staging and classification. *J Clin Oncol,* 27**,** 6199-206.

BARBIERI, M., BONAFE, M., FRANCESCHI, C. & PAOLISSO, G. (2003) Insulin/IGF-I-signaling pathway: an evolutionarily conserved mechanism of longevity from yeast to humans. *Am J Physiol Endocrinol Metab,* 285**,** E1064-71.

BASERGA, R. (2000) The contradictions of the insulin-like growth factor 1 receptor. *Oncogene,* 19**,** 5574-5581.

BASERGA, R. (2005) The insulin-like growth factor-I receptor as a target for cancer therapy. *Expert Opinion on Therapeutic Targets,* 9**,** 753-768.

BASERGA, R., HONGO, A., RUBINI, M., PRISCO, M. & VALENTINIS, B. (1997a) The IGF-I receptor in cell growth, transformation and apoptosis. *Biochim Biophys Acta,* 1332**,** F105-26.

BASERGA, R., RESNICOFF, M. & DEWS, M. (1997b) The IGF-I receptor and cancer. *Endocrine,* 7**,** 99-102.

BASU, B., OLMOS, D. & DE BONO, J. S. (2011) Targeting IGF-1R: throwing out the baby with the bathwater? *Br J Cancer,* 104**,** 1-3.

BATEMAN, K. E., CATTON, P. A., PENNOCK, P. W. & KRUTH, S. A. (1994a) 0-7-21 radiation therapy for the palliation of advanced cancer in dogs. *J Vet Intern Med,* 8**,** 394-9.

BATEMAN, K. E., CATTON, P. A., PENNOCK, P. W. & KRUTH, S. A. (1994b) 0-7-21 radiation therapy for the treatment of canine oral melanoma. *J Vet Intern Med,* 8**,** 267-72.

BAVETSIAS, V., CRUMPLER, S., SUN, C., AVERY, S., ATRASH, B., FAISAL, A., MOORE, A. S., KOSMOPOULOU, M., BROWN, N., SHELDRAKE, P. W., BUSH, K., HENLEY, A., BOX, G., VALENTI, M., DE HAVEN BRANDON, A., RAYNAUD, F. I., WORKMAN, P., ECCLES, S. A., BAYLISS, R., LINARDOPOULOS, S. & BLAGG, J. (2012) Optimization of imidazo[4,5-b]pyridine-based kinase inhibitors: identification of a dual FLT3/Aurora kinase inhibitor as an orally bioavailable preclinical development candidate for the treatment of acute myeloid leukemia. *J Med Chem,* 55**,** 8721-34.

BAXTER, R. C. (1988) Characterization of the acid-labile subunit of the growth hormone-dependent insulin-like growth factor binding protein complex. *J Clin Endocrinol Metab,* 67**,** 265-72.

BELFIORE, A., FRASCA, F., PANDINI, G., SCIACCA, L. & VIGNERI, R. (2009) Insulin receptor isoforms and insulin receptor/insulin-like growth factor receptor hybrids in physiology and disease. *Endocr Rev,* 30**,** 586-623.

BENINI, S., ZUNTINI, M., MANARA, M. C., COHEN, P., NICOLETTI, G., NANNI, P., OH, Y., PICCI, P. & SCOTLANDI, K. (2006) Insulin-like growth factor binding protein 3 as an anticancer molecule in Ewing's sarcoma. *Int J Cancer,* 119**,** 1039-46.

BENYOUCEF, S., SURINYA, K. H., HADASCHIK, D. & SIDDLE, K. (2007) Characterization of insulin/IGF hybrid receptors: contributions of the insulin receptor L2 and Fn1 domains and the alternatively spliced exon 11 sequence to ligand binding and receptor activation. *Biochem J,* 403**,** 603-13.

BERASI, S. P., XIU, M., YEE, A. S. & PAULSON, K. E. (2004) HBP1 repression of the p47phox gene: cell cycle regulation via the NADPH oxidase. *Mol Cell Biol,* 24**,** 3011-24.

BEREZIKOV, E., CUPPEN, E. & PLASTERK, R. H. (2006) Approaches to microRNA discovery. *Nat Genet,* 38 Suppl**,** S2-7.

BERGMAN, P. J., CAMPS-PALAU, M. A., MCKNIGHT, J. A., LEIBMAN, N. F., CRAFT, D. M., LEUNG, C., LIAO, J., RIVIERE, I., SADELAIN, M., HOHENHAUS, A. E., GREGOR, P., HOUGHTON, A. N., PERALES, M. A. & WOLCHOK, J. D. (2006) Development of a xenogeneic DNA vaccine program for canine malignant melanoma at the Animal Medical Center. *Vaccine,* 24**,** 4582-5.

BERGMAN, P. J., MCKNIGHT, J., NOVOSAD, A., CHARNEY, S., FARRELLY, J., CRAFT, D., WULDERK, M., JEFFERS, Y., SADELAIN, M., HOHENHAUS, A. E., SEGAL, N., GREGOR, P., ENGELHORN, M., RIVIERE, I., HOUGHTON, A.

N. & WOLCHOK, J. D. (2003) Long-term survival of dogs with advanced malignant melanoma after DNA vaccination with xenogeneic human tyrosinase: a phase I trial. *Clin Cancer Res,* 9**,** 1284-90.

BERGMAN, P. J. W., J. D (2008) Of Mice and Men (and Dogs): Development of a xenogeneic DNA vaccine for canine oral malignant melanoma. *Cancer Therapy,* 6**,** 817-826.

BIECHELE, T. L., CAMP, N. D., FASS, D. M., KULIKAUSKAS, R. M., ROBIN, N. C., WHITE, B. D., TARASKA, C. M., MOORE, E. C., MUSTER, J., KARMACHARYA, R., HAGGARTY, S. J., CHIEN, A. J. & MOON, R. T. (2010) Chemical-genetic screen identifies riluzole as an enhancer of Wnt/beta-catenin signaling in melanoma. *Chem Biol,* 17**,** 1177-82.

BIELEN, A., PERRYMAN, L., BOX, G. M., VALENTI, M., DE HAVEN BRANDON, A., MARTINS, V., JURY, A., POPOV, S., GOWAN, S., JEAY, S., RAYNAUD, F. I., HOFMANN, F., HARGRAVE, D., ECCLES, S. A. & JONES, C. (2011) Enhanced efficacy of IGF1R inhibition in pediatric glioblastoma by combinatorial targeting of PDGFRalpha/beta. *Mol Cancer Ther,* 10**,** 1407-18.

BITTNER, M., MELTZER, P., CHEN, Y., JIANG, Y., SEFTOR, E., HENDRIX, M., RADMACHER, M., SIMON, R., YAKHINI, Z., BEN-DOR, A., SAMPAS, N., DOUGHERTY, E., WANG, E., MARINCOLA, F., GOODEN, C., LUEDERS, J., GLATFELTER, A., POLLOCK, P., CARPTEN, J., GILLANDERS, E., LEJA, D., DIETRICH, K., BEAUDRY, C., BERENS, M., ALBERTS, D. & SONDAK, V. (2000) Molecular classification of cutaneous malignant melanoma by gene expression profiling. *Nature,* 406**,** 536-40.

BLACKWOOD, L. & DOBSON, J. M. (1996) Radiotherapy of oral malignant melanomas in dogs. *J Am Vet Med Assoc,* 209**,** 98-102.

BOGUNOVIC, D., O'NEILL, D. W., BELITSKAYA-LEVY, I., VACIC, V., YU, Y.-L., ADAMS, S., DARVISHIAN, F., BERMAN, R., SHAPIRO, R., PAVLICK, A. C., LONARDI, S., ZAVADIL, J., OSMAN, I. & BHARDWAJ, N. (2009) Immune profile and mitotic index of metastatic melanoma lesions enhance clinical staging in predicting patient survival. *Proceedings of the National Academy of Sciences,* 106**,** 20429-20434.

BOHULA, E. A., SALISBURY, A. J., SOHAIL, M., PLAYFORD, M. P., RIEDEMANN, J., SOUTHERN, E. M. & MACAULAY, V. M. (2003) The efficacy of small interfering RNAs targeted to the type 1 insulin-like growth factor receptor (IGF1R) is influenced by secondary structure in the IGF1R transcript. *J Biol Chem,* 278**,** 15991-7.

BOLON, B., CALDERWOOD MAYS, M. B. & HALL, B. J. (1990) Characteristics of canine melanomas and comparison of histology and DNA ploidy to their biologic behavior. *Vet Pathol,* 27**,** 96-102.

BOROVANSKY, J., HORAK, V., ELLEDER, M., FORTYN, K., SMIT, N. P. & KOLB, A. M. (2003) Biochemical characterization of a new melanoma model--the minipig MeLiM strain. *Melanoma Res,* 13**,** 543-8.

BORRELLI, S., CANDI, E., HU, B., DOLFINI, D., RAVO, M., GROBER, O. M. V., WEISZ, A., DOTTO, G. P., MELINO, G., VIGANO, M. A. & MANTOVANI, R. (2010) The p63 target HBP1 is required for skin differentiation and stratification. *Cell Death Differ,* 17**,** 1896-1907.

BOSS, D. S., WITTEVEEN, P. O., VAN DER SAR, J., LOLKEMA, M. P., VOEST, E. E., STOCKMAN, P. K., ATAMAN, O., WILSON, D., DAS, S. & SCHELLENS, J. H. (2011) Clinical evaluation of AZD1152, an i.v. inhibitor of Aurora B kinase, in patients with solid malignant tumors. *Ann Oncol,* 22**,** 431-7.

BOSTOCK, D. E. (1986) Neoplasms of the skin and subcutaneous tissues in dogs and cats. *Br Vet J,* 142**,** 1-19.

BRAHMER, J. R., TYKODI, S. S., CHOW, L. Q., HWU, W. J., TOPALIAN, S. L., HWU, P., DRAKE, C. G., CAMACHO, L. H., KAUH, J., ODUNSI, K., PITOT, H. C., HAMID, O., BHATIA, S., MARTINS, R., EATON, K., CHEN, S., SALAY, T. M., ALAPARTHY, S., GROSSO, J. F., KORMAN, A. J., PARKER, S. M., AGRAWAL, S., GOLDBERG, S. M., PARDOLL, D. M., GUPTA, A. & WIGGINTON, J. M. (2012) Safety and activity of anti-PD-L1 antibody in patients with advanced cancer. *N Engl J Med,* 366**,** 2455-65.

BRAR, S. S., KENNEDY, T. P., STURROCK, A. B., HUECKSTEADT, T. P., QUINN, M. T., WHORTON, A. R. & HOIDAL, J. R. (2002) An NAD(P)H oxidase regulates growth and transcription in melanoma cells. *Am J Physiol Cell Physiol,* 282**,** C1212-24.

BRAULKE, T. (1999) Type-2 IGF receptor: a multi-ligand binding protein. *Horm Metab Res,* 31**,** 242-6.

BRAZIL, D. P., YANG, Z. Z. & HEMMINGS, B. A. (2004) Advances in protein kinase B signalling: AKTion on multiple fronts. *Trends Biochem Sci,* 29**,** 233-42.

BRIGSTOCK, D. R. (2003) The CCN family: a new stimulus package. *J Endocrinol,* 178**,** 169-75.

BROSE, M. S., VOLPE, P., FELDMAN, M., KUMAR, M., RISHI, I., GERRERO, R., EINHORN, E., HERLYN, M., MINNA, J., NICHOLSON, A., ROTH, J. A., ALBELDA, S. M., DAVIES, H., COX, C., BRIGNELL, G., STEPHENS, P., FUTREAL, P. A., WOOSTER, R., STRATTON, M. R. & WEBER, B. L. (2002) BRAF and RAS mutations in human lung cancer and melanoma. *Cancer Res,* 62**,** 6997-7000.

BROWN-BORG, H. M., BORG, K. E., MELISKA, C. J. & BARTKE, A. (1996) Dwarf mice and the ageing process. *Nature,* 384**,** 33.

BRYJA, V., SCHULTE, G. & ARENAS, E. (2007) Wnt-3a utilizes a novel low dose and rapid pathway that does not require casein kinase 1-mediated phosphorylation of Dvl to activate beta-catenin. *Cell Signal,* 19**,** 610-6.

BUNDZA, A. & FELTMATE, T. E. (1990) Melanocytic cutaneous lesions and melanotic regional lymph nodes in slaughter swine. *Can J Vet Res,* 54**,** 301-4.

BURFEIND, P., CHERNICKY, C. L., RININSLAND, F. & ILAN, J. (1996) Antisense RNA to the type I insulin-like growth factor receptor suppresses tumor growth and prevents invasion by rat prostate cancer cells in vivo. *Proc Natl Acad Sci U S A,* 93**,** 7263-8.

BURGERS, A. M. G., BIERMASZ, N. R., SCHOONES, J. W., PEREIRA, A. M., RENEHAN, A. G., ZWAHLEN, M., EGGER, M. & DEKKERS, O. M. (2011) Meta-Analysis and Dose-Response Metaregression: Circulating Insulin-Like Growth Factor I (IGF-I) and Mortality. *Journal of Clinical Endocrinology & Metabolism,* 96**,** 2912-2920.

BURTRUM, D., ZHU, Z., LU, D., ANDERSON, D. M., PREWETT, M., PEREIRA, D. S., BASSI, R., ABDULLAH, R., HOOPER, A. T., KOO, H., JIMENEZ, X., JOHNSON, D., APBLETT, R., KUSSIE, P., BOHLEN, P., WITTE, L., HICKLIN, D. J. & LUDWIG, D. L. (2003) A Fully Human Monoclonal Antibody to the Insulin-Like Growth Factor I Receptor Blocks Ligand-Dependent Signaling and Inhibits Human Tumor Growth in Vivo. *Cancer Research,* 63**,** 8912-8921.

BYRON, S. A., HORWITZ, K. B., RICHER, J. K., LANGE, C. A., ZHANG, X. & YEE, D. (2006) Insulin receptor substrates mediate distinct biological responses to

insulin-like growth factor receptor activation in breast cancer cells. *Br J Cancer,* 95**,** 1220-8.

CALIN, G. A. & CROCE, C. M. (2006) MicroRNA signatures in human cancers. *Nat Rev Cancer,* 6**,** 857-866.

CAO, L., YU, Y., DARKO, I., CURRIER, D., MAYEENUDDIN, L. H., WAN, X., KHANNA, C. & HELMAN, L. J. (2008) Addiction to elevated insulin-like growth factor I receptor and initial modulation of the AKT pathway define the responsiveness of rhabdomyosarcoma to the targeting antibody. *Cancer Res,* 68**,** 8039-48.

CARBONI, J. M., WITTMAN, M., YANG, Z., LEE, F., GREER, A., HURLBURT, W., HILLERMAN, S., CAO, C., CANTOR, G. H., DELL-JOHN, J., CHEN, C., DISCENZA, L., MENARD, K., LI, A., TRAINOR, G., VYAS, D., KRAMER, R., ATTAR, R. M. & GOTTARDIS, M. M. (2009) BMS-754807, a small molecule inhibitor of insulin-like growth factor-1R/IR. *Mol Cancer Ther,* 8**,** 3341-9.

CARROLL, P. V., UMPLEBY, M., ALEXANDER, E. L., EGEL, V. A., CALLISON, K. V., SONKSEN, P. H. & RUSSELL-JONES, D. L. (1998) Recombinant human insulin-like growth factor-I (rhIGF-I) therapy in adults with type 1 diabetes mellitus: effects on IGFs, IGF-binding proteins, glucose levels and insulin treatment. *Clin Endocrinol (Oxf),* 49**,** 739-46.

CELEBI, J. T., SHENDRIK, I., SILVERS, D. N. & PEACOCKE, M. (2000) Identification of PTEN mutations in metastatic melanoma specimens. *Journal of Medical Genetics,* 37**,** 653-657.

CHAMBERS, C. A., KUHNS, M. S., EGEN, J. G. & ALLISON, J. P. (2001) CTLA-4-mediated inhibition in regulation of T cell responses: mechanisms and manipulation in tumor immunotherapy. *Annu Rev Immunol,* 19**,** 565-94.

CHAPMAN, P. B., HAUSCHILD, A., ROBERT, C., HAANEN, J. B., ASCIERTO, P., LARKIN, J., DUMMER, R., GARBE, C., TESTORI, A., MAIO, M., HOGG, D., LORIGAN, P., LEBBE, C., JOUARY, T., SCHADENDORF, D., RIBAS, A., O'DAY, S. J., SOSMAN, J. A., KIRKWOOD, J. M., EGGERMONT, A. M., DRENO, B., NOLOP, K., LI, J., NELSON, B., HOU, J., LEE, R. J., FLAHERTY, K. T. & MCARTHUR, G. A. (2011) Improved survival with vemurafenib in melanoma with BRAF V600E mutation. *N Engl J Med,* 364**,** 2507-16.

CHEATHAM, B. & KAHN, C. R. (1995) Insulin action and the insulin signaling network. *Endocr Rev,* 16**,** 117-42.

CHEN, J., WU, A., SUN, H., DRAKAS, R., GAROFALO, C., CASCIO, S., SURMACZ, E. & BASERGA, R. (2005) Functional significance of type 1 insulin-like growth factor-mediated nuclear translocation of the insulin receptor substrate-1 and beta-catenin. *J Biol Chem,* 280**,** 29912-20.

CHEN, L., MCGOWAN, P., ASHE, S., JOHNSTON, J., LI, Y., HELLSTROM, I. & HELLSTROM, K. E. (1994) Tumor immunogenicity determines the effect of B7 costimulation on T cell-mediated tumor immunity. *J Exp Med,* 179**,** 523-32.

CHEN, Y. C., ZHANG, X. W., NIU, X. H., XIN, D. Q., ZHAO, W. P., NA, Y. Q. & MAO, Z. B. (2010) Macrophage migration inhibitory factor is a direct target of HBP1-mediated transcriptional repression that is overexpressed in prostate cancer. *Oncogene,* 29**,** 3067-3078.

CHIEN, A. J., MOORE, E. C., LONSDORF, A. S., KULIKAUSKAS, R. M., ROTHBERG, B. G., BERGER, A. J., MAJOR, M. B., HWANG, S. T., RIMM, D. L. & MOON, R. T. (2009) Activated Wnt/beta-catenin signaling in melanoma is associated with decreased proliferation in patient tumors and a murine melanoma model. *Proc Natl Acad Sci U S A,* 106**,** 1193-8.

CHIN, L., POMERANTZ, J., POLSKY, D., JACOBSON, M., COHEN, C., CORDON-CARDO, C., HORNER, J. W., 2ND & DEPINHO, R. A. (1997) Cooperative effects of INK4a and ras in melanoma susceptibility in vivo. *Genes Dev,* 11**,** 2822-34.

CHIN, L., TAM, A., POMERANTZ, J., WONG, M., HOLASH, J., BARDEESY, N., SHEN, Q., O'HAGAN, R., PANTGINIS, J., ZHOU, H., HORNER, J. W., 2ND, CORDON-CARDO, C., YANCOPOULOS, G. D. & DEPINHO, R. A. (1999) Essential role for oncogenic Ras in tumour maintenance. *Nature,* 400**,** 468-72.

CHITNIS, M. M., YUEN, J. S. P., PROTHEROE, A. S., POLLAK, M. & MACAULAY, V. M. (2008) The Type 1 Insulin-Like Growth Factor Receptor Pathway. *Clin Cancer Res,* 14**,** 6364-6370.

CHOU, D. S., HSIAO, G., LAI, Y. A., TSAI, Y. J. & SHEU, J. R. (2009) Baicalein induces proliferation inhibition in B16F10 melanoma cells by generating reactive oxygen species via 12-lipoxygenase. *Free Radic Biol Med,* 46**,** 1197-203.

CHRISTOFORI, G., NAIK, P. & HANAHAN, D. (1994) A second signal supplied by insulin-like growth factor II in oncogene-induced tumorigenesis. *Nature,* 369**,** 414-8.

CHRISTOFORI, G., NAIK, P. & HANAHAN, D. (1995) Deregulation of both imprinted and expressed alleles of the insulin-like growth factor 2 gene during beta-cell tumorigenesis. *Nat Genet,* 10**,** 196-201.

CLEMMONS, D. R. (2007) Modifying IGF1 activity: an approach to treat endocrine disorders, atherosclerosis and cancer. *Nat Rev Drug Discov,* 6**,** 821-33.

COHEN, B. D., BAKER, D. A., SODERSTROM, C., TKALCEVIC, G., ROSSI, A. M., MILLER, P. E., TENGOWSKI, M. W., WANG, F., GUALBERTO, A., BEEBE, J. S. & MOYER, J. D. (2005) Combination Therapy Enhances the Inhibition of Tumor Growth with the Fully Human Anti-Type 1 Insulin-Like Growth Factor Receptor Monoclonal Antibody CP-751,871. *Clinical Cancer Research,* 11**,** 2063-2073.

COHEN, C., ZAVALA-POMPA, A., SEQUEIRA, J. H., SHOJI, M., SEXTON, D. G., COTSONIS, G., CERIMELE, F., GOVINDARAJAN, B., MACARON, N. & ARBISER, J. L. (2002) Mitogen-actived protein kinase activation is an early event in melanoma progression. *Clin Cancer Res,* 8**,** 3728-33.

COHEN, P. (2006) Insulin-Like Growth Factor Binding Protein-3: Insulin-Like Growth Factor Independence Comes of Age. *Endocrinology,* 147**,** 2109-2111.

COHEN, P., GRAVES, H. C., PEEHL, D. M., KAMAREI, M., GIUDICE, L. C. & ROSENFELD, R. G. (1992) Prostate-specific antigen (PSA) is an insulin-like growth factor binding protein-3 protease found in seminal plasma. *J Clin Endocrinol Metab,* 75**,** 1046-53.

COMIN-ANDUIX, B., CHODON, T., SAZEGAR, H., MATSUNAGA, D., MOCK, S., JALIL, J., ESCUIN-ORDINAS, H., CHMIELOWSKI, B., KOYA, R. C. & RIBAS, A. (2010) The oncogenic BRAF kinase inhibitor PLX4032/RG7204 does not affect the viability or function of human lymphocytes across a wide range of concentrations. *Clin Cancer Res,* 16**,** 6040-8.

CREIGHTON, C. J., CASA, A., LAZARD, Z., HUANG, S., TSIMELZON, A., HILSENBECK, S. G., OSBORNE, C. K. & LEE, A. V. (2008) Insulin-Like Growth Factor-I Activates Gene Transcription Programs Strongly Associated With Poor Breast Cancer Prognosis. *J Clin Oncol,* 26**,** 4078-4085.

CRUZADO, M. C., RISLER, N. R., MIATELLO, R. M., YAO, G., SCHIFFRIN, E. L. & TOUYZ, R. M. (2005) Vascular smooth muscle cell NAD(P)H oxidase activity

during the development of hypertension: Effect of angiotensin II and role of insulinlike growth factor-1 receptor transactivation. *Am J Hypertens,* 18**,** 81-7.

CURTIN, J. A., FRIDLYAND, J., KAGESHITA, T., PATEL, H. N., BUSAM, K. J., KUTZNER, H., CHO, K. H., AIBA, S., BROCKER, E. B., LEBOIT, P. E., PINKEL, D. & BASTIAN, B. C. (2005) Distinct sets of genetic alterations in melanoma. *N Engl J Med,* 353**,** 2135-47.

D'ERCOLE, A. J., APPLEWHITE, G. T. & UNDERWOOD, L. E. (1980) Evidence that somatomedin is synthesized by multiple tissues in the fetus. *Dev Biol,* 75**,** 315-28.

DA FORNO, P. D., PRINGLE, J. H., HUTCHINSON, P., OSBORN, J., HUANG, Q., POTTER, L., HANCOX, R. A., FLETCHER, A. & SALDANHA, G. S. (2008) WNT5A expression increases during melanoma progression and correlates with outcome. *Clin Cancer Res,* 14**,** 5825-32.

DAVIES, B. R., LOGIE, A., MCKAY, J. S., MARTIN, P., STEELE, S., JENKINS, R., COCKERILL, M., CARTLIDGE, S. & SMITH, P. D. (2007) AZD6244 (ARRY-142886), a potent inhibitor of mitogen-activated protein kinase/extracellular signal-regulated kinase kinase 1/2 kinases: mechanism of action in vivo, pharmacokinetic/pharmacodynamic relationship, and potential for combination in preclinical models. *Mol Cancer Ther,* 6**,** 2209-19.

DAVIES, H., BIGNELL, G. R., COX, C., STEPHENS, P., EDKINS, S., CLEGG, S., TEAGUE, J., WOFFENDIN, H., GARNETT, M. J., BOTTOMLEY, W., DAVIS, N., DICKS, E., EWING, R., FLOYD, Y., GRAY, K., HALL, S., HAWES, R., HUGHES, J., KOSMIDOU, V., MENZIES, A., MOULD, C., PARKER, A., STEVENS, C., WATT, S., HOOPER, S., WILSON, R., JAYATILAKE, H., GUSTERSON, B. A., COOPER, C., SHIPLEY, J., HARGRAVE, D., PRITCHARD-JONES, K., MAITLAND, N., CHENEVIX-TRENCH, G., RIGGINS, G. J., BIGNER, D. D., PALMIERI, G., COSSU, A., FLANAGAN, A., NICHOLSON, A., HO, J. W., LEUNG, S. Y., YUEN, S. T., WEBER, B. L., SEIGLER, H. F., DARROW, T. L., PATERSON, H., MARAIS, R., MARSHALL, C. J., WOOSTER, R., STRATTON, M. R. & FUTREAL, P. A. (2002) Mutations of the BRAF gene in human cancer. *Nature,* 417**,** 949-54.

DAVILA, D. & TORRES-ALEMAN, I. (2008) Neuronal death by oxidative stress involves activation of FOXO3 through a two-arm pathway that activates stress kinases and attenuates insulin-like growth factor I signaling. *Mol Biol Cell,* 19**,** 2014-25.

DAVIS, R. J. (1995) Transcriptional regulation by MAP kinases. *Mol Reprod Dev,* 42**,** 459-67.

DE LEON, D. D., WILSON, D. M., POWERS, M. & ROSENFELD, R. G. (1992) Effects of insulin-like growth factors (IGFs) and IGF receptor antibodies on the proliferation of human breast cancer cells. *Growth Factors,* 6**,** 327-36.

DE WIT, P. E. J., MORETTI, S., KOENDERS, P. G., WETERMAN, M. A. J., VAN MUIJEN, G. N. P., GIANOTTI, B. & RUITER, D. J. (1992) Increasing Epidermal Growth Factor Receptor Expression in Human Melanocytic Tumor Progression. *J Investig Dermatol,* 99**,** 168-173.

DEARTH, R. K., CUI, X., KIM, H. J., KUIATSE, I., LAWRENCE, N. A., ZHANG, X., DIVISOVA, J., BRITTON, O. L., MOHSIN, S., ALLRED, D. C., HADSELL, D. L. & LEE, A. V. (2006) Mammary tumorigenesis and metastasis caused by overexpression of insulin receptor substrate 1 (IRS-1) or IRS-2. *Mol Cell Biol,* 26**,** 9302-14.

DECHIARA, T. M., EFSTRATIADIS, A. & ROBERTSON, E. J. (1990) A growth-deficiency phenotype in heterozygous mice carrying an insulin-like growth factor II gene disrupted by targeting. *Nature,* 345**,** 78-80.

DECHIARA, T. M., ROBERTSON, E. J. & EFSTRATIADIS, A. (1991) Parental imprinting of the mouse insulin-like growth factor II gene. *Cell,* 64**,** 849-59.

DELAFONTAINE, P., SONG, Y. H. & LI, Y. (2004) Expression, regulation, and function of IGF-1, IGF-1R, and IGF-1 binding proteins in blood vessels. *Arterioscler Thromb Vasc Biol,* 24**,** 435-44.

DELMAS, V., BEERMANN, F., MARTINOZZI, S., CARREIRA, S., ACKERMANN, J., KUMASAKA, M., DENAT, L., GOODALL, J., LUCIANI, F., VIROS, A., DEMIRKAN, N., BASTIAN, B. C., GODING, C. R. & LARUE, L. (2007) Beta-catenin induces immortalization of melanocytes by suppressing p16INK4a expression and cooperates with N-Ras in melanoma development. *Genes Dev,* 21**,** 2923-35.

DENG, H., LIN, Y., BADIN, M., VASILCANU, D., STROMBERG, T., JERNBERG-WIKLUND, H., SEHAT, B. & LARSSON, O. (2011) Over-accumulation of nuclear IGF-1 receptor in tumor cells requires elevated expression of the receptor and the SUMO-conjugating enzyme Ubc9. *Biochem Biophys Res Commun,* 404**,** 667-71.

DESBOIS-MOUTHON, C., CADORET, A., BLIVET-VAN EGGELPOEL, M. J., BERTRAND, F., CHERQUI, G., PERRET, C. & CAPEAU, J. (2001) Insulin and IGF-1 stimulate the beta-catenin pathway through two signalling cascades involving GSK-3beta inhibition and Ras activation. *Oncogene,* 20**,** 252-9.

DESBOIS-MOUTHON, C. L., BARON, A., BLIVET-VAN EGGELPOÃ«L, M.-J., FARTOUX, L., VENOT, C., BLADT, F., HOUSSET, C. & ROSMORDUC, O. (2009) Insulin-Like Growth Factor-1 Receptor Inhibition Induces a Resistance Mechanism via the Epidermal Growth Factor Receptor/HER3/AKT Signaling Pathway: Rational Basis for Cotargeting Insulin-Like Growth Factor-1 Receptor and Epidermal Growth Factor Receptor in Hepatocellular Carcinoma. *Clinical Cancer Research,* 15**,** 5445-5456.

DEZFOULI, S., HATZINISIRIOU, I. & RALPH, S. J. (2003) Enhancing CTL responses to melanoma cell vaccines in vivo: synergistic increases obtained using IFN[ggr] primed and IFN[bgr] treated B7-1+ B16-F10 melanoma cells. *Immunol Cell Biol,* 81**,** 459-471.

DHOMEN, N., REIS-FILHO, J. S., DA ROCHA DIAS, S., HAYWARD, R., SAVAGE, K., DELMAS, V., LARUE, L., PRITCHARD, C. & MARAIS, R. (2009) Oncogenic Braf induces melanocyte senescence and melanoma in mice. *Cancer Cell,* 15**,** 294-303.

DIAMOND, J. R., ECKHARDT, S. G., TAN, A. C., NEWTON, T. P., SELBY, H. M., BRUNKOW, K. L., KACHAEVA, M. I., VARELLA-GARCIA, M., PITTS, T. M., BRAY, M. R., FLETCHER, G. C. & TENTLER, J. J. (2013) Predictive Biomarkers of Sensitivity to the Aurora and Angiogenic Kinase Inhibitor ENMD-2076 in Preclinical Breast Cancer Models. *Clin Cancer Res,* 19**,** 291-303.

DIMITRIADIS, G., PARRY-BILLINGS, M., BEVAN, S., DUNGER, D., PIVA, T., KRAUSE, U., WEGENER, G. & NEWSHOLME, E. A. (1992) Effects of insulin-like growth factor I on the rates of glucose transport and utilization in rat skeletal muscle in vitro. *Biochem J,* 285 (Pt 1)**,** 269-74.

DISSANAYAKE, S. K., WADE, M., JOHNSON, C. E., O'CONNELL, M. P., LEOTLELA, P. D., FRENCH, A. D., SHAH, K. V., HEWITT, K. J., ROSENTHAL, D. T., INDIG, F. E., JIANG, Y., NICKOLOFF, B. J., TAUB, D.

D., TRENT, J. M., MOON, R. T., BITTNER, M. & WEERARATNA, A. T. (2007) The Wnt5A/protein kinase C pathway mediates motility in melanoma cells via the inhibition of metastasis suppressors and initiation of an epithelial to mesenchymal transition. *J Biol Chem,* 282**,** 17259-71.

DISSEMOND, J., GOTTE, P., MORS, J., LINDEKE, A., GOOS, M., FERRONE, S. & WAGNER, S. N. (2003) Association of TAP1 downregulation in human primary melanoma lesions with lack of spontaneous regression. *Melanoma Res,* 13**,** 253-8.

DONG, A., KONG, M., MA, Z., QIAN, J., CHENG, H. & XU, X. (2008) Knockdown of insulin-like growth factor 1 receptor enhances chemosensitivity to cisplatin in human lung adenocarcinoma A549 cells. *Acta Biochim Biophys Sin (Shanghai),* 40**,** 497-504.

DONG, J., PHELPS, R. G., QIAO, R., YAO, S., BENARD, O., RONAI, Z. & AARONSON, S. A. (2003) BRAF oncogenic mutations correlate with progression rather than initiation of human melanoma. *Cancer Res,* 63**,** 3883-5.

DORN, C. R. & PRIESTER, W. A. (1976) Epidemiologic analysis of oral and pharyngeal cancer in dogs, cats, horses, and cattle. *J Am Vet Med Assoc,* 169**,** 1202-6.

DORN, C. R., TAYLOR, D. O., SCHNEIDER, R., HIBBARD, H. H. & KLAUBER, M. R. (1968) Survey of animal neoplasms in Alameda and Contra Costa Counties, California. II. Cancer morbidity in dogs and cats from Alameda County. *J Natl Cancer Inst,* 40**,** 307-18.

DOW, S. W., ELMSLIE, R. E., WILLSON, A. P., ROCHE, L., GORMAN, C. & POTTER, T. A. (1998) In vivo tumor transfection with superantigen plus cytokine genes induces tumor regression and prolongs survival in dogs with malignant melanoma. *J Clin Invest,* 101**,** 2406-14.

DRANSFIELD, D. T., COHEN, E. H., CHANG, Q., SPARROW, L. G., BENTLEY, J. D., DOLEZAL, O., XIAO, X., PEAT, T. S., NEWMAN, J., PILLING, P. A., PHAN, T., PRIEBE, I., BRIERLEY, G. V., KASTRAPELI, N., KOPACZ, K., MARTIK, D., WASSAF, D., RANK, D., CONLEY, G., HUANG, Y., ADAMS, T. E. & COSGROVE, L. (2010) A human monoclonal antibody against insulin-like growth factor-II blocks the growth of human hepatocellular carcinoma cell lines in vitro and in vivo. *Mol Cancer Ther,* 9**,** 1809-19.

DRICU, A., CARLBERG, M., WANG, M. & LARSSON, O. (1997) Inhibition of N-linked glycosylation using tunicamycin causes cell death in malignant cells: role of down-regulation of the insulin-like growth factor 1 receptor in induction of apoptosis. *Cancer Res,* 57**,** 543-8.

DU, J., PENG, T., SCHEIDEGGER, K. J. & DELAFONTAINE, P. (1999) Angiotensin II activation of insulin-like growth factor 1 receptor transcription is mediated by a tyrosine kinase-dependent redox-sensitive mechanism. *Arterioscler Thromb Vasc Biol,* 19**,** 2119-26.

DUDLEY, M. E., WUNDERLICH, J. R., YANG, J. C., SHERRY, R. M., TOPALIAN, S. L., RESTIFO, N. P., ROYAL, R. E., KAMMULA, U., WHITE, D. E., MAVROUKAKIS, S. A., ROGERS, L. J., GRACIA, G. J., JONES, S. A., MANGIAMELI, D. P., PELLETIER, M. M., GEA-BANACLOCHE, J., ROBINSON, M. R., BERMAN, D. M., FILIE, A. C., ABATI, A. & ROSENBERG, S. A. (2005) Adoptive cell transfer therapy following non-myeloablative but lymphodepleting chemotherapy for the treatment of patients with refractory metastatic melanoma. *J Clin Oncol,* 23**,** 2346-57.

DUMMER, R., HAUSCHILD, A., GUGGENHEIM, M., KEILHOLZ, U. & PENTHEROUDAKIS, G. (2012) Cutaneous melanoma: ESMO Clinical Practice

Guidelines for diagnosis, treatment and follow-up. *Ann Oncol,* 23 Suppl 7**,** vii86-91.

DUNN, S. E., HARDMAN, R. A., KARI, F. W. & BARRETT, J. C. (1997) Insulin-like growth factor 1 (IGF-1) alters drug sensitivity of HBL100 human breast cancer cells by inhibition of apoptosis induced by diverse anticancer drugs. *Cancer Res,* 57**,** 2687-93.

DUPONT, J., DUNN, S. E., BARRETT, J. C. & LEROITH, D. (2003) Microarray Analysis and Identification of Novel Molecules Involved in Insulin-like Growth Factor-1 Receptor Signaling and Gene Expression. *Recent Prog Horm Res,* 58**,** 325-342.

DUPONT, J. & LEROITH, D. (2001) Insulin and insulin-like growth factor I receptors: similarities and differences in signal transduction. *Horm Res,* 55 Suppl 2**,** 22-6.

EAGER, K. B., PFIZENMAIER, K. & RICCIARDI, R. P. (1989) Modulation of major histocompatibility complex (MHC) class I genes in adenovirus 12 transformed cells: interferon-gamma increases class I expression by a mechanism that circumvents E1A induced-repression and tumor necrosis factor enhances the effect of interferon-gamma. *Oncogene,* 4**,** 39-44.

EASTY, D. J. & BENNETT, D. C. (2000) Protein tyrosine kinases in malignant melanoma. *Melanoma Res,* 10**,** 401-11.

EASTY, D. J., GRAY, S. G., O'BYRNE, K. J., O'DONNELL, D. & BENNETT, D. C. (2011) Receptor tyrosine kinases and their activation in melanoma. *Pigment Cell Melanoma Res,* 24**,** 446-61.

ECCLES, S. A. (2011) The epidermal growth factor receptor/Erb-B/HER family in normal and malignant breast biology. *Int J Dev Biol,* 55**,** 685-96.

ECONOMOU, M. A., ALL-ERICSSON, C., BYKOV, V., GIRNITA, L., BARTOLAZZI, A., LARSSON, O. & SEREGARD, S. (2005) Receptors for the Liver Synthesized Growth Factors IGF-1 and HGF/SF in Uveal Melanoma: Intercorrelation and Prognostic Implications. *Invest. Ophthalmol. Vis. Sci.,* 46**,** 4372-4375.

EDEN, S., CONSTANCIA, M., HASHIMSHONY, T., DEAN, W., GOLDSTEIN, B., JOHNSON, A. C., KESHET, I., REIK, W. & CEDAR, H. (2001) An upstream repressor element plays a role in Igf2 imprinting. *EMBO J,* 20**,** 3518-25.

EGEN, J. G., KUHNS, M. S. & ALLISON, J. P. (2002) CTLA-4: new insights into its biological function and use in tumor immunotherapy. *Nat Immunol,* 3**,** 611-8.

EGGERMONT A. M, S. S., RUTKOWSKI P., J. MARSDEN, A. TESTORI, P. CORRIE, S. AAMDAL, P. A. ASCIERTO, P. PATEL, A. SPATZ AND EORTC MELANOMA GROUP (2010) Randomized phase III trial comparing postoperative adjuvant ganglioside GM2-KLH/QS-21 vaccination versus observation in stage II (T3-T4N0M0) melanoma: Final results of study EORTC 18961. . *Journal of Clinical Oncology,* 28**,** abstract 8505.

EGGERMONT, A. M., SUCIU, S., MACKIE, R., RUKA, W., TESTORI, A., KRUIT, W., PUNT, C. J., DELAUNEY, M., SALES, F., GROENEWEGEN, G., RUITER, D. J., JAGIELLO, I., STOITCHKOV, K., KEILHOLZ, U. & LIENARD, D. (2005) Post-surgery adjuvant therapy with intermediate doses of interferon alfa 2b versus observation in patients with stage IIb/III melanoma (EORTC 18952): randomised controlled trial. *Lancet,* 366**,** 1189-96.

EGGERMONT, A. M., SUCIU, S., SANTINAMI, M., TESTORI, A., KRUIT, W. H., MARSDEN, J., PUNT, C. J., SALES, F., GORE, M., MACKIE, R., KUSIC, Z., DUMMER, R., HAUSCHILD, A., MUSAT, E., SPATZ, A. & KEILHOLZ, U. (2008) Adjuvant therapy with pegylated interferon alfa-2b versus observation alone

in resected stage III melanoma: final results of EORTC 18991, a randomised phase III trial. *Lancet,* 372**,** 117-26.

EIGENTLER, T. K., CAROLI, U. M., RADNY, P. & GARBE, C. (2003) Palliative therapy of disseminated malignant melanoma: a systematic review of 41 randomised clinical trials. *Lancet Oncol,* 4**,** 748-59.

ELBASHIR, S. M., HARBORTH, J., LENDECKEL, W., YALCIN, A., WEBER, K. & TUSCHL, T. (2001) Duplexes of 21-nucleotide RNAs mediate RNA interference in cultured mammalian cells. *Nature,* 411**,** 494-8.

ELLOUK-ACHARD, S., DJENABI, S., DE OLIVEIRA, G. A., DESAUTY, G., DUC, H. T., ZOHAIR, M., TROJAN, J., CLAUDE, J. R., SARASIN, A. & LAFARGE-FRAYSSINET, C. (1998) Induction of apoptosis in rat hepatocarcinoma cells by expression of IGF-I antisense c-DNA. *J Hepatol,* 29**,** 807-18.

EPPIG, J. T., BLAKE, J. A., BULT, C. J., KADIN, J. A. & RICHARDSON, J. E. (2012) The Mouse Genome Database (MGD): comprehensive resource for genetics and genomics of the laboratory mouse. *Nucleic Acids Res,* 40**,** D881-6.

ESCAMILLA-POWERS, J. R., DANIEL, C. J., FARRELL, A., TAYLOR, K., ZHANG, X., BYERS, S. & SEARS, R. (2010) The Tumor Suppressor Protein HBP1 Is a Novel c-Myc-binding Protein That Negatively Regulates c-Myc Transcriptional Activity. *Journal of Biological Chemistry,* 285**,** 4847-4858.

ESCOBAR, H. M., GANTHER, K., RICHTER, A., SOLLER, J. T., WINKLER, S., NOLTE, I. & BULLERDIEK, J. (2004) Absence of Ras-gene Hot-spot Mutations in Canine Fibrosarcomas and Melanomas. *Anticancer Research,* 24**,** 3027-3028.

ESKANDARPOUR, M., HUANG, F., REEVES, K. A., CLARK, E. & HANSSON, J. (2009) Oncogenic NRAS has multiple effects on the malignant phenotype of human melanoma cells cultured in vitro. *International Journal of Cancer,* 124**,** 16-26.

ESSAGHIR, A., DIF, N., MARBEHANT, C. Y., COFFER, P. J. & DEMOULIN, J. B. (2009) The transcription of FOXO genes is stimulated by FOXO3 and repressed by growth factors. *J Biol Chem,* 284**,** 10334-42.

FANG, C. H., LI, B. G., SUN, X. & HASSELGREN, P. O. (2000) Insulin-like growth factor I reduces ubiquitin and ubiquitin-conjugating enzyme gene expression but does not inhibit muscle proteolysis in septic rats. *Endocrinology,* 141**,** 2743-51.

FAVONI, R. E., DE CUPIS, A., RAVERA, F., CANTONI, C., PIRANI, P., ARDIZZONI, A., NOONAN, D. & BIASSONI, R. (1994) Expression and function of the insulin-like growth factor I system in human non-small-cell lung cancer and normal lung cell lines. *Int J Cancer,* 56**,** 858-66.

FIRTH, S. M. & BAXTER, R. C. (2002) Cellular actions of the insulin-like growth factor binding proteins. *Endocr Rev,* 23**,** 824-854.

FISHER, P. B., GOPALKRISHNAN, R. V., CHADA, S., RAMESH, R., GRIMM, E. A., ROSENFELD, M. R., CURIEL, D. T. & DENT, P. (2003) mda-7/IL-24, a novel cancer selective apoptosis inducing cytokine gene: from the laboratory into the clinic. *Cancer Biol Ther,* 2**,** S23-37.

FISHER, P. B., SARKAR, D., LEBEDEVA, I. V., EMDAD, L., GUPTA, P., SAUANE, M., SU, Z. Z., GRANT, S., DENT, P., CURIEL, D. T., SENZER, N. & NEMUNAITIS, J. (2007) Melanoma differentiation associated gene-7/interleukin-24 (mda-7/IL-24): novel gene therapeutic for metastatic melanoma. *Toxicol Appl Pharmacol,* 224**,** 300-7.

FLAHERTY, K. T., ROBERT, C., HERSEY, P., NATHAN, P., GARBE, C., MILHEM, M., DEMIDOV, L. V., HASSEL, J. C., RUTKOWSKI, P., MOHR, P., DUMMER, R., TREFZER, U., LARKIN, J. M., UTIKAL, J., DRENO, B., NYAKAS, M.,

MIDDLETON, M. R., BECKER, J. C., CASEY, M., SHERMAN, L. J., WU, F. S., OUELLET, D., MARTIN, A. M., PATEL, K. & SCHADENDORF, D. (2012) Improved survival with MEK inhibition in BRAF-mutated melanoma. *N Engl J Med,* 367**,** 107-14.

FLEMING, M. G., HOWE, S. F. & GRAF, L. H., JR. (1994) Expression of insulin-like growth factor I (IGF-I) in nevi and melanomas. *Am J Dermatopathol,* 16**,** 383-91.

FLORES, J. F., WALKER, G. J., GLENDENING, J. M., HALUSKA, F. G., CASTRESANA, J. S., RUBIO, M. P., PASTORFIDE, G. C., BOYER, L. A., KAO, W. H., BULYK, M. L., BARNHILL, R. L., HAYWARD, N. K., HOUSMAN, D. E. & FOUNTAIN, J. W. (1996) Loss of the p16INK4a and p15INK4b genes, as well as neighboring 9p21 markers, in sporadic melanoma. *Cancer Res,* 56**,** 5023-32.

FOLEY, G. L., VALENTINE, B. A. & KINCAID, A. L. (1991) Congenital and acquired melanocytomas (benign melanomas) in eighteen young horses. *Vet Pathol,* 28**,** 363-9.

FONTIJN, D., DUYNDAM, M., BOSCH, L., GALLEGOZ RUIZ, M., VAN BERKEL, M., YUANA, Y., BROXTERMAN, H., SHAPIRO, L., PINEDO, H. & BOVEN, E. (2006) Basic fibroblast growth factor (bFGF) in melanoma cells can upregulate vascular endothelial growth factor (VEGF) and CD13/aminopeptidase N, which is associated with accelerated growth, invasion and vascularization. *Melanoma Research,* 16**,** S51.

FOUGEROUSSE, F., DURAND, M., LOPEZ, S., SUEL, L., DEMIGNON, J., THORNTON, C., OZAKI, H., KAWAKAMI, K., BARBET, P., BECKMANN, J. S. & MAIRE, P. (2002) Six and Eya expression during human somitogenesis and MyoD gene family activation. *J Muscle Res Cell Motil,* 23**,** 255-64.

FREEMAN, K. P., HAHN, K. A., HARRIS, F. D. & KING, G. K. (2003) Treatment of dogs with oral melanoma by hypofractionated radiation therapy and platinum-based chemotherapy (1987-1997). *J Vet Intern Med,* 17**,** 96-101.

FRIEDLANDER, M. R., CHEN, W., ADAMIDI, C., MAASKOLA, J., EINSPANIER, R., KNESPEL, S. & RAJEWSKY, N. (2008) Discovering microRNAs from deep sequencing data using miRDeep. *Nat Biotechnol,* 26**,** 407-15.

FRYSTYK, J. (2004) Free insulin-like growth factors -- measurements and relationships to growth hormone secretion and glucose homeostasis. *Growth Horm IGF Res,* 14**,** 337-75.

FUJIKI, H., SUGANUMA, M., IMAI, K. & NAKACHI, K. (2002) Green tea: cancer preventive beverage and/or drug. *Cancer Lett,* 188**,** 9-13.

FUKUDA, R., HIROTA, K., FAN, F., JUNG, Y. D., ELLIS, L. M. & SEMENZA, G. L. (2002) Insulin-like growth factor 1 induces hypoxia-inducible factor 1-mediated vascular endothelial growth factor expression, which is dependent on MAP kinase and phosphatidylinositol 3-kinase signaling in colon cancer cells. *J Biol Chem,* 277**,** 38205-11.

FURLANETTO, R. W., HARWELL, S. E. & BAGGS, R. B. (1993) Effects of Insulin-like Growth Factor Receptor Inhibition on Human Melanomas in Culture and in Athymic Mice. *Cancer Research,* 53**,** 2522-2526.

FURSTENBERGER, G. & SENN, H. J. (2002) Insulin-like growth factors and cancer. *Lancet Oncol,* 3**,** 298-302.

GADEA, B. B. & RUDERMAN, J. V. (2005) Aurora kinase inhibitor ZM447439 blocks chromosome-induced spindle assembly, the completion of chromosome condensation, and the establishment of the spindle integrity checkpoint in Xenopus egg extracts. *Mol Biol Cell,* 16**,** 1305-18.

GALLAGHER, S. J., KEFFORD, R. F. & RIZOS, H. (2006) The ARF tumour suppressor. *Int J Biochem Cell Biol,* 38**,** 1637-41.

GAO, J., CHESEBROUGH, J. W., CARTLIDGE, S. A., RICKETTS, S. A., INCOGNITO, L., VELDMAN-JONES, M., BLAKEY, D. C., TABRIZI, M., JALLAL, B., TRAIL, P. A., COATS, S., BOSSLET, K. & CHANG, Y. S. (2011) Dual IGF-I/II-neutralizing antibody MEDI-573 potently inhibits IGF signaling and tumor growth. *Cancer Res,* 71**,** 1029-40.

GARCIA-ECHEVERRIA, C., PEARSON, M. A., MARTI, A., MEYER, T., MESTAN, J., ZIMMERMANN, J., GAO, J., BRUEGGEN, J., CAPRARO, H. G., COZENS, R., EVANS, D. B., FABBRO, D., FURET, P., PORTA, D. G., LIEBETANZ, J., MARTINY-BARON, G., RUETZ, S. & HOFMANN, F. (2004) In vivo antitumor activity of NVP-AEW541-A novel, potent, and selective inhibitor of the IGF-IR kinase. *Cancer Cell,* 5**,** 231-9.

GARDAI, S. J., MCPHILLIPS, K. A., FRASCH, S. C., JANSSEN, W. J., STAREFELDT, A., MURPHY-ULLRICH, J. E., BRATTON, D. L., OLDENBORG, P.-A., MICHALAK, M. & HENSON, P. M. (2005) Cell-Surface Calreticulin Initiates Clearance of Viable or Apoptotic Cells through trans-Activation of LRP on the Phagocyte. *Cell,* 123**,** 321-334.

GARTEL, A. L., GOUFMAN, E., TEVOSIAN, S. G., SHIH, H., YEE, A. S. & TYNER, A. L. (1998) Activation and repression of p21(WAF1/CIP1) transcription by RB binding proteins. *Oncogene,* 17**,** 3463-9.

GE, N. L. & RUDIKOFF, S. (2000) Insulin-like growth factor I is a dual effector of multiple myeloma cell growth. *Blood,* 96**,** 2856-61.

GE, X., FU, Y. M. & MEADOWS, G. G. (2002) U0126, a mitogen-activated protein kinase kinase inhibitor, inhibits the invasion of human A375 melanoma cells. *Cancer Lett,* 179**,** 133-40.

GHERZI, R., TRABUCCHI, M., PONASSI, M., RUGGIERO, T., CORTE, G., MORONI, C., CHEN, C. Y., KHABAR, K. S., ANDERSEN, J. S. & BRIATA, P. (2006) The RNA-binding protein KSRP promotes decay of beta-catenin mRNA and is inactivated by PI3K-AKT signaling. *PLoS Biol,* 5**,** e5.

GIRNITA, A., GIRNITA, L., DEL PRETE, F., BARTOLAZZI, A., LARSSON, O. & AXELSON, M. (2004) Cyclolignans as inhibitors of the insulin-like growth factor-1 receptor and malignant cell growth. *Cancer Res,* 64**,** 236-42.

GIULIANI, C., SAJI, M., BUCCI, I., FIORE, G., LIBERATORE, M., SINGER, D. S., MONACO, F., KOHN, L. D. & NAPOLITANO, G. (2006) Transcriptional regulation of major histocompatibility complex class I gene by insulin and IGF-I in FRTL-5 thyroid cells. *J Endocrinol,* 189**,** 605-15.

GLUD, M., KLAUSEN, M., GNIADECKI, R., ROSSING, M., HASTRUP, N., NIELSEN, F. C. & DRZEWIECKI, K. T. (2009) MicroRNA expression in melanocytic nevi: the usefulness of formalin-fixed, paraffin-embedded material for miRNA microarray profiling. *J Invest Dermatol,* 129**,** 1219-24.

GOEL, V. K., LAZAR, A. J. F., WARNEKE, C. L., REDSTON, M. S. & HALUSKA, F. G. (2006) Examination of Mutations in BRAF, NRAS, and PTEN in Primary Cutaneous Melanoma. *J Invest Dermatol,* 126**,** 154-160.

GOLDSCHMIDT, M. H., ARMED FORCES INSTITUTE OF PATHOLOGY (U.S.), AMERICAN REGISTRY OF PATHOLOGY. & WHO COLLABORATING CENTER FOR WORLDWIDE REFERENCE ON COMPARATIVE ONCOLOGY. (1998) *Histological classification of epithelial and melanocytic tumors of the skin of domestic animals,* Washington, D.C., Armed Forces Institute of Pathology in cooperation with the American Registry of Pathology and the

World Health Organization Collaborating Center for Worldwide Reference on Comparative Oncology.

GOLDSCHMIDT, M. H. & SHOFER, F. S. (1998) *Skin tumors of the dog and cat,* Oxford, Butterworth-Heinemann.

GONG, Y., YAO, E., SHEN, R., GOEL, A., ARCILA, M., TERUYA-FELDSTEIN, J., ZAKOWSKI, M. F., FRANKEL, S., PEIFER, M., THOMAS, R. K., LADANYI, M. & PAO, W. (2009) High expression levels of total IGF-1R and sensitivity of NSCLC cells in vitro to an anti-IGF-1R antibody (R1507). *PLoS ONE,* 4**,** e7273.

GORDON, M. D. & NUSSE, R. (2006) Wnt Signaling: Multiple Pathways, Multiple Receptors, and Multiple Transcription Factors. *Journal of Biological Chemistry,* 281**,** 22429-22433.

GORELIK, E., PEPPOLONI, S., OVERTON, R. & HERBERMAN, R. B. (1985) Increase in H-2 Antigen Expression and Immunogenicity of BL6 Melanoma Cells Treated with N-Methyl-N'-nitronitrosoguanidine. *Cancer Res,* 45**,** 5341-5347.

GOYA, M., MIYAMOTO, S., NAGAI, K., OHKI, Y., NAKAMURA, K., SHITARA, K., MAEDA, H., SANGAI, T., KODAMA, K., ENDOH, Y., ISHII, G., HASEBE, T., YONOU, H., HATANO, T., OGAWA, Y. & OCHIAI, A. (2004) Growth inhibition of human prostate cancer cells in human adult bone implanted into nonobese diabetic/severe combined immunodeficient mice by a ligand-specific antibody to human insulin-like growth factors. *Cancer Res,* 64**,** 6252-8.

GROSENBAUGH, D. A., LEARD, A. T., BERGMAN, P. J., KLEIN, M. K., MELEO, K., SUSANECK, S., HESS, P. R., JANKOWSKI, M. K., JONES, P. D., LEIBMAN, N. F., JOHNSON, M. H., KURZMAN, I. D. & WOLCHOK, J. D. (2011) Safety and efficacy of a xenogeneic DNA vaccine encoding for human tyrosinase as adjunctive treatment for oral malignant melanoma in dogs following surgical excision of the primary tumor. *Am J Vet Res,* 72**,** 1631-8.

GUALBERTO, A., DOLLED-FILHART, M., GUSTAVSON, M., CHRISTIANSEN, J., WANG, Y.-F., HIXON, M. L., REYNOLDS, J., MCDONALD, S., ANG, A., RIMM, D. L., LANGER, C. J., BLAKELY, J., GARLAND, L., PAZ-ARES, L. G., KARP, D. D. & LEE, A. V. (2010) Molecular Analysis of Non-Small Cell Lung Cancer Identifies Subsets with Different Sensitivity to Insulin-like Growth Factor I Receptor Inhibition. *Clinical Cancer Research*.

GUALBERTO, A. & KARP, D. (2009) Development of the Monoclonal Antibody Figitumumab, Targeting the Insulin-like Growth Factor-1 Receptor, for the Treatment of Patients with Non–Small-Cell Lung Cancer. *Clinical Lung Cancer,* 10**,** 273-280.

GUEVARA-AGUIRRE, J., BALASUBRAMANIAN, P., GUEVARA-AGUIRRE, M., WEI, M., MADIA, F., CHENG, C. W., HWANG, D., MARTIN-MONTALVO, A., SAAVEDRA, J., INGLES, S., DE CABO, R., COHEN, P. & LONGO, V. D. (2011) Growth hormone receptor deficiency is associated with a major reduction in pro-aging signaling, cancer, and diabetes in humans. *Sci Transl Med,* 3**,** 70ra13.

GYORFFY, S., RODRIGUEZ-LECOMPTE, J. C., WOODS, J. P., FOLEY, R., KRUTH, S., LIAW, P. C. & GAULDIE, J. (2005) Bone marrow-derived dendritic cell vaccination of dogs with naturally occurring melanoma by using human gp100 antigen. *J Vet Intern Med,* 19**,** 56-63.

HAAPAJARVI, T., PITKANEN, K. & LAIHO, M. (1999) Human Melanoma Cell Line UV Responses Show Independency of p53 Function. *Cell Growth Differ,* 10**,** 163-171.

HAKAM, A., FANG, Q., KARL, R. & COPPOLA, D. (2003) Coexpression of IGF-1R and c-Src proteins in human pancreatic ductal adenocarcinoma. *Dig Dis Sci,* 48**,** 1972-8.

HAKAM, A., YEATMAN, T. J., LU, L., MORA, L., MARCET, G., NICOSIA, S. V., KARL, R. C. & COPPOLA, D. (1999) Expression of insulin-like growth factor-1 receptor in human colorectal cancer. *Hum Pathol,* 30**,** 1128-33.

HALABAN, R., FAN, B., AHN, J., FUNASAKA, Y., GITAY-GOREN, H. & NEUFELD, G. (1992a) Growth factors, receptor kinases, and protein tyrosine phosphatases in normal and malignant melanocytes. *J Immunother (1991),* 12**,** 154-61.

HALABAN, R., RUBIN, J. S., FUNASAKA, Y., COBB, M., BOULTON, T., FALETTO, D., ROSEN, E., CHAN, A., YOKO, K., WHITE, W. & ET AL. (1992b) Met and hepatocyte growth factor/scatter factor signal transduction in normal melanocytes and melanoma cells. *Oncogene,* 7**,** 2195-206.

HALUSKA, F. G., TSAO, H., WU, H., HALUSKA, F. S., LAZAR, A. & GOEL, V. (2006a) Genetic Alterations in Signaling Pathways in Melanoma. *Clinical Cancer Research,* 12**,** 2301s-2307s.

HALUSKA, P., CARBONI, J. M., LOEGERING, D. A., LEE, F. Y., WITTMAN, M., SAULNIER, M. G., FRENNESSON, D. B., KALLI, K. R., CONOVER, C. A., ATTAR, R. M., KAUFMANN, S. H., GOTTARDIS, M. & ERLICHMAN, C. (2006b) In vitro and in vivo antitumor effects of the dual insulin-like growth factor-I/insulin receptor inhibitor, BMS-554417. *Cancer Res,* 66**,** 362-71.

HAN, J. I., KIM, D. Y. & NA, K. J. (2010) Dysregulation of the Wnt/beta-catenin signaling pathway in canine cutaneous melanotic tumor. *Vet Pathol,* 47**,** 285-91.

HANAHAN, D. & WEINBERG, R. A. (2000) The Hallmarks of Cancer. *Cell,* 100**,** 57-70.

HANAHAN, D. & WEINBERG, R. A. (2011) Hallmarks of cancer: the next generation. *Cell,* 144**,** 646-74.

HANKINSON, S. E. & SCHERNHAMMER, E. S. (2003) Insulin-like growth factor and breast cancer risk: evidence from observational studies. *Breast Dis,* 17**,** 27-40.

HANKINSON, S. E., WILLETT, W. C., COLDITZ, G. A., HUNTER, D. J., MICHAUD, D. S., DEROO, B., ROSNER, B., SPEIZER, F. E. & POLLAK, M. (1998) Circulating concentrations of insulin-like growth factor-I and risk of breast cancer. *Lancet,* 351**,** 1393-6.

HANNAN, K. M., BRANDENBURGER, Y., JENKINS, A., SHARKEY, K., CAVANAUGH, A., ROTHBLUM, L., MOSS, T., POORTINGA, G., MCARTHUR, G. A., PEARSON, R. B. & HANNAN, R. D. (2003) mTOR-dependent regulation of ribosomal gene transcription requires S6K1 and is mediated by phosphorylation of the carboxy-terminal activation domain of the nucleolar transcription factor UBF. *Mol Cell Biol,* 23**,** 8862-77.

HAPPERFIELD, L. C., MILES, D. W., BARNES, D. M., THOMSEN, L. L., SMITH, P. & HANBY, A. (1997) The localization of the insulin-like growth factor receptor 1 (IGFR-1) in benign and malignant breast tissue. *J Pathol,* 183**,** 412-7.

HARRELA, M., KOISTINEN, H., KAPRIO, J., LEHTOVIRTA, M., TUOMILEHTO, J., ERIKSSON, J., TOIVANEN, L., KOSKENVUO, M., LEINONEN, P., KOISTINEN, R. & SEPPALA, M. (1996) Genetic and environmental components of interindividual variation in circulating levels of IGF-I, IGF-II, IGFBP-1, and IGFBP-3. *J Clin Invest,* 98**,** 2612-5.

HARVEY, H. J., MACEWEN, E. G., BRAUN, D., PATNAIK, A. K., WITHROW, S. J. & JONGEWARD, S. (1981) Prognostic criteria for dogs with oral melanoma. *J Am Vet Med Assoc,* 178**,** 580-2.

HASSAN, A. B. & MACAULAY, V. M. (2002) The insulin-like growth factor system as a therapeutic target in colorectal cancer. *Ann Oncol,* 13**,** 349-56.

HAUSCHILD, A., GROB, J. J., DEMIDOV, L. V., JOUARY, T., GUTZMER, R., MILLWARD, M., RUTKOWSKI, P., BLANK, C. U., MILLER, W. H., JR., KAEMPGEN, E., MARTIN-ALGARRA, S., KARASZEWSKA, B., MAUCH, C., CHIARION-SILENI, V., MARTIN, A. M., SWANN, S., HANEY, P., MIRAKHUR, B., GUCKERT, M. E., GOODMAN, V. & CHAPMAN, P. B. (2012) Dabrafenib in BRAF-mutated metastatic melanoma: a multicentre, open-label, phase 3 randomised controlled trial. *Lancet,* 380**,** 358-65.

HAY, N. & SONENBERG, N. (2004) Upstream and downstream of mTOR. *Genes Dev,* 18**,** 1926-45.

HAZAN, R. B., QIAO, R., KEREN, R., BADANO, I. & SUYAMA, K. (2004) Cadherin switch in tumor progression. *Ann N Y Acad Sci,* 1014**,** 155-63.

HE, T. C., SPARKS, A. B., RAGO, C., HERMEKING, H., ZAWEL, L., DA COSTA, L. T., MORIN, P. J., VOGELSTEIN, B. & KINZLER, K. W. (1998) Identification of c-MYC as a target of the APC pathway. *Science,* 281**,** 1509-12.

HEGDE, P. S., RUSNAK, D., BERTIAUX, M., ALLIGOOD, K., STRUM, J., GAGNON, R. & GILMER, T. M. (2007) Delineation of molecular mechanisms of sensitivity to lapatinib in breast cancer cell lines using global gene expression profiles. *Mol Cancer Ther,* 6**,** 1629-40.

HELLAWELL, G. O., TURNER, G. D., DAVIES, D. R., POULSOM, R., BREWSTER, S. F. & MACAULAY, V. M. (2002) Expression of the type 1 insulin-like growth factor receptor is up-regulated in primary prostate cancer and commonly persists in metastatic disease. *Cancer Res,* 62**,** 2942-50.

HELMS, M. W., KEMMING, D., CONTAG, C. H., POSPISIL, H., BARTKOWIAK, K., WANG, A., CHANG, S. Y., BUERGER, H. & BRANDT, B. H. (2009) TOB1 is regulated by EGF-dependent HER2 and EGFR signaling, is highly phosphorylated, and indicates poor prognosis in node-negative breast cancer. *Cancer Res,* 69**,** 5049-56.

HERLYN, M., THURIN, J., BALABAN, G., BENNICELLI, J. L., HERLYN, D., ELDER, D. E., BONDI, E., GUERRY, D., NOWELL, P., CLARK, W. H. & ET AL. (1985) Characteristics of cultured human melanocytes isolated from different stages of tumor progression. *Cancer Res,* 45**,** 5670-6.

HERMANS, I. F., SILK, J. D., YANG, J., PALMOWSKI, M. J., GILEADI, U., MCCARTHY, C., SALIO, M., RONCHESE, F. & CERUNDOLO, V. (2004) The VITAL assay: a versatile fluorometric technique for assessing CTL- and NKT-mediated cytotoxicity against multiple targets in vitro and in vivo. *Journal of Immunological Methods,* 285**,** 25-40.

HERSEY, P., MENZIES, S. W., HALLIDAY, G. M., NGUYEN, T., FARRELLY, M. L., DESILVA, C. & LETT, M. (2004) Phase I/II study of treatment with dendritic cell vaccines in patients with disseminated melanoma. *Cancer Immunol Immunother,* 53**,** 125-34.

HILMI, C., LARRIBERE, L., GIULIANO, S., BILLE, K., ORTONNE, J.-P., BALLOTTI, R. & BERTOLOTTO, C. (2007) IGF1 Promotes Resistance to Apoptosis in Melanoma Cells through an Increased Expression of BCL2, BCL-X(L), and Survivin. *J Invest Dermatol,* 128**,** 1499-1505.

HOA, N., TSUI, S., AFIFIYAN, N. F., SINHA HIKIM, A., LI, B., DOUGLAS, R. S. & SMITH, T. J. (2012) Nuclear targeting of IGF-1 receptor in orbital fibroblasts from Graves' disease: apparent role of ADAM17. *PLoS ONE,* 7**,** e34173.

HODI, F. S., O'DAY, S. J., MCDERMOTT, D. F., WEBER, R. W., SOSMAN, J. A., HAANEN, J. B., GONZALEZ, R., ROBERT, C., SCHADENDORF, D., HASSEL, J. C., AKERLEY, W., VAN DEN EERTWEGH, A. J., LUTZKY, J., LORIGAN, P., VAUBEL, J. M., LINETTE, G. P., HOGG, D., OTTENSMEIER, C. H., LEBBE, C., PESCHEL, C., QUIRT, I., CLARK, J. I., WOLCHOK, J. D., WEBER, J. S., TIAN, J., YELLIN, M. J., NICHOL, G. M., HOOS, A. & URBA, W. J. (2010a) Improved survival with ipilimumab in patients with metastatic melanoma. *N Engl J Med,* 363**,** 711-23.

HODI, F. S., O'DAY, S. J., MCDERMOTT, D. F., WEBER, R. W., SOSMAN, J. A., HAANEN, J. B., GONZALEZ, R., ROBERT, C., SCHADENDORF, D., HASSEL, J. C., AKERLEY, W., VAN DEN EERTWEGH, A. J. M., LUTZKY, J., LORIGAN, P., VAUBEL, J. M., LINETTE, G. P., HOGG, D., OTTENSMEIER, C. H., LEBBÃ©, C., PESCHEL, C., QUIRT, I., CLARK, J. I., WOLCHOK, J. D., WEBER, J. S., TIAN, J., YELLIN, M. J., NICHOL, G. M., HOOS, A. & URBA, W. J. (2010b) Improved Survival with Ipilimumab in Patients with Metastatic Melanoma. *New England Journal of Medicine,* 363**,** 711-723.

HOEK, K., RIMM, D. L., WILLIAMS, K. R., ZHAO, H., ARIYAN, S., LIN, A., KLUGER, H. M., BERGER, A. J., CHENG, E., TROMBETTA, E. S., WU, T., NIINOBE, M., YOSHIKAWA, K., HANNIGAN, G. E. & HALABAN, R. (2004) Expression Profiling Reveals Novel Pathways in the Transformation of Melanocytes to Melanomas. *Cancer Research,* 64**,** 5270-5282.

HOLMES, M. D., POLLAK, M. N., WILLETT, W. C. & HANKINSON, S. E. (2002) Dietary correlates of plasma insulin-like growth factor I and insulin-like growth factor binding protein 3 concentrations. *Cancer Epidemiol Biomarkers Prev,* 11**,** 852-61.

HOLZENBERGER, M., DUPONT, J., DUCOS, B., LENEUVE, P., GELOEN, A., EVEN, P. C., CERVERA, P. & LE BOUC, Y. (2003) IGF-1 receptor regulates lifespan and resistance to oxidative stress in mice. *Nature,* 421**,** 182-7.

HOSAKA, T., BIGGS, W. H., TIEU, D., BOYER, A. D., VARKI, N. M., CAVENEE, W. K. & ARDEN, K. C. (2004) Disruption of forkhead transcription factor (FOXO) family members in mice reveals their functional diversification. *Proceedings of the National Academy of Sciences of the United States of America,* 101**,** 2975-2980.

HOWE, L. R. & BROWN, A. M. (2004) Wnt signaling and breast cancer. *Cancer Biol Ther,* 3**,** 36-41.

HUANG, C., KIM, J., BERASI, S. P., WAZER, D. E., YEE, A. & PAULSON, K. E. (2006) Transcriptional repressor HBP1 inhibition of epidermal growth factor receptor signaling: Regulation of ligand-stimulated reactive oxygen species generation *Proc Amer Assoc Cancer Res,* 47**,** Abstract #4286.

HUANG, F., GREER, A., HURLBURT, W., HAN, X., HAFEZI, R., WITTENBERG, G. M., REEVES, K., CHEN, J., ROBINSON, D., LI, A., LEE, F. Y., GOTTARDIS, M. M., CLARK, E., HELMAN, L., ATTAR, R. M., DONGRE, A. & CARBONI, J. M. (2009) The mechanisms of differential sensitivity to an insulin-like growth factor-1 receptor inhibitor (BMS-536924) and rationale for combining with EGFR/HER2 inhibitors. *Cancer Res,* 69**,** 161-70.

HUANG, F., HURLBURT, W., GREER, A., REEVES, K. A., HILLERMAN, S., CHANG, H., FARGNOLI, J., GRAF FINCKENSTEIN, F., GOTTARDIS, M. M. & CARBONI, J. M. (2008) Differential Mechanisms of Acquired Resistance to Insulin-like Growth Factor-I Receptor Antibody Therapy or to a Small-Molecule Inhibitor, BMS-754807, in a Human Rhabdomyosarcoma Model. *Cancer Research***,** -.

HUSSUSSIAN, C. J., STRUEWING, J. P., GOLDSTEIN, A. M., HIGGINS, P. A., ALLY, D. S., SHEAHAN, M. D., CLARK, W. H., JR., TUCKER, M. A. & DRACOPOLI, N. C. (1994) Germline p16 mutations in familial melanoma. *Nat Genet,* 8**,** 15-21.

HWA, V., OH, Y. & ROSENFELD, R. G. (1999) The insulin-like growth factor-binding protein (IGFBP) superfamily. *Endocr Rev,* 20**,** 761-87.

IIIZUMI, M., ARAKAWA, H., MORI, T., ANDO, A. & NAKAMURA, Y. (2002) Isolation of a novel gene, CABC1, encoding a mitochondrial protein that is highly homologous to yeast activity of bc1 complex. *Cancer Res,* 62**,** 1246-50.

IKEDIOBI, O. N., DAVIES, H., BIGNELL, G., EDKINS, S., STEVENS, C., O'MEARA, S., SANTARIUS, T., AVIS, T., BARTHORPE, S., BRACKENBURY, L., BUCK, G., BUTLER, A., CLEMENTS, J., COLE, J., DICKS, E., FORBES, S., GRAY, K., HALLIDAY, K., HARRISON, R., HILLS, K., HINTON, J., HUNTER, C., JENKINSON, A., JONES, D., KOSMIDOU, V., LUGG, R., MENZIES, A., MIRONENKO, T., PARKER, A., PERRY, J., RAINE, K., RICHARDSON, D., SHEPHERD, R., SMALL, A., SMITH, R., SOLOMON, H., STEPHENS, P., TEAGUE, J., TOFTS, C., VARIAN, J., WEBB, T., WEST, S., WIDAA, S., YATES, A., REINHOLD, W., WEINSTEIN, J. N., STRATTON, M. R., FUTREAL, P. A. & WOOSTER, R. (2006) Mutation analysis of 24 known cancer genes in the NCI-60 cell line set. *Mol Cancer Ther,* 5**,** 2606-12.

INFANTE, J. R., FECHER, L. A., NALLAPAREDDY, S., GORDON, M. S., FLAHERTY, K. T., COX, D. S., DEMARINI, D. J., MORRIS, S. R., BURRIS, H. A. & MESSERSMITH, W. A. (2010) Safety and efficacy results from the first-in-human study of the oral MEK 1/2 inhibitor GSK1120212. *ASCO Meeting Abstracts,* 28**,** 2503.

ITO, T., ITO, N., BETTERMANN, A., TOKURA, Y., TAKIGAWA, M. & PAUS, R. (2004) Collapse and restoration of MHC class-I-dependent immune privilege: exploiting the human hair follicle as a model. *Am J Pathol,* 164**,** 623-34.

ITOH, S., HATTORI, T., HAYASHI, H., MIZUTANI, Y., TODO, M., TAKII, T., YANG, D., LEE, J. C., MATSUFUJI, S., MURAKAMI, Y., CHIBA, T. & ONOZAKI, K. (1999) Antiproliferative Effect of IL-1 Is Mediated by p38 Mitogen-Activated Protein Kinase in Human Melanoma Cell A375. *The Journal of Immunology,* 162**,** 7434-7440.

JACKSON-BOOTH, P. G., TERRY, C., LACKEY, B., LOPACZYNSKA, M. & NISSLEY, P. (2003) Inhibition of the biologic response to insulin-like growth factor I in MCF-7 breast cancer cells by a new monoclonal antibody to the insulin-like growth factor-I receptor. The importance of receptor down-regulation. *Horm Metab Res,* 35**,** 850-6.

JAMES, M. J. & ZOMERDIJK, J. C. (2004) Phosphatidylinositol 3-kinase and mTOR signaling pathways regulate RNA polymerase I transcription in response to IGF-1 and nutrients. *J Biol Chem,* 279**,** 8911-8.

JANEWAY CA JR, T. P., WALPORT M, ET AL.. (2001) General properties of armed effector T cells. *Immunobiology: The Immune System in Health and Disease***,** New York: Garland Science.

JARVIS, K., ASSIS-NASCIMENTO, P., MUDD, L. M. & MONTAGUE, J. R. (2007) Beta-amyloid toxicity and reversal in embryonic rat septal neurons. *Neurosci Lett,* 423**,** 184-8.

JASSEM, J. (2010) Randomised, open label, phase III trial of figitumumab in combination with paclitaxel and carboplatin versus paclitaxel and carboplatin in patients with non-small cell lung cancer (NSCLC). *Journal of Clinical Oncology***,** Abstract 7500.

JI, Q.-S., MULVIHILL, M. J., ROSENFELD-FRANKLIN, M., COOKE, A., FENG, L., MAK, G., O'CONNOR, M., YAO, Y., PIRRITT, C., BUCK, E., EYZAGUIRRE, A., ARNOLD, L. D., GIBSON, N. W. & PACHTER, J. A. (2007) A novel, potent, and selective insulin-like growth factor-I receptor kinase inhibitor blocks insulin-like growth factor-I receptor signaling in vitro and inhibits insulin-like growth factor-I receptor dependent tumor growth in vivo. *Mol Cancer Ther,* 6**,** 2158-2167.

JIANG, S., LI, Y., ZHU, Y. H., WU, X. Q., TANG, J., LI, Z., FENG, G. K., DENG, R., LI, D. D., LUO, R. Z., ZHANG, M. F., QIN, W., WANG, X., JIA, W. H. & ZHU, X. F. (2011) Intensive expression of UNC-51-like kinase 1 is a novel biomarker of poor prognosis in patients with esophageal squamous cell carcinoma. *Cancer Sci,* 102**,** 1568-75.

JONSSON, G., BUSCH, C., KNAPPSKOG, S., GEISLER, J., MILETIC, H., RINGNER, M., LILLEHAUG, J. R., BORG, A. & LONNING, P. E. (2010) Gene Expression Profiling-Based Identification of Molecular Subtypes in Stage IV Melanomas with Different Clinical Outcome. *Clinical Cancer Research,* 16**,** 3356-3367.

JUUL, A., SCHEIKE, T., DAVIDSEN, M., GYLLENBORG, J. & JÃ¸RGENSEN, T. (2002) Low Serum Insulin-Like Growth Factor I Is Associated With Increased Risk of Ischemic Heart Disease: A Population-Based Case-Control Study. *Circulation,* 106**,** 939-944.

KADARA, H., TAHARA, E., KIM, H. J., LOTAN, D., MYERS, J. & LOTAN, R. (2008) Involvement of Rac in fenretinide-induced apoptosis. *Cancer Res,* 68**,** 4416-23.

KAGESHITA, T., HAMBY, C. V., ISHIHARA, T., MATSUMOTO, K., SAIDA, T. & ONO, T. (2001) Loss of beta-catenin expression associated with disease progression in malignant melanoma. *Br J Dermatol,* 145**,** 210-6.

KALEBIC, T., TSOKOS, M. & HELMAN, L. J. (1994) In vivo treatment with antibody against IGF-1 receptor suppresses growth of human rhabdomyosarcoma and down-regulates p34cdc2. *Cancer Res,* 54**,** 5531-4.

KAMB, A., SHATTUCK-EIDENS, D., EELES, R., LIU, Q., GRUIS, N. A., DING, W., HUSSEY, C., TRAN, T., MIKI, Y., WEAVER-FELDHAUS, J. & ET AL. (1994) Analysis of the p16 gene (CDKN2) as a candidate for the chromosome 9p melanoma susceptibility locus. *Nat Genet,* 8**,** 23-6.

KANTER-LEWENSOHN, L., DRICU, A., GIRNITA, L., WEJDE, J. & LARSSON, O. (2000) Expression of Insulin-Like Growth Factor-1 Receptor (IGF-1R) and p27^Kip1 in Melanocyte Tumors: A Potential Regulatory Role of IGF-1 Pathway in Distribution of p27^Kip1between Different Cyclins. *Growth Factors,* 17**,** 193 - 202.

KANTER-LEWENSOHN, L., DRICU, A., WANG, M., WEJDE, J., KIESSLING, R. & LARSSON, O. (1998) Expression of the insulin-like growth factor-1 receptor and its anti-apoptotic effect in malignant melanoma: a potential therapeutic target. *Melanoma Res,* 8**,** 389-97.

KAPPEL, S., MATTHESS, Y., KAUFMANN, M. & STREBHARDT, K. (2007) Silencing of mammalian genes by tetracycline-inducible shRNA expression. *Nat Protoc,* 2**,** 3257-69.

KARASIC, T. B., HEI, T. K. & IVANOV, V. N. (2010) Disruption of IGF-1R signaling increases TRAIL-induced apoptosis: a new potential therapy for the treatment of melanoma. *Exp Cell Res,* 316**,** 1994-2007.

KEFFORD, R., ARKENAU, H., BROWN, M. P., MILLWARD, M., INFANTE, J. R., LONG, G. V., OUELLET, D., CURTIS, M., LEBOWITZ, P. F. & FALCHOOK, G. S. (2010) Phase I/II study of GSK2118436, a selective inhibitor of oncogenic

mutant BRAF kinase, in patients with metastatic melanoma and other solid tumors. *ASCO Meeting Abstracts,* 28**,** 8503.

KENT, M. S., COLLINS, C. J. & YE, F. (2009) Activation of the AKT and mammalian target of rapamycin pathways and the inhibitory effects of rapamycin on those pathways in canine malignant melanoma cell lines. *Am J Vet Res,* 70**,** 263-9.

KENYON, C., CHANG, J., GENSCH, E., RUDNER, A. & TABTIANG, R. (1993) A C. elegans mutant that lives twice as long as wild type. *Nature,* 366**,** 461-4.

KIM, H. S., NAGALLA, S. R., OH, Y., WILSON, E., ROBERTS, C. T., JR. & ROSENFELD, R. G. (1997) Identification of a family of low-affinity insulin-like growth factor binding proteins (IGFBPs): characterization of connective tissue growth factor as a member of the IGFBP superfamily. *Proc Natl Acad Sci U S A,* 94**,** 12981-6.

KIM, J., ZHANG, X., RIEGER-CHRIST, K. M., SUMMERHAYES, I. C., WAZER, D. E., PAULSON, K. E. & YEE, A. S. (2006) Suppression of Wnt signaling by the green tea compound (-)-epigallocatechin 3-gallate (EGCG) in invasive breast cancer cells. Requirement of the transcriptional repressor HBP1. *J Biol Chem,* 281**,** 10865-75.

KIRKWOOD, J. M., IBRAHIM, J. G., SOSMAN, J. A., SONDAK, V. K., AGARWALA, S. S., ERNSTOFF, M. S. & RAO, U. (2001) High-dose interferon alfa-2b significantly prolongs relapse-free and overall survival compared with the GM2-KLH/QS-21 vaccine in patients with resected stage IIB-III melanoma: results of intergroup trial E1694/S9512/C509801. *J Clin Oncol,* 19**,** 2370-80.

KIRKWOOD, J. M., LEE, S., MOSCHOS, S. J., ALBERTINI, M. R., MICHALAK, J. C., SANDER, C., WHITESIDE, T., BUTTERFIELD, L. H. & WEINER, L. (2009) Immunogenicity and antitumor effects of vaccination with peptide vaccine+/- granulocyte-monocyte colony-stimulating factor and/or IFN-alpha2b in advanced metastatic melanoma: Eastern Cooperative Oncology Group Phase II Trial E1696. *Clin Cancer Res,* 15**,** 1443-51.

KITCHELL, B. E., BROWN, D. M., LUCK, E. E., WOODS, L. L., ORENBERG, E. K. & BLOCH, D. A. (1994) Intralesional implant for treatment of primary oral malignant melanoma in dogs. *J Am Vet Med Assoc,* 204**,** 229-36.

KLAUS, A. & BIRCHMEIER, W. (2008) Wnt signalling and its impact on development and cancer. *Nat Rev Cancer,* 8**,** 387-398.

KLEIN, E. A. & ASSOIAN, R. K. (2008) Transcriptional regulation of the cyclin D1 gene at a glance. *J Cell Sci,* 121**,** 3853-3857.

KOENIG, A., BIANCO, S. R., FOSMIRE, S., WOJCIESZYN, J. & MODIANO, J. F. (2002) Expression and significance of p53, rb, p21/waf-1, p16/ink-4a, and PTEN tumor suppressors in canine melanoma. *Vet Pathol,* 39**,** 458-72.

KOIKE, N., PILON-THOMAS, S. & MULE, J. J. (2008) Nonmyeloablative chemotherapy followed by T-cell adoptive transfer and dendritic cell-based vaccination results in rejection of established melanoma. *J Immunother,* 31**,** 402-12.

KOOIJMAN, R. (2006) Regulation of apoptosis by insulin-like growth factor (IGF)-I. *Cytokine & Growth Factor Reviews,* 17**,** 305-323.

KORINEK, V., BARKER, N., MORIN, P. J., VAN WICHEN, D., DE WEGER, R., KINZLER, K. W., VOGELSTEIN, B. & CLEVERS, H. (1997) Constitutive transcriptional activation by a beta-catenin-Tcf complex in APC-/- colon carcinoma. *Science,* 275**,** 1784-7.

KRUMMEL, M. F. & ALLISON, J. P. (1996) CTLA-4 engagement inhibits IL-2 accumulation and cell cycle progression upon activation of resting T cells. *J Exp Med,* 183**,** 2533-40.

KULL, F. C., JR., JACOBS, S., SU, Y. F., SVOBODA, M. E., VAN WYK, J. J. & CUATRECASAS, P. (1983) Monoclonal antibodies to receptors for insulin and somatomedin-C. *J Biol Chem,* 258**,** 6561-6.

KURITA, S., MOTT, J. L., ALMADA, L. L., BRONK, S. F., WERNEBURG, N. W., SUN, S. Y., ROBERTS, L. R., FERNANDEZ-ZAPICO, M. E. & GORES, G. J. (2010) GLI3-dependent repression of DR4 mediates hedgehog antagonism of TRAIL-induced apoptosis. *Oncogene,* 29**,** 4848-58.

KUWAHARA, A., HIRABAYASHI, Y., KNOEPFLER, P. S., TAKETO, M. M., SAKAI, J., KODAMA, T. & GOTOH, Y. (2010) Wnt signaling and its downstream target N-myc regulate basal progenitors in the developing neocortex. *Development,* 137**,** 1035-44.

KUZUYA, H., MATSUURA, N., SAKAMOTO, M., MAKINO, H., SAKAMOTO, Y., KADOWAKI, T., SUZUKI, Y., KOBAYASHI, M., AKAZAWA, Y., NOMURA, M. & ET AL. (1993) Trial of insulinlike growth factor I therapy for patients with extreme insulin resistance syndromes. *Diabetes,* 42**,** 696-705.

LAEMMLI, U. K. (1970) Cleavage of structural proteins during the assembly of the head of bacteriophage T4. *Nature,* 227**,** 680-5.

LAFARGE-FRAYSSINET, C., DUC, H. T., FRAYSSINET, C., SARASIN, A., ANTHONY, D., GUO, Y. & TROJAN, J. (1997) Antisense insulin-like growth factor I transferred into a rat hepatoma cell line inhibits tumorigenesis by modulating major histocompatibility complex I cell surface expression. *Cancer Gene Ther,* 4**,** 276-85.

LAUGHLIN, G. A., BARRETT-CONNOR, E., CRIQUI, M. H. & KRITZ-SILVERSTEIN, D. (2004) The Prospective Association of Serum Insulin-Like Growth Factor I (IGF-I) and IGF-Binding Protein-1 Levels with All Cause and Cardiovascular Disease Mortality in Older Adults: The Rancho Bernardo Study. *Journal of Clinical Endocrinology & Metabolism,* 89**,** 114-120.

LAURO, D., KIDO, Y., HAYASHI, H., EBINA, Y. & ACCILI, D. (1999) Expression of kinase-inactive mutant insulin receptors does not rescue insulin receptor-deficient mice from perinatal death. *Diabetologia,* 42**,** 1441-1442.

LAVENDER, P., VANDEL, L., BANNISTER, A. J. & KOUZARIDES, T. (1997) The HMG-box transcription factor HBP1 is targeted by the pocket proteins and E1A. *Oncogene,* 14**,** 2721-8.

LAZAR-MOLNAR, E., HEGYESI, H., TOTH, S. & FALUS, A. (2000) Autocrine and paracrine regulation by cytokines and growth factors in melanoma. *Cytokine,* 12**,** 547-54.

LEACH, D. R., KRUMMEL, M. F. & ALLISON, J. P. (1996) Enhancement of antitumor immunity by CTLA-4 blockade. *Science,* 271**,** 1734-6.

LEE, A. V., HILSENBECK, S. G. & YEE, D. (1998) IGF system components as prognostic markers in breast cancer. *Breast Cancer Res Treat,* 47**,** 295-302.

LEE, J. K., EDDERKAOUI, M., TRUONG, P., OHNO, I., JANG, K. T., BERTI, A., PANDOL, S. J. & GUKOVSKAYA, A. S. (2007a) NADPH oxidase promotes pancreatic cancer cell survival via inhibiting JAK2 dephosphorylation by tyrosine phosphatases. *Gastroenterology,* 133**,** 1637-48.

LEE, S. K., KANG, J. S., JUNG DA, J., HUR, D. Y., KIM, J. E., HAHM, E., BAE, S., KIM, H. W., KIM, D., CHO, B. J., CHO, D., SHIN, D. H., HWANG, Y. I. & LEE, W. J. (2008) Vitamin C suppresses proliferation of the human melanoma cell SK-MEL-2 through the inhibition of cyclooxygenase-2 (COX-2) expression and the modulation of insulin-like growth factor II (IGF-II) production. *J Cell Physiol,* 216**,** 180-8.

LEE, Y. J., IMSUMRAN, A., PARK, M. Y., KWON, S. Y., YOON, H. I., LEE, J. H., YOO, C. G., KIM, Y. W., HAN, S. K., SHIM, Y. S., PIAO, W., YAMAMOTO, H., ADACHI, Y., CARBONE, D. P. & LEE, C. T. (2007b) Adenovirus expressing shRNA to IGF-1R enhances the chemosensitivity of lung cancer cell lines by blocking IGF-1 pathway. *Lung Cancer,* 55**,** 279-86.

LEMBO, G., ROCKMAN, H. A., HUNTER, J. J., STEINMETZ, H., KOCH, W. J., MA, L., PRINZ, M. P., ROSS, J., JR., CHIEN, K. R. & POWELL-BRAXTON, L. (1996) Elevated blood pressure and enhanced myocardial contractility in mice with severe IGF-1 deficiency. *J Clin Invest,* 98**,** 2648-55.

LEMERCIER, C., DUNCLIFFE, K., BOIBESSOT, I., ZHANG, H., VERDEL, A., ANGELOV, D. & KHOCHBIN, S. (2000) Involvement of retinoblastoma protein and HBP1 in histone H1(0) gene expression. *Mol Cell Biol,* 20**,** 6627-37.

LENS, M. B. & DAWES, M. (2004) Global perspectives of contemporary epidemiological trends of cutaneous malignant melanoma. *Br J Dermatol,* 150**,** 179-85.

LESAGE, F., HUGNOT, J. P., AMRI, E. Z., GRIMALDI, P., BARHANIN, J. & LAZDUNSKI, M. (1994) Expression cloning in K+ transport defective yeast and distribution of HBP1, a new putative HMG transcriptional regulator. *Nucleic Acids Res,* 22**,** 3685-8.

LI, G., SATYAMOORTHY, K., MEIER, F., BERKING, C., BOGENRIEDER, T. & HERLYN, M. (2003) Function and regulation of melanoma-stromal fibroblast interactions: when seeds meet soil. *Oncogene,* 22**,** 3162-71.

LI, H., WANG, W., LIU, X., PAULSON, K. E., YEE, A. S. & ZHANG, X. (2010) Transcriptional factor HBP1 targets P16INK4A, upregulating its expression and consequently is involved in Ras-induced premature senescence. *Oncogene,* 29**,** 5083-5094.

LI, L., YUAN, H., WEAVER, C. D., MAO, J., FARR, G. H., 3RD, SUSSMAN, D. J., JONKERS, J., KIMELMAN, D. & WU, D. (1999) Axin and Frat1 interact with dvl and GSK, bridging Dvl to GSK in Wnt-mediated regulation of LEF-1. *Embo J,* 18**,** 4233-40.

LI, M., CHIU, J.-F., GAGNE, J. & FUKAGAWA, N. K. (2008) Age-related differences in insulin-like growth factor-1 receptor signaling regulates Akt/FOXO3a and ERK/Fos pathways in vascular smooth muscle cells. *Journal of Cellular Physiology,* 217**,** 377-387.

LI, S. L., LIANG, S. J., GUO, N., WU, A. M. & FUJITA-YAMAGUCHI, Y. (2000) Single-chain antibodies against human insulin-like growth factor I receptor: expression, purification, and effect on tumor growth. *Cancer Immunol Immunother,* 49**,** 243-52.

LIAO, J. C., GREGOR, P., WOLCHOK, J. D., ORLANDI, F., CRAFT, D., LEUNG, C., HOUGHTON, A. N. & BERGMAN, P. J. (2006) Vaccination with human tyrosinase DNA induces antibody responses in dogs with advanced melanoma. *Cancer Immun,* 6**,** 8.

LIN, K. M., ZHAO, W. G., BHATNAGAR, J., ZHAO, W. D., LU, J. P., SIMKO, S., SCHUENEMAN, A. & AUSTIN, G. E. (2001) Cloning and expression of human HBP1, a high mobility group protein that enhances myeloperoxidase (MPO) promoter activity. *Leukemia,* 15**,** 601-12.

LIN, S.-Y., XIA, W., WANG, J. C., KWONG, K. Y., SPOHN, B., WEN, Y., PESTELL, R. G. & HUNG, M.-C. (2000) Î²-Catenin, a novel prognostic marker for breast cancer: Its roles in cyclin D1 expression and cancer progression. *Proceedings of the National Academy of Sciences,* 97**,** 4262-4266.

LIN, X., RUAN, X., ANDERSON, M. G., MCDOWELL, J. A., KROEGER, P. E., FESIK, S. W. & SHEN, Y. (2005) siRNA-mediated off-target gene silencing triggered by a 7 nt complementation. *Nucleic Acids Res,* 33**,** 4527-35.

LIN, Y., RICHARDS, F. M., KRIPPENDORFF, B. F., BRAMHALL, J. L., HARRINGTON, J. A., BAPIRO, T. E., ROBERTSON, A., ZHELEVA, D. & JODRELL, D. I. (2012) Paclitaxel and CYC3, an aurora kinase A inhibitor, synergise in pancreatic cancer cells but not bone marrow precursor cells. *Br J Cancer,* 107**,** 1692-701.

LING, X. & ARLINGHAUS, R. B. (2005) Knockdown of STAT3 Expression by RNA Interference Inhibits the Induction of Breast Tumors in Immunocompetent Mice. *Cancer Research,* 65**,** 2532-2536.

LITZENBURGER, B. C., CREIGHTON, C. J., TSIMELZON, A., CHAN, B. T., HILSENBECK, S. G., WANG, T., CARBONI, J. M., GOTTARDIS, M. M., HUANG, F., CHANG, J. C., LEWIS, M. T., RIMAWI, M. F. & LEE, A. V. (2011) High IGF-IR Activity in Triple-Negative Breast Cancer Cell Lines and Tumorgrafts Correlates with Sensitivity to Antiâ€“IGF-IR Therapy. *Clinical Cancer Research,* 17**,** 2314-2327.

LIU, B. Y., SOLOVIEV, I., HUANG, X., CHANG, P., ERNST, J. A., POLAKIS, P. & SAKANAKA, C. (2012) Mammary tumor regression elicited by Wnt signaling inhibitor requires IGFBP5. *Cancer Res,* 72**,** 1568-78.

LIU, J. L., BLAKESLEY, V. A., GUTKIND, J. S. & LEROITH, D. (1997) The constitutively active mutant Galpha13 transforms mouse fibroblast cells deficient in insulin-like growth factor-I receptor. *J Biol Chem,* 272**,** 29438-41.

LIU, J. P., BAKER, J., PERKINS, A. S., ROBERTSON, E. J. & EFSTRATIADIS, A. (1993) Mice carrying null mutations of the genes encoding insulin-like growth factor I (Igf-1) and type 1 IGF receptor (Igf1r). *Cell,* 75**,** 59-72.

LIU, W., BENNETT, M. & HELM, T. (2011) Canine melanoma: a comparison with human pigmented epithelioid melanocytoma. *Int J Dermatol,* 50**,** 1542-5.

LIU, X., TURBYVILLE, T., FRITZ, A. & WHITESELL, L. (1998) Inhibition of insulin-like growth factor I receptor expression in neuroblastoma cells induces the regression of established tumors in mice. *Cancer Res,* 58**,** 5432-8.

LIU, Y., WANG, H., ZHAO, J., MA, J., WEI, L., WU, S., XIE, T., SHEN, F., TROJAN, J., HABIB, N., ANTHONY, D. D., WU, M. & GUO, Y. (2000) Enhancement of immunogenicity of tumor cells by cotransfection with genes encoding antisense insulin-like growth factor-1 and B7.1 molecules. *Cancer Gene Ther,* 7**,** 456-65.

LLOYD, A. R., OPPENHEIM, J. J., KELVIN, D. J. & TAUB, D. D. (1996) Chemokines regulate T cell adherence to recombinant adhesion molecules and extracellular matrix proteins. *The Journal of Immunology,* 156**,** 932-8.

LOI, S., HAIBE-KAINS, B., DESMEDT, C., LALLEMAND, F., TUTT, A. M., GILLET, C., ELLIS, P., HARRIS, A., BERGH, J., FOEKENS, J. A., KLIJN, J. G., LARSIMONT, D., BUYSE, M., BONTEMPI, G., DELORENZI, M., PICCART, M. J. & SOTIRIOU, C. (2007) Definition of clinically distinct molecular subtypes in estrogen receptor-positive breast carcinomas through genomic grade. *J Clin Oncol,* 25**,** 1239-46.

LOI, S., HAIBE-KAINS, B., DESMEDT, C., WIRAPATI, P., LALLEMAND, F., TUTT, A. M., GILLET, C., ELLIS, P., RYDER, K., REID, J. F., DAIDONE, M. G., PIEROTTI, M. A., BERNS, E. M., JANSEN, M. P., FOEKENS, J. A., DELORENZI, M., BONTEMPI, G., PICCART, M. J. & SOTIRIOU, C. (2008) Predicting prognosis using molecular profiling in estrogen receptor-positive breast cancer treated with tamoxifen. *BMC Genomics,* 9**,** 239.

LOPEZ, T. & HANAHAN, D. (2002) Elevated levels of IGF-1 receptor convey invasive and metastatic capability in a mouse model of pancreatic islet tumorigenesis. *Cancer Cell,* 1**,** 339-53.

LUCERO, O., DAWSON, D., MOON, R. & CHIEN, A. A Re-evaluation of the "Oncogenic" Nature of Wnt/β-catenin Signaling in Melanoma and Other Cancers. *Current Oncology Reports,* 12**,** 314-318.

LUKAS, J., PARRY, D., AAGAARD, L., MANN, D. J., BARTKOVA, J., STRAUSS, M., PETERS, G. & BARTEK, J. (1995) Retinoblastoma-protein-dependent cell-cycle inhibition by the tumour suppressor p16. *Nature,* 375**,** 503-6.

LY, A., DUC, H. T., KALAMARIDES, M., TROJAN, L. A., PAN, Y., SHEVELEV, A., FRANCOIS, J. C., NOEL, T., KANE, A., HENIN, D., ANTHONY, D. D. & TROJAN, J. (2001) Human glioma cells transformed by IGF-I triple helix technology show immune and apoptotic characteristics determining cell selection for gene therapy of glioblastoma. *Mol Pathol,* 54**,** 230-239.

LY, A., FRANCOIS, J. C., UPEGUI-GONZALEZ, L. C., SWIERCZ, B., BEDEL, C., DUC, H. T., BOUT, D. & TROJAN, J. (2000) Alterations in tumorigenicity of embryonal carcinoma cells by IGF-I triple-helix induced changes in immunogenicity and apoptosis. *Life Sci,* 68**,** 307-19.

LYNCH, T. J., BELL, D. W., SORDELLA, R., GURUBHAGAVATULA, S., OKIMOTO, R. A., BRANNIGAN, B. W., HARRIS, P. L., HASERLAT, S. M., SUPKO, J. G., HALUSKA, F. G., LOUIS, D. N., CHRISTIANI, D. C., SETTLEMAN, J. & HABER, D. A. (2004) Activating mutations in the epidermal growth factor receptor underlying responsiveness of non-small-cell lung cancer to gefitinib. *N Engl J Med,* 350**,** 2129-39.

LYONS, A. B. & PARISH, C. R. (1994) Determination of lymphocyte division by flow cytometry. *J Immunol Methods,* 171**,** 131-7.

MA, J., POLLAK, M. N., GIOVANNUCCI, E., CHAN, J. M., TAO, Y., HENNEKENS, C. H. & STAMPFER, M. J. (1999) Prospective study of colorectal cancer risk in men and plasma levels of insulin-like growth factor (IGF)-I and IGF-binding protein-3. *J Natl Cancer Inst,* 91**,** 620-5.

MA, L., TERUYA-FELDSTEIN, J. & WEINBERG, R. A. (2007) Tumour invasion and metastasis initiated by microRNA-10b in breast cancer. *Nature,* 449**,** 682-8.

MACAULAY, V. M., EVERARD, M. J., TEALE, J. D., TROTT, P. A., VAN WYK, J. J., SMITH, I. E. & MILLAR, J. L. (1990) Autocrine function for insulin-like growth factor I in human small cell lung cancer cell lines and fresh tumor cells. *Cancer Res,* 50**,** 2511-7.

MACAULAY, V. M., MIDDLETON, M. R., PROTHEROE, A. S., TOLCHER, A., DIERAS, V., SESSA, C., BAHLEDA, R., BLAY, J. Y., LORUSSO, P., MERY-MIGNARD, D. & SORIA, J. C. (2012) Phase I study of humanized monoclonal antibody AVE1642 directed against the type 1 insulin-like growth factor receptor (IGF-1R), administered in combination with anticancer therapies to patients with advanced solid tumors. *Ann Oncol*.

MACEWEN, E. G., KURZMAN, I. D., VAIL, D. M., DUBIELZIG, R. R., EVERLITH, K., MADEWELL, B. R., RODRIGUEZ, C. O., JR., PHILLIPS, B., ZWAHLEN, C. H., OBRADOVICH, J., ROSENTHAL, R. C., FOX, L. E., ROSENBERG, M., HENRY, C. & FIDEL, J. (1999) Adjuvant therapy for melanoma in dogs: results of randomized clinical trials using surgery, liposome-encapsulated muramyl tripeptide, and granulocyte macrophage colony-stimulating factor. *Clin Cancer Res,* 5**,** 4249-58.

MACEWEN, E. G., PATNAIK, A. K., HARVEY, H. J., HAYES, A. A. & MATUS, R. (1986) Canine oral melanoma: comparison of surgery versus surgery plus Corynebacterium parvum. *Cancer Invest,* 4**,** 397-402.

MALONEY, E. K., MCLAUGHLIN, J. L., DAGDIGIAN, N. E., GARRETT, L. M., CONNORS, K. M., ZHOU, X. M., BLATTLER, W. A., CHITTENDEN, T. & SINGH, R. (2003) An anti-insulin-like growth factor I receptor antibody that is a potent inhibitor of cancer cell proliferation. *Cancer Res,* 63**,** 5073-83.

MAMALAKI, C., ELLIOTT, J., NORTON, T., YANNOUTSOS, N., TOWNSEND, A. R., CHANDLER, P., SIMPSON, E. & KIOUSSIS, D. (1993) Positive and negative selection in transgenic mice expressing a T-cell receptor specific for influenza nucleoprotein and endogenous superantigen. *Dev Immunol,* 3**,** 159-74.

MANLEY, C. A., LEIBMAN, N. F., WOLCHOK, J. D., RIVIERE, I. C., BARTIDO, S., CRAFT, D. M. & BERGMAN, P. J. (2011) Xenogeneic murine tyrosinase DNA vaccine for malignant melanoma of the digit of dogs. *J Vet Intern Med,* 25**,** 94-9.

MANNING, B. D. & CANTLEY, L. C. (2007) AKT/PKB signaling: navigating downstream. *Cell,* 129**,** 1261-74.

MAOR, S. B., ABRAMOVITCH, S., ERDOS, M. R., BRODY, L. C. & WERNER, H. (2000) BRCA1 suppresses insulin-like growth factor-I receptor promoter activity: potential interaction between BRCA1 and Sp1. *Mol Genet Metab,* 69**,** 130-6.

MASHHEDI, H., BLOUIN, M. J., ZAKIKHANI, M., DAVID, S., ZHAO, Y., BAZILE, M., BIRMAN, E., ALGIRE, C., ALIAGA, A., BEDELL, B. J. & POLLAK, M. (2011) Metformin abolishes increased tumor (18)F-2-fluoro-2-deoxy-D-glucose uptake associated with a high energy diet. *Cell Cycle,* 10**,** 2770-8.

MATTEI, S., COLOMBO, M. P., MELANI, C., SILVANI, A., PARMIANI, G. & HERLYN, M. (1994) Expression of cytokine/growth factors and their receptors in human melanoma and melanocytes. *International Journal of Cancer,* 56**,** 853-857.

MATTISKE, S., SUETANI, R. J., NEILSEN, P. M. & CALLEN, D. F. (2012) The oncogenic role of miR-155 in breast cancer. *Cancer Epidemiol Biomarkers Prev,* 21**,** 1236-43.

MAYR, B., SCHAFFNER, G., REIFINGER, M., ZWETKOFF, S. & PRODINGER, B. (2003) N-ras mutations in canine malignant melanomas. *Vet J,* 165**,** 169-71.

MCARTHUR, G., HAUSCHILD, A., ROBERT, C., HAANEN, J. B., ASCIERTO, P., LEE, R. J., NOLOP, K., NELSON, B., FLAHERTY, K. T. & CHAPMAN, P. B. (2011) Vemurafenlb Improves Overall Survival Compared to Dacarbazlne In Advanced BRAFV600E-mutated Melanoma: Updated Survival Results From a Phase III Randomised, Open-label, Multlcentre Trial. *European journal of cancer (Oxford, England : 1990),* 47**,** 14.

MEDEMA, R. H., KOPS, G. J., BOS, J. L. & BURGERING, B. M. (2000) AFX-like Forkhead transcription factors mediate cell-cycle regulation by Ras and PKB through p27kip1. *Nature,* 404**,** 782-7.

MEISTER, G., LANDTHALER, M., DORSETT, Y. & TUSCHL, T. (2004) Sequence-specific inhibition of microRNA- and siRNA-induced RNA silencing. *RNA,* 10**,** 544-50.

MELTZER, P. S. (2005) Cancer genomics: Small RNAs with big impacts. *Nature,* 435**,** 745-746.

MENG, D., LV, D. D. & FANG, J. (2008) Insulin-like growth factor-I induces reactive oxygen species production and cell migration through Nox4 and Rac1 in vascular smooth muscle cells. *Cardiovasc Res,* 80**,** 299-308.

MENU, E., JERNBERG-WIKLUND, H., STROMBERG, T., DE RAEVE, H., GIRNITA, L., LARSSON, O., AXELSON, M., ASOSINGH, K., NILSSON, K., VAN CAMP,

B. & VANDERKERKEN, K. (2006) Inhibiting the IGF-1 receptor tyrosine kinase with the cyclolignan PPP: an in vitro and in vivo study in the 5T33MM mouse model. *Blood,* 107**,** 655-60.

MEUTEN, D. J. (2002) *Tumors in domestic animals,* Ames, Iowa, Iowa State University Press.

MIDDLETON, M., HAUSCHILD, A., THOMSON, D., ANDERSON, R., BURDETTE-RADOUX, S., GEHLSEN, K., HELLSTRAND, K. & NAREDI, P. (2007) Results of a multicenter randomized study to evaluate the safety and efficacy of combined immunotherapy with interleukin-2, interferon-{alpha}2b and histamine dihydrochloride versus dacarbazine in patients with stage IV melanoma. *Ann Oncol,* 18**,** 1691-7.

MIDDLETON, M. R., GROB, J. J., AARONSON, N., FIERLBECK, G., TILGEN, W., SEITER, S., GORE, M., AAMDAL, S., CEBON, J., COATES, A., DRENO, B., HENZ, M., SCHADENDORF, D., KAPP, A., WEISS, J., FRAASS, U., STATKEVICH, P., MULLER, M. & THATCHER, N. (2000) Randomized phase III study of temozolomide versus dacarbazine in the treatment of patients with advanced metastatic malignant melanoma. *J Clin Oncol,* 18**,** 158-66.

MITCHELL, M. S., ABRAMS, J., THOMPSON, J. A., KASHANI-SABET, M., DECONTI, R. C., HWU, W. J., ATKINS, M. B., WHITMAN, E., ERNSTOFF, M. S., HALUSKA, F. G., JAKOWATZ, J. G., DAS GUPTA, T. K., RICHARDS, J. M., SAMLOWSKI, W. E., COSTANZI, J. J., ARONSON, F. R., DEISSEROTH, A. B., DUDEK, A. Z. & JONES, V. E. (2007) Randomized trial of an allogeneic melanoma lysate vaccine with low-dose interferon Alfa-2b compared with high-dose interferon Alfa-2b for Resected stage III cutaneous melanoma. *J Clin Oncol,* 25**,** 2078-85.

MITSIADES, C. S., MITSIADES, N. S., MCMULLAN, C. J., POULAKI, V., SHRINGARPURE, R., AKIYAMA, M., HIDESHIMA, T., CHAUHAN, D., JOSEPH, M., LIBERMANN, T. A., GARCIA-ECHEVERRIA, C., PEARSON, M. A., HOFMANN, F., ANDERSON, K. C. & KUNG, A. L. (2004) Inhibition of the insulin-like growth factor receptor-1 tyrosine kinase activity as a therapeutic strategy for multiple myeloma, other hematologic malignancies, and solid tumors. *Cancer Cell,* 5**,** 221-30.

MIZUSHIMA, N. (2010) The role of the Atg1/ULK1 complex in autophagy regulation. *Curr Opin Cell Biol,* 22**,** 132-9.

MODUR, V., NAGARAJAN, R., EVERS, B. M. & MILBRANDT, J. (2002a) FOXO Proteins Regulate Tumor Necrosis Factor-related Apoptosis Inducing Ligand Expression. *Journal of Biological Chemistry,* 277**,** 47928-47937.

MODUR, V., NAGARAJAN, R., EVERS, B. M. & MILBRANDT, J. (2002b) FOXO proteins regulate tumor necrosis factor-related apoptosis inducing ligand expression. Implications for PTEN mutation in prostate cancer. *J Biol Chem,* 277**,** 47928-37.

MOLENAAR, M., VAN DE WETERING, M., OOSTERWEGEL, M., PETERSON-MADURO, J., GODSAVE, S., KORINEK, V., ROOSE, J., DESTREE, O. & CLEVERS, H. (1996) XTcf-3 transcription factor mediates beta-catenin-induced axis formation in Xenopus embryos. *Cell,* 86**,** 391-9.

MOLHOEK, K. R., SHADA, A. L., SMOLKIN, M., CHOWBINA, S., PAPIN, J., BRAUTIGAN, D. L. & SLINGLUFF, C. L., JR. (2011) Comprehensive analysis of receptor tyrosine kinase activation in human melanomas reveals autocrine signaling through IGF-1R. *Melanoma Res,* 21**,** 274-84.

MONGROO, P. S. & RUSTGI, A. K. (2010) The role of the miR-200 family in epithelial-mesenchymal transition. *Cancer Biol Ther,* 10**,** 219-22.

MONTANO, X., SHAMSHER, M., WHITEHEAD, P., DAWSON, K. & NEWTON, J. (1994) Analysis of p53 in human cutaneous melanoma cell lines. *Oncogene,* 9**,** 1455-9.

MORETTI, S., MASSOBRIO, R., BROGELLI, L., NOVELLI, M., GIANNOTTI, B. & BERNENGO, M. G. (1990) Ki67 antigen expression correlates with tumor progression and HLA-DR antigen expression in melanocytic lesions. *J Invest Dermatol,* 95**,** 320-4.

MORGAN, C. D., MEASEL, J. W., JR., AMOSS, M. S., JR., RAO, A. & GREENE, J. F., JR. (1996) Immunophenotypic characterization of tumor infiltrating lymphocytes and peripheral blood lymphocytes isolated from melanomatous and non-melanomatous Sinclair miniature swine. *Vet Immunol Immunopathol,* 55**,** 189-203.

MORI, M., YAMAGUCHI, K., HONDA, S., NAGASAKI, K., UEDA, M., ABE, O. & ABE, K. (1991) Cancer cachexia syndrome developed in nude mice bearing melanoma cells producing leukemia-inhibitory factor. *Cancer Res,* 51**,** 6656-9.

MUKOHARA, T., SHIMADA, H., OGASAWARA, N., WANIKAWA, R., SHIMOMURA, M., NAKATSURA, T., ISHII, G., PARK, J. O., JÄNNE, P. A., SAIJO, N. & MINAMI, H. (2009) Sensitivity of breast cancer cell lines to the novel insulin-like growth factor-1 receptor (IGF-1R) inhibitor NVP-AEW541 is dependent on the level of IRS-1 expression. *Cancer Letters,* 282**,** 14-24.

MULLIGAN, C., ROCHFORD, J., DENYER, G., STEPHENS, R., YEO, G., FREEMAN, T., SIDDLE, K. & O'RAHILLY, S. (2002) Microarray analysis of insulin and insulin-like growth factor-1 (IGF-1) receptor signaling reveals the selective up-regulation of the mitogen heparin-binding EGF-like growth factor by IGF-1. *J Biol Chem,* 277**,** 42480-7.

MURPHY, S., HAYES, A. M., BLACKWOOD, L., MAGLENNON, G., PATTINSON, H. & SPARKES, A. H. (2005) Oral malignant melanoma - the effect of coarse fractionation radiotherapy alone or with adjuvant carboplatin therapy. *Vet Comp Oncol,* 3**,** 222-9.

NAKAE, J., KIDO, Y. & ACCILI, D. (2001) Distinct and overlapping functions of insulin and IGF-I receptors. *Endocr Rev,* 22**,** 818-35.

NEUDAUER, C. L. & MCCARTHY, J. B. (2003) Insulin-like growth factor I-stimulated melanoma cell migration requires phosphoinositide 3-kinase but not extracellular-regulated kinase activation. *Exp Cell Res,* 286**,** 128-37.

NISSLEY, S. P., HASKELL, J. F., SASAKI, N., DE VROEDE, M. A. & RECHLER, M. M. (1985) Insulin-like growth factor receptors. *J Cell Sci Suppl,* 3**,** 39-51.

O'CONNELL, M. P. & WEERARATNA, A. T. (2009) Hear the Wnt Ror: how melanoma cells adjust to changes in Wnt. *Pigment Cell Melanoma Res,* 22**,** 724-39.

O'CONNOR, R. (2003) Regulation of IGF-I receptor signaling in tumor cells. *Horm Metab Res,* 35**,** 771-7.

O'DELL, S. D. & DAY, I. N. (1998) Insulin-like growth factor II (IGF-II). *Int J Biochem Cell Biol,* 30**,** 767-71.

OBEID, M., PANARETAKIS, T., TESNIERE, A., JOZA, N., TUFI, R., APETOH, L., GHIRINGHELLI, F., ZITVOGEL, L. & KROEMER, G. (2007a) Leveraging the Immune System during Chemotherapy: Moving Calreticulin to the Cell Surface Converts Apoptotic Death from "Silent" to Immunogenic. *Cancer Res,* 67**,** 7941-7944.

OBEID, M., TESNIERE, A., GHIRINGHELLI, F., FIMIA, G. M., APETOH, L., PERFETTINI, J. L., CASTEDO, M., MIGNOT, G., PANARETAKIS, T.,

CASARES, N., METIVIER, D., LAROCHETTE, N., VAN ENDERT, P., CICCOSANTI, F., PIACENTINI, M., ZITVOGEL, L. & KROEMER, G. (2007b) Calreticulin exposure dictates the immunogenicity of cancer cell death. *Nat Med,* 13**,** 54-61.

OLIVE, V., JIANG, I. & HE, L. (2010) mir-17-92, a cluster of miRNAs in the midst of the cancer network. *Int J Biochem Cell Biol,* 42**,** 1348-54.

OLMOS, D., POSTEL-VINAY, S., MOLIFE, L. R., OKUNO, S. H., SCHUETZE, S. M., PACCAGNELLA, M. L., BATZEL, G. N., YIN, D., PRITCHARD-JONES, K., JUDSON, I., WORDEN, F. P., GUALBERTO, A., SCURR, M., DE BONO, J. S. & HALUSKA, P. (2010) Safety, pharmacokinetics, and preliminary activity of the anti-IGF-1R antibody figitumumab (CP-751,871) in patients with sarcoma and Ewing's sarcoma: a phase 1 expansion cohort study. *Lancet Oncol,* 11**,** 129-35.

OMHOLT, K., KARSBERG, S., PLATZ, A., KANTER, L., RINGBORG, U. & HANSSON, J. (2002) Screening of N-ras Codon 61 Mutations in Paired Primary and Metastatic Cutaneous Melanomas: Mutations Occur Early and Persist throughout Tumor Progression. *Clinical Cancer Research,* 8**,** 3468-3474.

ORLOVA, I. A., ALEXANDER, G. M., QURESHI, R. A., SACAN, A., GRAZIANO, A., BARRETT, J. E., SCHWARTZMAN, R. J. & AJIT, S. K. (2011) MicroRNA modulation in complex regional pain syndrome. *J Transl Med,* 9**,** 195.

OSTRAND-ROSENBERG, S., CLEMENTS, V. K., THAKUR, A. & COLE, G. A. (1989) Transfection of major histocompatibility complex class I and class II genes causes tumour rejection. *J Immunogenet,* 16**,** 343-9.

PACHER, M., SEEWALD, M. J., MIKULA, M., OEHLER, S., MOGG, M., VINATZER, U., EGER, A., SCHWEIFER, N., VARECKA, R., SOMMERGRUBER, W., MIKULITS, W. & SCHREIBER, M. (2007) Impact of constitutive IGF1/IGF2 stimulation on the transcriptional program of human breast cancer cells. *Carcinogenesis,* 28**,** 49-59.

PALSGAARD, J., BROWN, A. E., JENSEN, M., BORUP, R., WALKER, M. & DE MEYTS, P. (2009) Insulin-like growth factor I (IGF-I) is a more potent regulator of gene expression than insulin in primary human myoblasts and myotubes. *Growth Horm IGF Res,* 19**,** 168-78.

PANDINI, G., VIGNERI, R., COSTANTINO, A., FRASCA, F., IPPOLITO, A., FUJITA-YAMAGUCHI, Y., SIDDLE, K., GOLDFINE, I. D. & BELFIORE, A. (1999) Insulin and insulin-like growth factor-I (IGF-I) receptor overexpression in breast cancers leads to insulin/IGF-I hybrid receptor overexpression: evidence for a second mechanism of IGF-I signaling. *Clin Cancer Res,* 5**,** 1935-1944.

PARDOLL, D. M. (2002) Spinning molecular immunology into successful immunotherapy. *Nat Rev Immunol,* 2**,** 227-38.

PARISH, C. R. (1999) Fluorescent dyes for lymphocyte migration and proliferation studies. *Immunol Cell Biol,* 77**,** 499-508.

PARK, S. L., SETIAWAN, V. W., KANETSKY, P. A., ZHANG, Z. F., WILKENS, L. R., KOLONEL, L. N. & LE MARCHAND, L. (2011) Serum insulin-like growth factor-I and insulin-like growth factor binding protein-3 levels with risk of malignant melanoma. *Cancer Causes Control,* 22**,** 1267-75.

PARKER, A., CHEVILLE, J. C., LOHSE, C., CERHAN, J. R. & BLUTE, M. L. (2003) Expression of insulin-like growth factor I receptor and survival in patients with clear cell renal cell carcinoma. *J Urol,* 170**,** 420-4.

PARKER, A. S., CHEVILLE, J. C., JANNEY, C. A. & CERHAN, J. R. (2002) High expression levels of insulin-like growth factor-I receptor predict poor survival among women with clear-cell renal cell carcinomas. *Hum Pathol,* 33**,** 801-5.

PATEL, A. V., CHENG, I., CANZIAN, F., LE MARCHAND, L., THUN, M. J., BERG, C. D., BURING, J., CALLE, E. E., CHANOCK, S., CLAVEL-CHAPELON, F., COX, D. G., DORRONSORO, M., DOSSUS, L., HAIMAN, C. A., HANKINSON, S. E., HENDERSON, B. E., HOOVER, R., HUNTER, D. J., KAAKS, R., KOLONEL, L. N., KRAFT, P., LINSEISEN, J., LUND, E., MANJER, J., MCCARTY, C., PEETERS, P. H., PIKE, M. C., POLLAK, M., RIBOLI, E., STRAM, D. O., TJONNELAND, A., TRAVIS, R. C., TRICHOPOULOS, D., TUMINO, R., YEAGER, M., ZIEGLER, R. G. & FEIGELSON, H. S. (2008) IGF-1, IGFBP-1, and IGFBP-3 polymorphisms predict circulating IGF levels but not breast cancer risk: findings from the Breast and Prostate Cancer Cohort Consortium (BPC3). *PLoS One,* 3**,** e2578.

PAULSON, K. E., RIEGER-CHRIST, K., MCDEVITT, M. A., KUPERWASSER, C., KIM, J., UNANUE, V. E., ZHANG, X., HU, M., RUTHAZER, R., BERASI, S. P., HUANG, C.-Y., GIRI, D., KAUFMAN, S., DUGAN, J. M., BLUM, J., NETTO, G., WAZER, D. E., SUMMERHAYES, I. C. & YEE, A. S. (2007) Alterations of the HBP1 Transcriptional Repressor Are Associated with Invasive Breast Cancer. *Cancer Research,* 67**,** 6136-6145.

PAWITAN, Y., BJOHLE, J., AMLER, L., BORG, A. L., EGYHAZI, S., HALL, P., HAN, X., HOLMBERG, L., HUANG, F., KLAAR, S., LIU, E. T., MILLER, L., NORDGREN, H., PLONER, A., SANDELIN, K., SHAW, P. M., SMEDS, J., SKOOG, L., WEDREN, S. & BERGH, J. (2005) Gene expression profiling spares early breast cancer patients from adjuvant therapy: derived and validated in two population-based cohorts. *Breast Cancer Res,* 7**,** R953-64.

PEARL, R. A., PACIFICO, M. D., RICHMAN, P. I., STOTT, D. J., WILSON, G. D. & GROBBELAAR, A. O. (2007) Ki-67 expression in melanoma. A potential method of risk assessment for the patient with a positive sentinel node. *J Exp Clin Cancer Res,* 26**,** 109-15.

PEGGS, K. S., QUEZADA, S. A., KORMAN, A. J. & ALLISON, J. P. (2006) Principles and use of anti-CTLA4 antibody in human cancer immunotherapy. *Curr Opin Immunol,* 18**,** 206-13.

PENDE, M., UM, S. H., MIEULET, V., STICKER, M., GOSS, V. L., MESTAN, J., MUELLER, M., FUMAGALLI, S., KOZMA, S. C. & THOMAS, G. (2004) S6K1(-/-)/S6K2(-/-) mice exhibit perinatal lethality and rapamycin-sensitive 5'-terminal oligopyrimidine mRNA translation and reveal a mitogen-activated protein kinase-dependent S6 kinase pathway. *Mol Cell Biol,* 24**,** 3112-24.

PERER, E. S., MADAN, A. K., SHURIN, A., ZAKRIS, E., ROMEGUERA, K., PANG, Y. & BEECH, D. J. (2000) Insulin-like growth factor I receptor antagonism augments response to chemoradiation therapy in colon cancer cells. *J Surg Res,* 94**,** 1-5.

PEYRAT, J. P., BONNETERRE, J., BEUSCART, R., DJIANE, J. & DEMAILLE, A. (1988) Insulin-like growth factor 1 receptors in human breast cancer and their relation to estradiol and progesterone receptors. *Cancer Res,* 48**,** 6429-33.

PITTS, T. M., TAN, A. C., KULIKOWSKI, G. N., TENTLER, J. J., BROWN, A. M., FLANIGAN, S. A., LEONG, S., COLDREN, C. D., HIRSCH, F. R., VARELLA-GARCIA, M., KORCH, C. & ECKHARDT, S. G. (2010) Development of an integrated genomic classifier for a novel agent in colorectal cancer: approach to individualized therapy in early development. *Clin Cancer Res,* 16**,** 3193-204.

PLAYFORD, M. P., BICKNELL, D., BODMER, W. F. & MACAULAY, V. M. (2000) Insulin-like growth factor 1 regulates the location, stability, and transcriptional activity of beta-catenin. *Proc Natl Acad Sci U S A,* 97**,** 12103-8.

PLUTA, K., DIEHL, W., ZHANG, X. Y., KUTNER, R., BIALKOWSKA, A. & REISER, J. (2007) Lentiviral vectors encoding tetracycline-dependent repressors and transactivators for reversible knockdown of gene expression: a comparative study. *BMC Biotechnol,* 7**,** 41.

POLAKIS, P. (2000) Wnt signaling and cancer. *Genes & Development,* 14**,** 1837-1851.

POLAKIS, P. (2012) Wnt signaling in cancer. *Cold Spring Harb Perspect Biol,* 4.

POLAKIS, P. & MCCORMICK, F. (1993) Structural requirements for the interaction of p21ras with GAP, exchange factors, and its biological effector target. *J Biol Chem,* 268**,** 9157-60.

POLLAK, M. (2000) Insulin-like growth factor physiology and cancer risk. *Eur J Cancer,* 36**,** 1224-8.

POLLAK, M. N., SCHERNHAMMER, E. S. & HANKINSON, S. E. (2004) Insulin-like growth factors and neoplasia. *Nat Rev Cancer,* 4**,** 505-518.

POLLOCK, P. M., HARPER, U. L., HANSEN, K. S., YUDT, L. M., STARK, M., ROBBINS, C. M., MOSES, T. Y., HOSTETTER, G., WAGNER, U., KAKAREKA, J., SALEM, G., POHIDA, T., HEENAN, P., DURAY, P., KALLIONIEMI, O., HAYWARD, N. K., TRENT, J. M. & MELTZER, P. S. (2003) High frequency of BRAF mutations in nevi. *Nat Genet,* 33**,** 19-20.

POLLOCK, P. M. & HAYWARD, N. (2002) Mutations in exon 3 of the beta-catenin gene are rare in melanoma cell lines. *Melanoma Res,* 12**,** 183-6.

PORGADOR, A., FELDMAN, M. & EISENBACH, L. (1989) H-2Kb transfection of B16 melanoma cells results in reduced tumourigenicity and metastatic competence. *J Immunogenet,* 16**,** 291-303.

PRAVTCHEVA, D. D. & WISE, T. L. (1998) Metastasizing mammary carcinomas in H19 enhancers-Igf2 transgenic mice. *J Exp Zool,* 281**,** 43-57.

PREHN, R. T. & MAIN, J. M. (1957) Immunity to methylcholanthrene-induced sarcomas. *J Natl Cancer Inst,* 18**,** 769-78.

PUGLIELLI, L. (2008) Aging of the brain, neurotrophin signaling, and Alzheimer's disease: is IGF1-R the common culprit? *Neurobiol Aging,* 29**,** 795-811.

QUINTIN-COLONNA, F., DEVAUCHELLE, P., FRADELIZI, D., MOUROT, B., FAURE, T., KOURILSKY, P., ROTH, C. & MEHTALI, M. (1996) Gene therapy of spontaneous canine melanoma and feline fibrosarcoma by intratumoral administration of histoincompatible cells expressing human interleukin-2. *Gene Ther,* 3**,** 1104-12.

QUONG, R. Y., BICKFORD, S. T., ING, Y. L., TERMAN, B., HERLYN, M. & LASSAM, N. J. (1994) Protein kinases in normal and transformed melanocytes. *Melanoma Res,* 4**,** 313-9.

RAJAH, R., BHALA, A., NUNN, S. E., PEEHL, D. M. & COHEN, P. (1996) 7S nerve growth factor is an insulin-like growth factor-binding protein protease. *Endocrinology,* 137**,** 2676-82.

RAJSKI, M., ZANETTI-DALLENBACH, R., VOGEL, B., HERRMANN, R., ROCHLITZ, C. & BUESS, M. (2010) IGF-I induced genes in stromal fibroblasts predict the clinical outcome of breast and lung cancer patients. *BMC Medicine,* 8**,** 1-18.

RAKATZI, I., STOSIK, M., GROMKE, T., SIDDLE, K. & ECKEL, J. (2006) Differential phosphorylation of IRS-1 and IRS-2 by insulin and IGF-I receptors. *Arch Physiol Biochem,* 112**,** 37-47.

RAMBOW, F., MALEK, O., GEFFROTIN, C., LEPLAT, J. J., BOUET, S., PITON, G., HUGOT, K., BEVILACQUA, C., HORAK, V. & VINCENT-NAULLEAU, S. (2008a) Identification of differentially expressed genes in spontaneously regressing

melanoma using the MeLiM swine model. *Pigment Cell Melanoma Res,* 21**,** 147-61.

RAMBOW, F., PITON, G., BOUET, S., LEPLAT, J. J., BAULANDE, S., MARRAU, A., STAM, M., HORAK, V. & VINCENT-NAULLEAU, S. (2008b) Gene expression signature for spontaneous cancer regression in melanoma pigs. *Neoplasia,* 10**,** 714-26, 1 p following 726.

RAMOS-VARA, J. A., BEISSENHERZ, M. E., MILLER, M. A., JOHNSON, G. C., PACE, L. W., FARD, A. & KOTTLER, S. J. (2000) Retrospective study of 338 canine oral melanomas with clinical, histologic, and immunohistochemical review of 129 cases. *Vet Pathol,* 37**,** 597-608.

RAND, T. A., PETERSEN, S., DU, F. & WANG, X. (2005) Argonaute2 cleaves the anti-guide strand of siRNA during RISC activation. *Cell,* 123**,** 621-9.

RANGASAMY, D., TREMETHICK, D. J. & GREAVES, I. K. (2008) Gene knockdown by ecdysone-based inducible RNAi in stable mammalian cell lines. *Nat Protoc,* 3**,** 79-88.

RASSNICK, K. M., RUSLANDER, D. M., COTTER, S. M., AL-SARRAF, R., BRUYETTE, D. S., GAMBLIN, R. M., MELEO, K. A. & MOORE, A. S. (2001) Use of carboplatin for treatment of dogs with malignant melanoma: 27 cases (1989-2000). *J Am Vet Med Assoc,* 218**,** 1444-8.

REIDY, D. L., VAKIANI, E., FAKIH, M. G., SAIF, M. W., HECHT, J. R., GOODMAN-DAVIS, N., HOLLYWOOD, E., SHIA, J., SCHWARTZ, J., CHANDRAWANSA, K., DONTABHAKTUNI, A., YOUSSOUFIAN, H., SOLIT, D. B. & SALTZ, L. B. (2010) Randomized, phase II study of the insulin-like growth factor-1 receptor inhibitor IMC-A12, with or without cetuximab, in patients with cetuximab- or panitumumab-refractory metastatic colorectal cancer. *J Clin Oncol,* 28**,** 4240-6.

RENEHAN, A. G., ZWAHLEN, M., MINDER, C., O'DWYER, S. T., SHALET, S. M. & EGGER, M. (2004) Insulin-like growth factor (IGF)-I, IGF binding protein-3, and cancer risk: systematic review and meta-regression analysis. *Lancet,* 363**,** 1346-53.

RESNICOFF, M. (1998) Antitumor effects elicited by antisense-mediated downregulation of the insulin-like growth factor I receptor (review). *Int J Mol Med,* 1**,** 883-8.

RESNICOFF, M., ABRAHAM, D., YUTANAWIBOONCHAI, W., ROTMAN, H. L., KAJSTURA, J., RUBIN, R., ZOLTICK, P. & BASERGA, R. (1995a) The Insulin-like Growth Factor I Receptor Protects Tumor Cells from Apoptosis in Vivo. *Cancer Res,* 55**,** 2463-2469.

RESNICOFF, M., BURGAUD, J.-L., ROTMAN, H. L., ABRAHAM, D. & BASERGA, R. (1995b) Correlation between Apoptosis, Tumorigenesis, and Levels of Insulin-like Growth Factor I Receptors. *Cancer Res,* 55**,** 3739-3741.

RESNICOFF, M., COPPOLA, D., SELL, C., RUBIN, R., FERRONE, S. & BASERGA, R. (1994a) Growth inhibition of human melanoma cells in nude mice by antisense strategies to the type 1 insulin-like growth factor receptor. *Cancer Res,* 54**,** 4848-50.

RESNICOFF, M., LI, W., BASAK, S., HERLYN, D., BASERGA, R. & RUBIN, R. (1996a) Inhibition of rat C6 glioblastoma tumor growth by expression of insulin-like growth factor I receptor antisense mRNA. *Cancer Immunol Immunother,* 42**,** 64-8.

RESNICOFF, M., SELL, C., RUBINI, M., COPPOLA, D., AMBROSE, D., BASERGA, R. & RUBIN, R. (1994b) Rat glioblastoma cells expressing an antisense RNA to the insulin-like growth factor-1 (IGF-1) receptor are nontumorigenic and induce regression of wild-type tumors. *Cancer Res,* 54**,** 2218-22.

RESNICOFF, M., TJUVAJEV, J., ROTMAN, H. L., ABRAHAM, D., CURTIS, M., AIKEN, R. & BASERGA, R. (1996b) Regression of C6 rat brain tumors by cells expressing an antisense insulin-like growth factor I receptor RNA. *J Exp Ther Oncol,* 1**,** 385-9.

REVEL, A., ACHACHE, H., STEVENS, J., SMITH, Y. & REICH, R. (2011) MicroRNAs are associated with human embryo implantation defects. *Hum Reprod,* 26**,** 2830-40.

RICHTER, A., MURUA ESCOBAR, H., GUNTHER, K., SOLLER, J. T., WINKLER, S., NOLTE, I. & BULLERDIEK, J. (2005) RAS gene hot-spot mutations in canine neoplasias. *J Hered,* 96**,** 764-5.

RIEDEMANN, J. & MACAULAY, V. M. (2006) IGF1R signalling and its inhibition. *Endocrine-Related Cancer,* 13**,** S33-S43.

RIEDEMANN, J., SOHAIL, M. & MACAULAY, V. M. (2007a) Dual silencing of the EGF and type 1 IGF receptors suggests dominance of IGF signaling in human breast cancer cells. *Biochem Biophys Res Commun,* 355**,** 700-6.

RIEDEMANN, J., TAKIGUCHI, M., SOHAIL, M. & MACAULAY, V. M. (2007b) The EGF receptor interacts with the type 1 IGF receptor and regulates its stability. *Biochem Biophys Res Commun,* 355**,** 707-14.

RIMM, D. L., CACA, K., HU, G., HARRISON, F. B. & FEARON, E. R. (1999) Frequent nuclear/cytoplasmic localization of beta-catenin without exon 3 mutations in malignant melanoma. *Am J Pathol,* 154**,** 325-9.

ROBERT, C., THOMAS, L., BONDARENKO, I., O'DAY, S., M, D. J., GARBE, C., LEBBE, C., BAURAIN, J. F., TESTORI, A., GROB, J. J., DAVIDSON, N., RICHARDS, J., MAIO, M., HAUSCHILD, A., MILLER, W. H., JR., GASCON, P., LOTEM, M., HARMANKAYA, K., IBRAHIM, R., FRANCIS, S., CHEN, T. T., HUMPHREY, R., HOOS, A. & WOLCHOK, J. D. (2011) Ipilimumab plus dacarbazine for previously untreated metastatic melanoma. *N Engl J Med,* 364**,** 2517-26.

ROCHESTER, M. A., PATEL, N., TURNEY, B. W., DAVIES, D. R., ROBERTS, I. S., CREW, J., PROTHEROE, A. & MACAULAY, V. M. (2007) The type 1 insulin-like growth factor receptor is over-expressed in bladder cancer. *BJU Int,* 100**,** 1396-401.

ROCHESTER, M. A., RIEDEMANN, J., HELLAWELL, G. O., BREWSTER, S. F. & MACAULAY, V. M. (2005) Silencing of the IGF1R gene enhances sensitivity to DNA-damaging agents in both PTEN wild-type and mutant human prostate cancer. *Cancer Gene Ther,* 12**,** 90-100.

RODDAM, A. W., ALLEN, N. E., APPLEBY, P., KEY, T. J., FERRUCCI, L., CARTER, H. B., METTER, E. J., CHEN, C., WEISS, N. S., FITZPATRICK, A., HSING, A. W., LACEY, J. V., JR., HELZLSOUER, K., RINALDI, S., RIBOLI, E., KAAKS, R., JANSSEN, J. A., WILDHAGEN, M. F., SCHRODER, F. H., PLATZ, E. A., POLLAK, M., GIOVANNUCCI, E., SCHAEFER, C., QUESENBERRY, C. P., JR., VOGELMAN, J. H., SEVERI, G., ENGLISH, D. R., GILES, G. G., STATTIN, P., HALLMANS, G., JOHANSSON, M., CHAN, J. M., GANN, P., OLIVER, S. E., HOLLY, J. M., DONOVAN, J., MEYER, F., BAIRATI, I. & GALAN, P. (2008) Insulin-like growth factors, their binding proteins, and prostate cancer risk: analysis of individual patient data from 12 prospective studies. *Ann Intern Med,* 149**,** 461-71, W83-8.

RODECK, U. & HERLYN, M. (1988) Characteristics of cultured human melanocytes from different stages of tumor progression. *Cancer Treat Res,* 43**,** 3-16.

RODECK, U., HERLYN, M. & KOPROWSKI, H. (1987a) Interactions between growth factor receptors and corresponding monoclonal antibodies in human tumors. *J Cell Biochem,* 35**,** 315-320.

RODECK, U., HERLYN, M., MENSSEN, H. D., FURLANETTO, R. W. & KOPROWSKI, H. (1987b) Metastatic but not primary melanoma cell lines grow in vitro independently of exogenous growth factors. *International Journal of Cancer,* 40**,** 687-690.

ROMANELLI, R. J., LEBEAU, A. P., FULMER, C. G., LAZZARINO, D. A., HOCHBERG, A. & WOOD, T. L. (2007) Insulin-like Growth Factor Type-I Receptor Internalization and Recycling Mediate the Sustained Phosphorylation of Akt. *Journal of Biological Chemistry,* 282**,** 22513-22524.

ROTHER, K. I. & ACCILI, D. (2000) Role of insulin receptors and IGF receptors in growth and development. *Pediatr Nephrol,* 14**,** 558-61.

ROWINSKY, E. K., YOUSSOUFIAN, H., TONRA, J. R., SOLOMON, P., BURTRUM, D. & LUDWIG, D. L. (2007) IMC-A12, a human IgG1 monoclonal antibody to the insulin-like growth factor I receptor. *Clin Cancer Res,* 13**,** 5549s-5555s.

ROWLANDS, M. A., GUNNELL, D., HARRIS, R., VATTEN, L. J., HOLLY, J. M. & MARTIN, R. M. (2009) Circulating insulin-like growth factor peptides and prostate cancer risk: a systematic review and meta-analysis. *Int J Cancer,* 124**,** 2416-29.

RUSSO, V. C., GLUCKMAN, P. D., FELDMAN, E. L. & WERTHER, G. A. (2005) The insulin-like growth factor system and its pleiotropic functions in brain. *Endocr Rev,* 26**,** 916-43.

SACHDEV, D., LI, S. L., HARTELL, J. S., FUJITA-YAMAGUCHI, Y., MILLER, J. S. & YEE, D. (2003) A chimeric humanized single-chain antibody against the type I insulin-like growth factor (IGF) receptor renders breast cancer cells refractory to the mitogenic effects of IGF-I. *Cancer Res,* 63**,** 627-35.

SACHDEV, D., SINGH, R., FUJITA-YAMAGUCHI, Y. & YEE, D. (2006) Down-regulation of Insulin Receptor by Antibodies against the Type I Insulin-Like Growth Factor Receptor: Implications for Anti-Insulin-Like Growth Factor Therapy in Breast Cancer. *Cancer Res,* 66**,** 2391-2402.

SAITOH, T. & KATOH, M. (2001) FRAT1 and FRAT2, clustered in human chromosome 10q24.1 region, are up-regulated in gastric cancer. *Int J Oncol,* 19**,** 311-5.

SAJI, M., MORIARTY, J., BAN, T., SINGER, D. S. & KOHN, L. D. (1992) Major histocompatibility complex class I gene expression in rat thyroid cells is regulated by hormones, methimazole, and iodide as well as interferon. *J Clin Endocrinol Metab,* 75**,** 871-8.

SAKAI, H., YAMANE, T., YANAI, T., SHIRAI, N. & MASEGI, T. (2001) Expression of cyclin kinase inhibitor p27(Kip1) in skin tumours of dogs. *J Comp Pathol,* 125**,** 153-8.

SALTIEL, A. R. (1996) Diverse signaling pathways in the cellular actions of insulin. *Am J Physiol,* 270**,** E375-85.

SALTIEL, A. R. & KAHN, C. R. (2001) Insulin signalling and the regulation of glucose and lipid metabolism. *Nature,* 414**,** 799-806.

SAMANI, A. A., FALLAVOLLITA, L., JAALOUK, D. E., GALIPEAU, J. & BRODT, P. (2001) Inhibition of carcinoma cell growth and metastasis by a vesicular stomatitis virus G-pseudotyped retrovector expressing type I insulin-like growth factor receptor antisense. *Hum Gene Ther,* 12**,** 1969-77.

SAMPSON, E. M., HAQUE, Z. K., KU, M.-C., TEVOSIAN, S. G., ALBANESE, C., PESTELL, R. G., PAULSON, K. E. & YEE, A. S. (2001) Negative regulation of

the Wnt-[beta]-catenin pathway by the transcriptional repressor HBP1. *Embo J,* 20**,** 4500-4511.

SANTONOCITO, C., PARADISI, A., CAPIZZI, R., CONCOLINO, P., LAVIERI, M. M., LANZA SILVERI, S., DE LUCA, D., CATRICALA, C., DI CARLO, A., ZUPPI, C., AMEGLIO, F. & CAPOLUONGO, E. (2008) Insulin-like growth factor I (CA) repeats are associated with higher melanoma's Breslow index but not associated with the presence of the melanoma. A pilot study. *Clin Chim Acta,* 390**,** 104-9.

SARFSTEIN, R., PASMANIK-CHOR, M., YEHESKEL, A., EDRY, L., SHOMRON, N., WARMAN, N., WERTHEIMER, E., MAOR, S., SHOCHAT, L. & WERNER, H. (2012) Insulin-like growth factor-I receptor (IGF-IR) translocates to nucleus and autoregulates IGF-IR gene expression in breast cancer cells. *J Biol Chem,* 287**,** 2766-76.

SATO, S., NAKAMURA, M., CHO, D. H., TAPSCOTT, S. J., OZAKI, H. & KAWAKAMI, K. (2002) Identification of transcriptional targets for Six5: implication for the pathogenesis of myotonic dystrophy type 1. *Hum Mol Genet,* 11**,** 1045-58.

SATYAMOORTHY, K. & HERLYN, M. (2003) p16INK4A and familial melanoma. *Methods Mol Biol,* 222**,** 185-95.

SATYAMOORTHY, K., LI, G., GERRERO, M. R., BROSE, M. S., VOLPE, P., WEBER, B. L., VAN BELLE, P., ELDER, D. E. & HERLYN, M. (2003) Constitutive mitogen-activated protein kinase activation in melanoma is mediated by both BRAF mutations and autocrine growth factor stimulation. *Cancer Res,* 63**,** 756-9.

SATYAMOORTHY, K., LI, G., VAIDYA, B., KALABIS, J. & HERLYN, M. (2002) Insulin-like growth factor-I-induced migration of melanoma cells is mediated by interleukin-8 induction. *Cell Growth Differ,* 13**,** 87-93.

SATYAMOORTHY, K., LI, G., VAIDYA, B., PATEL, D. & HERLYN, M. (2001) Insulin-like growth factor-1 induces survival and growth of biologically early melanoma cells through both the mitogen-activated protein kinase and beta-catenin pathways. *Cancer Res,* 61**,** 7318-24.

SAUER, H., WARTENBERG, M. & HESCHELER, J. (2001) Reactive oxygen species as intracellular messengers during cell growth and differentiation. *Cell Physiol Biochem,* 11**,** 173-86.

SAXENA, S., JONSSON, Z. O. & DUTTA, A. (2003) Small RNAs with imperfect match to endogenous mRNA repress translation. Implications for off-target activity of small inhibitory RNA in mammalian cells. *J Biol Chem,* 278**,** 44312-9.

SCHEPELER, T., HOLM, A., HALVEY, P., NORDENTOFT, I., LAMY, P., RIISING, E. M., CHRISTENSEN, L. L., THORSEN, K., LIEBLER, D. C., HELIN, K., ORNTOFT, T. F. & ANDERSEN, C. L. (2012) Attenuation of the beta-catenin/TCF4 complex in colorectal cancer cells induces several growth-suppressive microRNAs that target cancer promoting genes. *Oncogene,* 31**,** 2750-60.

SCHERNHAMMER, E. S., HOLLY, J. M., HUNTER, D. J., POLLAK, M. N. & HANKINSON, S. E. (2006) Insulin-like growth factor-I, its binding proteins (IGFBP-1 and IGFBP-3), and growth hormone and breast cancer risk in The Nurses Health Study II. *Endocr Relat Cancer,* 13**,** 583-92.

SCHILLACI, R., SALATINO, M., CASSATARO, J., PROIETTI, C. J., GIAMBARTOLOMEI, G. H., RIVAS, M. A., CARNEVALE, R. P., CHARREAU, E. H. & ELIZALDE, P. V. (2006) Immunization with Murine Breast Cancer Cells Treated with Antisense Oligodeoxynucleotides to Type I Insulin-Like Growth Factor Receptor Induced an Antitumoral Effect Mediated by a

CD8+ Response Involving Fas/Fas Ligand Cytotoxic Pathway. *J Immunol,* 176**,** 3426-3437.

SCHRODER, K., HERTZOG, P. J., RAVASI, T. & HUME, D. A. (2004) Interferon-gamma: an overview of signals, mechanisms and functions. *J Leukoc Biol,* 75**,** 163-89.

SCHWARTZENTRUBER, D. J., LAWSON, D. H., RICHARDS, J. M., CONRY, R. M., MILLER, D. M., TREISMAN, J., GAILANI, F., RILEY, L., CONLON, K., POCKAJ, B., KENDRA, K. L., WHITE, R. L., GONZALEZ, R., KUZEL, T. M., CURTI, B., LEMING, P. D., WHITMAN, E. D., BALKISSOON, J., REINTGEN, D. S., KAUFMAN, H., MARINCOLA, F. M., MERINO, M. J., ROSENBERG, S. A., CHOYKE, P., VENA, D. & HWU, P. (2011) gp100 peptide vaccine and interleukin-2 in patients with advanced melanoma. *N Engl J Med,* 364**,** 2119-27.

SCIACCA, L., MINEO, R., PANDINI, G., MURABITO, A., VIGNERI, R. & BELFIORE, A. (2002) In IGF-I receptor-deficient leiomyosarcoma cells autocrine IGF-II induces cell invasion and protection from apoptosis via the insulin receptor isoform A. *Oncogene,* 21**,** 8240-50.

SCOTLANDI, K., BENINI, S., NANNI, P., LOLLINI, P. L., NICOLETTI, G., LANDUZZI, L., SERRA, M., MANARA, M. C., PICCI, P. & BALDINI, N. (1998) Blockage of insulin-like growth factor-I receptor inhibits the growth of Ewing's sarcoma in athymic mice. *Cancer Res,* 58**,** 4127-31.

SCOTLANDI, K., MAINI, C., MANARA, M. C., BENINI, S., SERRA, M., CERISANO, V., STRAMMIELLO, R., BALDINI, N., LOLLINI, P. L., NANNI, P., NICOLETTI, G. & PICCI, P. (2002) Effectiveness of insulin-like growth factor I receptor antisense strategy against Ewing's sarcoma cells. *Cancer Gene Ther,* 9**,** 296-307.

SCOTLANDI, K., MANARA, M. C., NICOLETTI, G., LOLLINI, P. L., LUKAS, S., BENINI, S., CROCI, S., PERDICHIZZI, S., ZAMBELLI, D., SERRA, M., GARCIA-ECHEVERRIA, C., HOFMANN, F. & PICCI, P. (2005) Antitumor activity of the insulin-like growth factor-I receptor kinase inhibitor NVP-AEW541 in musculoskeletal tumors. *Cancer Res,* 65**,** 3868-76.

SEGURA, M. F., BELITSKAYA-LEVY, I., ROSE, A. E., ZAKRZEWSKI, J., GAZIEL, A., HANNIFORD, D., DARVISHIAN, F., BERMAN, R. S., SHAPIRO, R. L., PAVLICK, A. C., OSMAN, I. & HERNANDO, E. (2010) Melanoma MicroRNA Signature Predicts Post-Recurrence Survival. *Clinical Cancer Research,* 16**,** 1577-1586.

SEHAT, B., TOFIGH, A., LIN, Y., TROCME, E., LILJEDAHL, U., LAGERGREN, J. & LARSSON, O. (2010) SUMOylation mediates the nuclear translocation and signaling of the IGF-1 receptor. *Sci Signal,* 3**,** ra10.

SELIGER, B. (2005) Strategies of tumor immune evasion. *BioDrugs,* 19**,** 347-54.

SELIGER, B., WOLLSCHEID, U., MOMBURG, F., BLANKENSTEIN, T. & HUBER, C. (2001) Characterization of the Major Histocompatibility Complex Class I Deficiencies in B16 Melanoma Cells. *Cancer Res,* 61**,** 1095-1099.

SELL, C., DUMENIL, G., DEVEAUD, C., MIURA, M., COPPOLA, D., DEANGELIS, T., RUBIN, R., EFSTRATIADIS, A. & BASERGA, R. (1994) Effect of a null mutation of the insulin-like growth factor I receptor gene on growth and transformation of mouse embryo fibroblasts. *Mol Cell Biol,* 14**,** 3604-12.

SELL, C., RUBINI, M., RUBIN, R., LIU, J. P., EFSTRATIADIS, A. & BASERGA, R. (1993) Simian virus 40 large tumor antigen is unable to transform mouse embryonic fibroblasts lacking type 1 insulin-like growth factor receptor. *Proc Natl Acad Sci U S A,* 90**,** 11217-11221.

SHANG, Y., MAO, Y., BATSON, J., SCALES, S. J., PHILLIPS, G., LACKNER, M. R., TOTPAL, K., WILLIAMS, S., YANG, J., TANG, Z., MODRUSAN, Z., TAN, C., LIANG, W. C., TSAI, S. P., VANDERBILT, A., KOZUKA, K., HOEFLICH, K., TIEN, J., ROSS, S., LI, C., LEE, S. H., SONG, A., WU, Y., STEPHAN, J. P., ASHKENAZI, A. & ZHA, J. (2008) Antixenograft tumor activity of a humanized anti-insulin-like growth factor-I receptor monoclonal antibody is associated with decreased AKT activation and glucose uptake. *Mol Cancer Ther,* 7**,** 2599-608.

SHAW, P. H., MAUGHAN, T. S. & CLARKE, A. R. (2011) Dual inhibition of epidermal growth factor and insulin-like 1 growth factor receptors reduce intestinal adenoma burden in the Apc(min/+) mouse. *Br J Cancer,* 105**,** 649-57.

SHELLY, S., CHIEN, M. B., YIP, B., KENT, M. S., THEON, A. P., MCCALLAN, J. L. & LONDON, C. A. (2005) Exon 15 BRAF mutations are uncommon in canine oral malignant melanomas. *Mamm Genome,* 16**,** 211-7.

SHEVELEV, A., BURFEIND, P., SCHULZE, E., RININSLAND, F., JOHNSON, T. R., TROJAN, J., CHERNICKY, C. L., HELENE, C. & ILAN, J. (1997) Potential triple helix-mediated inhibition of IGF-I gene expression significantly reduces tumorigenicity of glioblastoma in an animal model. *Cancer Gene Ther,* 4**,** 105-12.

SHI, H., MORICEAU, G., KONG, X., LEE, M. K., LEE, H., KOYA, R. C., NG, C., CHODON, T., SCOLYER, R. A., DAHLMAN, K. B., SOSMAN, J. A., KEFFORD, R. F., LONG, G. V., NELSON, S. F., RIBAS, A. & LO, R. S. (2012) Melanoma whole-exome sequencing identifies (V600E)B-RAF amplification-mediated acquired B-RAF inhibitor resistance. *Nat Commun,* 3**,** 724.

SHIH, H. H., TEVOSIAN, S. G. & YEE, A. S. (1998) Regulation of differentiation by HBP1, a target of the retinoblastoma protein. *Mol Cell Biol,* 18**,** 4732-43.

SHIH, H. H., XIU, M., BERASI, S. P., SAMPSON, E. M., LEITER, A., PAULSON, K. E. & YEE, A. S. (2001) HMG box transcriptional repressor HBP1 maintains a proliferation barrier in differentiated liver tissue. *Mol Cell Biol,* 21**,** 5723-32.

SHIH, I. M. & HERLYN, M. (1993) Role of growth factors and their receptors in the development and progression of melanoma. *J Invest Dermatol,* 100**,** 196S-203S.

SHIN, K. J., WALL, E. A., ZAVZAVADJIAN, J. R., SANTAT, L. A., LIU, J., HWANG, J. I., REBRES, R., ROACH, T., SEAMAN, W., SIMON, M. I. & FRASER, I. D. (2006) A single lentiviral vector platform for microRNA-based conditional RNA interference and coordinated transgene expression. *Proc Natl Acad Sci U S A,* 103**,** 13759-64.

SHINOZAKI, M., FUJIMOTO, A., MORTON, D. L. & HOON, D. S. (2004) Incidence of BRAF oncogene mutation and clinical relevance for primary cutaneous melanomas. *Clin Cancer Res,* 10**,** 1753-7.

SHTUTMAN, M., ZHURINSKY, J., SIMCHA, I., ALBANESE, C., D'AMICO, M., PESTELL, R. & BEN-ZE'EV, A. (1999) The cyclin D1 gene is a target of the beta-catenin/LEF-1 pathway. *Proc Natl Acad Sci U S A,* 96**,** 5522-7.

SLAABY, R., SCHAFFER, L., LAUTRUP-LARSEN, I., ANDERSEN, A. S., SHAW, A. C., MATHIASEN, I. S. & BRANDT, J. (2006) Hybrid Receptors Formed by Insulin Receptor (IR) and Insulin-like Growth Factor I Receptor (IGF-IR) Have Low Insulin and High IGF-1 Affinity Irrespective of the IR Splice Variant. *J. Biol. Chem.,* 281**,** 25869-25874.

SMYTH, G. K. (2004) Linear models and empirical bayes methods for assessing differential expression in microarray experiments. *Stat Appl Genet Mol Biol,* 3**,** Article3.

SMYTH, G. K. & SPEED, T. (2003) Normalization of cDNA microarray data. *Methods,* 31**,** 265-73.

SMYTH, G. K., YANG, Y. H. & SPEED, T. (2003) Statistical issues in cDNA microarray data analysis. *Methods Mol Biol,* 224**,** 111 - 136.

SOIFFER, R., HODI, F. S., HALUSKA, F., JUNG, K., GILLESSEN, S., SINGER, S., TANABE, K., DUDA, R., MENTZER, S., JAKLITSCH, M., BUENO, R., CLIFT, S., HARDY, S., NEUBERG, D., MULLIGAN, R., WEBB, I., MIHM, M. & DRANOFF, G. (2003) Vaccination with irradiated, autologous melanoma cells engineered to secrete granulocyte-macrophage colony-stimulating factor by adenoviral-mediated gene transfer augments antitumor immunity in patients with metastatic melanoma. *J Clin Oncol,* 21**,** 3343-50.

SPITZ, M. R., BARNETT, M. J., GOODMAN, G. E., THORNQUIST, M. D., WU, X. & POLLAK, M. (2002) Serum insulin-like growth factor (IGF) and IGF-binding protein levels and risk of lung cancer: a case-control study nested in the beta-Carotene and Retinol Efficacy Trial Cohort. *Cancer Epidemiol Biomarkers Prev,* 11**,** 1413-8.

SPORN, M. B. & ROBERTS, A. B. (1985) Autocrine growth factors and cancer. *Nature,* 313**,** 745-7.

SPRYNSKI, A. C., HOSE, D., KASSAMBARA, A., VINCENT, L., JOURDAN, M., ROSSI, J. F., GOLDSCHMIDT, H. & KLEIN, B. (2010) Insulin is a potent myeloma cell growth factor through insulin/IGF-1 hybrid receptor activation. *Leukemia,* 24**,** 1940-50.

STAUFFER, D., CHANG, B., HUANG, J., DUNN, A. & THAYER, M. (2007) p300/CREB-binding protein interacts with ATR and is required for the DNA replication checkpoint. *J Biol Chem,* 282**,** 9678-87.

STITT, T. N., DRUJAN, D., CLARKE, B. A., PANARO, F., TIMOFEYVA, Y., KLINE, W. O., GONZALEZ, M., YANCOPOULOS, G. D. & GLASS, D. J. (2004) The IGF-1/PI3K/Akt pathway prevents expression of muscle atrophy-induced ubiquitin ligases by inhibiting FOXO transcription factors. *Mol Cell,* 14**,** 395-403.

STRACKE, M. L., ENGEL, J. D., WILSON, L. W., RECHLER, M. M., LIOTTA, L. A. & SCHIFFMANN, E. (1989) The type I insulin-like growth factor receptor is a motility receptor in human melanoma cells. *J Biol Chem,* 264**,** 21544-9.

STRACKE, M. L., KOHN, E. C., AZNAVOORIAN, S. A., WILSON, L. L., SALOMON, D., KRUTZSCH, H. C., LIOTTA, L. A. & SCHIFFMANN, E. (1988) Insulin-like growth factors stimulate chemotaxis in human melanoma cells. *Biochemical and Biophysical Research Communications,* 153**,** 1076-1083.

STROMBERG, T., EKMAN, S., GIRNITA, L., DIMBERG, L. Y., LARSSON, O., AXELSON, M., LENNARTSSON, J., HELLMAN, U., CARLSON, K., OSTERBORG, A., VANDERKERKEN, K., NILSSON, K. & JERNBERG-WIKLUND, H. (2006) IGF-1 receptor tyrosine kinase inhibition by the cyclolignan PPP induces G2/M-phase accumulation and apoptosis in multiple myeloma cells. *Blood,* 107**,** 669-78.

STROS, M., LAUNHOLT, D. & GRASSER, K. D. (2007) The HMG-box: a versatile protein domain occurring in a wide variety of DNA-binding proteins. *Cell Mol Life Sci,* 64**,** 2590-606.

SUH, Y., ATZMON, G., CHO, M. O., HWANG, D., LIU, B., LEAHY, D. J., BARZILAI, N. & COHEN, P. (2008) Functionally significant insulin-like growth factor I receptor mutations in centenarians. *Proc Natl Acad Sci U S A,* 105**,** 3438-42.

SUMIMOTO, H., IMABAYASHI, F., IWATA, T. & KAWAKAMI, Y. (2006) The BRAF-MAPK signaling pathway is essential for cancer-immune evasion in human melanoma cells. *J Exp Med,* 203**,** 1651-6.

SUN, J. & JIN, T. (2008) Both Wnt and mTOR signaling pathways are involved in insulin-stimulated proto-oncogene expression in intestinal cells. *Cell Signal,* 20**,** 219-29.

SZEPIETOWSKI, J. C., REICH, A. & MCKENZIE, R. C. (2004) The multifunctional role of leukaemia inhibitory factor in cutaneous biology. *Acta Dermatovenerol Alp Panonica Adriat,* 13**,** 125-9.

SZPECHCINSKI, A., TRZOS, R., JAROCKI, P., TROJAN, L. A., OFICJALSKA, K., JUNKIERT, A., WEI, M. X., MAZUREK, M., CZAPIEWSKA, J. L., NIKLINSKI, J., KOPINSKI, P., CHYCZEWSKI, L., KASACKA, I. & TROJAN, J. (2004) Presence of MHC-I in rat glioma cells expressing antisense IGF-I-receptor RNA. *Rocz Akad Med Bialymst,* 49 Suppl 1**,** 98-104.

SZULC, J., WIZNEROWICZ, M., SAUVAIN, M.-O., TRONO, D. & AEBISCHER, P. (2006) A versatile tool for conditional gene expression and knockdown. *Nat Meth,* 3**,** 109-116.

TAKEDA, K., YASUMOTO, K., TAKADA, R., TAKADA, S., WATANABE, K., UDONO, T., SAITO, H., TAKAHASHI, K. & SHIBAHARA, S. (2000) Induction of melanocyte-specific microphthalmia-associated transcription factor by Wnt-3a. *J Biol Chem,* 275**,** 14013-6.

TALANTOV, D., MAZUMDER, A., YU, J. X., BRIGGS, T., JIANG, Y., BACKUS, J., ATKINS, D. & WANG, Y. (2005) Novel genes associated with malignant melanoma but not benign melanocytic lesions. *Clin Cancer Res,* 11**,** 7234-42.

TANAKA, K., GORELIK, E., WATANABE, M., HOZUMI, N. & JAY, G. (1988) Rejection of B16 melanoma induced by expression of a transfected major histocompatibility complex class I gene. *Mol. Cell. Biol.,* 8**,** 1857-1861.

TANAMI, H., IMOTO, I., HIRASAWA, A., YUKI, Y., SONODA, I., INOUE, J., YASUI, K., MISAWA-FURIHATA, A., KAWAKAMI, Y. & INAZAWA, J. (2004) Involvement of overexpressed wild-type BRAF in the growth of malignant melanoma cell lines. *Oncogene,* 23**,** 8796-8804.

TARHINI, A. A., GOGAS, H. & KIRKWOOD, J. M. (2012) IFN-alpha in the Treatment of Melanoma. *J Immunol,* 189**,** 3789-93.

TEN BERGE, D., BRUGMANN, S. A., HELMS, J. A. & NUSSE, R. (2008) Wnt and FGF signals interact to coordinate growth with cell fate specification during limb development. *Development,* 135**,** 3247-57.

TENG, L. (2009) Transcriptional regulation of p40PHOX and p47PHOX expression via HBP1 in endothelial cells. *Heart,* 96**,** e7.

TETSU, O. & MCCORMICK, F. (1999) Beta-catenin regulates expression of cyclin D1 in colon carcinoma cells. *Nature,* 398**,** 422-6.

TEVOSIAN, S. G., SHIH, H. H., MENDELSON, K. G., SHEPPARD, K. A., PAULSON, K. E. & YEE, A. S. (1997) HBP1: a HMG box transcriptional repressor that is targeted by the retinoblastoma family. *Genes Dev,* 11**,** 383-96.

THAMM, D. H., HUELSMEYER, M. K., MITZEY, A. M., QUROLLO, B., ROSE, B. J. & KURZMAN, I. D. (2010) RT-PCR-based tyrosine kinase display profiling of canine melanoma: IGF-1 receptor as a potential therapeutic target. *Melanoma Res,* 20**,** 35-42.

THISSEN, J. P., KETELSLEGERS, J. M. & UNDERWOOD, L. E. (1994) Nutritional regulation of the insulin-like growth factors. *Endocr Rev,* 15**,** 80-101.

THURISCH, B., LIANG, S. Y., SARIOGLU, N., SCHOMBURG, L., BUNGERT, J. R. & DAME, C. (2009) Transgenic mice expressing small interfering RNA against Gata4 point to a crucial role of Gata4 in the heart and gonads. *Journal of Molecular Endocrinology,* 43**,** 157-169.

TIAN, Q., FEETHAM, M. C., TAO, W. A., HE, X. C., LI, L., AEBERSOLD, R. & HOOD, L. (2004) Proteomic analysis identifies that 14-3-3zeta interacts with beta-catenin and facilitates its activation by Akt. *Proc Natl Acad Sci U S A,* 101**,** 15370-5.

TISSENBAUM, H. A. (2012) Genetics, life span, health span, and the aging process in Caenorhabditis elegans. *J Gerontol A Biol Sci Med Sci,* 67**,** 503-10.

TOMBOL, Z., EDER, K., KOVACS, A., SZABO, P. M., KULKA, J., LIKO, I., ZALATNAI, A., RACZ, G., TOTH, M., PATOCS, A., FALUS, A., RACZ, K. & IGAZ, P. (2010) MicroRNA expression profiling in benign (sporadic and hereditary) and recurring adrenal pheochromocytomas. *Mod Pathol,* 23**,** 1583-95.

TOPALIAN, S. L., HODI, F. S., BRAHMER, J. R., GETTINGER, S. N., SMITH, D. C., MCDERMOTT, D. F., POWDERLY, J. D., CARVAJAL, R. D., SOSMAN, J. A., ATKINS, M. B., LEMING, P. D., SPIGEL, D. R., ANTONIA, S. J., HORN, L., DRAKE, C. G., PARDOLL, D. M., CHEN, L., SHARFMAN, W. H., ANDERS, R. A., TAUBE, J. M., MCMILLER, T. L., XU, H., KORMAN, A. J., JURE-KUNKEL, M., AGRAWAL, S., MCDONALD, D., KOLLIA, G. D., GUPTA, A., WIGGINTON, J. M. & SZNOL, M. (2012) Safety, activity, and immune correlates of anti-PD-1 antibody in cancer. *N Engl J Med,* 366**,** 2443-54.

TRABADO, S., NGUYEN VAN BINH, P., MARTIN, C., LAFARGE-FRAYSSINET, C., THEVENIN, M., BAUDOUIN, F., WARNET, J. M. & DUC, H. T. (2006) Modulated expression of cell surface molecules and in vivo outgrowth of modified melanoma cells. *Biomedecine & Pharmacotherapy,* 60**,** 693-697.

TRABADO, S., VAN BINH, P. N., MARTIN, C., LAFARGE-FRAYSSINET, C., LONE, Y.-C., TROJAN, J., WARNET, J.-M. & DUC, H.-T. (2007) Stimulation of anti-melanoma immune effectors via modified tumour cells exhibiting inhibited IGF-I and low CD9. *Biomedicine & Pharmacotherapy,* 61**,** 494-498.

TREFZER, U., JOUARY, T., ROBERT, C., SANTINAMI, M., LEVCHENKO, E., SMITHERS, B., TESTORI, A., PEETERS, O., KIRKWOOD, J. & DRÃ©NO, B. (2010) FC13 DERMA Phase III trial of MAGE-A3 immunotherapy as adjuvant treatment in stage III melanoma: MAGE-A3 gene expression frequency and baseline demographics. *Melanoma Research,* 20**,** e34-e35 10.1097/01.cmr.0000382815.90748.46.

TROJAN, J., BLOSSEY, B. K., JOHNSON, T. R., RUDIN, S. D., TYKOCINSKI, M. & ILAN, J. (1992) Loss of tumorigenicity of rat glioblastoma directed by episome-based antisense cDNA transcription of insulin-like growth factor I. *Proceedings of the National Academy of Sciences,* 89**,** 4874-4878.

TROJAN, J., DUC, H. T., UPEGUI-GONZALEZ, L. C., HOR, F., GUO, Y., ANTHONY, D. & ILAN, J. (1996) Presence of MHC-I and B-7 molecules in rat and human glioma cells expressing antisense IGF-I mRNA. *Neurosci Lett,* 212**,** 9-12.

TROJAN, J., JOHNSON, T. R., RUDIN, S. D., BLOSSEY, B. K., KELLEY, K. M., SHEVELEV, A., ABDUL-KARIM, F. W., ANTHONY, D. D., TYKOCINSKI, M. L., ILAN, J. & ET AL. (1994) Gene therapy of murine teratocarcinoma: separate functions for insulin-like growth factors I and II in immunogenicity and differentiation. *Proc Natl Acad Sci U S A,* 91**,** 6088-92.

TROJAN, J., JOHNSON, T. R., RUDIN, S. D., ILAN, J. & TYKOCINSKI, M. L. (1993) Treatment and prevention of rat glioblastoma by immunogenic C6 cells expressing antisense insulin-like growth factor I RNA. *Science,* 259**,** 94-7.

TSAO, H., ZHANG, X., FOWLKES, K. & HALUSKA, F. G. (2000) Relative reciprocity of NRAS and PTEN/MMAC1 alterations in cutaneous melanoma cell lines. *Cancer Res,* 60**,** 1800-4.

UEKI, K., OKADA, T., HU, J., LIEW, C. W., ASSMANN, A., DAHLGREN, G. M., PETERS, J. L., SHACKMAN, J. G., ZHANG, M., ARTNER, I., SATIN, L. S., STEIN, R., HOLZENBERGER, M., KENNEDY, R. T., KAHN, C. R. & KULKARNI, R. N. (2006) Total insulin and IGF-I resistance in pancreatic beta cells causes overt diabetes. *Nat Genet,* 38**,** 583-8.

ULLRICH, A., GRAY, A., TAM, A. W., YANG-FENG, T., TSUBOKAWA, M., COLLINS, C., HENZEL, W., LE BON, T., KATHURIA, S., CHEN, E. & ET AL. (1986) Insulin-like growth factor I receptor primary structure: comparison with insulin receptor suggests structural determinants that define functional specificity. *EMBO J,* 5**,** 2503-12.

ULLRICH, E., BONMORT, M., MIGNOT, G., KROEMER, G. & ZITVOGEL, L. (2007) Tumor stress, cell death and the ensuing immune response. *Cell Death Differ,* 15**,** 21-28.

UPEGUI-GONZALEZ, L. C., DUC, H. T., BUISSON, Y., ARBORIO, M., LAFARGE-FRAYSSINET, C., JASMIN, C., GUO, Y. & TROJAN, J. (1998) Use of the IGF-I antisense strategy in the treatment of the hepatocarcinoma. *Adv Exp Med Biol,* 451**,** 35-42.

URSO, B., COPE, D. L., KALLOO-HOSEIN, H. E., HAYWARD, A. C., WHITEHEAD, J. P., O'RAHILLY, S. & SIDDLE, K. (1999) Differences in signaling properties of the cytoplasmic domains of the insulin receptor and insulin-like growth factor receptor in 3T3-L1 adipocytes. *J Biol Chem,* 274**,** 30864-73.

USUI, I., HARUTA, T., IWATA, M., TAKANO, A., UNO, T., KAWAHARA, J., UENO, E., SASAOKA, T. & KOBAYASHI, M. (2000) Retinoblastoma protein phosphorylation via PI 3-kinase and mTOR pathway regulates adipocyte differentiation. *Biochem Biophys Res Commun,* 275**,** 115-20.

VAIRA, V., LEE, C. W., GOEL, H. L., BOSARI, S., LANGUINO, L. R. & ALTIERI, D. C. (2006) Regulation of survivin expression by IGF-1//mTOR signaling. *Oncogene,* 26**,** 2678-2684.

VAN DER MERWE, P. A., MCNAMEE, P. N., DAVIES, E. A., BARCLAY, A. N. & DAVIS, S. J. (1995) Topology of the CD2-CD48 cell-adhesion molecule complex: implications for antigen recognition by T cells. *Curr Biol,* 5**,** 74-84.

VAN DUYVENVOORDE, H. A., VAN DOORN, J., KOENIG, J., GAUGUIN, L., OOSTDIJK, W., WADE, J. D., KARPERIEN, M., RUIVENKAMP, C. A., LOSEKOOT, M., VAN SETTEN, P. A., WALENKAMP, M. J., NOORDAM, C., DE MEYTS, P. & WIT, J. M. (2011) The severe short stature in two siblings with a heterozygous IGF1 mutation is not caused by a dominant negative effect of the putative truncated protein. *Growth Horm IGF Res,* 21**,** 44-50.

VAN DUYVENVOORDE, H. A., VAN SETTEN, P. A., WALENKAMP, M. J., VAN DOORN, J., KOENIG, J., GAUGUIN, L., OOSTDIJK, W., RUIVENKAMP, C. A., LOSEKOOT, M., WADE, J. D., DE MEYTS, P., KARPERIEN, M., NOORDAM, C. & WIT, J. M. (2010) Short stature associated with a novel heterozygous mutation in the insulin-like growth factor 1 gene. *J Clin Endocrinol Metab,* 95**,** E363-7.

VANDESOMPELE, J., DE PRETER, K., PATTYN, F., POPPE, B., VAN ROY, N., DE PAEPE, A. & SPELEMAN, F. (2002) Accurate normalization of real-time quantitative RT-PCR data by geometric averaging of multiple internal control genes. *Genome Biol,* 3**,** RESEARCH0034.

VANHAESEBROECK, B. & ALESSI, D. R. (2000) The PI3K-PDK1 connection: more than just a road to PKB. *Biochem J,* 346 Pt 3**,** 561-76.

VARDATSIKOS, G., SAHU, A. & SRIVASTAVA, A. K. (2009) The insulin-like growth factor family: molecular mechanisms, redox regulation, and clinical implications. *Antioxid Redox Signal,* 11**,** 1165-90.

VASAN, R. S., SULLIVAN, L. M., D'AGOSTINO, R. B., ROUBENOFF, R., HARRIS, T., SAWYER, D. B., LEVY, D. & WILSON, P. W. (2003) Serum insulin-like growth factor I and risk for heart failure in elderly individuals without a previous myocardial infarction: the Framingham Heart Study. *Ann Intern Med,* 139**,** 642-8.

VASILCANU, D., GIRNITA, A., GIRNITA, L., VASILCANU, R., AXELSON, M. & LARSSON, O. (2004) The cyclolignan PPP induces activation loop-specific inhibition of tyrosine phosphorylation of the insulin-like growth factor-1 receptor. Link to the phosphatidyl inositol-3 kinase/Akt apoptotic pathway. *Oncogene,* 23**,** 7854-62.

VELLA, V., PANDINI, G., SCIACCA, L., MINEO, R., VIGNERI, R., PEZZINO, V. & BELFIORE, A. (2002) A novel autocrine loop involving IGF-II and the insulin receptor isoform-A stimulates growth of thyroid cancer. *J Clin Endocrinol Metab,* 87**,** 245-54.

VENTURA, A., MEISSNER, A., DILLON, C. P., MCMANUS, M., SHARP, P. A., VAN PARIJS, L., JAENISCH, R. & JACKS, T. (2004) Cre-lox-regulated conditional RNA interference from transgenes. *Proc Natl Acad Sci U S A,* 101**,** 10380-5.

VERRAS, M. & SUN, Z. (2005) Beta-catenin is involved in insulin-like growth factor 1-mediated transactivation of the androgen receptor. *Mol Endocrinol,* 19**,** 391-8.

VILLAFUERTE, B. C., PHILLIPS, L. S., RANE, M. J. & ZHAO, W. (2004) Insulin-response element-binding protein 1: a novel Akt substrate involved in transcriptional action of insulin. *J Biol Chem,* 279**,** 36650-9.

VILLANUEVA, J., VULTUR, A., LEE, J. T., SOMASUNDARAM, R., FUKUNAGA-KALABIS, M., CIPOLLA, A. K., WUBBENHORST, B., XU, X., GIMOTTY, P. A., KEE, D., SANTIAGO-WALKER, A. E., LETRERO, R., D'ANDREA, K., PUSHPARAJAN, A., HAYDEN, J. E., BROWN, K. D., LAQUERRE, S., MCARTHUR, G. A., SOSMAN, J. A., NATHANSON, K. L. & HERLYN, M. (2010) Acquired resistance to BRAF inhibitors mediated by a RAF kinase switch in melanoma can be overcome by cotargeting MEK and IGF-1R/PI3K. *Cancer Cell,* 18**,** 683-95.

WAIN, H. M., BRUFORD, E. A., LOVERING, R. C., LUSH, M. J., WRIGHT, M. W. & POVEY, S. (2002) Guidelines for human gene nomenclature. *Genomics,* 79**,** 464-70.

WAN, P. T., GARNETT, M. J., ROE, S. M., LEE, S., NICULESCU-DUVAZ, D., GOOD, V. M., JONES, C. M., MARSHALL, C. J., SPRINGER, C. J., BARFORD, D. & MARAIS, R. (2004) Mechanism of activation of the RAF-ERK signaling pathway by oncogenic mutations of B-RAF. *Cell,* 116**,** 855-67.

WANG, L., SCHULZ, T. C., SHERRER, E. S., DAUPHIN, D. S., SHIN, S., NELSON, A. M., WARE, C. B., ZHAN, M., SONG, C. Z., CHEN, X., BRIMBLE, S. N., MCLEAN, A., GALEANO, M. J., UHL, E. W., D'AMOUR, K. A., CHESNUT, J. D., RAO, M. S., BLAU, C. A. & ROBINS, A. J. (2007) Self-renewal of human embryonic stem cells requires insulin-like growth factor-1 receptor and ERBB2 receptor signaling. *Blood,* 110**,** 4111-9.

WANG, W., CHEN, J. X., LIAO, R., DENG, Q., ZHOU, J. J., HUANG, S. & SUN, P. (2002) Sequential activation of the MEK-extracellular signal-regulated kinase and MKK3/6-p38 mitogen-activated protein kinase pathways mediates oncogenic ras-induced premature senescence. *Mol Cell Biol,* 22**,** 3389-403.

WANG, W., PAN, K., CHEN, Y., HUANG, C. & ZHANG, X. (2011) The acetylation of transcription factor HBP1 by p300/CBP enhances p16INK4A expression. *Nucleic Acids Res***,** 1-15.

WANG, Y., KLIJN, J. G., ZHANG, Y., SIEUWERTS, A. M., LOOK, M. P., YANG, F., TALANTOV, D., TIMMERMANS, M., MEIJER-VAN GELDER, M. E., YU, J., JATKOE, T., BERNS, E. M., ATKINS, D. & FOEKENS, J. A. (2005) Gene-expression profiles to predict distant metastasis of lymph-node-negative primary breast cancer. *Lancet,* 365**,** 671-9.

WARD, C. W. & GARRETT, T. P. (2004) Structural relationships between the insulin receptor and epidermal growth factor receptor families and other proteins. *Curr Opin Drug Discov Devel,* 7**,** 630-8.

WARSHAMANA-GREENE, G. S., LITZ, J., BUCHDUNGER, E., HOFMANN, F., GARCIA-ECHEVERRIA, C. & KRYSTAL, G. W. (2004) The insulin-like growth factor-I (IGF-I) receptor kinase inhibitor NVP-ADW742, in combination with STI571, delineates a spectrum of dependence of small cell lung cancer on IGF-I and stem cell factor signaling. *Mol Cancer Ther,* 3**,** 527-35.

WARSITO, D., SJOSTROM, S., ANDERSSON, S., LARSSON, O. & SEHAT, B. (2012) Nuclear IGF1R is a transcriptional co-activator of LEF1/TCF. *EMBO Rep,* 13**,** 244-50.

WEERARATNA, A. T. (2005) A Wnt-er Wonderland—The complexity of Wnt signaling in melanoma. *Cancer and Metastasis Reviews,* 24**,** 237-250.

WEERARATNA, A. T., JIANG, Y., HOSTETTER, G., ROSENBLATT, K., DURAY, P., BITTNER, M. & TRENT, J. M. (2002) Wnt5a signaling directly affects cell motility and invasion of metastatic melanoma. *Cancer Cell,* 1**,** 279-88.

WELLBROCK, C., KARASARIDES, M. & MARAIS, R. (2004) The RAF proteins take centre stage. *Nat Rev Mol Cell Biol,* 5**,** 875-885.

WERNER, H., KARNIELI, E., RAUSCHER, F. J. & LEROITH, D. (1996) Wild-type and mutant p53 differentially regulate transcription of the insulin-like growth factor I receptor gene. *Proc Natl Acad Sci U S A,* 93**,** 8318-23.

WERNER, H. & LE ROITH, D. (1997) The insulin-like growth factor-I receptor signaling pathways are important for tumorigenesis and inhibition of apoptosis. *Crit Rev Oncog,* 8**,** 71-92.

WHITE, M. F. (1998) The IRS-signaling system: a network of docking proteins that mediate insulin and cytokine action. *Recent Prog Horm Res,* 53**,** 119-38.

WIDLUND, H. R., HORSTMANN, M. A., PRICE, E. R., CUI, J., LESSNICK, S. L., WU, M., HE, X. & FISHER, D. E. (2002) Beta-catenin-induced melanoma growth requires the downstream target Microphthalmia-associated transcription factor. *J Cell Biol,* 158**,** 1079-87.

WIEDERSCHAIN, D., WEE, S., CHEN, L., LOO, A., YANG, G., HUANG, A., CHEN, Y., CAPONIGRO, G., YAO, Y. M., LENGAUER, C., SELLERS, W. R. & BENSON, J. D. (2009) Single-vector inducible lentiviral RNAi system for oncology target validation. *Cell Cycle,* 8**,** 498-504.

WILKER, E., BOL, D., KIGUCHI, K., RUPP, T., BELTRAN, L. & DIGIOVANNI, J. (1999) Enhancement of susceptibility to diverse skin tumor promoters by activation of the insulin-like growth factor-1 receptor in the epidermis of transgenic mice. *Mol Carcinog,* 25**,** 122-31.

WILLCOX, B. J., DONLON, T. A., HE, Q., CHEN, R., GROVE, J. S., YANO, K., MASAKI, K. H., WILLCOX, D. C., RODRIGUEZ, B. & CURB, J. D. (2008) FOXO3A genotype is strongly associated with human longevity. *Proc Natl Acad Sci U S A,* 105**,** 13987-92.

WITHROW, S. J. & VAIL, D. M. (2007) *Withrow & MacEwen's small animal clinical oncology,* St. Louis, Mo., Saunders Elsevier.

WIZNEROWICZ, M., SZULC, J. & TRONO, D. (2006) Tuning silence: conditional systems for RNA interference. *Nat Methods,* 3**,** 682-8.

WONDERLICH, J., SHEARER, G., LIVINGSTONE, A. & BROOKS, A. (2001) Induction and Measurement of Cytotoxic T Lymphocyte Activity. *Current Protocols in Immunology.* John Wiley & Sons, Inc.

WONG, C. H., ISKANDAR, K. B., YADAV, S. K., HIRPARA, J. L., LOH, T. & PERVAIZ, S. (2010) Simultaneous induction of non-canonical autophagy and apoptosis in cancer cells by ROS-dependent ERK and JNK activation. *PLoS ONE,* 5**,** e9996.

WONGKAJORNSILP, A., OUYPRASERTKUL, M., SANGRUCHI, T., HUABPRASERT, S., PAN, Y., TISAVIPAT, N., CHANYAVANICH, V., SANGRUCHI, S., CHOMSAMUT, K. & ANTHONY, D. D. (2001) The analysis of peri-tumor necrosis following the subcutaneous implantation of autologous tumor cells transfected with an episome transcribing an antisense insulin-like growth factor 1 RNA in a glioblastoma multiforme subject. *J Med Assoc Thai,* 84 Suppl 3**,** S740-7.

WU, J. D., HAUGK, K., COLEMAN, I., WOODKE, L., VESSELLA, R., NELSON, P., MONTGOMERY, R. B., LUDWIG, D. L. & PLYMATE, S. R. (2006) Combined in vivo effect of A12, a type 1 insulin-like growth factor receptor antibody, and docetaxel against prostate cancer tumors. *Clin Cancer Res,* 12**,** 6153-60.

WU, J. D., ODMAN, A., HIGGINS, L. M., HAUGK, K., VESSELLA, R., LUDWIG, D. L. & PLYMATE, S. R. (2005) In vivo effects of the human type I insulin-like growth factor receptor antibody A12 on androgen-dependent and androgen-independent xenograft human prostate tumors. *Clin Cancer Res,* 11**,** 3065-74.

WU, Y., YAKAR, S., ZHAO, L., HENNIGHAUSEN, L. & LEROITH, D. (2002) Circulating insulin-like growth factor-I levels regulate colon cancer growth and metastasis. *Cancer Res,* 62**,** 1030-5.

WU, Y. C., ZHU, M. & ROBERTSON, D. M. (2012) Novel nuclear localization and potential function of insulin-like growth factor-1 receptor/insulin receptor hybrid in corneal epithelial cells. *PLoS ONE,* 7**,** e42483.

XI, Y., NAKAJIMA, G., HAMIL, T., FODSTAD, O., RIKER, A. & JU, J. (2006) Association of insulin-like growth factor binding protein-3 expression with melanoma progression. *Mol Cancer Ther,* 5**,** 3078-84.

XIU, M., KIM, J., SAMPSON, E., HUANG, C.-Y., DAVIS, R. J., PAULSON, K. E. & YEE, A. S. (2003) The Transcriptional Repressor HBP1 Is a Target of the p38 Mitogen-Activated Protein Kinase Pathway in Cell Cycle Regulation. *Mol. Cell. Biol.,* 23**,** 8890-8901.

XU, L., SHEN, S. S., HOSHIDA, Y., SUBRAMANIAN, A., ROSS, K., BRUNET, J.-P., WAGNER, S. N., RAMASWAMY, S., MESIROV, J. P. & HYNES, R. O. (2008) Gene Expression Changes in an Animal Melanoma Model Correlate with Aggressiveness of Human Melanoma Metastases. *Molecular Cancer Research,* 6**,** 760-769.

XU, X., MARDELL, C., XIAN, C. J., ZOLA, H. & READ, L. C. (1995) Expression of functional insulin-like growth factor-1 receptor on lymphoid cell subsets of rats. *Immunology,* 85**,** 394-9.

YANG, H., HIGGINS, B., KOLINSKY, K., PACKMAN, K., GO, Z., IYER, R., KOLIS, S., ZHAO, S., LEE, R., GRIPPO, J. F., SCHOSTACK, K., SIMCOX, M. E., HEIMBROOK, D., BOLLAG, G. & SU, F. (2010) RG7204 (PLX4032), a selective

BRAFV600E inhibitor, displays potent antitumor activity in preclinical melanoma models. *Cancer Res,* 70**,** 5518-27.

YAO, C. J., WORKS, K., ROMAGNOLI, P. A. & AUSTIN, G. E. (2005) Effects of overexpression of HBP1 upon growth and differentiation of leukemic myeloid cells. *Leukemia : official journal of the Leukemia Society of America, Leukemia Research Fund, U.K,* 19**,** 1958-68.

YEE, A. S., SHIH, H. H. & TEVOSIAN, S. G. (1998) New perspectives on retinoblastoma family functions in differentiation. *Front Biosci,* 3**,** D532-47.

YEE, D., MORALES, F. R., HAMILTON, T. C. & VON HOFF, D. D. (1991) Expression of insulin-like growth factor I, its binding proteins, and its receptor in ovarian cancer. *Cancer Res,* 51**,** 5107-12.

YEH, A. H., BOHULA, E. A. & MACAULAY, V. M. (2006) Human melanoma cells expressing V600E B-RAF are susceptible to IGF1R targeting by small interfering RNAs. *Oncogene,* 25**,** 6574-6581.

YOUNG, A. R. (2004) Tanning devices--fast track to skin cancer? *Pigment Cell Res,* 17**,** 2-9.

YU, H. & ROHAN, T. (2000) Role of the insulin-like growth factor family in cancer development and progression. *J Natl Cancer Inst,* 92**,** 1472-89.

YUAN, Y. L., ZHOU, X. H., SONG, J., QIU, X. P., LI, J. & YE, L. F. (2008) Dual silencing of type 1 insulin-like growth factor and epidermal growth factor receptors to induce apoptosis of nasopharyngeal cancer cells. *The Journal of Laryngology & Otology,* 122**,** 952-960.

YUEN, J. S., COCKMAN, M. E., SULLIVAN, M., PROTHEROE, A., TURNER, G. D., ROBERTS, I. S., PUGH, C. W., WERNER, H. & MACAULAY, V. M. (2007) The VHL tumor suppressor inhibits expression of the IGF1R and its loss induces IGF1R upregulation in human clear cell renal carcinoma. *Oncogene,* 26**,** 6499-508.

ZAPF, J., HAURI, C., FUTO, E., HUSSAIN, M., RUTISHAUSER, J., MAACK, C. A. & FROESCH, E. R. (1995) Intravenously injected insulin-like growth factor (IGF) I/IGF binding protein-3 complex exerts insulin-like effects in hypophysectomized, but not in normal rats. *J Clin Invest,* 95**,** 179-86.

ZARAGOZA, D., GHAVIDEL, A., HEITMAN, J. & SCHULTZ, M. C. (1998) Rapamycin induces the G0 program of transcriptional repression in yeast by interfering with the TOR signaling pathway. *Mol Cell Biol,* 18**,** 4463-70.

ZEHAVI, L., AVRAHAM, R., BARZILAI, A., BAR-ILAN, D., NAVON, R., SIDI, Y., AVNI, D. & LEIBOWITZ-AMIT, R. (2012) Silencing of a large microRNA cluster on human chromosome 14q32 in melanoma: biological effects of mir-376a and mir-376c on insulin growth factor 1 receptor. *Mol Cancer,* 11**,** 44.

ZHA, J., O'BRIEN, C., SAVAGE, H., HUW, L.-Y., ZHONG, F., BERRY, L., LEWIS PHILLIPS, G. D., LUIS, E., CAVET, G., HU, X., AMLER, L. C. & LACKNER, M. R. (2009) Molecular predictors of response to a humanized anti-insulin-like growth factor-I receptor monoclonal antibody in breast and colorectal cancer. *Molecular Cancer Therapeutics,* 8**,** 2110-2121.

ZHANG, D., SAMANI, A. A. & BRODT, P. (2003) The role of the IGF-I receptor in the regulation of matrix metalloproteinases, tumor invasion and metastasis. *Horm Metab Res,* 35**,** 802-8.

ZHANG, J., TRENT, J. M. & MELTZER, P. S. (1993) Rapid isolation and characterization of amplified DNA by chromosome microdissection: identification of IGF1R amplification in malignant melanoma. *Oncogene,* 8**,** 2827-31.

ZHANG, X., KIM, J., RUTHAZER, R., MCDEVITT, M. A., WAZER, D. E., PAULSON, K. E. & YEE, A. S. (2006) The HBP1 Transcriptional Repressor Participates in RAS-Induced Premature Senescence. *Mol. Cell. Biol.,* 26**,** 8252-8266.

ZHOU, Y., CAPUCO, A. V. & JIANG, H. (2008) Involvement of connective tissue growth factor (CTGF) in insulin-like growth factor-I (IGF1) stimulation of proliferation of a bovine mammary epithelial cell line. *Domest Anim Endocrinol,* 35**,** 180-9.

ZHUMA, T., TYRRELL, R., SEKKALI, B., SKAVDIS, G., SAVELIEV, A., TOLAINI, M., RODERICK, K., NORTON, T., SMERDON, S., SEDGWICK, S., FESTENSTEIN, R. & KIOUSSIS, D. (1999) Human HMG box transcription factor HBP1: a role in hCD2 LCR function. *EMBO J,* 18**,** 6396-406.

ZOLLER, M. (1988) IFN-treatment of B16-F1 versus B16-F10: relative impact on non-adaptive and T-cell-mediated immune defense in metastatic spread. *Clin Exp Metastasis,* 6**,** 411-29.

log2 Fold Change	Moderated t statistic	P.Value	adj.P.Value	B-statistic	Illumina ID	ILMN_Gene	RefSeq_ID	Definition
0.677	6.239	2.62E-06	2.03E-02	4.508	1940647	HBP1	NM_012257.3	Hs HMG-box transcription factor 1 (HBP1), mRNA.
0.603	5.572	1.27E-05	3.37E-02	3.161	1170072	ZSWIM4	NM_023072.1	Hs zinc finger, SWIM-type containing 4 (ZSWIM4), mRNA.
0.522	5.995	4.64E-06	2.03E-02	4.022	5810672	SIX5	NM_175875.3	Hs SIX homeobox 5 (SIX5), mRNA.
0.486	5.489	1.55E-05	3.37E-02	2.988	3310504	PDK4	NM_002612.3	Hs pyruvate dehydrogenase kinase, isozyme 4 (PDK4), mRNA.
0.481	5.657	1.03E-05	3.21E-02	3.335	6220180	CABC1	NM_020247.4	Hs chaperone, ABC1 activity of bc1 complex homolog (S. pombe) (CABC1) mRNA.
0.451	6.113	3.52E-06	2.03E-02	4.259	7330026	FRAT2	NM_012083.2	Hs frequently rearranged in advanced T-cell lymphomas 2 (FRAT2), mRNA.
0.445	5.733	8.62E-06	3.12E-02	3.492	770746	ETV5	NM_004454.1	Hs ets variant gene 5 (ets-related molecule) (ETV5), mRNA.
0.424	6.471	1.53E-06	2.03E-02	4.961	770440	ULK1	NM_003565.1	Hs unc-51-like kinase 1 (C. elegans) (ULK1), mRNA.
0.320	5.448	1.71E-05	3.38E-02	2.904	1580309	SERF2	NM_001018108.2	Hs small EDRK-rich factor 2 (SERF2), mRNA.
-0.397	-5.503	1.49E-05	3.37E-02	3.018	2850551	RCAN1	NM_203417.1	Hs regulator of calcineurin 1 (RCAN1), tv: 2, mRNA.
-0.419	-5.993	4.66E-06	2.03E-02	4.018	1230646	THUMPD2	NM_025264.3	Hs THUMP domain containing 2 (THUMPD2), mRNA.

Appendix 1 – Genes differentially expressed at 3 hours in cells treated with IGF1R Inhibitor (AZ12253801)

log_2 Fold Change	Moderated t-statistic	P.Value	adj.P.Value	B-statistic	Illumina ID	ILMN_Gene	RefSeq_ID	Definition
1.953	15.116	3.26E-13	1.42E-09	19.783	5690687	CTGF	NM_001901.1	Hs connective tissue growth factor (CTGF), mRNA.
1.894	13.923	1.73E-12	4.69E-09	18.301	5270112	HMGCS1	NM_002130.6	Hs 3-hydroxy-3-methylglutaryl-Coenzyme A synthase 1 (soluble) (HMGCS1), tv: 2, mRNA.
1.759	11.084	1.51E-10	1.27E-07	14.190	2640292	CTGF	NM_001901.2	Hs connective tissue growth factor (CTGF), mRNA.
1.686	13.824	1.99E-12	4.82E-09	18.171	5670465	ADM	NM_001124.1	Hs adrenomedullin (ADM), mRNA.
1.626	16.082	9.14E-14	4.97E-10	20.892	2650390	LIF	NM_002309.2	Hs leukemia inhibitory factor (cholinergic differentiation factor) (LIF), mRNA.
1.534	19.313	2.00E-15	4.35E-11	24.095	3930605	CYR61	NM_001554.3	Hs cysteine-rich, angiogenic inducer, 61 (CYR61), mRNA.
1.506	9.634	2.05E-09	1.12E-06	11.719	3940673	LOC728285	XM_001127070.1	PREDICTED: Hs similar to keratin associated protein 2-4 (LOC728285), mRNA.
1.449	9.211	4.60E-09	2.23E-06	10.946	6370246	LOC644350	XM_927511.3	PREDICTED: Hs hypothetical LOC644350 (LOC644350), mRNA.
1.330	12.546	1.37E-11	1.86E-08	16.417	5860348	SC4MOL	NM_001017369.1	Hs sterol-C4-methyl oxidase-like (SC4MOL), tv: 2, mRNA.
1.318	11.341	9.74E-11	9.21E-08	14.600	4200037	SC4MOL	NM_006745.3	Hs sterol-C4-methyl oxidase-like (SC4MOL), tv: 1, mRNA.
1.179	9.054	6.26E-09	2.78E-06	10.650	360192	INSIG1	NM_198336.1	Hs insulin induced gene 1 (INSIG1), tv: 2, mRNA.
1.139	7.991	5.41E-08	1.43E-05	8.569	3400019	RGS2	NM_002923.1	Hs regulator of G-protein signalling 2, 24kDa (RGS2), mRNA.
1.131	8.411	2.27E-08	7.59E-06	9.411	7150563	ENC1	NM_003633.1	Hs ectodermal-neural cortex (with BTB-like domain) (ENC1), mRNA.
1.025	12.731	1.03E-11	1.60E-08	16.681	1340707	PLD6	NM_178836.2	Hs phospholipase D family, member 6 (PLD6), mRNA.
1.015	14.090	1.36E-12	4.22E-09	18.516	2850551	RCAN1	NM_203417.1	Hs regulator of calcineurin 1 (RCAN1), tv: 2, mRNA.
0.993	8.775	1.09E-08	4.08E-06	10.120	1990630	TRIB3	NM_021158.3	Hs tribbles homolog 3 (Drosophila) (TRIB3), mRNA.
0.979	6.225	2.71E-06	3.44E-04	4.756	6020382	KRTAP2-1	XM_926554.2	PREDICTED: Hs keratin associated protein 2-1 (KRTAP2-1), mRNA.
0.977	8.853	9.31E-09	3.82E-06	10.270	620239	RCAN1	NM_203418.1	Hs regulator of calcineurin 1 (RCAN1), tv: 3, mRNA.
0.975	12.004	3.25E-11	3.93E-08	15.621	7050068	SQLE	NM_003129.3	Hs squalene epoxidase (SQLE), mRNA.
0.950	10.058	9.32E-10	6.14E-07	12.471	6270646	MYC	NM_002467.3	Hs v-myc myelocytomatosis viral oncogene homolog (avian) (MYC), mRNA.
0.937	7.535	1.43E-07	3.13E-05	7.627	6960332	FOSL1	NM_005438.2	Hs FOS-like antigen 1 (FOSL1), mRNA.

Appendix 2 – Genes differentially expressed at 3 hours in cells treated with IGF1 ligand

0.937	13.066	6.14E-12	1.03E-08	17.152	3180307	NANOS1	NM_199461.2	Hs nanos homolog 1 (Drosophila) (NANOS1), mRNA.
0.933	7.282	2.48E-07	4.57E-05	7.089	5820601	CCND1	NM_053056.2	Hs cyclin D1 (CCND1), mRNA.
0.927	10.265	6.39E-10	4.63E-07	12.829	1440020	MVD	NM_002461.1	Hs mevalonate (diphospho) decarboxylase (MVD), mRNA.
0.897	8.223	3.33E-08	9.67E-06	9.039	3190148	DDIT4	NM_019058.2	Hs DNA-damage-inducible transcript 4 (DDIT4), mRNA.
0.887	7.996	5.35E-08	1.43E-05	8.579	2810059	KLF4	NM_004235.3	Hs Kruppel-like factor 4 (gut) (KLF4), mRNA.
0.887	6.175	3.04E-06	3.79E-04	4.641	4780128	ATF3	NM_001040619.1	Hs activating transcription factor 3 (ATF3), tv: 4, mRNA.
0.879	8.274	3.00E-08	9.25E-06	9.140	150438	MID1IP1	NM_021242.4	Hs MID1 interacting protein 1 (gastrulation specific G12 homolog (zebrafish)) (MID1IP1), tv:1, mRNA.
0.875	9.640	2.03E-09	1.12E-06	11.729	1820332	INSIG1	NM_198336.1	Hs insulin induced gene 1 (INSIG1), tv: 2, mRNA.
0.874	5.709	9.13E-06	8.95E-04	3.567	830619	DDIT3	NM_004083.4	Hs DNA-damage-inducible transcript 3 (DDIT3), mRNA.
0.866	6.168	3.09E-06	3.82E-04	4.627	6510377	TNFRSF12A	NM_016639.1	Hs tumor necrosis factor receptor superfamily, member 12A (TNFRSF12A), mRNA.
0.863	12.422	1.67E-11	2.13E-08	16.238	1820594	HBEGF	NM_001945.1	Hs heparin-binding EGF-like growth factor (HBEGF), mRNA.
0.857	6.042	4.15E-06	4.68E-04	4.338	4150148	LOC728934	XM_001128836.2	PREDICTED: Hs hypothetical LOC728934 (LOC728934), mRNA.
0.852	8.264	3.06E-08	9.25E-06	9.121	2640735	BHLHB2	NM_003670.1	Hs basic helix-loop-helix domain containing, class B, 2 (BHLHB2), mRNA.
0.850	10.678	3.06E-10	2.38E-07	13.525	1500082	CHAC1	NM_024111.2	Hs ChaC, cation transport regulator homolog 1 (E. coli) (CHAC1), mRNA.
0.843	8.115	4.17E-08	1.16E-05	8.821	4230431	CEBPG	NM_001806.2	Hs CCAAT/enhancer binding protein (C/EBP), gamma (CEBPG), mRNA.
0.842	7.308	2.34E-07	4.43E-05	7.145	5570102	DKK1	NM_012242.2	Hs dickkopf homolog 1 (Xenopus laevis) (DKK1), mRNA.
0.835	6.773	7.69E-07	1.24E-04	5.986	3990382	INO80C	NM_194281.3	Hs INO80 complex subunit C (INO80C), tv: 2, mRNA.
0.827	5.489	1.55E-05	1.34E-03	3.051	6380037	LOC100130516	XM_001720343.1	PREDICTED: Hs hypothetical protein LOC100130516 (LOC100130516), mRNA.
0.789	8.243	3.20E-08	9.43E-06	9.079	3120367	SQLE	NM_003129.3	Hs squalene epoxidase (SQLE), mRNA.
0.783	8.663	1.36E-08	5.01E-06	9.905	6510332	EPHA2	NM_004431.2	Hs EPH receptor A2 (EPHA2), mRNA.
0.774	5.775	7.80E-06	7.92E-04	3.720	3400332	RHOB	NM_004040.2	Hs ras homolog gene family, member B (RHOB), mRNA.
0.773	5.642	1.07E-05	1.02E-03	3.410	5810685	THBS1	NM_003246.2	Hs thrombospondin 1 (THBS1), mRNA.
0.772	6.760	7.93E-07	1.24E-04	5.956	5690066	XBP1	NM_005080.2	Hs X-box binding protein 1 (XBP1), tv: 1, mRNA.
0.765	6.315	2.19E-06	2.86E-04	4.961	4610433	ANGPTL4	NM_139314.1	Hs angiopoietin-like 4 (ANGPTL4), tv: 1, mRNA.
0.755	9.796	1.52E-09	9.03E-07	12.008	6650482	EPHA4	NM_004438.3	Hs EPH receptor A4 (EPHA4), mRNA.
0.745	6.816	6.98E-07	1.14E-04	6.080	3460097	HOXB2	NM_002145.3	Hs homeobox B2 (HOXB2), mRNA.
0.732	6.700	9.09E-07	1.35E-04	5.823	270538	PMP22	NM_153321.1	Hs peripheral myelin protein 22 (PMP22), tv: 2, mRNA.
0.730	8.477	1.98E-08	7.13E-06	9.542	1030333	CCL2	NM_002982.3	Hs chemokine (C-C motif) ligand 2 (CCL2), mRNA.
0.728	8.442	2.13E-08	7.34E-06	9.472	5550307	C6ORF145	XM_937537.2	PREDICTED: Hs chromosome 6 open reading frame 145 (C6orf145), mRNA.
0.721	7.511	1.51E-07	3.21E-05	7.575	5130750	HHEX	NM_002729.4	Hs hematopoietically expressed homeobox (HHEX), mRNA.
0.710	7.992	5.40E-08	1.43E-05	8.572	7150411	WNK4	NM_032387.3	Hs WNK lysine deficient protein kinase 4 (WNK4), mRNA.
0.708	7.409	1.88E-07	3.72E-05	7.360	7200195	TBX3	NM_005996.3	Hs T-box 3 (TBX3), tv: 1, mRNA.
0.694	6.852	6.44E-07	1.07E-04	6.158	610519	TPM1	NM_001018020.1	Hs tropomyosin 1 (alpha) (TPM1), tv: 7, mRNA.
0.683	7.000	4.62E-07	7.98E-05	6.482	2640670	IDI1	NM_004508.2	Hs isopentenyl-diphosphate delta isomerase 1 (IDI1), mRNA.
0.678	7.046	4.18E-07	7.39E-05	6.581	1780619	EHD1	NM_006795.2	Hs EH-domain containing 1 (EHD1), mRNA.
0.677	8.269	3.03E-08	9.25E-06	9.129	7050600	RARA	NM_000964.2	Hs retinoic acid receptor, alpha (RARA), tv: 1, mRNA.
0.671	6.046	4.11E-06	4.68E-04	4.346	6580121	MID1IP1	NM_021242.3	Hs MID1 interacting protein 1 (gastrulation specific G12 homolog (zebrafish)) (MID1IP1), mRNA.
0.669	8.143	3.93E-08	1.11E-05	8.878	1980474	PLD6	NM_178836.2	Hs phospholipase D family, member 6 (PLD6), mRNA.
0.668	8.301	2.84E-08	9.09E-06	9.193	1170170	STC2	NM_003714.2	Hs stanniocalcin 2 (STC2), mRNA.
0.665	7.548	1.39E-07	3.08E-05	7.654	5910600	FAM57A	NM_024792.1	Hs family with sequence similarity 57, member A (FAM57A), mRNA.

Appendix 2 – Genes differentially expressed at 3 hours in cells treated with IGF1 ligand

0.662	7.432	1.78E-07	3.66E-05	7.410	1300706	MTHFD2	NM_006636.3	Hs methylenetetrahydrofolate dehydrogenase (NADP+ dependent) 2, methenyltetrahydrofolate cyclohydrolase (MTHFD2), nuclear gene encoding mitochondrial protein, tv: 1, mRNA.
0.659	6.365	1.96E-06	2.56E-04	5.074	5560246	TPM1	NM_001018004.1	Hs tropomyosin 1 (alpha) (TPM1), tv: 3, mRNA.
0.658	6.215	2.77E-06	3.51E-04	4.732	2450156	XBP1	NM_001079539.1	Hs X-box binding protein 1 (XBP1), tv: 2, mRNA.
0.657	5.602	1.18E-05	1.10E-03	3.316	2030132	LOC653506	XM_927769.1	PREDICTED: Hs similar to meteorin, glial cell differentiation regulator-like (LOC653506), mRNA.
0.655	8.292	2.89E-08	9.12E-06	9.176	6400369	MAP3K14	NM_003954.2	Hs mitogen-activated protein kinase kinase kinase 14 (MAP3K14), mRNA.
0.654	6.682	9.47E-07	1.39E-04	5.782	6840477	HS.543887		AGENCOURT_14535501 NIH_MGC_191 Hs cDNA clone IMAGE:30415823 5, mRNA sequence
0.650	7.168	3.19E-07	5.73E-05	6.846	4260392	NSDHL	NM_015922.1	Hs NAD(P) dependent steroid dehydrogenase-like (NSDHL), mRNA.
0.644	5.564	1.29E-05	1.18E-03	3.227	270152	SLC7A5	NM_003486.5	Hs solute carrier family 7 (cationic amino acid transporter, y+ system), member 5 (SLC7A5), mRNA.
0.624	7.031	4.32E-07	7.56E-05	6.549	7330097	ADARB1	NM_001112.2	Hs adenosine deaminase, RNA-specific, B1 (RED1 homolog rat) (ADARB1), tv: 1, mRNA.
0.622	7.881	6.82E-08	1.73E-05	8.345	10487	SLC25A25	NM_052901.2	Hs solute carrier family 25 (mitochondrial carrier; phosphate carrier), member 25 (SLC25A25), nuclear gene encoding mitochondrial protein, tv: 1, mRNA.
0.621	5.946	5.20E-06	5.60E-04	4.117	5290397	CLCF1	NM_013246.2	Hs cardiotrophin-like cytokine factor 1 (CLCF1), tv: 1, mRNA.
0.618	6.460	1.57E-06	2.13E-04	5.287	4920110	GADD45B	NM_015675.2	Hs growth arrest and DNA-damage-inducible, beta (GADD45B), mRNA.
0.615	6.588	1.17E-06	1.68E-04	5.574	2480341	CDC25A	NM_001789.2	Hs cell division cycle 25 homolog A (S. pombe) (CDC25A), tv: 1, mRNA.
0.613	6.260	2.50E-06	3.21E-04	4.835	450168	SFRS7	NM_001031684.1	Hs splicing factor, arginine/serine-rich 7, 35kDa (SFRS7), mRNA.
0.608	6.865	6.26E-07	1.05E-04	6.186	5290148	GPT2	NM_133443.1	Hs glutamic pyruvate transaminase (alanine aminotransferase) 2 (GPT2), mRNA.
0.602	8.776	1.08E-08	4.08E-06	10.123	5890706	SHB	NM_003028.2	Hs Src homology 2 domain containing adaptor protein B (SHB), mRNA.
0.601	6.750	8.12E-07	1.25E-04	5.933	7150176	MAT2A	NM_005911.4	Hs methionine adenosyltransferase II, alpha (MAT2A), mRNA.
0.599	6.044	4.14E-06	4.68E-04	4.341	1400427	KCNG1	NM_002237.3	Hs potassium voltage-gated channel, subfamily G, member 1 (KCNG1), mRNA.
0.596	7.420	1.83E-07	3.71E-05	7.383	7560138	PMP22	NM_153321.1	Hs peripheral myelin protein 22 (PMP22), tv: 2, mRNA.
0.588	5.527	1.41E-05	1.25E-03	3.140	3130358	HS.25892		Hs cDNA FLJ38860 fis, clone MESAN2011977
0.586	6.025	4.33E-06	4.85E-04	4.297	6200670	LPIN1	NM_145693.1	Hs lipin 1 (LPIN1), mRNA.
0.585	6.616	1.10E-06	1.58E-04	5.637	6180465	SLC2A6	NM_017585.2	Hs solute carrier family 2 (facilitated glucose transporter), member 6 (SLC2A6), mRNA.
0.584	6.067	3.92E-06	4.54E-04	4.393	5420575	SLC3A2	NM_001013251.1	Hs solute carrier family 3 (activators of dibasic&neutral amino acid transport) 2 (SLC3A2), tv:6, mRNA.
0.584	7.528	1.45E-07	3.13E-05	7.611	6450154	LSS	NM_002340.3	Hs lanosterol synthase (2,3-oxidosqualene-lanosterol cyclase) (LSS), tv: 1, mRNA.
0.583	6.369	1.94E-06	2.56E-04	5.082	4760747	TPST1	NM_003596.2	Hs tyrosylprotein sulfotransferase 1 (TPST1), mRNA.
0.579	6.264	2.47E-06	3.20E-04	4.844	1110088	SLMO1	NM_006553.2	Hs slowmo homolog 1 (Drosophila) (SLMO1), mRNA.
0.577	5.531	1.40E-05	1.24E-03	3.150	60079	DNAJB1	NM_006145.1	Hs DnaJ (Hsp40) homolog, subfamily B, member 1 (DNAJB1), mRNA.
0.577	6.739	8.31E-07	1.26E-04	5.910	1690630	FAM43A	NM_153690.4	Hs family with sequence similarity 43, member A (FAM43A), mRNA.
0.575	6.838	6.64E-07	1.10E-04	6.128	510044	KLF4	NM_004235.3	Hs Kruppel-like factor 4 (gut) (KLF4), mRNA.
0.572	7.712	9.78E-08	2.36E-05	7.995	6620768	MVK	NM_000431.1	Hs mevalonate kinase (mevalonic aciduria) (MVK), mRNA.
0.559	8.882	8.78E-09	3.67E-06	10.325	4250678	MGC16121	XM_001128419.1	PREDICTED: Hs hypothetical protein MGC16121 (MGC16121), mRNA.
0.558	5.501	1.50E-05	1.31E-03	3.080	6270437	FJX1	NM_014344.2	Hs four jointed box 1 (Drosophila) (FJX1), mRNA.
0.556	9.237	4.38E-09	2.17E-06	10.993	2750280	CDK5R1	NM_003885.2	Hs cyclin-dependent kinase 5, regulatory subunit 1 (p35) (CDK5R1), mRNA.
0.545	5.684	9.70E-06	9.38E-04	3.508	1010047	RAB4B	NM_016154.3	Hs RAB4B, member RAS oncogene family (RAB4B), mRNA.
0.542	7.605	1.23E-07	2.84E-05	7.774	1300601	ST3GAL1	NM_003033.2	Hs ST3 beta-galactoside alpha-2,3-sialyltransferase 1 (ST3GAL1), tv: 1, mRNA.
0.539	7.418	1.84E-07	3.71E-05	7.381	2510224	ANKRD57	NM_023016.3	Hs ankyrin repeat domain 57 (ANKRD57), mRNA.
0.537	6.096	3.66E-06	4.33E-04	4.461	6550048	DHCR7	NM_001360.1	Hs 7-dehydrocholesterol reductase (DHCR7), mRNA.
0.536	7.323	2.26E-07	4.32E-05	7.179	1510296	ASNS	NM_133436.1	Hs asparagine synthetase (ASNS), tv: 1, mRNA.

Appendix 2 – Genes differentially expressed at 3 hours in cells treated with IGF1 ligand

0.535	5.954	5.11E-06	5.53E-04	4.135	5360678	DHCR7	NM_001360.2	Hs 7-dehydrocholesterol reductase (DHCR7), tv: 1, mRNA.
0.530	8.999	6.98E-09	2.98E-06	10.547	3610626	ADM2	NM_024866.4	Hs adrenomedullin 2 (ADM2), mRNA.
0.523	5.770	7.90E-06	7.93E-04	3.708	4150689	METRNL	XM_941466.2	PREDICTED: Hs meteorin, glial cell differentiation regulator-like (METRNL), mRNA.
0.522	6.618	1.10E-06	1.58E-04	5.640	3990026	CCNE1	NM_001238.1	Hs cyclin E1 (CCNE1), tv: 1, mRNA.
0.519	6.127	3.40E-06	4.07E-04	4.532	4260253	OBFC2A	NM_001031716.1	Hs oligonucleotide/oligosaccharide-binding fold containing 2A (OBFC2A), mRNA.
0.517	7.822	7.73E-08	1.93E-05	8.224	70035	ZFP42	NM_174900.3	Hs zinc finger protein 42 homolog (mouse) (ZFP42), mRNA.
0.517	5.825	6.93E-06	7.18E-04	3.836	7610433	SLC1A5	NM_005628.1	Hs solute carrier family 1 (neutral amino acid transporter), member 5 (SLC1A5), mRNA.
0.501	6.055	4.03E-06	4.64E-04	4.367	6370435	ETS1	NM_005238.2	Hs v-ets erythroblastosis virus E26 oncogene homolog 1 (avian) (ETS1), mRNA.
0.497	6.144	3.27E-06	3.97E-04	4.571	2070131	CCNE1	NM_057182.1	Hs cyclin E1 (CCNE1), tv: 2, mRNA.
0.494	5.606	1.17E-05	1.10E-03	3.325	1780367	C12ORF44	NM_001098673.1	Hs chromosome 12 open reading frame 44 (C12orf44), tv: 2, mRNA.
0.493	7.111	3.62E-07	6.45E-05	6.722	1440736	LDLR	NM_000527.2	Hs low density lipoprotein receptor (familial hypercholesterolemia) (LDLR), mRNA.
0.485	5.714	9.03E-06	8.89E-04	3.577	3120400	KANK2	NM_015493.4	Hs KN motif and ankyrin repeat domains 2 (KANK2), mRNA.
0.482	5.997	4.62E-06	5.13E-04	4.234	2970397	ZNF296	NM_145288.1	Hs zinc finger protein 296 (ZNF296), mRNA.
0.475	5.961	5.02E-06	5.47E-04	4.151	5050768	LONRF1	NM_152271.3	Hs LON peptidase N-terminal domain and ring finger 1 (LONRF1), mRNA.
0.472	5.553	1.33E-05	1.19E-03	3.202	6960382	ING2	NM_001564.2	Hs inhibitor of growth family, member 2 (ING2), mRNA.
0.471	5.740	8.48E-06	8.46E-04	3.639	60220	C16ORF79	NM_182563.2	Hs chromosome 16 open reading frame 79 (C16orf79), mRNA.
0.467	6.442	1.64E-06	2.20E-04	5.248	10440	MARS2	NM_138395.2	Hs methionyl-tRNA synthetase 2, mitochondrial (MARS2), mRNA.
0.461	5.560	1.30E-05	1.18E-03	3.218	6330754	UBE2Q1	NM_017582.5	Hs ubiquitin-conjugating enzyme E2Q (putative) 1 (UBE2Q1), mRNA.
0.460	5.569	1.27E-05	1.17E-03	3.240	840356	NUAK2	NM_030952.1	Hs NUAK family, SNF1-like kinase, 2 (NUAK2), mRNA.
0.448	6.759	7.95E-07	1.24E-04	5.954	6620292	C10ORF54	NM_022153.1	Hs chromosome 10 open reading frame 54 (C10orf54), mRNA.
0.442	5.801	7.34E-06	7.53E-04	3.780	150129	C1ORF135	NM_024037.1	Hs chromosome 1 open reading frame 135 (C1orf135), mRNA.
0.441	5.557	1.31E-05	1.18E-03	3.212	6980411	LOC100134259	NR_024452.1	Hs similar to hCG1987718 (LOC100134259), non-coding RNA.
0.439	7.574	1.31E-07	3.01E-05	7.707	4260687	SLCO4C1	NM_180991.4	Hs solute carrier organic anion transporter family, member 4C1 (SLCO4C1), mRNA.
0.437	5.641	1.07E-05	1.02E-03	3.407	670673	BCL2L1	NM_138578.1	Hs BCL2-like 1 (BCL2L1), nuclear gene encoding mitochondrial protein, tv: 1, mRNA.
0.436	6.019	4.38E-06	4.89E-04	4.284	1110722	BRIX1	NM_018321.3	Hs BRX1, biogenesis of ribosomes, homolog (S. cerevisiae) (BRIX1), mRNA.
0.418	6.748	8.14E-07	1.25E-04	5.930	1570273	NEDD4L	NM_015277.3	Hs neural precursor cell expressed, developmentally down-regulated 4-like (NEDD4L), mRNA.
0.408	5.932	5.38E-06	5.74E-04	4.083	6220600	LOC113386	NM_138781.2	Hs similar to envelope protein (LOC113386), mRNA.
0.403	6.195	2.90E-06	3.63E-04	4.688	60092	PUS1	NM_001002019.1	Hs pseudouridylate synthase 1 (PUS1), tv: 2, mRNA.
0.403	6.110	3.54E-06	4.21E-04	4.494	6330348	NT5DC3	NM_016575.1	Hs 5'-nucleotidase domain containing 3 (NT5DC3), tv: 2, mRNA.
0.402	6.396	1.82E-06	2.43E-04	5.143	730608	LOC285550	XR_017764.1	PREDICTED: Hs misc_RNA (LOC285550), miscRNA.
0.392	6.133	3.36E-06	4.03E-04	4.546	7610167	RAB4B	NM_016154.2	Hs RAB4B, member RAS oncogene family (RAB4B), mRNA.
0.378	6.378	1.90E-06	2.52E-04	5.103	3610228	PEA15	NM_003768.2	Hs phosphoprotein enriched in astrocytes 15 (PEA15), mRNA.
0.370	5.942	5.26E-06	5.64E-04	4.106	510577	TRIML2	NM_173553.1	Hs tripartite motif family-like 2 (TRIML2), mRNA.
0.368	5.579	1.24E-05	1.15E-03	3.263	4810653	YWHAH	NM_003405.3	Hs tyrosine 3-monooxygenase/tryptophan 5-monooxygenase activation protein (YWHAH), mRNA.
-0.314	-5.915	5.61E-06	5.93E-04	4.043	4050674	LOC145837	XM_934770.1	PREDICTED: Hs hypothetical protein LOC145837, tv: 2 (LOC145837), mRNA.
-0.339	-5.716	8.99E-06	8.89E-04	3.581	3370075	S1PR4	NM_003775.2	Hs sphingosine-1-phosphate receptor 4 (S1PR4), mRNA.
-0.378	-6.666	9.81E-07	1.43E-04	5.748	4480537	HS.13291		Hs cDNA FLJ35319 fis, clone PROST2011577
-0.389	-5.886	6.00E-06	6.31E-04	3.977	2630333	CYB5D2	NM_144611.2	Hs cytochrome b5 domain containing 2 (CYB5D2), mRNA.
-0.406	-5.642	1.07E-05	1.02E-03	3.410	5360672	CCNG2	NM_004354.1	Hs cyclin G2 (CCNG2), mRNA.
-0.408	-5.914	5.62E-06	5.93E-04	4.042	6200113	LOC653066	XM_930921.1	PREDICTED: Hs similar to inhibitor of growth family, member 5, tv: 4 (LOC653066), mRNA.

Appendix 2 – Genes differentially expressed at 3 hours in cells treated with IGF1 ligand

-0.424	-7.174	3.14E-07	5.69E-05	6.859	5810167	C17ORF44	NM_173621.1	Hs chromosome 17 open reading frame 44 (C17orf44), mRNA.
-0.427	-6.133	3.35E-06	4.03E-04	4.547	460427	TESK2	NM_007170.2	Hs testis-specific kinase 2 (TESK2), mRNA.
-0.430	-5.786	7.59E-06	7.76E-04	3.747	610152	DAB2	NM_001343.2	Hs disabled homolog 2, mitogen-responsive phosphoprotein (Drosophila) (DAB2), mRNA.
-0.445	-6.251	2.55E-06	3.26E-04	4.814	7510719	TRAF3IP2	NM_147686.1	Hs TRAF3 interacting protein 2 (TRAF3IP2), tv: 2, mRNA.
-0.454	-5.985	4.74E-06	5.24E-04	4.207	6840356	MGEA5	NM_012215.2	Hs meningioma expressed antigen 5 (hyaluronidase) (MGEA5), mRNA.
-0.460	-6.504	1.42E-06	1.97E-04	5.387	620619	TBC1D8	NM_007063.3	Hs TBC1 domain family, member 8 (with GRAM domain) (TBC1D8), mRNA.
-0.462	-5.823	6.96E-06	7.18E-04	3.831	3400646	FRAT1	NM_005479.2	Hs frequently rearranged in advanced T-cell lymphomas (FRAT1), mRNA.
-0.463	-5.626	1.11E-05	1.05E-03	3.372	1090438	ZMYND8	NM_183047.1	Hs zinc finger, MYND-type containing 8 (ZMYND8), tv: 1, mRNA.
-0.468	-6.082	3.78E-06	4.43E-04	4.428	6220438	RPS6KA5	NM_004755.2	Hs ribosomal protein S6 kinase, 90kDa, polypeptide 5 (RPS6KA5), tv: 1, mRNA.
-0.470	-6.078	3.81E-06	4.44E-04	4.421	3400598	WIPI1	NM_017983.4	Hs WD repeat domain, phosphoinositide interacting 1 (WIPI1), mRNA.
-0.474	-6.091	3.70E-06	4.35E-04	4.450	240682	ANKRD37	NM_181726.2	Hs ankyrin repeat domain 37 (ANKRD37), mRNA.
-0.478	-5.594	1.20E-05	1.11E-03	3.297	1510040	DYRK1B	NM_006484.1	Hs dual-specificity tyrosine-(Y)-phosphorylation regulated kinase 1B (DYRK1B), tv: c, mRNA.
-0.482	-6.772	7.72E-07	1.24E-04	5.982	2030403	OLIG1	NM_138983.1	Hs oligodendrocyte transcription factor 1 (OLIG1), mRNA.
-0.485	-5.513	1.46E-05	1.28E-03	3.108	6420017	SIN3A	NM_015477.1	Hs SIN3 homolog A, transcription regulator (yeast) (SIN3A), mRNA.
-0.486	-5.769	7.91E-06	7.93E-04	3.706	4230678	HIST2H2BE	NM_003528.2	Hs histone cluster 2, H2be (HIST2H2BE), mRNA.
-0.489	-5.960	5.03E-06	5.47E-04	4.149	7380673	MAT2B	NM_182796.1	Hs methionine adenosyltransferase II, beta (MAT2B), tv: 2, mRNA.
-0.490	-5.672	9.97E-06	9.60E-04	3.480	1690240	C5ORF4	NM_032385.3	Hs chromosome 5 open reading frame 4 (C5orf4), mRNA.
-0.491	-5.542	1.36E-05	1.22E-03	3.176	3990358	DEPDC7	NM_001077242.1	Hs DEP domain containing 7 (DEPDC7), tv: 1, mRNA.
-0.496	-5.699	9.35E-06	9.09E-04	3.543	3710647	MXD4	NM_006454.2	Hs MAX dimerization protein 4 (MXD4), mRNA.
-0.496	-5.829	6.87E-06	7.17E-04	3.844	2030324	SGK1	NM_005627.3	Hs serum/glucocorticoid regulated kinase 1 (SGK1), tv: 1, mRNA.
-0.500	-5.642	1.07E-05	1.02E-03	3.410	630400	OR51B4	NM_033179.1	Hs olfactory receptor, family 51, subfamily B, member 4 (OR51B4), mRNA.
-0.502	-6.573	1.21E-06	1.71E-04	5.540	3870543	PUM1	NM_014676.2	Hs pumilio homolog 1 (Drosophila) (PUM1), tv: 2, mRNA.
-0.509	-7.919	6.29E-08	1.61E-05	8.423	3140632	FAM117B	NM_173511.2	Hs family with sequence similarity 117, member B (FAM117B), mRNA.
-0.511	-6.577	1.20E-06	1.71E-04	5.550	770746	ETV5	NM_004454.1	Hs ets variant gene 5 (ets-related molecule) (ETV5), mRNA.
-0.512	-5.565	1.29E-05	1.18E-03	3.230	5870202	FBXO33	NM_203301.1	Hs F-box protein 33 (FBXO33), mRNA.
-0.518	-6.701	9.06E-07	1.35E-04	5.826	20358	MEIS2	NM_172315.1	Hs Meis homeobox 2 (MEIS2), tv: g, mRNA.
-0.535	-6.044	4.14E-06	4.68E-04	4.341	4150575	LETMD1	NM_001024668.1	Hs LETM1 domain containing 1 (LETMD1), tv: 2, mRNA.
-0.539	-5.604	1.17E-05	1.10E-03	3.321	3370450	BSDC1	NM_018045.5	Hs BSD domain containing 1 (BSDC1), mRNA.
-0.539	-6.515	1.39E-06	1.93E-04	5.410	7210450	LMO4	NM_006769.2	Hs LIM domain only 4 (LMO4), mRNA.
-0.540	-5.541	1.37E-05	1.22E-03	3.172	5220491	VGLL4	NM_014667.1	Hs vestigial like 4 (Drosophila) (VGLL4), mRNA.
-0.540	-8.202	3.48E-08	9.97E-06	8.996	7650209	BMF	NM_001003943.1	Hs Bcl2 modifying factor (BMF), tv: 4, mRNA.
-0.541	-9.119	5.51E-09	2.58E-06	10.773	580722	IRF2	NM_002199.3	Hs interferon regulatory factor 2 (IRF2), mRNA.
-0.542	-6.498	1.44E-06	1.98E-04	5.373	4210719	CART1	NM_006982.1	Hs cartilage paired-class homeoprotein 1 (CART1), mRNA.
-0.545	-6.877	6.08E-07	1.03E-04	6.214	130403	RNF19B	NM_153341.1	Hs ring finger protein 19B (RNF19B), mRNA.
-0.545	-7.486	1.59E-07	3.36E-05	7.523	6330730	SNAI2	NM_003068.3	Hs snail homolog 2 (Drosophila) (SNAI2), mRNA.
-0.546	-5.827	6.89E-06	7.17E-04	3.842	2470136	TLE4	NM_007005.3	Hs transducin-like enhancer of split 4 (E(sp1) homolog, Drosophila) (TLE4), mRNA.
-0.548	-5.983	4.77E-06	5.24E-04	4.203	4260189	TGIF1	NM_170695.2	Hs TGFB-induced factor homeobox 1 (TGIF1), tv: 1, mRNA.
-0.552	-6.710	8.88E-07	1.34E-04	5.845	110521	ALX1	NM_006982.2	Hs ALX homeobox 1 (ALX1), mRNA.
-0.554	-8.826	9.81E-09	3.95E-06	10.218	4070671	SOX5	NM_152989.2	Hs SRY (sex determining region Y)-box 5 (SOX5), tv: 2, mRNA.
-0.554	-7.688	1.03E-07	2.43E-05	7.945	3120292	FAM117B	NM_173511.2	Hs family with sequence similarity 117, member B (FAM117B), mRNA.

Appendix 2 – Genes differentially expressed at 3 hours in cells treated with IGF1 ligand

-0.555	-5.702	9.28E-06	9.06E-04	3.550	3190411	STARD13	NM_178006.1	Hs START domain containing 13 (STARD13), tv: alpha, mRNA.
-0.561	-7.301	2.38E-07	4.46E-05	7.130	2000504	CCDC28A	NM_015439.2	Hs coiled-coil domain containing 28A (CCDC28A), mRNA.
-0.585	-8.784	1.07E-08	4.08E-06	10.138	2060541	LOC148413	NR_015434.1	Hs hypothetical LOC148413 (LOC148413), non-coding RNA.
-0.593	-6.465	1.55E-06	2.13E-04	5.298	2490687	JMJD1C	NM_032776.1	Hs jumonji domain containing 1C (JMJD1C), tv: 1, mRNA.
-0.597	-6.196	2.90E-06	3.63E-04	4.689	2680097	YPEL5	NM_016061.1	Hs yippee-like 5 (Drosophila) (YPEL5), mRNA.
-0.601	-6.151	3.21E-06	3.95E-04	4.588	5310360	TLE4	NM_007005.3	Hs transducin-like enhancer of split 4 (E(sp1) homolog, Drosophila) (TLE4), mRNA.
-0.603	-7.388	1.96E-07	3.85E-05	7.316	4760300	ZMYND8	NM_183048.1	Hs zinc finger, MYND-type containing 8 (ZMYND8), tv: 3, mRNA.
-0.604	-9.114	5.57E-09	2.58E-06	10.763	110280	BMF	NM_033503.3	Hs Bcl2 modifying factor (BMF), tv: 2, mRNA.
-0.610	-7.028	4.35E-07	7.56E-05	6.543	6760255	MNT	NM_020310.2	Hs MAX binding protein (MNT), mRNA.
-0.612	-6.557	1.26E-06	1.77E-04	5.504	3840491	PELI2	NM_021255.2	Hs pellino homolog 2 (Drosophila) (PELI2), mRNA.
-0.619	-7.753	8.95E-08	2.19E-05	8.081	4760553	ISL1	NM_002202.1	Hs ISL1 transcription factor, LIM/homeodomain, (islet-1) (ISL1), mRNA.
-0.626	-7.369	2.05E-07	3.94E-05	7.276	5910523	LMO4	NM_006769.2	Hs LIM domain only 4 (LMO4), mRNA.
-0.626	-5.734	8.61E-06	8.56E-04	3.623	1430598	FBXO32	NM_058229.2	Hs F-box protein 32 (FBXO32), tv: 1, mRNA.
-0.627	-6.760	7.92E-07	1.24E-04	5.957	6620437	HOXA5	NM_019102.2	Hs homeobox A5 (HOXA5), mRNA.
-0.629	-9.895	1.26E-09	7.83E-07	12.185	2630554	JMY	NM_152405.2	Hs junction-mediating and regulatory protein (JMY), mRNA.
-0.630	-7.384	1.98E-07	3.85E-05	7.307	2370576	GATAD2B	NM_020699.1	Hs GATA zinc finger domain containing 2B (GATAD2B), mRNA.
-0.632	-5.774	7.83E-06	7.92E-04	3.717	5390102	SASH1	NM_015278.3	Hs SAM and SH3 domain containing 1 (SASH1), mRNA.
-0.635	-7.558	1.36E-07	3.05E-05	7.674	6110215	C12ORF76	NM_207435.1	Hs chromosome 12 open reading frame 76 (C12orf76), mRNA.
-0.635	-7.659	1.09E-07	2.56E-05	7.886	2510181	C12ORF76	NM_207435.1	Hs chromosome 12 open reading frame 76 (C12orf76), mRNA.
-0.643	-6.750	8.12E-07	1.25E-04	5.933	5080273	SOX2	NM_003106.2	Hs SRY (sex determining region Y)-box 2 (SOX2), mRNA.
-0.645	-8.324	2.71E-08	8.79E-06	9.239	5270132	CBLB	NM_170662.3	Hs Cas-Br-M (murine) ecotropic retroviral transforming sequence b (CBLB), mRNA.
-0.650	-7.454	1.70E-07	3.53E-05	7.455	5810672	SIX5	NM_175875.3	Hs SIX homeobox 5 (SIX5), mRNA.
-0.655	-6.701	9.06E-07	1.35E-04	5.826	7320471	TFAP2B	NM_003221.3	Hs transcription factor AP-2 beta (activating enhancer binding protein 2 beta) (TFAP2B), mRNA.
-0.655	-6.904	5.73E-07	9.75E-05	6.272	2640707	NR1D2	XM_001130839.1	PREDICTED: Hs nuclear receptor subfamily 1, group D, member 2 (NR1D2), mRNA.
-0.661	-7.927	6.18E-08	1.60E-05	8.440	1740373	ULK1	NM_003565.1	Hs unc-51-like kinase 1 (C. elegans) (ULK1), mRNA.
-0.667	-6.148	3.24E-06	3.96E-04	4.579	2570435	LETMD1	NM_015416.3	Hs LETM1 domain containing 1 (LETMD1), tv: 1, mRNA.
-0.670	-7.567	1.33E-07	3.02E-05	7.695	2450639	TSC22D1	NM_006022.2	Hs TSC22 domain family, member 1 (TSC22D1), tv: 2, mRNA.
-0.695	-10.606	3.47E-10	2.61E-07	13.405	770440	ULK1	NM_003565.1	Hs unc-51-like kinase 1 (C. elegans) (ULK1), mRNA.
-0.696	-9.080	5.95E-09	2.70E-06	10.699	1110465	YPEL2	NM_001005404.3	Hs yippee-like 2 (Drosophila) (YPEL2), mRNA.
-0.703	-9.016	6.75E-09	2.94E-06	10.579	1500647	SYF2	NM_015484.4	Hs SYF2 homolog, RNA splicing factor (S. cerevisiae) (SYF2), tv: 1, mRNA.
-0.710	-7.781	8.43E-08	2.08E-05	8.139	1660086	FAM100A	NM_145253.2	Hs family with sequence similarity 100, member A (FAM100A), mRNA.
-0.716	-7.412	1.86E-07	3.72E-05	7.367	4390300	TOB1	NM_005749.2	Hs transducer of ERBB2, 1 (TOB1), mRNA.
-0.732	-5.495	1.52E-05	1.33E-03	3.065	2650110	WDR48	NM_020839.2	Hs WD repeat domain 48 (WDR48), mRNA.
-0.734	-8.435	2.16E-08	7.34E-06	9.458	2690315	RNF44	NM_014901.4	Hs ring finger protein 44 (RNF44), mRNA.
-0.736	-7.528	1.45E-07	3.13E-05	7.611	4010020	ELF1	NM_172373.2	Hs E74-like factor 1 (ets domain transcription factor) (ELF1), mRNA.
-0.739	-6.940	5.29E-07	9.06E-05	6.351	4540072	C16ORF75	NM_152308.1	Hs chromosome 16 open reading frame 75 (C16orf75), mRNA.
-0.743	-6.771	7.73E-07	1.24E-04	5.981	5720040	EYA1	NM_172060.1	Hs eyes absent homolog 1 (Drosophila) (EYA1), tv: 1, mRNA.
-0.747	-8.793	1.05E-08	4.08E-06	10.154	6220180	CABC1	NM_020247.4	Hs ABC1 activity of bc1 complex homolog (S. pombe) (CABC1), mRNA.
-0.756	-7.987	5.45E-08	1.43E-05	8.562	150041	MANSC1	NM_018050.2	Hs MANSC domain containing 1 (MANSC1), mRNA.
-0.759	-9.692	1.84E-09	1.05E-06	11.822	70343	FRAT1	NM_005479.2	Hs frequently rearranged in advanced T-cell lymphomas (FRAT1), mRNA.

Appendix 2 – Genes differentially expressed at 3 hours in cells treated with IGF1 ligand

-0.761	-10.098	8.66E-10	5.89E-07	12.540	1780300	TSHZ1	NM_005786.4	Hs teashirt zinc finger homeobox 1 (TSHZ1), mRNA.
-0.762	-8.437	2.15E-08	7.34E-06	9.462	1570709	FZD7	NM_003507.1	Hs frizzled homolog 7 (Drosophila) (FZD7), mRNA.
-0.771	-7.460	1.68E-07	3.52E-05	7.468	3940148	CHMP1B	NM_020412.3	Hs chromatin modifying protein 1B (CHMP1B), mRNA.
-0.784	-11.426	8.43E-11	8.49E-08	14.734	7160435	EBF3	NM_001005463.1	Hs early B-cell factor 3 (EBF3), mRNA.
-0.785	-6.458	1.58E-06	2.13E-04	5.284	4670044	TFAP2B	NM_003221.3	Hs transcription factor AP-2 beta (activating enhancer binding protein 2 beta) (TFAP2B), mRNA.
-0.797	-8.472	2.00E-08	7.13E-06	9.532	4570524	ICK	NM_016513.3	Hs intestinal cell (MAK-like) kinase (ICK), tv: 2, mRNA.
-0.815	-9.553	2.39E-09	1.24E-06	11.572	7610746	NEUROG2	NM_024019.2	Hs neurogenin 2 (NEUROG2), mRNA.
-0.815	-8.106	4.25E-08	1.17E-05	8.802	3710397	EFNA1	NM_004428.2	Hs ephrin-A1 (EFNA1), tv: 1, mRNA.
-0.825	-8.359	2.52E-08	8.32E-06	9.308	7000142	KIAA0430	NM_014647.2	Hs KIAA0430 (KIAA0430), mRNA.
-0.828	-9.788	1.54E-09	9.03E-07	11.995	6860228	C5ORF41	NM_153607.1	Hs chromosome 5 open reading frame 41 (C5orf41), mRNA.
-0.856	-10.138	8.05E-10	5.65E-07	12.610	6400364	NR4A2	NM_006186.2	Hs nuclear receptor subfamily 4, group A, member 2 (NR4A2), tv: 1, mRNA.
-0.872	-7.294	2.42E-07	4.49E-05	7.115	520278	FAM100B	NM_182565.2	Hs family with sequence similarity 100, member B (FAM100B), mRNA.
-0.892	-8.242	3.21E-08	9.43E-06	9.076	3870603	ZSWIM4	NM_023072.1	Hs zinc finger, SWIM-type containing 4 (ZSWIM4), mRNA.
-0.893	-7.218	2.85E-07	5.22E-05	6.953	630091	NCOA7	NM_181782.2	Hs nuclear receptor coactivator 7 (NCOA7), mRNA.
-0.911	-11.212	1.21E-10	1.10E-07	14.396	5260754	TSC22D1	NM_006022.2	Hs TSC22 domain family, member 1 (TSC22D1), tv: 2, mRNA.
-0.916	-7.689	1.03E-07	2.43E-05	7.948	130309	CDKN1B	NM_004064.2	Hs cyclin-dependent kinase inhibitor 1B (p27, Kip1) (CDKN1B), mRNA.
-0.919	-9.949	1.14E-09	7.29E-07	12.280	670397	BRD8	NM_183359.1	Hs bromodomain containing 8 (BRD8), tv: 3, mRNA.
-0.919	-11.697	5.37E-11	6.15E-08	15.155	3420689	BRD8	NM_183359.1	Hs bromodomain containing 8 (BRD8), tv: 3, mRNA.
-0.940	-9.432	3.01E-09	1.52E-06	11.353	6840491	C5ORF41	NM_153607.1	Hs chromosome 5 open reading frame 41 (C5orf41), mRNA.
-0.962	-11.083	1.51E-10	1.27E-07	14.188	540390	ALPK1	NM_025144.2	Hs alpha-kinase 1 (ALPK1), mRNA.
-0.967	-13.114	5.71E-12	1.03E-08	17.218	7330026	FRAT2	NM_012083.2	Hs frequently rearranged in advanced T-cell lymphomas 2 (FRAT2), mRNA.
-0.971	-11.416	8.59E-11	8.49E-08	14.717	1410408	ARID5B	NM_032199.1	Hs AT rich interactive domain 5B (MRF1-like) (ARID5B), mRNA.
-0.972	-9.583	2.26E-09	1.20E-06	11.627	6200692	FOXO3	NM_201559.2	Hs forkhead box O3 (FOXO3), tv: 2, mRNA.
-1.063	-10.912	2.03E-10	1.64E-07	13.911	4850142	KIAA1370	NM_019600.2	Hs KIAA1370 (KIAA1370), mRNA.
-1.096	-11.647	5.84E-11	6.35E-08	15.078	6220113	DEPDC7	NM_139160.2	Hs DEP domain containing 7 (DEPDC7), tv: 2, mRNA.
-1.294	-14.610	6.52E-13	2.37E-09	19.170	3310504	PDK4	NM_002612.3	Hs pyruvate dehydrogenase kinase, isozyme 4 (PDK4), mRNA.
-1.329	-12.671	1.13E-11	1.64E-08	16.596	1990079	FBXO32	NM_148177.1	Hs F-box protein 32 (FBXO32), tv: 2, mRNA.
-1.343	-17.180	2.33E-14	2.53E-10	22.062	3780270	HBP1	NM_012257.3	Hs HMG-box transcription factor 1 (HBP1), mRNA.
-1.413	-13.432	3.54E-12	7.71E-09	17.651	2630669	DEPDC7	NM_001077242.1	Hs DEP domain containing 7 (DEPDC7), tv: 1, mRNA.
-1.438	-13.283	4.43E-12	8.76E-09	17.450	1170072	ZSWIM4	NM_023072.1	Hs zinc finger, SWIM-type containing 4 (ZSWIM4), mRNA.
-1.571	-5.506	1.48E-05	1.30E-03	3.092	1240440	TXNIP	NM_006472.2	Hs thioredoxin interacting protein (TXNIP), mRNA.
-1.828	-16.848	3.49E-14	2.53E-10	21.718	1940647	HBP1	NM_012257.3	Hs HMG-box transcription factor 1 (HBP1), mRNA.

Appendix 2 – Genes differentially expressed at 3 hours in cells treated with IGF1 ligand

log2 Fold Change	Moderated t statistic	P.Value	adj.P.Value	B-statistic	Illumina ID	ILMN_Gene	RefSeq_ID	Definition
0.741	7.309	2.33E-07	2.54E-03	5.718	4290201	IL24	NM_006850.2	Hs interleukin 24 (IL24), tv: 1, mRNA.
0.623	6.143	3.27E-06	1.43E-02	3.781	5900152	NOX4	NM_016931.2	Hs NADPH oxidase 4 (NOX4), mRNA.
0.599	8.018	5.11E-08	1.11E-03	6.776	1660746	IL24	NM_181339.1	Hs interleukin 24 (IL24), tv: 2, mRNA.
0.556	6.351	2.02E-06	1.10E-02	4.143	6520347	IL24	NM_006850.2	Hs interleukin 24 (IL24), tv: 1, mRNA.
-0.404	-6.678	9.54E-07	6.92E-03	4.699	3310520	MOXD1	NM_015529.2	Hs monooxygenase, DBH-like 1 (MOXD1), tv: 2, mRNA.
-0.490	-5.670	1.00E-05	3.63E-02	2.929	7330753	ACAT2	NM_005891.2	Hs acetyl-Coenzyme A acetyltransferase 2 (ACAT2), mRNA.

Appendix 3 – Genes differentially expressed at 24 hours in cells treated with IGF1R Inhibitor (AZ12253801)

log2 Fold Change	Moderated t statistic	P.Value	adj.P.Value	B-statistic	Illumina ID	ILMN_Gene	RefSeq_ID	Definition
2.775	10.225	6.87E-10	5.34E-08	12.806	6020195	UBC	NM_021009.3	Hs ubiquitin C (UBC), mRNA.
2.628	12.131	2.65E-11	5.16E-09	16.040	1570553	IL8	NM_000584.2	Hs interleukin 8 (IL8), mRNA.
2.581	22.400	8.51E-17	6.17E-13	28.081	3850433	HSPA1B	NM_005346.3	Hs heat shock 70kDa protein 1B (HSPA1B), mRNA.
2.414	12.470	1.54E-11	3.57E-09	16.574	5860039	CALB2	NM_007088.2	Hs calbindin 2 (CALB2), tv: CALB2c, mRNA.
2.302	8.251	3.15E-08	9.03E-07	8.976	1980309	IL8	NM_000584.2	Hs interleukin 8 (IL8), mRNA.
2.302	23.659	2.63E-17	2.87E-13	29.130	520682	CPA4	NM_016352.2	Hs carboxypeptidase A4 (CPA4), mRNA.
2.268	11.642	5.88E-11	8.95E-09	15.251	770133	LOC100134265	XM_001724386.1	PREDICTED: Hs similar to calbindin 2 full length protein (LOC100134265), mRNA.
2.161	18.804	3.51E-15	1.10E-11	24.662	1010450	RNY1	NR_004391.1	Hs RNA, Ro-associated Y1 (RNY1), small cytoplasmic RNA.
2.046	7.288	2.45E-07	4.33E-06	6.917	3520168	HS.579631		AGENCOURT_10229596 NIH_MGC_141 Hs cDNA clone IMAGE:6563923 5, mRNA sequence
2.007	16.274	7.15E-14	7.38E-11	21.805	1990577	GCLM	NM_002061.2	Hs glutamate-cysteine ligase, modifier subunit (GCLM), mRNA.
1.988	12.641	1.18E-11	3.14E-09	16.837	6370246	LOC644350	XM_927511.3	PREDICTED: Hs hypothetical LOC644350 (LOC644350), mRNA.
1.960	25.271	6.36E-18	1.38E-13	30.380	1070079	RNY4	NR_004393.1	Hs RNA, Ro-associated Y4 (RNY4), small cytoplasmic RNA.
1.910	11.022	1.68E-10	1.92E-08	14.210	830349	SNORD33	NR_000020.1	Hs small nucleolar RNA, C/D box 33 (SNORD33), small nucleolar RNA.
1.908	19.805	1.17E-15	6.38E-12	25.682	6380717	HSPA1A	NM_005345.4	Hs heat shock 70kDa protein 1A (HSPA1A), mRNA.
1.886	13.655	2.55E-12	1.11E-09	18.342	5080021	BIRC3	NM_001165.3	Hs baculoviral IAP repeat-containing 3 (BIRC3), tv: 1, mRNA.
1.843	10.340	5.58E-10	4.57E-08	13.013	5340224	SYPL1	NM_006754.2	Hs synaptophysin-like 1 (SYPL1), tv: 1, mRNA.
1.834	15.914	1.13E-13	9.80E-11	21.362	5570102	DKK1	NM_012242.2	Hs dickkopf homolog 1 (Xenopus laevis) (DKK1), mRNA.
1.757	9.871	1.32E-09	8.30E-08	12.158	6660601	HMOX1	NM_002133.1	Hs heme oxygenase (decycling) 1 (HMOX1), mRNA.
1.692	10.821	2.38E-10	2.49E-08	13.863	3940673	LOC728285	XM_001127070.1	PREDICTED: Hs similar to keratin associated protein 2-4 (LOC728285), mRNA.
1.685	18.378	5.68E-15	1.37E-11	24.210	2750050	RNY5	NR_001571.2	Hs RNA, Ro-associated Y5 (RNY5), small cytoplasmic RNA.
1.676	8.738	1.17E-08	4.31E-07	9.970	2470463	C11ORF54	NM_014039.2	Hs chromosome 11 open reading frame 54 (C11orf54), mRNA.
1.672	13.250	4.65E-12	1.69E-09	17.753	7050326	CDKN2D	NM_079421.2	Hs cyclin-dependent kinase inhibitor 2D (p19, inhibits CDK4) (CDKN2D), tv: 2, mRNA.
1.671	12.937	7.47E-12	2.23E-09	17.287	5690687	CTGF	NM_001901.1	Hs connective tissue growth factor (CTGF), mRNA.
1.612	10.973	1.83E-10	2.03E-08	14.126	6650079	C3ORF14	NM_020685.3	Hs chromosome 3 open reading frame 14 (C3orf14), mRNA.
1.575	11.247	1.14E-10	1.46E-08	14.593	3440253	SNAP25	NM_130811.1	Hs synaptosomal-associated protein, 25kDa (SNAP25), tv: 2, mRNA.
1.568	8.919	8.16E-09	3.29E-07	10.332	5490066	RPS26	NM_001029.3	Hs ribosomal protein S26 (RPS26), mRNA.
1.556	13.043	6.36E-12	2.01E-09	17.446	2230746	ABCC2	NM_000392.1	Hs ATP-binding cassette, sub-family C (CFTR/MRP), member 2 (ABCC2), mRNA.
1.546	8.791	1.05E-08	4.05E-07	10.076	4010270	LOC440731	XM_933693.2	PREDICTED: Hs hypothetical LOC440731, tv: 2 (LOC440731), mRNA.

Appendix 4 – Genes differentially expressed at 24 hours in cells treated with IGF1 ligand

1.527	9.920	1.20E-09	7.76E-08	12.249	870379	ZFAND2A	NM_182491.1	Hs zinc finger, AN1-type domain 2A (ZFAND2A), mRNA.
1.514	12.572	1.32E-11	3.22E-09	16.731	5720039	CXCL1	NM_001511.1	Hs chemokine (C-X-C motif) ligand 1 (melanoma growth stimulating activity, alpha) (CXCL1), mRNA.
1.504	14.406	8.67E-13	4.49E-10	19.394	5290397	CLCF1	NM_013246.2	Hs cardiotrophin-like cytokine factor 1 (CLCF1), tv: 1, mRNA.
1.475	10.348	5.50E-10	4.52E-08	13.028	3400019	RGS2	NM_002923.1	Hs regulator of G-protein signalling 2, 24kDa (RGS2), mRNA.
1.465	14.353	9.34E-13	4.73E-10	19.322	3890523	IL7R	XM_937367.1	PREDICTED: Hs interleukin 7 receptor (IL7R), mRNA.
1.457	13.044	6.35E-12	2.01E-09	17.447	7210632	AKR1C3	NM_003739.4	Hs aldo-keto reductase family 1, member C3 (3-alpha hydroxysteroid dehydrogenase, type II) (AKR1C3), m
1.456	9.993	1.05E-09	7.04E-08	12.382	4830520	KRT80	NM_182507.2	Hs keratin 80 (KRT80), tv: 1, mRNA.
1.456	11.158	1.33E-10	1.61E-08	14.443	4880673	GADD45A	NM_001924.2	Hs growth arrest and DNA-damage-inducible, alpha (GADD45A), mRNA.
1.454	9.163	5.06E-09	2.33E-07	10.810	2640292	CTGF	NM_001901.2	Hs connective tissue growth factor (CTGF), mRNA.
1.448	9.457	2.87E-09	1.45E-07	11.377	830619	DDIT3	NM_004083.4	Hs DNA-damage-inducible transcript 3 (DDIT3), mRNA.
1.444	9.770	1.59E-09	9.55E-08	11.969	3170068	APOBEC3B	NM_004900.3	Hs apolipoprotein B mRNA editing enzyme, catalytic polypeptide-like 3B (APOBEC3B), mRNA.
1.429	10.430	4.75E-10	4.08E-08	13.175	5810685	THBS1	NM_003246.2	Hs thrombospondin 1 (THBS1), mRNA.
1.422	8.294	2.88E-08	8.38E-07	9.065	5310161	MTHFD2L	NM_001004346.2	Hs methylenetetrahydrofolate dehydrogenase (NADP+ dependent) 2-like (MTHFD2L), mRNA.
1.422	11.655	5.76E-11	8.82E-09	15.273	2710370	SSR2	XM_945430.1	PREDICTED: Hs signal sequence receptor, beta (translocon-associated protein beta), tv: 4 (SSR2), mRNA.
1.421	10.715	2.87E-10	2.80E-08	13.678	780021	OPN3	NM_014322.2	Hs opsin 3 (OPN3), mRNA.
1.415	7.236	2.74E-07	4.71E-06	6.803	3360370	C11ORF54	NM_014039.2	Hs chromosome 11 open reading frame 54 (C11orf54), mRNA.
1.413	9.223	4.50E-09	2.12E-07	10.927	3780674	ZNF503	NM_032772.3	Hs zinc finger protein 503 (ZNF503), mRNA.
1.407	12.388	1.76E-11	3.79E-09	16.445	3440021	C21ORF51	NM_001042401.1	Hs chromosome 21 open reading frame 51 (C21orf51), tv: 2, mRNA.
1.401	12.542	1.38E-11	3.33E-09	16.685	5960358	PELO	NM_015946.4	Hs pelota homolog (Drosophila) (PELO), mRNA.
1.399	13.467	3.36E-12	1.36E-09	18.071	2810592	UPF2	NM_080599.1	Hs UPF2 regulator of nonsense transcripts homolog (yeast) (UPF2), tv: 1, mRNA.
1.389	9.150	5.19E-09	2.37E-07	10.784	4010086	OKL38	NM_013370.2	Hs pregnancy-induced growth inhibitor (OKL38), tv: 1, mRNA.
1.381	8.973	7.34E-09	3.04E-07	10.438	3060605	PRRG2	NM_000951.1	Hs proline rich Gla (G-carboxyglutamic acid) 2 (PRRG2), mRNA.
1.380	13.019	6.60E-12	2.05E-09	17.410	5860348	SC4MOL	NM_001017369.1	Hs sterol-C4-methyl oxidase-like (SC4MOL), tv: 2, mRNA.
1.369	9.249	4.28E-09	2.04E-07	10.978	3190537	POLR2J3	NM_001097615.1	Hs polymerase (RNA) II (DNA directed) polypeptide J3 (POLR2J3), mRNA.
1.369	9.539	2.46E-09	1.29E-07	11.533	6960402	LOC644100	XM_937388.1	PREDICTED: Hs similar to CG14464-PA.3 (LOC644100), mRNA.
1.361	12.269	2.12E-11	4.32E-09	16.259	6250192	COL6A3	NM_057165.2	Hs collagen, type VI, alpha 3 (COL6A3), tv: 3, mRNA.
1.358	9.026	6.62E-09	2.78E-07	10.542	6200072	GPR19	NM_006143.1	Hs G protein-coupled receptor 19 (GPR19), mRNA.
1.353	8.024	5.05E-08	1.29E-06	8.503	5690670	SNORA14B	NR_002956.1	Hs small nucleolar RNA, H/ACA box 14B (SNORA14B), small nucleolar RNA.
1.343	11.110	1.44E-10	1.72E-08	14.360	6040433	SYP	NM_003179.2	Hs synaptophysin (SYP), mRNA.
1.337	10.055	9.38E-10	6.60E-08	12.496	6550026	TICAM2	NM_021649.3	Hs toll-like receptor adaptor molecule 2 (TICAM2), mRNA.
1.337	9.276	4.06E-09	1.95E-07	11.031	4780504	RNU6-15	NR_028372.1	Hs RNA, U6 small nuclear 15 (RNU6-15), small nuclear RNA.
1.337	13.870	1.86E-12	8.27E-10	18.649	4220180	WDR68	NM_001003725.1	Hs WD repeat domain 68 (WDR68), tv: 2, mRNA.
1.330	10.184	7.40E-10	5.65E-08	12.732	3390082	LOC644100	XM_927327.1	PREDICTED: Hs similar to CG14464-PA.3 (LOC644100), mRNA.
1.325	12.694	1.09E-11	2.96E-09	16.918	60079	DNAJB1	NM_006145.1	Hs DnaJ (Hsp40) homolog, subfamily B, member 1 (DNAJB1), mRNA.
1.320	8.769	1.10E-08	4.16E-07	10.031	6380037	LOC100130516	XM_001720343.1	PREDICTED: Hs hypothetical protein LOC100130516 (LOC100130516), mRNA.
1.317	10.542	3.89E-10	3.51E-08	13.373	4670575	HTATIP2	NM_006410.3	Hs HIV-1 Tat interactive protein 2, 30kDa (HTATIP2), mRNA.
1.315	10.403	4.98E-10	4.25E-08	13.127	670255	GADD45A	NM_001924.2	Hs growth arrest and DNA-damage-inducible, alpha (GADD45A), mRNA.
1.315	9.354	3.50E-09	1.73E-07	11.179	1770402	PIR	NM_001018109.1	Hs pirin (iron-binding nuclear protein) (PIR), tv: 2, mRNA.
1.313	10.425	4.79E-10	4.10E-08	13.166	60630	GLA	NM_000169.2	Hs galactosidase, alpha (GLA), mRNA.
1.312	13.441	3.50E-12	1.38E-09	18.033	2640670	IDI1	NM_004508.2	Hs isopentenyl-diphosphate delta isomerase 1 (IDI1), mRNA.

Appendix 4 – Genes differentially expressed at 24 hours in cells treated with IGF1 ligand

1.309	11.442	8.21E-11	1.12E-08	14.921	2120037	PIR	NM_001018109.1	Hs pirin (iron-binding nuclear protein) (PIR), tv: 2, mRNA.
1.306	8.725	1.20E-08	4.40E-07	9.944	1010068	FKBP2	NM_004470.2	Hs FK506 binding protein 2, 13kDa (FKBP2), tv: 1, mRNA.
1.304	10.690	2.99E-10	2.88E-08	13.635	5670465	ADM	NM_001124.1	Hs adrenomedullin (ADM), mRNA.
1.301	15.003	3.80E-13	2.50E-10	20.196	6900398	FDPS	NM_002004.2	Hs farnesyl diphosphate synthase (farnesyl pyrophosphate synthetase, dimethylallyltranstransferase, geranylt
1.300	9.997	1.04E-09	7.01E-08	12.389	3830746	UQCRB	NM_006294.2	Hs ubiquinol-cytochrome c reductase binding protein (UQCRB), mRNA.
1.286	12.809	9.10E-12	2.64E-09	17.094	5550056	MRPL21	NM_181512.1	Hs mitochondrial ribosomal protein L21 (MRPL21), nuclear gene encoding mitochondrial protein, tv: 2, mR
1.282	8.327	2.69E-08	8.00E-07	9.134	6420465	GABARAPL1	NM_031412.2	Hs GABA(A) receptor-associated protein like 1 (GABARAPL1), mRNA.
1.275	10.509	4.12E-10	3.63E-08	13.316	3060255	BIRC3	NM_182962.1	Hs baculoviral IAP repeat-containing 3 (BIRC3), tv: 2, mRNA.
1.264	9.735	1.70E-09	9.95E-08	11.904	6980142	HS.571245		603034918F1 NIH_MGC_115 Hs cDNA clone IMAGE:5175893 5, mRNA sequence
1.264	10.493	4.24E-10	3.71E-08	13.287	1090538	LOC100128737	XM_001718329.1	PREDICTED: Hs hypothetical protein LOC100128737 (LOC100128737), mRNA.
1.263	9.780	1.56E-09	9.46E-08	11.987	6620750	ZC3HAV1	NM_020119.3	Hs zinc finger CCCH-type, antiviral 1 (ZC3HAV1), tv: 1, mRNA.
1.261	7.351	2.13E-07	3.89E-06	7.056	3460301	TAC1	NM_013997.1	Hs tachykinin, precursor 1 (substance K, substance P, neurokinin 1, neurokinin 2, neuromedin L, neurokinin
1.230	6.510	1.40E-06	1.76E-05	5.164	6860594	TAC1	NM_013996.1	Hs tachykinin, precursor 1 (substance K, substance P, neurokinin 1, neurokinin 2, neuromedin L, neurokinin
1.227	11.207	1.22E-10	1.55E-08	14.526	5900288	LOC728510	XM_001714650.1	PREDICTED: Hs hypothetical LOC728510 (LOC728510), mRNA.
1.222	7.714	9.72E-08	2.12E-06	7.845	2350465	RPL29	NM_000992.2	Hs ribosomal protein L29 (RPL29), mRNA.
1.214	5.926	5.46E-06	5.23E-05	3.801	3130397	TAC1	NM_003182.1	Hs tachykinin, precursor 1 (substance K, substance P, neurokinin 1, neurokinin 2, neuromedin L, neurokinin
1.214	12.810	9.09E-12	2.64E-09	17.094	3120598	AKR1C4	NM_001818.2	Hs aldo-keto reductase family 1, member C4 (chlordecone reductase; 3-alpha hydroxysteroid dehydrogenase,
1.213	16.344	6.55E-14	7.25E-11	21.889	6220739	GRAMD1B	NM_020716.1	Hs GRAM domain containing 1B (GRAMD1B), mRNA.
1.211	12.416	1.68E-11	3.74E-09	16.488	630086	CCDC23	NM_199342.1	Hs coiled-coil domain containing 23 (CCDC23), mRNA.
1.207	10.505	4.16E-10	3.65E-08	13.308	4610348	SGOL1	NM_138484.2	Hs shugoshin-like 1 (S. pombe) (SGOL1), tv: C2, mRNA.
1.200	12.714	1.05E-11	2.90E-09	16.949	1340400	C6ORF129	NM_138493.2	Hs chromosome 6 open reading frame 129 (C6orf129), mRNA.
1.200	9.112	5.59E-09	2.48E-07	10.711	2350091	LPXN	NM_004811.1	Hs leupaxin (LPXN), mRNA.
1.199	7.263	2.58E-07	4.49E-06	6.863	4230360	AP3B2	NM_004644.3	Hs adaptor-related protein complex 3, beta 2 subunit (AP3B2), mRNA.
1.197	9.568	2.32E-09	1.26E-07	11.589	3610279	RNU6-1	NR_004394.1	Hs RNA, U6 small nuclear 1 (RNU6-1), small nuclear RNA.
1.186	9.111	5.59E-09	2.48E-07	10.710	360192	INSIG1	NM_198336.1	Hs insulin induced gene 1 (INSIG1), tv: 2, mRNA.
1.185	16.929	3.16E-14	4.58E-11	22.586	2630474	MLLT11	NM_006818.3	Hs myeloid/lymphoid or mixed-lineage leukemia (trithorax homolog, Drosophila); translocated to, 11 (MLL
1.176	8.343	2.60E-08	7.78E-07	9.167	6220209	DMBT1	NM_017579.1	Hs deleted in malignant brain tumors 1 (DMBT1), tv: 3, mRNA.
1.174	8.680	1.31E-08	4.68E-07	9.854	2450167	RPL29	NM_000992.2	Hs ribosomal protein L29 (RPL29), mRNA.
1.173	8.322	2.72E-08	8.06E-07	9.124	5130594	WDR81	NM_152348.1	Hs WD repeat domain 81 (WDR81), mRNA.
1.167	7.789	8.30E-08	1.86E-06	8.004	2510253	C10ORF35	NM_145306.2	Hs chromosome 10 open reading frame 35 (C10orf35), mRNA.
1.167	8.536	1.76E-08	5.79E-07	9.562	2710161	SELK	NM_021237.3	Hs selenoprotein K (SELK), mRNA.
1.160	8.926	8.05E-09	3.26E-07	10.345	840253	ALDH2	NM_000690.2	Hs aldehyde dehydrogenase 2 family (mitochondrial) (ALDH2), nuclear gene encoding mitochondrial protei
1.158	12.601	1.26E-11	3.16E-09	16.775	1410113	ARL4A	NM_005738.3	Hs ADP-ribosylation factor-like 4A (ARL4A), tv: 1, mRNA.
1.156	7.291	2.43E-07	4.31E-06	6.924	6510367	JUN	NM_002228.3	Hs jun oncogene (JUN), mRNA.
1.154	10.594	3.55E-10	3.26E-08	13.465	2750685	LOC392437	XR_017149.2	PREDICTED: Hs misc_RNA (LOC392437), miscRNA.
1.150	9.124	5.46E-09	2.44E-07	10.735	3780717	SRXN1	NM_080725.1	Hs sulfiredoxin 1 homolog (S. cerevisiae) (SRXN1), mRNA.
1.143	9.837	1.40E-09	8.64E-08	12.095	4200037	SC4MOL	NM_006745.3	Hs sterol-C4-methyl oxidase-like (SC4MOL), tv: 1, mRNA.
1.143	9.436	2.99E-09	1.51E-07	11.337	1710504	NFKB2	NM_001077493.1	Hs nuclear factor of kappa light polypeptide gene enhancer in B-cells 2 (p49/p100) (NFKB2), tv: 3, mRNA.
1.137	9.296	3.91E-09	1.89E-07	11.069	1780719	PTGES3	NM_006601.4	Hs prostaglandin E synthase 3 (cytosolic) (PTGES3), mRNA.
1.136	9.240	4.35E-09	2.07E-07	10.961	670075	SNAP25	NM_130811.1	Hs synaptosomal-associated protein, 25kDa (SNAP25), tv: 2, mRNA.

Appendix 4 – Genes differentially expressed at 24 hours in cells treated with IGF1 ligand

1.133	10.794	2.49E-10	2.57E-08	13.817	7570673	UPP1	NM_003364.2	Hs uridine phosphorylase 1 (UPP1), tv: 1, mRNA.
1.131	8.306	2.81E-08	8.26E-07	9.091	730528	PLAUR	NM_002659.2	Hs plasminogen activator, urokinase receptor (PLAUR), tv: 1, mRNA.
1.129	9.633	2.06E-09	1.15E-07	11.711	6330753	XAGE1B	NM_001097595.1	Hs X antigen family, member 1B (XAGE1B), tv: 1, mRNA.
1.126	7.845	7.36E-08	1.70E-06	8.124	4780128	ATF3	NM_001040619.1	Hs activating transcription factor 3 (ATF3), tv: 4, mRNA.
1.116	10.731	2.79E-10	2.76E-08	13.706	3310615	NFKB2	NM_002502.3	Hs nuclear factor of kappa light polypeptide gene enhancer in B-cells 2 (p49/p100) (NFKB2), tv: 2, mRNA.
1.116	15.073	3.45E-13	2.42E-10	20.288	3850494	C9ORF25	NM_147202.1	Hs chromosome 9 open reading frame 25 (C9orf25), mRNA.
1.107	12.531	1.40E-11	3.36E-09	16.667	2370068	UBE2I	NM_194261.1	Hs ubiquitin-conjugating enzyme E2I (UBC9 homolog, yeast) (UBE2I), tv: 4, mRNA.
1.106	8.937	7.87E-09	3.21E-07	10.367	3840382	LOC643100	XM_931316.1	PREDICTED: Hs hypothetical protein LOC643100 (LOC643100), mRNA.
1.106	11.627	6.04E-11	9.02E-09	15.226	1940296	LOC387841	XM_932678.1	PREDICTED: Hs similar to ribosomal protein L13a, tv: 2 (LOC387841), mRNA.
1.106	7.667	1.08E-07	2.29E-06	7.743	5960411	BCYRN1	NR_001568.1	Hs brain cytoplasmic RNA 1 (non-protein coding) (BCYRN1), non-coding RNA.
1.104	6.303	2.26E-06	2.57E-05	4.684	270605	STRA13	NM_144998.2	Hs stimulated by retinoic acid 13 homolog (mouse) (STRA13), mRNA.
1.102	7.393	1.94E-07	3.64E-06	7.148	3520092	BAX	NM_138765.2	Hs BCL2-associated X protein (BAX), tv: sigma, mRNA.
1.101	11.140	1.37E-10	1.66E-08	14.412	7150128	SGOL1	NM_001012413.1	Hs shugoshin-like 1 (S. pombe) (SGOL1), tv: C1, mRNA.
1.098	12.007	3.24E-11	5.86E-09	15.842	4760747	TPST1	NM_003596.2	Hs tyrosylprotein sulfotransferase 1 (TPST1), mRNA.
1.096	12.363	1.83E-11	3.90E-09	16.405	7610433	SLC1A5	NM_005628.1	Hs solute carrier family 1 (neutral amino acid transporter), member 5 (SLC1A5), mRNA.
1.096	10.945	1.92E-10	2.12E-08	14.079	4490356	ULBP2	NM_025217.2	Hs UL16 binding protein 2 (ULBP2), mRNA.
1.086	7.122	3.52E-07	5.77E-06	6.551	7330544	ALDOC	NM_005165.2	Hs aldolase C, fructose-bisphosphate (ALDOC), mRNA.
1.086	11.180	1.28E-10	1.58E-08	14.480	1050762	TNFRSF10A	NM_003844.2	Hs tumor necrosis factor receptor superfamily, member 10a (TNFRSF10A), mRNA.
1.086	10.618	3.40E-10	3.15E-08	13.508	7650441	FGFBP1	NM_005130.3	Hs fibroblast growth factor binding protein 1 (FGFBP1), mRNA.
1.083	9.564	2.34E-09	1.26E-07	11.582	1990630	TRIB3	NM_021158.3	Hs tribbles homolog 3 (Drosophila) (TRIB3), mRNA.
1.080	12.955	7.27E-12	2.22E-09	17.314	6290609	RPS15	NM_001018.3	Hs ribosomal protein S15 (RPS15), mRNA.
1.080	10.998	1.75E-10	1.97E-08	14.169	630095	LOC651621	XM_940809.1	PREDICTED: Hs similar to hydroxysteroid (17-beta) dehydrogenase 7 (LOC651621), mRNA.
1.075	9.935	1.17E-09	7.62E-08	12.276	4590121	TRAPPC2P1	NR_002166.1	Hs trafficking protein particle complex 2 pseudogene 1 (TRAPPC2P1), non-coding RNA.
1.075	13.356	3.97E-12	1.51E-09	17.909	1170170	STC2	NM_003714.2	Hs stanniocalcin 2 (STC2), mRNA.
1.071	7.854	7.21E-08	1.69E-06	8.144	2570019	C11ORF82	NM_145018.2	Hs chromosome 11 open reading frame 82 (C11orf82), mRNA.
1.068	8.008	5.21E-08	1.31E-06	8.470	3460424	CHKA	NM_212469.1	Hs choline kinase alpha (CHKA), tv: 2, mRNA.
1.067	9.554	2.39E-09	1.27E-07	11.563	4250577	HSPD1	NM_002156.4	Hs heat shock 60kDa protein 1 (chaperonin) (HSPD1), nuclear gene encoding mitochondrial protein, tv: 1, m
1.067	12.008	3.23E-11	5.86E-09	15.845	6760762	CCDC84	NM_198489.1	Hs coiled-coil domain containing 84 (CCDC84), mRNA.
1.067	9.680	1.88E-09	1.07E-07	11.800	2370064	ASGR1	NM_001671.2	Hs asialoglycoprotein receptor 1 (ASGR1), mRNA.
1.062	8.064	4.64E-08	1.21E-06	8.587	20500	BRF2	NM_018310.2	Hs BRF2, subunit of RNA polymerase III transcription initiation factor, BRF1-like (BRF2), mRNA.
1.053	6.692	9.24E-07	1.26E-05	5.582	6020382	KRTAP2-1	XM_926554.2	PREDICTED: Hs keratin associated protein 2-1 (KRTAP2-1), mRNA.
1.053	8.981	7.23E-09	3.01E-07	10.453	3890521	DEDD2	NM_133328.2	Hs death effector domain containing 2 (DEDD2), mRNA.
1.052	10.047	9.52E-10	6.61E-08	12.481	5340129	AKR1C2	NM_001354.4	Hs aldo-keto reductase family 1, member C2 (dihydrodiol dehydrogenase 2; bile acid binding protein; 3-alph
1.049	10.942	1.93E-10	2.12E-08	14.073	2450477	ZNF682	NM_033196.2	Hs zinc finger protein 682 (ZNF682), tv: 1, mRNA.
1.049	6.581	1.19E-06	1.54E-05	5.326	7400279	CCNA1	NM_003914.2	Hs cyclin A1 (CCNA1), mRNA.
1.048	12.355	1.85E-11	3.91E-09	16.393	1090181	LOC441050	XM_496721.2	PREDICTED: Hs similar to unactive progesterone receptor, 23 kD (LOC441050), mRNA.
1.048	9.432	3.01E-09	1.52E-07	11.330	5260014	CDKN3	NM_005192.2	Hs cyclin-dependent kinase inhibitor 3 (CDK2-associated dual specificity phosphatase) (CDKN3), mRNA.
1.048	7.266	2.57E-07	4.47E-06	6.870	2750035	NUDT2	NM_147173.1	Hs nudix (nucleoside diphosphate linked moiety X)-type motif 2 (NUDT2), tv: 3, mRNA.
1.045	10.630	3.33E-10	3.12E-08	13.529	3610753	LOC85389	NR_001453.1	Hs RNA, small nucleolar (LOC85389), non-coding RNA.
1.042	7.551	1.38E-07	2.80E-06	7.494	2900725	CYP27B1	NM_000785.3	Hs cytochrome P450, family 27, subfamily B, polypeptide 1 (CYP27B1), nuclear gene encoding mitochondri

Appendix 4 – Genes differentially expressed at 24 hours in cells treated with IGF1 ligand

1.040	8.315	2.76E-08	8.18E-07	9.108	4590020	YOD1	NM_018566.3	Hs YOD1 OTU deubiquinating enzyme 1 homolog (S. cerevisiae) (YOD1), mRNA.
1.038	9.521	2.54E-09	1.32E-07	11.500	3190148	DDIT4	NM_019058.2	Hs DNA-damage-inducible transcript 4 (DDIT4), mRNA.
1.038	11.912	3.77E-11	6.57E-09	15.690	4280113	NFKBIA	NM_020529.1	Hs nuclear factor of kappa light polypeptide gene enhancer in B-cells inhibitor, alpha (NFKBIA), mRNA.
1.038	9.392	3.25E-09	1.63E-07	11.252	3400048	IL11	NM_000641.2	Hs interleukin 11 (IL11), mRNA.
1.037	8.409	2.27E-08	7.01E-07	9.303	1440324	PPARG	NM_138712.3	Hs peroxisome proliferator-activated receptor gamma (PPARG), tv: 1, mRNA.
1.036	9.035	6.50E-09	2.76E-07	10.559	5720725	ARG2	NM_001172.3	Hs arginase, type II (ARG2), nuclear gene encoding mitochondrial protein, mRNA.
1.031	8.051	4.77E-08	1.23E-06	8.560	50538	PIM3	XM_938171.2	PREDICTED: Hs pim-3 oncogene (PIM3), mRNA.
1.030	15.334	2.43E-13	1.82E-10	20.627	7380465	DPH3	NM_001047434.1	Hs DPH3, KTI11 homolog (S. cerevisiae) (DPH3), tv: 2, mRNA.
1.029	9.025	6.62E-09	2.78E-07	10.541	2030630	SKA1	NM_145060.3	Hs spindle and kinetochore associated complex subunit 1 (SKA1), tv: 2, mRNA.
1.025	9.117	5.54E-09	2.46E-07	10.720	4280048	WFDC3	NM_181522.1	Hs WAP four-disulfide core domain 3 (WFDC3), tv: 2, mRNA.
1.023	11.589	6.42E-11	9.38E-09	15.164	2260010	RIT1	NM_006912.4	Hs Ras-like without CAAX 1 (RIT1), mRNA.
1.009	10.694	2.97E-10	2.88E-08	13.641	520201	C6ORF136	NM_145029.1	Hs chromosome 6 open reading frame 136 (C6orf136), mRNA.
1.007	10.443	4.64E-10	4.02E-08	13.198	830019	PPARG	NM_015869.4	Hs peroxisome proliferator-activated receptor gamma (PPARG), tv: 2, mRNA.
1.005	9.699	1.82E-09	1.04E-07	11.836	840048	LOC729964	XM_001723531.1	PREDICTED: Hs similar to Cks1 protein homologue (LOC729964), mRNA.
1.003	8.398	2.33E-08	7.16E-07	9.279	3440446	C9ORF156	NM_016481.3	Hs chromosome 9 open reading frame 156 (C9orf156), mRNA.
1.003	11.090	1.49E-10	1.77E-08	14.326	6100278	RFESD	NM_173362.2	Hs Rieske (Fe-S) domain containing (RFESD), mRNA.
1.003	10.489	4.27E-10	3.72E-08	13.280	3440424	LOC653820	XM_930579.2	PREDICTED: Hs similar to family with sequence similarity 72, member A, tv: 1 (LOC653820), mRNA.
0.999	11.362	9.39E-11	1.23E-08	14.787	6840075	NP	NM_000270.1	Hs nucleoside phosphorylase (NP), mRNA.
0.989	9.006	6.88E-09	2.89E-07	10.502	7050332	HSP90AA1	NM_005348.2	Hs heat shock protein 90kDa alpha (cytosolic), class A member 1 (HSP90AA1), tv: 2, mRNA.
0.989	11.610	6.20E-11	9.12E-09	15.198	6200468	CKS2	NM_001827.1	Hs CDC28 protein kinase regulatory subunit 2 (CKS2), mRNA.
0.987	9.895	1.26E-09	8.01E-08	12.202	6280176	GBE1	NM_000158.2	Hs glucan (1,4-alpha-), branching enzyme 1 (glycogen branching enzyme, Andersen disease, glycogen storag
0.987	7.643	1.13E-07	2.38E-06	7.692	150100	S100A3	NM_002960.1	Hs S100 calcium binding protein A3 (S100A3), mRNA.
0.986	11.519	7.22E-11	1.01E-08	15.048	2600546	CT45A6	NM_001017438.1	Hs cancer/testis antigen family 45, member A6 (CT45A6), mRNA.
0.985	9.622	2.10E-09	1.16E-07	11.692	3180731	MGST1	NM_020300.3	Hs microsomal glutathione S-transferase 1 (MGST1), tv: 1b, mRNA.
0.985	11.354	9.52E-11	1.24E-08	14.773	7200243	SERPINB7	NM_003784.2	Hs serpin peptidase inhibitor, clade B (ovalbumin), member 7 (SERPINB7), tv: 1, mRNA.
0.984	11.391	8.94E-11	1.19E-08	14.836	3130619	FLJ40852	NM_173677.1	Hs hypothetical protein FLJ40852 (FLJ40852), mRNA.
0.984	8.482	1.96E-08	6.31E-07	9.453	4880193	KLRG1	NM_005810.3	Hs killer cell lectin-like receptor subfamily G, member 1 (KLRG1), mRNA.
0.982	7.852	7.25E-08	1.69E-06	8.140	5720056	MED10	NM_032286.2	Hs mediator complex subunit 10 (MED10), mRNA.
0.982	7.011	4.51E-07	7.03E-06	6.302	4570458	HERPUD1	NM_001010990.1	Hs homocysteine-inducible, endoplasmic reticulum stress-inducible, ubiquitin-like domain member 1 (HERP
0.981	10.042	9.61E-10	6.63E-08	12.472	1990047	C9ORF119	NM_001040011.1	Hs chromosome 9 open reading frame 119 (C9orf119), mRNA.
0.980	8.972	7.35E-09	3.04E-07	10.436	3390544	HSP90AA1	NM_001017963.2	Hs heat shock protein 90kDa alpha (cytosolic), class A member 1 (HSP90AA1), tv: 1, mRNA.
0.979	10.542	3.89E-10	3.51E-08	13.375	4280019	MAPK13	NM_002754.3	Hs mitogen-activated protein kinase 13 (MAPK13), mRNA.
0.978	9.557	2.38E-09	1.27E-07	11.567	5420441	TNFSF9	NM_003811.2	Hs tumor necrosis factor (ligand) superfamily, member 9 (TNFSF9), mRNA.
0.977	9.764	1.61E-09	9.63E-08	11.958	6350521	DGKG	NM_001080745.1	Hs diacylglycerol kinase, gamma 90kDa (DGKG), tv: 3, mRNA.
0.977	6.045	4.12E-06	4.17E-05	4.082	2940739	RASSF1	NM_170712.1	Hs Ras association (RalGDS/AF-6) domain family 1 (RASSF1), tv: B, mRNA.
0.975	9.193	4.77E-09	2.22E-07	10.870	7330280	SPANXB2	NM_145664.1	Hs SPANX family, member B2 (SPANXB2), mRNA.
0.974	14.461	8.03E-13	4.37E-10	19.470	3170064	MICB	NM_005931.2	Hs MHC class I polypeptide-related sequence B (MICB), mRNA.
0.973	8.359	2.52E-08	7.57E-07	9.201	2900348	ZFP36	NM_003407.2	Hs zinc finger protein 36, C3H type, homolog (mouse) (ZFP36), mRNA.
0.973	11.743	4.98E-11	7.90E-09	15.416	6510327	SNORD96A	NR_002592.1	Hs small nucleolar RNA, C/D box 96A (SNORD96A), small nucleolar RNA.
0.972	7.750	9.00E-08	1.99E-06	7.922	4390615	OPN3	NM_001030011.1	Hs opsin 3 (encephalopsin, panopsin) (OPN3), tv: 2, mRNA.

Appendix 4 – Genes differentially expressed at 24 hours in cells treated with IGF1 ligand

0.972	6.853	6.43E-07	9.32E-06	5.947	6350121	RASSF1	NM_170713.2	Hs Ras association (RalGDS/AF-6) domain family member 1 (RASSF1), tv: C, mRNA.
0.971	9.212	4.60E-09	2.15E-07	10.907	7380719	IGFBP6	NM_002178.2	Hs insulin-like growth factor binding protein 6 (IGFBP6), mRNA.
0.970	11.561	6.73E-11	9.74E-09	15.117	7400608	UXT	NM_153477.1	Hs ubiquitously-expressed transcript (UXT), tv: 1, mRNA.
0.969	7.352	2.13E-07	3.89E-06	7.059	6370019	TMEM170A	NM_145254.1	Hs transmembrane protein 170A (TMEM170A), mRNA.
0.969	8.739	1.17E-08	4.31E-07	9.972	6180019	ITGB1BP1	NM_004763.3	Hs integrin beta 1 binding protein 1 (ITGB1BP1), tv: 1, mRNA.
0.968	8.759	1.12E-08	4.20E-07	10.012	520195	TMEM79	NM_032323.1	Hs transmembrane protein 79 (TMEM79), mRNA.
0.966	10.035	9.72E-10	6.70E-08	12.460	5420575	SLC3A2	NM_001013251.1	Hs solute carrier family 3 (SLC3A2), tv: 6, mRNA.
0.964	10.210	7.06E-10	5.45E-08	12.779	3060619	MED8	NM_001001654.1	Hs mediator of RNA polymerase II transcription, subunit 8 homolog (S. cerevisiae) (MED8), tv: 5, mRNA.
0.963	9.557	2.37E-09	1.27E-07	11.568	240392	HS.202577		Hs cDNA FLJ34585 fis, clone KIDNE2008758
0.962	8.844	9.47E-09	3.72E-07	10.182	3610091	CUTC	NM_015960.2	Hs cutC copper transporter homolog (E. coli) (CUTC), mRNA.
0.961	5.581	1.24E-05	0.000102988	2.979	4830273	TWF1	NM_002822.3	Hs twinfilin, actin-binding protein, homolog 1 (Drosophila) (TWF1), mRNA.
0.956	12.609	1.24E-11	3.16E-09	16.788	5080131	MGST1	NM_145792.1	Hs microsomal glutathione S-transferase 1 (MGST1), tv: 1a, mRNA.
0.954	6.488	1.47E-06	1.84E-05	5.113	6660497	HSPA14	NM_016299.2	Hs heat shock 70kDa protein 14 (HSPA14), tv: 1, mRNA.
0.953	7.945	5.96E-08	1.46E-06	8.336	3890402	SLC25A24	NM_013386.3	Hs solute carrier family 25 (mitochondrial carrier; phosphate carrier), member 24 (SLC25A24), nuclear gene
0.948	10.162	7.70E-10	5.78E-08	12.692	990717	LOC642956	XM_938166.3	PREDICTED: Hs hypothetical LOC642956 (LOC642956), mRNA.
0.946	12.715	1.05E-11	2.90E-09	16.951	3370369	SPANXB1	NM_032461.2	Hs SPANX family, member B1 (SPANXB1), mRNA.
0.945	11.680	5.53E-11	8.53E-09	15.312	2750196	CSF2	NM_000758.2	Hs colony stimulating factor 2 (granulocyte-macrophage) (CSF2), mRNA.
0.945	11.834	4.29E-11	7.22E-09	15.564	6580630	HS.123214		hd27b07.y1 Human Retina cDNA (Un-normalized, unamplified): hd/he Hs cDNA clone hd27b07 5, mRNA s
0.944	6.397	1.82E-06	2.16E-05	4.903	3140577	RNPC3	NM_017619.3	Hs RNA-binding region (RNP1, RRM) containing 3 (RNPC3), mRNA.
0.943	8.897	8.52E-09	3.40E-07	10.288	2450156	XBP1	NM_001079539.1	Hs X-box binding protein 1 (XBP1), tv: 2, mRNA.
0.942	8.383	2.40E-08	7.32E-07	9.249	5860110	RABL3	NM_173825.3	Hs RAB, member of RAS oncogene family-like 3 (RABL3), mRNA.
0.942	9.265	4.15E-09	1.98E-07	11.010	5670594	NMB	NM_021077.3	Hs neuromedin B (NMB), tv: 1, mRNA.
0.941	9.355	3.49E-09	1.73E-07	11.183	1070709	PLEKHH3	NM_024927.3	Hs pleckstrin homology domain containing, family H (with MyTH4 domain) member 3 (PLEKHH3), mRNA
0.941	6.308	2.23E-06	2.55E-05	4.696	3840554	SPOCK2	NM_014767.1	Hs sparc/osteonectin, cwcv and kazal-like domains proteoglycan (testican) 2 (SPOCK2), mRNA.
0.939	7.190	3.04E-07	5.11E-06	6.701	2260196	LOC392437	XR_037197.1	PREDICTED: Hs misc_RNA (LOC392437), miscRNA.
0.938	6.840	6.62E-07	9.54E-06	5.918	4730181	FTHL12	NR_002205.1	Hs ferritin, heavy polypeptide-like 12 (FTHL12) on chromosome 9.
0.937	8.637	1.43E-08	5.01E-07	9.766	3190102	DSN1	NM_024918.2	Hs DSN1, MIND kinetochore complex component, homolog (S. cerevisiae) (DSN1), mRNA.
0.937	7.275	2.52E-07	4.41E-06	6.889	5960504	PSMC3IP	NM_016556.1	Hs PSMC3 interacting protein (PSMC3IP), tv: 2, mRNA.
0.936	7.707	9.87E-08	2.14E-06	7.829	1660309	THOC4	NM_005782.2	Hs THO complex 4 (THOC4), mRNA.
0.936	7.103	3.68E-07	5.99E-06	6.507	1410348	ATG12	NM_004707.2	Hs ATG12 autophagy related 12 homolog (S. cerevisiae) (ATG12), mRNA.
0.936	9.342	3.58E-09	1.76E-07	11.157	990500	AVPI1	NM_021732.1	Hs arginine vasopressin-induced 1 (AVPI1), mRNA.
0.935	5.926	5.45E-06	5.23E-05	3.801	4050400	HMMR	NM_012484.1	Hs hyaluronan-mediated motility receptor (RHAMM) (HMMR), tv: 1, mRNA.
0.933	12.409	1.70E-11	3.74E-09	16.478	540703	RFESD	NM_173362.2	Hs Rieske (Fe-S) domain containing (RFESD), mRNA.
0.931	9.125	5.45E-09	2.44E-07	10.736	6860671	RPL36A	NM_021029.4	Hs ribosomal protein L36a (RPL36A), mRNA.
0.929	7.316	2.30E-07	4.12E-06	6.979	1500010	CDC20	NM_001255.2	Hs cell division cycle 20 homolog (S. cerevisiae) (CDC20), mRNA.
0.928	6.377	1.90E-06	2.24E-05	4.858	3850021	CASP4	NM_001225.3	Hs caspase 4, apoptosis-related cysteine peptidase (CASP4), tv: alpha, mRNA.
0.928	7.608	1.22E-07	2.54E-06	7.615	4250204	SLC25A3	NM_213611.1	Hs solute carrier family 25 (mitochondrial carrier; phosphate carrier), member 3 (SLC25A3), nuclear gene en
0.924	12.629	1.20E-11	3.14E-09	16.818	1510296	ASNS	NM_133436.1	Hs asparagine synthetase (ASNS), tv: 1, mRNA.
0.921	8.719	1.22E-08	4.44E-07	9.932	6660333	ORC1L	NM_004153.2	Hs origin recognition complex, subunit 1-like (yeast) (ORC1L), mRNA.
0.920	7.854	7.22E-08	1.69E-06	8.143	6560204	RFC3	NM_181558.2	Hs replication factor C (activator 1) 3, 38kDa (RFC3), tv: 2, mRNA.

Appendix 4 – Genes differentially expressed at 24 hours in cells treated with IGF1 ligand

0.920	7.992	5.40E-08	1.35E-06	8.436	7560452	AGK	NM_018238.2	Hs acylglycerol kinase (AGK), mRNA.
0.919	6.142	3.28E-06	3.47E-05	4.310	3290537	FLJ36131	XM_001722366.1	PREDICTED: Hs hypothetical protein FLJ36131, tv: 2 (FLJ36131), mRNA.
0.918	9.597	2.20E-09	1.19E-07	11.644	4920110	GADD45B	NM_015675.2	Hs growth arrest and DNA-damage-inducible, beta (GADD45B), mRNA.
0.917	13.199	5.02E-12	1.76E-09	17.678	1820594	HBEGF	NM_001945.1	Hs heparin-binding EGF-like growth factor (HBEGF), mRNA.
0.916	7.869	6.99E-08	1.65E-06	8.176	60703	RELL2	NM_173828.3	Hs RELT-like 2 (RELL2), mRNA.
0.916	6.455	1.59E-06	1.94E-05	5.038	5670468	EIF5	NM_001969.3	Hs eukaryotic translation initiation factor 5 (EIF5), tv: 1, mRNA.
0.916	9.155	5.14E-09	2.36E-07	10.795	3310482	LOC285735	NM_001037231.1	Hs hypothetical protein LOC285735 (LOC285735), mRNA.
0.913	10.726	2.81E-10	2.77E-08	13.697	1240746	WFDC3	NM_080614.1	Hs WAP four-disulfide core domain 3 (WFDC3), mRNA.
0.911	11.453	8.07E-11	1.11E-08	14.937	2000148	IFIT1	NM_001548.3	Hs interferon-induced protein with tetratricopeptide repeats 1 (IFIT1), tv: 2, mRNA.
0.911	6.694	9.20E-07	1.25E-05	5.587	5270112	HMGCS1	NM_002130.6	Hs 3-hydroxy-3-methylglutaryl-Coenzyme A synthase 1 (soluble) (HMGCS1), tv: 2, mRNA.
0.909	6.577	1.20E-06	1.55E-05	5.319	2510324	NUDT2	NM_147173.1	Hs nudix (nucleoside diphosphate linked moiety X)-type motif 2 (NUDT2), tv: 3, mRNA.
0.908	9.858	1.35E-09	8.41E-08	12.133	6330170	CHKA	NM_212469.1	Hs choline kinase alpha (CHKA), tv: 2, mRNA.
0.906	7.431	1.79E-07	3.42E-06	7.231	6590598	LOC727837	XM_001125936.1	PREDICTED: Hs similar to synovial sarcoma, X breakpoint 2 isoform b (LOC727837), mRNA.
0.906	9.657	1.96E-09	1.10E-07	11.758	7330730	C10ORF75	XR_041972.1	PREDICTED: Hs misc_RNA (C10orf75), miscRNA.
0.906	7.602	1.24E-07	2.56E-06	7.602	4730138	GPX8	NM_001008397.2	Hs glutathione peroxidase 8 (putative) (GPX8), mRNA.
0.905	6.627	1.07E-06	1.42E-05	5.432	6760133	PRMT3	NM_005788.1	Hs protein arginine methyltransferase 3 (PRMT3), mRNA.
0.902	7.691	1.02E-07	2.20E-06	7.795	7510709	CEP55	NM_018131.3	Hs centrosomal protein 55kDa (CEP55), mRNA.
0.901	12.002	3.26E-11	5.86E-09	15.835	6250397	DPH3	NM_206831.1	Hs DPH3, KTI11 homolog (S. cerevisiae) (DPH3), tv: 1, mRNA.
0.901	7.246	2.68E-07	4.63E-06	6.825	3060682	BPGM	NM_001724.3	Hs 2,3-bisphosphoglycerate mutase (BPGM), tv: 1, mRNA.
0.900	9.660	1.95E-09	1.10E-07	11.762	3140500	OPN3	NM_014322.2	Hs opsin 3 (OPN3), mRNA.
0.899	7.125	3.51E-07	5.75E-06	6.556	730286	TXNRD1	NM_001093771.1	Hs thioredoxin reductase 1 (TXNRD1), tv: 5, mRNA.
0.899	6.589	1.17E-06	1.52E-05	5.345	5570427	GLS	NM_014905.2	Hs glutaminase (GLS), mRNA.
0.896	9.545	2.43E-09	1.28E-07	11.545	3800692	LOC652683	XM_942283.2	PREDICTED: Hs similar to sperm protein associated with the nucleus, X chromosome, family member B1 (I
0.896	5.813	7.13E-06	6.54E-05	3.533	270026	RASSF1	NM_007182.4	Hs Ras association (RalGDS/AF-6) domain family member 1 (RASSF1), tv: A, mRNA.
0.892	11.694	5.40E-11	8.39E-09	15.336	2030672	LOC158160	NM_001031744.1	Hs hypothetical protein LOC158160 (LOC158160), tv: 1, mRNA.
0.891	8.758	1.12E-08	4.21E-07	10.009	2350612	PHEX	NM_000444.3	Hs phosphate regulating endopeptidase homolog, X-linked (hypophosphatemia, vitamin D resistant rickets) (
0.890	6.830	6.76E-07	9.68E-06	5.896	6420040	CYB5D1	NM_144607.3	Hs cytochrome b5 domain containing 1 (CYB5D1), mRNA.
0.890	11.908	3.80E-11	6.57E-09	15.683	650307	HAUS8	NM_033417.1	Hs HAUS augmin-like complex, subunit 8 (HAUS8), tv: 1, mRNA.
0.889	11.165	1.31E-10	1.61E-08	14.454	5090368	HSPA4	NM_198431.1	Hs heat shock 70kDa protein 4 (HSPA4), tv: 2, mRNA.
0.888	6.921	5.51E-07	8.26E-06	6.101	5720184	KLF10	NM_005655.1	Hs Kruppel-like factor 10 (KLF10), tv: 1, mRNA.
0.886	12.443	1.61E-11	3.65E-09	16.530	1400019	CPA2	NM_001869.1	Hs carboxypeptidase A2 (pancreatic) (CPA2), mRNA.
0.886	10.148	7.90E-10	5.89E-08	12.667	1400358	HAUS8	NM_001011699.1	Hs HAUS augmin-like complex, subunit 8 (HAUS8), tv: 2, mRNA.
0.885	8.026	5.03E-08	1.29E-06	8.507	1660521	SPRR2D	NM_006945.3	Hs small proline-rich protein 2D (SPRR2D), mRNA.
0.885	6.692	9.25E-07	1.26E-05	5.582	70717	CIB3	NM_054113.2	Hs calcium and integrin binding family member 3 (CIB3), mRNA.
0.885	10.990	1.77E-10	1.98E-08	14.155	5570020	RAET1G	NM_001001788.2	Hs retinoic acid early transcript 1G (RAET1G), mRNA.
0.885	5.675	9.90E-06	8.54E-05	3.204	6100192	YWHAZ	NM_003406.2	Hs tyrosine 3-monooxygenase/tryptophan 5-monooxygenase activation protein, zeta polypeptide (YWHAZ),
0.884	5.844	6.63E-06	6.17E-05	3.606	6330215	HS.493947		Hs cDNA FLJ41455 fis, clone BRSTN2012284
0.883	6.380	1.89E-06	2.23E-05	4.865	1660220	LOC283932	NM_175901.3	Hs hypothetical protein LOC283932 (LOC283932), mRNA.
0.882	10.069	9.13E-10	6.53E-08	12.523	270358	FRAS1	NM_025074.4	Hs Fraser syndrome 1 (FRAS1), mRNA.
0.881	8.069	4.59E-08	1.20E-06	8.598	10546	RPS24	NM_001026.3	Hs ribosomal protein S24 (RPS24), tv: 2, mRNA.

Appendix 4 – Genes differentially expressed at 24 hours in cells treated with IGF1 ligand

0.880	8.918	8.18E-09	3.29E-07	10.329	610138	PSMB2	NM_002794.3	Hs proteasome (prosome, macropain) subunit, beta type, 2 (PSMB2), mRNA.
0.880	6.679	9.53E-07	1.29E-05	5.551	650300	CCDC86	NM_024098.1	Hs coiled-coil domain containing 86 (CCDC86), mRNA.
0.879	9.049	6.32E-09	2.70E-07	10.587	780528	CKS2	NM_001827.1	Hs CDC28 protein kinase regulatory subunit 2 (CKS2), mRNA.
0.878	8.964	7.46E-09	3.08E-07	10.421	3120014	ABHD4	NM_022060.2	Hs abhydrolase domain containing 4 (ABHD4), mRNA.
0.876	8.431	2.18E-08	6.82E-07	9.347	2900377	CBR1	NM_001757.2	Hs carbonyl reductase 1 (CBR1), mRNA.
0.875	7.185	3.07E-07	5.16E-06	6.690	2640324	SLC46A3	NM_181785.2	Hs solute carrier family 46, member 3 (SLC46A3), mRNA.
0.874	7.865	7.06E-08	1.66E-06	8.166	1660575	PPT2	NM_138717.1	Hs palmitoyl-protein thioesterase 2 (PPT2), tv: 2, mRNA.
0.874	8.246	3.18E-08	9.05E-07	8.967	6290086	NSUN3	NM_022072.3	Hs NOP2/Sun domain family, member 3 (NSUN3), mRNA.
0.874	9.229	4.45E-09	2.10E-07	10.939	940482	LOC100128309	XM_001717579.1	PREDICTED: Hs hypothetical protein LOC100128309 (LOC100128309), mRNA.
0.873	7.645	1.13E-07	2.38E-06	7.696	5690066	XBP1	NM_005080.2	Hs X-box binding protein 1 (XBP1), tv: 1, mRNA.
0.873	6.169	3.09E-06	3.31E-05	4.372	2030209	MTF1	NM_005955.2	Hs metal-regulatory transcription factor 1 (MTF1), mRNA.
0.870	9.050	6.31E-09	2.70E-07	10.590	1770603	TCN1	NM_001062.3	Hs transcobalamin I (vitamin B12 binding protein, R binder family) (TCN1), mRNA.
0.870	7.471	1.64E-07	3.19E-06	7.319	4120039	FTHL2	NR_002200.1	Hs ferritin, heavy polypeptide-like 2 (FTHL2) on chromosome 1.
0.869	8.910	8.31E-09	3.33E-07	10.313	5810609	KIAA1143	NM_020696.2	Hs KIAA1143 (KIAA1143), mRNA.
0.867	10.049	9.47E-10	6.61E-08	12.486	3850204	FTHL16	XR_041433.1	PREDICTED: Hs misc_RNA (FTHL16), miscRNA.
0.866	7.374	2.03E-07	3.74E-06	7.106	6220671	PLAUR	NM_001005376.1	Hs plasminogen activator, urokinase receptor (PLAUR), tv: 2, mRNA.
0.866	9.349	3.53E-09	1.74E-07	11.170	2320392	C12ORF65	NM_152269.2	Hs chromosome 12 open reading frame 65 (C12orf65), mRNA.
0.864	10.679	3.05E-10	2.90E-08	13.616	4260152	TOMM40L	NM_032174.4	Hs translocase of outer mitochondrial membrane 40 homolog (yeast)-like (TOMM40L), nuclear gene encodi
0.863	7.974	5.60E-08	1.39E-06	8.398	990162	C12ORF60	NM_175874.2	Hs chromosome 12 open reading frame 60 (C12orf60), mRNA.
0.862	10.202	7.17E-10	5.50E-08	12.764	4570451	LOC401233	NM_001013680.1	Hs similar to HIV TAT specific factor 1; cofactor required for Tat activation of HIV-1 transcription (LOC40
0.861	9.072	6.04E-09	2.62E-07	10.633	1940424	CT45A1	NM_001017417.1	Hs cancer/testis antigen family 45, member A1 (CT45A1), mRNA.
0.861	8.510	1.85E-08	6.03E-07	9.509	7650528	LOC650518	XM_937285.1	PREDICTED: Hs similar to Proteasome subunit alpha type 6 (Proteasome iota chain) (Macropain iota chain)
0.860	7.516	1.49E-07	2.96E-06	7.416	6860162	LOC441019	XM_498969.2	PREDICTED: Hs hypothetical LOC441019 (LOC441019), mRNA.
0.857	7.930	6.15E-08	1.49E-06	8.304	4640750	HIBCH	NM_198047.1	Hs 3-hydroxyisobutyryl-Coenzyme A hydrolase (HIBCH), nuclear gene encoding mitochondrial protein, tv:
0.853	12.121	2.69E-11	5.19E-09	16.024	3390326	ME1	NM_002395.3	Hs malic enzyme 1, NADP(+)-dependent, cytosolic (ME1), mRNA.
0.852	9.275	4.07E-09	1.95E-07	11.027	270196	OBFC2B	NM_024068.2	Hs oligonucleotide/oligosaccharide-binding fold containing 2B (OBFC2B), mRNA.
0.851	5.967	4.95E-06	4.82E-05	3.898	4480338	AKTIP	NM_001012398.1	Hs AKT interacting protein (AKTIP), tv: 1, mRNA.
0.850	9.098	5.74E-09	2.52E-07	10.684	6960653	SPANXA2	NM_145662.2	Hs SPANX family, member A2 (SPANXA2), mRNA.
0.848	7.702	9.98E-08	2.16E-06	7.818	3060523	NAMPT	NM_005746.2	Hs nicotinamide phosphoribosyltransferase (NAMPT), mRNA.
0.846	8.302	2.84E-08	8.31E-07	9.082	4890364	C19ORF40	NM_152266.1	Hs chromosome 19 open reading frame 40 (C19orf40), mRNA.
0.843	11.804	4.50E-11	7.42E-09	15.515	4480053	GCLM	NM_002061.2	Hs glutamate-cysteine ligase, modifier subunit (GCLM), mRNA.
0.842	10.032	9.78E-10	6.71E-08	12.454	4560164	PDLIM7	NM_213636.1	Hs PDZ and LIM domain 7 (enigma) (PDLIM7), tv: 4, mRNA.
0.839	6.117	3.48E-06	3.65E-05	4.251	7560364	LOC729779	XR_019592.2	PREDICTED: Hs misc_RNA (LOC729779), miscRNA.
0.839	8.238	3.23E-08	9.16E-07	8.951	2470161	PLEKHF1	NM_024310.4	Hs pleckstrin homology domain containing, family F (with FYVE domain) member 1 (PLEKHF1), mRNA.
0.836	8.260	3.09E-08	8.87E-07	8.997	3290609	HS.193784		Hs mRNA; cDNA DKFZp586K1922 (from clone DKFZp586K1922)
0.835	7.030	4.33E-07	6.81E-06	6.344	780187	C6ORF130	NM_145063.2	Hs chromosome 6 open reading frame 130 (C6orf130), mRNA.
0.835	7.519	1.48E-07	2.94E-06	7.424	1740753	CBWD3	NM_201453.2	Hs COBW domain containing 3 (CBWD3), mRNA.
0.833	7.293	2.42E-07	4.29E-06	6.928	2600025	PSMD14	NM_005805.3	Hs proteasome (prosome, macropain) 26S subunit, non-ATPase, 14 (PSMD14), mRNA.
0.833	10.333	5.66E-10	4.60E-08	13.001	7000692	MRPL52	NM_181306.1	Hs mitochondrial ribosomal protein L52 (MRPL52), nuclear gene encoding mitochondrial protein, tv: 6, mR
0.833	8.296	2.87E-08	8.36E-07	9.071	5960224	PTTG3P	NR_002734.1	Hs pituitary tumor-transforming 3 (pseudogene) (PTTG3P), non-coding RNA.

Appendix 4 – Genes differentially expressed at 24 hours in cells treated with IGF1 ligand

0.833	9.964	1.11E-09	7.33E-08	12.329	7160553	HOXA4	NM_002141.4	Hs homeobox A4 (HOXA4), mRNA.
0.832	7.750	9.01E-08	1.99E-06	7.921	520408	IFIT3	NM_001549.2	Hs interferon-induced protein with tetratricopeptide repeats 3 (IFIT3), mRNA.
0.832	7.829	7.61E-08	1.74E-06	8.090	4760450	C16ORF33	NM_024571.2	Hs chromosome 16 open reading frame 33 (C16orf33), mRNA.
0.832	9.618	2.11E-09	1.16E-07	11.684	4280162	SCNM1	NM_024041.2	Hs sodium channel modifier 1 (SCNM1), mRNA.
0.831	8.843	9.49E-09	3.72E-07	10.180	7160025	ING2	NM_001564.2	Hs inhibitor of growth family, member 2 (ING2), mRNA.
0.830	8.530	1.78E-08	5.84E-07	9.551	1240523	RPL41	NM_001035267.1	Hs ribosomal protein L41 (RPL41), tv: 2, mRNA.
0.830	9.031	6.54E-09	2.76E-07	10.552	5870202	FBXO33	NM_203301.1	Hs F-box protein 33 (FBXO33), mRNA.
0.829	10.529	3.98E-10	3.55E-08	13.351	6100241	C4ORF7	NM_152997.2	Hs chromosome 4 open reading frame 7 (C4orf7), mRNA.
0.829	7.354	2.12E-07	3.88E-06	7.062	6280341	PTS	NM_000317.1	Hs 6-pyruvoyltetrahydropterin synthase (PTS), mRNA.
0.828	7.939	6.04E-08	1.47E-06	8.323	870301	HKDC1	NM_025130.2	Hs hexokinase domain containing 1 (HKDC1), mRNA.
0.828	7.844	7.37E-08	1.70E-06	8.123	1240360	MRPL52	NM_180981.1	Hs mitochondrial ribosomal protein L52 (MRPL52), nuclear gene encoding mitochondrial protein, tv: 2, mR
0.827	7.535	1.43E-07	2.87E-06	7.457	5360446	MED27	NM_004269.2	Hs mediator complex subunit 27 (MED27), mRNA.
0.825	9.138	5.31E-09	2.42E-07	10.761	1440020	MVD	NM_002461.1	Hs mevalonate (diphospho) decarboxylase (MVD), mRNA.
0.824	9.792	1.53E-09	9.28E-08	12.010	6510279	DPH3	NM_001047434.1	Hs DPH3, KTI11 homolog (S. cerevisiae) (DPH3), tv: 2, mRNA.
0.823	5.943	5.24E-06	5.06E-05	3.841	2850020	DHRS2	NM_182908.3	Hs dehydrogenase/reductase (SDR family) member 2 (DHRS2), tv: 1, mRNA.
0.822	7.021	4.42E-07	6.91E-06	6.323	6560500	C10ORF75	XR_041972.1	PREDICTED: Hs misc_RNA (C10orf75), miscRNA.
0.821	8.024	5.05E-08	1.29E-06	8.503	6350348	BUB3	NM_001007793.1	Hs BUB3 budding uninhibited by benzimidazoles 3 homolog (yeast) (BUB3), tv: 2, mRNA.
0.821	7.963	5.74E-08	1.41E-06	8.374	830528	ASCC1	NM_015947.2	Hs activating signal cointegrator 1 complex subunit 1 (ASCC1), mRNA.
0.821	6.898	5.80E-07	8.60E-06	6.049	1580427	THEM2	NM_018473.2	Hs thioesterase superfamily member 2 (THEM2), mRNA.
0.820	6.243	2.60E-06	2.88E-05	4.544	5360148	LIPA	NM_000235.2	Hs lipase A, lysosomal acid, cholesterol esterase (LIPA), tv: 2, mRNA.
0.820	10.323	5.76E-10	4.64E-08	12.982	6980411	LOC100134259	NR_024452.1	Hs similar to hCG1987718 (LOC100134259), non-coding RNA.
0.819	7.968	5.67E-08	1.40E-06	8.386	7160180	UCHL3	NM_006002.3	Hs ubiquitin carboxyl-terminal esterase L3 (ubiquitin thiolesterase) (UCHL3), mRNA.
0.819	8.312	2.78E-08	8.21E-07	9.102	2710682	NQO2	NM_000904.2	Hs NAD(P)H dehydrogenase, quinone 2 (NQO2), mRNA.
0.818	7.538	1.42E-07	2.86E-06	7.463	4860240	DERPC	NM_017804.3	Hs decreased expression in renal and prostate (DERPC), mRNA.
0.816	10.672	3.09E-10	2.92E-08	13.604	7550220	S100A2	NM_005978.3	Hs S100 calcium binding protein A2 (S100A2), mRNA.
0.815	9.671	1.91E-09	1.08E-07	11.783	7210154	BIRC3	NM_001165.3	Hs baculoviral IAP repeat-containing 3 (BIRC3), tv: 1, mRNA.
0.813	10.064	9.21E-10	6.56E-08	12.514	6660369	GCNT2	NM_001491.2	Hs glucosaminyl (N-acetyl) transferase 2, I-branching enzyme (I blood group) (GCNT2), tv: 2, mRNA.
0.813	8.574	1.63E-08	5.47E-07	9.639	3940059	C20ORF29	NM_018347.1	Hs chromosome 20 open reading frame 29 (C20orf29), mRNA.
0.813	10.834	2.33E-10	2.46E-08	13.886	2970754	HAUS8	NM_033417.1	Hs HAUS augmin-like complex, subunit 8 (HAUS8), tv: 1, mRNA.
0.812	8.368	2.47E-08	7.51E-07	9.219	2030504	CSAG3B	NM_001080848.1	Hs CSAG family, member 3B (CSAG3B), mRNA.
0.812	6.791	7.39E-07	1.04E-05	5.807	4390390	PPIL3	NM_130906.1	Hs peptidylprolyl isomerase (cyclophilin)-like 3 (PPIL3), tv: PPIL3b, mRNA.
0.812	7.173	3.15E-07	5.26E-06	6.663	240437	CICE	XR_000206.4	PREDICTED: Hs cell death-inducing CIDE-like effector pseudogene (CICE), misc RNA.
0.812	5.723	8.83E-06	7.77E-05	3.319	4150148	LOC728934	XM_001128836.2	PREDICTED: Hs hypothetical LOC728934 (LOC728934), mRNA.
0.810	7.034	4.29E-07	6.76E-06	6.354	7160066	C20ORF196	NM_152504.2	Hs chromosome 20 open reading frame 196 (C20orf196), mRNA.
0.809	8.920	8.15E-09	3.29E-07	10.333	380014	SLC25A19	NM_021734.3	Hs solute carrier family 25 (mitochondrial thiamine pyrophosphate carrier), member 19 (SLC25A19), nuclea
0.809	8.602	1.54E-08	5.26E-07	9.696	3710653	TMUB2	NM_001076674.1	Hs transmembrane and ubiquitin-like domain containing 2 (TMUB2), tv: 3, mRNA.
0.808	8.123	4.10E-08	1.10E-06	8.710	1580129	MRPS7	NM_015971.2	Hs mitochondrial ribosomal protein S7 (MRPS7), nuclear gene encoding mitochondrial protein, mRNA.
0.808	7.466	1.66E-07	3.22E-06	7.307	450292	TUBB2A	NM_001069.2	Hs tubulin, beta 2A (TUBB2A), mRNA.
0.806	10.296	6.05E-10	4.83E-08	12.934	1740717	BOLA2	NM_001031827.1	Hs bolA homolog 2 (E. coli) (BOLA2), mRNA.
0.806	8.759	1.12E-08	4.20E-07	10.012	4220743	JMJD6	NM_015167.2	Hs jumonji domain containing 6 (JMJD6), tv: 2, mRNA.

Appendix 4 – Genes differentially expressed at 24 hours in cells treated with IGF1 ligand

0.805	8.290	2.90E-08	8.42E-07	9.058	7380725	GRB2	NM_002086.3	Hs growth factor receptor-bound protein 2 (GRB2), tv: 1, mRNA.
0.805	8.629	1.46E-08	5.05E-07	9.750	60148	BOLA2	NM_001031827.1	Hs bolA homolog 2 (E. coli) (BOLA2), mRNA.
0.802	9.082	5.93E-09	2.59E-07	10.652	3060059	TAF1A	NM_005681.2	Hs TATA box binding protein (TBP)-associated factor, RNA polymerase I, A, 48kDa (TAF1A), tv: 1, mRNA
0.801	9.552	2.40E-09	1.27E-07	11.558	3440689	ACYP1	NM_001107.3	Hs acylphosphatase 1, erythrocyte (common) type (ACYP1), tv: 1, mRNA.
0.801	8.423	2.21E-08	6.88E-07	9.331	5550037	CNN2	NM_201277.1	Hs calponin 2 (CNN2), tv: 2, mRNA.
0.801	6.392	1.84E-06	2.18E-05	4.891	1340075	BAG3	NM_004281.3	Hs BCL2-associated athanogene 3 (BAG3), mRNA.
0.800	12.625	1.21E-11	3.14E-09	16.812	1010161	ARL4A	NM_001037164.1	Hs ADP-ribosylation factor-like 4A (ARL4A), tv: 3, mRNA.
0.798	8.039	4.89E-08	1.26E-06	8.535	2650253	PRDX4	NM_006406.1	Hs peroxiredoxin 4 (PRDX4), mRNA.
0.798	7.000	4.62E-07	7.18E-06	6.278	4010129	CYB5R4	NM_016230.3	Hs cytochrome b5 reductase 4 (CYB5R4), mRNA.
0.796	8.064	4.65E-08	1.21E-06	8.586	1510008	GALR2	NM_003857.2	Hs galanin receptor 2 (GALR2), mRNA.
0.796	8.704	1.25E-08	4.51E-07	9.902	4050437	PTS	NM_000317.1	Hs 6-pyruvoyltetrahydropterin synthase (PTS), mRNA.
0.796	7.758	8.85E-08	1.96E-06	7.939	50382	PSMC3IP	NM_013290.5	Hs PSMC3 interacting protein (PSMC3IP), tv: 1, mRNA.
0.796	7.128	3.48E-07	5.72E-06	6.563	6040576	LOC100128163	XM_001722350.1	PREDICTED: Hs hypothetical protein LOC100128163 (LOC100128163), mRNA.
0.795	7.423	1.82E-07	3.46E-06	7.213	5910148	ACYP1	NM_001107.3	Hs acylphosphatase 1, erythrocyte (common) type (ACYP1), tv: 1, mRNA.
0.795	11.195	1.25E-10	1.56E-08	14.505	5260386	PCGF1	NM_032673.2	Hs polycomb group ring finger 1 (PCGF1), mRNA.
0.793	9.624	2.09E-09	1.16E-07	11.696	5220240	FTH1	NM_002032.2	Hs ferritin, heavy polypeptide 1 (FTH1), mRNA.
0.793	7.561	1.35E-07	2.76E-06	7.515	2360598	C1ORF31	NM_001012985.1	Hs chromosome 1 open reading frame 31 (C1orf31), mRNA.
0.793	7.542	1.41E-07	2.84E-06	7.472	4540382	ZC3HAV1	NM_020119.3	Hs zinc finger CCCH-type, antiviral 1 (ZC3HAV1), tv: 1, mRNA.
0.792	6.917	5.57E-07	8.33E-06	6.091	3870523	THAP1	NM_018105.2	Hs THAP domain containing, apoptosis associated protein 1 (THAP1), tv: 1, mRNA.
0.791	8.753	1.14E-08	4.23E-07	10.000	6510332	EPHA2	NM_004431.2	Hs EPH receptor A2 (EPHA2), mRNA.
0.791	7.965	5.71E-08	1.41E-06	8.378	4830056	ARPC5L	NM_030978.1	Hs actin related protein 2/3 complex, subunit 5-like (ARPC5L), mRNA.
0.790	6.024	4.33E-06	4.32E-05	4.032	4280661	TMUB2	NM_024107.2	Hs transmembrane and ubiquitin-like domain containing 2 (TMUB2), tv: 1, mRNA.
0.789	8.542	1.74E-08	5.74E-07	9.575	5090044	TFG	NM_006070.4	Hs TRK-fused gene (TFG), tv: 1, mRNA.
0.789	12.165	2.51E-11	5.00E-09	16.095	1980669	SNORD68	NR_002450.1	Hs small nucleolar RNA, C/D box 68 (SNORD68), small nucleolar RNA.
0.789	7.978	5.55E-08	1.38E-06	8.407	2690215	C1ORF77	NM_015607.2	Hs chromosome 1 open reading frame 77 (C1orf77), mRNA.
0.788	6.420	1.72E-06	2.07E-05	4.956	2750189	UPF2	NM_080599.1	Hs UPF2 regulator of nonsense transcripts homolog (yeast) (UPF2), tv: 1, mRNA.
0.786	7.440	1.76E-07	3.37E-06	7.250	2450020	SNORD56	NR_002739.1	Hs small nucleolar RNA, C/D box 56 (SNORD56), small nuclear RNA.
0.786	9.091	5.82E-09	2.55E-07	10.670	6840301	NT5DC2	NM_022908.1	Hs 5'-nucleotidase domain containing 2 (NT5DC2), mRNA.
0.786	9.965	1.11E-09	7.33E-08	12.332	7040470	PSMA6	NM_002791.1	Hs proteasome (prosome, macropain) subunit, alpha type, 6 (PSMA6), mRNA.
0.785	10.373	5.26E-10	4.42E-08	13.072	4280132	DSCR8	NM_203428.1	Hs Down syndrome critical region gene 8 (DSCR8), tv: 2, mRNA.
0.785	7.964	5.72E-08	1.41E-06	8.377	6280674	HAUS8	NM_033417.1	Hs HAUS augmin-like complex, subunit 8 (HAUS8), tv: 1, mRNA.
0.783	6.402	1.80E-06	2.14E-05	4.915	360475	PLAUR	NM_001005376.1	Hs plasminogen activator, urokinase receptor (PLAUR), tv: 2, mRNA.
0.782	8.411	2.26E-08	6.99E-07	9.308	4220246	CCL20	NM_004591.1	Hs chemokine (C-C motif) ligand 20 (CCL20), mRNA.
0.781	8.815	1.00E-08	3.91E-07	10.124	4760537	C20ORF24	NM_199483.1	Hs chromosome 20 open reading frame 24 (C20orf24), tv: 2, mRNA.
0.781	7.009	4.54E-07	7.06E-06	6.297	7160593	PPM1K	NM_152542.2	Hs protein phosphatase 1K (PP2C domain containing) (PPM1K), mRNA.
0.780	7.544	1.40E-07	2.83E-06	7.478	1260154	DOLPP1	NM_020438.3	Hs dolichyl pyrophosphate phosphatase 1 (DOLPP1), mRNA.
0.779	7.879	6.84E-08	1.62E-06	8.197	380528	CHORDC1	NM_012124.1	Hs cysteine and histidine-rich domain (CHORD)-containing 1 (CHORDC1), mRNA.
0.778	8.467	2.02E-08	6.45E-07	9.422	3170136	SAMD9L	NM_152703.2	Hs sterile alpha motif domain containing 9-like (SAMD9L), mRNA.
0.778	8.426	2.20E-08	6.84E-07	9.338	1430427	SNORD16	NR_002440.1	Hs small nucleolar RNA, C/D box 16 (SNORD16), small nucleolar RNA.
0.777	6.106	3.58E-06	3.72E-05	4.224	1170524	C2ORF7	NM_032319.1	Hs chromosome 2 open reading frame 7 (C2orf7), mRNA.

Appendix 4 – Genes differentially expressed at 24 hours in cells treated with IGF1 ligand

0.775	6.174	3.05E-06	3.27E-05	4.384	1230129	DDN	NM_015086.1	Hs dendrin (DDN), mRNA.
0.775	6.497	1.44E-06	1.81E-05	5.135	2710195	TARS	NM_152295.3	Hs threonyl-tRNA synthetase (TARS), mRNA.
0.774	6.680	9.50E-07	1.29E-05	5.555	4150189	CTSL1	NM_001912.3	Hs cathepsin L1 (CTSL1), tv: 1, mRNA.
0.774	7.097	3.73E-07	6.05E-06	6.494	620202	OSGIN1	NM_182980.2	Hs oxidative stress induced growth inhibitor 1 (OSGIN1), tv: 2, mRNA.
0.774	9.693	1.84E-09	1.05E-07	11.825	7040176	C20ORF24	NM_018840.2	Hs chromosome 20 open reading frame 24 (C20orf24), tv: 1, mRNA.
0.774	8.165	3.77E-08	1.03E-06	8.797	6560392	FLJ36848	XM_930136.2	PREDICTED: Hs hypothetical LOC647115 (FLJ36848), mRNA.
0.774	9.171	4.98E-09	2.31E-07	10.826	4900440	CIB1	NM_006384.2	Hs calcium and integrin binding 1 (calmyrin) (CIB1), mRNA.
0.774	8.873	8.94E-09	3.54E-07	10.240	1090102	ZNF274	NM_016324.2	Hs zinc finger protein 274 (ZNF274), tv: ZNF274b, mRNA.
0.773	7.787	8.32E-08	1.86E-06	8.001	4920398	SPPL2A	NM_032802.3	Hs signal peptide peptidase-like 2A (SPPL2A), mRNA.
0.772	9.106	5.65E-09	2.50E-07	10.699	4260253	OBFC2A	NM_001031716.1	Hs oligonucleotide/oligosaccharide-binding fold containing 2A (OBFC2A), mRNA.
0.772	7.681	1.04E-07	2.24E-06	7.773	3840397	POP1	NM_015029.1	Hs processing of precursor 1, ribonuclease P/MRP subunit (S. cerevisiae) (POP1), mRNA.
0.772	8.205	3.46E-08	9.68E-07	8.881	2230379	NAMPT	NM_005746.2	Hs nicotinamide phosphoribosyltransferase (NAMPT), mRNA.
0.771	6.820	6.93E-07	9.87E-06	5.871	940152	MKNK2	NM_017572.2	Hs MAP kinase interacting serine/threonine kinase 2 (MKNK2), tv: 1, mRNA.
0.771	6.177	3.03E-06	3.26E-05	4.391	3940477	TAP2	NM_000544.3	Hs transporter 2, ATP-binding cassette, sub-family B (MDR/TAP) (TAP2), tv: 1, mRNA.
0.771	8.016	5.13E-08	1.30E-06	8.486	460040	ATP5G1	NM_005175.2	Hs ATP synthase, H+ transporting, mitochondrial F0 complex, subunit C1 (subunit 9) (ATP5G1), nuclear ge
0.771	5.981	4.79E-06	4.69E-05	3.931	6450475	YRDC	NM_024640.3	Hs yrdC domain containing (E. coli) (YRDC), nuclear gene encoding mitochondrial protein, mRNA.
0.771	10.811	2.42E-10	2.52E-08	13.846	3870646	PDCL3	NM_024065.3	Hs phosducin-like 3 (PDCL3), mRNA.
0.770	8.961	7.51E-09	3.09E-07	10.415	2710121	LOC442597	XM_944534.1	PREDICTED: Hs hypothetical LOC442597 (LOC442597), mRNA.
0.770	8.135	4.00E-08	1.08E-06	8.736	2680706	PGAM1	NM_002629.2	Hs phosphoglycerate mutase 1 (brain) (PGAM1), mRNA.
0.770	5.763	8.04E-06	7.20E-05	3.412	460286	THOC4	XM_001134346.1	PREDICTED: Hs THO complex 4 (THOC4), mRNA.
0.769	7.553	1.37E-07	2.80E-06	7.497	730110	METTL4	NM_022840.3	Hs methyltransferase like 4 (METTL4), mRNA.
0.768	7.430	1.80E-07	3.42E-06	7.228	540215	C6ORF173	NM_001012507.1	Hs chromosome 6 open reading frame 173 (C6orf173), mRNA.
0.768	9.493	2.68E-09	1.38E-07	11.447	6130064	MEA1	NM_014623.2	Hs male-enhanced antigen 1 (MEA1), mRNA.
0.767	7.640	1.14E-07	2.40E-06	7.684	5900112	CCDC16	NM_052857.2	Hs coiled-coil domain containing 16 (CCDC16), mRNA.
0.766	7.501	1.54E-07	3.03E-06	7.384	3930592	CAP2	NM_006366.2	Hs CAP, adenylate cyclase-associated protein, 2 (yeast) (CAP2), mRNA.
0.765	7.900	6.56E-08	1.57E-06	8.240	2630743	BLOC1S2	NM_001001342.1	Hs biogenesis of lysosomal organelles complex-1, subunit 2 (BLOC1S2), tv: 2, mRNA.
0.764	6.224	2.71E-06	2.98E-05	4.501	2030162	CHTF8	NM_001040144.1	Hs CTF8, chromosome transmission fidelity factor 8 homolog (S. cerevisiae) (CHTF8), tv: 2, mRNA.
0.764	9.302	3.86E-09	1.87E-07	11.080	1990390	RAB3IP	NM_175624.2	Hs RAB3A interacting protein (rabin3) (RAB3IP), tv: beta 1, mRNA.
0.763	6.276	2.40E-06	2.70E-05	4.623	580609	ETFDH	NM_004453.1	Hs electron-transferring-flavoprotein dehydrogenase (ETFDH), nuclear gene encoding mitochondrial protein
0.763	6.146	3.25E-06	3.45E-05	4.319	1260086	ID2	NM_002166.4	Hs inhibitor of DNA binding 2, dominant negative helix-loop-helix protein (ID2), mRNA.
0.762	7.848	7.32E-08	1.70E-06	8.129	5360576	LOC100134189	XM_001722213.1	PREDICTED: Hs similar to LOC441089 protein, tv: 1 (LOC100134189), mRNA.
0.762	7.731	9.37E-08	2.06E-06	7.881	5360646	PSMC4	NM_006503.2	Hs proteasome (prosome, macropain) 26S subunit, ATPase, 4 (PSMC4), tv: 1, mRNA.
0.759	6.834	6.71E-07	9.62E-06	5.904	2470114	COL6A3	NM_004369.2	Hs collagen, type VI, alpha 3 (COL6A3), tv: 1, mRNA.
0.759	9.561	2.35E-09	1.27E-07	11.576	3930605	CYR61	NM_001554.3	Hs cysteine-rich, angiogenic inducer, 61 (CYR61), mRNA.
0.759	7.182	3.09E-07	5.18E-06	6.682	2480719	NSMCE2	NM_173685.1	Hs non-SMC element 2, MMS21 homolog (S. cerevisiae) (NSMCE2), mRNA.
0.759	7.519	1.48E-07	2.94E-06	7.422	7150692	LOC642732	XR_015408.1	PREDICTED: Hs misc_RNA (LOC642732), miscRNA.
0.759	6.701	9.07E-07	1.24E-05	5.601	3710671	KRT15	NM_002275.2	Hs keratin 15 (KRT15), mRNA.
0.759	7.176	3.13E-07	5.24E-06	6.670	4050239	KLHL18	NM_025010.3	Hs kelch-like 18 (Drosophila) (KLHL18), mRNA.
0.758	7.589	1.27E-07	2.62E-06	7.574	6650639	VAMP1	NM_199245.1	Hs vesicle-associated membrane protein 1 (synaptobrevin 1) (VAMP1), tv: 2, mRNA.
0.758	6.434	1.67E-06	2.02E-05	4.989	5570646	SCML1	NM_001037540.1	Hs sex comb on midleg-like 1 (Drosophila) (SCML1), tv: 1, mRNA.

Appendix 4 – Genes differentially expressed at 24 hours in cells treated with IGF1 ligand

0.757	9.383	3.31E-09	1.65E-07	11.235	4390301	TRPV2	NM_016113.3	Hs transient receptor potential cation channel, subfamily V, member 2 (TRPV2), mRNA.
0.757	7.226	2.80E-07	4.80E-06	6.780	4210220	TMEM111	NM_018447.1	Hs transmembrane protein 111 (TMEM111), mRNA.
0.756	6.682	9.46E-07	1.28E-05	5.558	770102	C5ORF34	NM_198566.1	Hs chromosome 5 open reading frame 34 (C5orf34), mRNA.
0.756	5.759	8.11E-06	7.25E-05	3.404	3170452	ORMDL1	NM_016467.3	Hs ORM1-like 1 (S. cerevisiae) (ORMDL1), mRNA.
0.756	9.168	5.01E-09	2.32E-07	10.820	5490019	GPX3	NM_002084.3	Hs glutathione peroxidase 3 (plasma) (GPX3), mRNA.
0.756	9.471	2.80E-09	1.42E-07	11.404	4210102	C3ORF75	NM_001031703.2	Hs chromosome 3 open reading frame 75 (C3orf75), mRNA.
0.755	6.925	5.47E-07	8.21E-06	6.109	5090491	CXORF38	NM_144970.1	Hs chromosome X open reading frame 38 (CXorf38), mRNA.
0.755	6.123	3.43E-06	3.60E-05	4.265	3990382	INO80C	NM_194281.3	Hs INO80 complex subunit C (INO80C), tv: 2, mRNA.
0.755	8.595	1.56E-08	5.31E-07	9.681	2970475	NARFL	NM_022493.1	Hs nuclear prelamin A recognition factor-like (NARFL), mRNA.
0.755	8.462	2.04E-08	6.47E-07	9.410	7210326	PSMB8	NM_004159.4	Hs proteasome (prosome, macropain) subunit, beta type, 8 (large multifunctional peptidase 7) (PSMB8), tv: 1
0.754	5.650	1.05E-05	9.00E-05	3.145	4610189	HERPUD1	NM_001010990.1	Hs homocysteine-inducible, endoplasmic reticulum stress-inducible, ubiquitin-like domain member 1 (HERP
0.754	6.069	3.90E-06	3.98E-05	4.138	670386	ID1	NM_181353.1	Hs inhibitor of DNA binding 1, dominant negative helix-loop-helix protein (ID1), tv: 2, mRNA.
0.753	7.689	1.03E-07	2.21E-06	7.791	1770519	PDRG1	NM_030815.2	Hs p53 and DNA-damage regulated 1 (PDRG1), mRNA.
0.753	9.753	1.64E-09	9.77E-08	11.938	4280343	COASY	NM_025233.5	Hs Coenzyme A synthase (COASY), nuclear gene encoding mitochondrial protein, tv: 1, mRNA.
0.753	7.785	8.36E-08	1.87E-06	7.996	3370202	ANXA2P1	NR_001562.1	Hs annexin A2 pseudogene 1 (ANXA2P1) on chromosome 4.
0.753	7.190	3.03E-07	5.11E-06	6.702	5310471	UBE2C	NM_181803.1	Hs ubiquitin-conjugating enzyme E2C (UBE2C), tv: 6, mRNA.
0.753	6.809	7.09E-07	1.01E-05	5.848	6370474	CDCA3	NM_031299.3	Hs cell division cycle associated 3 (CDCA3), mRNA.
0.752	7.902	6.52E-08	1.56E-06	8.246	4900270	EBAG9	NM_004215.3	Hs estrogen receptor binding site associated, antigen, 9 (EBAG9), tv: 1, mRNA.
0.752	7.460	1.68E-07	3.25E-06	7.296	6250280	PRDX1	NM_181696.1	Hs peroxiredoxin 1 (PRDX1), tv: 2, mRNA.
0.752	8.620	1.48E-08	5.11E-07	9.732	6220014	C3ORF75	NM_001031703.2	Hs chromosome 3 open reading frame 75 (C3orf75), mRNA.
0.751	7.418	1.84E-07	3.48E-06	7.203	1740471	TINF2	NM_012461.1	Hs TERF1 (TRF1)-interacting nuclear factor 2 (TINF2), mRNA.
0.751	7.914	6.35E-08	1.53E-06	8.272	5960181	ASNS	NM_133436.1	Hs asparagine synthetase (ASNS), tv: 1, mRNA.
0.750	7.495	1.56E-07	3.06E-06	7.371	7330392	TAP1	NM_000593.5	Hs transporter 1, ATP-binding cassette, sub-family B (MDR/TAP) (TAP1), mRNA.
0.750	5.661	1.02E-05	8.79E-05	3.170	1230048	ABCB1	NM_000927.3	Hs ATP-binding cassette, sub-family B (MDR/TAP), member 1 (ABCB1), mRNA.
0.750	7.509	1.51E-07	2.99E-06	7.402	6280152	UTP11L	NM_016037.2	Hs UTP11-like, U3 small nucleolar ribonucleoprotein, (yeast) (UTP11L), mRNA.
0.748	8.640	1.42E-08	4.99E-07	9.773	3180521	SPRYD3	NM_032840.1	Hs SPRY domain containing 3 (SPRYD3), mRNA.
0.747	7.349	2.14E-07	3.90E-06	7.051	6450647	MRPS28	NM_014018.2	Hs mitochondrial ribosomal protein S28 (MRPS28), nuclear gene encoding mitochondrial protein, mRNA.
0.747	5.860	6.38E-06	5.97E-05	3.644	2810082	C20ORF111	NM_016470.6	Hs chromosome 20 open reading frame 111 (C20orf111), mRNA.
0.747	7.078	3.89E-07	6.24E-06	6.451	5860504	CSAG3B	NM_001080848.1	Hs CSAG family, member 3B (CSAG3B), mRNA.
0.747	6.664	9.87E-07	1.32E-05	5.517	2450725	SLC3A2	NM_001013251.1	Hs solute carrier family 3 (activators of dibasic and neutral amino acid transport), member 2 (SLC3A2), tv: 6
0.747	7.816	7.82E-08	1.78E-06	8.063	2450358	CKS1B	NM_001826.1	Hs CDC28 protein kinase regulatory subunit 1B (CKS1B), mRNA.
0.746	8.166	3.76E-08	1.03E-06	8.800	270692	LOC643668	XR_016986.1	PREDICTED: Hs similar to peptidase (prosome, macropain) 26S subunit, ATPase 1 (LOC643668), mRNA.
0.745	7.112	3.61E-07	5.89E-06	6.527	1260259	LOC100131647	XM_001714166.1	PREDICTED: Hs similar to hCG1653500 (LOC100131647), mRNA.
0.744	5.988	4.72E-06	4.63E-05	3.946	6220441	CISD1	NM_018464.2	Hs CDGSH iron sulfur domain 1 (CISD1), mRNA.
0.744	7.326	2.25E-07	4.06E-06	7.001	1510468	GRPEL1	NM_025196.2	Hs GrpE-like 1, mitochondrial (E. coli) (GRPEL1), nuclear gene encoding mitochondrial protein, mRNA.
0.742	8.717	1.22E-08	4.44E-07	9.929	4210088	CKS1B	NM_001826.1	Hs CDC28 protein kinase regulatory subunit 1B (CKS1B), mRNA.
0.741	8.766	1.11E-08	4.17E-07	10.025	5080605	SNRPA1	NM_003090.2	Hs small nuclear ribonucleoprotein polypeptide A' (SNRPA1), mRNA.
0.741	9.127	5.43E-09	2.44E-07	10.740	6180446	PRDX1	NM_181696.1	Hs peroxiredoxin 1 (PRDX1), tv: 2, mRNA.
0.741	6.797	7.29E-07	1.03E-05	5.820	510239	CBWD5	NM_001024916.2	Hs COBW domain containing 5 (CBWD5), mRNA.
0.740	7.172	3.16E-07	5.27E-06	6.661	270133	C1ORF128	NM_020362.3	Hs chromosome 1 open reading frame 128 (C1orf128), mRNA.

Appendix 4 – Genes differentially expressed at 24 hours in cells treated with IGF1 ligand

0.739	7.661	1.09E-07	2.31E-06	7.730	1850739	SIRT6	NM_016539.1	Hs sirtuin (silent mating type information regulation 2 homolog) 6 (S. cerevisiae) (SIRT6), mRNA.
0.738	9.897	1.25E-09	8.00E-08	12.206	6660551	HS.575603		NISC_gf01f08.y1 NCI_CGAP_Kid12 Hs cDNA clone IMAGE:3252614 5, mRNA sequence
0.738	6.813	7.04E-07	1.00E-05	5.856	6270634	TMEM120A	NM_031925.1	Hs transmembrane protein 120A (TMEM120A), mRNA.
0.736	6.605	1.13E-06	1.47E-05	5.383	4230619	GCA	NM_012198.2	Hs grancalcin, EF-hand calcium binding protein (GCA), mRNA.
0.736	6.350	2.03E-06	2.36E-05	4.793	4280136	ADRM1	NM_175573.1	Hs adhesion regulating molecule 1 (ADRM1), tv: 2, mRNA.
0.736	9.136	5.33E-09	2.42E-07	10.757	4220544	FAM54A	NM_001099286.1	Hs family with sequence similarity 54, member A (FAM54A), tv: 1, mRNA.
0.735	8.112	4.20E-08	1.12E-06	8.687	4260392	NSDHL	NM_015922.1	Hs NAD(P) dependent steroid dehydrogenase-like (NSDHL), mRNA.
0.735	6.032	4.25E-06	4.27E-05	4.050	7550639	GNPDA2	NM_138335.1	Hs glucosamine-6-phosphate deaminase 2 (GNPDA2), mRNA.
0.734	7.785	8.37E-08	1.87E-06	7.995	4920767	FTL	NM_000146.3	Hs ferritin, light polypeptide (FTL), mRNA.
0.733	7.412	1.86E-07	3.52E-06	7.190	3440224	YRDC	NM_024640.3	Hs yrdC domain containing (E. coli) (YRDC), nuclear gene encoding mitochondrial protein, mRNA.
0.733	7.970	5.65E-08	1.40E-06	8.389	3420097	TRMU	NM_018006.4	Hs tRNA 5-methylaminomethyl-2-thiouridylate methyltransferase (TRMU), nuclear gene encoding mitochor
0.733	9.280	4.04E-09	1.94E-07	11.037	1570328	MRPL27	NM_148570.1	Hs mitochondrial ribosomal protein L27 (MRPL27), nuclear gene encoding mitochondrial protein, tv: 3, mR
0.733	10.738	2.75E-10	2.75E-08	13.718	2490017	ZC3H12A	NM_025079.1	Hs zinc finger CCCH-type containing 12A (ZC3H12A), mRNA.
0.733	7.811	7.91E-08	1.79E-06	8.052	2650164	FLJ10986	NM_018291.2	Hs hypothetical protein FLJ10986 (FLJ10986), mRNA.
0.732	6.150	3.23E-06	3.43E-05	4.327	2570035	C17ORF49	NM_174893.1	Hs chromosome 17 open reading frame 49 (C17orf49), mRNA.
0.730	7.512	1.50E-07	2.98E-06	7.407	2750202	HS.537002		Hs cDNA clone IMAGE:4811759
0.728	7.829	7.61E-08	1.74E-06	8.091	540487	PUS7L	NM_001098615.1	Hs pseudouridylate synthase 7 homolog (S. cerevisiae)-like (PUS7L), tv: 1, mRNA.
0.728	7.196	2.99E-07	5.05E-06	6.715	6020093	SARS	NM_006513.2	Hs seryl-tRNA synthetase (SARS), mRNA.
0.727	6.025	4.32E-06	4.32E-05	4.034	4200204	C9ORF37	NM_032937.3	Hs chromosome 9 open reading frame 37 (C9orf37), mRNA.
0.726	9.754	1.64E-09	9.77E-08	11.939	3060487	PSMC1	NM_002802.2	Hs proteasome (prosome, macropain) 26S subunit, ATPase, 1 (PSMC1), mRNA.
0.726	6.106	3.57E-06	3.72E-05	4.225	7330546	MED8	NM_201542.2	Hs mediator of RNA polymerase II transcription, subunit 8 homolog (S. cerevisiae) (MED8), tv: 1, mRNA.
0.726	8.373	2.45E-08	7.45E-07	9.228	4850731	TFPI	NM_006287.4	Hs tissue factor pathway inhibitor (lipoprotein-associated coagulation inhibitor) (TFPI), tv: 1, mRNA.
0.726	8.367	2.48E-08	7.51E-07	9.216	6280471	HSPA1L	NM_005527.3	Hs heat shock 70kDa protein 1-like (HSPA1L), mRNA.
0.726	6.132	3.36E-06	3.55E-05	4.286	5340050	UBE2V2	NM_003350.2	Hs ubiquitin-conjugating enzyme E2 variant 2 (UBE2V2), mRNA.
0.725	5.780	7.71E-06	6.95E-05	3.454	3520754	SGOL2	NM_152524.3	Hs shugoshin-like 2 (S. pombe) (SGOL2), mRNA.
0.724	8.703	1.25E-08	4.51E-07	9.901	6620634	UBE2S	NM_014501.2	Hs ubiquitin-conjugating enzyme E2S (UBE2S), mRNA.
0.724	6.342	2.06E-06	2.39E-05	4.777	4640239	UPF3B	NM_023010.2	Hs UPF3 regulator of nonsense transcripts homolog B (yeast) (UPF3B), tv: 2, mRNA.
0.723	6.766	7.82E-07	1.09E-05	5.750	4150048	FABP5	NM_001444.1	Hs fatty acid binding protein 5 (psoriasis-associated) (FABP5), mRNA.
0.723	8.031	4.97E-08	1.27E-06	8.518	3290017	C1ORF26	NM_017673.5	Hs chromosome 1 open reading frame 26 (C1orf26), mRNA.
0.722	6.866	6.25E-07	9.11E-06	5.975	4260075	LSM3	NM_014463.1	Hs LSM3 homolog, U6 small nuclear RNA associated (S. cerevisiae) (LSM3), mRNA.
0.721	8.459	2.05E-08	6.50E-07	9.405	160274	LOC642513	XR_016174.2	PREDICTED: Hs misc_RNA (LOC642513), miscRNA.
0.721	8.288	2.92E-08	8.45E-07	9.053	6270373	CCDC90A	NM_001031713.2	Hs coiled-coil domain containing 90A (CCDC90A), mRNA.
0.720	6.219	2.74E-06	3.00E-05	4.490	270152	SLC7A5	NM_003486.5	Hs solute carrier family 7 (cationic amino acid transporter, y+ system), member 5 (SLC7A5), mRNA.
0.720	5.970	4.92E-06	4.80E-05	3.903	4070026	KATNA1	NM_007044.2	Hs katanin p60 (ATPase-containing) subunit A 1 (KATNA1), mRNA.
0.720	6.360	1.98E-06	2.31E-05	4.817	6770541	CCDC18	NM_206886.2	Hs coiled-coil domain containing 18 (CCDC18), mRNA.
0.720	6.509	1.40E-06	1.76E-05	5.163	620168	ATG4A	NM_178270.1	Hs ATG4 autophagy related 4 homolog A (S. cerevisiae) (ATG4A), tv: 2, mRNA.
0.720	6.527	1.35E-06	1.71E-05	5.203	3870092	AKT1S1	NM_032375.2	Hs AKT1 substrate 1 (proline-rich) (AKT1S1), mRNA.
0.719	6.031	4.26E-06	4.28E-05	4.048	3180619	LOC643438	XR_015310.1	PREDICTED: Hs misc_RNA (LOC643438), miscRNA.
0.719	6.792	7.38E-07	1.04E-05	5.808	840717	CTSL1	NM_001912.3	Hs cathepsin L1 (CTSL1), tv: 1, mRNA.
0.718	8.633	1.44E-08	5.02E-07	9.759	2570379	LOC100130932	XM_001726766.1	PREDICTED: Hs similar to Sm protein G (LOC100130932), mRNA.

Appendix 4 – Genes differentially expressed at 24 hours in cells treated with IGF1 ligand

0.718	7.847	7.32E-08	1.70E-06	8.129	4560541	MLKL	NM_152649.1	Hs mixed lineage kinase domain-like (MLKL), mRNA.
0.718	6.757	7.98E-07	1.11E-05	5.729	2120201	C20ORF152	NM_080834.1	Hs chromosome 20 open reading frame 152 (C20orf152), mRNA.
0.717	7.132	3.45E-07	5.68E-06	6.572	6760685	TAF1A	NM_005681.2	Hs TATA box binding protein (TBP)-associated factor, RNA polymerase I, A, 48kDa (TAF1A), tv: 1, mRNA
0.717	8.036	4.93E-08	1.27E-06	8.527	3830095	DFFB	NM_004402.2	Hs DNA fragmentation factor, 40kDa, beta polypeptide (caspase-activated DNase) (DFFB), mRNA.
0.717	11.473	7.80E-11	1.09E-08	14.971	2060528	LOC649604	XM_945148.1	PREDICTED: Hs similar to ADP-ribosylation factor-like protein 4A, tv: 2 (LOC649604), mRNA.
0.716	8.247	3.17E-08	9.05E-07	8.969	5690280	FXR2	NM_004860.2	Hs fragile X mental retardation, autosomal homolog 2 (FXR2), mRNA.
0.715	6.916	5.58E-07	8.34E-06	6.088	6900475	ABHD2	NM_152924.3	Hs abhydrolase domain containing 2 (ABHD2), tv: 2, mRNA.
0.715	8.929	8.01E-09	3.26E-07	10.350	6060358	ATG4A	NM_178270.1	Hs ATG4 autophagy related 4 homolog A (S. cerevisiae) (ATG4A), tv: 2, mRNA.
0.714	6.288	2.34E-06	2.64E-05	4.651	5360326	SIP1	NM_001009182.1	Hs survival of motor neuron protein interacting protein 1 (SIP1), tv: beta, mRNA.
0.714	8.812	1.01E-08	3.92E-07	10.118	4120341	ITGAE	NM_002208.4	Hs integrin, alpha E (antigen CD103, human mucosal lymphocyte antigen 1; alpha polypeptide) (ITGAE), m
0.714	6.792	7.37E-07	1.04E-05	5.809	1030102	RGS16	NM_002928.2	Hs regulator of G-protein signalling 16 (RGS16), mRNA.
0.714	10.610	3.45E-10	3.18E-08	13.494	2230433	TMEM154	NM_152680.1	Hs transmembrane protein 154 (TMEM154), mRNA.
0.713	6.883	6.01E-07	8.87E-06	6.015	520630	CLN3	NM_001042432.1	Hs ceroid-lipofuscinosis, neuronal 3 (CLN3), tv: 1, mRNA.
0.713	7.856	7.19E-08	1.69E-06	8.147	1820332	INSIG1	NM_198336.1	Hs insulin induced gene 1 (INSIG1), tv: 2, mRNA.
0.713	6.000	4.58E-06	4.53E-05	3.976	1430288	LOC100129668	XM_001713607.1	PREDICTED: Hs hypothetical protein LOC100129668 (LOC100129668), mRNA.
0.711	7.090	3.79E-07	6.12E-06	6.478	1430152	SCML1	NM_001037540.1	Hs sex comb on midleg-like 1 (Drosophila) (SCML1), tv: 1, mRNA.
0.710	7.229	2.79E-07	4.78E-06	6.786	3930114	MOCS2	NM_004531.3	Hs molybdenum cofactor synthesis 2 (MOCS2), tv: 3, mRNA.
0.710	8.748	1.15E-08	4.25E-07	9.989	1780564	CDC42	NM_001039802.1	Hs cell division cycle 42 (GTP binding protein, 25kDa) (CDC42), tv: 3, mRNA.
0.709	7.668	1.07E-07	2.28E-06	7.746	3830349	IL7R	NM_002185.2	Hs interleukin 7 receptor (IL7R), mRNA.
0.709	6.950	5.17E-07	7.84E-06	6.165	6760600	LOC729608	XM_001714722.1	PREDICTED: Hs similar to Brix domain containing 1 (LOC729608), mRNA.
0.709	8.590	1.58E-08	5.35E-07	9.671	4060468	CENPL	NM_033319.1	Hs centromere protein L (CENPL), mRNA.
0.708	7.496	1.55E-07	3.06E-06	7.374	3290170	PAAF1	NM_025155.1	Hs proteasomal ATPase-associated factor 1 (PAAF1), mRNA.
0.708	8.245	3.19E-08	9.07E-07	8.964	3450630	SNORD83B	NR_000028.1	Hs small nucleolar RNA, C/D box 83B (SNORD83B), small nucleolar RNA.
0.707	7.611	1.21E-07	2.53E-06	7.622	3940168	SSX2	NM_003147.4	Hs synovial sarcoma, X breakpoint 2 (SSX2), tv: 1, mRNA.
0.707	5.623	1.12E-05	9.49E-05	3.079	7150739	FAM172A	NM_032042.4	Hs family with sequence similarity 172, member A (FAM172A), mRNA.
0.707	7.740	9.20E-08	2.02E-06	7.900	4260139	AKR1B1	NM_001628.2	Hs aldo-keto reductase family 1, member B1 (aldose reductase) (AKR1B1), mRNA.
0.707	7.034	4.29E-07	6.76E-06	6.354	3190735	SSNA1	NM_003731.1	Hs Sjogren syndrome nuclear autoantigen 1 (SSNA1), mRNA.
0.707	9.849	1.37E-09	8.51E-08	12.116	430523	MED8	NM_001001651.1	Hs mediator of RNA polymerase II transcription, subunit 8 homolog (S. cerevisiae) (MED8), tv: 3, mRNA.
0.706	7.012	4.50E-07	7.02E-06	6.304	2900487	CYP11A1	NM_000781.2	Hs cytochrome P450, family 11, subfamily A, polypeptide 1 (CYP11A1), nuclear gene encoding mitochondr
0.705	6.290	2.33E-06	2.63E-05	4.654	3130494	WDR20	NM_181291.1	Hs WD repeat domain 20 (WDR20), tv: 1, mRNA.
0.705	7.096	3.74E-07	6.06E-06	6.491	2690411	GOLSYN	NM_001099743.1	Hs Golgi-localized protein (GOLSYN), tv: 7, mRNA.
0.704	7.390	1.96E-07	3.65E-06	7.142	5910195	RBM18	NM_033117.2	Hs RNA binding motif protein 18 (RBM18), mRNA.
0.704	7.673	1.06E-07	2.26E-06	7.756	6660400	NDRG3	NM_022477.2	Hs NDRG family member 3 (NDRG3), tv: 2, mRNA.
0.704	6.702	9.04E-07	1.24E-05	5.604	7550494	SELK	NM_021237.3	Hs selenoprotein K (SELK), mRNA.
0.703	6.939	5.30E-07	8.00E-06	6.141	5390121	GDPD3	NM_024307.2	Hs glycerophosphodiester phosphodiesterase domain containing 3 (GDPD3), mRNA.
0.703	6.390	1.85E-06	2.19E-05	4.886	780743	UPF3B	NM_080632.1	Hs UPF3 regulator of nonsense transcripts homolog B (yeast) (UPF3B), tv: 1, mRNA.
0.703	7.246	2.68E-07	4.63E-06	6.825	5570524	LRRC42	NM_052940.3	Hs leucine rich repeat containing 42 (LRRC42), mRNA.
0.702	8.884	8.74E-09	3.47E-07	10.262	1430626	KCTD9	NM_017634.2	Hs potassium channel tetramerisation domain containing 9 (KCTD9), mRNA.
0.701	8.157	3.82E-08	1.04E-06	8.782	7560382	ELK4	NM_001973.2	Hs ELK4, ETS-domain protein (SRF accessory protein 1) (ELK4), tv: a, mRNA.
0.700	8.261	3.08E-08	8.87E-07	8.998	5560347	UPF2	NM_080599.1	Hs UPF2 regulator of nonsense transcripts homolog (yeast) (UPF2), tv: 1, mRNA.

Appendix 4 – Genes differentially expressed at 24 hours in cells treated with IGF1 ligand

0.699	9.105	5.67E-09	2.50E-07	10.697	3990148	PSMC3IP	NM_016556.1	Hs PSMC3 interacting protein (PSMC3IP), tv: 2, mRNA.
0.698	7.088	3.80E-07	6.13E-06	6.475	70167	LY96	NM_015364.2	Hs lymphocyte antigen 96 (LY96), mRNA.
0.698	8.182	3.63E-08	1.00E-06	8.834	5960471	BCL9L	NM_182557.2	Hs B-cell CLL/lymphoma 9-like (BCL9L), mRNA.
0.697	6.985	4.79E-07	7.36E-06	6.243	1690289	PGBD4	NM_152595.3	Hs piggyBac transposable element derived 4 (PGBD4), mRNA.
0.697	8.161	3.80E-08	1.04E-06	8.789	5910397	LIAS	NM_006859.2	Hs lipoic acid synthetase (LIAS), nuclear gene encoding mitochondrial protein, tv: 1, mRNA.
0.696	6.307	2.24E-06	2.55E-05	4.694	4860379	C5ORF21	NM_032042.3	Hs chromosome 5 open reading frame 21 (C5orf21), mRNA.
0.696	6.894	5.87E-07	8.69E-06	6.038	610408	HSPA4L	NM_014278.2	Hs heat shock 70kDa protein 4-like (HSPA4L), mRNA.
0.696	7.896	6.61E-08	1.58E-06	8.233	6370068	GNL1	NM_005275.2	Hs guanine nucleotide binding protein-like 1 (GNL1), mRNA.
0.695	7.249	2.66E-07	4.62E-06	6.832	1010333	MSX1	NM_002448.3	Hs msh homeobox 1 (MSX1), mRNA.
0.695	6.064	3.94E-06	4.02E-05	4.126	3310471	TMEM99	NM_145274.2	Hs transmembrane protein 99 (TMEM99), mRNA.
0.695	6.607	1.12E-06	1.47E-05	5.386	3990598	DRAP1	NM_006442.2	Hs DR1-associated protein 1 (negative cofactor 2 alpha) (DRAP1), mRNA.
0.694	7.388	1.97E-07	3.66E-06	7.137	3310639	C14ORF124	NM_020195.1	Hs chromosome 14 open reading frame 124 (C14orf124), mRNA.
0.694	5.590	1.21E-05	0.000101326	3.000	6330176	KBTBD4	NM_018095.3	Hs kelch repeat and BTB (POZ) domain containing 4 (KBTBD4), tv: 1, mRNA.
0.694	7.494	1.56E-07	3.07E-06	7.368	4560554	C20ORF24	NM_018840.2	Hs chromosome 20 open reading frame 24 (C20orf24), tv: 1, mRNA.
0.693	5.848	6.57E-06	6.12E-05	3.615	6370278	MPV17L2	NM_032683.2	Hs MPV17 mitochondrial membrane protein-like 2 (MPV17L2), nuclear gene encoding mitochondrial protei
0.692	7.197	2.99E-07	5.05E-06	6.716	3890326	SOD2	NM_001024465.1	Hs superoxide dismutase 2, mitochondrial (SOD2), nuclear gene encoding mitochondrial protein, tv: 2, mRN
0.692	6.374	1.91E-06	2.25E-05	4.851	6350070	SCNM1	NM_024041.2	Hs sodium channel modifier 1 (SCNM1), mRNA.
0.691	7.717	9.67E-08	2.11E-06	7.850	1580544	PIGH	NM_004569.3	Hs phosphatidylinositol glycan anchor biosynthesis, class H (PIGH), mRNA.
0.691	7.848	7.31E-08	1.70E-06	8.131	4490753	LOC644761	XR_039630.1	PREDICTED: Hs misc_RNA (LOC644761), miscRNA.
0.690	8.452	2.09E-08	6.58E-07	9.390	2030315	RFC4	NM_181573.1	Hs replication factor C (activator 1) 4, 37kDa (RFC4), tv: 2, mRNA.
0.690	5.565	1.29E-05	0.000106316	2.941	4670273	SCARNA12	NR_003010.1	Hs small Cajal body-specific RNA 12 (SCARNA12), guide RNA.
0.688	8.114	4.18E-08	1.11E-06	8.692	1580093	SCYL1	NM_020680.3	Hs SCY1-like 1 (S. cerevisiae) (SCYL1), tv: A, mRNA.
0.688	7.815	7.85E-08	1.79E-06	8.059	1580435	TGM2	NM_004613.2	Hs transglutaminase 2 (C polypeptide, protein-glutamine-gamma-glutamyltransferase) (TGM2), tv: 1, mRNA
0.687	7.329	2.24E-07	4.03E-06	7.008	610243	THOC3	NM_032361.1	Hs THO complex 3 (THOC3), mRNA.
0.685	5.865	6.31E-06	5.91E-05	3.655	7040609	SIP1	NM_001009182.1	Hs survival of motor neuron protein interacting protein 1 (SIP1), tv: beta, mRNA.
0.684	6.829	6.78E-07	9.70E-06	5.893	2570300	IFI44	NM_006417.3	Hs interferon-induced protein 44 (IFI44), mRNA.
0.684	7.640	1.14E-07	2.40E-06	7.685	270408	P4HA2	NM_001017974.1	Hs prolyl 4-hydroxylase, alpha polypeptide II (P4HA2), tv: 3, mRNA.
0.683	6.716	8.76E-07	1.20E-05	5.635	2940040	BCCIP	NM_016567.2	Hs BRCA2 and CDKN1A interacting protein (BCCIP), tv: A, mRNA.
0.682	6.747	8.16E-07	1.13E-05	5.707	6480563	SSX1	NM_005635.2	Hs synovial sarcoma, X breakpoint 1 (SSX1), mRNA.
0.682	8.123	4.11E-08	1.10E-06	8.710	3390521	UBXN8	NM_005671.2	Hs UBX domain protein 8 (UBXN8), mRNA.
0.681	6.955	5.12E-07	7.78E-06	6.176	2940577	HSPA2	NM_021979.3	Hs heat shock 70kDa protein 2 (HSPA2), mRNA.
0.681	6.326	2.14E-06	2.47E-05	4.738	3870181	MID1	NM_033290.2	Hs midline 1 (Opitz/BBB syndrome) (MID1), tv: 3, mRNA.
0.680	5.856	6.43E-06	6.01E-05	3.636	6250196	CENPP	NM_001012267.1	Hs centromere protein P (CENPP), mRNA.
0.679	7.886	6.75E-08	1.60E-06	8.212	7610259	LOC100131531	XM_001717228.1	PREDICTED: Hs similar to hCG1644658 (LOC100131531), mRNA.
0.679	7.424	1.82E-07	3.45E-06	7.215	1990327	TUBB4Q	NM_020040.3	Hs tubulin, beta polypeptide 4, member Q (TUBB4Q), mRNA.
0.678	7.263	2.58E-07	4.49E-06	6.863	5720438	LOC493869	NM_001008397.1	Hs similar to RIKEN cDNA 2310016C16 (LOC493869), mRNA.
0.677	7.001	4.61E-07	7.16E-06	6.280	5130615	SSX4B	NM_001034832.2	Hs synovial sarcoma, X breakpoint 4B (SSX4B), tv: 1, mRNA.
0.677	5.828	6.87E-06	6.35E-05	3.569	6350431	SSX3	NM_021014.2	Hs synovial sarcoma, X breakpoint 3 (SSX3), tv: 1, mRNA.
0.676	6.051	4.07E-06	4.12E-05	4.095	6960538	NOP2	NM_006170.2	Hs NOP2 nucleolar protein homolog (yeast) (NOP2), tv: 1, mRNA.
0.676	6.981	4.83E-07	7.41E-06	6.234	2900504	C7ORF20	NM_015949.2	Hs chromosome 7 open reading frame 20 (C7orf20), mRNA. XM_946081 XM_946082 XM_946083

Appendix 4 – Genes differentially expressed at 24 hours in cells treated with IGF1 ligand

0.675	9.129	5.41E-09	2.44E-07	10.743	4540475	FABP5L2	XM_001721172.1	PREDICTED: Hs fatty acid binding protein 5-like 2 (FABP5L2), mRNA.
0.675	6.856	6.39E-07	9.27E-06	5.953	6580131	MRPL22	NM_001014990.1	Hs mitochondrial ribosomal protein L22 (MRPL22), nuclear gene encoding mitochondrial protein, tv: 2, mR
0.675	7.863	7.08E-08	1.67E-06	8.163	6200273	C10ORF41	XM_210876.4	PREDICTED: Hs chromosome 10 open reading frame 41 (C10orf41), mRNA.
0.674	6.426	1.70E-06	2.05E-05	4.970	1770376	SERPINB8	NM_002640.3	Hs serpin peptidase inhibitor, clade B (ovalbumin), member 8 (SERPINB8), tv: 1, mRNA.
0.674	7.930	6.15E-08	1.49E-06	8.305	6960382	ING2	NM_001564.2	Hs inhibitor of growth family, member 2 (ING2), mRNA.
0.673	8.121	4.13E-08	1.10E-06	8.705	7400619	SPATA5L1	NM_024063.1	Hs spermatogenesis associated 5-like 1 (SPATA5L1), mRNA.
0.673	8.101	4.29E-08	1.14E-06	8.665	870731	C2ORF49	NM_024093.1	Hs chromosome 2 open reading frame 49 (C2orf49), mRNA.
0.672	6.746	8.18E-07	1.13E-05	5.705	3140768	TMEM93	NM_001014764.1	Hs transmembrane protein 93 (TMEM93), tv: 1, mRNA.
0.672	7.213	2.89E-07	4.91E-06	6.751	1300608	SNHG9	NR_003142.2	Hs small nucleolar RNA host gene 9 (non-protein coding) (SNHG9), non-coding RNA.
0.672	8.395	2.34E-08	7.17E-07	9.275	5700017	KBTBD4	NM_018095.3	Hs kelch repeat and BTB (POZ) domain containing 4 (KBTBD4), tv: 1, mRNA.
0.671	6.332	2.11E-06	2.44E-05	4.752	730228	VDAC3	NM_005662.4	Hs voltage-dependent anion channel 3 (VDAC3), mRNA.
0.671	5.722	8.85E-06	7.78E-05	3.317	5490356	NXF1	NM_001081491.1	Hs nuclear RNA export factor 1 (NXF1), tv: 2, mRNA.
0.670	8.092	4.38E-08	1.16E-06	8.645	3780246	EEF1B2	NM_001959.3	Hs eukaryotic translation elongation factor 1 beta 2 (EEF1B2), tv: 1, mRNA.
0.670	5.686	9.65E-06	8.37E-05	3.230	7510731	WBP5	NM_001006612.1	Hs WW domain binding protein 5 (WBP5), tv: 2, mRNA.
0.669	5.771	7.87E-06	7.07E-05	3.433	5420347	HCFC1R1	NM_001002018.1	Hs host cell factor C1 regulator 1 (XPO1 dependent) (HCFC1R1), tv: 3, mRNA.
0.669	6.128	3.39E-06	3.57E-05	4.277	3420561	RPA2	NM_002946.3	Hs replication protein A2, 32kDa (RPA2), mRNA.
0.668	7.794	8.19E-08	1.84E-06	8.016	2060612	MRPL27	NM_148571.1	Hs mitochondrial ribosomal protein L27 (MRPL27), nuclear gene encoding mitochondrial protein, tv: 2, mR
0.668	8.268	3.04E-08	8.77E-07	9.013	5960079	HS.374257		Hs mRNA; cDNA DKFZp779K2051 (from clone DKFZp779K2051)
0.668	6.209	2.81E-06	3.06E-05	4.466	6250064	IRF1	NM_002198.1	Hs interferon regulatory factor 1 (IRF1), mRNA.
0.667	5.558	1.31E-05	0.000107815	2.923	7320767	LOC645822	XM_001724973.1	PREDICTED: Hs similar to ubiquitin specific peptidase 32 (LOC645822), mRNA.
0.666	6.938	5.31E-07	8.01E-06	6.138	1070053	SFRS14	NM_001017392.2	Hs splicing factor, arginine/serine-rich 14 (SFRS14), tv: 1, mRNA.
0.666	7.059	4.05E-07	6.45E-06	6.410	1500678	TFPT	NM_013342.2	Hs TCF3 (E2A) fusion partner (in childhood Leukemia) (TFPT), mRNA.
0.666	6.037	4.21E-06	4.24E-05	4.062	3400209	ARL14	NM_025047.1	Hs ADP-ribosylation factor-like 14 (ARL14), mRNA.
0.665	11.292	1.06E-10	1.37E-08	14.670	1500762	C3ORF37	NM_020187.2	Hs chromosome 3 open reading frame 37 (C3orf37), tv: 2, mRNA.
0.664	6.935	5.35E-07	8.05E-06	6.132	4290592	PTK9	NM_198974.1	Hs PTK9 protein tyrosine kinase 9 (PTK9), tv: 2, mRNA.
0.664	8.347	2.58E-08	7.73E-07	9.175	7610142	HSD17B7P2	NR_003086.1	Hs hydroxysteroid (17-beta) dehydrogenase 7 pseudogene 2 (HSD17B7P2), non-coding RNA.
0.664	9.310	3.81E-09	1.85E-07	11.095	1300601	ST3GAL1	NM_003033.2	Hs ST3 beta-galactoside alpha-2,3-sialyltransferase 1 (ST3GAL1), tv: 1, mRNA.
0.663	5.941	5.26E-06	5.07E-05	3.837	1510291	PTTG1	NM_004219.2	Hs pituitary tumor-transforming 1 (PTTG1), mRNA.
0.663	6.302	2.26E-06	2.57E-05	4.683	1190026	APOBEC3G	NM_021822.1	Hs apolipoprotein B mRNA editing enzyme, catalytic polypeptide-like 3G (APOBEC3G), mRNA.
0.663	6.484	1.49E-06	1.85E-05	5.104	1660215	ATP6V0A1	NM_005177.3	Hs ATPase, H+ transporting, lysosomal V0 subunit a1 (ATP6V0A1), tv: 3, mRNA.
0.662	7.916	6.34E-08	1.52E-06	8.274	4780519	ZC3HC1	NM_016478.3	Hs zinc finger, C3HC-type containing 1 (ZC3HC1), mRNA.
0.661	6.553	1.27E-06	1.62E-05	5.263	2340605	C12ORF60	NM_175874.2	Hs chromosome 12 open reading frame 60 (C12orf60), mRNA.
0.660	8.764	1.11E-08	4.17E-07	10.023	4830328	CYB561D2	NM_007022.3	Hs cytochrome b-561 domain containing 2 (CYB561D2), mRNA.
0.660	5.655	1.04E-05	8.90E-05	3.157	3120332	OR7E156P	NR_002171.1	Hs olfactory receptor, family 7, subfamily E, member 156 pseudogene (OR7E156P), non-coding RNA.
0.660	6.904	5.73E-07	8.50E-06	6.062	4540181	LOC100130308	XR_036947.1	PREDICTED: Hs misc_RNA (LOC100130308), miscRNA.
0.660	5.689	9.59E-06	8.33E-05	3.236	20521	MASTL	NM_032844.1	Hs microtubule associated serine/threonine kinase-like (MASTL), mRNA.
0.659	6.079	3.80E-06	3.91E-05	4.162	5090053	FDX1L	NM_001031734.2	Hs ferredoxin 1-like (FDX1L), mRNA.
0.659	8.576	1.62E-08	5.47E-07	9.643	7570176	TEK	NM_000459.2	Hs TEK tyrosine kinase, endothelial (venous malformations, multiple cutaneous and mucosal) (TEK), mRNA
0.658	6.815	7.00E-07	9.96E-06	5.862	130037	PHF5A	NM_032758.3	Hs PHD finger protein 5A (PHF5A), mRNA.
0.658	6.395	1.82E-06	2.17E-05	4.900	4490228	SSX2	NM_003147.4	Hs synovial sarcoma, X breakpoint 2 (SSX2), tv: 1, mRNA.

Appendix 4 – Genes differentially expressed at 24 hours in cells treated with IGF1 ligand

0.658	7.042	4.22E-07	6.68E-06	6.370	3060133	PPP2R4	NM_021131.3	Hs protein phosphatase 2A activator, regulatory subunit 4 (PPP2R4), tv: 3, mRNA.
0.657	8.684	1.30E-08	4.65E-07	9.862	3460431	LIG3	NM_013975.2	Hs ligase III, DNA, ATP-dependent (LIG3), nuclear gene encoding mitochondrial protein, tv: alpha, mRNA.
0.657	6.148	3.24E-06	3.44E-05	4.322	4050315	LOC646817	XM_929774.2	PREDICTED: Hs similar to Protein SET (Phosphatase 2A inhibitor I2PP2A) (I-2PP2A) (Template-activating
0.657	6.789	7.43E-07	1.05E-05	5.801	5720142	ATG12	NM_004707.2	Hs ATG12 autophagy related 12 homolog (S. cerevisiae) (ATG12), mRNA.
0.657	5.940	5.28E-06	5.08E-05	3.834	2190470	KLF10	NM_005655.1	Hs Kruppel-like factor 10 (KLF10), tv: 1, mRNA.
0.656	6.869	6.20E-07	9.07E-06	5.984	2350594	UBXN8	NM_005671.2	Hs UBX domain protein 8 (UBXN8), mRNA.
0.656	7.790	8.28E-08	1.86E-06	8.006	3460731	TCP10L	NM_144659.4	Hs t-complex 10 (mouse)-like (TCP10L), mRNA.
0.656	7.154	3.29E-07	5.44E-06	6.620	1500280	IFIT3	NM_001031683.1	Hs interferon-induced protein with tetratricopeptide repeats 3 (IFIT3), mRNA.
0.655	6.384	1.87E-06	2.21E-05	4.872	5080451	PSMA5	NM_002790.2	Hs proteasome (prosome, macropain) subunit, alpha type, 5 (PSMA5), mRNA.
0.655	5.887	5.98E-06	5.65E-05	3.708	4390121	ADRM1	NM_175573.1	Hs adhesion regulating molecule 1 (ADRM1), tv: 2, mRNA.
0.655	5.795	7.44E-06	6.76E-05	3.490	5570300	C10ORF78	NM_145247.4	Hs chromosome 10 open reading frame 78 (C10orf78), tv: 2, mRNA.
0.654	7.325	2.25E-07	4.06E-06	7.000	4220520	TMEM57	NM_018202.3	Hs transmembrane protein 57 (TMEM57), mRNA.
0.654	6.454	1.59E-06	1.94E-05	5.036	460086	PARD6A	NM_001037281.1	Hs par-6 partitioning defective 6 homolog alpha (C. elegans) (PARD6A), tv: 2, mRNA.
0.654	7.222	2.83E-07	4.83E-06	6.772	60768	FBXL12	NM_017703.1	Hs F-box and leucine-rich repeat protein 12 (FBXL12), mRNA.
0.653	7.036	4.27E-07	6.75E-06	6.358	2120402	TES	NM_015641.2	Hs testis derived transcript (3 LIM domains) (TES), tv: 1, mRNA.
0.653	6.386	1.86E-06	2.20E-05	4.878	990128	MBNL2	NM_207304.1	Hs muscleblind-like 2 (Drosophila) (MBNL2), tv: 3, mRNA.
0.653	7.247	2.68E-07	4.63E-06	6.827	6110348	C11ORF24	NM_022338.2	Hs chromosome 11 open reading frame 24 (C11orf24), mRNA.
0.652	7.092	3.77E-07	6.10E-06	6.484	2120079	EIF2AK2	NM_002759.1	Hs eukaryotic translation initiation factor 2-alpha kinase 2 (EIF2AK2), mRNA.
0.652	5.790	7.53E-06	6.82E-05	3.478	20392	CISD1	NM_018464.2	Hs CDGSH iron sulfur domain 1 (CISD1), mRNA.
0.652	6.376	1.91E-06	2.24E-05	4.855	6110025	FHL2	NM_201557.2	Hs four and a half LIM domains 2 (FHL2), tv: 4, mRNA.
0.652	9.102	5.70E-09	2.51E-07	10.691	4290072	SERTAD1	NM_013376.3	Hs SERTA domain containing 1 (SERTAD1), mRNA.
0.651	5.889	5.96E-06	5.63E-05	3.713	1710349	LOC651143	XM_942536.1	PREDICTED: Hs hypothetical protein LOC651143, tv: 1 (LOC651143), mRNA.
0.650	8.637	1.43E-08	5.01E-07	9.767	1820471	FKBPL	NM_022110.3	Hs FK506 binding protein like (FKBPL), mRNA.
0.649	8.162	3.79E-08	1.04E-06	8.791	3180014	NFKBIB	NM_001001716.1	Hs nuclear factor of kappa light polypeptide gene enhancer in B-cells inhibitor, beta (NFKBIB), tv: 2, mRNA
0.649	7.087	3.81E-07	6.15E-06	6.471	7330463	SNORA3	NR_002580.1	Hs small nucleolar RNA, H/ACA box 3 (SNORA3), small nucleolar RNA.
0.649	7.046	4.18E-07	6.63E-06	6.380	6510189	VKORC1L1	NM_173517.3	Hs vitamin K epoxide reductase complex, subunit 1-like 1 (VKORC1L1), mRNA.
0.647	7.312	2.32E-07	4.14E-06	6.971	1300326	TEK	NM_000459.1	Hs TEK tyrosine kinase, endothelial (venous malformations, multiple cutaneous and mucosal) (TEK), mRNA
0.646	9.481	2.74E-09	1.40E-07	11.423	4150553	TAF13	NM_005645.3	Hs TAF13 RNA polymerase II, TATA box binding protein (TBP)-associated factor, 18kDa (TAF13), mRNA
0.646	6.417	1.74E-06	2.08E-05	4.949	4250544	BTBD10	NM_032320.5	Hs BTB (POZ) domain containing 10 (BTBD10), mRNA.
0.645	5.811	7.16E-06	6.55E-05	3.528	290309	FAM125A	NM_138401.2	Hs family with sequence similarity 125, member A (FAM125A), mRNA.
0.645	7.241	2.71E-07	4.68E-06	6.813	1300706	MTHFD2	NM_006636.3	Hs methylenetetrahydrofolate dehydrogenase (NADP+ dependent) 2, methenyltetrahydrofolate cyclohydrolas
0.645	5.752	8.25E-06	7.37E-05	3.386	1410524	PCNA	NM_002592.2	Hs proliferating cell nuclear antigen (PCNA), tv: 1, mRNA.
0.645	6.492	1.46E-06	1.82E-05	5.124	6620397	ISCU	NM_014301.2	Hs iron-sulfur cluster scaffold homolog (E. coli) (ISCU), nuclear gene encoding mitochondrial protein, tv: 1,
0.643	6.924	5.48E-07	8.22E-06	6.107	6560435	LOC100128163	XM_001719960.1	PREDICTED: Hs hypothetical protein LOC100128163 (LOC100128163), mRNA.
0.643	7.647	1.12E-07	2.37E-06	7.699	990288	FHL2	NM_201555.1	Hs four and a half LIM domains 2 (FHL2), tv: 2, mRNA.
0.642	6.853	6.43E-07	9.32E-06	5.947	3520040	YARS	NM_003680.2	Hs tyrosyl-tRNA synthetase (YARS), mRNA.
0.642	6.316	2.19E-06	2.51E-05	4.714	2750128	SLC7A11	NM_014331.3	Hs solute carrier family 7, (cationic amino acid transporter, y+ system) member 11 (SLC7A11), mRNA.
0.641	5.556	1.31E-05	0.000108008	2.920	3450326	NAGK	NM_017567.2	Hs N-acetylglucosamine kinase (NAGK), mRNA.
0.641	6.084	3.76E-06	3.88E-05	4.173	430209	NLN	NM_020726.3	Hs neurolysin (metallopeptidase M3 family) (NLN), mRNA.
0.641	6.572	1.22E-06	1.56E-05	5.306	6220050	STIL	NM_003035.2	Hs SCL/TAL1 interrupting locus (STIL), tv: 2, mRNA.

Appendix 4 – Genes differentially expressed at 24 hours in cells treated with IGF1 ligand

0.640	6.005	4.53E-06	4.49E-05	3.988	730253	CCDC49	NM_017748.3	Hs coiled-coil domain containing 49 (CCDC49), mRNA.
0.639	6.400	1.81E-06	2.15E-05	4.910	6350148	LOC652826	XM_942509.2	PREDICTED: Hs similar to 26S protease regulatory subunit 6B (MIP224) (MB67-interacting protein) (TAT-
0.639	6.393	1.84E-06	2.18E-05	4.893	160241	LOC345645	XR_016204.2	PREDICTED: Hs similar to hCG2002932 (LOC345645), mRNA.
0.638	6.951	5.15E-07	7.82E-06	6.169	5810743	LOC387882	NM_207376.1	Hs hypothetical protein (LOC387882), mRNA.
0.638	5.811	7.16E-06	6.55E-05	3.528	7650278	TRMT1	NM_017722.2	Hs TRM1 tRNA methyltransferase 1 homolog (S. cerevisiae) (TRMT1), mRNA.
0.638	7.449	1.72E-07	3.32E-06	7.270	2490364	LUM	NM_002345.3	Hs lumican (LUM), mRNA.
0.638	6.521	1.37E-06	1.73E-05	5.188	6840477	HS.543887		AGENCOURT_14535501 NIH_MGC_191 Hs cDNA clone IMAGE:30415823 5, mRNA sequence
0.638	6.665	9.84E-07	1.32E-05	5.519	1300719	C14ORF149	NM_144581.1	Hs chromosome 14 open reading frame 149 (C14orf149), mRNA.
0.637	5.695	9.44E-06	8.22E-05	3.251	2360630	FDFT1	NM_004462.3	Hs farnesyl-diphosphate farnesyltransferase 1 (FDFT1), mRNA.
0.637	6.229	2.68E-06	2.96E-05	4.513	3180048	IDH1	NM_005896.2	Hs isocitrate dehydrogenase 1 (NADP+), soluble (IDH1), mRNA.
0.636	6.913	5.62E-07	8.38E-06	6.082	4260368	UBE2C	NM_181800.1	Hs ubiquitin-conjugating enzyme E2C (UBE2C), tv: 3, mRNA.
0.636	6.927	5.45E-07	8.19E-06	6.113	3990307	MIR302C	NR_029858.1	Hs microRNA 302c (MIR302C), microRNA.
0.636	9.034	6.51E-09	2.76E-07	10.558	5690113	NUFIP2	NM_020772.1	Hs nuclear fragile X mental retardation protein interacting protein 2 (NUFIP2), mRNA.
0.636	7.621	1.19E-07	2.48E-06	7.644	2490343	GRK4	NM_001004057.1	Hs G protein-coupled receptor kinase 4 (GRK4), tv: 3, mRNA.
0.635	7.940	6.03E-08	1.47E-06	8.325	5090289	EFNB2	NM_004093.2	Hs ephrin-B2 (EFNB2), mRNA.
0.635	7.214	2.88E-07	4.89E-06	6.755	1850500	C3ORF75	NM_001031703.2	Hs chromosome 3 open reading frame 75 (C3orf75), mRNA.
0.634	6.432	1.68E-06	2.02E-05	4.985	870400	MGAT2	NM_002408.3	Hs mannosyl (alpha-1,6-)-glycoprotein beta-1,2-N-acetylglucosaminyltransferase (MGAT2), mRNA.
0.633	8.163	3.77E-08	1.03E-06	8.795	6450154	LSS	NM_002340.3	Hs lanosterol synthase (2,3-oxidosqualene-lanosterol cyclase) (LSS), tv: 1, mRNA.
0.633	7.099	3.71E-07	6.03E-06	6.498	2810367	ABCB6	NM_005689.1	Hs ATP-binding cassette, sub-family B (MDR/TAP), member 6 (ABCB6), nuclear gene encoding mitochond
0.633	5.741	8.46E-06	7.52E-05	3.362	4850673	UTP23	NM_032334.1	Hs UTP23, small subunit (SSU) processome component, homolog (yeast) (UTP23), mRNA.
0.633	7.729	9.41E-08	2.06E-06	7.877	3170139	PHACTR1	NM_030948.1	Hs phosphatase and actin regulator 1 (PHACTR1), mRNA.
0.633	7.537	1.42E-07	2.86E-06	7.463	2650156	TAP2	NM_018833.2	Hs transporter 2, ATP-binding cassette, sub-family B (MDR/TAP) (TAP2), tv: 2, mRNA.
0.632	6.720	8.68E-07	1.19E-05	5.645	2120682	GPR89C	NM_001097616.1	Hs G protein-coupled receptor 89C (GPR89C), mRNA.
0.632	6.107	3.57E-06	3.72E-05	4.226	580100	CD163L1	NM_174941.4	Hs CD163 molecule-like 1 (CD163L1), mRNA.
0.631	5.548	1.34E-05	0.000109565	2.900	2650092	JOSD2	NM_138334.1	Hs Josephin domain containing 2 (JOSD2), mRNA.
0.631	6.313	2.20E-06	2.52E-05	4.709	4780541	RAE1	NM_003610.3	Hs RAE1 RNA export 1 homolog (S. pombe) (RAE1), tv: 1, mRNA.
0.631	5.746	8.36E-06	7.44E-05	3.374	7000703	POLR3K	NM_016310.2	Hs polymerase (RNA) III (DNA directed) polypeptide K, 12.3 kDa (POLR3K), mRNA.
0.630	7.855	7.21E-08	1.69E-06	8.145	1340491	SP110	NM_004510.2	Hs SP110 nuclear body protein (SP110), tv: b, mRNA.
0.630	7.988	5.45E-08	1.36E-06	8.426	6270475	DUS3L	NM_020175.1	Hs dihydrouridine synthase 3-like (S. cerevisiae) (DUS3L), mRNA.
0.629	7.494	1.56E-07	3.07E-06	7.368	2570307	TTLL7	NM_024686.4	Hs tubulin tyrosine ligase-like family, member 7 (TTLL7), mRNA.
0.628	7.571	1.32E-07	2.72E-06	7.535	4890731	RFC5	NM_007370.3	Hs replication factor C (activator 1) 5, 36.5kDa (RFC5), tv: 1, mRNA.
0.628	5.770	7.90E-06	7.09E-05	3.430	5080600	LOC100132457	XM_001721497.1	PREDICTED: Hs similar to Sm protein G (LOC100132457), mRNA.
0.627	6.838	6.65E-07	9.56E-06	5.913	3800040	PHAX	NM_032177.2	Hs phosphorylated adaptor for RNA export (PHAX), mRNA.
0.627	6.647	1.02E-06	1.36E-05	5.478	4560592	SLIT2	NM_004787.1	Hs slit homolog 2 (Drosophila) (SLIT2), mRNA.
0.627	6.124	3.42E-06	3.60E-05	4.268	3460056	C1ORF57	NM_032324.1	Hs chromosome 1 open reading frame 57 (C1orf57), mRNA.
0.627	6.839	6.63E-07	9.55E-06	5.915	450463	SERPINB7	NM_003784.2	Hs serpin peptidase inhibitor, clade B (ovalbumin), member 7 (SERPINB7), tv: 1, mRNA.
0.627	5.764	8.00E-06	7.18E-05	3.417	4880750	SOCS5	NM_144949.2	Hs suppressor of cytokine signaling 5 (SOCS5), tv: 2, mRNA.
0.626	8.448	2.10E-08	6.62E-07	9.383	6620768	MVK	NM_000431.1	Hs mevalonate kinase (mevalonic aciduria) (MVK), mRNA.
0.625	7.465	1.66E-07	3.23E-06	7.305	1240273	SNORD110	NR_003078.1	Hs small nucleolar RNA, C/D box 110 (SNORD110), small nucleolar RNA.
0.625	7.082	3.85E-07	6.19E-06	6.462	7570671	UNKL	NM_023076.3	Hs unkempt homolog (Drosophila)-like (UNKL), tv: 1, mRNA.

Appendix 4 – Genes differentially expressed at 24 hours in cells treated with IGF1 ligand

0.624	6.295	2.30E-06	2.61E-05	4.667	1850487	LOC730324	XM_001722095.1	PREDICTED: Hs hypothetical LOC730324 (LOC730324), mRNA.
0.624	6.593	1.16E-06	1.51E-05	5.355	3190129	XAGE1	NM_133431.1	Hs X antigen family, member 1 (XAGE1), tv: 2, mRNA.
0.624	10.656	3.18E-10	2.99E-08	13.576	5080348	WDFY2	NM_052950.2	Hs WD repeat and FYVE domain containing 2 (WDFY2), mRNA.
0.623	5.543	1.36E-05	0.000110714	2.888	1050600	MAP2K1	NM_002755.2	Hs mitogen-activated protein kinase kinase 1 (MAP2K1), mRNA.
0.622	7.188	3.05E-07	5.13E-06	6.696	1340746	SLC45A3	NM_033102.2	Hs solute carrier family 45, member 3 (SLC45A3), mRNA.
0.622	8.220	3.36E-08	9.43E-07	8.913	3930386	C2ORF76	NM_001017927.2	Hs chromosome 2 open reading frame 76 (C2orf76), mRNA.
0.622	5.801	7.33E-06	6.69E-05	3.504	3940136	NUDT15	NM_018283.1	Hs nudix (nucleoside diphosphate linked moiety X)-type motif 15 (NUDT15), mRNA.
0.621	6.339	2.08E-06	2.40E-05	4.769	4050040	TUBB3	NM_006086.2	Hs tubulin, beta 3 (TUBB3), mRNA.
0.621	6.498	1.44E-06	1.80E-05	5.136	7560554	DGCR14	NM_022719.1	Hs DiGeorge syndrome critical region gene 14 (DGCR14), mRNA.
0.620	5.720	8.89E-06	7.82E-05	3.312	2710328	MLKL	XM_001126647.1	PREDICTED: Hs mixed lineage kinase domain-like (MLKL), mRNA.
0.619	8.144	3.93E-08	1.07E-06	8.754	840204	HAS2	NM_005328.1	Hs hyaluronan synthase 2 (HAS2), mRNA.
0.618	6.783	7.53E-07	1.06E-05	5.787	2450255	LOC391532	XR_017653.1	PREDICTED: Hs misc_RNA (LOC391532), miscRNA.
0.617	5.675	9.91E-06	8.55E-05	3.203	6370523	KBTBD8	NM_032505.1	Hs kelch repeat and BTB (POZ) domain containing 8 (KBTBD8), mRNA.
0.617	7.109	3.63E-07	5.92E-06	6.522	5900240	MRPL18	NM_014161.2	Hs mitochondrial ribosomal protein L18 (MRPL18), nuclear gene encoding mitochondrial protein, mRNA.
0.617	6.741	8.29E-07	1.15E-05	5.692	520609	KIAA1324	NM_020775.2	Hs KIAA1324 (KIAA1324), mRNA.
0.617	8.803	1.03E-08	3.97E-07	10.100	5910554	ADAL	NM_001012969.1	Hs adenosine deaminase-like (ADAL), mRNA.
0.616	5.579	1.24E-05	0.000103193	2.975	50129	FHOD1	NM_013241.2	Hs formin homology 2 domain containing 1 (FHOD1), mRNA.
0.616	6.864	6.27E-07	9.13E-06	5.972	3440189	ZBTB20	NM_015642.3	Hs zinc finger and BTB domain containing 20 (ZBTB20), mRNA.
0.616	6.963	5.02E-07	7.66E-06	6.194	6760707	LOC652685	XM_942289.1	PREDICTED: Hs similar to PMS1 protein homolog 2 (DNA mismatch repair protein PMS2) (LOC652685),
0.615	8.119	4.14E-08	1.10E-06	8.701	3190561	SNORD35B	NR_001285.1	Hs small nucleolar RNA, C/D box 35B (SNORD35B), small nucleolar RNA.
0.615	6.267	2.46E-06	2.75E-05	4.600	1470242	NUDT5	NM_014142.2	Hs nudix (nucleoside diphosphate linked moiety X)-type motif 5 (NUDT5), mRNA.
0.615	5.697	9.41E-06	8.20E-05	3.255	6660086	LOC441089	NR_003665.1	Hs CRSP8 pseudogene (LOC441089), non-coding RNA.
0.614	6.666	9.82E-07	1.32E-05	5.521	990725	DONSON	NM_017613.2	Hs downstream neighbor of SON (DONSON), mRNA.
0.614	7.392	1.95E-07	3.64E-06	7.146	5910187	SDHALP1	NR_003264.1	Hs succinate dehydrogenase complex, subunit A, flavoprotein pseudogene 1 (SDHALP1) on chromosome 3.
0.614	7.977	5.57E-08	1.38E-06	8.403	6840546	PAWR	NM_002583.2	Hs PRKC, apoptosis, WT1, regulator (PAWR), mRNA.
0.614	6.520	1.37E-06	1.73E-05	5.187	6840100	C11ORF51	NM_014042.1	Hs chromosome 11 open reading frame 51 (C11orf51), mRNA.
0.614	6.209	2.81E-06	3.06E-05	4.466	7560731	SNORA64	NR_002326.1	Hs small nucleolar RNA, H/ACA box 64 (SNORA64), small nucleolar RNA.
0.613	7.969	5.67E-08	1.40E-06	8.387	6620181	MRPL43	NM_176792.1	Hs mitochondrial ribosomal protein L43 (MRPL43), nuclear gene encoding mitochondrial protein, tv: 2, mR
0.613	8.186	3.60E-08	9.97E-07	8.843	5270156	BCCIP	NM_078469.1	Hs BRCA2 and CDKN1A interacting protein (BCCIP), tv: C, mRNA.
0.612	5.829	6.86E-06	6.34E-05	3.572	1400682	EFHA1	NM_152726.1	Hs EF-hand domain family, member A1 (EFHA1), mRNA.
0.612	6.280	2.38E-06	2.68E-05	4.631	5220731	TXNL4B	NM_017853.1	Hs thioredoxin-like 4B (TXNL4B), mRNA.
0.612	6.344	2.05E-06	2.38E-05	4.781	5720327	PSMA3	NM_002788.2	Hs proteasome (prosome, macropain) subunit, alpha type, 3 (PSMA3), tv: 1, mRNA.
0.612	7.674	1.06E-07	2.26E-06	7.757	6840706	ANAPC10	NM_014885.3	Hs anaphase promoting complex subunit 10 (ANAPC10), mRNA.
0.611	6.105	3.58E-06	3.72E-05	4.222	4590370	SLC2A1	NM_006516.1	Hs solute carrier family 2 (facilitated glucose transporter), member 1 (SLC2A1), mRNA.
0.610	6.583	1.19E-06	1.53E-05	5.332	5490592	HS.385784		Hs cDNA clone IMAGE:5418341, partial cds
0.610	6.734	8.40E-07	1.16E-05	5.677	270612	AIFM2	NM_032797.4	Hs apoptosis-inducing factor, mitochondrion-associated, 2 (AIFM2), nuclear gene encoding mitochondrial pr
0.610	6.576	1.20E-06	1.55E-05	5.316	5820471	C14ORF149	NM_144581.1	Hs chromosome 14 open reading frame 149 (C14orf149), mRNA.
0.610	6.670	9.73E-07	1.31E-05	5.531	6250131	CABYR	NM_153768.1	Hs calcium binding tyrosine-(Y)-phosphorylation regulated (CABYR), tv: 2, mRNA.
0.610	5.821	6.99E-06	6.44E-05	3.552	380468	GMEB1	NM_024482.1	Hs glucocorticoid modulatory element binding protein 1 (GMEB1), tv: 2, mRNA.
0.609	7.028	4.34E-07	6.82E-06	6.341	730689	LOC652595	XM_942117.1	PREDICTED: Hs similar to U2 small nuclear ribonucleoprotein A (U2 snRNP-A) (LOC652595), mRNA.

Appendix 4 – Genes differentially expressed at 24 hours in cells treated with IGF1 ligand

0.609	7.545	1.40E-07	2.83E-06	7.480	6100301	CDC123	NM_006023.1	Hs cell division cycle 123 homolog (S. cerevisiae) (CDC123), mRNA.
0.608	6.414	1.75E-06	2.09E-05	4.943	160639	EBAG9	NM_198120.1	Hs estrogen receptor binding site associated, antigen, 9 (EBAG9), tv: 2, mRNA.
0.608	7.153	3.30E-07	5.45E-06	6.618	5220484	MLX	NM_198204.1	Hs MAX-like protein X (MLX), tv: 2, mRNA.
0.608	6.339	2.08E-06	2.40E-05	4.769	460487	FAM55C	NM_145037.1	Hs family with sequence similarity 55, member C (FAM55C), mRNA.
0.608	7.042	4.22E-07	6.68E-06	6.370	5860050	LOC388564	XM_498725.3	PREDICTED: Hs hypothetical gene supported by BC052596 (LOC388564), mRNA.
0.607	5.636	1.09E-05	9.26E-05	3.110	150274	THAP10	NM_020147.2	Hs THAP domain containing 10 (THAP10), mRNA.
0.607	6.228	2.69E-06	2.96E-05	4.510	2260296	SCAND2	NR_003654.1	Hs SCAN domain containing 2 (SCAND2) on chromosome 15.
0.606	6.543	1.30E-06	1.65E-05	5.240	6020441	SMTN	NM_006932.3	Hs smoothelin (SMTN), tv: 3, mRNA.
0.606	6.131	3.37E-06	3.55E-05	4.284	4830048	RGP1	NM_001080496.1	Hs RGP1 retrograde golgi transport homolog (S. cerevisiae) (RGP1), mRNA.
0.605	7.761	8.80E-08	1.96E-06	7.944	5960014	C15ORF57	NM_052849.2	Hs chromosome 15 open reading frame 57 (C15orf57), tv: 2, mRNA.
0.605	6.304	2.26E-06	2.57E-05	4.686	6450274	POLR3G	NM_006467.2	Hs polymerase (RNA) III (DNA directed) polypeptide G (32kD) (POLR3G), mRNA.
0.605	8.907	8.37E-09	3.35E-07	10.306	4760209	MMAA	NM_172250.1	Hs methylmalonic aciduria (cobalamin deficiency) cblA type (MMAA), mRNA.
0.604	7.027	4.35E-07	6.82E-06	6.339	5560112	RNMTL1	NM_018146.2	Hs RNA methyltransferase like 1 (RNMTL1), mRNA.
0.603	6.437	1.66E-06	2.01E-05	4.995	4880161	SLC3A2	NM_001012661.1	Hs solute carrier family 3 (activators of dibasic and neutral amino acid transport), member 2 (SLC3A2), tv: 1
0.603	6.093	3.69E-06	3.81E-05	4.193	5560253	LOC642897	XR_017554.1	PREDICTED: Hs misc_RNA (LOC642897), miscRNA.
0.603	7.156	3.27E-07	5.42E-06	6.626	5810022	MLKL	XM_001126647.1	PREDICTED: Hs mixed lineage kinase domain-like (MLKL), mRNA.
0.602	6.018	4.40E-06	4.38E-05	4.017	4040437	NANP	NM_152667.1	Hs N-acetylneuraminic acid phosphatase (NANP), mRNA.
0.602	7.319	2.29E-07	4.10E-06	6.986	4390349	ZNF256	NM_005773.2	Hs zinc finger protein 256 (ZNF256), mRNA.
0.602	6.422	1.72E-06	2.06E-05	4.961	5310369	LYAR	NM_017816.1	Hs Ly1 antibody reactive homolog (mouse) (LYAR), mRNA.
0.602	6.911	5.64E-07	8.41E-06	6.077	4040114	TEF	NM_003216.2	Hs thyrotrophic embryonic factor (TEF), tv: 1, mRNA.
0.601	5.559	1.31E-05	0.000107708	2.926	4260187	CRTC2	NM_181715.1	Hs CREB regulated transcription coactivator 2 (CRTC2), mRNA.
0.601	5.981	4.80E-06	4.69E-05	3.930	3420373	SOD2	NM_001024466.1	Hs superoxide dismutase 2, mitochondrial (SOD2), nuclear gene encoding mitochondrial protein, tv: 3, mRN
0.601	6.170	3.07E-06	3.29E-05	4.376	780500	CAB39L	NM_001079670.1	Hs calcium binding protein 39-like (CAB39L), tv: 2, mRNA.
0.601	6.279	2.39E-06	2.68E-05	4.630	1850433	SPTY2D1	NM_194285.2	Hs SPT2, Suppressor of Ty, domain containing 1 (S. cerevisiae) (SPTY2D1), mRNA.
0.601	7.563	1.35E-07	2.76E-06	7.518	6900025	POLR2D	NM_004805.2	Hs polymerase (RNA) II (DNA directed) polypeptide D (POLR2D), mRNA.
0.599	5.553	1.33E-05	0.000108742	2.912	4730343	ATP6V0E1	NM_003945.3	Hs ATPase, H+ transporting, lysosomal 9kDa, V0 subunit e1 (ATP6V0E1), mRNA.
0.599	5.944	5.23E-06	5.05E-05	3.842	4780524	ZNF274	NM_016324.2	Hs zinc finger protein 274 (ZNF274), tv: ZNF274b, mRNA.
0.598	6.214	2.78E-06	3.04E-05	4.477	2640088	ALDOA	NM_184041.1	Hs aldolase A, fructose-bisphosphate (ALDOA), tv: 2, mRNA.
0.598	5.961	5.02E-06	4.88E-05	3.884	5490634	CACYBP	NM_001007214.1	Hs calcyclin binding protein (CACYBP), tv: 2, mRNA.
0.597	5.540	1.37E-05	0.000111515	2.880	5420520	MDC1	NM_014641.1	Hs mediator of DNA damage checkpoint 1 (MDC1), mRNA.
0.597	5.746	8.36E-06	7.44E-05	3.374	6660279	DOHH	NM_031304.3	Hs deoxyhypusine hydroxylase/monooxygenase (DOHH), mRNA.
0.597	6.599	1.14E-06	1.49E-05	5.370	3850255	ZSWIM3	NM_080752.2	Hs zinc finger, SWIM-type containing 3 (ZSWIM3), mRNA.
0.597	5.719	8.92E-06	7.84E-05	3.309	1450634	TINAGL1	NM_022164.1	Hs tubulointerstitial nephritis antigen-like 1 (TINAGL1), mRNA.
0.596	6.590	1.17E-06	1.52E-05	5.347	430672	HSPA8	NM_153201.1	Hs heat shock 70kDa protein 8 (HSPA8), tv: 2, mRNA.
0.596	5.938	5.30E-06	5.10E-05	3.830	4010095	CSAG3A	NM_203311.1	Hs CSAG family, member 3A (CSAG3A), mRNA.
0.596	7.226	2.80E-07	4.80E-06	6.782	2100209	FAM24B	NM_152644.1	Hs family with sequence similarity 24, member B (FAM24B), mRNA.
0.596	6.491	1.46E-06	1.82E-05	5.121	5290408	MCEE	NM_032601.2	Hs methylmalonyl CoA epimerase (MCEE), mRNA.
0.595	6.184	2.98E-06	3.21E-05	4.408	450072	CHCHD6	NM_032343.1	Hs coiled-coil-helix-coiled-coil-helix domain containing 6 (CHCHD6), mRNA.
0.595	7.503	1.53E-07	3.02E-06	7.388	5570575	C15ORF57	NM_001080791.1	Hs chromosome 15 open reading frame 57 (C15orf57), tv: 3, mRNA.
0.594	7.638	1.14E-07	2.40E-06	7.681	1340537	ALKBH2	NM_001001655.1	Hs alkB, alkylation repair homolog 2 (E. coli) (ALKBH2), mRNA.

Appendix 4 – Genes differentially expressed at 24 hours in cells treated with IGF1 ligand

0.594	5.709	9.13E-06	8.00E-05	3.285	7550402	TIMM44	NM_006351.2	Hs translocase of inner mitochondrial membrane 44 homolog (yeast) (TIMM44), nuclear gene encoding mito
0.594	8.991	7.09E-09	2.96E-07	10.473	2630563	SLC39A14	NM_015359.2	Hs solute carrier family 39 (zinc transporter), member 14 (SLC39A14), mRNA.
0.593	6.620	1.09E-06	1.44E-05	5.417	4920129	RTN3	NM_201430.1	Hs reticulon 3 (RTN3), tv: 4, mRNA.
0.593	5.882	6.05E-06	5.70E-05	3.697	6110079	CRYAB	NM_001885.1	Hs crystallin, alpha B (CRYAB), mRNA.
0.593	5.969	4.93E-06	4.80E-05	3.903	2100161	FAM98A	NM_015475.3	Hs family with sequence similarity 98, member A (FAM98A), mRNA.
0.593	8.745	1.15E-08	4.26E-07	9.985	2370241	TRIM16	NM_006470.3	Hs tripartite motif-containing 16 (TRIM16), mRNA.
0.592	5.935	5.34E-06	5.13E-05	3.823	360161	TMEM11	NM_003876.1	Hs transmembrane protein 11 (TMEM11), mRNA.
0.592	8.607	1.52E-08	5.23E-07	9.705	2510348	PCNA	NM_182649.1	Hs proliferating cell nuclear antigen (PCNA), tv: 2, mRNA.
0.592	6.045	4.13E-06	4.17E-05	4.081	1980424	LOC647349	XR_019572.1	PREDICTED: Hs similar to AP-3 complex subunit sigma-1 (Adapter-related protein complex 3 sigma-1 subu
0.592	6.260	2.49E-06	2.78E-05	4.586	580358	FABP5L2	XM_001134012.2	PREDICTED: Hs fatty acid binding protein 5-like 2 (FABP5L2), mRNA.
0.591	5.699	9.34E-06	8.16E-05	3.262	5220224	DIABLO	NM_019887.3	Hs diablo homolog (Drosophila) (DIABLO), nuclear gene encoding mitochondrial protein, tv: 1, mRNA.
0.591	8.022	5.06E-08	1.29E-06	8.500	4830373	GMNN	NM_015895.3	Hs geminin, DNA replication inhibitor (GMNN), mRNA.
0.590	5.834	6.79E-06	6.28E-05	3.582	7650402	C15ORF56	NM_001039905.1	Hs chromosome 15 open reading frame 56 (C15orf56), mRNA.
0.589	6.469	1.54E-06	1.90E-05	5.069	1580133	CUGBP1	NM_001025596.1	Hs CUG triplet repeat, RNA binding protein 1 (CUGBP1), tv: 3, mRNA.
0.589	5.861	6.36E-06	5.95E-05	3.648	5090025	C12ORF66	NM_152440.4	Hs chromosome 12 open reading frame 66 (C12orf66), mRNA.
0.588	6.655	1.01E-06	1.34E-05	5.497	4860673	DDX39	NM_005804.2	Hs DEAD (Asp-Glu-Ala-Asp) box polypeptide 39 (DDX39), mRNA.
0.588	7.167	3.19E-07	5.30E-06	6.651	6650220	FASTKD5	NM_021826.4	Hs FAST kinase domains 5 (FASTKD5), mRNA.
0.586	6.464	1.56E-06	1.91E-05	5.057	3370722	ELOVL1	NM_022821.2	Hs elongation of very long chain fatty acids (FEN1/Elo2, SUR4/Elo3, yeast)-like 1 (ELOVL1), mRNA.
0.586	6.473	1.53E-06	1.89E-05	5.079	3400095	IL20RB	NM_144717.2	Hs interleukin 20 receptor beta (IL20RB), mRNA.
0.586	7.293	2.42E-07	4.29E-06	6.929	2970397	ZNF296	NM_145288.1	Hs zinc finger protein 296 (ZNF296), mRNA.
0.585	7.210	2.90E-07	4.93E-06	6.746	7150382	NR2C2	NM_003298.3	Hs nuclear receptor subfamily 2, group C, member 2 (NR2C2), mRNA.
0.584	8.137	3.99E-08	1.08E-06	8.740	6110095	CCDC15	NM_025004.1	Hs coiled-coil domain containing 15 (CCDC15), mRNA.
0.584	5.639	1.08E-05	9.20E-05	3.118	7560189	RNF5P1	NR_003129.1	Hs ring finger protein 5 pseudogene 1 (RNF5P1), non-coding RNA.
0.583	6.617	1.10E-06	1.45E-05	5.409	6020719	RAB23	NM_016277.3	Hs RAB23, member RAS oncogene family (RAB23), tv: 1, mRNA.
0.583	6.385	1.87E-06	2.21E-05	4.876	2030441	SPATS2	NM_023071.1	Hs spermatogenesis associated, serine-rich 2 (SPATS2), mRNA.
0.583	7.444	1.74E-07	3.35E-06	7.259	2000445	PSMB10	NM_002801.2	Hs proteasome (prosome, macropain) subunit, beta type, 10 (PSMB10), mRNA.
0.582	5.899	5.82E-06	5.52E-05	3.735	1110095	CLTB	NM_007097.2	Hs clathrin, light chain (Lcb) (CLTB), tv: 2, mRNA.
0.582	6.768	7.79E-07	1.09E-05	5.754	4590424	PDCD2L	NM_032346.1	Hs programmed cell death 2-like (PDCD2L), mRNA.
0.582	8.684	1.30E-08	4.65E-07	9.862	2140154	CYB5A	NM_001914.2	Hs cytochrome b5 type A (microsomal) (CYB5A), tv: 2, mRNA.
0.582	7.400	1.91E-07	3.59E-06	7.164	2060477	AGPAT9	NM_032717.3	Hs 1-acylglycerol-3-phosphate O-acyltransferase 9 (AGPAT9), mRNA.
0.582	5.641	1.07E-05	9.17E-05	3.124	4200270	TMUB2	NM_001076674.1	Hs transmembrane and ubiquitin-like domain containing 2 (TMUB2), tv: 3, mRNA.
0.581	6.212	2.79E-06	3.04E-05	4.473	3400577	EIF2S2	NM_003908.3	Hs eukaryotic translation initiation factor 2, subunit 2 beta, 38kDa (EIF2S2), mRNA.
0.581	5.793	7.48E-06	6.78E-05	3.484	7150280	LOC145853	XM_096885.9	PREDICTED: Hs hypothetical LOC145853 (LOC145853), mRNA.
0.581	7.808	7.95E-08	1.80E-06	8.046	3840593	SP110	NM_004510.2	Hs SP110 nuclear body protein (SP110), tv: b, mRNA.
0.580	7.438	1.76E-07	3.38E-06	7.246	10220	ANAPC11	NM_001002246.1	Hs anaphase promoting complex subunit 11 (ANAPC11), tv: 4, mRNA.
0.580	6.091	3.70E-06	3.82E-05	4.190	1240176	PPP1R13L	NM_006663.2	Hs protein phosphatase 1, regulatory (inhibitor) subunit 13 like (PPP1R13L), mRNA.
0.580	5.980	4.80E-06	4.70E-05	3.929	7560746	FAM103A1	NM_031452.2	Hs family with sequence similarity 103, member A1 (FAM103A1), mRNA.
0.580	5.580	1.24E-05	0.000103193	2.976	5050181	ERCC6L	NM_017669.2	Hs excision repair cross-complementing rodent repair deficiency, complementation group 6-like (ERCC6L),
0.580	7.020	4.43E-07	6.92E-06	6.322	990136	C12ORF48	NM_017915.2	Hs chromosome 12 open reading frame 48 (C12orf48), mRNA.
0.579	6.015	4.43E-06	4.40E-05	4.011	10341	SHMT2	NM_005412.4	Hs serine hydroxymethyltransferase 2 (mitochondrial) (SHMT2), nuclear gene encoding mitochondrial prote

Appendix 4 – Genes differentially expressed at 24 hours in cells treated with IGF1 ligand

0.579	6.655	1.01E-06	1.34E-05	5.496	6580646	PSMC5	NM_002805.4	Hs proteasome (prosome, macropain) 26S subunit, ATPase, 5 (PSMC5), mRNA.
0.578	7.074	3.92E-07	6.28E-06	6.443	5310348	CCDC21	NM_022778.2	Hs coiled-coil domain containing 21 (CCDC21), mRNA.
0.577	6.881	6.03E-07	8.88E-06	6.011	4250367	UCA1	NR_015379.2	Hs urothelial cancer associated 1 (non-protein coding) (UCA1), non-coding RNA.
0.577	5.580	1.24E-05	0.000103183	2.977	6110168	PGAM4	NM_001029891.2	Hs phosphoglycerate mutase family member 4 (PGAM4), mRNA.
0.577	6.462	1.56E-06	1.92E-05	5.054	7200348	DISP2	NM_033510.1	Hs dispatched homolog 2 (Drosophila) (DISP2), mRNA.
0.576	6.722	8.64E-07	1.19E-05	5.650	1090370	UCHL5IP	NM_017518.5	Hs UCHL5 interacting protein (UCHL5IP), tv: 1, mRNA.
0.576	6.478	1.51E-06	1.87E-05	5.090	1240221	POLR2H	NM_006232.2	Hs polymerase (RNA) II (DNA directed) polypeptide H (POLR2H), mRNA.
0.575	6.465	1.55E-06	1.91E-05	5.060	3060184	MRPL43	NM_032112.2	Hs mitochondrial ribosomal protein L43 (MRPL43), nuclear gene encoding mitochondrial protein, tv: 1, mR
0.574	7.055	4.09E-07	6.51E-06	6.400	5080326	PSMA6	NM_002791.1	Hs proteasome (prosome, macropain) subunit, alpha type, 6 (PSMA6), mRNA.
0.574	5.963	5.01E-06	4.86E-05	3.887	4230053	GPATCH3	NM_022078.1	Hs G patch domain containing 3 (GPATCH3), mRNA.
0.574	6.845	6.55E-07	9.46E-06	5.928	6900600	MFSD5	NM_032889.3	Hs major facilitator superfamily domain containing 5 (MFSD5), mRNA.
0.574	5.585	1.23E-05	0.000102273	2.988	520403	PRO1853	NM_144736.3	Hs hypothetical protein PRO1853 (PRO1853), tv: 1, mRNA.
0.573	6.090	3.71E-06	3.83E-05	4.186	5560279	LOC728069	XM_001128421.1	PREDICTED: Hs hypothetical LOC728069 (LOC728069), mRNA.
0.573	6.367	1.95E-06	2.28E-05	4.833	4120114	IL12A	NM_000882.2	Hs interleukin 12A (natural killer cell stimulatory factor 1, cytotoxic lymphocyte maturation factor 1, p35) (I
0.573	6.294	2.30E-06	2.61E-05	4.665	1510609	NME1-NME2	NM_001018136.1	Hs NME1-NME2 readthrough (NME1-NME2), mRNA.
0.572	6.657	1.00E-06	1.34E-05	5.502	2970561	LOC644877	XR_038951.1	PREDICTED: Hs misc_RNA (LOC644877), miscRNA.
0.572	5.921	5.52E-06	5.28E-05	3.790	6040709	CCDC19	NM_012337.2	Hs coiled-coil domain containing 19 (CCDC19), mRNA.
0.571	7.278	2.50E-07	4.39E-06	6.895	6180070	FTHL11	NR_002204.1	Hs ferritin, heavy polypeptide-like 11 (FTHL11) on chromosome 8.
0.571	7.289	2.44E-07	4.32E-06	6.919	2630408	LETM2	NM_144652.1	Hs leucine zipper-EF-hand containing transmembrane protein 2 (LETM2), mRNA.
0.571	7.340	2.18E-07	3.97E-06	7.031	1430475	EID2	NM_153232.3	Hs EP300 interacting inhibitor of differentiation 2 (EID2), mRNA.
0.570	6.483	1.49E-06	1.85E-05	5.102	2470465	TRAF2	NM_021138.3	Hs TNF receptor-associated factor 2 (TRAF2), mRNA.
0.570	5.563	1.29E-05	0.000106685	2.937	2370291	LPCAT3	NM_005768.5	Hs lysophosphatidylcholine acyltransferase 3 (LPCAT3), mRNA.
0.569	7.463	1.67E-07	3.24E-06	7.302	3180484	OIP5	NM_007280.1	Hs Opa interacting protein 5 (OIP5), mRNA.
0.569	5.968	4.95E-06	4.82E-05	3.899	1050446	NME2	NM_001018137.1	Hs non-metastatic cells 2, protein (NM23B) expressed in (NME2), tv: 2, mRNA.
0.569	5.615	1.14E-05	9.63E-05	3.060	2680113	DCUN1D5	NM_032299.2	Hs DCN1, defective in cullin neddylation 1, domain containing 5 (S. cerevisiae) (DCUN1D5), mRNA.
0.569	6.310	2.22E-06	2.54E-05	4.702	7200598	MED6	NM_005466.2	Hs mediator complex subunit 6 (MED6), mRNA.
0.568	6.078	3.82E-06	3.92E-05	4.159	830674	LOC100134189	XM_001722214.1	PREDICTED: Hs similar to cofactor required for Sp1 transcriptional activation, subunit 8, 34kDa, tv: 2 (LOC
0.567	7.375	2.02E-07	3.73E-06	7.108	1450647	ATG4D	NM_032885.4	Hs ATG4 autophagy related 4 homolog D (S. cerevisiae) (ATG4D), mRNA.
0.567	5.614	1.15E-05	9.65E-05	3.058	6290253	C19ORF52	NM_138358.2	Hs chromosome 19 open reading frame 52 (C19orf52), mRNA.
0.565	5.903	5.76E-06	5.47E-05	3.747	3120367	SQLE	NM_003129.3	Hs squalene epoxidase (SQLE), mRNA.
0.564	6.371	1.93E-06	2.26E-05	4.843	2450139	RHEB	NM_005614.3	Hs Ras homolog enriched in brain (RHEB), mRNA.
0.564	6.287	2.34E-06	2.64E-05	4.649	6200014	ZNF165	NM_003447.2	Hs zinc finger protein 165 (ZNF165), mRNA.
0.564	7.282	2.48E-07	4.36E-06	6.905	670673	BCL2L1	NM_138578.1	Hs BCL2-like 1 (BCL2L1), nuclear gene encoding mitochondrial protein, tv: 1, mRNA.
0.564	6.393	1.83E-06	2.18E-05	4.894	6270670	IDH1	NM_005896.2	Hs isocitrate dehydrogenase 1 (NADP+), soluble (IDH1), mRNA.
0.564	7.566	1.34E-07	2.75E-06	7.525	3370592	SIRT7	NM_016538.1	Hs sirtuin (silent mating type information regulation 2 homolog) 7 (S. cerevisiae) (SIRT7), mRNA.
0.563	6.606	1.12E-06	1.47E-05	5.385	6580682	CLN3	NM_000086.2	Hs ceroid-lipofuscinosis, neuronal 3 (CLN3), tv: 2, mRNA.
0.563	6.647	1.03E-06	1.36E-05	5.478	1340039	TFPI	NM_006287.4	Hs tissue factor pathway inhibitor (lipoprotein-associated coagulation inhibitor) (TFPI), tv: 1, mRNA.
0.562	6.284	2.36E-06	2.66E-05	4.641	1260398	EME1	NM_152463.1	Hs essential meiotic endonuclease 1 homolog 1 (S. pombe) (EME1), mRNA.
0.562	5.858	6.41E-06	5.99E-05	3.640	1710753	ARL5B	NM_178815.3	Hs ADP-ribosylation factor-like 5B (ARL5B), mRNA.
0.560	6.897	5.82E-07	8.62E-06	6.046	7050068	SQLE	NM_003129.3	Hs squalene epoxidase (SQLE), mRNA.

Appendix 4 – Genes differentially expressed at 24 hours in cells treated with IGF1 ligand

0.560	5.741	8.46E-06	7.52E-05	3.361	240524	PHC3	NM_024947.2	Hs polyhomeotic homolog 3 (Drosophila) (PHC3), mRNA.
0.560	6.923	5.50E-07	8.24E-06	6.104	2640554	EEF1B2	NM_021121.2	Hs eukaryotic translation elongation factor 1 beta 2 (EEF1B2), tv: 2, mRNA.
0.560	6.039	4.18E-06	4.22E-05	4.067	7160148	ZNF329	NM_024620.3	Hs zinc finger protein 329 (ZNF329), mRNA.
0.559	6.236	2.64E-06	2.92E-05	4.529	4210647	ESRRAP2	NR_000033.2	Hs estrogen-related receptor alpha pseudogene 2 (ESRRAP2) on chromosome 13.
0.558	6.117	3.48E-06	3.65E-05	4.250	2000300	IFI30	NM_006332.3	Hs interferon, gamma-inducible protein 30 (IFI30), mRNA.
0.558	6.547	1.29E-06	1.64E-05	5.248	1300136	LZIC	NM_032368.3	Hs leucine zipper and CTNNBIP1 domain containing (LZIC), mRNA.
0.557	6.213	2.79E-06	3.04E-05	4.474	3460239	HVCN1	NM_032369.2	Hs hydrogen voltage-gated channel 1 (HVCN1), tv: 2, mRNA.
0.557	6.806	7.15E-07	1.01E-05	5.840	5130487	SRRD	NM_001013694.2	Hs SRR1 domain containing (SRRD), mRNA.
0.556	6.207	2.82E-06	3.07E-05	4.461	3170332	DPP9	NM_139159.3	Hs dipeptidyl-peptidase 9 (DPP9), mRNA.
0.556	8.307	2.80E-08	8.26E-07	9.093	6580707	TFE3	NM_006521.3	Hs transcription factor binding to IGHM enhancer 3 (TFE3), mRNA.
0.555	6.406	1.78E-06	2.13E-05	4.923	2940367	TBC1D7	NM_016495.2	Hs TBC1 domain family, member 7 (TBC1D7), mRNA.
0.555	6.398	1.81E-06	2.16E-05	4.907	4220576	SLC4A1AP	NM_018158.1	Hs solute carrier family 4 (anion exchanger), member 1, adaptor protein (SLC4A1AP), mRNA.
0.554	6.733	8.43E-07	1.16E-05	5.674	5390497	C7ORF53	NM_182597.1	Hs chromosome 7 open reading frame 53 (C7orf53), mRNA.
0.554	7.337	2.20E-07	3.98E-06	7.025	7560288	DCUN1D3	NM_173475.1	Hs DCN1, defective in cullin neddylation 1, domain containing 3 (S. cerevisiae) (DCUN1D3), mRNA.
0.553	7.335	2.21E-07	3.99E-06	7.021	4830156	TM4SF18	NM_138786.1	Hs transmembrane 4 L six family member 18 (TM4SF18), mRNA.
0.553	6.211	2.80E-06	3.05E-05	4.470	5260168	PMS2	NR_003085.1	Hs PMS2 postmeiotic segregation increased 2 (S. cerevisiae) (PMS2), tv: 2, transcribed RNA.
0.553	6.093	3.68E-06	3.81E-05	4.194	2900692	GSG2	NM_031965.2	Hs germ cell associated 2 (haspin) (GSG2), mRNA.
0.553	6.645	1.03E-06	1.37E-05	5.473	1300491	POLE3	NM_017443.3	Hs polymerase (DNA directed), epsilon 3 (p17 subunit) (POLE3), mRNA.
0.553	6.883	6.01E-07	8.87E-06	6.014	430431	TRIP10	NM_004240.2	Hs thyroid hormone receptor interactor 10 (TRIP10), mRNA.
0.552	5.886	6.01E-06	5.66E-05	3.705	5810328	FTL	NM_000146.3	Hs ferritin, light polypeptide (FTL), mRNA.
0.552	6.228	2.69E-06	2.96E-05	4.510	3800202	LOC390530	XM_372543.2	PREDICTED: Hs similar to Ig heavy chain V-I region HG3 precursor (LOC390530), mRNA.
0.552	5.748	8.32E-06	7.42E-05	3.378	3710719	MRPL45	NM_032351.3	Hs mitochondrial ribosomal protein L45 (MRPL45), nuclear gene encoding mitochondrial protein, mRNA.
0.551	7.079	3.88E-07	6.23E-06	6.455	240682	ANKRD37	NM_181726.2	Hs ankyrin repeat domain 37 (ANKRD37), mRNA.
0.551	7.371	2.04E-07	3.76E-06	7.099	6330044	ANXA7	NM_004034.1	Hs annexin A7 (ANXA7), tv: 2, mRNA.
0.551	6.310	2.22E-06	2.54E-05	4.701	2320053	SAP30L	NM_024632.4	Hs SAP30-like (SAP30L), mRNA.
0.551	5.786	7.61E-06	6.88E-05	3.468	7100280	C11ORF48	NM_024099.3	Hs chromosome 11 open reading frame 48 (C11orf48), mRNA.
0.551	7.819	7.78E-08	1.78E-06	8.068	3390239	LOC651158	XM_940286.1	PREDICTED: Hs similar to apolipoprotein B mRNA editing enzyme, catalytic polypeptide-like 3F isoform a
0.550	6.375	1.91E-06	2.25E-05	4.851	1110440	WDR77	NM_024102.2	Hs WD repeat domain 77 (WDR77), mRNA.
0.549	6.221	2.73E-06	2.99E-05	4.494	2600059	GNPDA1	NM_005471.3	Hs glucosamine-6-phosphate deaminase 1 (GNPDA1), mRNA.
0.548	6.950	5.17E-07	7.84E-06	6.165	10487	SLC25A25	NM_052901.2	Hs solute carrier family 25 (mitochondrial carrier; phosphate carrier), member 25 (SLC25A25), nuclear gene
0.548	6.239	2.62E-06	2.90E-05	4.536	1450370	DCP1A	NM_018403.4	Hs DCP1 decapping enzyme homolog A (S. cerevisiae) (DCP1A), mRNA.
0.547	7.351	2.13E-07	3.89E-06	7.057	2750392	EPM2A	NM_005670.3	Hs epilepsy, progressive myoclonus type 2A, Lafora disease (laforin) (EPM2A), tv: 1, mRNA.
0.547	7.435	1.77E-07	3.39E-06	7.240	3850136	CLCN6	NM_001286.2	Hs chloride channel 6 (CLCN6), tv: ClC-6a, mRNA.
0.546	5.652	1.05E-05	8.96E-05	3.150	2750647	C20ORF27	NM_001039140.1	Hs chromosome 20 open reading frame 27 (C20orf27), mRNA.
0.546	8.198	3.51E-08	9.78E-07	8.868	2120026	LOC100134300	XR_038277.1	PREDICTED: Hs misc_RNA (LOC100134300), miscRNA.
0.546	6.296	2.30E-06	2.60E-05	4.669	6510685	LOC100127983	XM_001722508.1	PREDICTED: Hs hypothetical protein LOC100127983 (LOC100127983), mRNA.
0.546	6.208	2.82E-06	3.07E-05	4.463	3520239	KDM6B	NM_001080424.1	Hs lysine (K)-specific demethylase 6B (KDM6B), mRNA.
0.545	8.718	1.22E-08	4.44E-07	9.930	2570240	SULF1	NM_015170.1	Hs sulfatase 1 (SULF1), mRNA.
0.545	6.836	6.68E-07	9.59E-06	5.909	6020600	PHC3	NM_024947.2	Hs polyhomeotic homolog 3 (Drosophila) (PHC3), mRNA.
0.545	5.805	7.27E-06	6.63E-05	3.513	1470093	LOC440776	XM_496483.3	PREDICTED: Hs hypothetical LOC440776 (LOC440776), mRNA.

Appendix 4 – Genes differentially expressed at 24 hours in cells treated with IGF1 ligand

0.545	5.727	8.76E-06	7.73E-05	3.327	4780615	ANXA2	NM_001002858.1	Hs annexin A2 (ANXA2), tv: 1, mRNA.
0.544	6.468	1.54E-06	1.90E-05	5.067	2060646	MRPL20	NM_017971.2	Hs mitochondrial ribosomal protein L20 (MRPL20), nuclear gene encoding mitochondrial protein, mRNA.
0.543	5.999	4.59E-06	4.54E-05	3.973	430731	WDR53	NM_182627.1	Hs WD repeat domain 53 (WDR53), mRNA.
0.542	5.912	5.65E-06	5.39E-05	3.766	620072	DNAJC27	NM_016544.1	Hs DnaJ (Hsp40) homolog, subfamily C, member 27 (DNAJC27), mRNA.
0.542	5.629	1.10E-05	9.37E-05	3.094	2480338	DBI	NM_020548.4	Hs diazepam binding inhibitor (GABA receptor modulator, acyl-Coenzyme A binding protein) (DBI), mRNA
0.542	6.772	7.72E-07	1.08E-05	5.762	2750040	ZNF526	NM_133444.1	Hs zinc finger protein 526 (ZNF526), mRNA.
0.541	7.444	1.74E-07	3.35E-06	7.260	3710332	PSMB3	NM_002795.2	Hs proteasome (prosome, macropain) subunit, beta type, 3 (PSMB3), mRNA.
0.541	7.512	1.50E-07	2.98E-06	7.407	730497	CC2D1B	NM_032449.1	Hs coiled-coil and C2 domain containing 1B (CC2D1B), mRNA.
0.541	5.557	1.31E-05	0.000108008	2.920	1440639	SNRNP25	NM_024571.3	Hs small nuclear ribonucleoprotein 25kDa (U11/U12) (SNRNP25), mRNA.
0.541	5.774	7.83E-06	7.04E-05	3.439	160204	RPP40	NM_006638.2	Hs ribonuclease P/MRP 40kDa subunit (RPP40), mRNA.
0.540	5.945	5.22E-06	5.04E-05	3.846	4570333	YARS2	NM_001040436.1	Hs tyrosyl-tRNA synthetase 2, mitochondrial (YARS2), nuclear gene encoding mitochondrial protein, mRNA
0.540	5.895	5.88E-06	5.56E-05	3.726	3780131	C19ORF50	NM_024069.2	Hs chromosome 19 open reading frame 50 (C19orf50), mRNA.
0.540	7.286	2.46E-07	4.34E-06	6.913	6370468	BOLA2	NM_001031827.1	Hs bolA homolog 2 (E. coli) (BOLA2), mRNA.
0.539	5.758	8.13E-06	7.26E-05	3.402	6660152	KLHL12	NM_021633.2	Hs kelch-like 12 (Drosophila) (KLHL12), mRNA.
0.539	5.553	1.33E-05	0.000108794	2.911	6220736	FANCB	NM_152633.2	Hs Fanconi anemia, complementation group B (FANCB), tv: 2, mRNA.
0.539	6.168	3.09E-06	3.31E-05	4.370	1230487	SRGAP3	NM_001033117.1	Hs SLIT-ROBO Rho GTPase activating protein 3 (SRGAP3), tv: 2, mRNA.
0.539	6.150	3.22E-06	3.43E-05	4.328	3060440	NME1	NM_198175.1	Hs non-metastatic cells 1, protein (NM23A) expressed in (NME1), tv: 1, mRNA.
0.538	5.830	6.86E-06	6.34E-05	3.572	4150482	DOM3Z	NM_005510.3	Hs dom-3 homolog Z (C. elegans) (DOM3Z), mRNA.
0.538	6.471	1.53E-06	1.89E-05	5.075	1090451	PAX8	NM_003466.3	Hs paired box 8 (PAX8), tv: PAX8A, mRNA.
0.538	6.680	9.51E-07	1.29E-05	5.553	6940521	MRPL43	NM_032112.2	Hs mitochondrial ribosomal protein L43 (MRPL43), nuclear gene encoding mitochondrial protein, tv: 1, mR
0.538	8.503	1.88E-08	6.11E-07	9.494	5130441	CA5BP	NR_026551.1	Hs carbonic anhydrase VB pseudogene (CA5BP), non-coding RNA.
0.537	6.171	3.07E-06	3.29E-05	4.376	1240452	PINX1	NM_017884.4	Hs PIN2-interacting protein 1 (PINX1), mRNA.
0.536	6.449	1.61E-06	1.96E-05	5.024	2360364	LOC440356	XM_934751.1	PREDICTED: Hs hypothetical gene supported by AK131031; BC070380, tv: 2 (LOC440356), mRNA.
0.536	7.468	1.65E-07	3.21E-06	7.312	5860477	CANX	NM_001024649.1	Hs calnexin (CANX), tv: 2, mRNA.
0.536	6.166	3.11E-06	3.32E-05	4.365	5900491	ZNF34	NM_030580.2	Hs zinc finger protein 34 (ZNF34), mRNA.
0.536	6.332	2.11E-06	2.44E-05	4.753	3450598	TM4SF19	XM_001134247.1	PREDICTED: Hs transmembrane 4 L six family member 19, tv: 2 (TM4SF19), mRNA.
0.535	5.685	9.66E-06	8.37E-05	3.228	5910138	NGDN	NM_001042635.1	Hs neuroguidin, EIF4E binding protein (NGDN), tv: 1, mRNA.
0.534	5.911	5.65E-06	5.39E-05	3.766	3360681	TNFAIP3	NM_006290.2	Hs tumor necrosis factor, alpha-induced protein 3 (TNFAIP3), mRNA.
0.534	6.175	3.04E-06	3.27E-05	4.386	6770608	BNIP3	NM_004052.2	Hs BCL2/adenovirus E1B 19kDa interacting protein 3 (BNIP3), nuclear gene encoding mitochondrial protei
0.534	6.570	1.22E-06	1.57E-05	5.303	4730204	FCRLB	NM_001002901.2	Hs Fc receptor-like B (FCRLB), mRNA.
0.533	5.871	6.21E-06	5.83E-05	3.671	510544	RAD51C	NM_058216.1	Hs RAD51 homolog C (S. cerevisiae) (RAD51C), tv: 1, mRNA.
0.532	5.572	1.27E-05	0.000104814	2.959	6220504	CTH	NM_001902.4	Hs cystathionase (cystathionine gamma-lyase) (CTH), tv: 1, mRNA.
0.532	7.597	1.25E-07	2.58E-06	7.593	3120176	CNOT7	NM_013354.5	Hs CCR4-NOT transcription complex, subunit 7 (CNOT7), tv: 1, mRNA.
0.531	7.280	2.49E-07	4.37E-06	6.900	3520343	C10ORF140	NM_207371.3	Hs chromosome 10 open reading frame 140 (C10orf140), mRNA.
0.531	8.083	4.46E-08	1.18E-06	8.626	3180037	GTDC1	NM_024659.2	Hs glycosyltransferase-like domain containing 1 (GTDC1), tv: 2, mRNA.
0.530	5.815	7.10E-06	6.52E-05	3.537	2230541	CCDC16	NM_052857.2	Hs coiled-coil domain containing 16 (CCDC16), mRNA.
0.530	5.880	6.09E-06	5.73E-05	3.691	6560608	C7ORF20	NM_015949.2	Hs chromosome 7 open reading frame 20 (C7orf20), mRNA. XM_946081 XM_946082 XM_946083
0.530	6.969	4.96E-07	7.58E-06	6.207	6520075	GDE1	NM_016641.3	Hs glycerophosphodiester phosphodiesterase 1 (GDE1), mRNA.
0.529	5.912	5.64E-06	5.38E-05	3.768	7200402	AP3S1	NM_001002924.1	Hs adaptor-related protein complex 3, sigma 1 subunit (AP3S1), tv: 2, mRNA.
0.529	6.017	4.41E-06	4.39E-05	4.014	4150711	USP37	NM_020935.1	Hs ubiquitin specific peptidase 37 (USP37), mRNA.

Appendix 4 – Genes differentially expressed at 24 hours in cells treated with IGF1 ligand

0.529	6.312	2.21E-06	2.53E-05	4.707	6270717	SNRPC	NM_003093.1	Hs small nuclear ribonucleoprotein polypeptide C (SNRPC), mRNA.
0.529	5.835	6.76E-06	6.26E-05	3.586	3710189	LIAS	NM_194451.1	Hs lipoic acid synthetase (LIAS), nuclear gene encoding mitochondrial protein, tv: 2, mRNA.
0.528	6.451	1.61E-06	1.96E-05	5.027	540139	NFKBIE	NM_004556.2	Hs nuclear factor of kappa light polypeptide gene enhancer in B-cells inhibitor, epsilon (NFKBIE), mRNA.
0.528	5.992	4.68E-06	4.60E-05	3.955	5310465	MRPS12	NM_033362.2	Hs mitochondrial ribosomal protein S12 (MRPS12), nuclear gene encoding mitochondrial protein, tv: 2, mR
0.528	6.303	2.26E-06	2.57E-05	4.684	4120025	CHCHD8	NM_016565.2	Hs coiled-coil-helix-coiled-coil-helix domain containing 8 (CHCHD8), mRNA.
0.527	6.308	2.23E-06	2.55E-05	4.697	7650020	AADACL1	NM_020792.3	Hs arylacetamide deacetylase-like 1 (AADACL1), mRNA.
0.526	6.748	8.15E-07	1.13E-05	5.708	130446	SNX11	NM_152244.1	Hs sorting nexin 11 (SNX11), tv: 1, mRNA.
0.526	6.703	9.02E-07	1.23E-05	5.606	1820196	OVGP1	NM_002557.3	Hs oviductal glycoprotein 1, 120kDa (OVGP1), mRNA.
0.525	6.821	6.91E-07	9.85E-06	5.874	2570707	N6AMT1	NM_013240.3	Hs N-6 adenine-specific DNA methyltransferase 1 (putative) (N6AMT1), tv: 1, mRNA.
0.525	5.993	4.66E-06	4.59E-05	3.960	5360039	BPNT1	NM_006085.4	Hs 3'(2'), 5'-bisphosphate nucleotidase 1 (BPNT1), mRNA.
0.524	5.804	7.28E-06	6.64E-05	3.512	7560164	GCAT	NM_014291.2	Hs glycine C-acetyltransferase (2-amino-3-ketobutyrate coenzyme A ligase) (GCAT), nuclear gene encoding
0.524	7.594	1.26E-07	2.60E-06	7.585	4920215	C9ORF64	NM_032307.3	Hs chromosome 9 open reading frame 64 (C9orf64), mRNA.
0.523	6.176	3.03E-06	3.26E-05	4.389	6100154	C2ORF44	NM_025203.1	Hs chromosome 2 open reading frame 44 (C2orf44), mRNA.
0.523	7.538	1.42E-07	2.86E-06	7.465	5550612	BRP44	NM_015415.2	Hs brain protein 44 (BRP44), tv: 2, mRNA.
0.522	5.723	8.83E-06	7.77E-05	3.319	3610156	CDKL3	NM_016508.2	Hs cyclin-dependent kinase-like 3 (CDKL3), mRNA.
0.522	5.594	1.20E-05	0.000100655	3.009	2070093	LIG4	NM_206937.1	Hs ligase IV, DNA, ATP-dependent (LIG4), tv: 2, mRNA.
0.522	6.036	4.21E-06	4.24E-05	4.061	6900392	CHCHD5	NM_032309.2	Hs coiled-coil-helix-coiled-coil-helix domain containing 5 (CHCHD5), mRNA.
0.522	7.533	1.44E-07	2.88E-06	7.453	1980768	SIAH2	NM_005067.5	Hs seven in absentia homolog 2 (Drosophila) (SIAH2), mRNA.
0.522	6.677	9.58E-07	1.30E-05	5.546	50487	BUD13	NM_032725.2	Hs BUD13 homolog (S. cerevisiae) (BUD13), mRNA.
0.522	6.443	1.63E-06	1.98E-05	5.010	7330270	ADNP2	NM_014913.2	Hs ADNP homeobox 2 (ADNP2), mRNA.
0.521	6.986	4.77E-07	7.35E-06	6.246	2940746	NNMT	NM_006169.2	Hs nicotinamide N-methyltransferase (NNMT), mRNA.
0.521	6.032	4.25E-06	4.27E-05	4.051	3780600	SPCS3	NM_021928.2	Hs signal peptidase complex subunit 3 homolog (S. cerevisiae) (SPCS3), mRNA.
0.520	5.526	1.42E-05	0.000114917	2.847	4220026	NUBP1	NM_002484.2	Hs nucleotide binding protein 1 (MinD homolog, E. coli) (NUBP1), mRNA.
0.520	6.334	2.10E-06	2.43E-05	4.758	6480669	DONSON	NM_017613.2	Hs downstream neighbor of SON (DONSON), mRNA.
0.520	5.857	6.43E-06	6.01E-05	3.636	290332	TAF13	NM_005645.3	Hs TAF13 RNA polymerase II, TATA box binding protein (TBP)-associated factor, 18kDa (TAF13), mRNA
0.519	5.956	5.08E-06	4.92E-05	3.872	3440386	ECM1	NM_004425.2	Hs extracellular matrix protein 1 (ECM1), tv: 1, mRNA.
0.519	8.812	1.01E-08	3.92E-07	10.119	3610626	ADM2	NM_024866.4	Hs adrenomedullin 2 (ADM2), mRNA.
0.519	7.292	2.42E-07	4.29E-06	6.927	3940167	CNRIP1	NM_015463.2	Hs cannabinoid receptor interacting protein 1 (CNRIP1), tv: CRIP1a, mRNA.
0.519	6.471	1.53E-06	1.89E-05	5.074	4230044	LOC730173	XR_039686.1	PREDICTED: Hs misc_RNA (LOC730173), miscRNA.
0.519	6.950	5.18E-07	7.84E-06	6.164	4260364	PHAX	NM_032177.2	Hs phosphorylated adaptor for RNA export (PHAX), mRNA.
0.518	7.284	2.47E-07	4.35E-06	6.908	6770309	MYL6	NM_021019.3	Hs myosin, light chain 6, alkali, smooth muscle and non-muscle (MYL6), tv: 1, mRNA.
0.518	6.939	5.30E-07	8.00E-06	6.140	2710524	MAP1B	NM_032010.1	Hs microtubule-associated protein 1B (MAP1B), tv: 2, mRNA.
0.517	5.741	8.46E-06	7.52E-05	3.362	4040563	LOC441241	XM_935516.1	PREDICTED: Hs chaperonin containing TCP1, subunit 6A (zeta 1)-like (LOC441241), mRNA.
0.517	6.430	1.68E-06	2.03E-05	4.980	2140360	INF2	NM_032714.1	Hs inverted formin, FH2 and WH2 domain containing (INF2), tv: 3, mRNA.
0.515	7.439	1.76E-07	3.37E-06	7.250	730100	UFD1L	NM_001035247.1	Hs ubiquitin fusion degradation 1 like (yeast) (UFD1L), tv: 2, mRNA.
0.514	5.813	7.13E-06	6.54E-05	3.533	2100224	RHBDD3	NM_012265.1	Hs rhomboid domain containing 3 (RHBDD3), mRNA.
0.513	8.900	8.48E-09	3.39E-07	10.293	6370369	CD14	NM_001040021.1	Hs CD14 molecule (CD14), tv: 2, mRNA.
0.513	5.937	5.32E-06	5.11E-05	3.827	620767	MRPL49	NM_004927.2	Hs mitochondrial ribosomal protein L49 (MRPL49), nuclear gene encoding mitochondrial protein, mRNA.
0.512	6.869	6.20E-07	9.07E-06	5.984	6250386	LOC653147	XM_926208.2	PREDICTED: Hs similar to 60S ribosomal protein L26-like 1 (LOC653147), mRNA.
0.512	8.067	4.61E-08	1.20E-06	8.594	6250451	CENPI	NM_006733.2	Hs centromere protein I (CENPI), mRNA.

Appendix 4 – Genes differentially expressed at 24 hours in cells treated with IGF1 ligand

0.512	5.580	1.24E-05	0.000103193	2.976	3400674	MRPS15	NM_031280.2	Hs mitochondrial ribosomal protein S15 (MRPS15), nuclear gene encoding mitochondrial protein, mRNA.
0.511	5.963	5.00E-06	4.86E-05	3.888	6620026	CD83	NM_004233.3	Hs CD83 molecule (CD83), tv: 1, mRNA.
0.511	5.702	9.28E-06	8.11E-05	3.269	670561	DHRS7B	NM_015510.3	Hs dehydrogenase/reductase (SDR family) member 7B (DHRS7B), mRNA.
0.511	6.390	1.85E-06	2.19E-05	4.886	3930053	COX10	NM_001303.2	Hs COX10 homolog, cytochrome c oxidase assembly protein, heme A: farnesyltransferase (yeast) (COX10),
0.509	6.146	3.26E-06	3.45E-05	4.318	6350131	CTRL	NM_001907.1	Hs chymotrypsin-like (CTRL), mRNA.
0.508	6.398	1.81E-06	2.16E-05	4.906	1010521	SP4	NM_003112.3	Hs Sp4 transcription factor (SP4), mRNA.
0.508	7.330	2.23E-07	4.02E-06	7.010	290594	LOC644760	XM_932354.1	PREDICTED: Hs hypothetical protein LOC644760 (LOC644760), mRNA.
0.507	5.733	8.62E-06	7.63E-05	3.343	20195	SUV39H1	NM_003173.2	Hs suppressor of variegation 3-9 homolog 1 (Drosophila) (SUV39H1), mRNA.
0.507	5.664	1.02E-05	8.76E-05	3.176	7200437	MOCS2	NM_176806.2	Hs molybdenum cofactor synthesis 2 (MOCS2), tv: 1, mRNA.
0.507	6.060	3.98E-06	4.05E-05	4.117	510327	ELK4	NM_001973.2	Hs ELK4, ETS-domain protein (SRF accessory protein 1) (ELK4), tv: a, mRNA.
0.506	5.808	7.22E-06	6.60E-05	3.520	6660270	MRPL17	NM_022061.2	Hs mitochondrial ribosomal protein L17 (MRPL17), nuclear gene encoding mitochondrial protein, mRNA.
0.504	6.531	1.34E-06	1.70E-05	5.212	6380463	OSTF1	NM_012383.3	Hs osteoclast stimulating factor 1 (OSTF1), mRNA.
0.504	6.542	1.30E-06	1.65E-05	5.239	6200753	SWAP70	NM_015055.2	Hs SWAP switching B-cell complex 70kDa subunit (SWAP70), mRNA.
0.503	6.482	1.49E-06	1.86E-05	5.100	5270367	CTSC	NM_001814.2	Hs cathepsin C (CTSC), tv: 1, mRNA.
0.502	6.434	1.67E-06	2.02E-05	4.988	4230296	PSMC2	NM_002803.2	Hs proteasome (prosome, macropain) 26S subunit, ATPase, 2 (PSMC2), mRNA.
0.501	6.663	9.87E-07	1.32E-05	5.516	380056	B3GNT2	NM_006577.5	Hs UDP-GlcNAc:betaGal beta-1,3-N-acetylglucosaminyltransferase 2 (B3GNT2), mRNA.
0.501	6.250	2.55E-06	2.84E-05	4.562	1010630	NOP2	NM_006170.2	Hs NOP2 nucleolar protein homolog (yeast) (NOP2), tv: 1, mRNA.
0.501	5.968	4.95E-06	4.82E-05	3.899	1410079	CDC26	NM_139286.3	Hs cell division cycle 26 homolog (S. cerevisiae) (CDC26), mRNA.
0.501	5.733	8.63E-06	7.63E-05	3.341	3180348	SCYL3	NM_020423.4	Hs SCY1-like 3 (S. cerevisiae) (SCYL3), tv: 1, mRNA.
0.500	6.752	8.07E-07	1.12E-05	5.718	3360181	SMTN	NM_134269.1	Hs smoothelin (SMTN), tv: 2, mRNA.
0.500	5.878	6.11E-06	5.74E-05	3.688	4760398	CCDC107	NM_174923.1	Hs coiled-coil domain containing 107 (CCDC107), mRNA.
0.500	6.115	3.50E-06	3.67E-05	4.245	2060082	MRPS10	NM_018141.2	Hs mitochondrial ribosomal protein S10 (MRPS10), nuclear gene encoding mitochondrial protein, mRNA.
0.500	5.822	6.97E-06	6.42E-05	3.555	7560215	LOC100129685	XM_001723814.1	PREDICTED: Hs hypothetical protein LOC100129685 (LOC100129685), mRNA.
-0.500	-5.852	6.51E-06	6.07E-05	3.624	2190541	GATS	NM_178831.4	Hs opposite strand transcription unit to STAG3 (GATS), mRNA.
-0.500	-6.377	1.90E-06	2.24E-05	4.856	6060477	ZFP112	NM_001083335.1	Hs zinc finger protein 112 homolog (mouse) (ZFP112), tv: 1, mRNA.
-0.501	-5.839	6.71E-06	6.23E-05	3.594	940162	ZFHX4	NM_024721.3	Hs zinc finger homeobox 4 (ZFHX4), mRNA.
-0.501	-6.331	2.12E-06	2.44E-05	4.749	2940687	C9ORF5	NM_032012.3	Hs chromosome 9 open reading frame 5 (C9orf5), mRNA.
-0.502	-6.580	1.19E-06	1.54E-05	5.324	540379	DLG3	NM_021120.2	Hs discs, large homolog 3 (Drosophila) (DLG3), tv: 1, mRNA.
-0.502	-8.453	2.08E-08	6.56E-07	9.394	3370075	S1PR4	NM_003775.2	Hs sphingosine-1-phosphate receptor 4 (S1PR4), mRNA.
-0.502	-6.576	1.21E-06	1.55E-05	5.315	870161	CXADR	NM_001338.3	Hs coxsackie virus and adenovirus receptor (CXADR), mRNA.
-0.503	-5.576	1.25E-05	0.000103857	2.968	2120112	TRIM9	NM_015163.4	Hs tripartite motif-containing 9 (TRIM9), tv: 1, mRNA.
-0.504	-5.527	1.41E-05	0.0001147	2.849	6900612	DSTN	NM_001011546.1	Hs destrin (actin depolymerizing factor) (DSTN), tv: 2, mRNA.
-0.504	-7.425	1.81E-07	3.45E-06	7.218	4070296	BCORL1	NM_021946.2	Hs BCL6 co-repressor-like 1 (BCORL1), mRNA.
-0.504	-6.255	2.53E-06	2.81E-05	4.573	4120019	PLSCR4	NM_020353.1	Hs phospholipid scramblase 4 (PLSCR4), mRNA.
-0.505	-5.527	1.41E-05	0.0001147	2.849	1440037	BID	NM_197966.1	Hs BH3 interacting domain death agonist (BID), tv: 1, mRNA.
-0.506	-6.146	3.26E-06	3.45E-05	4.318	110521	ALX1	NM_006982.2	Hs ALX homeobox 1 (ALX1), mRNA.
-0.507	-7.804	8.02E-08	1.81E-06	8.038	2640601	GIT1	NM_014030.3	Hs G protein-coupled receptor kinase interacting ArfGAP 1 (GIT1), tv: 2, mRNA.
-0.507	-5.947	5.20E-06	5.03E-05	3.849	1940487	STAT5A	NM_003152.2	Hs signal transducer and activator of transcription 5A (STAT5A), mRNA.
-0.507	-7.923	6.24E-08	1.51E-06	8.290	4280129	ELP2	NM_018255.1	Hs elongation protein 2 homolog (S. cerevisiae) (ELP2), mRNA.
-0.508	-7.851	7.27E-08	1.70E-06	8.136	6180050	STK24	NM_003576.3	Hs serine/threonine kinase 24 (STE20 homolog, yeast) (STK24), tv: 1, mRNA.

Appendix 4 – Genes differentially expressed at 24 hours in cells treated with IGF1 ligand

-0.508	-6.089	3.72E-06	3.84E-05	4.184	1090477	BTRC	NM_033637.2	Hs beta-transducin repeat containing (BTRC), tv: 1, mRNA.
-0.508	-7.939	6.03E-08	1.47E-06	8.325	4150176	LOC644544	XM_927666.1	PREDICTED: Hs hypothetical protein LOC644544 (LOC644544), mRNA.
-0.509	-6.221	2.74E-06	3.00E-05	4.493	2260373	SOX5	NM_006940.4	Hs SRY (sex determining region Y)-box 5 (SOX5), tv: 1, mRNA.
-0.510	-7.980	5.54E-08	1.38E-06	8.410	580121	SNX1	NM_003099.3	Hs sorting nexin 1 (SNX1), tv: 1, mRNA.
-0.510	-8.204	3.47E-08	9.68E-07	8.879	3440491	GALC	NM_000153.2	Hs galactosylceramidase (GALC), tv: 1, mRNA.
-0.511	-6.161	3.15E-06	3.36E-05	4.353	3170491	PDIA5	NM_006810.2	Hs protein disulfide isomerase family A, member 5 (PDIA5), mRNA.
-0.511	-5.529	1.40E-05	0.000114157	2.855	7400689	C20ORF11	NM_017896.2	Hs chromosome 20 open reading frame 11 (C20orf11), mRNA.
-0.511	-6.274	2.41E-06	2.70E-05	4.619	4780239	NID1	NM_002508.2	Hs nidogen 1 (NID1), mRNA.
-0.512	-6.416	1.74E-06	2.08E-05	4.947	10768	LARGE	NM_004737.3	Hs like-glycosyltransferase (LARGE), tv: 1, mRNA.
-0.512	-5.940	5.28E-06	5.08E-05	3.834	4730082	LOC731096	XM_001129635.1	PREDICTED: Hs similar to Elongation factor 1-gamma (EF-1-gamma) (eEF-1B gamma) (LOC731096), mR
-0.512	-5.990	4.69E-06	4.61E-05	3.952	6580753	MIB2	NM_080875.1	Hs mindbomb homolog 2 (Drosophila) (MIB2), mRNA.
-0.512	-6.191	2.93E-06	3.16E-05	4.425	5260477	LOC100133163	XM_001726385.1	PREDICTED: Hs similar to breakpoint cluster region (LOC100133163), mRNA.
-0.512	-5.593	1.20E-05	0.000100692	3.008	1940670	FAM86B1	NM_001083537.1	Hs family with sequence similarity 86, member B1 (FAM86B1), tv: 1, mRNA.
-0.513	-6.101	3.62E-06	3.75E-05	4.212	2510546	C10ORF125	NM_198472.2	Hs chromosome 10 open reading frame 125 (C10orf125), tv: 2, mRNA.
-0.513	-6.945	5.23E-07	7.92E-06	6.153	7570196	TSPAN9	NM_006675.3	Hs tetraspanin 9 (TSPAN9), mRNA.
-0.513	-6.786	7.48E-07	1.05E-05	5.795	4490180	BEXL1	XM_936467.2	PREDICTED: Hs brain expressed X-linked-like 1 (BEXL1), mRNA.
-0.513	-7.819	7.77E-08	1.78E-06	8.069	7570195	KIAA0355	NM_014686.3	Hs KIAA0355 (KIAA0355), mRNA.
-0.513	-6.056	4.02E-06	4.08E-05	4.108	780133	SH3D19	NM_001009555.2	Hs SH3 domain containing 19 (SH3D19), mRNA.
-0.514	-6.914	5.60E-07	8.36E-06	6.085	7000338	LOC552889	NM_001136262.1	Hs hypothetical protein LOC552889 (LOC552889), mRNA.
-0.514	-5.616	1.14E-05	9.62E-05	3.062	3870349	LOC388279	XM_373688.4	PREDICTED: Hs hypothetical LOC388279 (LOC388279), mRNA.
-0.515	-5.995	4.63E-06	4.57E-05	3.964	2710725	HP1BP3	NM_016287.3	Hs heterochromatin protein 1, binding protein 3 (HP1BP3), mRNA.
-0.515	-6.025	4.33E-06	4.32E-05	4.033	1430711	KLF12	NM_007249.4	Hs Kruppel-like factor 12 (KLF12), mRNA.
-0.515	-5.793	7.48E-06	6.78E-05	3.484	2970164	EDNRB	NM_000115.1	Hs endothelin receptor type B (EDNRB), tv: 1, mRNA.
-0.516	-6.106	3.57E-06	3.72E-05	4.225	4050593	MRC2	NM_006039.3	Hs mannose receptor, C type 2 (MRC2), mRNA.
-0.516	-7.454	1.70E-07	3.29E-06	7.282	1570661	CYP2J2	NM_000775.2	Hs cytochrome P450, family 2, subfamily J, polypeptide 2 (CYP2J2), mRNA.
-0.517	-6.382	1.88E-06	2.22E-05	4.868	5960544	SEPHS1	NM_012247.3	Hs selenophosphate synthetase 1 (SEPHS1), mRNA.
-0.517	-6.198	2.89E-06	3.13E-05	4.439	130551	PRKCZ	NM_002744.4	Hs protein kinase C, zeta (PRKCZ), tv: 1, mRNA.
-0.517	-7.068	3.97E-07	6.34E-06	6.431	3420471	CAMK2D	NM_172128.1	Hs calcium/calmodulin-dependent protein kinase (CaM kinase) II delta (CAMK2D), tv: 2, mRNA.
-0.518	-5.548	1.34E-05	0.000109565	2.901	2340240	C15ORF38	NM_182616.1	Hs chromosome 15 open reading frame 38 (C15orf38), mRNA.
-0.518	-5.976	4.85E-06	4.74E-05	3.919	3060754	SEMA4F	NM_004263.3	Hs sema domain, immunoglobulin domain (Ig), transmembrane domain (TM) and short cytoplasmic domain,
-0.518	-6.160	3.15E-06	3.36E-05	4.351	2810372	NPR2	NM_003995.3	Hs natriuretic peptide receptor B/guanylate cyclase B (atrionatriuretic peptide receptor B) (NPR2), mRNA.
-0.519	-6.074	3.85E-06	3.94E-05	4.150	4210382	DLL3	NM_016941.2	Hs delta-like 3 (Drosophila) (DLL3), tv: 1, mRNA.
-0.520	-6.194	2.91E-06	3.15E-05	4.431	4390382	KIAA0182	NM_014615.1	Hs KIAA0182 (KIAA0182), mRNA.
-0.521	-5.839	6.71E-06	6.23E-05	3.593	1440601	HS.556994		zx42c01.r1 Soares_total_fetus_Nb2HF8_9w Hs cDNA clone IMAGE:789120 5, mRNA sequence
-0.521	-6.029	4.28E-06	4.29E-05	4.044	1690240	C5ORF4	NM_032385.3	Hs chromosome 5 open reading frame 4 (C5orf4), mRNA.
-0.521	-5.548	1.34E-05	0.000109565	2.901	830010	SLC6A10P	NR_003083.2	Hs solute carrier family 6 (neurotransmitter transporter, creatine), member 10 (pseudogene) (SLC6A10P) on
-0.522	-5.688	9.61E-06	8.34E-05	3.234	6860291	GAS8	NM_001481.1	Hs growth arrest-specific 8 (GAS8), mRNA.
-0.522	-5.841	6.67E-06	6.20E-05	3.599	3930670	LOC100132323	XM_001720619.1	PREDICTED: Hs hypothetical protein LOC100132323 (LOC100132323), mRNA.
-0.522	-6.757	7.98E-07	1.11E-05	5.730	4290278	WT1	NM_000378.3	Hs Wilms tumor 1 (WT1), tv: A, mRNA.
-0.523	-5.870	6.23E-06	5.85E-05	3.667	1410538	CYP2R1	NM_024514.4	Hs cytochrome P450, family 2, subfamily R, polypeptide 1 (CYP2R1), mRNA.

Appendix 4 – Genes differentially expressed at 24 hours in cells treated with IGF1 ligand

-0.523	-6.368	1.94E-06	2.27E-05	4.836	4610546	PCDHGA5	NM_018918.2	Hs protocadherin gamma subfamily A, 5 (PCDHGA5), tv: 1, mRNA.
-0.524	-6.027	4.31E-06	4.31E-05	4.038	6330397	TRIM7	NM_033342.2	Hs tripartite motif-containing 7 (TRIM7), tv: 6, mRNA.
-0.524	-5.558	1.31E-05	0.000107815	2.923	6940280	GPR177	NM_001002292.1	Hs G protein-coupled receptor 177 (GPR177), tv: 2, mRNA.
-0.525	-5.795	7.43E-06	6.76E-05	3.491	2760202	AP3M1	NM_012095.4	Hs adaptor-related protein complex 3, mu 1 subunit (AP3M1), tv: 2, mRNA.
-0.525	-6.125	3.42E-06	3.60E-05	4.268	3390129	C9ORF103	NM_001001551.1	Hs chromosome 9 open reading frame 103 (C9orf103), mRNA.
-0.526	-5.529	1.41E-05	0.000114337	2.853	4560072	TUB	NM_177972.1	Hs tubby homolog (mouse) (TUB), tv: 2, mRNA.
-0.527	-6.704	9.01E-07	1.23E-05	5.608	3420689	BRD8	NM_183359.1	Hs bromodomain containing 8 (BRD8), tv: 3, mRNA.
-0.527	-6.860	6.33E-07	9.21E-06	5.962	160411	NCOA1	NM_147223.2	Hs nuclear receptor coactivator 1 (NCOA1), tv: 2, mRNA.
-0.527	-5.730	8.70E-06	7.68E-05	3.334	3930195	MYST3	NM_006766.2	Hs MYST histone acetyltransferase (monocytic leukemia) 3 (MYST3), mRNA.
-0.528	-5.852	6.50E-06	6.07E-05	3.625	5670288	IFT88	NM_006531.3	Hs intraflagellar transport 88 homolog (Chlamydomonas) (IFT88), tv: 2, mRNA.
-0.529	-6.108	3.56E-06	3.71E-05	4.230	4540689	ANKRD10	NM_017664.2	Hs ankyrin repeat domain 10 (ANKRD10), mRNA.
-0.529	-7.651	1.11E-07	2.35E-06	7.710	5420110	KIAA1279	NM_015634.2	Hs KIAA1279 (KIAA1279), mRNA.
-0.530	-6.909	5.67E-07	8.43E-06	6.073	1110465	YPEL2	NM_001005404.3	Hs yippee-like 2 (Drosophila) (YPEL2), mRNA.
-0.530	-5.604	1.17E-05	9.85E-05	3.034	5860605	PDCD6IP	NM_013374.3	Hs programmed cell death 6 interacting protein (PDCD6IP), mRNA.
-0.531	-6.391	1.84E-06	2.18E-05	4.890	940296	LOC653841	XM_935522.2	PREDICTED: Hs similar to integrator complex subunit 4 (LOC653841), mRNA.
-0.532	-6.035	4.23E-06	4.25E-05	4.057	510224	LPIN2	NM_014646.2	Hs lipin 2 (LPIN2), mRNA.
-0.532	-6.184	2.98E-06	3.21E-05	4.407	1260767	FAM3C	NM_001040020.1	Hs family with sequence similarity 3, member C (FAM3C), tv: 2, mRNA.
-0.532	-6.850	6.47E-07	9.36E-06	5.940	2350722	PLA2G4B	NM_005090.2	Hs phospholipase A2, group IVB (cytosolic) (PLA2G4B), mRNA.
-0.532	-5.965	4.98E-06	4.84E-05	3.893	160605	RASA3	NM_007368.2	Hs RAS p21 protein activator 3 (RASA3), mRNA.
-0.533	-5.548	1.34E-05	0.000109565	2.900	7320066	HECTD1	NM_015382.1	Hs HECT domain containing 1 (HECTD1), mRNA.
-0.533	-6.026	4.31E-06	4.31E-05	4.037	2140064	GTF3C2	NM_001521.2	Hs general transcription factor IIIC, polypeptide 2, beta 110kDa (GTF3C2), tv: 1, mRNA.
-0.534	-6.662	9.91E-07	1.33E-05	5.513	5050437	SCAND1	NM_016558.2	Hs SCAN domain containing 1 (SCAND1), tv: 1, mRNA.
-0.534	-6.758	7.97E-07	1.11E-05	5.731	5690053	TK2	NM_004614.3	Hs thymidine kinase 2, mitochondrial (TK2), nuclear gene encoding mitochondrial protein, mRNA.
-0.534	-5.672	9.97E-06	8.59E-05	3.197	3400367	USP4	NM_003363.2	Hs ubiquitin specific peptidase 4 (proto-oncogene) (USP4), tv: 1, mRNA.
-0.534	-7.385	1.98E-07	3.67E-06	7.131	4210196	TGIF1	NM_003244.2	Hs TGFB-induced factor homeobox 1 (TGIF1), tv: 4, mRNA.
-0.536	-6.423	1.71E-06	2.06E-05	4.962	1740373	ULK1	NM_003565.1	Hs unc-51-like kinase 1 (C. elegans) (ULK1), mRNA.
-0.536	-7.421	1.83E-07	3.47E-06	7.210	4780647	TMEM150A	NM_001031738.1	Hs transmembrane protein 150A (TMEM150A), tv: 1, mRNA.
-0.536	-6.028	4.29E-06	4.30E-05	4.041	2600470	WDR60	NM_018051.3	Hs WD repeat domain 60 (WDR60), mRNA.
-0.538	-8.081	4.48E-08	1.18E-06	8.622	270706	COL4A5	NM_000495.3	Hs collagen, type IV, alpha 5 (COL4A5), tv: 1, mRNA.
-0.538	-7.678	1.05E-07	2.25E-06	7.768	1110364	CAMK2D	NM_001221.2	Hs calcium/calmodulin-dependent protein kinase (CaM kinase) II delta (CAMK2D), tv: 3, mRNA.
-0.538	-7.220	2.84E-07	4.84E-06	6.768	1580520	PTPN13	NM_080684.1	Hs protein tyrosine phosphatase, non-receptor type 13 (APO-1/CD95 (Fas)-associated phosphatase) (PTPN1
-0.538	-5.950	5.16E-06	5.00E-05	3.856	5720537	ACPL2	NM_152282.3	Hs acid phosphatase-like 2 (ACPL2), tv: 1, mRNA.
-0.539	-5.682	9.75E-06	8.43E-05	3.220	6220722	MSRA	NM_012331.2	Hs methionine sulfoxide reductase A (MSRA), mRNA.
-0.539	-5.723	8.82E-06	7.77E-05	3.319	6330243	VPS33B	NM_018668.3	Hs vacuolar protein sorting 33 homolog B (yeast) (VPS33B), mRNA.
-0.539	-5.781	7.69E-06	6.94E-05	3.457	4290403	CMTM7	NM_181472.1	Hs CKLF-like MARVEL transmembrane domain containing 7 (CMTM7), tv: 2, mRNA.
-0.539	-5.635	1.09E-05	9.26E-05	3.109	6040743	ZADH2	NM_175907.3	Hs zinc binding alcohol dehydrogenase domain containing 2 (ZADH2), mRNA.
-0.539	-5.853	6.49E-06	6.06E-05	3.627	4670019	ITFG1	NM_030790.3	Hs integrin alpha FG-GAP repeat containing 1 (ITFG1), mRNA.
-0.539	-6.640	1.04E-06	1.38E-05	5.462	1820747	DAAM2	NM_015345.2	Hs dishevelled associated activator of morphogenesis 2 (DAAM2), mRNA.
-0.540	-6.165	3.12E-06	3.33E-05	4.362	6520347	IL24	NM_006850.2	Hs interleukin 24 (IL24), tv: 1, mRNA.
-0.541	-5.709	9.14E-06	8.01E-05	3.284	2370279	MACROD1	NM_014067.2	Hs MACRO domain containing 1 (MACROD1), mRNA.

Appendix 4 – Genes differentially expressed at 24 hours in cells treated with IGF1 ligand

-0.541	-7.873	6.94E-08	1.64E-06	8.184	3370632	OSMR	NM_003999.1	Hs oncostatin M receptor (OSMR), mRNA.
-0.541	-6.099	3.64E-06	3.77E-05	4.208	4900386	TOP3B	NM_003935.3	Hs topoisomerase (DNA) III beta (TOP3B), mRNA.
-0.541	-5.555	1.32E-05	0.000108448	2.916	7560377	SLC37A3	NM_207113.1	Hs solute carrier family 37 (glycerol-3-phosphate transporter), member 3 (SLC37A3), tv: 1, mRNA.
-0.543	-6.432	1.68E-06	2.02E-05	4.984	6400364	NR4A2	NM_006186.2	Hs nuclear receptor subfamily 4, group A, member 2 (NR4A2), tv: 1, mRNA.
-0.544	-7.377	2.01E-07	3.73E-06	7.113	5890440	PKP4	NM_003628.3	Hs plakophilin 4 (PKP4), tv: 1, mRNA.
-0.544	-6.306	2.24E-06	2.55E-05	4.692	2360328	FBXO46	XM_934743.2	PREDICTED: Hs F-box protein 46, tv: 5 (FBXO46), mRNA.
-0.544	-5.814	7.12E-06	6.53E-05	3.534	2100706	SORCS1	NM_001013031.1	Hs sortilin-related VPS10 domain containing receptor 1 (SORCS1), tv: 2, mRNA.
-0.545	-6.793	7.36E-07	1.04E-05	5.811	4590743	SNX1	NM_003099.3	Hs sorting nexin 1 (SNX1), tv: 1, mRNA.
-0.546	-6.061	3.97E-06	4.04E-05	4.119	2970463	CASC3	NM_007359.3	Hs cancer susceptibility candidate 3 (CASC3), mRNA.
-0.546	-6.017	4.41E-06	4.39E-05	4.015	1300239	TRIM44	NM_017583.3	Hs tripartite motif-containing 44 (TRIM44), mRNA.
-0.547	-7.305	2.35E-07	4.19E-06	6.956	7200609	PCSK1	NM_000439.3	Hs proprotein convertase subtilisin/kexin type 1 (PCSK1), mRNA.
-0.548	-5.706	9.19E-06	8.04E-05	3.279	6940059	LOC375295	XM_374020.4	PREDICTED: Hs hypothetical gene supported by BC013438 (LOC375295), mRNA.
-0.549	-8.704	1.25E-08	4.51E-07	9.903	2650753	KIAA1324L	NM_152748.2	Hs KIAA1324-like (KIAA1324L), tv: 2, mRNA.
-0.549	-6.455	1.59E-06	1.94E-05	5.038	940021	PEX11B	NM_003846.1	Hs peroxisomal biogenesis factor 11 beta (PEX11B), mRNA.
-0.550	-5.947	5.19E-06	5.02E-05	3.851	1990546	MLEC	NM_014730.2	Hs malectin (MLEC), mRNA.
-0.552	-6.592	1.16E-06	1.51E-05	5.353	2360672	TNFRSF19	NM_148957.2	Hs tumor necrosis factor receptor superfamily, member 19 (TNFRSF19), tv: 2, mRNA.
-0.552	-6.471	1.53E-06	1.89E-05	5.073	5220672	KIAA1600	NM_020940.2	Hs KIAA1600 (KIAA1600), mRNA.
-0.552	-6.093	3.68E-06	3.81E-05	4.195	940280	CTNNBL1	NM_030877.3	Hs catenin, beta like 1 (CTNNBL1), mRNA.
-0.554	-6.476	1.51E-06	1.88E-05	5.087	4050221	YJEFN3	NM_198537.2	Hs YjeF N-terminal domain containing 3 (YJEFN3), nuclear gene encoding mitochondrial protein, mRNA.
-0.554	-6.520	1.37E-06	1.73E-05	5.187	5910523	LMO4	NM_006769.2	Hs LIM domain only 4 (LMO4), mRNA.
-0.556	-6.588	1.17E-06	1.52E-05	5.344	6580487	HSD17B11	NM_016245.2	Hs hydroxysteroid (17-beta) dehydrogenase 11 (HSD17B11), mRNA.
-0.556	-7.664	1.08E-07	2.29E-06	7.737	1410020	TMCO3	NM_017905.3	Hs transmembrane and coiled-coil domains 3 (TMCO3), mRNA.
-0.556	-6.108	3.55E-06	3.71E-05	4.231	3170593	PTPRA	NM_080840.2	Hs protein tyrosine phosphatase, receptor type, A (PTPRA), tv: 2, mRNA.
-0.557	-8.069	4.59E-08	1.20E-06	8.598	540113	CDC14B	NM_033331.2	Hs CDC14 cell division cycle 14 homolog B (S. cerevisiae) (CDC14B), tv: 2, mRNA.
-0.558	-6.225	2.71E-06	2.98E-05	4.502	4220347	LRRC1	NM_018214.4	Hs leucine rich repeat containing 1 (LRRC1), mRNA.
-0.558	-6.066	3.93E-06	4.00E-05	4.131	6580019	LOC731954	XR_015662.2	PREDICTED: Hs similar to supervillin (LOC731954), mRNA.
-0.558	-7.108	3.63E-07	5.93E-06	6.520	3850139	FOXD3	NM_012183.1	Hs forkhead box D3 (FOXD3), mRNA.
-0.559	-5.636	1.09E-05	9.26E-05	3.110	2760427	PYGL	NM_002863.3	Hs phosphorylase, glycogen, liver (PYGL), mRNA.
-0.559	-5.736	8.56E-06	7.58E-05	3.350	1980259	C15ORF28	XR_001373.1	PREDICTED: Hs chromosome 15 open reading frame 28 (C15orf28), misc RNA.
-0.559	-6.545	1.29E-06	1.65E-05	5.245	1500189	CD81	NM_004356.3	Hs CD81 molecule (CD81), mRNA.
-0.559	-6.153	3.20E-06	3.40E-05	4.336	3460121	TOMM20	NM_014765.1	Hs translocase of outer mitochondrial membrane 20 homolog (yeast) (TOMM20), nuclear gene encoding mit
-0.559	-8.517	1.83E-08	5.97E-07	9.523	2480487	STX6	NM_005819.4	Hs syntaxin 6 (STX6), mRNA.
-0.560	-7.553	1.37E-07	2.80E-06	7.498	1230201	CTLA4	NM_005214.3	Hs cytotoxic T-lymphocyte-associated protein 4 (CTLA4), tv: 1, mRNA.
-0.560	-6.258	2.51E-06	2.79E-05	4.580	3400372	PRRX1	NM_006902.3	Hs paired related homeobox 1 (PRRX1), tv: pmx-1a, mRNA.
-0.560	-6.082	3.79E-06	3.89E-05	4.167	6180133	ITPR3	NM_002224.2	Hs inositol 1,4,5-triphosphate receptor, type 3 (ITPR3), mRNA.
-0.561	-5.824	6.94E-06	6.40E-05	3.560	3130196	KCTD15	NM_024076.1	Hs potassium channel tetramerisation domain containing 15 (KCTD15), mRNA.
-0.561	-5.884	6.03E-06	5.68E-05	3.701	160364	ZNF282	NM_003575.2	Hs zinc finger protein 282 (ZNF282), mRNA.
-0.561	-5.987	4.73E-06	4.64E-05	3.944	6060646	CRYZL1	NM_145858.2	Hs crystallin, zeta (quinone reductase)-like 1 (CRYZL1), mRNA.
-0.561	-7.934	6.10E-08	1.48E-06	8.313	2710064	LOC387763	XM_941665.2	PREDICTED: Hs hypothetical LOC387763 (LOC387763), mRNA.
-0.561	-6.155	3.19E-06	3.40E-05	4.339	4120176	C9ORF23	NM_148179.1	Hs chromosome 9 open reading frame 23 (C9orf23), tv: 2, mRNA.

Appendix 4 – Genes differentially expressed at 24 hours in cells treated with IGF1 ligand

-0.562	-6.495	1.45E-06	1.81E-05	5.130	940180	RBBP5	NM_005057.2	Hs retinoblastoma binding protein 5 (RBBP5), mRNA.
-0.564	-5.661	1.02E-05	8.79E-05	3.171	4890328	SIDT2	NM_001040455.1	Hs SID1 transmembrane family, member 2 (SIDT2), mRNA.
-0.566	-6.398	1.81E-06	2.16E-05	4.905	1110370	KIAA1430	NM_020827.1	Hs KIAA1430 (KIAA1430), mRNA.
-0.566	-7.384	1.98E-07	3.67E-06	7.129	3130128	GPRASP2	NM_001004051.1	Hs G protein-coupled receptor associated sorting protein 2 (GPRASP2), tv: 1, mRNA.
-0.567	-6.983	4.80E-07	7.38E-06	6.240	6510576	CTPS2	NM_175859.1	Hs CTP synthase II (CTPS2), tv: 2, mRNA.
-0.567	-8.227	3.31E-08	9.32E-07	8.928	1570647	LOC442041	XR_037431.1	PREDICTED: Hs misc_RNA (LOC442041), partial miscRNA.
-0.567	-7.037	4.26E-07	6.75E-06	6.359	6130537	IP6K1	NM_153273.3	Hs inositol hexakisphosphate kinase 1 (IP6K1), tv: 1, mRNA.
-0.567	-7.885	6.76E-08	1.61E-06	8.209	3610647	URG4	NM_001077664.1	Hs up-regulated gene 4 (URG4), nuclear gene encoding mitochondrial protein, tv: 2, mRNA.
-0.568	-6.127	3.40E-06	3.58E-05	4.274	7650468	TMEM168	NM_022484.4	Hs transmembrane protein 168 (TMEM168), mRNA.
-0.568	-5.706	9.19E-06	8.04E-05	3.279	2340040	SNUPN	NM_001042581.1	Hs snurportin 1 (SNUPN), tv: 2, mRNA.
-0.568	-5.970	4.93E-06	4.80E-05	3.903	5260632	UBE2D4	NM_015983.2	Hs ubiquitin-conjugating enzyme E2D 4 (putative) (UBE2D4), mRNA.
-0.568	-6.856	6.39E-07	9.27E-06	5.953	2070095	HIF1AN	NM_017902.2	Hs hypoxia inducible factor 1, alpha subunit inhibitor (HIF1AN), mRNA.
-0.570	-5.933	5.37E-06	5.16E-05	3.817	6110736	IRS2	NM_003749.2	Hs insulin receptor substrate 2 (IRS2), mRNA.
-0.570	-6.149	3.23E-06	3.43E-05	4.326	7150537	GGT7	NM_178026.2	Hs gamma-glutamyltransferase 7 (GGT7), mRNA.
-0.571	-7.778	8.48E-08	1.89E-06	7.982	3610273	C12ORF51	NM_001109662.1	Hs chromosome 12 open reading frame 51 (C12orf51), mRNA.
-0.571	-8.778	1.08E-08	4.14E-07	10.050	1090497	CREG1	NM_003851.2	Hs cellular repressor of E1A-stimulated genes 1 (CREG1), mRNA.
-0.571	-6.054	4.04E-06	4.10E-05	4.101	10504	FGFBP2	NM_031950.2	Hs fibroblast growth factor binding protein 2 (FGFBP2), mRNA.
-0.572	-6.112	3.53E-06	3.68E-05	4.238	1240615	LPHN2	NM_012302.2	Hs latrophilin 2 (LPHN2), mRNA.
-0.572	-6.176	3.03E-06	3.26E-05	4.389	3120767	CNIH	NM_005776.2	Hs cornichon homolog (Drosophila) (CNIH), mRNA.
-0.573	-6.314	2.20E-06	2.52E-05	4.710	2710646	MSRB2	NM_012228.2	Hs methionine sulfoxide reductase B2 (MSRB2), mRNA.
-0.573	-6.774	7.67E-07	1.08E-05	5.769	5720112	TOM1L1	NM_005486.1	Hs target of myb1 (chicken)-like 1 (TOM1L1), mRNA.
-0.574	-7.705	9.91E-08	2.15E-06	7.825	940685	NAV1	NM_020443.2	Hs neuron navigator 1 (NAV1), mRNA.
-0.574	-6.872	6.17E-07	9.04E-06	5.989	4180544	ROPN1L	NM_031916.2	Hs ropporin 1-like (ROPN1L), mRNA.
-0.574	-7.450	1.72E-07	3.31E-06	7.272	5690520	CHMP6	NM_024591.3	Hs chromatin modifying protein 6 (CHMP6), mRNA.
-0.575	-6.607	1.12E-06	1.47E-05	5.387	3610100	LUC7L	NM_018032.3	Hs LUC7-like (S. cerevisiae) (LUC7L), tv: 1, mRNA.
-0.575	-6.890	5.91E-07	8.75E-06	6.030	4210719	CART1	NM_006982.1	Hs cartilage paired-class homeoprotein 1 (CART1), mRNA.
-0.575	-6.019	4.38E-06	4.36E-05	4.021	3360280	THYN1	NM_014174.2	Hs thymocyte nuclear protein 1 (THYN1), tv: 1, mRNA.
-0.575	-7.391	1.95E-07	3.65E-06	7.144	510066	HS.574453		Hs cDNA FLJ14337 fis, clone PLACE4000494
-0.575	-6.099	3.63E-06	3.77E-05	4.208	5670181	TMEM181	NM_020823.1	Hs transmembrane protein 181 (TMEM181), mRNA.
-0.575	-6.369	1.94E-06	2.27E-05	4.838	4280093	LOC440157	NM_001013701.1	Hs hypothetical gene supported by AK096951; BC066547 (LOC440157), mRNA.
-0.576	-7.814	7.85E-08	1.79E-06	8.059	450376	TSC2	NM_001077183.1	Hs tuberous sclerosis 2 (TSC2), tv: 4, mRNA.
-0.576	-5.548	1.34E-05	0.000109565	2.900	3170725	C2ORF79	NM_001013663.1	Hs chromosome 2 open reading frame 79 (C2orf79), mRNA.
-0.576	-5.919	5.55E-06	5.31E-05	3.783	870632	HS.66187		Hs clone 23700 mRNA sequence
-0.576	-6.746	8.18E-07	1.13E-05	5.705	1510040	DYRK1B	NM_006484.1	Hs dual-specificity tyrosine-(Y)-phosphorylation regulated kinase 1B (DYRK1B), tv: c, mRNA.
-0.577	-7.505	1.52E-07	3.02E-06	7.392	150681	ZNHIT6	NM_017953.2	Hs zinc finger, HIT type 6 (ZNHIT6), mRNA.
-0.577	-5.890	5.94E-06	5.61E-05	3.716	5810673	ATPAF1	NM_001042546.1	Hs ATP synthase mitochondrial F1 complex assembly factor 1 (ATPAF1), nuclear gene encoding mitochond
-0.578	-7.679	1.05E-07	2.25E-06	7.768	4480546	ADO	NM_032804.5	Hs 2-aminoethanethiol (cysteamine) dioxygenase (ADO), mRNA.
-0.578	-6.986	4.77E-07	7.35E-06	6.247	730523	CLIP2	NM_032421.2	Hs CAP-GLY domain containing linker protein 2 (CLIP2), tv: 2, mRNA.
-0.579	-5.785	7.62E-06	6.88E-05	3.466	3520504	TFAP4	NM_003223.1	Hs transcription factor AP-4 (activating enhancer binding protein 4) (TFAP4), mRNA.
-0.580	-6.147	3.25E-06	3.44E-05	4.320	1850575	CHD6	NM_032221.3	Hs chromodomain helicase DNA binding protein 6 (CHD6), mRNA.

Appendix 4 – Genes differentially expressed at 24 hours in cells treated with IGF1 ligand

-0.580	-6.584	1.18E-06	1.53E-05	5.334	2370500	HS.569175		DA697821 NT2NE2 Hs cDNA clone NT2NE2019092 5, mRNA sequence
-0.581	-7.886	6.75E-08	1.60E-06	8.211	3840598	LOC643531	XR_019563.2	PREDICTED: Hs misc_RNA (LOC643531), miscRNA.
-0.581	-6.587	1.18E-06	1.52E-05	5.341	3930452	CDC2L6	NM_015076.3	Hs cell division cycle 2-like 6 (CDK8-like) (CDC2L6), mRNA.
-0.581	-7.456	1.70E-07	3.28E-06	7.285	6110253	SUMF2	NM_001042470.1	Hs sulfatase modifying factor 2 (SUMF2), tv: 4, mRNA.
-0.581	-7.434	1.78E-07	3.40E-06	7.238	3710240	CELSR2	NM_001408.1	Hs cadherin, EGF LAG seven-pass G-type receptor 2 (flamingo homolog, Drosophila) (CELSR2), mRNA.
-0.581	-6.034	4.23E-06	4.25E-05	4.056	510341	VEZF1	NM_007146.2	Hs vascular endothelial zinc finger 1 (VEZF1), mRNA.
-0.582	-7.392	1.95E-07	3.64E-06	7.146	6420161	STK36	NM_015690.2	Hs serine/threonine kinase 36, fused homolog (Drosophila) (STK36), mRNA.
-0.582	-6.520	1.37E-06	1.73E-05	5.188	2710754	CD96	NM_198196.2	Hs CD96 molecule (CD96), tv: 1, mRNA.
-0.582	-7.429	1.80E-07	3.42E-06	7.227	7610598	TRAF5	NM_004619.3	Hs TNF receptor-associated factor 5 (TRAF5), tv: 1, mRNA.
-0.582	-5.954	5.11E-06	4.95E-05	3.867	1820195	ZCCHC3	NM_033089.6	Hs zinc finger, CCHC domain containing 3 (ZCCHC3), mRNA.
-0.583	-6.444	1.63E-06	1.98E-05	5.011	1110544	GPHN	NM_001024218.1	Hs gephyrin (GPHN), tv: 2, mRNA.
-0.583	-6.549	1.28E-06	1.64E-05	5.253	1170093	EML1	NM_004434.2	Hs echinoderm microtubule associated protein like 1 (EML1), tv: 2, mRNA.
-0.583	-6.102	3.60E-06	3.74E-05	4.216	1500504	AKR1A1	NM_006066.2	Hs aldo-keto reductase family 1, member A1 (aldehyde reductase) (AKR1A1), tv: 1, mRNA.
-0.584	-7.783	8.39E-08	1.88E-06	7.992	520491	HS.562504		PM3-DT0037-231299-001-e06 DT0037 Hs cDNA, mRNA sequence
-0.584	-6.248	2.57E-06	2.85E-05	4.557	2260674	LOC100132289	XR_037745.1	PREDICTED: Hs misc_RNA (LOC100132289), miscRNA.
-0.584	-6.941	5.28E-07	7.97E-06	6.145	7200240	ARHGAP4	NM_001666.2	Hs Rho GTPase activating protein 4 (ARHGAP4), mRNA.
-0.584	-6.973	4.92E-07	7.53E-06	6.216	270201	MEGF10	NM_032446.1	Hs multiple EGF-like-domains 10 (MEGF10), mRNA.
-0.585	-6.326	2.14E-06	2.47E-05	4.738	4760672	LPAR3	NM_012152.2	Hs lysophosphatidic acid receptor 3 (LPAR3), mRNA.
-0.586	-6.138	3.31E-06	3.50E-05	4.301	6400711	ZNF573	NM_152360.2	Hs zinc finger protein 573 (ZNF573), mRNA.
-0.586	-5.993	4.66E-06	4.59E-05	3.959	3890482	ZNF581	NM_016535.3	Hs zinc finger protein 581 (ZNF581), mRNA.
-0.586	-6.439	1.65E-06	2.00E-05	5.001	7150070	ARHGEF11	NM_014784.2	Hs Rho guanine nucleotide exchange factor (GEF) 11 (ARHGEF11), tv: 1, mRNA.
-0.586	-5.541	1.37E-05	0.000111331	2.882	6130730	FAM96A	NM_032231.4	Hs family with sequence similarity 96, member A (FAM96A), tv: 1, mRNA.
-0.587	-7.896	6.61E-08	1.58E-06	8.233	3440288	DNAJC4	NM_005528.3	Hs DnaJ (Hsp40) homolog, subfamily C, member 4 (DNAJC4), mRNA.
-0.587	-8.894	8.57E-09	3.41E-07	10.282	2630333	CYB5D2	NM_144611.2	Hs cytochrome b5 domain containing 2 (CYB5D2), mRNA.
-0.587	-6.829	6.79E-07	9.70E-06	5.891	6110484	GEMIN5	NM_015465.1	Hs gem (nuclear organelle) associated protein 5 (GEMIN5), mRNA.
-0.587	-7.678	1.05E-07	2.25E-06	7.767	6550754	EVL	NM_016337.2	Hs Enah/Vasp-like (EVL), mRNA.
-0.588	-6.026	4.31E-06	4.31E-05	4.037	5220491	VGLL4	NM_014667.1	Hs vestigial like 4 (Drosophila) (VGLL4), mRNA.
-0.588	-5.681	9.75E-06	8.44E-05	3.219	2030041	DDEF2	NM_003887.1	Hs development and differentiation enhancing factor 2 (DDEF2), mRNA.
-0.589	-6.522	1.36E-06	1.72E-05	5.191	6900528	RHOT1	NM_001033568.1	Hs ras homolog gene family, member T1 (RHOT1), tv: 1, mRNA.
-0.589	-6.004	4.54E-06	4.50E-05	3.986	3390292	KLF9	NM_001206.2	Hs Kruppel-like factor 9 (KLF9), mRNA.
-0.589	-6.449	1.61E-06	1.96E-05	5.024	5130164	RASA1	NM_002890.1	Hs RAS p21 protein activator (GTPase activating protein) 1 (RASA1), tv: 1, mRNA.
-0.589	-7.129	3.47E-07	5.71E-06	6.565	4610280	MEIS3P1	NR_002211.1	Hs Meis homeobox 3 pseudogene 1 (MEIS3P1), non-coding RNA.
-0.590	-7.370	2.04E-07	3.76E-06	7.098	6420133	DYNC1I2	NM_001378.1	Hs dynein, cytoplasmic 1, intermediate chain 2 (DYNC1I2), mRNA.
-0.590	-6.078	3.82E-06	3.92E-05	4.158	1070414	DHRS4L2	NM_198083.2	Hs dehydrogenase/reductase (SDR family) member 4 like 2 (DHRS4L2), mRNA.
-0.590	-7.204	2.94E-07	4.97E-06	6.733	2970209	SLC47A1	NM_018242.2	Hs solute carrier family 47, member 1 (SLC47A1), mRNA.
-0.590	-5.661	1.03E-05	8.79E-05	3.169	7150689	LOC644907	NM_001090027.1	Hs hCG18290 (LOC644907), mRNA.
-0.590	-5.837	6.73E-06	6.24E-05	3.590	1260575	C13ORF23	NM_025138.3	Hs chromosome 13 open reading frame 23 (C13orf23), tv: 1, mRNA.
-0.591	-6.460	1.57E-06	1.92E-05	5.049	130669	BAG5	NM_004873.2	Hs BCL2-associated athanogene 5 (BAG5), tv: 2, mRNA.
-0.591	-5.867	6.28E-06	5.88E-05	3.660	4200291	TCF12	NM_207038.1	Hs transcription factor 12 (TCF12), tv: 4, mRNA.
-0.593	-6.377	1.90E-06	2.24E-05	4.857	7330142	TGFB1I1	NM_015927.3	Hs transforming growth factor beta 1 induced transcript 1 (TGFB1I1), tv: 2, mRNA.

Appendix 4 – Genes differentially expressed at 24 hours in cells treated with IGF1 ligand

-0.594	-6.236	2.64E-06	2.92E-05	4.529	6900630	ATP2B4	NM_001684.3	Hs ATPase, Ca++ transporting, plasma membrane 4 (ATP2B4), tv: 2, mRNA.
-0.594	-5.554	1.32E-05	0.00010856	2.914	5690328	MRPS33	NM_016071.2	Hs mitochondrial ribosomal protein S33 (MRPS33), nuclear gene encoding mitochondrial protein, tv: 1, mR
-0.594	-5.998	4.61E-06	4.55E-05	3.970	5570377	LOC100131578	XM_001725660.1	PREDICTED: Hs hypothetical protein LOC100131578 (LOC100131578), mRNA.
-0.595	-9.517	2.56E-09	1.33E-07	11.492	870750	LOC100009676	NR_024407.1	Hs hypothetical LOC100009676 (LOC100009676), non-coding RNA.
-0.595	-7.085	3.82E-07	6.16E-06	6.469	1340288	RICS	NM_014715.2	Hs Rho GTPase-activating protein (RICS), mRNA.
-0.595	-5.591	1.21E-05	0.000101129	3.002	7150292	TRNP1	NM_001013642.2	Hs TMF1-regulated nuclear protein 1 (TRNP1), mRNA.
-0.595	-7.982	5.51E-08	1.38E-06	8.414	620255	FZD4	NM_012193.2	Hs frizzled homolog 4 (Drosophila) (FZD4), mRNA.
-0.595	-6.139	3.31E-06	3.50E-05	4.302	6280601	C6ORF48	NM_016947.1	Hs chromosome 6 open reading frame 48 (C6orf48), mRNA.
-0.595	-8.985	7.16E-09	2.98E-07	10.462	2750386	RPGR	NM_000328.2	Hs retinitis pigmentosa GTPase regulator (RPGR), tv: A, mRNA.
-0.596	-7.357	2.10E-07	3.86E-06	7.070	20475	TBC1D19	NM_018317.1	Hs TBC1 domain family, member 19 (TBC1D19), mRNA.
-0.596	-7.728	9.43E-08	2.06E-06	7.875	2190128	RAB32	NM_006834.2	Hs RAB32, member RAS oncogene family (RAB32), mRNA.
-0.597	-8.070	4.59E-08	1.20E-06	8.599	2480468	RANBP10	NM_020850.1	Hs RAN binding protein 10 (RANBP10), mRNA.
-0.598	-6.737	8.36E-07	1.15E-05	5.683	2190564	FAM160B2	NM_022749.5	Hs family with sequence similarity 160, member B2 (FAM160B2), mRNA.
-0.598	-6.463	1.56E-06	1.92E-05	5.056	450762	FCGR2A	NM_021642.2	Hs Fc fragment of IgG, low affinity IIa, receptor (CD32) (FCGR2A), mRNA.
-0.599	-6.183	2.98E-06	3.22E-05	4.406	6760706	MCOLN3	NM_018298.9	Hs mucolipin 3 (MCOLN3), mRNA.
-0.599	-6.870	6.19E-07	9.07E-06	5.985	3140167	ZNF146	NM_007145.1	Hs zinc finger protein 146 (ZNF146), mRNA.
-0.599	-5.648	1.06E-05	9.04E-05	3.140	1170162	DSTYK	NM_015375.2	Hs dual serine/threonine and tyrosine protein kinase (DSTYK), tv: 1, mRNA.
-0.599	-7.880	6.84E-08	1.62E-06	8.198	2630553	COX4NB	NM_006067.3	Hs COX4 neighbor (COX4NB), mRNA.
-0.600	-8.443	2.12E-08	6.67E-07	9.373	1260497	RFTN1	NM_015150.1	Hs raftlin, lipid raft linker 1 (RFTN1), mRNA.
-0.600	-5.905	5.73E-06	5.45E-05	3.751	2470608	LLGL1	NM_004140.3	Hs lethal giant larvae homolog 1 (Drosophila) (LLGL1), mRNA.
-0.601	-8.012	5.18E-08	1.31E-06	8.477	2100767	COLEC12	NM_130386.1	Hs collectin sub-family member 12 (COLEC12), mRNA.
-0.601	-7.401	1.91E-07	3.59E-06	7.167	7160292	ST3GAL2	NM_006927.3	Hs ST3 beta-galactoside alpha-2,3-sialyltransferase 2 (ST3GAL2), mRNA.
-0.601	-7.823	7.71E-08	1.76E-06	8.078	3610286	GLTSCR2	NM_015710.3	Hs glioma tumor suppressor candidate region gene 2 (GLTSCR2), mRNA.
-0.601	-5.589	1.22E-05	0.000101463	2.998	2760292	PPP1CC	NM_002710.1	Hs protein phosphatase 1, catalytic subunit, gamma isoform (PPP1CC), mRNA.
-0.602	-7.398	1.92E-07	3.61E-06	7.158	4230021	NCK2	NM_001004720.1	Hs NCK adaptor protein 2 (NCK2), tv: 2, mRNA.
-0.602	-6.090	3.71E-06	3.83E-05	4.187	3840440	C11ORF58	NM_001142705.1	Hs chromosome 11 open reading frame 58 (C11orf58), tv: 2, mRNA.
-0.602	-7.270	2.54E-07	4.44E-06	6.878	3610039	DGAT1	NM_012079.2	Hs diacylglycerol O-acyltransferase homolog 1 (mouse) (DGAT1), mRNA.
-0.603	-7.290	2.44E-07	4.31E-06	6.922	6200437	AP3M1	NM_207012.2	Hs adaptor-related protein complex 3, mu 1 subunit (AP3M1), tv: 1, mRNA.
-0.603	-7.768	8.67E-08	1.93E-06	7.959	3440133	RNF150	NM_020724.1	Hs ring finger protein 150 (RNF150), mRNA.
-0.603	-6.468	1.54E-06	1.90E-05	5.067	7610494	CDCA4	NM_017955.2	Hs cell division cycle associated 4 (CDCA4), tv: 13, mRNA.
-0.603	-6.759	7.95E-07	1.11E-05	5.733	6330088	USF2	NM_207291.1	Hs upstream transcription factor 2, c-fos interacting (USF2), tv: 2, mRNA.
-0.603	-6.627	1.07E-06	1.42E-05	5.432	5290768	HS.483906		Hs mRNA; cDNA DKFZp667L2214 (from clone DKFZp667L2214)
-0.603	-6.536	1.32E-06	1.68E-05	5.223	6200215	TTC13	NM_024525.2	Hs tetratricopeptide repeat domain 13 (TTC13), mRNA.
-0.604	-10.175	7.52E-10	5.70E-08	12.716	1570669	LACTB	NM_032857.2	Hs lactamase, beta (LACTB), nuclear gene encoding mitochondrial protein, tv: 1, mRNA.
-0.604	-5.563	1.30E-05	0.000106772	2.935	2030577	TIMP3	NM_000362.4	Hs TIMP metallopeptidase inhibitor 3 (TIMP3), mRNA.
-0.604	-7.450	1.72E-07	3.31E-06	7.273	5420343	ATF6	NM_007348.2	Hs activating transcription factor 6 (ATF6), mRNA.
-0.604	-9.340	3.59E-09	1.76E-07	11.153	780097	INPP5F	NM_014937.2	Hs inositol polyphosphate-5-phosphatase F (INPP5F), tv: 1, mRNA.
-0.605	-8.418	2.24E-08	6.92E-07	9.321	3420739	SNTB1	NM_021021.2	Hs syntrophin, beta 1 (dystrophin-associated protein A1, 59kDa, basic component 1) (SNTB1), mRNA.
-0.605	-6.206	2.83E-06	3.07E-05	4.460	2340709	ZMYM3	NM_201599.1	Hs zinc finger, MYM-type 3 (ZMYM3), tv: 2, mRNA.
-0.605	-9.627	2.08E-09	1.16E-07	11.700	6200376	ITIH5L	NM_198510.1	Hs inter-alpha (globulin) inhibitor H5-like (ITIH5L), mRNA.

Appendix 4 – Genes differentially expressed at 24 hours in cells treated with IGF1 ligand

-0.606	-7.044	4.19E-07	6.65E-06	6.376	6480722	NACC1	NM_052876.2	Hs nucleus accumbens associated 1, BEN and BTB (POZ) domain containing (NACC1), mRNA.
-0.607	-7.340	2.18E-07	3.97E-06	7.032	3460010	MYL5	NM_002477.1	Hs myosin, light chain 5, regulatory (MYL5), mRNA.
-0.607	-6.738	8.33E-07	1.15E-05	5.686	3180736	ARHGEF1	NM_199002.1	Hs Rho guanine nucleotide exchange factor (GEF) 1 (ARHGEF1), tv: 1, mRNA.
-0.607	-7.387	1.97E-07	3.66E-06	7.135	2600692	TTC8	NM_144596.2	Hs tetratricopeptide repeat domain 8 (TTC8), tv: 1, mRNA.
-0.607	-5.584	1.23E-05	0.00010249	2.985	4570398	F2R	NM_001992.2	Hs coagulation factor II (thrombin) receptor (F2R), mRNA.
-0.608	-6.345	2.05E-06	2.38E-05	4.783	4220504	SERPINB6	NM_004568.4	Hs serpin peptidase inhibitor, clade B (ovalbumin), member 6 (SERPINB6), mRNA.
-0.609	-7.382	1.99E-07	3.69E-06	7.125	290296	FAM113A	NM_022760.3	Hs family with sequence similarity 113, member A (FAM113A), mRNA.
-0.609	-6.756	7.99E-07	1.11E-05	5.728	780332	FAM3C	NM_001040020.1	Hs family with sequence similarity 3, member C (FAM3C), tv: 2, mRNA.
-0.609	-6.302	2.26E-06	2.57E-05	4.684	2850347	LOC729680	XR_040503.1	PREDICTED: Hs misc_RNA (LOC729680), miscRNA.
-0.609	-5.970	4.92E-06	4.80E-05	3.905	7550411	TBC1D9B	NM_015043.3	Hs TBC1 domain family, member 9B (with GRAM domain) (TBC1D9B), tv: 2, mRNA.
-0.609	-6.768	7.79E-07	1.09E-05	5.754	2650019	FAM53C	NM_016605.1	Hs family with sequence similarity 53, member C (FAM53C), mRNA.
-0.609	-7.296	2.40E-07	4.27E-06	6.936	5310278	PABPC4	NM_003819.2	Hs poly(A) binding protein, cytoplasmic 4 (inducible form) (PABPC4), mRNA.
-0.610	-6.415	1.74E-06	2.08E-05	4.945	540129	KDELR3	NM_016657.1	Hs KDEL (Lys-Asp-Glu-Leu) endoplasmic reticulum protein retention receptor 3 (KDELR3), tv: 2, mRNA.
-0.611	-7.482	1.60E-07	3.13E-06	7.343	2190364	WDR13	NM_017883.3	Hs WD repeat domain 13 (WDR13), mRNA.
-0.611	-6.265	2.47E-06	2.75E-05	4.597	580148	CYLN2	NM_032421.1	Hs cytoplasmic linker 2 (CYLN2), tv: 2, mRNA.
-0.611	-8.483	1.96E-08	6.31E-07	9.453	1240392	GPR137B	NM_003272.1	Hs G protein-coupled receptor 137B (GPR137B), mRNA.
-0.612	-5.604	1.17E-05	9.85E-05	3.034	1430598	FBXO32	NM_058229.2	Hs F-box protein 32 (FBXO32), tv: 1, mRNA.
-0.612	-7.029	4.33E-07	6.81E-06	6.343	6480349	SSBP2	NM_012446.2	Hs single-stranded DNA binding protein 2 (SSBP2), mRNA.
-0.612	-6.624	1.08E-06	1.42E-05	5.426	4670021	NPEPL1	NM_024663.3	Hs aminopeptidase-like 1 (NPEPL1), mRNA.
-0.613	-8.097	4.34E-08	1.15E-06	8.655	2030681	RPL32	NM_001007074.1	Hs ribosomal protein L32 (RPL32), tv: 3, mRNA.
-0.613	-6.276	2.40E-06	2.70E-05	4.623	6560484	VPS41	NM_014396.2	Hs vacuolar protein sorting 41 (yeast) (VPS41), tv: 1, mRNA.
-0.613	-5.674	9.93E-06	8.56E-05	3.202	7150348	NKX2-5	NM_004387.2	Hs NK2 transcription factor related, locus 5 (Drosophila) (NKX2-5), mRNA.
-0.614	-6.153	3.20E-06	3.40E-05	4.335	840544	RBM4	NM_002896.2	Hs RNA binding motif protein 4 (RBM4), mRNA.
-0.614	-7.231	2.77E-07	4.76E-06	6.792	4590390	FAM38A	NM_014745.1	Hs family with sequence similarity 38, member A (FAM38A), mRNA.
-0.615	-7.339	2.19E-07	3.97E-06	7.030	6370594	PPAPDC2	NM_203453.2	Hs phosphatidic acid phosphatase type 2 domain containing 2 (PPAPDC2), mRNA.
-0.615	-7.271	2.54E-07	4.44E-06	6.879	3780762	FAM44B	NM_138369.1	Hs family with sequence similarity 44, member B (FAM44B), mRNA.
-0.615	-8.463	2.04E-08	6.47E-07	9.412	870390	DEPDC6	NM_022783.1	Hs DEP domain containing 6 (DEPDC6), mRNA.
-0.616	-7.405	1.90E-07	3.57E-06	7.174	2750324	PRKCZ	NM_002744.4	Hs protein kinase C, zeta (PRKCZ), tv: 1, mRNA.
-0.616	-6.685	9.39E-07	1.28E-05	5.566	1450356	ERCC1	NM_001983.2	Hs excision repair cross-complementing rodent repair deficiency, complementation group 1 (includes overlap
-0.616	-6.738	8.34E-07	1.15E-05	5.685	7200044	SH3BGRL2	NM_031469.2	Hs SH3 domain binding glutamic acid-rich protein like 2 (SH3BGRL2), mRNA.
-0.616	-6.944	5.24E-07	7.92E-06	6.153	7000184	SLC38A9	NM_173514.1	Hs solute carrier family 38, member 9 (SLC38A9), mRNA.
-0.616	-6.515	1.38E-06	1.74E-05	5.176	2970301	FAM92A1	NM_145269.3	Hs family with sequence similarity 92, member A1 (FAM92A1), mRNA.
-0.617	-6.465	1.55E-06	1.91E-05	5.060	6590661	MED22	NM_181491.1	Hs mediator complex subunit 22 (MED22), tv: c, mRNA.
-0.618	-7.491	1.57E-07	3.09E-06	7.361	7320494	ZFPM1	NM_153813.2	Hs zinc finger protein, multitype 1 (ZFPM1), mRNA.
-0.618	-6.288	2.34E-06	2.64E-05	4.651	5490692	SEZ6L2	NM_201575.1	Hs seizure related 6 homolog (mouse)-like 2 (SEZ6L2), tv: 2, mRNA.
-0.618	-7.529	1.45E-07	2.90E-06	7.445	5310717	NIN	NM_020921.3	Hs ninein (GSK3B interacting protein) (NIN), tv: 2, mRNA.
-0.619	-6.857	6.37E-07	9.26E-06	5.956	6420239	CYFIP1	NM_001033028.1	Hs cytoplasmic FMR1 interacting protein 1 (CYFIP1), tv: 2, mRNA.
-0.619	-6.761	7.91E-07	1.11E-05	5.738	4810008	PEX13	NM_002618.2	Hs peroxisome biogenesis factor 13 (PEX13), mRNA.
-0.619	-6.840	6.61E-07	9.54E-06	5.918	1850041	DPM2	NM_003863.2	Hs dolichyl-phosphate mannosyltransferase polypeptide 2, regulatory subunit (DPM2), mRNA.
-0.619	-6.866	6.24E-07	9.10E-06	5.977	1170398	C10ORF57	NM_025125.2	Hs chromosome 10 open reading frame 57 (C10orf57), mRNA.

Appendix 4 – Genes differentially expressed at 24 hours in cells treated with IGF1 ligand

-0.619	-5.958	5.05E-06	4.91E-05	3.877	1260730	EPHB4	NM_004444.4	Hs EPH receptor B4 (EPHB4), mRNA.
-0.620	-6.325	2.15E-06	2.47E-05	4.735	4590661	COPS7B	NM_022730.1	Hs COP9 constitutive photomorphogenic homolog subunit 7B (Arabidopsis) (COPS7B), mRNA.
-0.620	-8.527	1.79E-08	5.87E-07	9.544	6290725	FYN	NM_002037.3	Hs FYN oncogene related to SRC, FGR, YES (FYN), tv: 1, mRNA.
-0.620	-6.123	3.44E-06	3.60E-05	4.264	2690022	CIAO1	NM_004804.2	Hs cytosolic iron-sulfur protein assembly 1 homolog (S. cerevisiae) (CIAO1), mRNA.
-0.621	-6.825	6.84E-07	9.77E-06	5.884	2260619	MIB2	NM_080875.1	Hs mindbomb homolog 2 (Drosophila) (MIB2), mRNA.
-0.621	-7.969	5.67E-08	1.40E-06	8.386	4880554	SALL2	NM_005407.1	Hs sal-like 2 (Drosophila) (SALL2), mRNA.
-0.621	-7.496	1.55E-07	3.06E-06	7.373	2140193	EDG7	NM_012152.1	Hs endothelial differentiation, lysophosphatidic acid G-protein-coupled receptor, 7 (EDG7), mRNA.
-0.621	-9.055	6.24E-09	2.68E-07	10.600	7160435	EBF3	NM_001005463.1	Hs early B-cell factor 3 (EBF3), mRNA.
-0.622	-7.007	4.55E-07	7.08E-06	6.293	4280543	LOC283755	NM_001024682.1	Hs hypothetical protein LOC283755 (LOC283755), mRNA.
-0.622	-6.636	1.05E-06	1.39E-05	5.453	1400376	WWC3	NM_015691.2	Hs WWC family member 3 (WWC3), mRNA.
-0.622	-7.047	4.16E-07	6.62E-06	6.383	4830424	MYLIP	NM_013262.3	Hs myosin regulatory light chain interacting protein (MYLIP), mRNA.
-0.623	-7.152	3.30E-07	5.45E-06	6.617	380102	TMEM51	NM_018022.1	Hs transmembrane protein 51 (TMEM51), mRNA.
-0.624	-8.820	9.93E-09	3.88E-07	10.135	620619	TBC1D8	NM_007063.3	Hs TBC1 domain family, member 8 (with GRAM domain) (TBC1D8), mRNA.
-0.624	-5.594	1.20E-05	0.000100644	3.009	6480059	ACTA2	NM_001613.1	Hs actin, alpha 2, smooth muscle, aorta (ACTA2), mRNA.
-0.627	-5.733	8.62E-06	7.63E-05	3.343	2470619	AKT1	NM_001014432.1	Hs v-akt murine thymoma viral oncogene homolog 1 (AKT1), tv: 2, mRNA.
-0.628	-5.585	1.23E-05	0.000102214	2.989	6760021	SNHG7	NR_003672.2	Hs small nucleolar RNA host gene 7 (non-protein coding) (SNHG7), tv: 1, non-coding RNA.
-0.629	-5.691	9.53E-06	8.29E-05	3.242	130537	EPHA3	NM_182644.1	Hs EPH receptor A3 (EPHA3), tv: 2, mRNA.
-0.629	-6.055	4.03E-06	4.09E-05	4.105	5870687	ZNF629	XM_034819.6	PREDICTED: Hs zinc finger protein 629 (ZNF629), mRNA.
-0.630	-8.311	2.78E-08	8.21E-07	9.101	2750706	NTSR1	NM_002531.2	Hs neurotensin receptor 1 (high affinity) (NTSR1), mRNA.
-0.630	-7.855	7.20E-08	1.69E-06	8.146	2900132	RBL1	NM_002895.2	Hs retinoblastoma-like 1 (p107) (RBL1), tv: 1, mRNA.
-0.630	-9.120	5.50E-09	2.46E-07	10.727	130754	PTPRZ1	NM_002851.2	Hs protein tyrosine phosphatase, receptor-type, Z polypeptide 1 (PTPRZ1), mRNA.
-0.630	-6.874	6.13E-07	9.00E-06	5.994	2490687	JMJD1C	NM_032776.1	Hs jumonji domain containing 1C (JMJD1C), tv: 1, mRNA.
-0.631	-6.036	4.21E-06	4.24E-05	4.060	7650243	OSBPL1A	NM_080597.2	Hs oxysterol binding protein-like 1A (OSBPL1A), tv: OSBPL1B, mRNA.
-0.632	-7.265	2.57E-07	4.48E-06	6.866	5690246	SPIRE1	NM_020148.2	Hs spire homolog 1 (Drosophila) (SPIRE1), tv: 2, mRNA.
-0.632	-6.083	3.78E-06	3.88E-05	4.170	5270446	RBM41	NM_018301.2	Hs RNA binding motif protein 41 (RBM41), mRNA.
-0.632	-6.350	2.02E-06	2.35E-05	4.795	4670671	ACP6	NM_016361.2	Hs acid phosphatase 6, lysophosphatidic (ACP6), mRNA.
-0.633	-7.285	2.46E-07	4.34E-06	6.911	1850021	SLC25A43	NM_145305.1	Hs solute carrier family 25, member 43 (SLC25A43), mRNA.
-0.633	-7.918	6.31E-08	1.52E-06	8.279	780270	TIMP2	NM_003255.4	Hs TIMP metallopeptidase inhibitor 2 (TIMP2), mRNA.
-0.633	-7.300	2.38E-07	4.23E-06	6.945	7040168	TTC19	NM_017775.2	Hs tetratricopeptide repeat domain 19 (TTC19), mRNA.
-0.633	-5.786	7.60E-06	6.88E-05	3.468	5960017	DRG2	NM_001388.3	Hs developmentally regulated GTP binding protein 2 (DRG2), mRNA.
-0.633	-7.911	6.39E-08	1.53E-06	8.265	1440142	TMEM77	NM_178454.3	Hs transmembrane protein 77 (TMEM77), mRNA.
-0.634	-6.389	1.85E-06	2.19E-05	4.886	7210674	DBNDD1	NM_001042610.1	Hs dysbindin (dystrobrevin binding protein 1) domain containing 1 (DBNDD1), tv: 1, mRNA.
-0.634	-6.643	1.03E-06	1.37E-05	5.470	1400044	HSPA12A	NM_025015.2	Hs heat shock 70kDa protein 12A (HSPA12A), mRNA.
-0.634	-5.684	9.69E-06	8.39E-05	3.226	3940458	CRYL1	NM_015974.2	Hs crystallin, lambda 1 (CRYL1), mRNA.
-0.634	-6.130	3.38E-06	3.56E-05	4.280	2190400	DNAJC18	NM_152686.2	Hs DnaJ (Hsp40) homolog, subfamily C, member 18 (DNAJC18), mRNA.
-0.635	-6.086	3.74E-06	3.86E-05	4.178	1770243	IGF2BP3	NM_006547.2	Hs insulin-like growth factor 2 mRNA binding protein 3 (IGF2BP3), mRNA.
-0.635	-7.519	1.48E-07	2.94E-06	7.423	2490379	RPL34	NM_000995.2	Hs ribosomal protein L34 (RPL34), tv: 1, mRNA.
-0.635	-6.633	1.06E-06	1.40E-05	5.446	460411	IPO8	NM_006390.2	Hs importin 8 (IPO8), mRNA.
-0.636	-5.617	1.14E-05	9.60E-05	3.064	3190671	ATP5D	NM_001687.4	Hs ATP synthase, H+ transporting, mitochondrial F1 complex, delta subunit (ATP5D), nuclear gene encodin
-0.636	-6.359	1.98E-06	2.32E-05	4.816	2570041	WASF3	NM_006646.4	Hs WAS protein family, member 3 (WASF3), mRNA.

Appendix 4 – Genes differentially expressed at 24 hours in cells treated with IGF1 ligand

-0.637	-8.623	1.47E-08	5.08E-07	9.739	7150209	SLC4A11	NM_032034.2	Hs solute carrier family 4, sodium borate transporter, member 11 (SLC4A11), mRNA.
-0.637	-9.733	1.70E-09	9.96E-08	11.900	7550563	TRPC4AP	NM_015638.2	Hs transient receptor potential cation channel, subfamily C, member 4 associated protein (TRPC4AP), tv: 1,
-0.638	-5.813	7.13E-06	6.54E-05	3.533	2230382	HS.4988		Hs mRNA; cDNA DKFZp686B24166 (from clone DKFZp686B24166)
-0.638	-10.623	3.37E-10	3.13E-08	13.518	5690239	TRIL	NM_014817.3	Hs TLR4 interactor with leucine rich repeats (TRIL), mRNA.
-0.639	-6.501	1.43E-06	1.79E-05	5.143	5310707	EI24	NM_004879.3	Hs etoposide induced 2.4 mRNA (EI24), tv: 1, mRNA.
-0.639	-7.760	8.82E-08	1.96E-06	7.942	4390450	SGK	NM_005627.2	Hs serum/glucocorticoid regulated kinase (SGK), mRNA.
-0.639	-5.699	9.35E-06	8.16E-05	3.262	10685	ANTXR2	NM_058172.3	Hs anthrax toxin receptor 2 (ANTXR2), mRNA.
-0.640	-6.706	8.97E-07	1.23E-05	5.613	3390092	PLEKHM2	NM_015164.1	Hs pleckstrin homology domain containing, family M (with RUN domain) member 2 (PLEKHM2), mRNA.
-0.640	-5.838	6.72E-06	6.23E-05	3.593	7200647	MGC70857	NM_001001795.1	Hs similar to RIKEN cDNA C030006K11 gene (MGC70857), mRNA.
-0.642	-6.223	2.72E-06	2.99E-05	4.498	1170647	ACADVL	NM_001033859.1	Hs acyl-Coenzyme A dehydrogenase, very long chain (ACADVL), nuclear gene encoding mitochondrial pro
-0.642	-5.795	7.44E-06	6.76E-05	3.490	1170619	PFDN5	NM_002624.3	Hs prefoldin subunit 5 (PFDN5), tv: 1, mRNA.
-0.642	-6.689	9.31E-07	1.27E-05	5.575	6250427	C17ORF96	NM_001130677.1	Hs chromosome 17 open reading frame 96 (C17orf96), mRNA.
-0.642	-6.730	8.48E-07	1.17E-05	5.669	3290458	FEZ1	NM_005103.3	Hs fasciculation and elongation protein zeta 1 (zygin I) (FEZ1), tv: 1, mRNA.
-0.642	-8.014	5.15E-08	1.30E-06	8.482	6520128	GPX4	NM_001039847.1	Hs glutathione peroxidase 4 (phospholipid hydroperoxidase) (GPX4), tv: 2, mRNA.
-0.643	-8.708	1.24E-08	4.49E-07	9.910	1070184	PRKD1	NM_002742.2	Hs protein kinase D1 (PRKD1), mRNA.
-0.643	-8.135	4.00E-08	1.08E-06	8.736	7000328	LOC100129550	NR_024618.1	Hs hypothetical LOC100129550 (LOC100129550), non-coding RNA.
-0.644	-8.299	2.85E-08	8.33E-07	9.077	2850382	TMTC4	NM_001079669.1	Hs transmembrane and tetratricopeptide repeat containing 4 (TMTC4), tv: 2, mRNA.
-0.644	-7.438	1.76E-07	3.38E-06	7.247	7610091	ZDHHC14	NM_024630.2	Hs zinc finger, DHHC-type containing 14 (ZDHHC14), tv: 1, mRNA.
-0.645	-5.735	8.59E-06	7.61E-05	3.346	4480575	FOXO4	NM_005938.2	Hs forkhead box O4 (FOXO4), mRNA.
-0.645	-6.179	3.01E-06	3.24E-05	4.396	130519	STAT2	NM_005419.2	Hs signal transducer and activator of transcription 2, 113kDa (STAT2), mRNA.
-0.645	-7.220	2.84E-07	4.84E-06	6.769	5340646	ASAP2	NM_003887.2	Hs ArfGAP with SH3 domain, ankyrin repeat and PH domain 2 (ASAP2), tv: 1, mRNA.
-0.646	-6.667	9.79E-07	1.32E-05	5.524	6900176	TSEN2	NM_025265.2	Hs tRNA splicing endonuclease 2 homolog (S. cerevisiae) (TSEN2), mRNA.
-0.646	-7.546	1.39E-07	2.83E-06	7.482	4070239	ATHL1	NM_025092.3	Hs ATH1, acid trehalase-like 1 (yeast) (ATHL1), mRNA.
-0.646	-7.110	3.62E-07	5.92E-06	6.523	4860458	UBE2Z	NM_023079.3	Hs ubiquitin-conjugating enzyme E2Z (UBE2Z), mRNA.
-0.646	-6.451	1.60E-06	1.95E-05	5.029	7380338	UST	NM_005715.1	Hs uronyl-2-sulfotransferase (UST), mRNA.
-0.647	-5.981	4.79E-06	4.69E-05	3.931	6760386	LOC283267	NR_015451.1	Hs hypothetical LOC283267 (LOC283267), non-coding RNA.
-0.647	-7.629	1.17E-07	2.44E-06	7.660	6660047	KIAA0090	NM_015047.1	Hs KIAA0090 (KIAA0090), mRNA.
-0.647	-6.320	2.17E-06	2.49E-05	4.725	2600240	RAB26	NM_014353.4	Hs RAB26, member RAS oncogene family (RAB26), mRNA.
-0.648	-5.838	6.73E-06	6.24E-05	3.591	4010647	AIF1L	NM_031426.2	Hs allograft inflammatory factor 1-like (AIF1L), tv: 1, mRNA.
-0.648	-5.781	7.69E-06	6.94E-05	3.458	610201	HES6	NM_018645.3	Hs hairy and enhancer of split 6 (Drosophila) (HES6), mRNA.
-0.648	-5.822	6.97E-06	6.42E-05	3.555	6110608	DHX30	NM_014966.2	Hs DEAH (Asp-Glu-Ala-His) box polypeptide 30 (DHX30), tv: 2, mRNA.
-0.648	-6.264	2.47E-06	2.76E-05	4.595	6580674	HS.21177		Hs mRNA full length insert cDNA clone EUROIMAGE 966164
-0.649	-6.835	6.70E-07	9.61E-06	5.906	5080066	BRWD1	NM_001007246.1	Hs bromodomain and WD repeat domain containing 1 (BRWD1), tv: 3, mRNA.
-0.649	-6.112	3.53E-06	3.68E-05	4.238	3870102	HNMT	NM_001024074.1	Hs histamine N-methyltransferase (HNMT), tv: 2, mRNA.
-0.651	-7.252	2.65E-07	4.59E-06	6.838	160291	MVP	NM_017458.2	Hs major vault protein (MVP), tv: 1, mRNA.
-0.651	-8.035	4.93E-08	1.27E-06	8.526	870324	ARHGEF1	NM_004706.3	Hs Rho guanine nucleotide exchange factor (GEF) 1 (ARHGEF1), tv: 2, mRNA.
-0.651	-6.973	4.91E-07	7.52E-06	6.217	7400259	IDUA	NM_000203.3	Hs iduronidase, alpha-L- (IDUA), mRNA.
-0.652	-6.959	5.07E-07	7.72E-06	6.185	6760593	OSBPL10	NM_017784.3	Hs oxysterol binding protein-like 10 (OSBPL10), mRNA.
-0.652	-7.880	6.84E-08	1.62E-06	8.198	5560360	RIPK5	NM_199462.1	Hs receptor interacting protein kinase 5 (RIPK5), tv: 2, mRNA.
-0.654	-7.304	2.36E-07	4.21E-06	6.952	4250079	TMEM67	NM_153704.3	Hs transmembrane protein 67 (TMEM67), mRNA.

Appendix 4 – Genes differentially expressed at 24 hours in cells treated with IGF1 ligand

-0.655	-6.469	1.54E-06	1.90E-05	5.069	1410209	SGK1	NM_005627.3	Hs serum/glucocorticoid regulated kinase 1 (SGK1), tv: 1, mRNA.
-0.655	-6.954	5.13E-07	7.79E-06	6.174	4060576	SLC35D2	NM_007001.1	Hs solute carrier family 35, member D2 (SLC35D2), mRNA.
-0.655	-6.642	1.04E-06	1.38E-05	5.467	3060474	SLC23A2	NM_203327.1	Hs solute carrier family 23 (nucleobase transporters), member 2 (SLC23A2), tv: 2, mRNA.
-0.656	-7.888	6.72E-08	1.60E-06	8.216	3390379	ACCS	NM_032592.3	Hs 1-aminocyclopropane-1-carboxylate synthase homolog (Arabidopsis)(non-functional) (ACCS), tv: 1, mR
-0.656	-5.590	1.21E-05	0.000101212	3.001	990382	C1ORF53	NM_001024594.1	Hs chromosome 1 open reading frame 53 (C1orf53), mRNA.
-0.656	-6.832	6.74E-07	9.65E-06	5.898	6940088	DGKA	NM_201554.1	Hs diacylglycerol kinase, alpha 80kDa (DGKA), tv: 4, mRNA.
-0.656	-7.489	1.58E-07	3.10E-06	7.357	1110707	LOC100130633	XM_001725169.1	PREDICTED: Hs similar to ZMYM6 protein (LOC100130633), mRNA.
-0.656	-5.635	1.09E-05	9.26E-05	3.109	430243	KIAA1202	NM_020717.1	Hs KIAA1202 protein (KIAA1202), mRNA.
-0.656	-7.234	2.75E-07	4.73E-06	6.799	4230470	CHES1	NM_005197.2	Hs checkpoint suppressor 1 (CHES1), mRNA.
-0.657	-7.333	2.22E-07	4.00E-06	7.017	2470634	PBX3	NM_006195.4	Hs pre-B-cell leukemia homeobox 3 (PBX3), mRNA.
-0.658	-5.737	8.54E-06	7.57E-05	3.352	650348	METTL1	NM_005371.5	Hs methyltransferase like 1 (METTL1), tv: 1, mRNA.
-0.658	-5.972	4.89E-06	4.78E-05	3.910	3140750	RBM38	NM_183425.1	Hs RNA binding motif protein 38 (RBM38), tv: 2, mRNA.
-0.658	-9.478	2.76E-09	1.40E-07	11.418	2710392	ABCA8	NM_007168.2	Hs ATP-binding cassette, sub-family A (ABC1), member 8 (ABCA8), mRNA.
-0.658	-5.923	5.50E-06	5.27E-05	3.793	6560066	MTHFS	NM_006441.1	Hs 5,10-methenyltetrahydrofolate synthetase (5-formyltetrahydrofolate cyclo-ligase) (MTHFS), mRNA.
-0.658	-8.025	5.04E-08	1.29E-06	8.504	7160100	PPRC1	NM_015062.3	Hs peroxisome proliferator-activated receptor gamma, coactivator-related 1 (PPRC1), mRNA.
-0.659	-7.278	2.50E-07	4.39E-06	6.896	5310168	HLA-B	NM_005514.5	Hs major histocompatibility complex, class I, B (HLA-B), mRNA.
-0.659	-10.734	2.77E-10	2.75E-08	13.712	1690487	C3ORF70	NM_001025266.1	Hs chromosome 3 open reading frame 70 (C3orf70), mRNA.
-0.659	-6.598	1.15E-06	1.49E-05	5.367	4220630	PFDN5	NM_145897.2	Hs prefoldin subunit 5 (PFDN5), tv: 3, mRNA.
-0.660	-8.644	1.41E-08	4.97E-07	9.780	3870543	PUM1	NM_014676.2	Hs pumilio homolog 1 (Drosophila) (PUM1), tv: 2, mRNA.
-0.660	-10.347	5.51E-10	4.52E-08	13.027	2370438	A2M	NM_000014.4	Hs alpha-2-macroglobulin (A2M), mRNA.
-0.660	-5.614	1.15E-05	9.65E-05	3.057	4850403	LOC648980	XM_941280.2	PREDICTED: Hs similar to breakpoint cluster region, tv: 1 (LOC648980), mRNA.
-0.660	-8.160	3.80E-08	1.04E-06	8.787	6760280	ZC4H2	NM_018684.1	Hs zinc finger, C4H2 domain containing (ZC4H2), mRNA.
-0.661	-5.725	8.78E-06	7.75E-05	3.324	5360193	SIRPA	NM_080792.2	Hs signal-regulatory protein alpha (SIRPA), tv: 3, mRNA.
-0.662	-9.939	1.16E-09	7.59E-08	12.282	2060541	LOC148413	NR_015434.1	Hs hypothetical LOC148413 (LOC148413), non-coding RNA.
-0.662	-7.174	3.14E-07	5.25E-06	6.665	3830156	GTF3C3	NM_012086.2	Hs general transcription factor IIIC, polypeptide 3, 102kDa (GTF3C3), mRNA.
-0.662	-6.225	2.70E-06	2.97E-05	4.504	5310379	TMEM115	NM_007024.4	Hs transmembrane protein 115 (TMEM115), mRNA.
-0.662	-5.561	1.30E-05	0.000107124	2.932	4150079	PRKAA1	NM_006251.5	Hs protein kinase, AMP-activated, alpha 1 catalytic subunit (PRKAA1), tv: 1, mRNA.
-0.664	-7.029	4.33E-07	6.81E-06	6.343	7160725	SPRY4	NM_030964.2	Hs sprouty homolog 4 (Drosophila) (SPRY4), mRNA.
-0.664	-7.125	3.51E-07	5.75E-06	6.556	2450634	POLR3H	NM_001018052.1	Hs polymerase (RNA) III (DNA directed) polypeptide H (22.9kD) (POLR3H), tv: 2, mRNA.
-0.664	-6.371	1.93E-06	2.26E-05	4.842	7200373	S100A1	NM_006271.1	Hs S100 calcium binding protein A1 (S100A1), mRNA.
-0.664	-6.605	1.13E-06	1.48E-05	5.382	1110372	CSRNP2	NM_030809.1	Hs cysteine-serine-rich nuclear protein 2 (CSRNP2), mRNA.
-0.664	-8.247	3.18E-08	9.05E-07	8.968	6040554	WDR67	NM_145647.2	Hs WD repeat domain 67 (WDR67), mRNA.
-0.665	-8.640	1.42E-08	4.99E-07	9.773	3840497	DCAF10	NM_024345.3	Hs DDB1 and CUL4 associated factor 10 (DCAF10), mRNA.
-0.665	-8.501	1.89E-08	6.13E-07	9.491	1500358	ANKRD29	NM_173505.2	Hs ankyrin repeat domain 29 (ANKRD29), mRNA.
-0.665	-8.297	2.86E-08	8.36E-07	9.073	5900286	ZFP90	NM_133458.2	Hs zinc finger protein 90 homolog (mouse) (ZFP90), mRNA.
-0.667	-6.499	1.44E-06	1.80E-05	5.139	3190239	GRK5	NM_005308.2	Hs G protein-coupled receptor kinase 5 (GRK5), mRNA.
-0.667	-7.247	2.68E-07	4.63E-06	6.827	1470601	PFKFB3	NM_004566.2	Hs 6-phosphofructo-2-kinase/fructose-2,6-biphosphatase 3 (PFKFB3), mRNA.
-0.668	-6.853	6.44E-07	9.32E-06	5.946	3840465	EDNRB	NM_003991.1	Hs endothelin receptor type B (EDNRB), tv: 2, mRNA.
-0.668	-6.029	4.28E-06	4.29E-05	4.043	4070088	CNIH	NM_005776.2	Hs cornichon homolog (Drosophila) (CNIH), mRNA.
-0.668	-6.915	5.59E-07	8.34E-06	6.088	6660711	C13ORF23	NM_025138.3	Hs chromosome 13 open reading frame 23 (C13orf23), tv: 1, mRNA.

Appendix 4 – Genes differentially expressed at 24 hours in cells treated with IGF1 ligand

-0.668	-7.402	1.91E-07	3.58E-06	7.169	4220059	HS.443490		Hs cDNA FLJ32174 fis, clone PLACE6001064
-0.669	-5.785	7.61E-06	6.88E-05	3.467	5340021	KPNA6	NM_012316.3	Hs karyopherin alpha 6 (importin alpha 7) (KPNA6), mRNA.
-0.669	-8.855	9.27E-09	3.66E-07	10.203	1690520	LOC145783	XM_934388.2	PREDICTED: Hs hypothetical protein LOC145783, tv: 2 (LOC145783), mRNA.
-0.670	-6.248	2.57E-06	2.85E-05	4.557	6100050	NECAP2	NM_018090.3	Hs NECAP endocytosis associated 2 (NECAP2), mRNA.
-0.671	-8.939	7.84E-09	3.21E-07	10.371	4610561	CSGALNACT1	NM_018371.3	Hs chondroitin sulfate N-acetylgalactosaminyltransferase 1 (CSGALNACT1), mRNA.
-0.671	-9.238	4.37E-09	2.07E-07	10.956	6290717	DMRTA1	NM_022160.1	Hs DMRT-like family A1 (DMRTA1), mRNA.
-0.672	-6.684	9.42E-07	1.28E-05	5.563	3710397	EFNA1	NM_004428.2	Hs ephrin-A1 (EFNA1), tv: 1, mRNA.
-0.672	-7.170	3.17E-07	5.28E-06	6.657	4920463	ARID2	NM_152641.2	Hs AT rich interactive domain 2 (ARID, RFX-like) (ARID2), mRNA.
-0.673	-7.847	7.34E-08	1.70E-06	8.127	620497	ZNF473	NM_015428.1	Hs zinc finger protein 473 (ZNF473), tv: 1, mRNA.
-0.674	-6.271	2.43E-06	2.72E-05	4.612	1260020	TP53I3	NM_147184.1	Hs tumor protein p53 inducible protein 3 (TP53I3), tv: 2, mRNA.
-0.674	-9.119	5.51E-09	2.46E-07	10.725	520184	HPCAL1	NM_134421.1	Hs hippocalcin-like 1 (HPCAL1), tv: 2, mRNA.
-0.674	-5.885	6.01E-06	5.67E-05	3.703	1980672	IL1A	NM_000575.3	Hs interleukin 1, alpha (IL1A), mRNA.
-0.675	-5.667	1.01E-05	8.69E-05	3.185	4810048	ABCB10	NM_012089.1	Hs ATP-binding cassette, sub-family B (MDR/TAP), member 10 (ABCB10), nuclear gene encoding mitocho
-0.675	-7.527	1.45E-07	2.90E-06	7.441	7100561	FAM176B	NM_018166.1	Hs family with sequence similarity 176, member B (FAM176B), mRNA.
-0.676	-5.550	1.33E-05	0.000109242	2.906	5670280	LOC728755	XM_001128377.2	PREDICTED: Hs similar to hCG1984907 (LOC728755), mRNA.
-0.676	-6.807	7.13E-07	1.01E-05	5.842	6380079	FAM53B	NM_014661.3	Hs family with sequence similarity 53, member B (FAM53B), mRNA.
-0.676	-6.682	9.45E-07	1.28E-05	5.559	6100630	MUM1	NM_032853.2	Hs melanoma associated antigen (mutated) 1 (MUM1), mRNA.
-0.676	-6.280	2.38E-06	2.68E-05	4.631	1230397	TMEM69	NM_016486.2	Hs transmembrane protein 69 (TMEM69), mRNA.
-0.677	-5.965	4.98E-06	4.84E-05	3.893	1580487	CHD7	NM_017780.2	Hs chromodomain helicase DNA binding protein 7 (CHD7), mRNA.
-0.677	-5.767	7.95E-06	7.13E-05	3.424	3940615	PUS7	NM_019042.3	Hs pseudouridylate synthase 7 homolog (S. cerevisiae) (PUS7), mRNA.
-0.678	-8.213	3.40E-08	9.54E-07	8.898	1050309	HLX	NM_021958.2	Hs H2.0-like homeobox (HLX), mRNA.
-0.678	-5.654	1.04E-05	8.93E-05	3.153	1820093	HNRPA1P4	XM_939887.2	PREDICTED: Hs heterogeneous nuclear ribonucleoprotein A1 pseudogene 4 (HNRPA1P4), mRNA.
-0.678	-7.159	3.25E-07	5.39E-06	6.632	6330438	PLXNB1	NM_002673.3	Hs plexin B1 (PLXNB1), mRNA.
-0.678	-9.056	6.23E-09	2.68E-07	10.601	7610152	UBAP2L	NM_014847.2	Hs ubiquitin associated protein 2-like (UBAP2L), mRNA.
-0.678	-6.269	2.44E-06	2.73E-05	4.606	4860646	FAM20C	NM_020223.2	Hs family with sequence similarity 20, member C (FAM20C), mRNA.
-0.679	-6.622	1.08E-06	1.43E-05	5.422	5490131	NIPSNAP1	NM_003634.1	Hs nipsnap homolog 1 (C. elegans) (NIPSNAP1), mRNA.
-0.679	-8.293	2.89E-08	8.38E-07	9.064	870437	TRPM4	NM_017636.2	Hs transient receptor potential cation channel, subfamily M, member 4 (TRPM4), mRNA.
-0.680	-5.789	7.55E-06	6.83E-05	3.476	20040	PSEN2	NM_000447.1	Hs presenilin 2 (Alzheimer disease 4) (PSEN2), tv: 1, mRNA.
-0.680	-7.365	2.07E-07	3.80E-06	7.086	1980164	DHX32	NM_018180.2	Hs DEAH (Asp-Glu-Ala-His) box polypeptide 32 (DHX32), mRNA.
-0.680	-6.241	2.61E-06	2.89E-05	4.540	3450037	LOC729375	NR_024252.1	Hs family with sequence similarity 86, member A pseudogene (LOC729375), non-coding RNA.
-0.680	-6.843	6.58E-07	9.50E-06	5.923	7050136	RAB22A	NM_020673.2	Hs RAB22A, member RAS oncogene family (RAB22A), mRNA.
-0.681	-8.559	1.68E-08	5.61E-07	9.609	3360008	ZNF275	NM_001080485.1	Hs zinc finger protein 275 (ZNF275), mRNA.
-0.681	-7.823	7.71E-08	1.76E-06	8.077	6770168	CRTAP	NM_006371.3	Hs cartilage associated protein (CRTAP), mRNA.
-0.681	-7.685	1.03E-07	2.22E-06	7.782	630400	OR51B4	NM_033179.1	Hs olfactory receptor, family 51, subfamily B, member 4 (OR51B4), mRNA.
-0.681	-7.543	1.40E-07	2.84E-06	7.476	290685	SLC6A15	NM_182767.3	Hs solute carrier family 6, member 15 (SLC6A15), tv: 1, mRNA.
-0.681	-6.757	7.98E-07	1.11E-05	5.730	6860653	HBXIP	NM_006402.2	Hs hepatitis B virus x interacting protein (HBXIP), mRNA.
-0.683	-7.814	7.86E-08	1.79E-06	8.057	2750209	GLI4	NM_138465.3	Hs GLI family zinc finger 4 (GLI4), mRNA.
-0.683	-6.084	3.76E-06	3.87E-05	4.174	2230189	FKRP	NM_024301.3	Hs fukutin related protein (FKRP), tv: 1, mRNA.
-0.684	-7.901	6.54E-08	1.56E-06	8.243	2450446	TRIM33	NM_015906.3	Hs tripartite motif-containing 33 (TRIM33), tv: a, mRNA.
-0.685	-6.077	3.83E-06	3.92E-05	4.156	2120463	PKIG	NM_007066.3	Hs protein kinase (cAMP-dependent, catalytic) inhibitor gamma (PKIG), tv: 2, mRNA.

Appendix 4 – Genes differentially expressed at 24 hours in cells treated with IGF1 ligand

-0.686	-8.590	1.58E-08	5.35E-07	9.672	6520243	ATRN	NM_139321.1	Hs attractin (ATRN), tv: 1, mRNA.
-0.687	-8.293	2.88E-08	8.38E-07	9.065	5570139	QPCT	NM_012413.3	Hs glutaminyl-peptide cyclotransferase (QPCT), mRNA.
-0.687	-7.485	1.59E-07	3.11E-06	7.349	6020246	UBXN11	NM_183008.2	Hs UBX domain protein 11 (UBXN11), tv: 2, mRNA.
-0.687	-6.288	2.34E-06	2.64E-05	4.649	1240242	CPOX	NM_000097.4	Hs coproporphyrinogen oxidase (CPOX), mRNA.
-0.687	-8.514	1.84E-08	5.99E-07	9.517	3190753	ARSG	NM_014960.2	Hs arylsulfatase G (ARSG), mRNA.
-0.687	-6.591	1.16E-06	1.51E-05	5.351	4760594	TRPV4	NM_021625.3	Hs transient receptor potential cation channel, subfamily V, member 4 (TRPV4), tv: 1, mRNA.
-0.687	-6.906	5.70E-07	8.47E-06	6.067	2760735	SYNM	NM_015286.5	Hs synemin, intermediate filament protein (SYNM), tv: B, mRNA.
-0.687	-6.664	9.85E-07	1.32E-05	5.518	5960376	FAM20C	NM_020223.2	Hs family with sequence similarity 20, member C (FAM20C), mRNA.
-0.688	-6.489	1.47E-06	1.83E-05	5.116	2030048	HS.294103		Hs mRNA; cDNA DKFZp686P23119 (from clone DKFZp686P23119)
-0.688	-5.799	7.37E-06	6.72E-05	3.499	4260414	H2AFY	NM_004893.2	Hs H2A histone family, member Y (H2AFY), tv: 2, mRNA.
-0.688	-6.869	6.21E-07	9.07E-06	5.982	1770170	CTDSPL	NM_005808.2	Hs CTD (carboxy-terminal domain, RNA polymerase II, polypeptide A) small phosphatase-like (CTDSPL), t
-0.688	-9.322	3.72E-09	1.82E-07	11.119	3180315	ZNF319	NM_020807.1	Hs zinc finger protein 319 (ZNF319), mRNA.
-0.688	-7.990	5.42E-08	1.36E-06	8.430	1780133	TMTC4	NM_032813.2	Hs transmembrane and tetratricopeptide repeat containing 4 (TMTC4), tv: 1, mRNA.
-0.689	-6.149	3.23E-06	3.43E-05	4.327	5720465	DNAJC12	NM_021800.2	Hs DnaJ (Hsp40) homolog, subfamily C, member 12 (DNAJC12), tv: 1, mRNA.
-0.689	-6.566	1.23E-06	1.58E-05	5.293	1990079	FBXO32	NM_148177.1	Hs F-box protein 32 (FBXO32), tv: 2, mRNA.
-0.690	-7.998	5.33E-08	1.34E-06	8.447	1300139	GNG7	NM_052847.2	Hs guanine nucleotide binding protein (G protein), gamma 7 (GNG7), mRNA.
-0.690	-6.678	9.55E-07	1.29E-05	5.549	4560332	SNHG11	NR_003239.1	Hs small nucleolar RNA host gene 11 (non-protein coding) (SNHG11), non-coding RNA.
-0.690	-5.798	7.39E-06	6.72E-05	3.497	7380706	NINJ1	NM_004148.3	Hs ninjurin 1 (NINJ1), mRNA.
-0.690	-7.548	1.39E-07	2.82E-06	7.485	6100482	ATP2B4	NM_001001396.1	Hs ATPase, Ca++ transporting, plasma membrane 4 (ATP2B4), tv: 1, mRNA.
-0.691	-9.076	6.00E-09	2.61E-07	10.640	7610138	DDX5	NM_004396.2	Hs DEAD (Asp-Glu-Ala-Asp) box polypeptide 5 (DDX5), mRNA.
-0.692	-7.759	8.83E-08	1.96E-06	7.941	2140239	CMTM7	NM_181472.1	Hs CKLF-like MARVEL transmembrane domain containing 7 (CMTM7), tv: 2, mRNA.
-0.694	-6.783	7.53E-07	1.06E-05	5.788	1660341	FLJ39632	XR_015133.1	PREDICTED: Hs misc_RNA (FLJ39632), miscRNA.
-0.694	-6.970	4.94E-07	7.56E-06	6.211	6380112	GRAMD4	NM_015124.2	Hs GRAM domain containing 4 (GRAMD4), mRNA.
-0.695	-6.445	1.63E-06	1.97E-05	5.015	3710154	SLC7A2	NM_001008539.2	Hs solute carrier family 7 (cationic amino acid transporter, y+ system), member 2 (SLC7A2), tv: 2, mRNA.
-0.695	-6.609	1.12E-06	1.47E-05	5.391	5690324	DENND4B	NM_014856.2	Hs DENN/MADD domain containing 4B (DENND4B), mRNA.
-0.696	-6.243	2.60E-06	2.88E-05	4.545	7550743	LOC203547	NM_001017980.2	Hs hypothetical protein LOC203547 (LOC203547), mRNA.
-0.696	-8.383	2.40E-08	7.32E-07	9.249	5700189	TCTN1	NM_001082538.1	Hs tectonic family member 1 (TCTN1), tv: 1, mRNA.
-0.696	-7.389	1.96E-07	3.65E-06	7.140	6420450	LIME1	NM_017806.1	Hs Lck interacting transmembrane adaptor 1 (LIME1), mRNA.
-0.696	-6.111	3.53E-06	3.68E-05	4.238	1050544	SCAMP1	NM_004866.4	Hs secretory carrier membrane protein 1 (SCAMP1), mRNA.
-0.697	-6.284	2.36E-06	2.66E-05	4.641	770687	FASTK	NM_033015.2	Hs Fas-activated serine/threonine kinase (FASTK), tv: 4, mRNA.
-0.697	-8.548	1.72E-08	5.69E-07	9.586	1780402	SEPN1	NM_206926.1	Hs selenoprotein N, 1 (SEPN1), tv: 2, mRNA.
-0.698	-7.365	2.07E-07	3.80E-06	7.086	5700088	KLF11	XM_001129527.1	PREDICTED: Hs Kruppel-like factor 11 (KLF11), mRNA.
-0.698	-7.568	1.33E-07	2.74E-06	7.529	3460161	RAB3IL1	NM_013401.2	Hs RAB3A interacting protein (rabin3)-like 1 (RAB3IL1), mRNA.
-0.699	-7.028	4.34E-07	6.82E-06	6.341	6580711	AEBP1	NM_001129.3	Hs AE binding protein 1 (AEBP1), mRNA.
-0.700	-6.268	2.45E-06	2.74E-05	4.604	2470528	C9ORF116	NM_144654.2	Hs chromosome 9 open reading frame 116 (C9orf116), tv: 2, mRNA.
-0.700	-5.798	7.38E-06	6.72E-05	3.498	460220	ITGA1	NM_181501.1	Hs integrin, alpha 1 (ITGA1), mRNA.
-0.700	-8.427	2.19E-08	6.84E-07	9.340	1770148	FLJ20444	XM_933028.2	PREDICTED: Hs hypothetical protein FLJ20444, tv: 2 (FLJ20444), mRNA.
-0.701	-5.906	5.72E-06	5.44E-05	3.754	6580202	C19ORF43	NM_024038.2	Hs chromosome 19 open reading frame 43 (C19orf43), mRNA.
-0.701	-6.888	5.94E-07	8.78E-06	6.026	2000224	FAM89B	NM_001098784.1	Hs family with sequence similarity 89, member B (FAM89B), tv: 3, mRNA.
-0.702	-6.467	1.55E-06	1.90E-05	5.066	4250372	KLHDC3	NM_057161.2	Hs kelch domain containing 3 (KLHDC3), mRNA.

Appendix 4 – Genes differentially expressed at 24 hours in cells treated with IGF1 ligand

-0.702	-6.557	1.26E-06	1.61E-05	5.273	2470050	KRAS	NM_033360.2	Hs v-Ki-ras2 Kirsten rat sarcoma viral oncogene homolog (KRAS), tv: a, mRNA.
-0.703	-7.151	3.31E-07	5.46E-06	6.614	1980328	CACNB3	NM_000725.2	Hs calcium channel, voltage-dependent, beta 3 subunit (CACNB3), mRNA.
-0.703	-8.420	2.23E-08	6.90E-07	9.325	4560576	MYD88	NM_002468.3	Hs myeloid differentiation primary response gene (88) (MYD88), mRNA.
-0.703	-8.249	3.16E-08	9.05E-07	8.972	6480630	ATP9A	NM_006045.1	Hs ATPase, class II, type 9A (ATP9A), mRNA.
-0.704	-6.358	1.99E-06	2.32E-05	4.813	3310022	IRX5	NM_005853.5	Hs iroquois homeobox 5 (IRX5), mRNA.
-0.704	-7.438	1.76E-07	3.38E-06	7.247	70037	CLUAP1	NM_015041.1	Hs clusterin associated protein 1 (CLUAP1), tv: 1, mRNA.
-0.704	-7.072	3.94E-07	6.29E-06	6.440	70601	CUL1	NM_003592.2	Hs cullin 1 (CUL1), mRNA.
-0.705	-7.334	2.21E-07	4.00E-06	7.018	50332	MDFIC	NM_199072.3	Hs MyoD family inhibitor domain containing (MDFIC), mRNA.
-0.705	-6.802	7.21E-07	1.02E-05	5.832	460463	SMARCD3	NM_001003802.1	Hs SWI/SNF related, matrix associated, actin dependent regulator of chromatin, subfamily d, member 3 (SM
-0.705	-6.399	1.81E-06	2.15E-05	4.908	6220164	CENTG3	NM_031946.3	Hs centaurin, gamma 3 (CENTG3), mRNA.
-0.705	-8.290	2.91E-08	8.42E-07	9.057	2320243	ABCA2	NM_212533.2	Hs ATP-binding cassette, sub-family A (ABC1), member 2 (ABCA2), tv: 2, mRNA.
-0.706	-7.410	1.87E-07	3.53E-06	7.185	6760433	RNF135	NM_032322.3	Hs ring finger protein 135 (RNF135), tv: 1, mRNA.
-0.706	-8.654	1.38E-08	4.89E-07	9.801	2120280	LOC400657	NM_001008234.1	Hs hypothetical gene supported by BC036588 (LOC400657), mRNA.
-0.706	-6.559	1.25E-06	1.60E-05	5.276	3420332	SLC37A3	NM_032295.2	Hs solute carrier family 37 (glycerol-3-phosphate transporter), member 3 (SLC37A3), tv: 2, mRNA.
-0.706	-10.349	5.50E-10	4.52E-08	13.029	290333	CDCA4	NM_145701.1	Hs cell division cycle associated 4 (CDCA4), tv: 14, mRNA.
-0.706	-6.639	1.04E-06	1.38E-05	5.461	6060356	RPL13A	NM_012423.2	Hs ribosomal protein L13a (RPL13A), mRNA.
-0.706	-6.678	9.55E-07	1.29E-05	5.550	7000193	HS.370359		Hs mRNA; cDNA DKFZp686F09166 (from clone DKFZp686F09166)
-0.707	-8.356	2.54E-08	7.61E-07	9.194	4480731	RASL12	NM_016563.2	Hs RAS-like, family 12 (RASL12), mRNA.
-0.707	-7.981	5.53E-08	1.38E-06	8.412	4250445	RPL4	NM_000968.2	Hs ribosomal protein L4 (RPL4), mRNA.
-0.707	-7.955	5.84E-08	1.43E-06	8.357	5570152	ATP1A1	NM_000701.6	Hs ATPase, Na+/K+ transporting, alpha 1 polypeptide (ATP1A1), tv: 1, mRNA.
-0.707	-5.697	9.41E-06	8.20E-05	3.255	1430243	PRCC	NM_005973.4	Hs papillary renal cell carcinoma (translocation-associated) (PRCC), tv: 1, mRNA.
-0.707	-7.564	1.34E-07	2.75E-06	7.521	70102	ALDH7A1	NM_001182.2	Hs aldehyde dehydrogenase 7 family, member A1 (ALDH7A1), mRNA.
-0.708	-7.688	1.03E-07	2.21E-06	7.788	990075	BMP4	NM_130851.1	Hs bone morphogenetic protein 4 (BMP4), tv: 3, mRNA.
-0.709	-7.856	7.20E-08	1.69E-06	8.147	510326	TAZ	NM_181312.1	Hs tafazzin (cardiomyopathy, dilated 3A (X-linked); endocardial fibroelastosis 2; Barth syndrome) (TAZ), tv
-0.709	-8.239	3.23E-08	9.15E-07	8.952	4390113	UNC84A	NM_025154.3	Hs unc-84 homolog A (C. elegans) (UNC84A), mRNA.
-0.710	-7.674	1.06E-07	2.26E-06	7.757	620240	ABR	NM_001092.3	Hs active BCR-related gene (ABR), tv: 2, mRNA.
-0.710	-8.242	3.21E-08	9.12E-07	8.957	5260403	ST3GAL5	NM_001042437.1	Hs ST3 beta-galactoside alpha-2,3-sialyltransferase 5 (ST3GAL5), tv: 2, mRNA.
-0.711	-6.675	9.62E-07	1.30E-05	5.542	5130414	C9ORF23	NM_148178.1	Hs chromosome 9 open reading frame 23 (C9orf23), tv: 1, mRNA.
-0.711	-7.487	1.58E-07	3.10E-06	7.354	7570309	SPRY4	NM_030964.2	Hs sprouty homolog 4 (Drosophila) (SPRY4), mRNA.
-0.711	-5.618	1.13E-05	9.58E-05	3.067	1850554	NPDC1	NM_015392.2	Hs neural proliferation, differentiation and control, 1 (NPDC1), mRNA.
-0.712	-8.757	1.13E-08	4.21E-07	10.008	2190333	HS.155736		Hs cDNA FLJ38396 fis, clone FEBRA2007957
-0.712	-7.400	1.91E-07	3.59E-06	7.165	2970730	MYADM	NM_001020820.1	Hs myeloid-associated differentiation marker (MYADM), tv: 4, mRNA.
-0.712	-8.304	2.82E-08	8.28E-07	9.088	1980709	ACSS2	NM_018677.2	Hs acyl-CoA synthetase short-chain family member 2 (ACSS2), tv: 1, mRNA.
-0.712	-8.390	2.37E-08	7.24E-07	9.263	1240609	TMEM16D	NM_178826.2	Hs transmembrane protein 16D (TMEM16D), mRNA.
-0.713	-7.426	1.81E-07	3.44E-06	7.220	630259	VPS37D	NM_001077621.1	Hs vacuolar protein sorting 37 homolog D (S. cerevisiae) (VPS37D), mRNA.
-0.713	-6.548	1.29E-06	1.64E-05	5.251	3990324	TANC1	NM_033394.1	Hs tetratricopeptide repeat, ankyrin repeat and coiled-coil containing 1 (TANC1), mRNA.
-0.713	-5.794	7.46E-06	6.77E-05	3.488	2340703	LOC100133372	XR_039042.1	PREDICTED: Hs misc_RNA (LOC100133372), miscRNA.
-0.713	-6.424	1.71E-06	2.06E-05	4.965	6330270	GPC4	NM_001448.2	Hs glypican 4 (GPC4), mRNA.
-0.713	-7.026	4.36E-07	6.83E-06	6.336	630017	ZNF783	NM_001004302.2	Hs zinc finger family member 783 (ZNF783), mRNA.
-0.713	-5.933	5.37E-06	5.16E-05	3.817	3310451	PIGO	NM_152850.2	Hs phosphatidylinositol glycan anchor biosynthesis, class O (PIGO), tv: 2, mRNA.

Appendix 4 – Genes differentially expressed at 24 hours in cells treated with IGF1 ligand

-0.713	-8.170	3.72E-08	1.02E-06	8.808	840239	ZNF589	NM_016089.2	Hs zinc finger protein 589 (ZNF589), mRNA.
-0.714	-6.195	2.90E-06	3.14E-05	4.433	3930731	DHRS7	NM_016029.1	Hs dehydrogenase/reductase (SDR family) member 7 (DHRS7), mRNA.
-0.714	-6.729	8.50E-07	1.17E-05	5.666	2470689	SPHK1	NM_021972.2	Hs sphingosine kinase 1 (SPHK1), tv: 1, mRNA.
-0.715	-8.089	4.41E-08	1.16E-06	8.639	4040605	PSEN2	NM_012486.1	Hs presenilin 2 (Alzheimer disease 4) (PSEN2), tv: 2, mRNA.
-0.715	-7.815	7.84E-08	1.79E-06	8.061	3400593	SMARCD1	NM_003076.3	Hs SWI/SNF related, matrix associated, actin dependent regulator of chromatin, subfamily d, member 1 (SM
-0.715	-8.073	4.55E-08	1.19E-06	8.607	2070470	C1ORF21	NM_030806.3	Hs chromosome 1 open reading frame 21 (C1orf21), mRNA.
-0.716	-5.793	7.47E-06	6.78E-05	3.486	730687	TCHP	NM_032300.2	Hs trichoplein, keratin filament binding (TCHP), mRNA.
-0.716	-7.977	5.58E-08	1.38E-06	8.403	5390494	EIF4B	NM_001417.4	Hs eukaryotic translation initiation factor 4B (EIF4B), mRNA.
-0.717	-7.106	3.65E-07	5.95E-06	6.515	2360494	HS.485155		Hs cDNA: FLJ22515 fis, clone HRC12122, highly similar to AF052101 Hs clone 23872 mRNA sequence
-0.718	-6.813	7.03E-07	1.00E-05	5.857	7610072	BTBD2	NM_017797.3	Hs BTB (POZ) domain containing 2 (BTBD2), mRNA.
-0.718	-8.395	2.34E-08	7.17E-07	9.274	1850079	KIAA1267	NM_015443.2	Hs KIAA1267 (KIAA1267), mRNA.
-0.718	-6.014	4.44E-06	4.41E-05	4.007	6400333	CTLA4	NM_005214.3	Hs cytotoxic T-lymphocyte-associated protein 4 (CTLA4), tv: 1, mRNA.
-0.719	-8.172	3.71E-08	1.02E-06	8.813	6110301	KDELC2	NM_153705.4	Hs KDEL (Lys-Asp-Glu-Leu) containing 2 (KDELC2), mRNA.
-0.720	-7.097	3.72E-07	6.05E-06	6.495	2320463	MGC52000	NM_198943.1	Hs CXYorf1-related protein (MGC52000), mRNA.
-0.720	-6.848	6.50E-07	9.40E-06	5.935	4280044	LOC100131609	XR_038433.1	PREDICTED: Hs misc_RNA (LOC100131609), miscRNA.
-0.721	-6.447	1.62E-06	1.97E-05	5.019	360377	TGFA	NM_003236.1	Hs transforming growth factor, alpha (TGFA), mRNA.
-0.722	-7.747	9.06E-08	2.00E-06	7.915	3890458	MGC4294	XR_017834.1	PREDICTED: Hs hypothetical protein MGC4294 (MGC4294), misc RNA.
-0.722	-8.383	2.40E-08	7.32E-07	9.249	2230288	TST	NM_003312.4	Hs thiosulfate sulfurtransferase (rhodanese) (TST), nuclear gene encoding mitochondrial protein, mRNA.
-0.722	-7.630	1.16E-07	2.44E-06	7.663	2680086	USP22	NM_015276.1	Hs ubiquitin specific peptidase 22 (USP22), mRNA.
-0.723	-6.020	4.38E-06	4.36E-05	4.021	1090653	C1ORF133	NR_024337.1	Hs chromosome 1 open reading frame 133 (C1orf133), non-coding RNA. XM_001720763
-0.723	-8.030	4.98E-08	1.28E-06	8.516	7400243	KIAA0892	NM_015329.3	Hs KIAA0892 (KIAA0892), mRNA.
-0.724	-5.663	1.02E-05	8.76E-05	3.175	1940056	RIMKLB	NM_020734.2	Hs ribosomal modification protein rimK-like family member B (RIMKLB), mRNA.
-0.724	-7.270	2.54E-07	4.44E-06	6.879	290132	C20ORF117	NM_199181.2	Hs chromosome 20 open reading frame 117 (C20orf117), tv: 2, mRNA.
-0.724	-8.129	4.06E-08	1.09E-06	8.722	5550452	KCNMA1	NM_002247.2	Hs potassium large conductance calcium-activated channel, subfamily M, alpha member 1 (KCNMA1), tv: 2
-0.724	-7.193	3.02E-07	5.09E-06	6.707	2230630	CMTM4	NM_181521.2	Hs CKLF-like MARVEL transmembrane domain containing 4 (CMTM4), tv: 2, mRNA.
-0.726	-7.148	3.33E-07	5.48E-06	6.607	3840204	LASS1	NM_198207.2	Hs LAG1 homolog, ceramide synthase 1 (LASS1), tv: 2, mRNA.
-0.726	-6.483	1.49E-06	1.85E-05	5.101	6760719	EMILIN1	NM_007046.1	Hs elastin microfibril interfacer 1 (EMILIN1), mRNA.
-0.726	-7.062	4.03E-07	6.43E-06	6.415	2450411	DNAJC12	NM_021800.2	Hs DnaJ (Hsp40) homolog, subfamily C, member 12 (DNAJC12), tv: 1, mRNA.
-0.726	-8.360	2.52E-08	7.57E-07	9.202	4200035	RBM45	NM_152945.2	Hs RNA binding motif protein 45 (RBM45), mRNA.
-0.727	-6.389	1.85E-06	2.19E-05	4.884	5080682	CTDSP1	NM_021198.1	Hs CTD (carboxy-terminal domain, RNA polymerase II, polypeptide A) small phosphatase 1 (CTDSP1), tv:
-0.727	-6.868	6.22E-07	9.09E-06	5.980	2480288	GPAA1	NM_003801.3	Hs glycosylphosphatidylinositol anchor attachment protein 1 homolog (yeast) (GPAA1), mRNA.
-0.728	-8.041	4.87E-08	1.25E-06	8.540	4480592	CHMP6	XM_001132548.1	PREDICTED: Hs chromatin modifying protein 6 (CHMP6), mRNA.
-0.728	-6.528	1.35E-06	1.71E-05	5.204	6020653	BTBD3	NM_014962.2	Hs BTB (POZ) domain containing 3 (BTBD3), tv: 1, mRNA.
-0.729	-9.430	3.02E-09	1.52E-07	11.326	4150544	ALDH7A1	NM_001182.2	Hs aldehyde dehydrogenase 7 family, member A1 (ALDH7A1), mRNA.
-0.729	-6.112	3.52E-06	3.68E-05	4.239	4490142	NRBP2	NM_178564.2	Hs nuclear receptor binding protein 2 (NRBP2), mRNA.
-0.730	-6.995	4.68E-07	7.25E-06	6.266	5130253	HGS	NM_004712.3	Hs hepatocyte growth factor-regulated tyrosine kinase substrate (HGS), mRNA.
-0.731	-6.967	4.98E-07	7.61E-06	6.203	2850497	MUS81	NM_025128.3	Hs MUS81 endonuclease homolog (S. cerevisiae) (MUS81), mRNA.
-0.732	-6.663	9.87E-07	1.32E-05	5.516	4280228	IVNS1ABP	NM_006469.4	Hs influenza virus NS1A binding protein (IVNS1ABP), mRNA.
-0.733	-5.608	1.16E-05	9.77E-05	3.043	3830168	LOC100133469	XM_001724642.1	PREDICTED: Hs hypothetical protein LOC100133469 (LOC100133469), mRNA.
-0.733	-6.289	2.34E-06	2.64E-05	4.652	1410603	RAB3IP	NM_001024647.2	Hs RAB3A interacting protein (rabin3) (RAB3IP), tv: A, mRNA.

Appendix 4 – Genes differentially expressed at 24 hours in cells treated with IGF1 ligand

-0.733	-5.720	8.90E-06	7.82E-05	3.311	2940066	LOC388275	XM_928429.1	PREDICTED: Hs similar to Heterogeneous nuclear ribonucleoprotein A1 (Helix-destabilizing protein) (Sing
-0.734	-8.100	4.31E-08	1.14E-06	8.662	5260278	PPAPDC3	NM_032728.2	Hs phosphatidic acid phosphatase type 2 domain containing 3 (PPAPDC3), mRNA.
-0.734	-8.184	3.62E-08	1.00E-06	8.837	3180343	C17ORF85	NM_018553.1	Hs chromosome 17 open reading frame 85 (C17orf85), mRNA.
-0.734	-6.984	4.80E-07	7.38E-06	6.241	2320129	CSDA	NM_003651.3	Hs cold shock domain protein A (CSDA), mRNA.
-0.735	-7.206	2.93E-07	4.96E-06	6.736	7650523	SHISA2	NM_001007538.1	Hs shisa homolog 2 (Xenopus laevis) (SHISA2), mRNA.
-0.735	-6.453	1.60E-06	1.95E-05	5.033	7400743	KIAA1618	NM_020954.2	Hs KIAA1618 (KIAA1618), mRNA.
-0.736	-6.721	8.66E-07	1.19E-05	5.648	3990201	OTUD4	NM_199324.1	Hs OTU domain containing 4 (OTUD4), tv: 1, mRNA.
-0.737	-7.054	4.10E-07	6.52E-06	6.399	460767	BGN	NM_001711.3	Hs biglycan (BGN), mRNA.
-0.737	-8.923	8.10E-09	3.27E-07	10.339	1580402	SLC35B2	NM_178148.1	Hs solute carrier family 35, member B2 (SLC35B2), mRNA.
-0.737	-7.704	9.94E-08	2.15E-06	7.822	4810348	C1ORF188	NM_173795.2	Hs chromosome 1 open reading frame 188 (C1orf188), mRNA.
-0.737	-6.744	8.23E-07	1.14E-05	5.699	3450747	DHRS11	NM_024308.3	Hs dehydrogenase/reductase (SDR family) member 11 (DHRS11), mRNA.
-0.737	-6.636	1.05E-06	1.39E-05	5.453	5420482	C9ORF58	NM_001002260.1	Hs chromosome 9 open reading frame 58 (C9orf58), tv: 2, mRNA.
-0.737	-7.163	3.22E-07	5.35E-06	6.641	6180204	FUK	NM_145059.2	Hs fucokinase (FUK), mRNA.
-0.738	-7.560	1.35E-07	2.77E-06	7.512	6510634	C14ORF169	NM_024644.2	Hs chromosome 14 open reading frame 169 (C14orf169), mRNA.
-0.738	-7.285	2.46E-07	4.34E-06	6.910	4290201	IL24	NM_006850.2	Hs interleukin 24 (IL24), tv: 1, mRNA.
-0.738	-8.769	1.10E-08	4.16E-07	10.032	2140735	RALGDS	NM_006266.2	Hs ral guanine nucleotide dissociation stimulator (RALGDS), tv: 1, mRNA.
-0.738	-7.608	1.22E-07	2.54E-06	7.615	2710093	ZNF74	NM_003426.2	Hs zinc finger protein 74 (ZNF74), tv: 1, mRNA.
-0.739	-7.028	4.35E-07	6.82E-06	6.340	1690370	TMEM132A	NM_178031.2	Hs transmembrane protein 132A (TMEM132A), tv: 2, mRNA.
-0.739	-7.647	1.12E-07	2.37E-06	7.701	2850537	TBC1D9B	NM_015043.3	Hs TBC1 domain family, member 9B (with GRAM domain) (TBC1D9B), tv: 2, mRNA.
-0.739	-7.112	3.60E-07	5.89E-06	6.528	2810364	KLHDC2	NM_014315.2	Hs kelch domain containing 2 (KLHDC2), mRNA.
-0.739	-6.977	4.87E-07	7.46E-06	6.226	1770685	MYH10	NM_005964.1	Hs myosin, heavy chain 10, non-muscle (MYH10), mRNA.
-0.739	-6.839	6.63E-07	9.55E-06	5.915	7320386	TTL	NM_153712.4	Hs tubulin tyrosine ligase (TTL), mRNA.
-0.739	-6.291	2.32E-06	2.62E-05	4.657	4040653	LOC728855	NR_024510.1	Hs hypothetical LOC728855 (LOC728855), non-coding RNA.
-0.741	-8.656	1.38E-08	4.88E-07	9.804	5420427	TUG1	NR_002323.1	Hs taurine upregulated 1 (non-protein coding) (TUG1), non-coding RNA.
-0.742	-8.427	2.19E-08	6.84E-07	9.339	6660600	COQ9	NM_020312.1	Hs coenzyme Q9 homolog (S. cerevisiae) (COQ9), mRNA.
-0.742	-7.801	8.08E-08	1.82E-06	8.030	2710546	COG4	NM_015386.2	Hs component of oligomeric golgi complex 4 (COG4), mRNA.
-0.743	-8.748	1.15E-08	4.25E-07	9.990	6020746	CMTM3	NM_001048251.1	Hs CKLF-like MARVEL transmembrane domain containing 3 (CMTM3), tv: 5, mRNA.
-0.743	-9.148	5.21E-09	2.37E-07	10.782	4260093	ZCCHC11	NM_001009882.1	Hs zinc finger, CCHC domain containing 11 (ZCCHC11), tv: 3, mRNA.
-0.744	-6.995	4.68E-07	7.25E-06	6.267	5570653	TM7SF2	NM_003273.2	Hs transmembrane 7 superfamily member 2 (TM7SF2), mRNA.
-0.745	-6.589	1.17E-06	1.52E-05	5.346	3140603	SVIL	NM_003174.3	Hs supervillin (SVIL), tv: 1, mRNA.
-0.745	-6.379	1.89E-06	2.23E-05	4.862	1430402	NUP85	NM_024844.3	Hs nucleoporin 85kDa (NUP85), mRNA.
-0.745	-6.325	2.15E-06	2.47E-05	4.736	5490524	ZNF302	NM_018443.2	Hs zinc finger protein 302 (ZNF302), tv: 1, mRNA.
-0.745	-13.403	3.70E-12	1.44E-09	17.977	6650736	WRNIP1	NM_130395.1	Hs Werner helicase interacting protein 1 (WRNIP1), tv: 2, mRNA.
-0.746	-7.314	2.31E-07	4.14E-06	6.974	7050014	TMEM231	NM_001077419.1	Hs transmembrane protein 231 (TMEM231), tv: 3, mRNA.
-0.746	-10.097	8.69E-10	6.32E-08	12.573	6110187	CSNK2A2	NM_001896.2	Hs casein kinase 2, alpha prime polypeptide (CSNK2A2), mRNA.
-0.747	-7.171	3.16E-07	5.27E-06	6.660	3990521	LOC728635	XM_001131304.1	PREDICTED: Hs similar to peroxisomal short-chain alcohol dehydrogenase, tv: 1 (LOC728635), mRNA.
-0.747	-5.773	7.84E-06	7.05E-05	3.437	4890270	LY6E	NM_002346.1	Hs lymphocyte antigen 6 complex, locus E (LY6E), mRNA.
-0.747	-6.861	6.31E-07	9.18E-06	5.965	70070	GRINA	NM_000837.1	Hs glutamate receptor, ionotropic, N-methyl D-aspartate-associated protein 1 (glutamate binding) (GRINA),
-0.747	-6.907	5.69E-07	8.46E-06	6.069	5700735	PARP9	NM_031458.1	Hs poly (ADP-ribose) polymerase family, member 9 (PARP9), mRNA.
-0.748	-9.748	1.66E-09	9.85E-08	11.928	270129	TMEM8	NM_021259.1	Hs transmembrane protein 8 (five membrane-spanning domains) (TMEM8), mRNA.

Appendix 4 – Genes differentially expressed at 24 hours in cells treated with IGF1 ligand

-0.749	-8.379	2.42E-08	7.36E-07	9.242	2650064	SMARCE1	NM_003079.4	Hs SWI/SNF related, matrix associated, actin dependent regulator of chromatin, subfamily e, member 1 (SM
-0.749	-5.945	5.22E-06	5.04E-05	3.845	4250048	CMTM7	NM_138410.2	Hs CKLF-like MARVEL transmembrane domain containing 7 (CMTM7), tv: 1, mRNA.
-0.750	-5.839	6.71E-06	6.23E-05	3.593	3400709	HS.531457		Hs cDNA FLJ37595 fis, clone BRCOC2007864
-0.750	-7.343	2.17E-07	3.95E-06	7.039	3450136	RNF144	NM_014746.2	Hs ring finger protein 144 (RNF144), mRNA.
-0.750	-8.627	1.46E-08	5.06E-07	9.746	5870307	LOC440359	XM_496143.2	PREDICTED: Hs similar to muscle Y-box protein YB2 (LOC440359), mRNA.
-0.750	-8.363	2.50E-08	7.54E-07	9.209	2070669	CDC42EP3	NM_006449.3	Hs CDC42 effector protein (Rho GTPase binding) 3 (CDC42EP3), mRNA.
-0.751	-6.522	1.36E-06	1.72E-05	5.192	2600291	MTAP	NM_002451.3	Hs methylthioadenosine phosphorylase (MTAP), mRNA.
-0.751	-7.225	2.81E-07	4.80E-06	6.779	3800431	RCOR3	NM_018254.2	Hs REST corepressor 3 (RCOR3), mRNA.
-0.751	-6.346	2.04E-06	2.37E-05	4.785	5820240	FNTB	NM_002028.3	Hs farnesyltransferase, CAAX box, beta (FNTB), mRNA.
-0.751	-7.946	5.95E-08	1.45E-06	8.338	670446	FAM86C	NM_152563.2	Hs family with sequence similarity 86, member C (FAM86C), tv: 2, mRNA.
-0.752	-7.562	1.35E-07	2.76E-06	7.516	6900491	TCF7L2	NM_030756.2	Hs transcription factor 7-like 2 (T-cell specific, HMG-box) (TCF7L2), mRNA.
-0.752	-8.439	2.14E-08	6.72E-07	9.364	4490273	KLHDC5	NM_020782.1	Hs kelch domain containing 5 (KLHDC5), mRNA.
-0.752	-8.847	9.42E-09	3.71E-07	10.187	3120162	ALAD	NM_001003945.1	Hs aminolevulinate, delta-, dehydratase (ALAD), tv: 1, mRNA.
-0.753	-8.773	1.09E-08	4.16E-07	10.041	6370014	B3GAT1	NM_018644.3	Hs beta-1,3-glucuronyltransferase 1 (glucuronosyltransferase P) (B3GAT1), tv: 1, mRNA.
-0.753	-6.294	2.31E-06	2.61E-05	4.664	6180246	COX7A2L	NM_004718.2	Hs cytochrome c oxidase subunit VIIa polypeptide 2 like (COX7A2L), nuclear gene encoding mitochondrial
-0.753	-8.180	3.64E-08	1.01E-06	8.830	4560092	FNBP1L	NM_001024948.1	Hs formin binding protein 1-like (FNBP1L), tv: 1, mRNA.
-0.753	-6.669	9.75E-07	1.31E-05	5.529	6110609	FAM39DP	NR_003659.1	Hs family with sequence similarity 39, member D pseudogene (FAM39DP) on chromosome 15.
-0.754	-7.737	9.26E-08	2.03E-06	7.893	4830427	PPIL5	NM_152329.3	Hs peptidylprolyl isomerase (cyclophilin)-like 5 (PPIL5), tv: 1, mRNA.
-0.754	-7.197	2.99E-07	5.05E-06	6.715	2900204	RFX1	NM_002918.3	Hs regulatory factor X, 1 (influences HLA class II expression) (RFX1), mRNA.
-0.755	-7.703	9.95E-08	2.15E-06	7.821	5340414	LGTN	NM_006893.2	Hs ligatin (LGTN), mRNA.
-0.755	-5.860	6.38E-06	5.97E-05	3.644	5690711	TMEM134	NM_001078651.1	Hs transmembrane protein 134 (TMEM134), tv: 3, mRNA.
-0.758	-8.815	1.00E-08	3.91E-07	10.124	1010129	C10ORF61	NM_001013840.1	Hs chromosome 10 open reading frame 61 (C10orf61), tv: 1, mRNA.
-0.758	-5.794	7.46E-06	6.77E-05	3.487	1070300	OGT	NM_181673.1	Hs O-linked N-acetylglucosamine (GlcNAc) transferase (UDP-N-acetylglucosamine:polypeptide-N-acetylglu
-0.759	-8.116	4.17E-08	1.11E-06	8.696	5870445	LOC644517	XR_037472.1	PREDICTED: Hs misc_RNA (LOC644517), miscRNA.
-0.760	-8.631	1.45E-08	5.03E-07	9.755	2000577	DCAF7	NM_005828.3	Hs DDB1 and CUL4 associated factor 7 (DCAF7), mRNA.
-0.761	-8.262	3.08E-08	8.87E-07	9.000	6420731	SLC20A1	NM_005415.3	Hs solute carrier family 20 (phosphate transporter), member 1 (SLC20A1), mRNA.
-0.761	-6.993	4.70E-07	7.26E-06	6.262	770187	LOC286512	XR_038196.1	PREDICTED: Hs misc_RNA (LOC286512), miscRNA.
-0.762	-6.051	4.07E-06	4.12E-05	4.096	2570091	PHF19	NM_015651.1	Hs PHD finger protein 19 (PHF19), tv: 1, mRNA.
-0.762	-8.023	5.06E-08	1.29E-06	8.500	5270575	MAPK8IP3	NM_001040439.1	Hs mitogen-activated protein kinase 8 interacting protein 3 (MAPK8IP3), tv: 2, mRNA.
-0.763	-8.075	4.54E-08	1.19E-06	8.609	3460451	SH3PXD2A	NM_014631.2	Hs SH3 and PX domains 2A (SH3PXD2A), mRNA.
-0.764	-11.165	1.31E-10	1.61E-08	14.454	1940021	GRN	NM_002087.2	Hs granulin (GRN), mRNA.
-0.764	-6.407	1.78E-06	2.12E-05	4.926	2450187	GPD1L	NM_015141.2	Hs glycerol-3-phosphate dehydrogenase 1-like (GPD1L), mRNA.
-0.765	-9.918	1.21E-09	7.77E-08	12.244	7040327	ALDH5A1	NM_001080.3	Hs aldehyde dehydrogenase 5 family, member A1 (ALDH5A1), nuclear gene encoding mitochondrial protei
-0.765	-5.681	9.77E-06	8.44E-05	3.218	2230187	MAPBPIP	NM_014017.1	Hs mitogen-activated protein-binding protein-interacting protein (MAPBPIP), mRNA.
-0.765	-8.865	9.09E-09	3.59E-07	10.223	6420215	STRA6	NM_022369.2	Hs stimulated by retinoic acid gene 6 homolog (mouse) (STRA6), mRNA.
-0.765	-9.058	6.21E-09	2.68E-07	10.604	1940053	ATP2A2	NM_001681.2	Hs ATPase, Ca++ transporting, cardiac muscle, slow twitch 2 (ATP2A2), tv: 2, mRNA.
-0.765	-10.546	3.87E-10	3.51E-08	13.380	4890278	MGC3032	XM_933539.2	PREDICTED: Hs hypothetical protein MGC3032, tv: 3 (MGC3032), mRNA.
-0.767	-7.027	4.35E-07	6.82E-06	6.339	5820193	TYRO3	NM_006293.2	Hs TYRO3 protein tyrosine kinase (TYRO3), mRNA.
-0.767	-10.046	9.54E-10	6.61E-08	12.479	4490014	TTC13	NM_024525.2	Hs tetratricopeptide repeat domain 13 (TTC13), mRNA.
-0.767	-5.530	1.40E-05	0.000114142	2.856	2640014	PLEKHG4	NM_015432.2	Hs pleckstrin homology domain containing, family G (with RhoGef domain) member 4 (PLEKHG4), mRNA

Appendix 4 – Genes differentially expressed at 24 hours in cells treated with IGF1 ligand

-0.770	-7.840	7.44E-08	1.71E-06	8.114	7650735	VPS72	NM_005997.1	Hs vacuolar protein sorting 72 homolog (S. cerevisiae) (VPS72), mRNA.
-0.771	-6.438	1.65E-06	2.00E-05	4.997	1190626	ZMYND11	NM_006624.3	Hs zinc finger, MYND domain containing 11 (ZMYND11), tv: 1, mRNA.
-0.771	-5.905	5.74E-06	5.46E-05	3.750	3180446	MED16	NM_005481.2	Hs mediator complex subunit 16 (MED16), mRNA.
-0.771	-6.457	1.58E-06	1.94E-05	5.041	7650189	LAMB2	NM_002292.3	Hs laminin, beta 2 (laminin S) (LAMB2), mRNA.
-0.771	-9.064	6.14E-09	2.65E-07	10.617	2030324	SGK1	NM_005627.3	Hs serum/glucocorticoid regulated kinase 1 (SGK1), tv: 1, mRNA.
-0.772	-7.947	5.93E-08	1.45E-06	8.341	1940743	RPL13	NM_033251.1	Hs ribosomal protein L13 (RPL13), tv: 2, mRNA.
-0.772	-6.344	2.05E-06	2.38E-05	4.781	2940075	STRADB	NM_018571.5	Hs STE20-related kinase adaptor beta (STRADB), mRNA.
-0.772	-8.427	2.19E-08	6.84E-07	9.340	3290113	ADRBK1	NM_001619.3	Hs adrenergic, beta, receptor kinase 1 (ADRBK1), mRNA.
-0.773	-8.957	7.57E-09	3.11E-07	10.407	3120379	DPY19L1	NM_015283.1	Hs dpy-19-like 1 (C. elegans) (DPY19L1), mRNA.
-0.773	-8.141	3.95E-08	1.07E-06	8.749	1820044	ALDH9A1	NM_000696.3	Hs aldehyde dehydrogenase 9 family, member A1 (ALDH9A1), mRNA.
-0.774	-6.609	1.12E-06	1.47E-05	5.391	2030754	GHDC	NM_032484.3	Hs GH3 domain containing (GHDC), mRNA.
-0.775	-7.458	1.69E-07	3.26E-06	7.291	2190730	CEPT1	NM_001007794.1	Hs choline/ethanolamine phosphotransferase 1 (CEPT1), tv: 2, mRNA.
-0.777	-5.795	7.45E-06	6.77E-05	3.489	3190022	KATNB1	NM_005886.2	Hs katanin p80 (WD repeat containing) subunit B 1 (KATNB1), mRNA.
-0.777	-7.321	2.27E-07	4.08E-06	6.991	4210411	NDRG2	NM_201539.1	Hs NDRG family member 2 (NDRG2), tv: 6, mRNA.
-0.777	-6.505	1.42E-06	1.78E-05	5.152	6650100	WDR36	NM_139281.2	Hs WD repeat domain 36 (WDR36), mRNA.
-0.777	-7.838	7.47E-08	1.72E-06	8.110	6620241	LOC340970	XR_038494.1	PREDICTED: Hs misc_RNA (LOC340970), miscRNA.
-0.777	-8.772	1.09E-08	4.16E-07	10.038	6980477	CLUAP1	NM_015041.1	Hs clusterin associated protein 1 (CLUAP1), tv: 1, mRNA.
-0.778	-8.767	1.10E-08	4.16E-07	10.029	6580164	PHF21A	NM_016621.2	Hs PHD finger protein 21A (PHF21A), mRNA.
-0.779	-7.608	1.22E-07	2.54E-06	7.616	5570523	C1ORF159	NM_017891.2	Hs chromosome 1 open reading frame 159 (C1orf159), mRNA.
-0.779	-6.880	6.05E-07	8.90E-06	6.007	7510025	TSPAN3	NM_005724.4	Hs tetraspanin 3 (TSPAN3), tv: 1, mRNA.
-0.780	-5.641	1.07E-05	9.17E-05	3.122	6520594	ARHGEF11	NM_014784.2	Hs Rho guanine nucleotide exchange factor (GEF) 11 (ARHGEF11), tv: 1, mRNA.
-0.780	-9.704	1.80E-09	1.04E-07	11.846	770561	C20ORF108	NM_080821.2	Hs chromosome 20 open reading frame 108 (C20orf108), mRNA.
-0.781	-8.651	1.39E-08	4.91E-07	9.795	7510356	DGKQ	NM_001347.2	Hs diacylglycerol kinase, theta 110kDa (DGKQ), mRNA.
-0.781	-8.362	2.50E-08	7.54E-07	9.207	3060176	ZNF746	NM_152557.3	Hs zinc finger protein 746 (ZNF746), mRNA.
-0.781	-8.727	1.20E-08	4.39E-07	9.948	1770008	FRMD4A	NM_018027.3	Hs FERM domain containing 4A (FRMD4A), mRNA.
-0.782	-5.677	9.86E-06	8.52E-05	3.208	6980475	EFTUD2	NM_004247.2	Hs elongation factor Tu GTP binding domain containing 2 (EFTUD2), mRNA.
-0.782	-7.609	1.22E-07	2.54E-06	7.617	4920300	MAP3K12	NM_006301.2	Hs mitogen-activated protein kinase kinase kinase 12 (MAP3K12), mRNA.
-0.782	-7.521	1.47E-07	2.93E-06	7.427	6420736	DNAJC12	NM_201262.1	Hs DnaJ (Hsp40) homolog, subfamily C, member 12 (DNAJC12), tv: 2, mRNA.
-0.783	-6.471	1.53E-06	1.89E-05	5.074	7210192	ADA	NM_000022.2	Hs adenosine deaminase (ADA), mRNA.
-0.784	-9.704	1.80E-09	1.04E-07	11.846	1230347	RERE	NM_012102.3	Hs arginine-glutamic acid dipeptide (RE) repeats (RERE), tv: 1, mRNA.
-0.784	-7.365	2.06E-07	3.80E-06	7.088	2510682	LOC645146	XM_928177.2	PREDICTED: Hs similar to Kinase suppressor of Ras 1 (LOC645146), mRNA.
-0.785	-6.270	2.44E-06	2.73E-05	4.608	6560301	SH2B3	NM_005475.1	Hs SH2B adaptor protein 3 (SH2B3), mRNA.
-0.786	-7.375	2.02E-07	3.73E-06	7.109	60022	C3ORF39	NM_032806.4	Hs chromosome 3 open reading frame 39 (C3orf39), mRNA.
-0.786	-8.128	4.06E-08	1.09E-06	8.721	2030446	SNAPC3	NM_003084.1	Hs small nuclear RNA activating complex, polypeptide 3, 50kDa (SNAPC3), mRNA.
-0.787	-5.739	8.50E-06	7.55E-05	3.356	5860112	FGFRL1	NM_001004358.1	Hs fibroblast growth factor receptor-like 1 (FGFRL1), tv: 2, mRNA.
-0.787	-8.207	3.45E-08	9.65E-07	8.886	6940433	STAT5B	NM_012448.3	Hs signal transducer and activator of transcription 5B (STAT5B), mRNA.
-0.788	-10.024	9.93E-10	6.75E-08	12.439	4220184	HS.326560		PREDICTED: Hs LOC440151 (LOC440151), mRNA
-0.788	-6.317	2.19E-06	2.51E-05	4.717	2190463	ADCY6	NM_020983.2	Hs adenylate cyclase 6 (ADCY6), tv: 2, mRNA.
-0.790	-7.306	2.35E-07	4.19E-06	6.958	3400070	ZNF7	NM_003416.1	Hs zinc finger protein 7 (ZNF7), mRNA.
-0.790	-7.239	2.72E-07	4.69E-06	6.809	3930593	ACSL3	NM_004457.3	Hs acyl-CoA synthetase long-chain family member 3 (ACSL3), tv: 1, mRNA.

Appendix 4 – Genes differentially expressed at 24 hours in cells treated with IGF1 ligand

-0.791	-7.591	1.27E-07	2.61E-06	7.579	2340414	HS.568777		AGENCOURT_8210259 NIH_MGC_112 Hs cDNA clone IMAGE:6258046 5, mRNA sequence
-0.791	-8.711	1.24E-08	4.47E-07	9.915	4920148	ALDH1A3	NM_000693.1	Hs aldehyde dehydrogenase 1 family, member A3 (ALDH1A3), mRNA.
-0.791	-5.909	5.68E-06	5.41E-05	3.760	540441	LOC100133999	XM_001716785.1	PREDICTED: Hs hypothetical protein LOC100133999 (LOC100133999), mRNA.
-0.791	-6.228	2.69E-06	2.96E-05	4.511	1110605	FTSJ1	NM_012280.2	Hs FtsJ homolog 1 (E. coli) (FTSJ1), tv: 1, mRNA.
-0.791	-6.883	6.02E-07	8.87E-06	6.013	150241	MAN2C1	NM_006715.2	Hs mannosidase, alpha, class 2C, member 1 (MAN2C1), mRNA.
-0.791	-5.988	4.71E-06	4.63E-05	3.948	940435	TRIM8	NM_030912.2	Hs tripartite motif-containing 8 (TRIM8), mRNA.
-0.791	-9.822	1.44E-09	8.84E-08	12.066	6100382	RTKN	NM_033046.2	Hs rhotekin (RTKN), tv: 2, mRNA.
-0.792	-6.001	4.57E-06	4.53E-05	3.978	5290626	C14ORF4	NM_024496.2	Hs chromosome 14 open reading frame 4 (C14orf4), mRNA.
-0.793	-7.207	2.92E-07	4.96E-06	6.738	670671	TMEM134	NM_001078650.1	Hs transmembrane protein 134 (TMEM134), tv: 2, mRNA.
-0.794	-6.875	6.13E-07	8.99E-06	5.995	2480661	SUV420H1	NM_017635.3	Hs suppressor of variegation 4-20 homolog 1 (Drosophila) (SUV420H1), tv: 1, mRNA.
-0.794	-8.023	5.05E-08	1.29E-06	8.502	6840475	HS.397465		Hs mRNA; cDNA DKFZp686F1546 (from clone DKFZp686F1546)
-0.794	-12.502	1.47E-11	3.43E-09	16.623	4780414	RPL32	NM_001007073.1	Hs ribosomal protein L32 (RPL32), tv: 2, mRNA.
-0.795	-6.083	3.77E-06	3.88E-05	4.171	3890196	PIGO	NM_152850.2	Hs phosphatidylinositol glycan anchor biosynthesis, class O (PIGO), tv: 2, mRNA.
-0.795	-7.850	7.29E-08	1.70E-06	8.134	2450286	DHX33	NM_020162.2	Hs DEAH (Asp-Glu-Ala-His) box polypeptide 33 (DHX33), mRNA.
-0.796	-6.301	2.27E-06	2.58E-05	4.681	6020669	LOC391811	XR_018614.1	PREDICTED: Hs similar to DNA polymerase delta subunit 2 (DNA polymerase delta subunit p50) (LOC391
-0.796	-6.410	1.76E-06	2.11E-05	4.933	5960682	RBPMS2	NM_194272.1	Hs RNA binding protein with multiple splicing 2 (RBPMS2), mRNA.
-0.796	-8.540	1.74E-08	5.75E-07	9.570	4810181	ZBTB42	NM_001137601.1	Hs zinc finger and BTB domain containing 42 (ZBTB42), mRNA.
-0.796	-8.195	3.54E-08	9.84E-07	8.860	5050382	SPARC	NM_003118.2	Hs secreted protein, acidic, cysteine-rich (osteonectin) (SPARC), mRNA.
-0.797	-7.275	2.52E-07	4.41E-06	6.889	7330435	CCDC6	NM_005436.2	Hs coiled-coil domain containing 6 (CCDC6), mRNA.
-0.797	-7.450	1.72E-07	3.31E-06	7.273	6200431	AKT1	NM_001014431.1	Hs v-akt murine thymoma viral oncogene homolog 1 (AKT1), tv: 3, mRNA.
-0.798	-6.780	7.58E-07	1.06E-05	5.781	1850092	PODXL	NM_001018111.1	Hs podocalyxin-like (PODXL), tv: 1, mRNA.
-0.798	-6.317	2.19E-06	2.51E-05	4.717	5820598	MED16	NM_005481.2	Hs mediator complex subunit 16 (MED16), mRNA.
-0.799	-8.563	1.66E-08	5.57E-07	9.617	3840491	PELI2	NM_021255.2	Hs pellino homolog 2 (Drosophila) (PELI2), mRNA.
-0.800	-7.178	3.12E-07	5.22E-06	6.674	2690484	WDR35	NM_001006657.1	Hs WD repeat domain 35 (WDR35), tv: 1, mRNA.
-0.801	-8.687	1.30E-08	4.64E-07	9.867	4900332	FOXJ2	NM_018416.2	Hs forkhead box J2 (FOXJ2), mRNA.
-0.801	-9.296	3.91E-09	1.89E-07	11.069	4490615	TSPAN3	NM_005724.4	Hs tetraspanin 3 (TSPAN3), tv: 1, mRNA.
-0.803	-9.929	1.18E-09	7.66E-08	12.264	4610296	CLUAP1	NM_024793.1	Hs clusterin associated protein 1 (CLUAP1), tv: 2, mRNA.
-0.804	-9.693	1.84E-09	1.05E-07	11.824	2510181	C12ORF76	NM_207435.1	Hs chromosome 12 open reading frame 76 (C12orf76), mRNA.
-0.806	-7.479	1.61E-07	3.14E-06	7.336	870041	SNAPIN	NM_012437.3	Hs SNAP-associated protein (SNAPIN), mRNA.
-0.806	-6.408	1.77E-06	2.12E-05	4.928	6380286	GTF2IP1	NR_002206.1	Hs general transcription factor II, i, pseudogene 1 (GTF2IP1) on chromosome 7.
-0.806	-7.216	2.86E-07	4.88E-06	6.759	5090221	HS.556255		Hs clone TESTIS-609 mRNA sequence
-0.807	-7.756	8.90E-08	1.97E-06	7.933	6510397	WDR19	NM_025132.3	Hs WD repeat domain 19 (WDR19), mRNA.
-0.807	-8.021	5.08E-08	1.29E-06	8.497	6960379	SFRP1	NM_003012.3	Hs secreted frizzled-related protein 1 (SFRP1), mRNA.
-0.808	-6.665	9.83E-07	1.32E-05	5.521	3610487	UBQLN4	NM_020131.3	Hs ubiquilin 4 (UBQLN4), mRNA.
-0.808	-8.123	4.10E-08	1.10E-06	8.710	3180719	FLJ10916	NM_018271.2	Hs hypothetical protein FLJ10916 (FLJ10916), mRNA.
-0.811	-7.720	9.60E-08	2.10E-06	7.858	4560736	SLCO4A1	NM_016354.3	Hs solute carrier organic anion transporter family, member 4A1 (SLCO4A1), mRNA.
-0.811	-7.487	1.59E-07	3.10E-06	7.353	6220368	POGK	NM_017542.3	Hs pogo transposable element with KRAB domain (POGK), mRNA.
-0.812	-7.103	3.68E-07	5.99E-06	6.507	2850630	C19ORF48	NM_199250.1	Hs chromosome 19 open reading frame 48 (C19orf48), mRNA.
-0.812	-10.178	7.48E-10	5.69E-08	12.722	1230470	RHOU	NM_021205.4	Hs ras homolog gene family, member U (RHOU), mRNA.
-0.813	-9.312	3.79E-09	1.84E-07	11.100	2570112	ABLIM1	NM_006720.3	Hs actin binding LIM protein 1 (ABLIM1), tv: 4, mRNA.

Appendix 4 – Genes differentially expressed at 24 hours in cells treated with IGF1 ligand

-0.813	-8.178	3.66E-08	1.01E-06	8.826	6660161	RNF144A	NM_014746.3	Hs ring finger protein 144A (RNF144A), mRNA.
-0.814	-8.660	1.37E-08	4.85E-07	9.813	4810288	INTS5	NM_030628.1	Hs integrator complex subunit 5 (INTS5), mRNA.
-0.814	-6.209	2.81E-06	3.06E-05	4.466	70239	AGGF1	NM_018046.3	Hs angiogenic factor with G patch and FHA domains 1 (AGGF1), mRNA.
-0.814	-9.580	2.27E-09	1.23E-07	11.612	6280435	ZNF605	NM_183238.2	Hs zinc finger protein 605 (ZNF605), mRNA.
-0.815	-5.995	4.64E-06	4.57E-05	3.964	1440209	RGS10	NM_001005339.1	Hs regulator of G-protein signaling 10 (RGS10), tv: 1, mRNA.
-0.815	-9.510	2.59E-09	1.34E-07	11.479	4250167	SOX13	NM_005686.2	Hs SRY (sex determining region Y)-box 13 (SOX13), mRNA.
-0.815	-8.422	2.22E-08	6.88E-07	9.329	3290685	DPYSL2	NM_001386.4	Hs dihydropyrimidinase-like 2 (DPYSL2), mRNA.
-0.816	-8.768	1.10E-08	4.16E-07	10.031	4830433	LARP6	NM_018357.2	Hs La ribonucleoprotein domain family, member 6 (LARP6), tv: 1, mRNA.
-0.816	-9.712	1.77E-09	1.03E-07	11.860	7570341	LOC100133887	XM_001718657.1	PREDICTED: Hs hypothetical protein LOC100133887 (LOC100133887), partial mRNA.
-0.816	-6.836	6.68E-07	9.59E-06	5.908	2470367	INPPL1	NM_001567.2	Hs inositol polyphosphate phosphatase-like 1 (INPPL1), mRNA.
-0.817	-8.187	3.60E-08	9.97E-07	8.843	5690156	TTC31	NM_022492.3	Hs tetratricopeptide repeat domain 31 (TTC31), mRNA.
-0.818	-7.756	8.89E-08	1.97E-06	7.935	2970332	WEE1	NM_003390.2	Hs WEE1 homolog (S. pombe) (WEE1), mRNA.
-0.819	-9.745	1.67E-09	9.87E-08	11.921	4860468	ARL1	NM_001177.3	Hs ADP-ribosylation factor-like 1 (ARL1), mRNA.
-0.819	-9.315	3.77E-09	1.84E-07	11.104	6520139	FGFR3	NM_022965.1	Hs fibroblast growth factor receptor 3 (achondroplasia, thanatophoric dwarfism) (FGFR3), tv: 2, mRNA.
-0.819	-9.547	2.42E-09	1.28E-07	11.550	6250553	ITFG3	NM_032039.1	Hs integrin alpha FG-GAP repeat containing 3 (ITFG3), mRNA.
-0.819	-6.191	2.93E-06	3.16E-05	4.424	1690259	PAPSS2	NM_004670.3	Hs 3'-phosphoadenosine 5'-phosphosulfate synthase 2 (PAPSS2), tv: 1, mRNA.
-0.819	-9.360	3.46E-09	1.72E-07	11.191	770520	TAF4	NM_003185.3	Hs TAF4 RNA polymerase II, TATA box binding protein (TBP)-associated factor, 135kDa (TAF4), mRNA.
-0.820	-6.852	6.45E-07	9.34E-06	5.943	7040709	IGF2BP2	NM_006548.4	Hs insulin-like growth factor 2 mRNA binding protein 2 (IGF2BP2), tv: 1, mRNA.
-0.820	-7.356	2.11E-07	3.87E-06	7.067	10470	GTF2IP1	NR_002206.1	Hs general transcription factor II, i, pseudogene 1 (GTF2IP1) on chromosome 7.
-0.820	-5.816	7.09E-06	6.51E-05	3.539	5310309	ZNF252	NR_023392.1	Hs zinc finger protein 252 (ZNF252), non-coding RNA.
-0.821	-9.865	1.33E-09	8.38E-08	12.146	4180468	ZBED1	NM_004729.3	Hs zinc finger, BED-type containing 1 (ZBED1), mRNA.
-0.822	-7.165	3.21E-07	5.33E-06	6.646	870110	C15ORF39	NM_015492.4	Hs chromosome 15 open reading frame 39 (C15orf39), mRNA.
-0.822	-7.650	1.12E-07	2.36E-06	7.706	2350685	HEY2	NM_012259.1	Hs hairy/enhancer-of-split related with YRPW motif 2 (HEY2), mRNA.
-0.824	-6.926	5.46E-07	8.21E-06	6.110	3840288	LRFN3	NM_024509.1	Hs leucine rich repeat and fibronectin type III domain containing 3 (LRFN3), mRNA.
-0.825	-7.549	1.39E-07	2.82E-06	7.488	2850433	SPSB3	NM_080861.3	Hs splA/ryanodine receptor domain and SOCS box containing 3 (SPSB3), mRNA.
-0.825	-9.962	1.11E-09	7.33E-08	12.326	580465	VASH1	NM_014909.3	Hs vasohibin 1 (VASH1), mRNA.
-0.825	-8.342	2.61E-08	7.78E-07	9.166	1510685	DOK4	NM_018110.2	Hs docking protein 4 (DOK4), mRNA.
-0.825	-9.133	5.37E-09	2.43E-07	10.751	7000228	LOC400455	XR_018793.1	PREDICTED: Hs hypothetical LOC400455 (LOC400455), mRNA.
-0.826	-8.495	1.91E-08	6.17E-07	9.479	270678	DNAL4	NM_005740.2	Hs dynein, axonemal, light chain 4 (DNAL4), mRNA.
-0.826	-7.707	9.87E-08	2.14E-06	7.830	6100433	SOX18	NM_018419.2	Hs SRY (sex determining region Y)-box 18 (SOX18), mRNA.
-0.827	-12.047	3.03E-11	5.73E-09	15.907	5550554	BBS1	NM_024649.4	Hs Bardet-Biedl syndrome 1 (BBS1), mRNA.
-0.827	-11.019	1.69E-10	1.92E-08	14.204	6900278	FYCO1	NM_024513.1	Hs FYVE and coiled-coil domain containing 1 (FYCO1), mRNA.
-0.828	-7.011	4.51E-07	7.03E-06	6.302	2760706	C16ORF48	NM_032140.1	Hs chromosome 16 open reading frame 48 (C16orf48), mRNA.
-0.828	-7.390	1.96E-07	3.65E-06	7.141	6480095	SNX27	NM_030918.5	Hs sorting nexin family member 27 (SNX27), mRNA.
-0.828	-8.467	2.02E-08	6.45E-07	9.422	4200343	CYFIP1	NM_001033028.1	Hs cytoplasmic FMR1 interacting protein 1 (CYFIP1), tv: 2, mRNA.
-0.830	-7.077	3.89E-07	6.24E-06	6.451	4890689	CTHRC1	NM_138455.2	Hs collagen triple helix repeat containing 1 (CTHRC1), mRNA.
-0.830	-6.477	1.51E-06	1.88E-05	5.087	6450075	TFAP2C	NM_003222.3	Hs transcription factor AP-2 gamma (activating enhancer binding protein 2 gamma) (TFAP2C), mRNA.
-0.830	-8.073	4.56E-08	1.20E-06	8.605	4730152	DSTYK	NM_199462.2	Hs dual serine/threonine and tyrosine protein kinase (DSTYK), tv: 2, mRNA.
-0.831	-9.492	2.69E-09	1.39E-07	11.444	4760593	CD59	NM_000611.4	Hs CD59 molecule, complement regulatory protein (CD59), tv: 2, mRNA.
-0.831	-8.517	1.83E-08	5.97E-07	9.523	2490551	POU3F2	NM_005604.2	Hs POU class 3 homeobox 2 (POU3F2), mRNA.

Appendix 4 – Genes differentially expressed at 24 hours in cells treated with IGF1 ligand

-0.831	-10.748	2.70E-10	2.72E-08	13.737	1240441	FAM39DP	NR_003659.1	Hs family with sequence similarity 39, member D pseudogene (FAM39DP) on chromosome 15.
-0.832	-8.715	1.22E-08	4.45E-07	9.924	3520121	RPL28	NM_000991.3	Hs ribosomal protein L28 (RPL28), mRNA.
-0.833	-10.162	7.71E-10	5.78E-08	12.692	1780239	OLIG2	NM_005806.2	Hs oligodendrocyte lineage transcription factor 2 (OLIG2), mRNA.
-0.833	-12.297	2.03E-11	4.25E-09	16.303	6400243	ABLIM1	NM_001003407.1	Hs actin binding LIM protein 1 (ABLIM1), tv: 2, mRNA.
-0.834	-7.242	2.71E-07	4.67E-06	6.816	4290010	DPH5	NM_001077395.1	Hs DPH5 homolog (S. cerevisiae) (DPH5), tv: 3, mRNA.
-0.834	-8.815	1.00E-08	3.91E-07	10.124	2360437	ZNF532	NM_018181.4	Hs zinc finger protein 532 (ZNF532), mRNA.
-0.834	-8.803	1.03E-08	3.97E-07	10.099	3400612	WDFY1	NM_020830.3	Hs WD repeat and FYVE domain containing 1 (WDFY1), mRNA.
-0.834	-7.211	2.90E-07	4.92E-06	6.747	6200132	FZD9	NM_003508.2	Hs frizzled homolog 9 (Drosophila) (FZD9), mRNA.
-0.837	-9.811	1.47E-09	8.97E-08	12.046	650619	FAM125B	NM_033446.1	Hs family with sequence similarity 125, member B (FAM125B), tv: 1, mRNA.
-0.837	-6.752	8.07E-07	1.12E-05	5.718	2140392	ZNF580	NM_016202.2	Hs zinc finger protein 580 (ZNF580), tv: 1, mRNA.
-0.839	-6.249	2.56E-06	2.84E-05	4.560	1430176	OGT	NM_181672.1	Hs O-linked N-acetylglucosamine (GlcNAc) transferase (UDP-N-acetylglucosamine:polypeptide-N-acetylglu
-0.840	-8.484	1.95E-08	6.31E-07	9.455	2710324	HELZ	NM_014877.3	Hs helicase with zinc finger (HELZ), mRNA.
-0.842	-6.780	7.58E-07	1.06E-05	5.781	7050189	PRPF19	NM_014502.3	Hs PRP19/PSO4 pre-mRNA processing factor 19 homolog (S. cerevisiae) (PRPF19), mRNA.
-0.842	-8.256	3.12E-08	8.95E-07	8.987	150092	RBM33	NM_001008408.3	Hs RNA binding motif protein 33 (RBM33), tv: 1, mRNA.
-0.843	-9.532	2.49E-09	1.30E-07	11.521	2810390	SMO	NM_005631.3	Hs smoothened homolog (Drosophila) (SMO), mRNA.
-0.844	-8.302	2.83E-08	8.31E-07	9.082	7040037	CUEDC2	NM_024040.2	Hs CUE domain containing 2 (CUEDC2), mRNA.
-0.845	-6.041	4.16E-06	4.20E-05	4.073	6250114	LOC650737	XM_944786.1	PREDICTED: Hs hypothetical protein LOC650737, tv: 1 (LOC650737), mRNA.
-0.845	-9.489	2.70E-09	1.39E-07	11.440	1990292	NEURL4	NM_032442.2	Hs neuralized homolog 4 (Drosophila) (NEURL4), tv: 1, mRNA.
-0.846	-11.520	7.21E-11	1.01E-08	15.049	5560411	ZNF212	NM_012256.2	Hs zinc finger protein 212 (ZNF212), mRNA.
-0.846	-5.996	4.63E-06	4.57E-05	3.966	3120544	METRN	NM_024042.2	Hs meteorin, glial cell differentiation regulator (METRN), mRNA.
-0.846	-9.729	1.72E-09	1.00E-07	11.892	3710647	MXD4	NM_006454.2	Hs MAX dimerization protein 4 (MXD4), mRNA.
-0.848	-10.074	9.05E-10	6.50E-08	12.531	5560075	MFGE8	NM_005928.1	Hs milk fat globule-EGF factor 8 protein (MFGE8), mRNA.
-0.848	-5.796	7.42E-06	6.75E-05	3.492	20609	SLC29A2	NM_001532.2	Hs solute carrier family 29 (nucleoside transporters), member 2 (SLC29A2), mRNA.
-0.848	-7.273	2.53E-07	4.42E-06	6.885	1240661	KIAA0528	NM_014802.1	Hs KIAA0528 (KIAA0528), mRNA.
-0.848	-6.995	4.68E-07	7.25E-06	6.266	3440367	ACSL3	NM_004457.3	Hs acyl-CoA synthetase long-chain family member 3 (ACSL3), tv: 1, mRNA.
-0.849	-5.918	5.56E-06	5.32E-05	3.781	4150142	SUCLG1	NM_003849.2	Hs succinate-CoA ligase, alpha subunit (SUCLG1), mRNA.
-0.849	-6.297	2.29E-06	2.60E-05	4.671	870113	PTGES2	NM_198938.1	Hs prostaglandin E synthase 2 (PTGES2), tv: 2, mRNA.
-0.850	-10.056	9.36E-10	6.60E-08	12.498	4560292	LOC650034	XM_939124.1	PREDICTED: Hs similar to uncharacterized protein family UPF0227 member RGD1359682 (LOC650034),
-0.850	-7.614	1.20E-07	2.51E-06	7.629	3400397	EML3	NM_153265.2	Hs echinoderm microtubule associated protein like 3 (EML3), mRNA.
-0.851	-9.775	1.58E-09	9.50E-08	11.978	7610050	ABCC5	NM_001023587.1	Hs ATP-binding cassette, sub-family C (CFTR/MRP), member 5 (ABCC5), tv: 2, mRNA.
-0.852	-9.744	1.67E-09	9.87E-08	11.920	7320731	MAP3K4	NM_005922.2	Hs mitogen-activated protein kinase kinase kinase 4 (MAP3K4), tv: 1, mRNA.
-0.852	-8.939	7.85E-09	3.21E-07	10.370	6900450	QDPR	NM_000320.1	Hs quinoid dihydropteridine reductase (QDPR), mRNA.
-0.853	-7.865	7.06E-08	1.66E-06	8.166	1070435	GAS7	NM_201433.1	Hs growth arrest-specific 7 (GAS7), tv: c, mRNA.
-0.854	-11.768	4.78E-11	7.76E-09	15.457	2230528	MMS19L	NM_022362.2	Hs MMS19-like (MET18 homolog, S. cerevisiae) (MMS19L), mRNA.
-0.854	-7.319	2.28E-07	4.10E-06	6.987	1470184	CLSTN1	NM_001009566.1	Hs calsyntenin 1 (CLSTN1), tv: 1, mRNA.
-0.854	-6.289	2.33E-06	2.63E-05	4.653	3890747	LOC158345	XR_017130.1	PREDICTED: Hs similar to ribosomal protein L4 (LOC158345), mRNA.
-0.854	-7.322	2.27E-07	4.08E-06	6.992	4570707	TRAK1	NM_001042646.1	Hs trafficking protein, kinesin binding 1 (TRAK1), tv: 1, mRNA.
-0.855	-6.611	1.11E-06	1.46E-05	5.396	4250246	KCTD3	NM_016121.3	Hs potassium channel tetramerisation domain containing 3 (KCTD3), mRNA.
-0.857	-10.307	5.92E-10	4.76E-08	12.954	2230471	LOC100133756	XM_001718451.1	PREDICTED: Hs hypothetical protein LOC100133756 (LOC100133756), partial mRNA.
-0.857	-8.048	4.80E-08	1.24E-06	8.554	3520093	LTBP3	NM_021070.2	Hs latent transforming growth factor beta binding protein 3 (LTBP3), mRNA.

Appendix 4 – Genes differentially expressed at 24 hours in cells treated with IGF1 ligand

-0.859	-6.076	3.84E-06	3.93E-05	4.153	3460008	TMEM173	NM_198282.1	Hs transmembrane protein 173 (TMEM173), nuclear gene encoding mitochondrial protein, mRNA.
-0.859	-6.171	3.07E-06	3.29E-05	4.377	1740242	FVT1	NM_002035.1	Hs follicular lymphoma variant translocation 1 (FVT1), mRNA.
-0.860	-7.087	3.81E-07	6.15E-06	6.472	2630376	RNF135	NM_197939.1	Hs ring finger protein 135 (RNF135), tv: 2, mRNA.
-0.860	-6.875	6.11E-07	8.98E-06	5.997	5490307	LOC100133542	XM_001719794.1	PREDICTED: Hs hypothetical protein LOC100133542 (LOC100133542), partial mRNA.
-0.860	-8.471	2.00E-08	6.42E-07	9.430	6770242	MARCKSL1	NM_023009.4	Hs MARCKS-like 1 (MARCKSL1), mRNA.
-0.861	-11.399	8.83E-11	1.19E-08	14.848	2230129	CLUAP1	NM_024793.1	Hs clusterin associated protein 1 (CLUAP1), tv: 2, mRNA.
-0.861	-7.729	9.42E-08	2.06E-06	7.876	7210196	FARP1	NM_005766.2	Hs FERM, RhoGEF (ARHGEF) and pleckstrin domain protein 1 (chondrocyte-derived) (FARP1), tv: 1, mR
-0.862	-8.236	3.25E-08	9.18E-07	8.946	2750598	ANKRD46	NM_198401.2	Hs ankyrin repeat domain 46 (ANKRD46), mRNA.
-0.863	-9.266	4.15E-09	1.98E-07	11.010	6940402	CUTL1	NM_181552.1	Hs cut-like 1, CCAAT displacement protein (Drosophila) (CUTL1), tv: 1, mRNA.
-0.864	-10.010	1.02E-09	6.88E-08	12.414	5360424	RPS6KA2	NM_001006932.1	Hs ribosomal protein S6 kinase, 90kDa, polypeptide 2 (RPS6KA2), tv: 2, mRNA.
-0.864	-7.338	2.19E-07	3.97E-06	7.028	2900240	SOHLH2	NM_017826.1	Hs spermatogenesis and oogenesis specific basic helix-loop-helix 2 (SOHLH2), mRNA.
-0.864	-7.955	5.84E-08	1.43E-06	8.356	4590554	KCTD3	NM_016121.3	Hs potassium channel tetramerisation domain containing 3 (KCTD3), mRNA.
-0.864	-6.992	4.71E-07	7.27E-06	6.260	5670075	PAFAH1B1	NM_000430.2	Hs platelet-activating factor acetylhydrolase, isoform Ib, alpha subunit 45kDa (PAFAH1B1), mRNA.
-0.865	-6.676	9.59E-07	1.30E-05	5.545	730671	ACAD8	NM_014384.2	Hs acyl-Coenzyme A dehydrogenase family, member 8 (ACAD8), nuclear gene encoding mitochondrial prot
-0.866	-7.161	3.24E-07	5.37E-06	6.636	4730370	ABCA9	NM_080283.3	Hs ATP-binding cassette, sub-family A (ABC1), member 9 (ABCA9), mRNA.
-0.867	-11.883	3.96E-11	6.78E-09	15.643	4830253	BAT2L	NM_013318.3	Hs HLA-B associated transcript 2-like (BAT2L), mRNA.
-0.867	-9.077	5.99E-09	2.60E-07	10.642	2120450	HS.356079		Hs cDNA FLJ42149 fis, clone THYMU1000692
-0.867	-7.808	7.96E-08	1.80E-06	8.045	730458	LRP3	NM_002333.1	Hs low density lipoprotein receptor-related protein 3 (LRP3), mRNA.
-0.868	-6.658	1.00E-06	1.34E-05	5.503	650110	APP	NM_201414.1	Hs amyloid beta (A4) precursor protein (APP), tv: 3, mRNA.
-0.869	-10.030	9.81E-10	6.71E-08	12.451	1990446	KIAA0040	NM_014656.1	Hs KIAA0040 (KIAA0040), mRNA.
-0.869	-8.958	7.56E-09	3.11E-07	10.408	4060139	PLXNB3	NM_005393.1	Hs plexin B3 (PLXNB3), mRNA.
-0.869	-10.350	5.49E-10	4.52E-08	13.031	6110215	C12ORF76	NM_207435.1	Hs chromosome 12 open reading frame 76 (C12orf76), mRNA.
-0.870	-6.905	5.72E-07	8.48E-06	6.065	10008	RERE	NM_001042682.1	Hs arginine-glutamic acid dipeptide (RE) repeats (RERE), tv: 3, mRNA.
-0.871	-10.256	6.50E-10	5.08E-08	12.863	6220180	CABC1	NM_020247.4	Hs chaperone, ABC1 activity of bc1 complex homolog (S. pombe) (CABC1), nuclear gene encoding mitocho
-0.872	-7.090	3.79E-07	6.12E-06	6.478	2260020	SLC1A1	NM_004170.4	Hs solute carrier family 1 (neuronal/epithelial high affinity glutamate transporter, system Xag), member 1 (Sl
-0.872	-6.331	2.11E-06	2.44E-05	4.751	6840148	CREBBP	NM_001079846.1	Hs CREB binding protein (CREBBP), tv: 2, mRNA.
-0.872	-8.227	3.31E-08	9.32E-07	8.928	2450148	PARP4	NM_006437.3	Hs poly (ADP-ribose) polymerase family, member 4 (PARP4), mRNA.
-0.873	-6.464	1.56E-06	1.91E-05	5.058	1510202	RWDD1	NM_001007464.1	Hs RWD domain containing 1 (RWDD1), tv: 3, mRNA.
-0.873	-7.563	1.35E-07	2.76E-06	7.517	5390180	ASXL1	NM_015338.4	Hs additional sex combs like 1 (Drosophila) (ASXL1), mRNA.
-0.874	-6.585	1.18E-06	1.53E-05	5.338	4290615	ZBTB33	NM_006777.3	Hs zinc finger and BTB domain containing 33 (ZBTB33), mRNA.
-0.875	-11.625	6.05E-11	9.02E-09	15.223	3460278	C22ORF13	NM_031444.2	Hs chromosome 22 open reading frame 13 (C22orf13), mRNA.
-0.875	-7.958	5.80E-08	1.42E-06	8.363	4540682	PALM	NM_002579.2	Hs paralemmin (PALM), tv: 1, mRNA.
-0.876	-6.667	9.80E-07	1.32E-05	5.523	6900706	AKAP12	NM_144497.1	Hs A kinase (PRKA) anchor protein (gravin) 12 (AKAP12), tv: 2, mRNA.
-0.876	-7.565	1.34E-07	2.75E-06	7.523	7200706	LOXL3	NM_032603.2	Hs lysyl oxidase-like 3 (LOXL3), mRNA.
-0.876	-6.139	3.31E-06	3.50E-05	4.301	610148	GSDMD	NM_024736.5	Hs gasdermin D (GSDMD), mRNA.
-0.877	-13.983	1.58E-12	7.32E-10	18.809	4070671	SOX5	NM_152989.2	Hs SRY (sex determining region Y)-box 5 (SOX5), tv: 2, mRNA.
-0.878	-6.515	1.39E-06	1.75E-05	5.175	7650315	JMJD8	NM_001005920.2	Hs jumonji domain containing 8 (JMJD8), mRNA.
-0.878	-7.995	5.37E-08	1.35E-06	8.441	5900725	PHLDA1	NM_007350.3	Hs pleckstrin homology-like domain, family A, member 1 (PHLDA1), mRNA.
-0.879	-6.828	6.80E-07	9.70E-06	5.891	6760008	DBN1	NM_004395.2	Hs drebrin 1 (DBN1), tv: 1, mRNA.
-0.879	-8.546	1.72E-08	5.71E-07	9.582	4010021	FN3KRP	NM_024619.2	Hs fructosamine-3-kinase-related protein (FN3KRP), mRNA.

Appendix 4 – Genes differentially expressed at 24 hours in cells treated with IGF1 ligand

-0.879	-6.647	1.02E-06	1.36E-05	5.479	1260068	FST	NM_006350.2	Hs follistatin (FST), tv: FST317, mRNA.
-0.880	-6.077	3.82E-06	3.92E-05	4.157	1440630	CEP110	NM_007018.4	Hs centrosomal protein 110kDa (CEP110), mRNA.
-0.880	-7.801	8.08E-08	1.82E-06	8.031	3520066	FZD1	NM_003505.1	Hs frizzled homolog 1 (Drosophila) (FZD1), mRNA.
-0.880	-6.215	2.77E-06	3.03E-05	4.480	1240639	FLJ20254	NM_017727.3	Hs hypothetical protein FLJ20254 (FLJ20254), mRNA.
-0.881	-6.876	6.10E-07	8.97E-06	5.999	5820601	CCND1	NM_053056.2	Hs cyclin D1 (CCND1), mRNA.
-0.881	-7.003	4.60E-07	7.15E-06	6.283	2630189	PHF16	NM_001077445.1	Hs PHD finger protein 16 (PHF16), tv: 2, mRNA.
-0.881	-8.037	4.91E-08	1.26E-06	8.530	2690187	AFAP1	NM_198595.2	Hs actin filament associated protein 1 (AFAP1), tv: 2, mRNA.
-0.882	-8.527	1.79E-08	5.87E-07	9.543	2630601	HS.475334		Human mRNA for KIAA0280 gene, partial cds
-0.883	-7.633	1.16E-07	2.42E-06	7.670	2120161	C9ORF116	NM_144654.2	Hs chromosome 9 open reading frame 116 (C9orf116), tv: 2, mRNA.
-0.884	-8.540	1.74E-08	5.75E-07	9.569	6590575	SPRY2	NM_005842.2	Hs sprouty homolog 2 (Drosophila) (SPRY2), mRNA.
-0.884	-8.141	3.95E-08	1.07E-06	8.749	3290639	RAB7B	NM_177403.3	Hs RAB7B, member RAS oncogene family (RAB7B), mRNA.
-0.884	-8.270	3.03E-08	8.75E-07	9.016	1710189	RHBDF1	NM_022450.2	Hs rhomboid 5 homolog 1 (Drosophila) (RHBDF1), mRNA.
-0.884	-8.624	1.47E-08	5.07E-07	9.742	4060364	MGAT4B	NM_054013.2	Hs mannosyl (alpha-1,3-)-glycoprotein beta-1,4-N-acetylglucosaminyltransferase, isozyme B (MGAT4B), tv
-0.884	-7.929	6.16E-08	1.49E-06	8.302	3460066	ROBLD3	NM_014017.2	Hs roadblock domain containing 3 (ROBLD3), mRNA.
-0.885	-9.820	1.45E-09	8.86E-08	12.062	5870577	S100A13	NM_005979.2	Hs S100 calcium binding protein A13 (S100A13), tv: 2, mRNA.
-0.885	-8.804	1.03E-08	3.97E-07	10.102	4250711	GPR177	NM_024911.4	Hs G protein-coupled receptor 177 (GPR177), tv: 1, mRNA.
-0.886	-8.223	3.34E-08	9.39E-07	8.919	6960630	CD97	NM_078481.2	Hs CD97 molecule (CD97), tv: 1, mRNA.
-0.887	-11.787	4.63E-11	7.57E-09	15.488	7610754	GSPT2	NM_018094.2	Hs G1 to S phase transition 2 (GSPT2), mRNA.
-0.887	-8.137	3.98E-08	1.08E-06	8.740	2490411	ITGB5	NM_002213.3	Hs integrin, beta 5 (ITGB5), mRNA. XM_944688 XM_944693
-0.888	-11.533	7.06E-11	1.00E-08	15.070	830253	FOXR2	NM_198451.1	Hs forkhead box R2 (FOXR2), mRNA.
-0.888	-6.025	4.32E-06	4.32E-05	4.035	1110114	DIMT1L	NM_014473.2	Hs DIM1 dimethyladenosine transferase 1-like (S. cerevisiae) (DIMT1L), mRNA.
-0.888	-9.620	2.11E-09	1.16E-07	11.687	7650358	TGFBI	NM_000358.1	Hs transforming growth factor, beta-induced, 68kDa (TGFBI), mRNA.
-0.890	-11.541	6.96E-11	9.96E-09	15.084	5860707	SAAL1	NM_138421.2	Hs serum amyloid A-like 1 (SAAL1), mRNA.
-0.890	-10.332	5.67E-10	4.60E-08	12.998	2450246	OSBPL5	NM_145638.1	Hs oxysterol binding protein-like 5 (OSBPL5), tv: 2, mRNA.
-0.891	-9.860	1.35E-09	8.41E-08	12.136	770538	LYSMD2	NM_153374.1	Hs LysM, putative peptidoglycan-binding, domain containing 2 (LYSMD2), mRNA.
-0.891	-8.330	2.68E-08	7.96E-07	9.140	4810520	TRIB1	NM_025195.2	Hs tribbles homolog 1 (Drosophila) (TRIB1), mRNA.
-0.892	-6.376	1.91E-06	2.24E-05	4.855	2350315	DCTN1	NM_023019.1	Hs dynactin 1 (p150, glued homolog, Drosophila) (DCTN1), tv: 2, mRNA.
-0.892	-7.209	2.91E-07	4.93E-06	6.743	1780678	LOC374395	NM_199337.1	Hs similar to RIKEN cDNA 1810059G22 (LOC374395), mRNA.
-0.892	-9.898	1.25E-09	8.00E-08	12.207	2680070	EFNB3	NM_001406.3	Hs ephrin-B3 (EFNB3), mRNA.
-0.893	-9.429	3.03E-09	1.52E-07	11.323	70161	PKD2	NM_000297.2	Hs polycystic kidney disease 2 (autosomal dominant) (PKD2), mRNA.
-0.893	-7.525	1.46E-07	2.92E-06	7.436	7050626	PCNX	NM_014982.2	Hs pecanex homolog (Drosophila) (PCNX), mRNA.
-0.894	-7.840	7.44E-08	1.71E-06	8.114	650689	CLIP3	NM_015526.1	Hs CAP-GLY domain containing linker protein 3 (CLIP3), mRNA.
-0.894	-8.234	3.26E-08	9.22E-07	8.941	2630746	LAMB1	NM_002291.1	Hs laminin, beta 1 (LAMB1), mRNA.
-0.896	-5.762	8.04E-06	7.20E-05	3.412	5080164	GEMIN6	NM_024775.9	Hs gem (nuclear organelle) associated protein 6 (GEMIN6), mRNA.
-0.896	-7.418	1.84E-07	3.48E-06	7.203	1500047	RIN1	NM_004292.2	Hs Ras and Rab interactor 1 (RIN1), mRNA.
-0.898	-7.036	4.27E-07	6.75E-06	6.358	3420296	TGFA	NM_001099691.1	Hs transforming growth factor, alpha (TGFA), tv: 2, mRNA.
-0.898	-9.045	6.37E-09	2.71E-07	10.580	2710446	CRLS1	NM_019095.3	Hs cardiolipin synthase 1 (CRLS1), mRNA.
-0.898	-7.848	7.31E-08	1.70E-06	8.131	2370482	GSN	NM_198252.2	Hs gelsolin (amyloidosis, Finnish type) (GSN), tv: 2, mRNA.
-0.900	-7.380	2.00E-07	3.70E-06	7.119	940168	GTPBP8	NM_014170.2	Hs GTP-binding protein 8 (putative) (GTPBP8), tv: 1, mRNA.
-0.900	-10.628	3.34E-10	3.12E-08	13.526	6380553	SLC35B4	NM_032826.3	Hs solute carrier family 35, member B4 (SLC35B4), mRNA.

Appendix 4 – Genes differentially expressed at 24 hours in cells treated with IGF1 ligand

-0.901	-7.677	1.05E-07	2.25E-06	7.765	4050128	SULF2	NM_018837.2	Hs sulfatase 2 (SULF2), tv: 1, mRNA.
-0.903	-10.377	5.22E-10	4.41E-08	13.080	1710019	ICA1	NM_004968.2	Hs islet cell autoantigen 1, 69kDa (ICA1), tv: 2, mRNA.
-0.903	-9.063	6.15E-09	2.66E-07	10.614	5910431	COL4A1	NM_001845.4	Hs collagen, type IV, alpha 1 (COL4A1), mRNA.
-0.903	-10.016	1.01E-09	6.83E-08	12.425	650681	CTDSP2	NM_005730.3	Hs CTD (carboxy-terminal domain, RNA polymerase II, polypeptide A) small phosphatase 2 (CTDSP2), mR
-0.903	-10.157	7.78E-10	5.82E-08	12.682	6290292	POMT2	NM_013382.3	Hs protein-O-mannosyltransferase 2 (POMT2), mRNA.
-0.904	-10.048	9.50E-10	6.61E-08	12.483	270114	FAM134B	NM_001034850.1	Hs family with sequence similarity 134, member B (FAM134B), tv: 1, mRNA.
-0.905	-7.354	2.11E-07	3.87E-06	7.064	6760661	CAPN5	NM_004055.4	Hs calpain 5 (CAPN5), mRNA.
-0.905	-7.760	8.82E-08	1.96E-06	7.942	2360671	ANKLE2	NM_015114.1	Hs ankyrin repeat and LEM domain containing 2 (ANKLE2), mRNA.
-0.906	-6.549	1.28E-06	1.64E-05	5.255	3890255	TOP2B	NM_001068.2	Hs topoisomerase (DNA) II beta 180kDa (TOP2B), mRNA.
-0.907	-12.155	2.55E-11	5.04E-09	16.079	3390373	TIMM22	NM_013337.2	Hs translocase of inner mitochondrial membrane 22 homolog (yeast) (TIMM22), nuclear gene encoding mito
-0.908	-9.336	3.62E-09	1.77E-07	11.146	5220482	CA11	NM_001217.3	Hs carbonic anhydrase XI (CA11), mRNA.
-0.909	-8.498	1.90E-08	6.15E-07	9.484	1260615	SETD2	NM_014159.4	Hs SET domain containing 2 (SETD2), mRNA.
-0.911	-7.604	1.23E-07	2.55E-06	7.607	1340193	DHX30	NM_138615.1	Hs DEAH (Asp-Glu-Ala-His) box polypeptide 30 (DHX30), tv: 1, mRNA.
-0.913	-10.995	1.76E-10	1.97E-08	14.164	2190020	GNG2	NM_053064.3	Hs guanine nucleotide binding protein (G protein), gamma 2 (GNG2), mRNA.
-0.914	-8.550	1.71E-08	5.69E-07	9.590	7560047	CIRBP	NM_001280.1	Hs cold inducible RNA binding protein (CIRBP), mRNA.
-0.915	-6.495	1.45E-06	1.81E-05	5.129	2320672	LOC728820	XR_038223.1	PREDICTED: Hs misc_RNA (LOC728820), miscRNA.
-0.915	-10.778	2.56E-10	2.63E-08	13.789	4490133	SFRS2B	NM_032102.2	Hs splicing factor, arginine/serine-rich 2B (SFRS2B), mRNA.
-0.915	-5.814	7.11E-06	6.53E-05	3.535	7000274	LOC644039	XM_929431.1	PREDICTED: Hs similar to 60S ribosomal protein L10 (QM protein) (Tumor suppressor QM) (Laminin rece
-0.915	-10.924	1.99E-10	2.17E-08	14.042	430333	NLRX1	NM_170722.1	Hs NLR family member X1 (NLRX1), tv: 2, mRNA.
-0.916	-8.713	1.23E-08	4.46E-07	9.921	2320093	PIGY	NM_001042616.1	Hs phosphatidylinositol glycan anchor biosynthesis, class Y (PIGY), tv: 2, mRNA.
-0.916	-6.329	2.12E-06	2.45E-05	4.747	4490528	CKAP4	NM_006825.2	Hs cytoskeleton-associated protein 4 (CKAP4), mRNA.
-0.916	-6.292	2.32E-06	2.62E-05	4.660	1300110	GPR153	NM_207370.1	Hs G protein-coupled receptor 153 (GPR153), mRNA.
-0.916	-9.607	2.16E-09	1.18E-07	11.664	4180500	TP53	NM_000546.3	Hs tumor protein p53 (TP53), mRNA.
-0.920	-7.930	6.15E-08	1.49E-06	8.304	50274	MRFAP1L1	NM_203462.1	Hs Morf4 family associated protein 1-like 1 (MRFAP1L1), tv: 2, mRNA.
-0.920	-8.172	3.71E-08	1.02E-06	8.813	5090739	NPAL3	NM_020448.3	Hs NIPA-like domain containing 3 (NPAL3), mRNA.
-0.920	-6.027	4.31E-06	4.31E-05	4.038	4730541	SLC44A1	NM_080546.3	Hs solute carrier family 44, member 1 (SLC44A1), mRNA.
-0.920	-6.962	5.03E-07	7.66E-06	6.193	620066	MGAT4B	NM_014275.3	Hs mannosyl (alpha-1,3-)-glycoprotein beta-1,4-N-acetylglucosaminyltransferase, isozyme B (MGAT4B), tv
-0.920	-8.412	2.26E-08	6.99E-07	9.308	6270037	RAPGEF1	NM_198679.1	Hs Rap guanine nucleotide exchange factor (GEF) 1 (RAPGEF1), tv: 2, mRNA.
-0.920	-6.218	2.75E-06	3.01E-05	4.487	3400215	B3GNT1	NM_006876.2	Hs UDP-GlcNAc:betaGal beta-1,3-N-acetylglucosaminyltransferase 1 (B3GNT1), mRNA.
-0.920	-12.005	3.25E-11	5.86E-09	15.840	3710035	PDZD2	NM_178140.2	Hs PDZ domain containing 2 (PDZD2), mRNA.
-0.920	-7.430	1.79E-07	3.42E-06	7.229	4180204	NCOR2	NM_001077261.1	Hs nuclear receptor co-repressor 2 (NCOR2), tv: 2, mRNA.
-0.921	-9.124	5.46E-09	2.44E-07	10.734	150309	SLC24A3	NM_020689.3	Hs solute carrier family 24 (sodium/potassium/calcium exchanger), member 3 (SLC24A3), mRNA.
-0.922	-9.485	2.72E-09	1.40E-07	11.431	6660131	TSPAN13	NM_014399.3	Hs tetraspanin 13 (TSPAN13), mRNA.
-0.922	-7.169	3.18E-07	5.29E-06	6.654	1110228	TMEM136	NM_174926.1	Hs transmembrane protein 136 (TMEM136), mRNA.
-0.922	-8.599	1.55E-08	5.28E-07	9.690	2120634	CMTM4	NM_181521.2	Hs CKLF-like MARVEL transmembrane domain containing 4 (CMTM4), tv: 2, mRNA.
-0.923	-8.052	4.76E-08	1.23E-06	8.562	510180	FOXD2	NM_004474.3	Hs forkhead box D2 (FOXD2), mRNA.
-0.925	-9.171	4.98E-09	2.31E-07	10.826	7320139	SOX8	NM_014587.2	Hs SRY (sex determining region Y)-box 8 (SOX8), mRNA.
-0.926	-7.742	9.16E-08	2.02E-06	7.904	50450	TMEM179B	NM_199337.2	Hs transmembrane protein 179B (TMEM179B), mRNA.
-0.926	-7.800	8.10E-08	1.82E-06	8.028	5360243	ITGB5	NM_002213.3	Hs integrin, beta 5 (ITGB5), mRNA. XM_944688 XM_944693
-0.926	-10.399	5.02E-10	4.25E-08	13.119	3360504	EEF1A1	NM_001402.5	Hs eukaryotic translation elongation factor 1 alpha 1 (EEF1A1), mRNA.

Appendix 4 – Genes differentially expressed at 24 hours in cells treated with IGF1 ligand

-0.927	-10.834	2.33E-10	2.46E-08	13.886	1500192	HIST3H2A	NM_033445.2	Hs histone cluster 3, H2a (HIST3H2A), mRNA.
-0.927	-6.577	1.20E-06	1.55E-05	5.319	3120600	ADCY6	NM_020983.2	Hs adenylate cyclase 6 (ADCY6), tv: 2, mRNA.
-0.929	-5.996	4.62E-06	4.57E-05	3.966	780324	ZNF337	NM_015655.2	Hs zinc finger protein 337 (ZNF337), mRNA.
-0.930	-9.046	6.36E-09	2.71E-07	10.582	380369	TRRAP	NM_003496.1	Hs transformation/transcription domain-associated protein (TRRAP), mRNA.
-0.931	-7.788	8.30E-08	1.86E-06	8.003	520278	FAM100B	NM_182565.2	Hs family with sequence similarity 100, member B (FAM100B), mRNA.
-0.933	-10.062	9.25E-10	6.56E-08	12.510	5130093	PHLDB1	NM_015157.1	Hs pleckstrin homology-like domain, family B, member 1 (PHLDB1), mRNA.
-0.933	-6.733	8.42E-07	1.16E-05	5.675	7380367	C9ORF69	NM_152833.2	Hs chromosome 9 open reading frame 69 (C9orf69), mRNA.
-0.933	-9.033	6.53E-09	2.76E-07	10.555	7550722	ZMYM6	NM_007167.2	Hs zinc finger, MYM-type 6 (ZMYM6), mRNA.
-0.933	-7.174	3.14E-07	5.25E-06	6.665	520332	B4GALT7	NM_007255.1	Hs xylosylprotein beta 1,4-galactosyltransferase, polypeptide 7 (galactosyltransferase I) (B4GALT7), mRNA
-0.933	-7.831	7.57E-08	1.74E-06	8.095	130309	CDKN1B	NM_004064.2	Hs cyclin-dependent kinase inhibitor 1B (p27, Kip1) (CDKN1B), mRNA.
-0.934	-8.017	5.12E-08	1.29E-06	8.489	6370039	RAVER2	NM_018211.2	Hs ribonucleoprotein, PTB-binding 2 (RAVER2), mRNA.
-0.935	-8.564	1.66E-08	5.57E-07	9.619	430609	NCRNA00094	NR_015427.1	Hs non-protein coding RNA 94 (NCRNA00094), non-coding RNA.
-0.937	-10.128	8.21E-10	6.05E-08	12.629	5960451	WDR70	NM_018034.2	Hs WD repeat domain 70 (WDR70), mRNA.
-0.940	-7.314	2.31E-07	4.14E-06	6.974	1940273	SGSM2	NM_014853.2	Hs small G protein signaling modulator 2 (SGSM2), tv: 1, mRNA.
-0.940	-5.794	7.46E-06	6.77E-05	3.488	4260022	PSMG2	NM_020232.3	Hs proteasome (prosome, macropain) assembly chaperone 2 (PSMG2), mRNA.
-0.940	-11.025	1.67E-10	1.92E-08	14.215	6110167	NPAS2	NM_002518.3	Hs neuronal PAS domain protein 2 (NPAS2), mRNA.
-0.941	-7.479	1.61E-07	3.14E-06	7.336	6560576	OCRL	NM_001587.3	Hs oculocerebrorenal syndrome of Lowe (OCRL), tv: b, mRNA.
-0.941	-7.252	2.65E-07	4.59E-06	6.838	6060767	AASDHPPT	NM_015423.2	Hs aminoadipate-semialdehyde dehydrogenase-phosphopantetheinyl transferase (AASDHPPT), mRNA.
-0.941	-5.806	7.25E-06	6.62E-05	3.516	7040220	RDH14	NM_020905.2	Hs retinol dehydrogenase 14 (all-trans/9-cis/11-cis) (RDH14), mRNA.
-0.941	-10.289	6.13E-10	4.87E-08	12.921	1940326	CSRNP2	NM_030809.1	Hs cysteine-serine-rich nuclear protein 2 (CSRNP2), mRNA.
-0.942	-9.736	1.69E-09	9.95E-08	11.905	580403	DFNA5	NM_004403.2	Hs deafness, autosomal dominant 5 (DFNA5), tv: 1, mRNA.
-0.942	-8.465	2.03E-08	6.46E-07	9.418	7400546	PPP3CB	NM_021132.1	Hs protein phosphatase 3 (formerly 2B), catalytic subunit, beta isoform (PPP3CB), mRNA.
-0.943	-7.528	1.45E-07	2.90E-06	7.443	6280411	ARID1A	NM_139135.2	Hs AT rich interactive domain 1A (SWI-like) (ARID1A), tv: 2, mRNA.
-0.944	-7.605	1.23E-07	2.55E-06	7.610	7160253	LAMA4	NM_002290.2	Hs laminin, alpha 4 (LAMA4), mRNA.
-0.944	-7.337	2.19E-07	3.98E-06	7.026	6520035	LOC402112	XR_019262.2	PREDICTED: Hs misc_RNA (LOC402112), miscRNA.
-0.946	-12.463	1.56E-11	3.57E-09	16.563	3360112	TMEM2	NM_013390.1	Hs transmembrane protein 2 (TMEM2), mRNA.
-0.947	-10.882	2.14E-10	2.29E-08	13.969	3360646	MVP	NM_005115.3	Hs major vault protein (MVP), tv: 2, mRNA.
-0.948	-10.063	9.24E-10	6.56E-08	12.511	1260451	VWA5A	NM_198315.2	Hs von Willebrand factor A domain containing 5A (VWA5A), tv: 2, mRNA.
-0.950	-8.718	1.22E-08	4.44E-07	9.930	1030278	C10ORF33	NM_032709.1	Hs chromosome 10 open reading frame 33 (C10orf33), mRNA.
-0.952	-7.414	1.86E-07	3.51E-06	7.193	520324	REEP5	NM_005669.4	Hs receptor accessory protein 5 (REEP5), mRNA.
-0.953	-8.115	4.18E-08	1.11E-06	8.693	670639	LONP2	NM_031490.2	Hs lon peptidase 2, peroxisomal (LONP2), mRNA.
-0.953	-10.259	6.46E-10	5.07E-08	12.868	1660300	PRCP	NM_199418.2	Hs prolylcarboxypeptidase (angiotensinase C) (PRCP), tv: 2, mRNA.
-0.953	-7.665	1.08E-07	2.29E-06	7.739	4760328	FASTK	NM_033015.2	Hs Fas-activated serine/threonine kinase (FASTK), tv: 4, mRNA.
-0.954	-7.283	2.47E-07	4.35E-06	6.907	6110154	RNF187	XM_928029.2	PREDICTED: Hs ring finger protein 187 (RNF187), mRNA.
-0.956	-7.408	1.88E-07	3.54E-06	7.182	7380026	FAM39E	NM_182905.2	Hs family with sequence similarity 39, member E (FAM39E), mRNA.
-0.957	-5.550	1.34E-05	0.000109326	2.905	4200601	TMEM48	NM_018087.3	Hs transmembrane protein 48 (TMEM48), mRNA.
-0.957	-9.616	2.12E-09	1.16E-07	11.679	1430487	MGP	NM_000900.2	Hs matrix Gla protein (MGP), mRNA.
-0.957	-6.472	1.53E-06	1.89E-05	5.076	4010411	RHOT1	NM_001033566.1	Hs ras homolog gene family, member T1 (RHOT1), tv: 2, mRNA.
-0.960	-9.620	2.11E-09	1.16E-07	11.688	6660259	RBBP9	NM_006606.2	Hs retinoblastoma binding protein 9 (RBBP9), mRNA.
-0.960	-12.648	1.17E-11	3.14E-09	16.848	5490070	TGFBR2	NM_001024847.1	Hs transforming growth factor, beta receptor II (70/80kDa) (TGFBR2), tv: 1, mRNA.

Appendix 4 – Genes differentially expressed at 24 hours in cells treated with IGF1 ligand

-0.960	-12.587	1.28E-11	3.18E-09	16.754	6380040	COL9A2	NM_001852.3	Hs collagen, type IX, alpha 2 (COL9A2), mRNA.
-0.961	-7.376	2.02E-07	3.73E-06	7.112	6650324	PLEKHA1	NM_001001974.1	Hs pleckstrin homology domain containing, family A (phosphoinositide binding specific) member 1 (PLEKH
-0.964	-6.910	5.66E-07	8.42E-06	6.075	2810044	MGC72104	NM_207350.1	Hs similar to FRG1 protein (FSHD region gene 1 protein) (MGC72104), mRNA.
-0.964	-10.251	6.56E-10	5.12E-08	12.853	4570524	ICK	NM_016513.3	Hs intestinal cell (MAK-like) kinase (ICK), tv: 2, mRNA.
-0.967	-8.061	4.67E-08	1.21E-06	8.581	6620711	AFAP1L2	NM_032550.2	Hs actin filament associated protein 1-like 2 (AFAP1L2), tv: 2, mRNA.
-0.969	-6.865	6.26E-07	9.12E-06	5.974	5490202	LOC646688	XR_037673.1	PREDICTED: Hs misc_RNA (LOC646688), miscRNA.
-0.969	-8.604	1.53E-08	5.25E-07	9.699	1340538	SGSH	NM_000199.2	Hs N-sulfoglucosamine sulfohydrolase (sulfamidase) (SGSH), mRNA.
-0.970	-9.552	2.39E-09	1.27E-07	11.559	3130220	TMEM158	NM_015444.2	Hs transmembrane protein 158 (TMEM158), mRNA.
-0.970	-6.251	2.55E-06	2.84E-05	4.564	6510025	NSMCE4A	NM_017615.1	Hs non-SMC element 4 homolog A (S. cerevisiae) (NSMCE4A), mRNA.
-0.971	-6.194	2.91E-06	3.15E-05	4.430	3940050	FLJ46906	XM_928441.1	PREDICTED: Hs hypothetical gene supported by AK128874; BC071813 (FLJ46906), mRNA.
-0.972	-7.084	3.83E-07	6.17E-06	6.466	6980220	LOC644322	XM_933391.1	PREDICTED: Hs similar to Ribosome biogenesis protein BMS1 homolog, tv: 2 (LOC644322), mRNA.
-0.974	-10.204	7.14E-10	5.49E-08	12.769	7040270	ZNF362	NM_152493.2	Hs zinc finger protein 362 (ZNF362), mRNA.
-0.975	-9.631	2.06E-09	1.15E-07	11.708	2140139	BRWD2	NM_018117.10	Hs bromodomain and WD repeat domain containing 2 (BRWD2), mRNA.
-0.975	-9.951	1.14E-09	7.44E-08	12.305	3370730	CDC42EP5	NM_145057.2	Hs CDC42 effector protein (Rho GTPase binding) 5 (CDC42EP5), mRNA.
-0.975	-6.437	1.66E-06	2.01E-05	4.995	4780129	CENPF	NM_016343.3	Hs centromere protein F, 350/400ka (mitosin) (CENPF), mRNA.
-0.976	-10.098	8.66E-10	6.32E-08	12.576	2760452	RPS29	NM_001030001.1	Hs ribosomal protein S29 (RPS29), tv: 2, mRNA.
-0.977	-9.079	5.95E-09	2.60E-07	10.647	1500524	PHC2	NM_004427.3	Hs polyhomeotic homolog 2 (Drosophila) (PHC2), tv: 2, mRNA.
-0.977	-6.196	2.90E-06	3.13E-05	4.436	770221	C20ORF177	NM_022106.1	Hs chromosome 20 open reading frame 177 (C20orf177), mRNA.
-0.979	-9.152	5.16E-09	2.37E-07	10.790	4640131	PQLC1	NM_025078.3	Hs PQ loop repeat containing 1 (PQLC1), mRNA.
-0.981	-9.833	1.41E-09	8.69E-08	12.086	5890538	FEM1A	NM_018708.2	Hs fem-1 homolog a (C. elegans) (FEM1A), mRNA.
-0.981	-7.712	9.77E-08	2.13E-06	7.840	4060176	KIF11	NM_004523.2	Hs kinesin family member 11 (KIF11), mRNA.
-0.982	-7.386	1.97E-07	3.67E-06	7.133	6590132	IGFBP3	NM_000598.4	Hs insulin-like growth factor binding protein 3 (IGFBP3), tv: 2, mRNA.
-0.988	-6.833	6.72E-07	9.63E-06	5.902	2650474	CAPS	NM_004058.2	Hs calcyphosine (CAPS), tv: 1, mRNA.
-0.988	-7.990	5.42E-08	1.36E-06	8.431	7040315	STX16	NM_001001433.1	Hs syntaxin 16 (STX16), tv: 1, mRNA.
-0.990	-7.412	1.86E-07	3.52E-06	7.191	2690292	NCOA5	NM_020967.2	Hs nuclear receptor coactivator 5 (NCOA5), mRNA.
-0.992	-7.843	7.39E-08	1.71E-06	8.120	6270382	DYRK4	NM_003845.1	Hs dual-specificity tyrosine-(Y)-phosphorylation regulated kinase 4 (DYRK4), mRNA.
-0.992	-7.483	1.60E-07	3.12E-06	7.345	830201	TSKU	NM_015516.3	Hs tsukushin (TSKU), mRNA.
-0.992	-7.082	3.85E-07	6.19E-06	6.462	4010041	MPI	NM_002435.1	Hs mannose phosphate isomerase (MPI), mRNA.
-0.992	-5.599	1.19E-05	9.95E-05	3.022	5490301	PABPC1L	XM_001722078.1	PREDICTED: Hs poly(A) binding protein, cytoplasmic 1-like (PABPC1L), mRNA.
-0.993	-8.004	5.26E-08	1.32E-06	8.462	4570736	GTF2I	NM_033001.1	Hs general transcription factor II, i (GTF2I), tv: 3, mRNA.
-0.994	-9.933	1.17E-09	7.63E-08	12.271	6330504	SERTAD4	NM_019605.2	Hs SERTA domain containing 4 (SERTAD4), mRNA.
-0.994	-8.204	3.47E-08	9.68E-07	8.880	6040600	TMEM98	NM_015544.2	Hs transmembrane protein 98 (TMEM98), tv: 1, mRNA.
-0.994	-8.430	2.18E-08	6.82E-07	9.346	3310692	SPRY1	NM_199327.1	Hs sprouty homolog 1, antagonist of FGF signaling (Drosophila) (SPRY1), tv: 2, mRNA.
-0.994	-10.826	2.36E-10	2.48E-08	13.872	450088	SOX10	NM_006941.3	Hs SRY (sex determining region Y)-box 10 (SOX10), mRNA.
-0.995	-7.636	1.15E-07	2.41E-06	7.676	2900551	NVL	NM_206840.1	Hs nuclear VCP-like (NVL), tv: 2, mRNA.
-0.995	-13.234	4.77E-12	1.70E-09	17.729	6510400	CPN1	NM_001308.2	Hs carboxypeptidase N, polypeptide 1 (CPN1), mRNA.
-0.996	-10.687	3.01E-10	2.88E-08	13.629	3990220	LOC100128675	NR_024562.1	Hs hypothetical LOC100128675 (LOC100128675), tv: 2, non-coding RNA.
-0.996	-6.749	8.13E-07	1.13E-05	5.711	1820048	TMEM214	NM_017727.4	Hs transmembrane protein 214 (TMEM214), tv: 1, mRNA.
-1.001	-10.892	2.10E-10	2.26E-08	13.986	5260288	DUSP6	NM_022652.2	Hs dual specificity phosphatase 6 (DUSP6), tv: 2, mRNA.
-1.001	-6.275	2.41E-06	2.70E-05	4.620	6110487	PACSIN3	NM_016223.3	Hs protein kinase C and casein kinase substrate in neurons 3 (PACSIN3), mRNA.

Appendix 4 – Genes differentially expressed at 24 hours in cells treated with IGF1 ligand

-1.002	-7.531	1.44E-07	2.89E-06	7.449	3390411	TFAP2C	NM_003222.3	Hs transcription factor AP-2 gamma (activating enhancer binding protein 2 gamma) (TFAP2C), mRNA.
-1.005	-7.832	7.57E-08	1.74E-06	8.096	1410021	AIF1L	NM_031426.2	Hs allograft inflammatory factor 1-like (AIF1L), tv: 1, mRNA.
-1.005	-8.553	1.70E-08	5.67E-07	9.597	1440575	OSBPL7	NM_145798.2	Hs oxysterol binding protein-like 7 (OSBPL7), tv: 1, mRNA.
-1.006	-7.313	2.31E-07	4.14E-06	6.973	2480576	RHOT1	NM_001033566.1	Hs ras homolog gene family, member T1 (RHOT1), tv: 2, mRNA.
-1.008	-9.462	2.84E-09	1.44E-07	11.387	3890551	CMTM3	NM_144601.2	Hs CKLF-like MARVEL transmembrane domain containing 3 (CMTM3), tv: 1, mRNA.
-1.012	-7.151	3.30E-07	5.45E-06	6.616	3440201	TTC5	NM_138376.1	Hs tetratricopeptide repeat domain 5 (TTC5), mRNA.
-1.012	-6.020	4.38E-06	4.36E-05	4.021	3990674	SSFA2	NM_006751.4	Hs sperm specific antigen 2 (SSFA2), mRNA.
-1.013	-6.297	2.29E-06	2.60E-05	4.670	4010414	PPFIBP1	NM_003622.2	Hs PTPRF interacting protein, binding protein 1 (liprin beta 1) (PPFIBP1), tv: 1, mRNA.
-1.013	-10.703	2.92E-10	2.84E-08	13.658	150041	MANSC1	NM_018050.2	Hs MANSC domain containing 1 (MANSC1), mRNA.
-1.013	-11.759	4.85E-11	7.82E-09	15.442	6400639	MGC18216	XM_927732.1	PREDICTED: Hs hypothetical protein MGC18216 (MGC18216), mRNA.
-1.014	-8.473	2.00E-08	6.42E-07	9.433	3180661	FAM134B	NM_001034850.1	Hs family with sequence similarity 134, member B (FAM134B), tv: 1, mRNA.
-1.014	-8.635	1.44E-08	5.02E-07	9.763	130368	PRKAR1A	NM_212472.1	Hs protein kinase, cAMP-dependent, regulatory, type I, alpha (tissue specific extinguisher 1) (PRKAR1A), tv
-1.015	-11.065	1.56E-10	1.83E-08	14.284	4280524	LEPREL1	NM_018192.2	Hs leprecan-like 1 (LEPREL1), mRNA.
-1.015	-10.091	8.77E-10	6.36E-08	12.563	4480504	ZNF828	NM_032436.1	Hs zinc finger protein 828 (ZNF828), mRNA.
-1.016	-11.955	3.52E-11	6.23E-09	15.759	2190689	OSBPL5	NM_020896.2	Hs oxysterol binding protein-like 5 (OSBPL5), tv: 1, mRNA.
-1.019	-8.608	1.52E-08	5.23E-07	9.707	4760754	LOC100132528	XR_038720.1	PREDICTED: Hs misc_RNA (LOC100132528), miscRNA.
-1.020	-12.015	3.19E-11	5.86E-09	15.856	3450753	RXRG	NM_006917.3	Hs retinoid X receptor, gamma (RXRG), tv: 1, mRNA.
-1.021	-7.635	1.15E-07	2.42E-06	7.674	4040332	DUS1L	NM_022156.3	Hs dihydrouridine synthase 1-like (S. cerevisiae) (DUS1L), mRNA.
-1.023	-6.740	8.30E-07	1.15E-05	5.690	3310291	POU3F2	NM_005604.2	Hs POU class 3 homeobox 2 (POU3F2), mRNA.
-1.024	-7.066	3.99E-07	6.37E-06	6.425	5090014	CCDC90B	NM_021825.3	Hs coiled-coil domain containing 90B (CCDC90B), mRNA.
-1.025	-7.350	2.13E-07	3.89E-06	7.055	2760079	FOXC1	NM_001453.1	Hs forkhead box C1 (FOXC1), mRNA.
-1.028	-8.575	1.63E-08	5.47E-07	9.640	610324	DDX1	NM_004939.1	Hs DEAD (Asp-Glu-Ala-Asp) box polypeptide 1 (DDX1), mRNA.
-1.029	-6.614	1.11E-06	1.46E-05	5.402	240400	PMEPA1	NM_199169.1	Hs prostate transmembrane protein, androgen induced 1 (PMEPA1), tv: 2, mRNA.
-1.031	-7.697	1.01E-07	2.18E-06	7.807	7610097	SETMAR	NM_006515.1	Hs SET domain and mariner transposase fusion gene (SETMAR), mRNA.
-1.032	-8.995	7.03E-09	2.94E-07	10.481	5810142	CITED4	NM_133467.2	Hs Cbp/p300-interacting transactivator, with Glu/Asp-rich carboxy-terminal domain, 4 (CITED4), mRNA.
-1.032	-9.161	5.07E-09	2.33E-07	10.808	3830092	RGS10	NM_001005339.1	Hs regulator of G-protein signaling 10 (RGS10), tv: 1, mRNA.
-1.032	-8.778	1.08E-08	4.14E-07	10.049	4210703	RPL15	NM_002948.2	Hs ribosomal protein L15 (RPL15), mRNA.
-1.033	-11.179	1.28E-10	1.58E-08	14.479	5420592	SRC	NM_198291.1	Hs v-src sarcoma (Schmidt-Ruppin A-2) viral oncogene homolog (avian) (SRC), tv: 2, mRNA.
-1.034	-8.045	4.83E-08	1.25E-06	8.547	1470685	ITGB3	NM_000212.2	Hs integrin, beta 3 (platelet glycoprotein IIIa, antigen CD61) (ITGB3), mRNA.
-1.034	-16.061	9.39E-14	8.89E-11	21.543	70753	C9ORF123	NM_033428.1	Hs chromosome 9 open reading frame 123 (C9orf123), mRNA.
-1.034	-5.695	9.43E-06	8.22E-05	3.252	2070291	PGM1	NM_002633.2	Hs phosphoglucomutase 1 (PGM1), mRNA.
-1.035	-7.536	1.43E-07	2.87E-06	7.459	5700707	SPRED1	NM_152594.1	Hs sprouty-related, EVH1 domain containing 1 (SPRED1), mRNA.
-1.040	-8.131	4.03E-08	1.09E-06	8.728	1570520	DHX16	NM_003587.3	Hs DEAH (Asp-Glu-Ala-His) box polypeptide 16 (DHX16), mRNA.
-1.041	-7.523	1.47E-07	2.93E-06	7.431	1780647	ADCK2	NM_052853.3	Hs aarF domain containing kinase 2 (ADCK2), mRNA.
-1.042	-9.725	1.73E-09	1.01E-07	11.885	4290605	SLC44A1	NM_080546.3	Hs solute carrier family 44, member 1 (SLC44A1), mRNA.
-1.044	-6.562	1.24E-06	1.59E-05	5.284	1110551	F8A1	NM_012151.3	Hs coagulation factor VIII-associated (intronic transcript) 1 (F8A1), mRNA.
-1.044	-9.978	1.08E-09	7.21E-08	12.354	7570500	COQ5	NM_032314.3	Hs coenzyme Q5 homolog, methyltransferase (S. cerevisiae) (COQ5), mRNA.
-1.044	-9.198	4.73E-09	2.21E-07	10.878	7050064	RAMP1	NM_005855.2	Hs receptor (G protein-coupled) activity modifying protein 1 (RAMP1), mRNA.
-1.045	-8.353	2.55E-08	7.65E-07	9.188	2940301	HPS6	NM_024747.4	Hs Hermansky-Pudlak syndrome 6 (HPS6), mRNA.
-1.045	-6.353	2.01E-06	2.34E-05	4.802	7000377	PHIP	NM_017934.4	Hs pleckstrin homology domain interacting protein (PHIP), mRNA.

Appendix 4 – Genes differentially expressed at 24 hours in cells treated with IGF1 ligand

-1.047	-9.540	2.45E-09	1.29E-07	11.535	7380689	RPL22	NM_000983.3	Hs ribosomal protein L22 (RPL22), mRNA.
-1.047	-6.236	2.64E-06	2.92E-05	4.530	7160246	JMJD8	NM_001005920.2	Hs jumonji domain containing 8 (JMJD8), mRNA.
-1.047	-10.714	2.87E-10	2.80E-08	13.677	5310360	TLE4	NM_007005.3	Hs transducin-like enhancer of split 4 (E(sp1) homolog, Drosophila) (TLE4), mRNA.
-1.047	-6.911	5.65E-07	8.41E-06	6.076	1580356	TMED1	NM_006858.2	Hs transmembrane emp24 protein transport domain containing 1 (TMED1), mRNA.
-1.050	-14.576	6.84E-13	3.91E-10	19.626	4220097	DEM1	NM_022774.1	Hs defects in morphology 1 homolog (S. cerevisiae) (DEM1), mRNA.
-1.054	-11.454	8.05E-11	1.11E-08	14.940	4120053	PFKFB3	NM_004566.2	Hs 6-phosphofructo-2-kinase/fructose-2,6-biphosphatase 3 (PFKFB3), mRNA.
-1.054	-15.012	3.75E-13	2.50E-10	20.207	3930020	CTSF	NM_003793.2	Hs cathepsin F (CTSF), mRNA.
-1.055	-8.549	1.71E-08	5.69E-07	9.588	2970632	RP9	NM_203288.1	Hs retinitis pigmentosa 9 (autosomal dominant) (RP9), mRNA.
-1.056	-8.917	8.20E-09	3.29E-07	10.327	3290551	EIF4G3	NM_003760.3	Hs eukaryotic translation initiation factor 4 gamma, 3 (EIF4G3), mRNA.
-1.056	-11.109	1.44E-10	1.72E-08	14.359	380070	RPS23	NM_001025.4	Hs ribosomal protein S23 (RPS23), mRNA.
-1.059	-6.105	3.58E-06	3.72E-05	4.223	5080347	MRPS2	NM_016034.2	Hs mitochondrial ribosomal protein S2 (MRPS2), nuclear gene encoding mitochondrial protein, mRNA.
-1.059	-8.796	1.04E-08	4.01E-07	10.087	50327	ZNF589	NM_016089.2	Hs zinc finger protein 589 (ZNF589), mRNA.
-1.064	-6.433	1.67E-06	2.02E-05	4.986	1240551	ACADVL	NM_000018.2	Hs acyl-Coenzyme A dehydrogenase, very long chain (ACADVL), nuclear gene encoding mitochondrial pro
-1.064	-9.219	4.54E-09	2.13E-07	10.919	4260520	METAP2	NM_006838.3	Hs methionyl aminopeptidase 2 (METAP2), mRNA.
-1.065	-7.717	9.66E-08	2.11E-06	7.851	6280168	SERPINA3	NM_001085.4	Hs serpin peptidase inhibitor, clade A (alpha-1 antiproteinase, antitrypsin), member 3 (SERPINA3), mRNA.
-1.067	-14.867	4.57E-13	2.93E-10	20.016	4120386	PCOLCE	NM_002593.2	Hs procollagen C-endopeptidase enhancer (PCOLCE), mRNA.
-1.068	-10.328	5.70E-10	4.61E-08	12.993	2360196	DOCK1	NM_001380.3	Hs dedicator of cytokinesis 1 (DOCK1), mRNA.
-1.070	-10.272	6.31E-10	4.99E-08	12.892	6550647	COG2	NM_007357.1	Hs component of oligomeric golgi complex 2 (COG2), mRNA.
-1.070	-7.076	3.91E-07	6.26E-06	6.447	2970674	LEO1	NM_138792.2	Hs Leo1, Paf1/RNA polymerase II complex component, homolog (S. cerevisiae) (LEO1), mRNA.
-1.072	-5.876	6.14E-06	5.77E-05	3.683	4480220	FGFRL1	NM_021923.3	Hs fibroblast growth factor receptor-like 1 (FGFRL1), tv: 3, mRNA.
-1.074	-7.752	8.96E-08	1.98E-06	7.926	2320626	FLRT3	NM_198391.1	Hs fibronectin leucine rich transmembrane protein 3 (FLRT3), tv: 2, mRNA.
-1.079	-8.147	3.91E-08	1.06E-06	8.760	2940646	REPIN1	NM_014374.1	Hs replication initiator 1 (REPIN1), tv: 2, mRNA.
-1.081	-10.401	5.00E-10	4.25E-08	13.124	2450129	FLOT2	NM_004475.2	Hs flotillin 2 (FLOT2), mRNA.
-1.083	-12.950	7.34E-12	2.22E-09	17.306	6560091	TGFBR2	NM_001024847.2	Hs transforming growth factor, beta receptor II (70/80kDa) (TGFBR2), tv: 1, mRNA.
-1.085	-6.665	9.84E-07	1.32E-05	5.519	7050576	COMMD7	NM_001099339.1	Hs COMM domain containing 7 (COMMD7), tv: 2, mRNA.
-1.085	-14.655	6.13E-13	3.69E-10	19.732	2360551	ALDH1A3	NM_000693.2	Hs aldehyde dehydrogenase 1 family, member A3 (ALDH1A3), mRNA.
-1.086	-11.388	9.00E-11	1.19E-08	14.829	7210377	GPR37	NM_005302.2	Hs G protein-coupled receptor 37 (endothelin receptor type B-like) (GPR37), mRNA.
-1.086	-10.083	8.90E-10	6.41E-08	12.549	3710196	DDR1	NM_013993.2	Hs discoidin domain receptor tyrosine kinase 1 (DDR1), tv: 1, mRNA.
-1.089	-7.553	1.37E-07	2.80E-06	7.497	4890491	ATPAF1	NM_022745.3	Hs ATP synthase mitochondrial F1 complex assembly factor 1 (ATPAF1), nuclear gene encoding mitochond
-1.092	-9.954	1.13E-09	7.42E-08	12.311	5720040	EYA1	NM_172060.1	Hs eyes absent homolog 1 (Drosophila) (EYA1), tv: 1, mRNA.
-1.096	-9.165	5.04E-09	2.33E-07	10.814	6510408	FRMD8	NM_031904.3	Hs FERM domain containing 8 (FRMD8), mRNA.
-1.098	-7.189	3.04E-07	5.11E-06	6.699	7000746	C3ORF31	NM_138807.2	Hs chromosome 3 open reading frame 31 (C3orf31), mRNA.
-1.102	-9.558	2.37E-09	1.27E-07	11.571	3520278	GALK1	NM_000154.1	Hs galactokinase 1 (GALK1), mRNA.
-1.103	-12.278	2.09E-11	4.30E-09	16.273	5700646	CRTAP	NM_006371.3	Hs cartilage associated protein (CRTAP), mRNA.
-1.103	-5.927	5.45E-06	5.23E-05	3.803	2320079	NME4	NM_005009.2	Hs non-metastatic cells 4, protein expressed in (NME4), nuclear gene encoding mitochondrial protein, mRN
-1.104	-10.801	2.46E-10	2.55E-08	13.829	5050520	SPATA20	NM_022827.2	Hs spermatogenesis associated 20 (SPATA20), mRNA.
-1.104	-6.355	2.00E-06	2.34E-05	4.805	7400341	C11ORF2	NM_013265.2	Hs chromosome 11 open reading frame 2 (C11orf2), mRNA.
-1.107	-14.409	8.64E-13	4.49E-10	19.398	7160707	TBC1D14	NM_020773.1	Hs TBC1 domain family, member 14 (TBC1D14), mRNA.
-1.108	-11.026	1.67E-10	1.92E-08	14.218	2000064	CTPS2	NM_175859.1	Hs CTP synthase II (CTPS2), tv: 2, mRNA.
-1.109	-11.117	1.43E-10	1.71E-08	14.373	2320653	ECHDC2	NM_018281.2	Hs enoyl Coenzyme A hydratase domain containing 2 (ECHDC2), mRNA.

Appendix 4 – Genes differentially expressed at 24 hours in cells treated with IGF1 ligand

-1.109	-9.743	1.67E-09	9.87E-08	11.918	60324	OCRL	NM_000276.3	Hs oculocerebrorenal syndrome of Lowe (OCRL), tv: a, mRNA.
-1.114	-10.357	5.41E-10	4.52E-08	13.044	5810605	CCNI	NM_006835.2	Hs cyclin I (CCNI), mRNA.
-1.114	-8.769	1.10E-08	4.16E-07	10.032	2450390	FASTK	NM_006712.3	Hs Fas-activated serine/threonine kinase (FASTK), tv: 1, mRNA.
-1.117	-10.528	3.98E-10	3.55E-08	13.350	4050121	ICA1	NM_004968.2	Hs islet cell autoantigen 1, 69kDa (ICA1), tv: 2, mRNA.
-1.120	-10.684	3.03E-10	2.89E-08	13.624	5550592	LOC728661	XM_001717735.1	PREDICTED: Hs similar to solute carrier family 35, member E2 (LOC728661), mRNA.
-1.126	-10.526	4.00E-10	3.55E-08	13.346	4570255	LEF1	NM_016269.2	Hs lymphoid enhancer-binding factor 1 (LEF1), mRNA.
-1.131	-9.897	1.25E-09	8.00E-08	12.206	4040544	EPHA3	NM_005233.3	Hs EPH receptor A3 (EPHA3), tv: 1, mRNA.
-1.133	-11.948	3.56E-11	6.25E-09	15.748	730673	PCMTD2	NM_018257.1	Hs protein-L-isoaspartate (D-aspartate) O-methyltransferase domain containing 2 (PCMTD2), mRNA.
-1.135	-10.028	9.85E-10	6.72E-08	12.447	7050300	ZFP36L2	NM_006887.3	Hs zinc finger protein 36, C3H type-like 2 (ZFP36L2), mRNA.
-1.135	-9.371	3.38E-09	1.69E-07	11.213	3930541	PLEKHA1	NM_021622.3	Hs pleckstrin homology domain containing, family A (phosphoinositide binding specific) member 1 (PLEKH
-1.142	-10.146	7.94E-10	5.90E-08	12.662	1400465	POFUT1	NM_015352.1	Hs protein O-fucosyltransferase 1 (POFUT1), tv: 1, mRNA.
-1.143	-10.005	1.03E-09	6.93E-08	12.404	4210670	PAM	NM_138821.1	Hs peptidylglycine alpha-amidating monooxygenase (PAM), tv: 3, mRNA.
-1.149	-12.715	1.05E-11	2.90E-09	16.950	1570709	FZD7	NM_003507.1	Hs frizzled homolog 7 (Drosophila) (FZD7), mRNA.
-1.150	-8.338	2.63E-08	7.85E-07	9.156	60537	NAT14	NM_020378.2	Hs N-acetyltransferase 14 (GCN5-related, putative) (NAT14), mRNA.
-1.151	-12.753	9.92E-12	2.84E-09	17.009	3060450	RBM5	NM_005778.1	Hs RNA binding motif protein 5 (RBM5), mRNA.
-1.152	-11.701	5.34E-11	8.35E-09	15.347	2570291	IFNGR2	NM_005534.2	Hs interferon gamma receptor 2 (interferon gamma transducer 1) (IFNGR2), mRNA.
-1.152	-8.749	1.14E-08	4.25E-07	9.993	2570328	TRIB2	NM_021643.1	Hs tribbles homolog 2 (Drosophila) (TRIB2), mRNA.
-1.154	-6.453	1.60E-06	1.95E-05	5.033	2070520	CDCA7	NM_031942.4	Hs cell division cycle associated 7 (CDCA7), tv: 1, mRNA.
-1.154	-8.366	2.48E-08	7.51E-07	9.215	2650349	C19ORF48	NM_199250.1	Hs chromosome 19 open reading frame 48 (C19orf48), mRNA.
-1.154	-11.559	6.76E-11	9.74E-09	15.113	770164	RPAIN	NM_032308.1	Hs RPA interacting protein (RPAIN), tv: 2, mRNA.
-1.157	-12.504	1.46E-11	3.43E-09	16.625	6420309	FAM134B	NM_001034850.1	Hs family with sequence similarity 134, member B (FAM134B), tv: 1, mRNA.
-1.158	-12.412	1.69E-11	3.74E-09	16.482	6280332	CXCL16	NM_022059.1	Hs chemokine (C-X-C motif) ligand 16 (CXCL16), mRNA.
-1.158	-6.073	3.86E-06	3.95E-05	4.146	7610538	H1FX	NM_006026.2	Hs H1 histone family, member X (H1FX), mRNA.
-1.158	-10.347	5.51E-10	4.52E-08	13.027	6040767	PIGQ	NM_004204.2	Hs phosphatidylinositol glycan anchor biosynthesis, class Q (PIGQ), tv: 2, mRNA.
-1.160	-8.600	1.54E-08	5.28E-07	9.691	1990278	FCGR2A	NM_021642.2	Hs Fc fragment of IgG, low affinity IIa, receptor (CD32) (FCGR2A), mRNA.
-1.161	-7.813	7.87E-08	1.79E-06	8.057	7200703	KAT2B	NM_003884.4	Hs K(lysine) acetyltransferase 2B (KAT2B), mRNA.
-1.164	-9.703	1.80E-09	1.04E-07	11.844	6860544	FOXK1	NM_001037165.1	Hs forkhead box K1 (FOXK1), mRNA.
-1.170	-8.677	1.32E-08	4.70E-07	9.847	7400669	ZC3H5	XM_940903.2	PREDICTED: Hs zinc finger CCCH-type containing 5 (ZC3H5), mRNA.
-1.172	-10.914	2.02E-10	2.19E-08	14.024	5490376	NCOR2	NM_006312.3	Hs nuclear receptor co-repressor 2 (NCOR2), tv: 1, mRNA.
-1.174	-8.061	4.67E-08	1.21E-06	8.581	1510703	MFSD3	NM_138431.1	Hs major facilitator superfamily domain containing 3 (MFSD3), mRNA.
-1.174	-12.392	1.75E-11	3.79E-09	16.451	4670544	ACSS2	NM_018677.2	Hs acyl-CoA synthetase short-chain family member 2 (ACSS2), tv: 1, mRNA.
-1.177	-7.229	2.78E-07	4.78E-06	6.788	2630064	ACTR10	NM_018477.2	Hs actin-related protein 10 homolog (S. cerevisiae) (ACTR10), mRNA.
-1.178	-10.568	3.71E-10	3.39E-08	13.421	60014	FAM84B	NM_174911.3	Hs family with sequence similarity 84, member B (FAM84B), mRNA.
-1.179	-10.295	6.05E-10	4.83E-08	12.933	1340750	SRP68	NM_014230.2	Hs signal recognition particle 68kDa (SRP68), mRNA.
-1.180	-8.022	5.07E-08	1.29E-06	8.499	6840372	IGFBP3	NM_001013398.1	Hs insulin-like growth factor binding protein 3 (IGFBP3), tv: 1, mRNA.
-1.180	-7.760	8.81E-08	1.96E-06	7.943	4830577	MRPS16	NM_016065.3	Hs mitochondrial ribosomal protein S16 (MRPS16), nuclear gene encoding mitochondrial protein, mRNA.
-1.181	-8.976	7.30E-09	3.03E-07	10.443	990113	LOC100127888	NR_024470.1	Hs hypothetical protein LOC100127888 (LOC100127888), non-coding RNA.
-1.184	-7.542	1.41E-07	2.84E-06	7.472	2900292	RANGAP1	NM_002883.2	Hs Ran GTPase activating protein 1 (RANGAP1), mRNA.
-1.187	-14.730	5.52E-13	3.43E-10	19.833	730543	RPAIN	NM_001033002.2	Hs RPA interacting protein (RPAIN), mRNA.
-1.188	-13.118	5.67E-12	1.87E-09	17.558	4570768	TRAF1	NM_005658.3	Hs TNF receptor-associated factor 1 (TRAF1), mRNA.

Appendix 4 – Genes differentially expressed at 24 hours in cells treated with IGF1 ligand

-1.189	-9.642	2.02E-09	1.13E-07	11.729	6760669	SPRY1	NM_005841.1	Hs sprouty homolog 1, antagonist of FGF signaling (Drosophila) (SPRY1), tv: 1, mRNA.
-1.190	-8.188	3.58E-08	9.96E-07	8.847	6960022	Sep-05	NM_002688.4	Hs septin 5 (SEPT5), mRNA.
-1.191	-6.223	2.72E-06	2.99E-05	4.498	2320187	MED16	NM_005481.2	Hs mediator complex subunit 16 (MED16), mRNA.
-1.194	-10.999	1.75E-10	1.97E-08	14.170	2850291	GARNL4	NM_015085.3	Hs GTPase activating Rap/RanGAP domain-like 4 (GARNL4), mRNA.
-1.201	-11.254	1.13E-10	1.45E-08	14.606	3130154	AMACR	NM_203382.1	Hs alpha-methylacyl-CoA racemase (AMACR), tv: 2, mRNA.
-1.201	-7.916	6.33E-08	1.52E-06	8.275	3360468	SNX17	NM_014748.2	Hs sorting nexin 17 (SNX17), mRNA.
-1.202	-9.480	2.75E-09	1.40E-07	11.421	940471	C5ORF13	NM_004772.1	Hs chromosome 5 open reading frame 13 (C5orf13), mRNA.
-1.203	-11.391	8.96E-11	1.19E-08	14.834	6980164	NKIRAS2	NM_017595.4	Hs NFKB inhibitor interacting Ras-like 2 (NKIRAS2), tv: 2, mRNA.
-1.203	-8.247	3.17E-08	9.05E-07	8.969	6660626	BRD3	NM_007371.2	Hs bromodomain containing 3 (BRD3), mRNA.
-1.203	-7.528	1.45E-07	2.90E-06	7.444	1440437	LOC151162	NR_024275.1	Hs hypothetical LOC151162 (LOC151162), non-coding RNA.
-1.210	-9.208	4.64E-09	2.17E-07	10.898	6370356	EEF1A2	NM_001958.2	Hs eukaryotic translation elongation factor 1 alpha 2 (EEF1A2), mRNA.
-1.211	-8.476	1.99E-08	6.38E-07	9.439	940458	SYTL5	NM_138780.1	Hs synaptotagmin-like 5 (SYTL5), mRNA.
-1.215	-6.633	1.06E-06	1.40E-05	5.446	5870113	THOC7	NM_025075.1	Hs THO complex 7 homolog (Drosophila) (THOC7), mRNA.
-1.216	-9.702	1.80E-09	1.04E-07	11.842	2760494	PHF2	NM_005392.3	Hs PHD finger protein 2 (PHF2), mRNA.
-1.217	-8.644	1.41E-08	4.97E-07	9.781	2650114	ITGB5	NM_002213.3	Hs integrin, beta 5 (ITGB5), mRNA. XM_944688 XM_944693
-1.219	-8.216	3.38E-08	9.50E-07	8.905	1230682	BIRC5	NM_001168.2	Hs baculoviral IAP repeat-containing 5 (BIRC5), tv: 1, mRNA.
-1.220	-11.831	4.31E-11	7.22E-09	15.559	1070133	CLDN12	NM_012129.2	Hs claudin 12 (CLDN12), mRNA.
-1.222	-9.861	1.34E-09	8.41E-08	12.138	6110053	ZNF32	NM_001005368.1	Hs zinc finger protein 32 (ZNF32), tv: 2, mRNA.
-1.222	-14.277	1.04E-12	5.14E-10	19.217	4040176	LAMA5	NM_005560.3	Hs laminin, alpha 5 (LAMA5), mRNA.
-1.225	-12.248	2.20E-11	4.42E-09	16.226	4490524	ACSS2	NM_001076552.1	Hs acyl-CoA synthetase short-chain family member 2 (ACSS2), tv: 2, mRNA.
-1.227	-8.954	7.63E-09	3.12E-07	10.399	4050156	ERBB2	NM_004448.2	Hs v-erb-b2 erythroblastic leukemia viral oncogene homolog 2, neuro/glioblastoma derived oncogene homol
-1.235	-7.706	9.89E-08	2.15E-06	7.827	2480037	CMTM8	NM_178868.3	Hs CKLF-like MARVEL transmembrane domain containing 8 (CMTM8), mRNA.
-1.235	-10.171	7.58E-10	5.73E-08	12.708	3170519	HARS2	NM_012208.2	Hs histidyl-tRNA synthetase 2, mitochondrial (putative) (HARS2), nuclear gene encoding mitochondrial prot
-1.236	-10.767	2.61E-10	2.67E-08	13.770	7200707	PRMT6	NM_018137.1	Hs protein arginine methyltransferase 6 (PRMT6), mRNA.
-1.237	-8.578	1.61E-08	5.45E-07	9.648	6620544	TACO1	NM_016360.2	Hs translational activator of mitochondrially encoded cytochrome c oxidase I (TACO1), nuclear gene encodi
-1.240	-15.831	1.26E-13	1.02E-10	21.259	840670	STK32B	NM_018401.1	Hs serine/threonine kinase 32B (STK32B), mRNA.
-1.241	-11.064	1.56E-10	1.83E-08	14.283	1430524	LTA4H	NM_000895.1	Hs leukotriene A4 hydrolase (LTA4H), mRNA.
-1.241	-9.620	2.11E-09	1.16E-07	11.687	2810601	LEF1	NM_016269.2	Hs lymphoid enhancer-binding factor 1 (LEF1), mRNA.
-1.244	-8.071	4.58E-08	1.20E-06	8.601	6940541	CCDC117	NM_173510.1	Hs coiled-coil domain containing 117 (CCDC117), mRNA.
-1.246	-8.587	1.58E-08	5.37E-07	9.666	3830041	PMEPA1	NM_199169.1	Hs prostate transmembrane protein, androgen induced 1 (PMEPA1), tv: 2, mRNA.
-1.252	-10.756	2.66E-10	2.70E-08	13.751	5820768	DEF8	NM_207514.1	Hs differentially expressed in FDCP 8 homolog (mouse) (DEF8), tv: 1, mRNA.
-1.254	-9.230	4.45E-09	2.10E-07	10.940	5890025	GNG12	NM_018841.4	Hs guanine nucleotide binding protein (G protein), gamma 12 (GNG12), mRNA.
-1.258	-8.464	2.03E-08	6.47E-07	9.415	3610112	RAB11FIP3	NM_014700.2	Hs RAB11 family interacting protein 3 (class II) (RAB11FIP3), mRNA.
-1.260	-10.108	8.51E-10	6.24E-08	12.593	5860519	CSPG4	NM_001897.4	Hs chondroitin sulfate proteoglycan 4 (CSPG4), mRNA.
-1.260	-10.431	4.74E-10	4.08E-08	13.177	3450114	FAM69B	XM_001130258.1	PREDICTED: Hs family with sequence similarity 69, member B (FAM69B), mRNA.
-1.261	-8.499	1.89E-08	6.14E-07	9.488	2850039	TBC1D2B	NM_015079.2	Hs TBC1 domain family, member 2B (TBC1D2B), mRNA.
-1.262	-8.549	1.71E-08	5.69E-07	9.588	1850047	FAM189B	NM_006589.2	Hs family with sequence similarity 189, member B (FAM189B), tv: 1, mRNA.
-1.264	-9.842	1.39E-09	8.60E-08	12.102	6380086	GORASP1	NM_031899.2	Hs golgi reassembly stacking protein 1, 65kDa (GORASP1), mRNA.
-1.264	-6.955	5.12E-07	7.78E-06	6.176	1850468	CCDC56	NM_001040431.1	Hs coiled-coil domain containing 56 (CCDC56), mRNA.
-1.265	-7.100	3.70E-07	6.02E-06	6.501	2710431	GTPBP3	NM_032620.1	Hs GTP binding protein 3 (mitochondrial) (GTPBP3), nuclear gene encoding mitochondrial protein, tv: V, m

Appendix 4 – Genes differentially expressed at 24 hours in cells treated with IGF1 ligand

-1.266	-9.039	6.45E-09	2.74E-07	10.567	510576	BCOR	NM_017745.4	Hs BCL6 co-repressor (BCOR), tv: 1, mRNA.
-1.267	-10.211	7.05E-10	5.45E-08	12.781	1710630	ST6GAL1	NM_003032.2	Hs ST6 beta-galactosamide alpha-2,6-sialyltranferase 1 (ST6GAL1), tv: 2, mRNA.
-1.269	-13.165	5.29E-12	1.80E-09	17.627	5900019	CRTC3	NM_022769.3	Hs CREB regulated transcription coactivator 3 (CRTC3), tv: 1, mRNA.
-1.269	-10.130	8.18E-10	6.05E-08	12.633	1940129	SIRPA	NM_001040023.1	Hs signal-regulatory protein alpha (SIRPA), tv: 2, mRNA.
-1.271	-10.260	6.45E-10	5.07E-08	12.870	3610398	MMACHC	NM_015506.2	Hs methylmalonic aciduria (cobalamin deficiency) cblC type, with homocystinuria (MMACHC), mRNA.
-1.276	-9.871	1.32E-09	8.30E-08	12.158	3840079	RAB3GAP1	NM_012233.1	Hs RAB3 GTPase activating protein subunit 1 (catalytic) (RAB3GAP1), mRNA.
-1.278	-12.598	1.26E-11	3.16E-09	16.771	5900152	NOX4	NM_016931.2	Hs NADPH oxidase 4 (NOX4), mRNA.
-1.280	-9.976	1.08E-09	7.21E-08	12.351	2260220	B3GNT6	NM_006876.1	Hs UDP-GlcNAc:betaGal beta-1,3-N-acetylglucosaminyltransferase 6 (B3GNT6), mRNA.
-1.282	-15.078	3.43E-13	2.42E-10	20.294	730612	HTRA1	NM_002775.3	Hs HtrA serine peptidase 1 (HTRA1), mRNA.
-1.283	-8.769	1.10E-08	4.16E-07	10.033	4230520	DNCL1	NM_003746.1	Hs dynein, cytoplasmic, light polypeptide 1 (DNCL1), mRNA.
-1.291	-7.243	2.70E-07	4.66E-06	6.819	1580477	C11ORF74	NM_138787.2	Hs chromosome 11 open reading frame 74 (C11orf74), mRNA.
-1.292	-10.761	2.64E-10	2.69E-08	13.758	6250468	DUSP6	NM_001946.2	Hs dual specificity phosphatase 6 (DUSP6), tv: 1, mRNA.
-1.293	-6.513	1.39E-06	1.75E-05	5.171	770541	EI24	NM_001007277.1	Hs etoposide induced 2.4 mRNA (EI24), tv: 2, mRNA.
-1.293	-10.089	8.80E-10	6.36E-08	12.559	5560561	TNS3	NM_022748.10	Hs tensin 3 (TNS3), mRNA.
-1.299	-13.475	3.32E-12	1.36E-09	18.083	4280669	RBL2	NM_005611.2	Hs retinoblastoma-like 2 (p130) (RBL2), mRNA.
-1.301	-7.928	6.17E-08	1.49E-06	8.301	6280100	GPSM1	XM_939186.2	PREDICTED: Hs G-protein signalling modulator 1 (AGS3-like, C. elegans) (GPSM1), mRNA.
-1.305	-8.569	1.64E-08	5.51E-07	9.630	360114	CTXN1	NM_206833.2	Hs cortexin 1 (CTXN1), mRNA.
-1.305	-11.226	1.18E-10	1.51E-08	14.557	1070551	CSRP2BP	NM_020536.2	Hs CSRP2 binding protein (CSRP2BP), tv: 1, mRNA.
-1.308	-12.290	2.05E-11	4.26E-09	16.291	3930154	H2AFY	NM_138609.2	Hs H2A histone family, member Y (H2AFY), tv: 1, mRNA.
-1.313	-14.471	7.92E-13	4.37E-10	19.483	360731	LOC728661	NM_001110781.1	Hs similar to solute carrier family 35, member E2 (LOC728661), mRNA.
-1.323	-11.872	4.03E-11	6.85E-09	15.626	4780139	PLP1	NM_199478.1	Hs proteolipid protein 1 (PLP1), tv: 2, mRNA.
-1.324	-8.927	8.04E-09	3.26E-07	10.347	2900041	H2AFY2	NM_018649.2	Hs H2A histone family, member Y2 (H2AFY2), mRNA.
-1.329	-13.166	5.28E-12	1.80E-09	17.628	6770204	MEN1	NM_130799.1	Hs multiple endocrine neoplasia I (MEN1), tv: 2, mRNA.
-1.331	-7.934	6.10E-08	1.48E-06	8.312	4880014	TCEA2	NM_198723.1	Hs transcription elongation factor A (SII), 2 (TCEA2), tv: 2, mRNA.
-1.331	-14.638	6.27E-13	3.69E-10	19.710	940735	MGP	NM_000900.2	Hs matrix Gla protein (MGP), mRNA.
-1.337	-8.735	1.18E-08	4.33E-07	9.963	1510414	MGRN1	NM_015246.1	Hs mahogunin, ring finger 1 (MGRN1), mRNA.
-1.339	-8.894	8.58E-09	3.41E-07	10.281	5870286	AMACR	NM_203382.1	Hs alpha-methylacyl-CoA racemase (AMACR), tv: 2, mRNA.
-1.339	-11.752	4.90E-11	7.84E-09	15.431	4490673	TWIST1	NM_000474.3	Hs twist homolog 1 (Drosophila) (TWIST1), mRNA.
-1.344	-9.597	2.20E-09	1.19E-07	11.644	6020286	FST	NM_013409.1	Hs follistatin (FST), tv: FST344, mRNA.
-1.353	-7.694	1.02E-07	2.19E-06	7.801	3610630	CRBN	NM_016302.2	Hs cereblon (CRBN), mRNA.
-1.356	-11.421	8.51E-11	1.16E-08	14.885	7610615	SLC6A10P	NR_003083.2	Hs solute carrier family 6 (neurotransmitter transporter, creatine), member 10 (pseudogene) (SLC6A10P) on
-1.357	-12.058	2.98E-11	5.69E-09	15.924	6940647	C16ORF58	NM_022744.1	Hs chromosome 16 open reading frame 58 (C16orf58), mRNA.
-1.358	-17.756	1.17E-14	2.12E-11	23.530	3800095	DEPDC6	NM_022783.1	Hs DEP domain containing 6 (DEPDC6), mRNA.
-1.370	-12.008	3.23E-11	5.86E-09	15.843	4590133	AFAP1L2	NM_001001936.1	Hs actin filament associated protein 1-like 2 (AFAP1L2), tv: 1, mRNA.
-1.370	-6.651	1.02E-06	1.35E-05	5.488	5220347	BCKDK	NM_005881.1	Hs branched chain ketoacid dehydrogenase kinase (BCKDK), mRNA.
-1.371	-9.856	1.35E-09	8.42E-08	12.129	6110195	ZCCHC24	NM_153367.2	Hs zinc finger, CCHC domain containing 24 (ZCCHC24), mRNA.
-1.373	-14.238	1.10E-12	5.31E-10	19.164	1170349	LAD1	NM_005558.3	Hs ladinin 1 (LAD1), mRNA.
-1.375	-11.974	3.42E-11	6.09E-09	15.789	1190091	DMRT2	NM_006557.4	Hs doublesex and mab-3 related transcription factor 2 (DMRT2), tv: 1, mRNA.
-1.390	-8.660	1.37E-08	4.85E-07	9.812	6220086	DYNLL1	NM_001037494.1	Hs dynein, light chain, LC8-type 1 (DYNLL1), tv: 1, mRNA.
-1.392	-7.665	1.08E-07	2.29E-06	7.739	1780554	TMUB1	NM_031434.2	Hs transmembrane and ubiquitin-like domain containing 1 (TMUB1), mRNA.

Appendix 4 – Genes differentially expressed at 24 hours in cells treated with IGF1 ligand

-1.401	-11.617	6.13E-11	9.07E-09	15.210	3890066	DPH5	NM_001077394.1	Hs DPH5 homolog (S. cerevisiae) (DPH5), tv: 1, mRNA.
-1.410	-9.777	1.57E-09	9.48E-08	11.983	5690523	RNASEH2C	NM_032193.3	Hs ribonuclease H2, subunit C (RNASEH2C), mRNA.
-1.411	-8.408	2.28E-08	7.01E-07	9.301	2060202	HAPLN1	NM_001884.2	Hs hyaluronan and proteoglycan link protein 1 (HAPLN1), mRNA.
-1.424	-6.933	5.37E-07	8.08E-06	6.128	1450524	NUP205	NM_015135.1	Hs nucleoporin 205kDa (NUP205), mRNA.
-1.424	-8.634	1.44E-08	5.02E-07	9.760	6510204	SLC35A1	NM_006416.3	Hs solute carrier family 35 (CMP-sialic acid transporter), member A1 (SLC35A1), mRNA.
-1.441	-9.670	1.92E-09	1.08E-07	11.782	1470706	C8ORF55	NM_016647.2	Hs chromosome 8 open reading frame 55 (C8orf55), mRNA.
-1.447	-6.218	2.75E-06	3.01E-05	4.486	1510181	PTGES	NM_004878.3	Hs prostaglandin E synthase (PTGES), mRNA.
-1.465	-8.686	1.30E-08	4.64E-07	9.866	1010048	CXXC5	NM_016463.5	Hs CXXC finger 5 (CXXC5), mRNA.
-1.476	-6.987	4.76E-07	7.34E-06	6.249	450348	GNG10	NM_001017998.2	Hs guanine nucleotide binding protein (G protein), gamma 10 (GNG10), mRNA.
-1.483	-8.363	2.50E-08	7.54E-07	9.208	3710039	MRPL54	NM_172251.1	Hs mitochondrial ribosomal protein L54 (MRPL54), nuclear gene encoding mitochondrial protein, mRNA.
-1.488	-8.746	1.15E-08	4.26E-07	9.987	3930086	UCKL1	NM_017859.2	Hs uridine-cytidine kinase 1-like 1 (UCKL1), mRNA.
-1.490	-11.815	4.43E-11	7.35E-09	15.533	6860026	ZNF358	NM_018083.4	Hs zinc finger protein 358 (ZNF358), mRNA.
-1.490	-10.914	2.02E-10	2.19E-08	14.025	3780554	CRBN	NM_016302.2	Hs cereblon (CRBN), mRNA.
-1.505	-10.740	2.74E-10	2.75E-08	13.722	520544	AMACR	NM_014324.4	Hs alpha-methylacyl-CoA racemase (AMACR), tv: 1, mRNA.
-1.514	-11.638	5.93E-11	8.96E-09	15.243	3890095	SOD3	NM_003102.2	Hs superoxide dismutase 3, extracellular (SOD3), mRNA.
-1.525	-9.086	5.88E-09	2.58E-07	10.659	1660477	CALM1	NM_006888.3	Hs calmodulin 1 (phosphorylase kinase, delta) (CALM1), mRNA.
-1.535	-11.719	5.18E-11	8.17E-09	15.376	510471	FAM175B	NM_032182.3	Hs family with sequence similarity 175, member B (FAM175B), mRNA.
-1.538	-15.889	1.17E-13	9.80E-11	21.331	10433	ITGA10	NM_003637.3	Hs integrin, alpha 10 (ITGA10), mRNA.
-1.540	-16.241	7.46E-14	7.38E-11	21.765	7150634	APOD	NM_001647.2	Hs apolipoprotein D (APOD), mRNA.
-1.541	-10.052	9.43E-10	6.61E-08	12.491	3940471	CCDC106	NM_013301.2	Hs coiled-coil domain containing 106 (CCDC106), mRNA.
-1.569	-11.412	8.64E-11	1.17E-08	14.869	4540064	C17ORF70	NM_025161.3	Hs chromosome 17 open reading frame 70 (C17orf70), mRNA.
-1.593	-16.968	3.01E-14	4.58E-11	22.632	7150017	C6ORF48	NM_001040437.1	Hs chromosome 6 open reading frame 48 (C6orf48), tv: 1, mRNA.
-1.612	-8.771	1.09E-08	4.16E-07	10.037	3310445	MRPS26	NM_030811.3	Hs mitochondrial ribosomal protein S26 (MRPS26), nuclear gene encoding mitochondrial protein, mRNA.
-1.617	-10.510	4.12E-10	3.63E-08	13.317	1050279	CXXC5	NM_016463.7	Hs CXXC finger 5 (CXXC5), mRNA.
-1.619	-13.317	4.21E-12	1.58E-09	17.852	4670044	TFAP2B	NM_003221.3	Hs transcription factor AP-2 beta (activating enhancer binding protein 2 beta) (TFAP2B), mRNA.
-1.622	-9.545	2.43E-09	1.28E-07	11.545	4590154	ZDHHC8	NM_013373.2	Hs zinc finger, DHHC-type containing 8 (ZDHHC8), mRNA.
-1.624	-11.060	1.57E-10	1.83E-08	14.275	580431	PRRX1	NM_006902.3	Hs paired related homeobox 1 (PRRX1), tv: pmx-1a, mRNA.
-1.630	-15.718	1.47E-13	1.14E-10	21.116	4180209	PLAGL2	NM_002657.2	Hs pleiomorphic adenoma gene-like 2 (PLAGL2), mRNA.
-1.640	-9.130	5.40E-09	2.44E-07	10.745	630278	H1F0	NM_005318.2	Hs H1 histone family, member 0 (H1F0), mRNA.
-1.645	-13.260	4.58E-12	1.69E-09	17.767	4150519	FAM108C1	NM_021214.1	Hs family with sequence similarity 108, member C1 (FAM108C1), mRNA.
-1.648	-13.917	1.74E-12	7.89E-10	18.715	3890187	PRMT6	NM_018137.1	Hs protein arginine methyltransferase 6 (PRMT6), mRNA.
-1.655	-8.327	2.69E-08	8.00E-07	9.133	4670398	TEAD2	NM_003598.1	Hs TEA domain family member 2 (TEAD2), mRNA.
-1.658	-8.470	2.01E-08	6.42E-07	9.429	70044	JTB	NM_006694.2	Hs jumping translocation breakpoint (JTB), mRNA.
-1.660	-14.101	1.34E-12	6.32E-10	18.974	4540326	PYGB	NM_002862.3	Hs phosphorylase, glycogen; brain (PYGB), mRNA.
-1.689	-8.582	1.60E-08	5.41E-07	9.656	6130747	PRPSAP1	NM_002766.1	Hs phosphoribosyl pyrophosphate synthetase-associated protein 1 (PRPSAP1), mRNA.
-1.693	-17.314	1.98E-14	3.31E-11	23.032	7320471	TFAP2B	NM_003221.3	Hs transcription factor AP-2 beta (activating enhancer binding protein 2 beta) (TFAP2B), mRNA.
-1.694	-13.551	2.97E-12	1.24E-09	18.192	7040497	ART3	NM_001179.3	Hs ADP-ribosyltransferase 3 (ART3), mRNA.
-1.715	-17.820	1.08E-14	2.12E-11	23.601	1940162	GBP2	NM_004120.3	Hs guanylate binding protein 2, interferon-inducible (GBP2), mRNA.
-1.720	-10.863	2.21E-10	2.36E-08	13.936	4640689	EIF4A2	NM_001967.3	Hs eukaryotic translation initiation factor 4A, isoform 2 (EIF4A2), mRNA.
-1.775	-10.123	8.28E-10	6.08E-08	12.621	5390333	TMEM98	NM_001033504.1	Hs transmembrane protein 98 (TMEM98), tv: 2, mRNA.

Appendix 4 – Genes differentially expressed at 24 hours in cells treated with IGF1 ligand

-1.804	-11.197	1.24E-10	1.56E-08	14.508	4560288	ERBB3	NM_001982.2	Hs v-erb-b2 erythroblastic leukemia viral oncogene homolog 3 (avian) (ERBB3), tv: 1, mRNA.
-1.851	-10.531	3.97E-10	3.55E-08	13.354	4590537	ERAL1	NM_005702.2	Hs Era G-protein-like 1 (E. coli) (ERAL1), mRNA.
-1.854	-13.571	2.88E-12	1.23E-09	18.222	290086	LZTR1	NM_006767.3	Hs leucine-zipper-like transcription regulator 1 (LZTR1), mRNA.
-1.881	-16.027	9.81E-14	8.89E-11	21.502	1340066	RXRG	NM_001009598.1	Hs retinoid X receptor, gamma (RXRG), tv: 2, mRNA.
-1.885	-16.364	6.38E-14	7.25E-11	21.914	4390414	SPRY4	NM_030964.2	Hs sprouty homolog 4 (Drosophila) (SPRY4), mRNA.
-1.901	-16.629	4.58E-14	6.01E-11	22.232	4880204	SPRYD5	NM_032681.1	Hs SPRY domain containing 5 (SPRYD5), mRNA.
-1.935	-9.883	1.29E-09	8.16E-08	12.180	770474	LPHN1	NM_014921.3	Hs latrophilin 1 (LPHN1), tv: 2, mRNA.
-1.951	-16.608	4.70E-14	6.01E-11	22.207	110181	KIAA1199	NM_018689.1	Hs KIAA1199 (KIAA1199), mRNA.
-1.984	-13.148	5.42E-12	1.82E-09	17.603	3180187	SOX11	NM_003108.3	Hs SRY (sex determining region Y)-box 11 (SOX11), mRNA.
-1.995	-19.527	1.58E-15	6.89E-12	25.405	730576	SPRY4	NM_030964.2	Hs sprouty homolog 4 (Drosophila) (SPRY4), mRNA.
-2.046	-13.083	5.98E-12	1.94E-09	17.506	4860546	CTHRC1	NM_138455.2	Hs collagen triple helix repeat containing 1 (CTHRC1), mRNA.
-2.085	-12.129	2.66E-11	5.16E-09	16.038	5050681	TESC	NM_017899.2	Hs tescalcin (TESC), mRNA.
-2.204	-18.674	4.06E-15	1.10E-11	24.526	670041	AKAP12	NM_144497.1	Hs A kinase (PRKA) anchor protein (gravin) 12 (AKAP12), tv: 2, mRNA.
-2.219	-18.748	3.73E-15	1.10E-11	24.604	4390102	PRKAR1A	NM_212471.1	Hs protein kinase, cAMP-dependent, regulatory, type I, alpha (tissue specific extinguisher 1) (PRKAR1A), tv
-2.313	-17.809	1.10E-14	2.12E-11	23.589	4150477	LOXL4	NM_032211.6	Hs lysyl oxidase-like 4 (LOXL4), mRNA.
-2.516	-16.330	6.66E-14	7.25E-11	21.873	2190709	ASAP3	NM_017707.2	Hs ArfGAP with SH3 domain, ankyrin repeat and PH domain 3 (ASAP3), mRNA.

Appendix 4 – Genes differentially expressed at 24 hours in cells treated with IGF1 ligand

***IGF signatures*(1=present, 0=absent)**					
A375 IGF up regulated gene signature for 24 hours	**A375 IGF up regulated gene signature for 3 hours**	**MCF IGF up regulated gene signature**	**Number of signatures containing gene**	**hgnc_symbol**	**Description**
1	1	1	3	SLC3A2	solute carrier family 3 (activators of dibasic and neutral amino acid transport), member 2 11026]
1	1	1	3	CDC25A	cell division cycle 25 homolog A (S. pombe) 1725]
1	1	1	3	HMGCS1	3-hydroxy-3-methylglutaryl-CoA synthase 1 (soluble) 5007]
1	1	1	3	MVD	mevalonate (diphospho) decarboxylase 7529]
1	1	1	3	SLC7A5	solute carrier family 7 (amino acid transporter light chain, L system), member 5 11063]
1	1	1	3	DDIT3	DNA-damage-inducible transcript 3 2726]
1	1	1	3	IDI1	isopentenyl-diphosphate delta isomerase 1 5387]
1	1	1	3	PSPH	phosphoserine phosphatase 9577]
1	1	1	3	SLC1A5	solute carrier family 1 (neutral amino acid transporter), member 5 10943]
1	1	1	3	DDIT4	DNA-damage-inducible transcript 4 24944]
1	1	1	3	TRIB3	tribbles homolog 3 (Drosophila) 16228]
1	1	1	3	ASNS	asparagine synthetase (glutamine-hydrolyzing) 753]
1	1	1	3	INSIG1	insulin induced gene 1 6083]
1	1	1	3	FHL2	four and a half LIM domains 2 3703]
1	0	1	2	PNP	purine nucleoside phosphorylase 7892]
1	1	0	2	MVK	mevalonate kinase 7530]
1	1	0	2	IL8	interleukin 8 6025]
1	0	1	2	CYP27B1	cytochrome P450, family 27, subfamily B, polypeptide 1 2606]
1	0	1	2	CACYBP	calcyclin binding protein 30423]
1	0	1	2	GEMIN2	gem (nuclear organelle) associated protein 2 10884]
1	0	1	2	SRRD	SRR1 domain containing 33910]
1	1	0	2	MSMO1	methylsterol monooxygenase 1 10545]
1	0	1	2	P4HA2	prolyl 4-hydroxylase, alpha polypeptide II 8547]
1	0	1	2	NME2	NME/NM23 nucleoside diphosphate kinase 2 7850]
1	1	0	2	NABP1	nucleic acid binding protein 1 26232]

Appendix 5 – Genes common to MCF7 and A375 IGF induced up regulated gene signatures

1	0	1	2	BOLA2	bolA homolog 2 (E. coli) 29488]
1	0	1	2	TUBB2A	tubulin, beta 2A class IIa 12412]
1	0	1	2	TUBG1	tubulin, gamma 1 12417]
1	0	1	2	DBI	diazepam binding inhibitor (GABA receptor modulator, acyl-CoA binding protein) 2690]
1	0	1	2	WDR62	WD repeat domain 62 24502]
1	1	0	2	ADM	adrenomedullin 259]
1	0	1	2	DUSP4	dual specificity phosphatase 4 3070]
1	0	1	2	FABP5	fatty acid binding protein 5 (psoriasis-associated) 3560]
1	1	0	2	CYR61	cysteine-rich, angiogenic inducer, 61 2654]
1	0	1	2	CTSC	cathepsin C 2528]
1	1	0	2	CTGF	connective tissue growth factor 2500]
1	1	0	2	HBEGF	heparin-binding EGF-like growth factor 3059]
1	0	1	2	FDPS	farnesyl diphosphate synthase 3631]
1	0	1	2	GARS	glycyl-tRNA synthetase 4162]
1	1	0	2	ID2	inhibitor of DNA binding 2, dominant negative helix-loop-helix protein 5361]
1	0	1	2	ITGAE	integrin, alpha E (antigen CD103, human mucosal lymphocyte antigen 1; alpha polypeptide) 6147]
1	1	0	2	LSS	lanosterol synthase (2,3-oxidosqualene-lanosterol cyclase) 6708]
1	1	0	2	RGS2	regulator of G-protein signaling 2, 24kDa 9998]
1	1	0	2	ST3GAL1	ST3 beta-galactoside alpha-2,3-sialyltransferase 1 10862]
1	0	1	2	SNRPA1	small nuclear ribonucleoprotein polypeptide A' 11152]
1	1	0	2	SQLE	squalene epoxidase 11279]
1	1	0	2	TAC1	tachykinin, precursor 1 11517]
1	1	0	2	THBS1	thrombospondin 1 11785]
1	1	0	2	TPST1	tyrosylprotein sulfotransferase 1 12020]
1	0	1	2	YARS	tyrosyl-tRNA synthetase 12840]
1	1	0	2	STC2	stanniocalcin 2 11374]
1	0	1	2	CCNA1	cyclin A1 1577]
1	0	1	2	ORC1	origin recognition complex, subunit 1 8487]
1	0	1	2	CNN2	calponin 2 2156]
1	1	0	2	EPHA2	EPH receptor A2 3386]

Appendix 5 – Genes common to MCF7 and A375 IGF induced up regulated gene signatures

1	0	1	2	FDFT1	farnesyl-diphosphate farnesyltransferase 1 3629]
1	0	1	2	ITGB1BP1	integrin beta 1 binding protein 1 23927]
1	1	0	2	XBP1	X-box binding protein 1 12801]
1	0	1	2	ISG15	ISG15 ubiquitin-like modifier 4053]
1	1	0	2	ETS1	v-ets erythroblastosis virus E26 oncogene homolog 1 (avian) 3488]
1	0	1	2	HRAS	v-Ha-ras Harvey rat sarcoma viral oncogene homolog 5173]
1	0	1	2	SHMT2	serine hydroxymethyltransferase 2 (mitochondrial) 10852]
1	0	1	2	UCHL3	ubiquitin carboxyl-terminal esterase L3 (ubiquitin thiolesterase) 12515]
1	0	1	2	TUBA1A	tubulin, alpha 1a 20766]
1	0	1	2		Tubulin beta-3 chain [Source:UniProtKB/Swiss-Prot;Acc:Q13509]
1	0	1	2	TUBB4B	tubulin, beta 4B class IVb 20771]
1	1	0	2	DNAJB1	DnaJ (Hsp40) homolog, subfamily B, member 1 5270]
1	0	1	2	TIMM44	translocase of inner mitochondrial membrane 44 homolog (yeast) 17316]
1	0	1	2	SARS	seryl-tRNA synthetase 10537]
1	0	1	2	EBP	emopamil binding protein (sterol isomerase) 3133]
1	1	0	2	MTHFD2	methylenetetrahydrofolate dehydrogenase (NADP+ dependent) 2, methenyltetrahydrofolate cyclohydrolase 7434]
1	0	1	2	MLLT11	myeloid/lymphoid or mixed-lineage leukemia (trithorax homolog, Drosophila); translocated to, 11 16997]
1	0	1	2	CLTB	clathrin, light chain B 2091]
1	0	1	2	RASSF1	Ras association (RalGDS/AF-6) domain family member 1 9882]
1	0	1	2	RFC5	replication factor C (activator 1) 5, 36.5kDa 9973]
1	0	1	2	CHORDC1	cysteine and histidine-rich domain (CHORD) containing 1 14525]
1	1	0	2	DKK1	dickkopf 1 homolog (Xenopus laevis) 2891]
1	0	1	2	RAD54B	RAD54 homolog B (S. cerevisiae) 17228]
1	1	0	2	CLCF1	cardiotrophin-like cytokine factor 1 17412]
1	0	1	2	PSMC3IP	PSMC3 interacting protein 17928]
1	0	1	2	SLC7A11	solute carrier family 7 (anionic amino acid transporter light chain, xc- system), member 11 11059]
1	0	1	2	UBE2S	ubiquitin-conjugating enzyme E2S 17895]
1	0	1	2	SMG5	smg-5 homolog, nonsense mediated mRNA decay factor (C. elegans) 24644]
1	0	1	2	SLC39A14	solute carrier family 39 (zinc transporter), member 14 20858]
1	1	0	2	GADD45B	growth arrest and DNA-damage-inducible, beta 4096]

Appendix 5 – Genes common to MCF7 and A375 IGF induced up regulated gene signatures

1	0	1	2	GMNN	geminin, DNA replication inhibitor 17493]
1	1	0	2	NSDHL	NAD(P) dependent steroid dehydrogenase-like 13398]
1	0	1	2	GLRX2	glutaredoxin 2 16065]
1	0	1	2	POLR3K	polymerase (RNA) III (DNA directed) polypeptide K, 12.3 kDa 14121]
1	1	0	2	HSD17B7	hydroxysteroid (17-beta) dehydrogenase 7 5215]
1	0	1	2	HAUS7	HAUS augmin-like complex, subunit 7 32979]
1	0	1	2	TIPIN	TIMELESS interacting protein 30750]
1	0	1	2	ATAD3A	ATPase family, AAA domain containing 3A 25567]
1	0	1	2	C20orf24	chromosome 20 open reading frame 24 15870]
1	0	1	2	KCTD5	potassium channel tetramerisation domain containing 5 21423]
1	0	1	2	C12orf4	chromosome 12 open reading frame 4 1184]
1	0	1	2	C11orf24	chromosome 11 open reading frame 24 1174]
1	0	1	2	TOR3A	torsin family 3, member A 11997]
1	0	1	2	CCDC86	coiled-coil domain containing 86 28359]
1	0	1	2	SLC52A2	solute carrier family 52, riboflavin transporter, member 2 30224]
1	0	1	2	YRDC	yrdC domain containing (E. coli) 28905]
1	1	0	2	ADM2	adrenomedullin 2 28898]
1	0	1	2	CDT1	chromatin licensing and DNA replication factor 1 24576]
1	0	1	2	ARPC5L	actin related protein 2/3 complex, subunit 5-like 23366]
1	0	1	2	MAK16	MAK16 homolog (S. cerevisiae) 13703]
1	1	0	2	SLC25A25	solute carrier family 25 (mitochondrial carrier; phosphate carrier), member 25 20663]
1	0	1	2	RAD51C	RAD51 homolog C (S. cerevisiae) 9820]
1	0	1	2	TARS	threonyl-tRNA synthetase 11572]
1	0	1	2	ADRM1	adhesion regulating molecule 1 15759]
1	0	1	2	ATG4A	autophagy related 4A, cysteine peptidase 16489]
1	1	0	2	ID1	inhibitor of DNA binding 1, dominant negative helix-loop-helix protein 5360]
1	0	1	2	RFC3	replication factor C (activator 1) 3, 38kDa 9971]
1	1	0	2	ATF4	activating transcription factor 4 (tax-responsive enhancer element B67) 786]
1	0	1	2	ALDOA	aldolase A, fructose-bisphosphate 414]
1	1	0	2	INO80C	INO80 complex subunit C 26994]

Appendix 5 – Genes common to MCF7 and A375 IGF induced up regulated gene signatures

1	0	1	2	NME1	NME/NM23 nucleoside diphosphate kinase 1 7849]
1	0	1	2	PDLIM7	PDZ and LIM domain 7 (enigma) 22958]
0	1	1	2	LDLR	low density lipoprotein receptor 6547]
0	1	1	2	C12orf44	chromosome 12 open reading frame 44 25679]
0	1	1	2	DHCR7	7-dehydrocholesterol reductase 2860]
0	1	1	2	CEBPG	CCAAT/enhancer binding protein (C/EBP), gamma 1837]
0	1	1	2	TNFRSF12A	tumor necrosis factor receptor superfamily, member 12A 18152]
0	1	1	2	MID1IP1	MID1 interacting protein 1 20715]
0	1	1	2	AEN	apoptosis enhancing nuclease 25722]

IGF signatures **(1=present, 0=absent)**

A375 IGF down regulated gene signature for 24 hours	A375 IGF down regulated gene signature for 3 hours	MCF IGF down regulated gene signature	Number of signatures containing gene	hgnc_symbol	Description
1	1	1	3	EFNA1	ephrin-A1 3221]
1	1	1	3	ADCK3	aarF domain containing kinase 3 16812]
1	1	1	3	C5orf4	chromosome 5 open reading frame 4 1334]
1	0	1	2	GALC	galactosylceramidase 4115]
1	0	1	2	TGFBI	transforming growth factor, beta-induced, 68kDa 11771]
1	0	1	2	TIMP3	TIMP metallopeptidase inhibitor 3 11822]
1	0	1	2	CD55	CD55 molecule, decay accelerating factor for complement (Cromer blood group) 2665]
1	0	1	2	LTA4H	leukotriene A4 hydrolase 6710]
1	0	1	2	ATP2B4	ATPase, Ca++ transporting, plasma membrane 4 817]
1	0	1	2	ZNF280D	zinc finger protein 280D 25953]
1	0	1	2	ZNF32	zinc finger protein 32 13095]
1	1	0	2	YPEL2	yippee-like 2 (Drosophila) 18326]
1	1	0	2	EBF3	early B-cell factor 3 19087]
1	0	1	2	BRWD1	bromodomain and WD repeat domain containing 1 12760]
1	0	1	2	HNMT	histamine N-methyltransferase 5028]
1	1	0	2	RPS29	ribosomal protein S29 10419]
1	0	1	2	FAM134B	family with sequence similarity 134, member B 25964]
1	0	1	2	SIDT2	SID1 transmembrane family, member 2 24272]
1	0	1	2	PHF16	PHD finger protein 16 22982]
1	0	1	2	SLC35E2B	solute carrier family 35, member E2B 33941]
1	0	1	2	ALDH7A1	aldehyde dehydrogenase 7 family, member A1 877]
1	0	1	2	FZD2	frizzled family receptor 2 4040]
1	0	1	2	EIF4A2	eukaryotic translation initiation factor 4A2 3284]
1	0	1	2	ERBB3	v-erb-b2 erythroblastic leukemia viral oncogene homolog 3 (avian) 3431]
1	0	1	2	GRN	granulin 4601]

Appendix 6 – Genes common to the MCF7 and A375 IGF induced down regulated gene signatures

1	0	1	2	ITGB5	integrin, beta 5 6160]
1	0	1	2	KCNMA1	potassium large conductance calcium-activated channel, subfamily M, alpha member 1 6284]
1	0	1	2	LAMB1	laminin, beta 1 6486]
1	0	1	2	SMARCE1	SWI/SNF related, matrix associated, actin dependent regulator of chromatin, subfamily e, member 1 11109]
1	0	1	2	SNX1	sorting nexin 1 11172]
1	1	0	2	TFAP2B	transcription factor AP-2 beta (activating enhancer binding protein 2 beta) 11743]
1	1	0	2	TGIF1	TGFB-induced factor homeobox 1 11776]
1	0	1	2	GPR137B	G protein-coupled receptor 137B 11862]
1	0	1	2	NRIP1	nuclear receptor interacting protein 1 8001]
1	1	0	2	FZD7	frizzled family receptor 7 4045]
1	1	0	2	ULK1	unc-51-like kinase 1 (C elegans) 12558]
1	0	1	2	PKP4	plakophilin 4 9026]
1	0	1	2	IRS2	insulin receptor substrate 2 6126]
1	0	1	2	CTSF	cathepsin F 2531]
1	1	0	2	CDKN1B	cyclin-dependent kinase inhibitor 1B (p27, Kip1) 1785]
1	0	1	2	LARGE	like-glycosyltransferase 6511]
1	0	1	2	NREP	neuronal regeneration related protein homolog (rat) 16834]
1	0	1	2	FEZ1	fasciculation and elongation protein zeta 1 (zygin I) 3659]
1	0	1	2	TOM1L1	target of myb1 (chicken)-like 1 11983]
1	0	1	2	NFIB	nuclear factor I/B 7785]
1	0	1	2	RBL2	retinoblastoma-like 2 (p130) 9894]
1	1	0	2	SGK1	serum/glucocorticoid regulated kinase 1 10810]
1	0	1	2	CTDSP2	CTD (carboxy-terminal domain, RNA polymerase II, polypeptide A) small phosphatase 2 17077]
1	0	1	2	SPRY1	sprouty homolog 1, antagonist of FGF signaling (Drosophila) 11269]
1	0	1	2	RAMP1	receptor (G protein-coupled) activity modifying protein 1 9843]
1	0	1	2	LANCL1	LanC lantibiotic synthetase component C-like 1 (bacterial) 6508]
1	1	0	2	NR4A2	nuclear receptor subfamily 4, group A, member 2 7981]
1	0	1	2	PARP4	poly (ADP-ribose) polymerase family, member 4 271]
1	1	0	2	MXD4	MAX dimerization protein 4 13906]
1	1	0	2	SSFA2	sperm specific antigen 2 11319]

Appendix 6 – Genes common to the MCF7 and A375 IGF induced down regulated gene signatures

1	1	0	2	LMO4	LIM domain only 4 6644]
1	1	0	2	SOX5	SRY (sex determining region Y)-box 5 11201]
1	0	1	2	ZNF33B	zinc finger protein 33B 13097]
1	1	0	2	ALX1	ALX homeobox 1 1494]
1	0	1	2	SLC35D2	solute carrier family 35, member D2 20799]
1	1	0	2	TLE4	transducin-like enhancer of split 4 (E(sp1) homolog, Drosophila) 11840]
1	0	1	2	ZMYM6	zinc finger, MYM-type 6 13050]
1	0	1	2	KLHDC2	kelch domain containing 2 20231]
1	0	1	2	VPS41	vacuolar protein sorting 41 homolog (S cerevisiae) 12713]
1	1	0	2	VGLL4	vestigial like 4 (Drosophila) 28966]
1	1	0	2	PUM1	pumilio homolog 1 (Drosophila) 14957]
1	0	1	2	ARHGAP32	Rho GTPase activating protein 32 17399]
1	0	1	2	KIAA0528	KIAA0528 29062]
1	0	1	2	CDK19	cyclin-dependent kinase 19 19338]
1	0	1	2	CRYL1	crystallin, lambda 1 18246]
1	0	1	2	DYNC2LI1	dynein, cytoplasmic 2, light intermediate chain 1 24595]
1	0	1	2	HSD17B11	hydroxysteroid (17-beta) dehydrogenase 11 22960]
1	1	0	2	CRBN	cereblon 30185]
1	1	0	2	ICK	intestinal cell (MAK-like) kinase 21219]
1	0	1	2	ANKRD10	ankyrin repeat domain 10 20265]
1	0	1	2	WDR70	WD repeat domain 70 25495]
1	1	0	2	AGGF1	angiogenic factor with G patch and FHA domains 1 24684]
1	1	0	2	MANSC1	MANSC domain containing 1 25505]
1	0	1	2	PCMTD2	protein-L-isoaspartate (D-aspartate) O-methyltransferase domain containing 2 15882]
1	0	1	2	TBC1D19	TBC1 domain family, member 19 25624]
1	0	1	2	ZNF302	zinc finger protein 302 13848]
1	1	0	2	SERTAD4	SERTA domain containing 4 25236]
1	0	1	2	PLSCR4	phospholipid scramblase 4 16497]
1	0	1	2	SLC24A3	solute carrier family 24 (sodium/potassium/calcium exchanger), member 3 10977]
1	0	1	2	CCPG1	cell cycle progression 1 24227]

Appendix 6 – Genes common to the MCF7 and A375 IGF induced down regulated gene signatures

1	1	0	2	PELI2	pellino E3 ubiquitin protein ligase family member 2 8828]
1	0	1	2	DEPTOR	DEP domain containing MTOR-interacting protein 22953]
1	0	1	2	FYCO1	FYVE and coiled-coil domain containing 1 14673]
1	0	1	2	C10orf57	chromosome 10 open reading frame 57 25804]
1	0	1	2	WDR19	WD repeat domain 19 18340]
1	0	1	2	TRIM8	tripartite motif containing 8 15579]
1	1	0	2	JMJD1C	jumonji domain containing 1C 12313]
1	1	0	2	OR51B4	olfactory receptor, family 51, subfamily B, member 4 14708]
1	1	0	2	ANTXR2	anthrax toxin receptor 2 21732]
1	1	0	2	FBXO32	F-box protein 32 16731]
1	0	1	2	OSBPL1A	oxysterol binding protein-like 1A 16398]
1	0	1	2	PTPN13	protein tyrosine phosphatase, non-receptor type 13 (APO-1/CD95 (Fas)-associated phosphatase) 9646]
1	0	1	2	SPSB3	splA/ryanodine receptor domain and SOCS box containing 3 30629]
1	0	1	2	NEK7	NIMA (never in mitosis gene a)-related kinase 7 13386]
1	1	0	2	AKAP12	A kinase (PRKA) anchor protein 12 370]
1	0	1	2	CRYZL1	crystallin, zeta (quinone reductase)-like 1 2420]
1	1	0	2	EYA1	eyes absent homolog 1 (Drosophila) 3519]
1	1	0	2	CCDC117	coiled-coil domain containing 117 26599]
1	1	0	2	FAM100B	family with sequence similarity 100, member B 28438]
1	0	1	2	PRCP	prolylcarboxypeptidase (angiotensinase C) 9344]
1	1	0	2	C12orf76	chromosome 12 open reading frame 76 33790]
0	1	1	2	PTCH1	patched 1 9585]
0	1	1	2	FRAT1	frequently rearranged in advanced T-cell lymphomas 3944]
0	1	1	2	FRAT2	frequently rearranged in advanced T-cell lymphomas 2 16048]
0	1	1	2	HBP1	HMG-box transcription factor 1 23200]
0	1	1	2	KIAA0430	KIAA0430 29562]
0	1	1	2	PHF3	PHD finger protein 3 8921]
0	1	1	2	LETMD1	LETM1 domain containing 1 24241]
0	1	1	2	CCDC28A	coiled-coil domain containing 28A 21098]
0	1	1	2	SYF2	SYF2 homolog, RNA splicing factor (S cerevisiae) 19824]

Appendix 6 – Genes common to the MCF7 and A375 IGF induced down regulated gene signatures

0	1	1	2	YPEL5	yippee-like 5 (Drosophila) 18329]
0	1	1	2	MNT	MAX binding protein 7188]
0	1	1	2	WDR48	WD repeat domain 48 30914]
0	1	1	2	TBC1D15	TBC1 domain family, member 15 25694]
0	1	1	2	ANKRA2	ankyrin repeat, family A (RFXANK-like), 2 13208]
0	1	1	2	DHX40	DEAH (Asp-Glu-Ala-His) box polypeptide 40 18018]
0	1	1	2	GABARAPL1	GABA(A) receptor-associated protein like 1 4068]
0	1	1	2	ARID5B	AT rich interactive domain 5B (MRF1-like) 17362]
0	1	1	2	CBLB	Cbl proto-oncogene, E3 ubiquitin protein ligase B 1542]